INTERNATIONAL DOCTORAL
SCHOOL OF THE USC

Ricardo
Rodiño Balboa

PhD Thesis

Palladium-Catalyzed Transformations of Alkylidenecyclopropanes

Santiago de Compostela, 2025

Doctoral Programme in Chemical Science and Technology

ESCOLA DE DOUTORAMENTO
INTERNACIONAL DA USC

DOCTORAL THESIS

PALLADIUM-CATALYZED TRANSFORMATIONS OF ALKYLIDENECYCLOPROPANES

Author

Ricardo Rodiño Balboa

Supervisors: Fernando José López García, José Luis Mascareñas Cid

Tutor: José Luis Mascareñas Cid

PHD PROGRAMME IN CHEMICAL SCIENCE AND TECHNOLOGY

SANTIAGO DE COMPOSTELA

Acknowledgments/ Agradecimientos

Parece que llega a su fin la larga y emocionante aventura que es hacer una tesis doctoral; y como se suele decir, *de ben nacidos é ser agradecidos*.

Quiero comenzar mencionando a José Luis, y agradecerle el haberme transmitido la pasión y la curiosidad por la química orgánica que me han llevado a comenzar este camino. Gracias a Fernando, quien siempre ha confiado en mí, y me ha apoyado a lo largo de todos estos años. Sin su guía, esta tesis no habría sido posible.

Al comenzar en un laboratorio hay mucho que aprender. Por ello, valoro especialmente la paciencia de Jaime, y sobre todo de Felipe, durante mis primeros años en el grado y máster. Dr. Verdugo, gracias por permitirme acompañarte hasta el día de hoy explorando las maravillas de los ACPs, no solo como compañero, sino también como amigo. Muchas gracias también a Martín, quien me ayudó a adentrarme en el mundo de los cálculos DFT y perfiles de reacción que ahora *aliñan* mi trabajo experimental.

Agradezco la buena acogida por parte de todo el grupo, que me dio la seguridad para continuar la carrera investigadora hasta el doctorado, especialmente a Borja, Marcote y Xandro. Más tarde llegaron Edu, vecino de agonías con los ACPs y otras *cacas*; y Jose, el viejo y sabio castor que me ayudó a racionar la cantidad de sustrato en catálisis. Más allá de lo personal, ambos han sido referentes a nivel profesional. También merecen su hueco aquí Andrés, Sara, Soraya y Mache; por sus consejos y buenos momentos. Gracias.

Tuve la suerte de conocer a Andy, una persona con gran pasión y curiosidad, un amigo con quien compartí muchos momentos dentro y fuera del laboratorio. ¡Sigue siendo tan caótico y divertido! Dani también merece un lugar especial (que no aparte), pues comenzamos juntos el grado, y continuamos en el máster y el doctorado a la par. He conocido a poca gente tan *buena* como él, en diversos sentidos, y solo le deseo lo mejor. Gracias por todo, chicos.

Con el tiempo, el P3L3 se ha convertido en un segundo hogar. Álex, máis alá das charlas de química, calculos e outras rabuñadas, as nosas conversas abstractas foron fundamentais para manter a locura que se precisa para facer unha tese. Carlos, gracias por tus plantas, consejos y ese característico sentido del humor que te hace tan especial. Sergio, como legítimo heredero de la vitrina 2, apúntate a crossfit. Fuera bromas, vales *oro* (recuerda que eso es bueno). Iván, gracias por ser un *nakama*. Ojalá la vida te dé buenas *cartas* y pocos racematos (o no). Laura, ¡sigue siempre con esa energía! Gracias por mantener un poco el orden dentro del caos del P3L3. Pablo, gracias por darme los momentos más absurdos del laboratorio, que hacen trabajar un poco más divertido. María y Domingo, disfrutad de esta etapa, que es dura, pero también bonita. Sebas [inserte dinosaurio].

Mencionar también a la peñita del P3L4 y P3L5, en particular a Xulián, una amistad que me llevo del grado, y que con su energía y buen humor es capaz de animar cualquier sala o evento. A Cinzia, por tener siempre una sonrisa y un hueco para un abrazo; a Fer, por sus reflexiones; y a mis otros compañeros: Leo, Adrián, Alejandra, Clara, Álvaro, Manuel José, David, Laura y Ximena. Gracias y, ¡mucho ánimo a todos! Gracias también a Alba, por salir bien en las fotos; a Celia, por su buen rollo; y a Mery, por llamarme Charlie. Gracias también a Lara, Rebeca y Mauro. Gracias a Paula, por darme un abrazo cuando lo necesitaba; y a Zeko, por ser un gran compañero de congresos, y otras actividades extracurriculares. Recordaré con cariño el comité CiQUS, los cafés COVID, los juegos de mesa en casa de Andrés o los lunes de Perk.

Gracias a la Universidad de Santiago y al CiQUS por todas sus infraestructuras y servicios, en especial a Mencha, Paula, Andrea, Noela y Arcadio. A Adrián por haberme ayudado tanto con el papeleo (qué paciencia). A la fundación "Segundo Gil Dávila", al Ministerio de Universidades (becas *FPU*), y a MetBioCat, quienes me han permitido realizar la tesis doctoral y financiar mi estancia en el extranjero.

Thanks to Professor Tomislav Rovis, who let me explore NYC and know how is researching in a such outstanding university as is Columbia University. Xiao, Tairin, Leo, Ben, thanks for making those three months easier.

Gracias a mi familia, por haber *financiado* esta carrera de fondo con táperes y con cariño, y haberme apoyado cuando lo necesitaba. A María, por haber aguantado mis cambios de humor en esta última etapa. A mis amigos, por haber entendido mis ausencias. Gracias a toda esa gente que en algún momento me ha ayudado.

Table of contents

Abbreviations and Acronyms

Ac	Acetyl (CH_3CO-)
acac	Acetylacetonate
ACP	Alkylidenecyclopropane
ADTMCs	2-Alkylidenetrimethylene carbonates
Alk	Alkyl
Ar	Aryl
AcOH	Acetic acid
BArF	Tetrakis(3,5-bis(trifluoromethyl)phenyl) borate
BINAP	2,2'-Bis(diphenylphosphino)-1,1'-binaphthalene
BINOL	1,1'-Bi(2-naphthol)
Bn	Benzyl/$C_6H_5CH_2$
Boc	*tert*-Butyloxycarbonyl ($C_5H_9O_2$)
br	Broad
BrettPhos	2-(Dicyclohexylphosphino) 3,6-Dimethoxy-2',4',6'-triisopropyl-1,1'-biphenyl
Bz	Benzoyl (C_6H_5CO-)
BzOH	Benzoic acid
Cbz	Benzyloxycarbonyl
CCDC	Cambridge crystallographic Data centre
Cin.	Cinnamyl
COD	1,5-Cyclooctadiene
Conv.	Conversion
COT	Cyclooctatriene
CPA	Chiral phosphoric acid
CPBA	Chloroperoxybenzoic acid
Cp	Cyclopentadienyl
Cy	Cyclohexyl (C_6H_{11}-)
DAD	Diode array detector
d	Doublet
dd	Double doublet
ddd	Doublet of doublet of doublets
dioxane	1,4-Dioxane
dppe	1,2-Bis(diphenylphosphino)ethane
dppf	1,1'-Bis(diphenylphosphino)ferrocene
dq	Doublet of quartet
dt	Doublet of triplets
dba	Dibenzylideneacetone
DAD	Diode array detector
DCE	1,2-Dichloroethane
DEAD	Diethyl azodicarboxylate
DFT	Density functional theory
DIAD	Diisopropyl azodicarboxylate
DMA	Dimethylacetamide
DMAP	4-dimethylaminopyridine
DME	Dimethoxy ethane
DMF	*N,N*-Dimethyl formamide
DMSO	Dimethyl sulfoxide
dppe	1,2-Bis(diphenylphosphino)ethane
dr	Diastereomeric ratio
EA	Energy activation
ee	Enantiomeric excess
equiv.	Equivalents
er	Enantiomeric ratio
ESI	Electrospray
EWG	Electron-withdrawing group
GC-MS	Gas chromatography mass spectrometry
HOMO	Highest occupied molecular orbital
HPLC	High performance liquid chromatography
HRMS	High resolution mass spectra
IMes	1,3-Bis(2,4,6-trimethylphenyl)-1,3-

	dihydro-2*H*-imidazol-2-ylidene
^{i}Pr	Isopropyl (C_3H_7-)
LRMS	Low resolution mass spectra
LUMO	Lowest unoccupied molecular orbital
m	Multiplet
MCP	Methylenecyclopropane
Ms	Methanesulfonyl/mesyl
MS	Molecular sieves
n.a.	Not available
Napht	Naphthyl
NBD	Norbornadiene
NHC	*N*-heterocyclic carbene
NMR	Nuclear magnetic resonance
Ns	Nosyl
Nu	Nucleophile
p	Pentet
pent	Pentyl
Phth	Phthalimide
Pin	Pinacolato
phen	1,10-phenanthroline
Py	Piridine
q	Quartet
qd	Quartet of doublets
rt	Room temperature
RuPhos	2-Dicyclohexylphosphino-2',6'-diisopropoxybiphenyl
s	Singlet
SDP	Chiral spiro diphosphine
t	Triplet
t	Time
T	Temperature
TBS	*tert*-butyldimethylsilyl
^{t}Am	*tert*-amyl
^{t}Bu	*tert*-butyl
^{t}BuBrettPhos	2-(Di-*tert*-butylphosphino)-2',4',6'- Triisopropyl-3,6-dimethoxy-1,1'-biphenyl
^{t}BuXPhos	2-Di-tert-butylphosphino-2',4',6'-triisopropylbiphenyl
td	Triple doublet
Tf	Triflate
TFA	Trifluoroacetic acid
THF	Tetrahydrofuran
TLC	Thin layer chromatography
TMC	Transition metal-catalyzed
TMEDA	Tetramethylethylenediamine
TMS	Trimethylsilyl
TMM	Trimethylenemethane
Tol	Tolyl
TS	Transition state
Ts	*Para*-toluenesulfonyl/Tosyl
VAPOL	2,2'-Diphenyl-(4-biphenanthrol)
VANOL	3,3'-Diphenyl-2,2'-bi-1-naphthalol
VCP	Vinylcyclopropane
VDCP	Vinylidenecyclopropane
XPhos	2-Dicyclohexylphosphino-2',4',6'-triisopropylbiphenyl

Disclaimer

Throughout this thesis, when referring to cycloadditions we use the Huisgen notation, using parenthesis, where the numbers refer to the atoms involved in the forming ring [for instance in (4+3), (4+2), (2+2) cycloadditions] to distinguish from the Woodward-Hoffman notation, using brackets, where the numbers refer to the electrons involved in bonding changes.[1] However, in some specific examples we use the brackets notation that is also acceptable.

[1] a) Huisgen, R. Cycloadditions — Definition, Classification, and Characterization. *Angew. Chem. Int. Ed.* **1968**, *7*, 321.; b) Limanto, J.; Khuong, K. S.; Houk, K. N.; Snapper, M. L. Intramolecular Cycloadditions of Cyclobutadiene with Dienes: Experimental and Computational Studies of the Competing (2 + 2) and (4 + 2) Modes of Reaction. *J. Am. Chem. Soc.* **2003**, *125*, 16310.

Summary / Resumo

Summary

Organic synthesis has profoundly impacted fields such as medicinal chemistry, materials science, and agriculture by enabling the creation of complex molecular structures beyond those found in nature. In recent years, the field has embraced sustainable practices aligned with the principles of Green Chemistry, prioritizing efficiency, environmental responsibility, and atom economy. In this context, catalysis has emerged as a key synthetic tool, driving more selective and efficient reactions, often under milder conditions, and reducing waste and energy consumption.

Among homogeneous catalytic methods, in which catalysts and reactants are in the same phase, those based on complexes featuring transition metals stand out for their tunable electronic and steric properties. Advances in this field have allowed to broaden significantly the catalogue of chemical transformations available in the toolbox of synthetic chemistry. Therefore, palladium-catalyzed cross-coupling reactions are indispensable tools in organic synthesis. Pioneered in the 1970s by Heck, Negishi, and Suzuki, these transformations enable the creation of C-C bonds by coupling organic halides with partners such as alkenes, alkynes, organozinc, or organoboron reagents. Their groundbreaking work has been recognized with the 2010 Nobel Prize in Chemistry. Related advancements, such as the Buchwald-Hartwig amination for C-N bond formation, among many others, continue to expand the utility of cross-couplings.

Cycloaddition reactions are powerful transformations for constructing cyclic frameworks, particularly heterocycles, by generating at least two σ-bonds in a single step. Traditional cycloadditions, like the Diels-Alder reaction, are well-understood but often require activating functional groups and harsh conditions, limiting their scope. Transition metal catalysis has addressed these limitations by enabling formal cycloadditions under milder conditions, and introducing new reaction types, while including enantioselective processes when chiral ligands are employed. This is particularly relevant for applications related to medicinal chemistry, since opposite enantiomers usually hold different biological profiles. The importance of asymmetric catalysis with transition metals became visible with the Nobel Prize award of 2001, which was shared by W. Knowles, R. Noyori and B. Sharpless.

Alkylidenecyclopropanes (ACPs) are relevant organic scaffolds, featuring a three-membered ring with an *exo*-cyclic double bond. These structural features make ACPs highly strained systems, facilitating the insertion of transition metals into one of their C-C bonds. Additionally, the double bond can also be used as a handle for triggering the metal-catalyzed transformations.

Therefore, ACPs can behave as olefins, reacting as 2C synthons in different cycloadditions or, more interestingly, as 3C components. While cycloadditions of ACPs catalyzed by heat or Lewis acids are well-established, those promoted by transition metal catalysts are still scarce. Binger developed pioneering examples in the eighties, in particular, intermolecular Pd-catalyzed (3+2) cycloadditions of methylenecyclopropane (MCP) and strained alkenes. Mechanistically, the authors proposed the participation palladacyclobutane and trimethylmethane (TMM) species as key intermediates (**Scheme 1**).

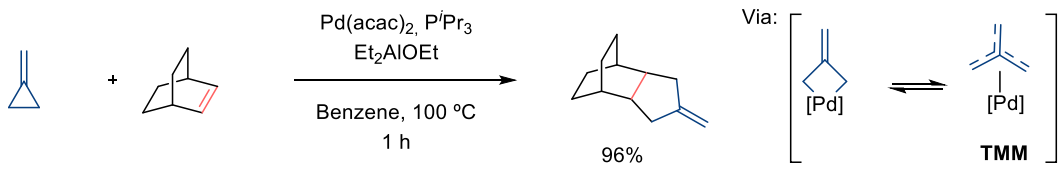

Scheme 1. Pd(0)-catalyzed formal (3+2) cycloaddition between MCPs and strained alkenes.

These and additional studies were primarily focused on such intermolecular processes. The development of intramolecular variants, enabling the synthesis of more complex polycyclic structures, was pioneered by our group in the early 2000s. The methods included a range of TMC intramolecular cycloadditions using ACPs tethered to carbon-based unsaturated partners, such as

alkenes, alkynes, dienes and allenes. Moreover, intermolecular and intramolecular multicomponent (3+2+2) cycloadditions were also developed, allowing the construction of larger polycyclic scaffolds.

In contrast to TMC cycloadditions of ACPs with C-C unsaturated systems, the number of related ACP cycloadditions involving heteroatom-containing partners is extremely low and essentially limited to the pioneering cases reported in 2001 by Yamamoto and coworkers. In particular, these authors reported a Pd(0)-catalyzed intermolecular (3+2) cycloaddition of ACPs with aldehydes and tosyl imines, to respectively afford tetrahydrofurans and pyrrolidines. However, the scope and versatility of these processes is very limited, while the reaction conditions are not synthetically convenient (**Scheme 2**).

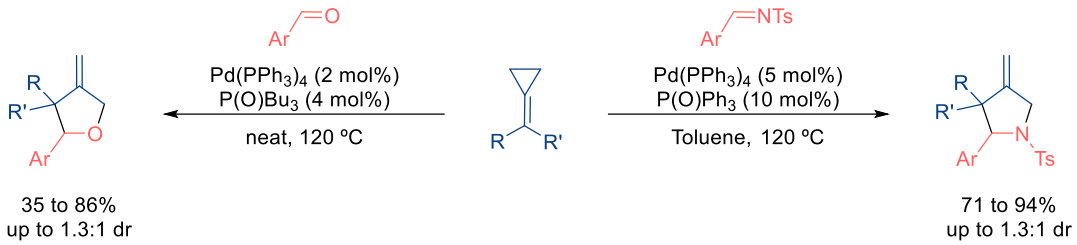

Scheme 2. Pd(0)-catalyzed intermolecular (3+2) heterocycloadditions of ACPs reported by Yamamoto.

At the first stages of my PhD work, our group explored the development of intramolecular heterocycloadditions of ACPs, describing a Pd(0)-catalyzed (3+2) cycloaddition of ACP-tethered carbonyls, to deliver polycyclic tetrahydrofuran scaffolds with high efficiency (**Scheme 3a**). The use of Pd(0) catalysts bearing Buchwald ligands proved crucial for the cycloaddition, although the mechanistic basis for such efficiency remained unclear. Preliminary results of Dr. Verdugo revealed that the same catalytic system was also effective to promote the intramolecular (3+2) aza-cycloaddition of ACPs when oxime ethers were used as counterparts, forming bicyclic pyrrolidine frameworks (**Scheme 3b**). These preliminary results set the basis for new objectives that were addressed in this PhD work.

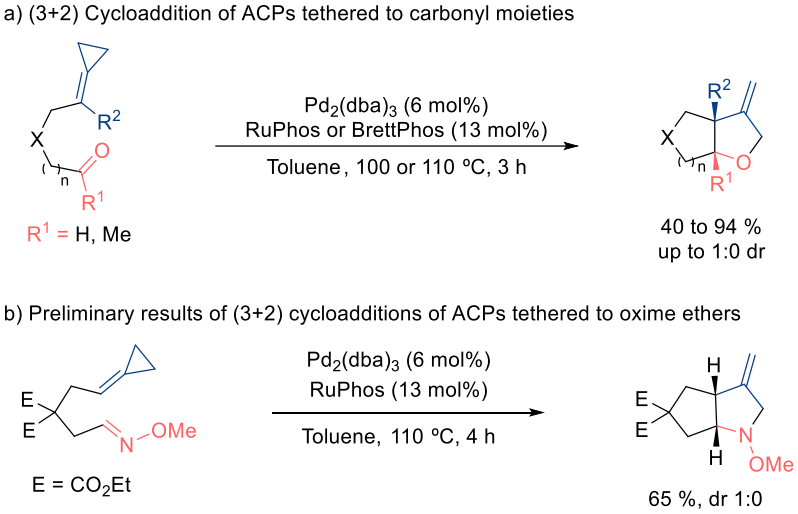

Scheme 3. Pd(0)-catalyzed intramolecular (3+2) heterocycloadditions of ACPs explored by our group.

Cycloisomerization reactions of ACPs have also been explored using transition metal catalysts, offering new pathways to complex cyclic frameworks. For example, in 2018, Evans reported a Rh(I)-catalyzed ene-cycloisomerization of ACPs tethered to substituted allyl sulfides, achieving high yields and good diastereoselectivities (**Scheme 4**).

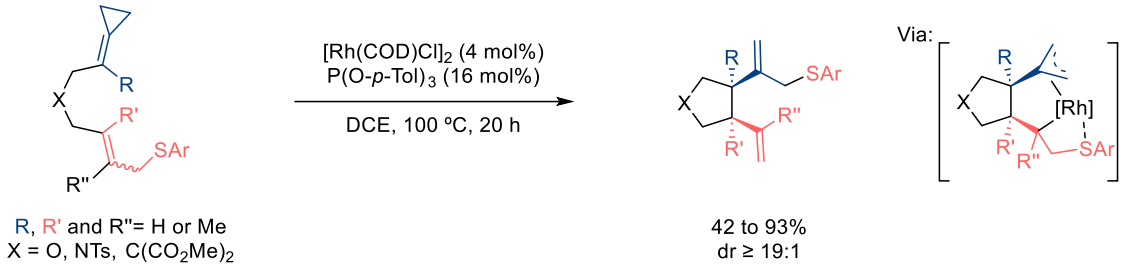

Scheme 4. Rh(I)-catalyzed ene-cycloisomerization of ACPs with intramolecular β-sulfide elimination.

Despite the synthetic potential of this and other ACP cycloisomerizations, tandem and multicomponent processes, particularly with heteroatom-containing partners, remained underexplored.

Tandem ring-opening/addition reactions of ACPs can be promoted by transition metal catalysts such as Ni, Rh, or Pd, forming allylic and homoallylic compounds through selective hydrofunctionalization processes. A seminal example by Yamamoto in the late 1990s involves a Pd(0)-catalyzed hydrofunctionalization with malonate nucleophiles, to yield 1,1-disubstituted alkenes. Mechanistically, an initial palladium hydride species and and π-allyl Pd(II) intermediates were proposed (**Scheme 5**). Later, Yamamoto and others extended this strategy to various nucleophiles.

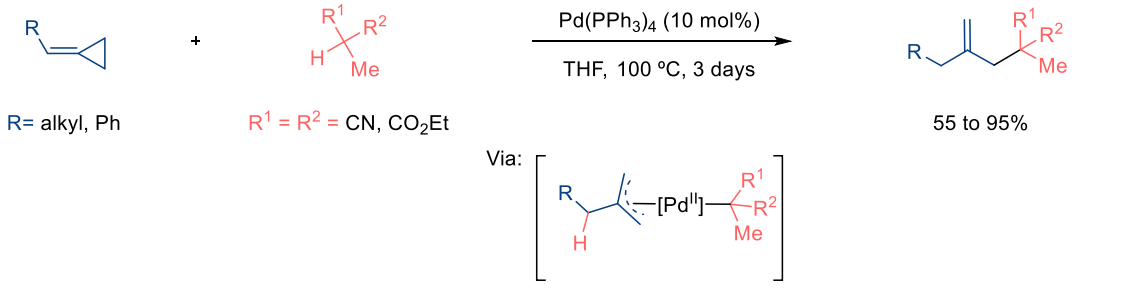

Scheme 5. Pd(0)-catalyzed hydrocarbonation of ACPs with malonate-type nucleophiles.

Based on these precedents, this PhD thesis aimed to expand the metal-catalyzed chemistry of ACPs addressing three primary objectives.:

- **Discovery novel cycloaddition reactions of ACPs with hetero-unsaturated partners**, focusing on functionalized pyrrolidines, and use of DFT studies to elucidate mechanistic details, for both oxa- and aza-cycloadditions.
- **Development of tandem cycloisomerization processes of ACPs** to access new cyclic scaffolds, supported by computational studies
- **Perform multicomponent cycloadditions of ACPs with heteroatom partners** to uncover new methodologies for synthesizing medium-sized heterocycles.

Pd(0)-Catalyzed (3+2) Cycloadditions between ACPs and Imines

Pyrrolidine scaffolds play a crucial role in medicinal chemistry, as they constitute the core of numerous biologically active molecules. Although various synthetic methods exist, many require multistep processes, underscoring the need for more efficient and direct catalytic approaches. In this regard, transition-metal-catalyzed (TMC) cycloadditions stand out for their ability to construct cyclic frameworks from simple acyclic precursors, often with high regio- and stereocontrol.

ACPs can participate as counterparts in TMC cycloadditions with unsaturated heteroatom containing partners to form five-membered aza-heterocycles; however, such examples are scarce and of very limited scope. In this context, our group envisioned the development of an intramolecular

cycloadditions using ACPs tethered to oxime ethers. In preliminary investigations, Dr. Verdugo discovered that the catalyst generated from $Pd_2(dba)_3$ and RuPhos can promote the desired annulation to yield pyrrolidine products (see **Scheme 3b**, page 10). The use of bulky phosphite ligands also enabled the formation of the cycloadducts. Notably, by employing Pd(0)-catalysts with chiral phosphoramidite ligands the cycloaddition of a model precursor led to the desired heterocycle with promising enantioselectivities.

Based on these precedents, we aimed to thoroughly explore the Pd(0)-catalyzed intramolecular cycloaddition between ACPs and oxime derivatives, as well as to develop an intermolecular variant that could overcome the important limitations of the previously reported method. Moreover, we combined this experimental research with a computational analysis of the hetero-cycloadditions, trying to elucidate key mechanistic information.

Regarding the intramolecular transformation, the Pd(0)-catalyzed (3+2) cycloaddition between ACPs and oxime ethers proved to be highly sensitive to structural features of the substrates (**Scheme 6**). The desired cycloadducts were only obtained with aldoxime precursors bearing a diester moiety at the tether. In many case, dienic side-products were also obtained. We hypothesized that the limited scope arose from the challenges associated with the migratory insertion of the C=N bond in the oxime ether. Attempts to enhance reactivity using acidic additives and electron-poor imines were unsuccessful.

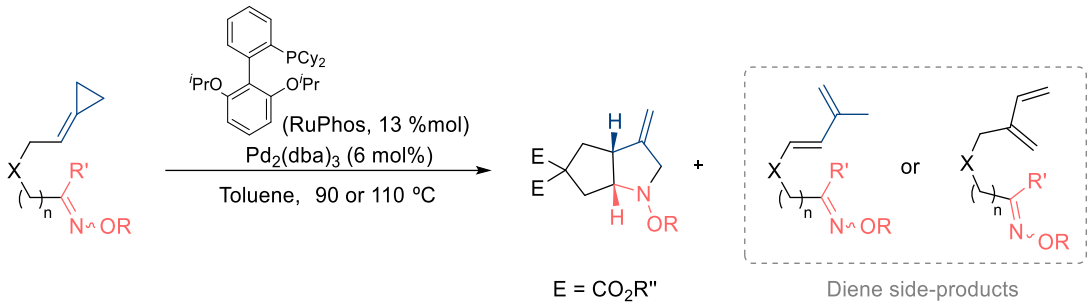

Scheme 6. Pd(0)-catalyzed intramolecular (3+2) heterocycloaddition of ACPs tethered to oxime ethers.

We carried out mechanistic DFT studies using Pd(0)-*t*BuXPhos as model catalyst, which confirmed that these cycloadditions occur via an initial insertion of the Pd complex into the distal C–C bond of the ACP, followed by a metallo–ene rearrangement and a final reductive elimination. Remarkably, computations showed the critical role of the hemilabile interactions between the Pd center and the ligand, as well as the relevance of the ligand conformation, in stabilizing key reaction intermediates.

Deuterium labeling experiments revealed a new reactivity pattern for ACPs, a stepwise rearrangement which leads to some of the diene obtained as side-products (**Scheme 7**). DFT calculations supported this pathway, showing a minimal energy difference between the cycloaddition and diene-forming pathways, which is consistent with the formation of these dienes in many cases.

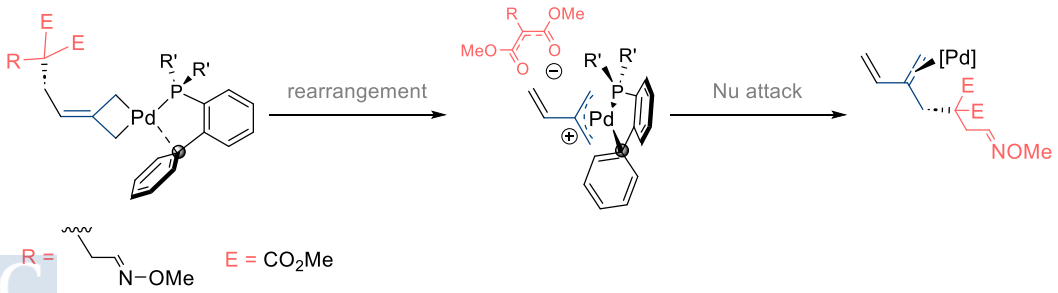

Scheme 7. Mechanistic proposal for diene by-products formation based on DFT studies.

For the intermolecular variant, a catalytic system consisting of $Pd_2(dba)_3$ and a phosphoramidite ligand facilitated the (3+2) cycloaddition between ACPs and sulfonyl imines (**Scheme 8**). The method tolerates different substituents at the ACP and a wide range of cyclic and acyclic imines as partners, including ketimines, to afford functionalized pyrrolidines in high yields. Additionally, enantioselective studies with a model substrate, led to the identification of a (S)-VAPOL-derived phosphoramidite that affords an 83% yield and an enantioselectivity of 78%.

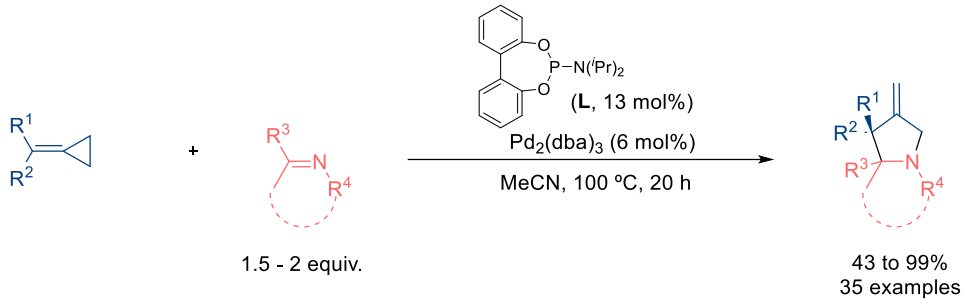

Scheme 8. Pd(0)-catalyzed intermolecular (3+2) heterocycloaddition of ACPs and various imine partners.

DFT studies supported a palladaene mechanism similar to that proposed for the intramolecular cycloaddition. These computations emphasized the role of hemilabile interactions between the Pd center and the bulky ancillary ligand, which help to stabilize key intermediates and to determine the selectivity of the heterocycloaddition.

A DFT Mechanistic Study of Pd(0)-Catalyzed (3+2) Cycloadditions between ACPs and Carbonyls

Transition-metal-catalyzed (TMC) cycloadditions between ACPs and carbonyl partners are very scarce. To address this gap, our group investigated intramolecular cycloadditions of ACPs with aldehydes and ketones. Initial ligand screenings revealed that common ligands used for related (3+2) cycloadditions with alkenes failed to deliver satisfactory yields. However, Buchwald's biaryl monophosphines, such as BrettPhos or RuPhos, proved to be highly effective, enabling the synthesis of 5,5- and 6,5-fused bicyclic THFs with excellent yields, *syn* selectivity and broad scope (see **Scheme 3a**, page 10). Moreover, these catalytic systems also promoted efficiently the intermolecular (3+2) cycloadditions between ACPs and trifluoromethyl ketones, to afford β-methylene THFs in high yields.

Based on these foundations, we computationally investigated the mechanism of these heterocycloadditions, specifically focusing on uncovering the key role of Buchwald ligands in enabling these reactions. Therefore, we explored Pd(0)-catalyzed (3+2) cycloadditions between ACPs and carbonyl partners, both intra- and intermolecularly. For comparative purposes, we employed the simple Pd(0)-PH_3 complex to get simple idea of the different alternatives and the a realistic catalysts, comprising ^{t}BuXPhos as ligand, to determine the specific role of this type of ligands.

For the intramolecular transformation, we have evaluated the most plausible pathways: a metalloene process (a) or an isomerization/migratory insertion process (b, **Scheme 9**).

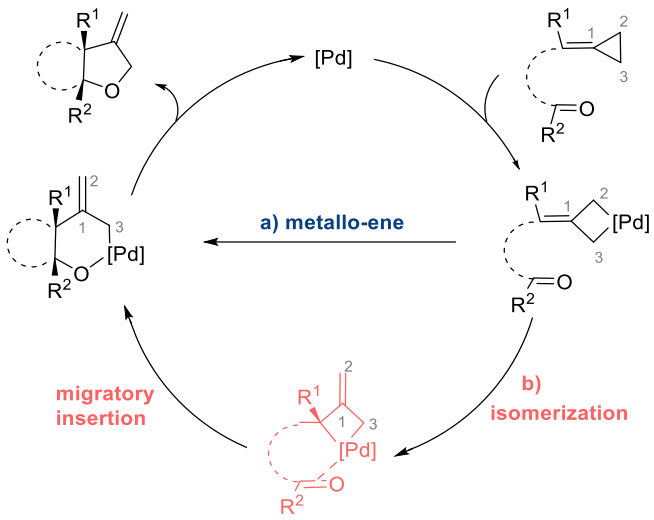

Scheme 9. Evaluated pathways for the Pd(0)-catalyzed intramolecular (3+2) cycloaddition.

Studies with Pd(0)-PH_3 suggested that the metalloene pathway (path a) might be energetically preferred. These conclusion was further confirmed using Pd(0)-*t*BuXPhos as catalyst. Notably, the Buchwald ligands appear to be crucial for the heterocycloaddition, as various hemilabile interactions between the palladium center and specific atoms of the ligand (Pd-H and Pd-C_{ipso} of the biaryl), stabilize the different intermediates throughout the catalytic cycle (**Figure 1**). In this regard, the biaryl conformation of the Buchwald ligand plays a key role, as its "inward" conformation facilitates the afore mentioned secondary interactions, ultimately favoring a less energetic overall reaction pathway.

Additional studies on migratory insertion and reductive elimination confirmed the importance of these hemilabile interactions in the stabilization of key intermediates.

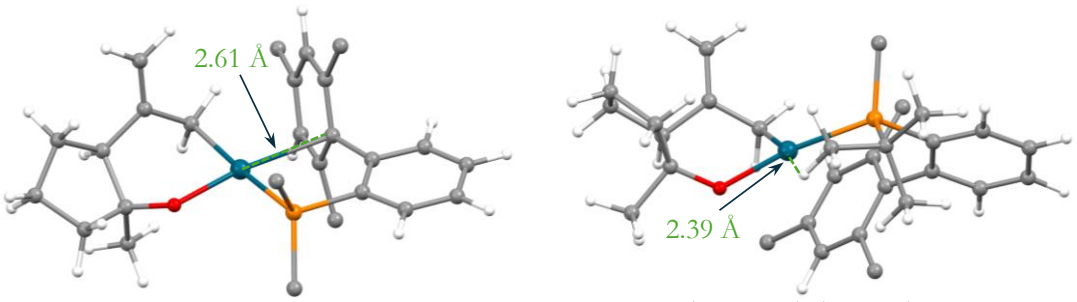

Pd-C_{ipso} interaction facilitated by an *inward* biaryl conformation

Pd-H agostic interaction

Figure 1. 3D examples of key Pd-*t*BuXPhos interactions stabilizing palladacyclic intermediates.

For the intermolecular cycloaddition, we examined the metalloene pathway using both acetophenone and 2,2,2-trifluoroacetophenone as carbonyl partners, as well as Pd(0)-PH_3 and Pd(0)-*t*BuXPhos as catalyst. Remarkably, the fluorinated carbonyl partner significantly facilitated the migratory insertion with both Pd(0)-catalysts. Studies with Pd(0)-*t*BuXPhos suggested that the Buchwald ligand could play a role in improving the selectivity of the cycloaddition, suppressing side pathways. Moreover, these studies showed again the importance of hemilabile secondary interactions between the ligand and the metal center, and the relevance of the "inward" ligand conformation.

Pd(0)-Catalyzed Tandem Cycloisomerization/Allylic Substitution Reactions of ACPs tethered to Carbonyl and Imine partners

Palladium-catalyzed reactions involving π-allyl intermediates have become pivotal in organic synthesis, enabling the efficient formation of C–C and C–heteroatom bonds. These intermediates, which are typically obtained via oxidative addition of allylic substrates with leaving groups, can react with various nucleophiles including organometallic reagents (e.g. organoboron or organozinc reagents), to give the corresponding allyl cross-coupling products. Strained systems like ACPs can also generate π-allyl intermediates under palladium catalysis, so these intermediates could be trapped by appropriate nucleophiles. However, the exploration of this type of tandem processes, especially when using organometallic reagents, remains underexplored.

In this context, our group developed a tandem cycloisomerization and cross-coupling methodology that intercepts π-allyl-Pd(II) intermediates, generated from ACPs tethered to carbonyl moieties, with boronic acids, to yield highly functionalized cyclopentanols (**Scheme 10**). Using a catalyst generated in situ from $Pd_2(dba)_3$ and an electron-poor phosphine, the transformation showed a broad scope and high stereoselectivities.

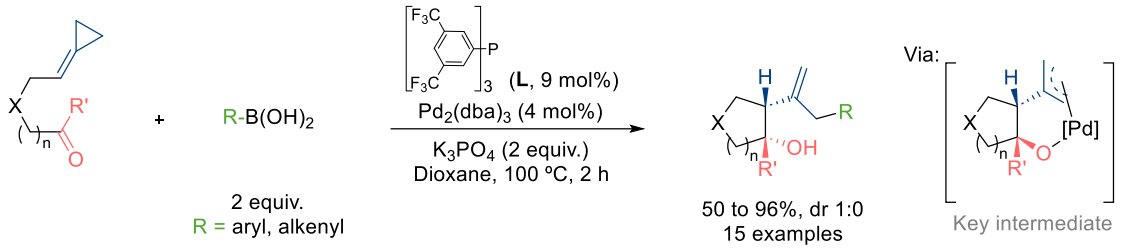

Scheme 10. Tandem cycloisomerization / cross coupling between keto-ACPs and boronic acids.

Preliminary results further showed that 1,3-dicarbonyls can serve as nucleophiles under similar catalytic conditions, yielding cyclic alcohols efficiently.

On these bases, we planned to explore the scope of these cycloisomerization / cross-coupling reactions using 1,3-dicarbonyls and phenols as nucleophiles. Moreover, we aimed to develop tandem processes with analogue ACP-imine partners, and shed light on the mechanism of these transformations through DFT computational studies.

Thus, using a catalyst generated from $Pd_2(dba)_3$ and an electron-poor phosphine, the reaction of ACPs-tethered carbonyls with a variety of 1,3-dicarbonyl nucleophiles provided the expected cyclic alcohols in good-to-excellent yields and high *syn* selectivity for most cases (**Scheme 11**).

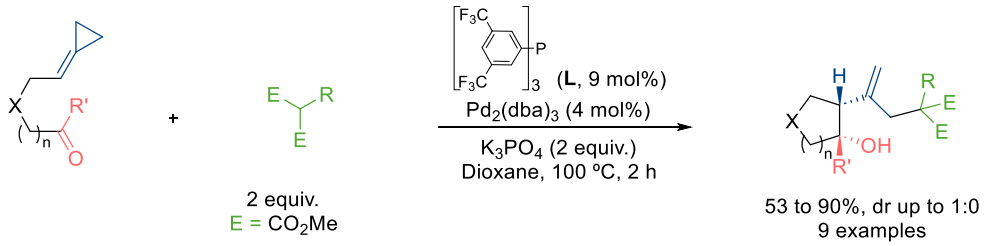

Scheme 11. Tandem cycloisomerization / cross-coupling between keto-ACPs and 1,3-dicarbonyl compounds.

The use of a phosphoramidite as ligand, instead of the electron-poor phosphine, enabled the participation of alcohols as nucleophiles, providing the corresponding products in good yields and total *syn* selectivity (**Scheme 12**).

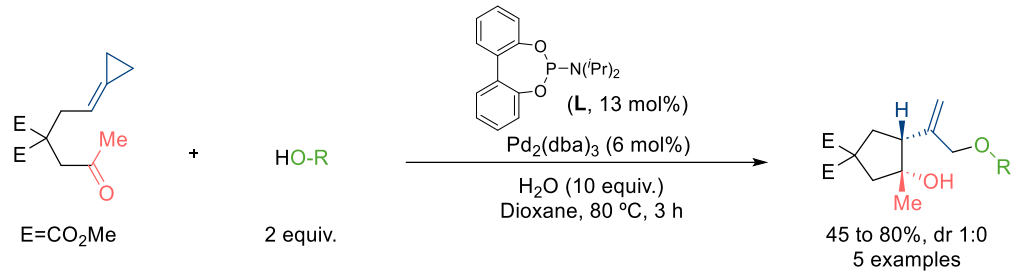

Scheme 12. Tandem cycloisomerization / cross coupling between keto-ACPs and alcohols.

Additionally, we have developed a tandem cycloisomerization/cross-coupling process of ACPs tethered to sulfinyl imines, and aryl boronic acids, using a catalyst generated from $Pd_2(dba)_3$ and a bulky phosphite. Although more restricted compared to the analogous reaction with ACPs tethered to carbonyl moieties, the transformation provided the corresponding cyclic amines in good-to-excellent yields and complete *syn* selectivity (**Scheme 13**).

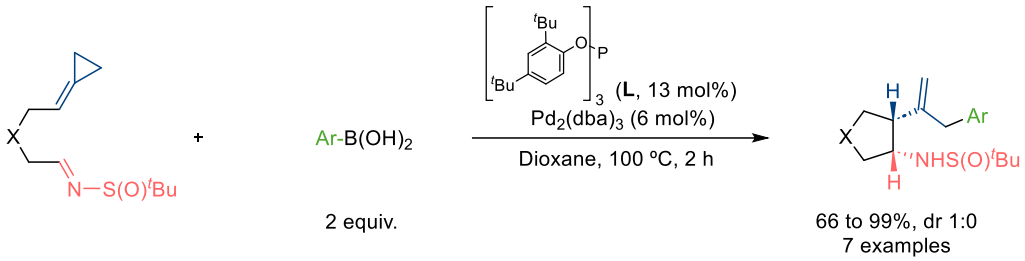

Scheme 13. Tandem cycloisomerization / cross coupling between imine-ACPs and aryl boronic acids.

DFT computations of tandem processes involving keto-ACPs, using Pd(0)-$P(OMe)_3$ as model catalyst, revealed that Pd(II)-allyl intermediates preferentially proceed via transmetalation with the boronic acid rather than through a C–O reductive elimination. In contrast, the use of Pd(0)-^{t}BuXPhos promotes the formation of σ-allyl oxapalladacyclic intermediates, which energetically favor the reductive elimination toward the (3+2) adduct. Consistently, calculations with Pd(0)-$P(OMe)_3$ revealed that the out-of-sphere attack of dimethyl malonate on the Pd(II)-allylic intermediate is energetically preferred over the competitive C-O reductive elimination. These findings align well with experimental results, as electron-poor monophosphines favor the formation of tandem products, whereas Buchwald ligands such as ^{t}BuXPhos promote the (3+2) intramolecular cycloadducts. Preliminary DFT analysis of ACPs tethered to imines and boronic acids also revealed a mechanistic pathway similar to that proposed for keto-ACPs.

Pd(0)-Catalyzed Cross-Coupling between ACPs and Boronic Acids

The Pd(0)-catalyzed hydrofunctionalization of ACPs is a versatile approach for synthesizing 1,1-difunctionalized alkenes via ring-opening reactions that generate Pd π-allyl intermediates. This method has been applied predominantly to relatively acidic hydrogen-containing pronucleophiles such as alcohols, amines, and amides, whereas the use of carbon-based nucleophiles is underexplored and limited to malonates or electron-rich heteroaromatics. Mechanistically, the process is proposed to proceed through a palladium hydride species that, after a hydropalladation delivers a σ-cyclopropyl intermediate. A subsequent β-carbon elimination leads to a key π-allyl species that is trapped by the nucleophile. However, alternative pathways involving palladacyclobutane intermediates have been suggested in specific cases (**Scheme 14**).

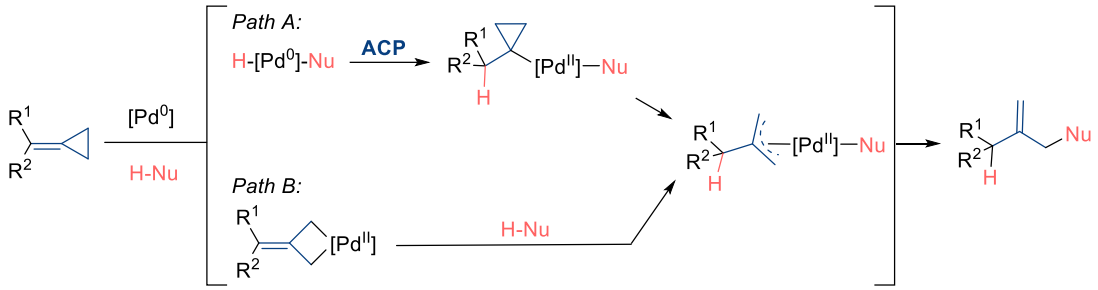

Scheme 14. Possible mechanisms for Pd(0) catalyzed hydrofuncionalizations of ACPs.

Despite its potential, the scope of nucleophiles remains narrow, and the use of organometallic reagents such as boronic acids has not yet been explored. Building on prior work involving the cross-coupling of ACP-carbonyl compounds with boronic acids, we aimed to develop a Pd(0)-catalyzed allyl cross-coupling reaction between ACPs and boronic acids. This approach involved intercepting acyclic π-allyl Pd intermediates, resulting from the alcohol addition to ACPs, with boron-based carbon nucleophiles.

Screening of reaction conditions demonstrated that a Pd(0)/phosphoramidite catalytic system effectively facilitates the reaction, enabling the use of various ACPs and aryl or alkenyl boronic acids to produce 1,1-disubstituted alkenes with high efficiency and selectivity (**Scheme 15**). Notably, the reaction can be conducted either in the presence of base or with an acidic additive like phenol.

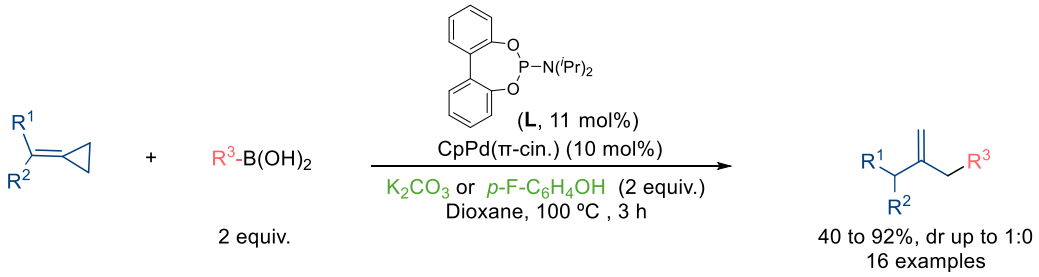

Scheme 15. Allylic cross-coupling reaction between ACPs and boronic acids.

DFT computations were conducted to discern between the possible reaction pathways. Using Pd(0)-$P(OMe)_3$ as a model catalyst indicated that, regardless of the reaction conditions (basic or acidic conditions), the pathway involving oxidative addition of the ACP to the Pd(0) species, followed by protonation of the resulting alkylidenepalladacyclobutane intermediate (see **Scheme 14** , *Path B*), is energetically more favorable than the alternative hydropalladation route, involving palladium hydride species (see **Scheme 14** , *Path A*).

Pd(0)-Catalyzed (3+2+2) Cycloaddition between ACPs tethered to Carbonyl Moieties and Isocyanates

Dipolar cycloadditions between 1,*n*-dipoles and dipolarophiles are a key tool in organic synthesis, enabling the construction of diverse carbo- and heterocyclic frameworks, including medium-sized ring systems. While early work focused on stable 1,3-dipoles like azides or nitrile oxides, recent advances have expanded the field to include *in situ*-generated 1,*n*-dipoles, often leveraging transition metal catalytic methods. Zwitterionic π-allyl palladium complexes, generated from vinylcyclopropanes, epoxides, or carbonates have proven particularly versatile, participating as 1,3-dipoles in several [3+n] formal cycloadditions. However, the development of methodologies utilizing 1,4- or 1,5-dipoles remains underexplored, with notable exceptions involving vinyl carbonate-derived precursors.

Building on our previous mechanistic studies on Pd-catalyzed transformations involving ACPs and carbonyls, which revealed the formation of allyl oxapalladacyclic intermediates, we aimed to develop

novel cycloadditions in which these intermediates could behave as formal 1,5-dipoles. Specifically, our objective involved the development of a Pd(0)-catalyzed (3+2+*n*) cycloaddition between keto-ACPs and an external unsaturated partner. This approach aimed to expand the repertoire of ACP multicomponent annulations, enabling the direct synthesis of heterocycloadducts with *exo*cyclic double bonds.

An initial evaluation of the reactivity of an ACP-tethered carbonyl with a Pd(0)/phosphoramidite catalyst was conducted using a wide range of partners, including activated alkenes, dienes, allenes, and hetero-unsaturated substrates such as carbonyl compounds, imines or isocyanates. Most of the partners did not participate in the reaction, leading to diene side-products. However, using an aryl isocyanate as partner, we observed a formal (5+2) cycloaddition to afford fused-cyclic carbamates in good yield and complete *syn* diastereoselectivity.

An optimization of the reaction conditions enabled the use of various keto-ACPs and aryl isocyanates to provide the corresponding bicyclic or tricyclic structures, containing a carbamate functionality, in good yields and high diastereoselectivity (**Scheme 16**).

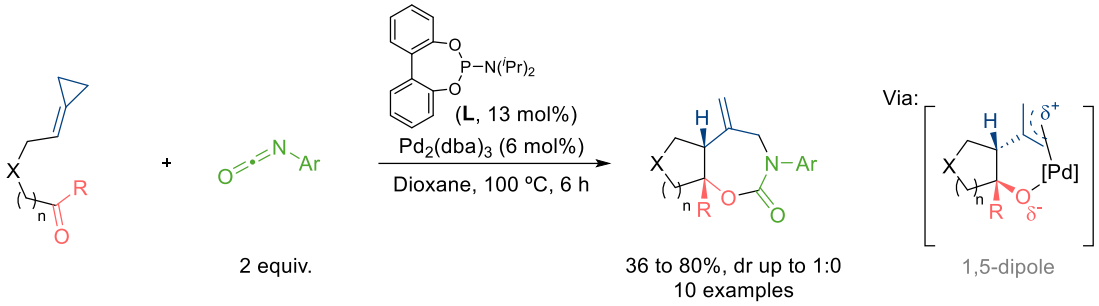

Scheme 16. Pd(0)-catalyzed (3+2+2) cycloaddition between keto-ACPs and aryl isocyanates.

Preliminary studies on an asymmetric transformation, employing a Pd(0)-catalysts bearing a chiral phosphoramidite showed modest enantioinduction. DFT computations supported the *in situ* generation of a palladium π-allyl 1,5-dipole, which reacts selectively with an isocyanate partner, with preference to the C-O reductive elimination pathway that would deliver the intramolecular (3+2) cycloadduct.

Resumo

A síntese orgánica tivo un gran impacto en campos como a química médica, a ciencia dos materiais e a agricultura, ao permitir a creación de estruturas moleculares complexas máis aló das atopadas na natureza. Nos últimos anos, este campo adoptou prácticas sostibles aliñadas cos principios da química verde, priorizando a eficiencia, a responsabilidade ambiental e a economía atómica. Neste contexto, a catálise emerxeu como unha ferramenta sintética clave, impulsando reaccións máis selectivas e eficientes, a miúdo baixo condicións máis suaves, reducindo así os refugallos e o consumo de enerxía.

Entre os métodos catalíticos homoxéneos, onde catalizadores e reactivos están na mesma fase, aqueles baseados en complexos que conteñen metais de transición destacan polas súas propiedades electrónicas e estéricas modulables. Os avances neste campo permitiron ampliar significativamente o catálogo de transformacións químicas dispoñibles na caixa de ferramentas da química sintética. Así, as reaccións de acoplamento cruzado catalizadas por paladio son ferramentas indispensables na síntese orgánica. Desenvolvidas de forma pioneira na década de 1970 por Heck, Negishi e Suzuki, estas transformacións permiten a formación de ligazóns C-C ao acoplar haluros orgánicos con compoñentes como alquenos, alquinos, organozinc e organoboranos. O seu rompedor traballo foi recoñecido co Premio Nobel de Química en 2010. Avances relacionados, como a aminación de Buchwald-Hartwig para a formación de enlaces C-N, entre moitos outros, continúan expandindo a utilidade dos acoplamentos cruzados.

As reaccións de cicloadición son transformacións útiles para construír estruturas cíclicas, particularmente heterociclos, ao xerar polo menos dous enlaces σ nun só paso. As cicloadicións tradicionais, como a reacción de Diels-Alder, están ben desenvolvidas, pero frecuentemente requiren grupos funcionais activadores e condicións de reacción severas, o que limita o seu alcance. A catálise con metais de transición aborda estas limitacións, permitindo cicloadicións baixo condicións máis suaves e introducindo novos tipos de reaccións, incluídos procesos enantioselectivos cando se empregan ligandos quirais. Isto último é particularmente interesante para aplicacións relacionadas coa química médica, xa que enantiómeros opostos con frecuencia mostran perfís biolóxicos diferentes. A importancia da catálise asimétrica con metais de transición foi visible co Premio Nobel de Química en 2001, compartido entre W. Knowles, R. Noyori e B. Sharpless.

Os alquilidenociclopropanos (ACPs) son estruturas orgánicas relevantes, que conteñen un anel de tres membros cun dobre enlace exocíclico. Estas características estruturais fan aos ACPs sistemas altamente tensionados, facilitando a inserción de metais de transición nun dos enlaces C-C. Ademais, o dobre enlace pode tamén desencadear transformacións catalizadas por metais.

Así, os ACPs poden comportarse como olefinas típicas, reaccionando como sintóns de 2C en diferentes cicloadicións ou, de xeito máis interesante, como sintóns de 3C. Aínda que as cicloadicións de ACPs catalizadas termicamente ou mediante ácidos de Lewis están ben establecidas, aquelas promovidas por metais de transición son aínda escasas. Como exemplo pioneiro, en 1980 Binger desenvolveu unha reacción (3+2) intermolecular catalizada por Pd entre metilenociclopropanos (MCPs) e alquenos tensionados. Mecanisticamente, os autores propoñen a participación de especies de paladaciclobutano e trimetilmetano (TMM) como intermedios clave (**Esquema 17**).

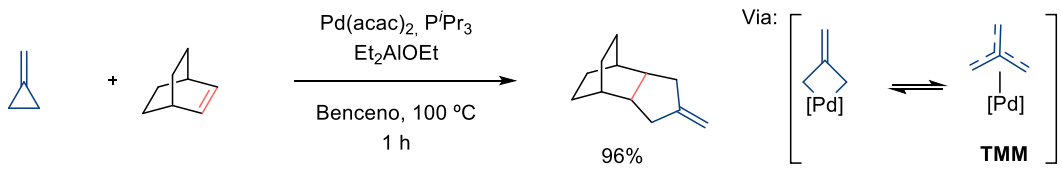

Esquema 17. Cicloadición formal (3+2) catalizada por Pd(0) entre MCPs e alquenos tensionados.

Este e outros estudos centráronse principalmente en procesos intermoleculares. O desenvolvemento de variantes intramoleculares, que permiten a síntese de estruturas policíclicas máis complexas, foi iniciado polo noso grupo a principios dos anos 2000. Estas transformacións incluíron unha serie de cicloadicións intramoleculares catalizadas por metais de transición (TMC), empregando ACPs (alquilidenociclopropanos) unidos a compoñentes insaturados baseados en carbono, como alquenos, alquinos, dienos e alenos. Ademais, tamén se desenvolveron cicloadicións (3+2+2) multicompoñente, tanto intermoleculares como intramoleculares, o que permitiu construír esqueletos policíclicos de maior tamaño.

En contraste coas cicloadicións TMC de ACPs con sistemas insaturados C-C, o número de cicloadicións relacionadas que involucran compoñentes con heteroátomos é extremadamente reducido, e limítase esencialmente aos casos pioneiros descritos en 2001 por Yamamoto e colaboradores. En particular, estes autores reportaron unha cicloadición intermolecular (3+2) catalizada por Pd(0) entre ACPs e aldehídos ou iminas tosiladas, obténdose respectivamente tetrahidrofuranos e pirrolidinas. Con todo, o alcance e a versatilidade destes procesos é moi limitado, ademais de que as condicións de reacción non resultan sinteticamente convenientes (**Esquema 18**).

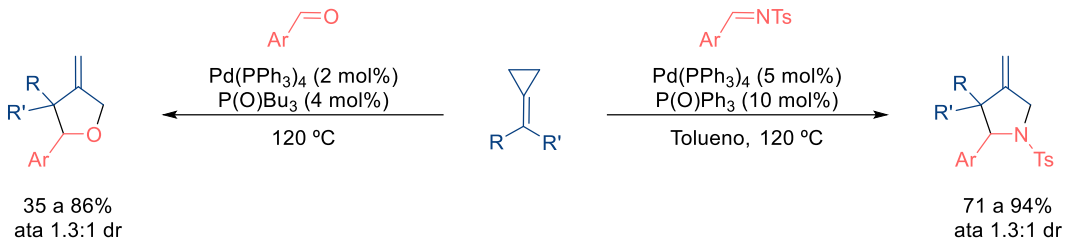

Esquema 18. Heterocicloadicións intermoleculares (3+2) de ACPs e compoñentes hetero-insaturados.

Nas primeiras etapas do meu PhD, o noso grupo explorou o desenvolvemento de heterocicloadicións de ACPs intramoleculares, describindo unha cicloadición (3+2) catalizada por Pd(0) de ACPs conectados a grupos carbonilo, proporcionando esqueletos policíclicos de tetrahidrofurano con alta eficiencia (**Esquema 19a**). O uso de catalizadores de Pd(0) con ligandos de Buchwald foi determinante para a cicloadición, aínda que a base mecanística da súa eficiencia segue sen estar completamente clara. Os resultados preliminares do Dr. Verdugo tamén revelaron que o mesmo sistema catalítico é eficaz para promover a aza-cicloadición (3+2) intramolecular de ACPs cando se empregan éteres de oxima como compañeiros, formando esqueletos bicíclicos de pirrolidina (**Esquema 19b**). Estes resultados preliminares sentaron as bases para novos obxectivos que están expostos nesta tese.

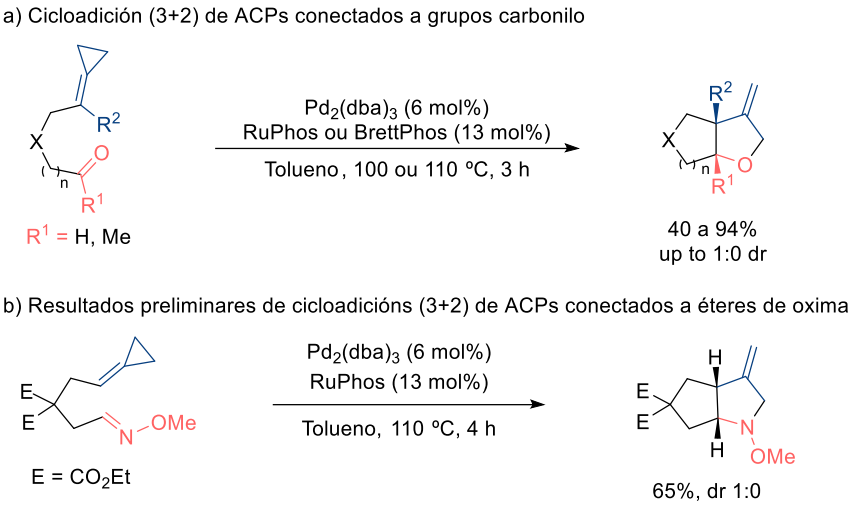

Esquema 19. Heterocicloadicións intramoleculares (3+2) catalizadas por Pd(0) de ACPs exploradas polo grupo.

As reaccións de cicloisomerización de ACPs tamén foron exploradas utilizando catalizadores de metais de transición, abrindo novas vías para a construción de esqueletos cíclicos complexos. Como exemplo, en 2018, Evans reportou unha ene-cicloisomerización catalizada por Rh(I) de ACPs conectados a sulfuros alílicos substituídos, logrando altos rendementos e diastereoselectividades. (**Esquema 20**).

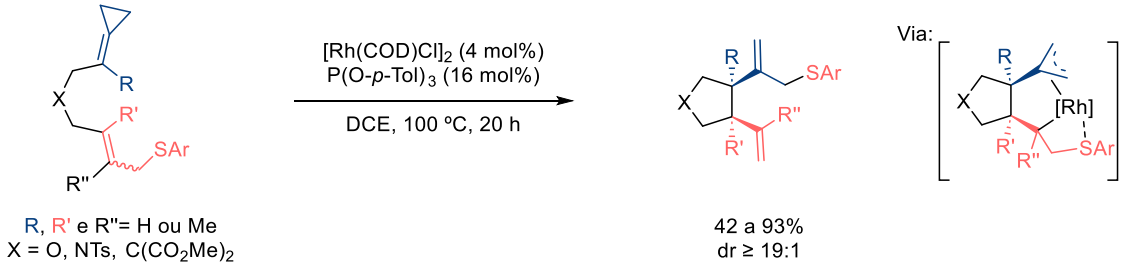

Esquema 20. Ene-cicloisomerización catalizada por Rh(I) de ACPs con eliminación intramolecular de β-sulfuro.

A pesar do potencial sintético das cicloisomerizacións de ACPs, os procesos en tándem e as reaccións multicompoñente, particularmente con compoñentes que conteñen heteroátomos, permanecen pouco exploradas.

As reaccións en tándem de apertura de anel/adición de ACPs poden ser promovidas por catalizadores de metais de transición como Ni, Rh ou Pd, formando compostos alílicos e homoalílicos a través de procesos de hidrofuncionalización selectivos. Un exemplo pioneiro, reportado por Yamamoto a finais da década de 1990, implicou a hidrofuncionalización de ACPs catalizada por Pd(0) con nucleófilos de tipo malonato, xerando alquenos 1,1-disustituidos a través de intermedios de hidruro de paladio e especies π-alílicas de Pd(II) (**Esquema 21**). Posteriormente, Yamamoto e outros ampliaron esta metodoloxía a diferentes nucleófilos.

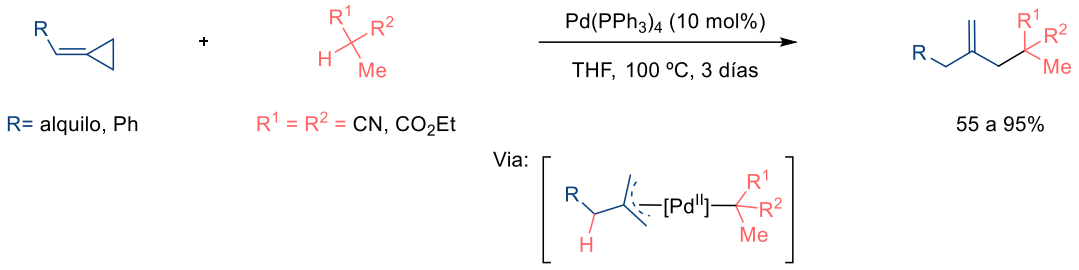

Esquema 21. Hidrocarbonación de ACPs catalizada por Pd(0) con nucleófilos tipo malonato.

En base a este precedentes, esta tese doutoral ten como obxectivo expandir a química de ACPs catalizada por metais de transición a través de tres obxectivos principais:

- **Descubrir novas reaccións de cicloadición de ACPs con compoñentes heteroinsaturados**, centrándonos en pirrolidinas funcionalizadas, e empregando estudos de DFT para elucidar detalles mecanísticos, tanto para as oxa- como aza-cicloadicións.

- **Desenvolver procesos en tándem de cicloisomerización de ACPs** para acceder a novos esqueletos cíclicos, apoiados por estudos computacionais.

- **Explorar cicloadicións multicompoñente de ACPs con compoñentes con heteroátomos** para descubrir novas metodoloxías para a síntese de heterociclos de tamaño medio.

Cicloadicións (3+2) Catalizadas por Pd(0) entre ACPs e Iminas

Os esqueletos de pirrolidina desempeñan un papel crucial en química médica, xa que constitúen o núcleo de moitas moléculas con actividade biolóxica. Aínda que existen diversos métodos sintéticos, moitos deles requiren procesos multietapa, o que pon de manifesto a necesidade de desenvolver enfoques catalíticos máis eficientes e directos. Neste sentido, as cicloadicións catalizadas por metais de transición (TMC) destacan pola súa capacidade para construír estruturas cíclicas a partir de precursores acíclicos simples, frecuentemente cun alto control rexio- e estereoselectivo.

Os ACPs poden participar como compoñentes en cicloadicións TMC con sistemas insaturados que conteñen heteroátomos, permitindo acceder a aza-heterociclos de cinco membros; con todo, estes exemplos son escasos e de alcance moi limitado. Neste contexto, o noso grupo propuxo o desenvolvemento dunha cicloadición intramolecular utilizando ACPs unidos a éteres de oxima. En estudos preliminares, o Dr. Verdugo descubriu que o catalizador xerado a partir de $Pd_2(dba)_3$ e RuPhos é capaz de promover a anulación desexada para formar produtos de pirrolidina (véxase **Esquema 19b**, páxina 21). O uso de ligandos fosfito voluminosos tamén permitiu a formación dos cicloadutos. De xeito destacado, ao empregar catalizadores de Pd(0) con ligandos fosforamidita quirais, a cicloadición dun precursor modelo conduciu ao heterociclo desexado con prometedoras enantioselectividades.

Baseándonos nestes precedentes, propuxémonos explorar en profundidade a cicloadición intramolecular catalizada por Pd(0) entre ACPs e derivados de oxima, así como desenvolver unha variante intermolecular que puidese superar as importantes limitacións dos métodos previamente reportados. Ademais, combinamos esta investigación experimental cunha análise computacional das heterocicloadicións, tratando de esclarecer aspectos clave do mecanismo.

En canto á transformación intramolecular, a cicloadición (3+2) catalizada por Pd(0) entre ACPs e éteres de oxima resultou ser altamente sensible ás características estruturais dos substratos (**Esquema 22**). Os cicloadutos desexados só se obtiveron a partir de aldoximas que presentan unha unidade diéster no conector. En moitos casos, tamén se observaron subprodutos de tipo dieno.

Hipotetizamos que o alcance limitado da transformación débese ás dificultades asociadas á inserción migratoria do enlace C=N da oxima. Os intentos de mellorar a reactividade mediante aditivos ácidos e iminas electrodeficientes non tiveron éxito.

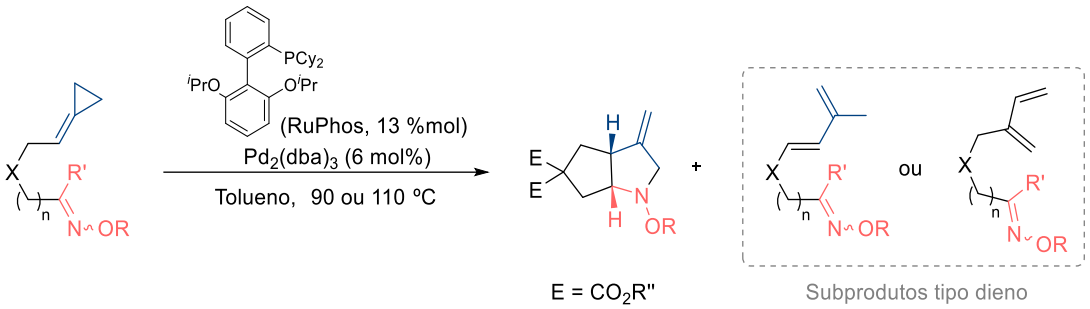

Esquema 22. Heterocicloadición (3+2) intramolecular catalizada por Pd(0) de ACPs conectados a éteres de oxima.

Levamos a cabo estudos mecanísticos DFT utilizando Pd(0)-*t*BuXPhos como catalizador modelo, os cales confirmaron que estas cicloadicións teñen lugar mediante unha inserción inicial do complexo de Pd no enlace C–C distal do ACP, seguida dun reordenamento tipo metalo–eno e, finalmente, unha eliminación redutora. Os cálculos mostraron o papel crítico das interaccións hemilábiles entre o centro de Pd e o ligando, así como a importancia da conformación do ligando, na estabilización de intermedios de reacción clave.

Experimentos de marcaxe con deuterio revelaron un novo patrón de reactividade para os ACPs: un reordenamento en dous pasos que conduce a certos dienos obtidos como subprodutos (**Esquema 23**). Os cálculos de DFT apoiaron este camiño, mostrando unha mínima diferenza enerxética entre a vía de cicloadición e a de formación de dienos, o cal é consistente coa aparición destes subprodutos en numerosos casos.

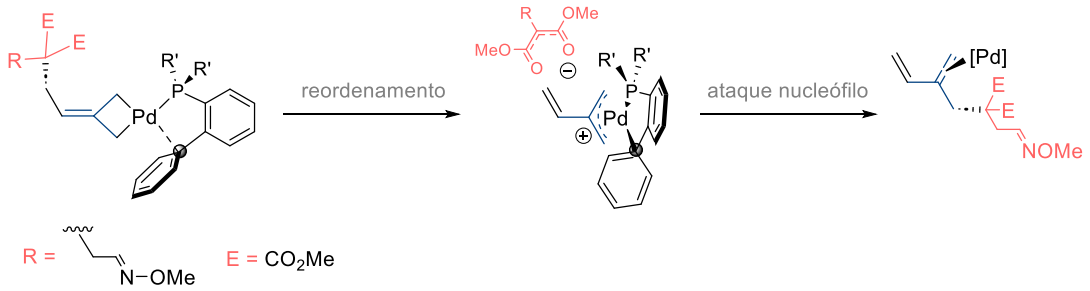

Esquema 23. Proposta mecanística para a formación subprodutos diénicos baseada en estudios DFT.

Para a variante intermolecular, un sistema catalítico composto por $Pd_2(dba)_3$ e un ligando fosforamidita facilitou a cicloadición (3+2) entre ACPs e sulfonil iminas (**Esquema 24**). O método tolera diversas substitucións no ACP e unha variedade de iminas cíclicas e acíclicas, incluídas as cetiminas, logrando pirrolidinas funcionalizadas con altos rendementos. Ademais, estudos enantioselectivos co substrato modelo, mostraron que o uso dunha fosforamidita derivada do (*S*)-VAPOL proporciona o cicloaduto cun 83% de rendemento e un 78% de enantioselectividade.

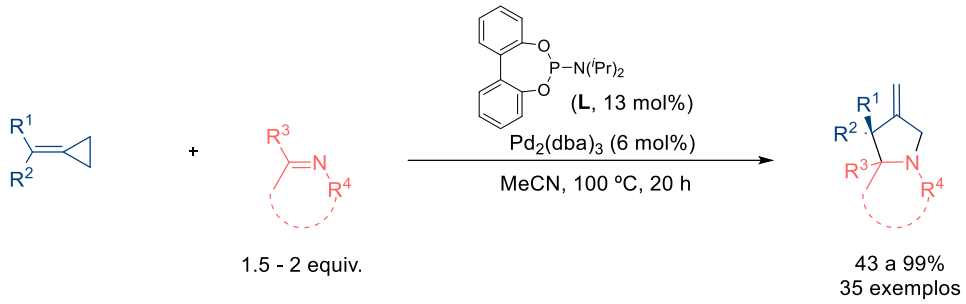

Esquema 24. Heterocicloadición (3+2) catalizada por Pd(0) entre ACPs e varios compoñentes imina.

Os estudos DFT apoiaron un mecanismo de pallada-eno similar ao da cicloadición intramolecular. Estes cálculos destacaron o papel das interaccións hemilábiles entre o centro de Pd e os ligandos auxiliares voluminosos, os cales estabilizan intermedios clave e determinan a selectividade da heterocicloadición.

Un Estudio Mecanístico DFT de Cicloadicións (3+2) Catalizadas por Pd(0) entre ACPs e Carbonilos

As cicloadicións catalizadas por metais de transición (TMC) entre ACPs e compostos carbonílicos son extremadamente escasas. Para abordar esta carencia, o noso grupo investigou cicloadicións intramoleculares de ACPs con aldehídos e cetonas. Os estudos iniciais de cribado de ligandos revelaron que os ligandos comunmente empregados en cicloadiciones (3+2) relacionadas con alquenos non permitían obter rendementos satisfactorios. Con todo, as monofosfinas biarilo de Buchwald, como BrettPhos ou RuPhos, demostraron ser altamente eficaces, permitindo a síntese de sistemas biciclos 5,5- e 6,5-fusionados de THFs con excelentes rendementos, selectividade *syn* e un amplo alcance (véxase **Esquema 19a**, páxina 21). Ademais, estes sistemas catalíticos tamén promoveron de forma eficiente as cicloadicións (3+2) intermoleculares entre ACPs e cetonas trifluorometiladas, proporcionando THFs β-metilénicos con altos rendementos.

Sobre esta base, investigamos computacionalmente o mecanismo destas heterocicloadicións, centrándonos en desentrañar o papel crave dos ligandos de Buchwald para facer posibles estas reaccións. Así, exploramos as cicloadicións (3+2) catalizadas por Pd(0) entre ACPs e compostos carbonílicos, tanto en procesos intra- como intermoleculares. Con fins comparativos, empregamos un complexo sinxelo, Pd(0)-PH_3, para obter unha visión básica das posibles alternativas; e un catalizador máis realista, que inclúe *t*BuXPhos como ligando, co obxectivo de determinar o papel específico deste tipo de ligandos.

Para a transformación intramolecular, avaliamos os camiños máis plausibles: un proceso metaloeno (a) ou un proceso de isomerización/inserción migratoria (b, **Esquema 25**).

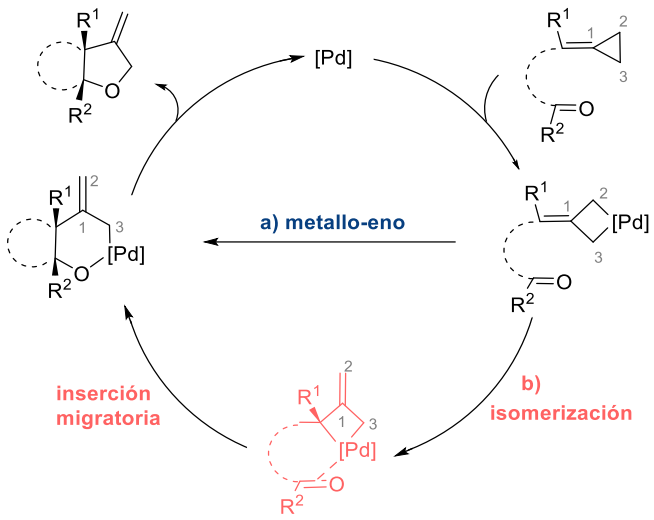

Esquema 25. Camiños avaliados para a cicloadición (3+2) intramolecular catalizada por Pd(0).

Estudos con Pd(0)-PH_3 suxeriron que o camiño metaloeno (camiño A) é enerxeticamente máis favorecido na formación do cicloaduto. Estas conclusións foron máis tarde confirmadas utilizando Pd(0)-*t*BuXPhos como catalizador. É importante destacar que o uso dos ligandos de Buchwald parece ser crucial para a heterocicloadición, xa que diferentes interaccións hemilábiles entre o centro de paladio e átomos específicos do ligando (Pd-H e Pd-C_{ipso} do biarilo), estabilizan diferentes intermedios a través do ciclo catalítico (**Figura 2**). Ademais, a conformación do biarilo do ligando de Buchwald desempeña un papel crave, dado que a súa conformación "cara a dentro" facilita as mencionadas interaccións secundarias, favorecendo un camiño de reacción global menos enerxético.

Estudos adicionais sobre a inserción migratoria e a eliminación redutora confirmaron a importancia destas interaccións hemilábiles para estabilizar intermediarios clave.

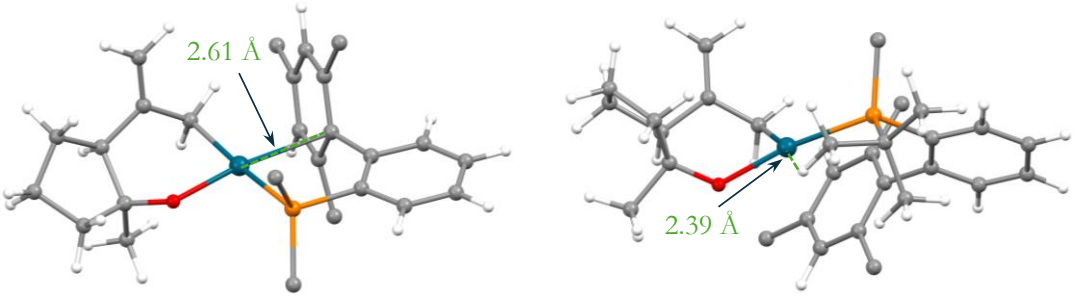

Interacción Pd-C_{ipso} facilitada por unha conformación *cara adentro* do biarilo

Interacción agóstica Pd-H

Figura 2. Exemplos 3D de interaccións Pd-*t*BuXPhos clave estabilizando intermedios paladacíclicos.

Para a cicloadición intermolecular, examinamos a proposta metaloeno utilizando tanto acetofenona como 2,2,2-trifluoroacetofenona como compoñentes carbonílicos, así como Pd(0)-PH_3 e Pd(0)-*t*BuXPhos. De maneira notable, o compoñente carbonílico fluorado facilitou significativamente a inserción migratoria con ambos catalizadores de Pd(0). Os estudos con Pd(0)-*t*BuXPhos suxeriron que o ligando de Buchwald poderían desempeñar un papel na mellora da selectividade da cicloadición, suprimindo camiños secundarios. Ademais, estes estudos destacaron novamente a importancia das interaccións secundarias hemilábiles entre o ligando de Buchwald e o centro metálico, así como a relevancia da conformación "cara a dentro" do ligando.

Reaccións en Tándem de Cicloisomerización/Substitución Alílica Catalizadas por Pd(0) de ACPs conectados a Compoñentes Carbonilo e Imina

As reaccións catalizadas por paladio que implican intermedios π-alilo convertéronse en ferramentas clave en síntese orgánica, xa que permiten a formación eficiente de enlaces C–C e C–heteroátomo. Estes intermedios, que normalmente se xeran mediante adición oxidativa de substratos alílicos con grupos saíntes, poden reaccionar con diversos nucleófilos, incluídos reactivos organometálicos (p.e., reactivos de organoboro ou organozinc), dando lugar aos correspondentes produtos de acoplamento cruzado alílico. Sistemas tensionados como os ACPs tamén poden xerar intermedios π-alilo baixo catálise con paladio, polo que ditos intermedios poderían atraparse cos nucleófilos adecuados. Con todo, a exploración deste tipo de procesos en tándem, especialmente utilizando reactivos organometálicos, segue estando pouco desenvolvida.

Neste contexto, o noso grupo desenvolveu unha metodoloxía de cicloisomerización e acoplamento cruzado en tándem que intercepta intermedios π-alilo-Pd(II), xerados a partir de ACPs unidos a grupos carbonilo, con ácidos borónicos, para producir ciclopentanos altamente funcionalizados (**Esquema 26**). Utilizando un catalizador xerado *in situ* a partir de $Pd_2(dba)_3$ e unha fosfina deficiente en electróns, a transformación mostrou un amplo alcance e altas selectividades.

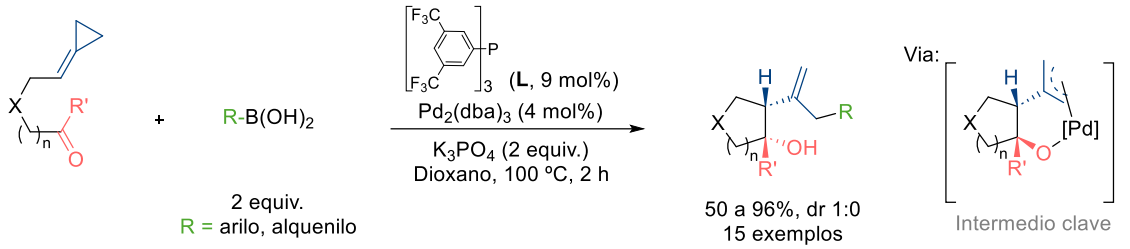

Esquema 26. Cicloisomerización/ acoplamento cruzado en tándem entre ceto-ACPs e ácidos borónicos.

Resultados preliminares mostraron ademais que os 1,3-dicarbonilos poden actuar como nucleófilos baixo condicións catalíticas similares, xerando alcois cíclicos de xeito eficiente.

Sobre estas bases, propuxémonos explorar o alcance das reaccións de cicloisomerización e acoplamento cruzado utilizando 1,3-dicarbonilos e fenois como nucleófilos. Ademais, tamén decidimos explorar procesos en tándem con substratos ACP-iminas análogos, e dilucidar os aspectos mecanísticos destas transformacións mediante estudos computacionais de DFT.

Así, empregando o catalizador derivado de $Pd_2(dba)_3$ e unha fosfina deficiente en electróns, a reacción de ACPs conectados a carbonilos, e unha gran variedade de nucleófilos 1,3-dicarbonilo, proporcionou os correspondentes alcois cíclicos en rendementos de bos a excelentes, e alta selectividade *syn* na maioría dos casos (**Esquema 27**).

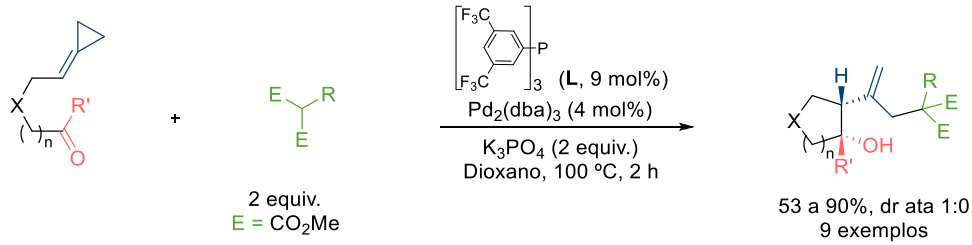

Esquema 27. Cicloisomerización/ acoplamento cruzado en tándem entre ceto-ACPs e compostos 1,3-dicarbonilo.

O uso de fosforamiditas como ligando, en lugar de fosfinas deficientes en electróns, permitiu o uso de alcois como socios de reacción, proporcionando os correspondentes produtos en bos rendementos e total selectividade *syn* (**Esquema 28**).

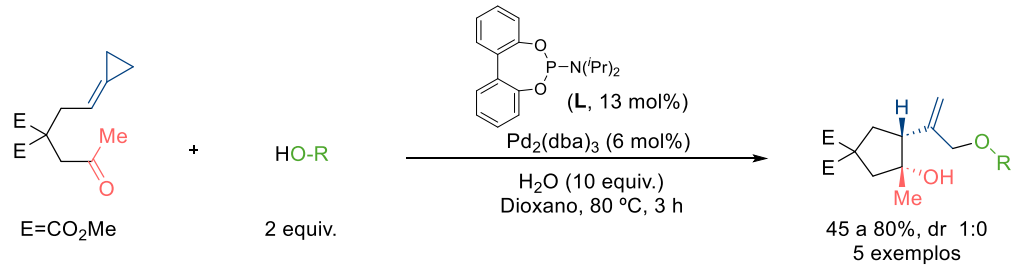

Esquema 28. Cicloisomerización/ acoplamento cruzado en tándem entre ceto-ACPs e alcois.

Ademais, desenvolvemos un proceso en tándem de cicloisomerización/acoplamento cruzado entre ACPs unidos a iminas sulfinílicas, e ácidos borónicos arílicos, utilizando o catalizador xerado con $Pd_2(dba)_3$ e un fosfito voluminoso. Aínda que máis restrinxida que a reacción análoga con ACPs unidos a motivos carbonílicos, a transformación proporcionou as aminas cíclicas correspondentes con rendementos de bos a excelentes e unha selectividade *syn* total (**Esquema 29**).

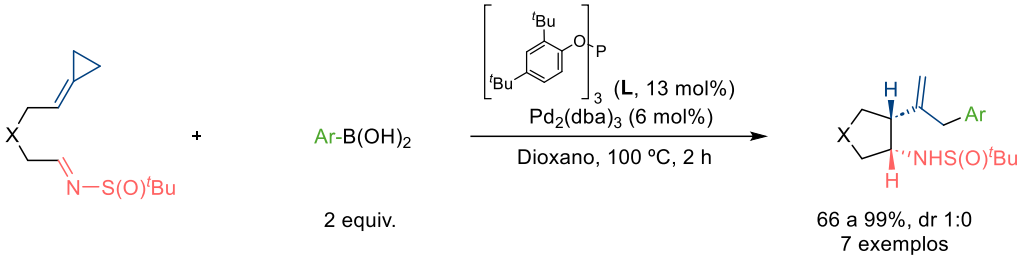

Esquema 29. Cicloisomerización/ acoplamento cruzado en tándem entre imino-ACPs e ácidos borónicos.

Os cálculos DFT de procesos en tándem que involucran ceto-ACPs, utilizando Pd(0)-$P(OMe)_3$ como catalizador modelo, revelaron que os intermedios alílicos-Pd(II) evolucionan preferentemente a través dunha transmetalación co ácido borónico en lugar da eliminación redutora C–O intramolecular. En contraste, o uso de Pd(0)-*t*BuXPhos promove a formación de intermedios σ-alílicos oxapalladacíclicos, o que favorece enerxeticamente a eliminación redutora cara o aduto (3+2). Consistentemente, os cálculos con Pd(0)-$P(OMe)_3$ mostraron que o ataque fóra-de-esfera do dimetil malonato sobre o intermedio alílico-Pd(II) é enerxeticamente preferido sobre a eliminación redutora C-O competitiva. Estes achados coinciden cos resultados experimentais, onde as monofosfinas electronicamente pobres favorecen a formación de produtos en tándem, mentres que os ligandos de Buchwald promoven os cicloadutos (3+2) intramoleculares. Unha análise DFT preliminar de ACPs conectados a iminas e ácidos borónicos revelou unha ruta mecanística similar á proposta para ceto-ACPs.

Acoplamento Cruzado Catalizado por Pd(0) entre ACPs e Ácidos Borónicos

A hidrofuncionalización de ACPs catalizada por Pd(0) é unha estratexia versátil para a síntese de alquenos 1,1-difuncionalizados mediante reaccións de apertura de anel que xeran intermedios π-alilo de paladio. Este método aplicouse principalmente a pronucleófilos que conteñen hidróxeno relativamente ácido, como alcois, aminas e amidas, mentres que o uso de nucleófilos de base carbonada está pouco explorado e limítase a malonatos ou heteroaromáticos ricos en electróns. Desde un punto de vista mecanístico, proponse que o proceso transcorre a través dunha especie hidruro de paladio que, tras unha hidropaladación, xera un intermedio σ-ciclopropilo. Posteriormente, unha eliminación β-carbónica conduce a unha especie π-alilo clave, que é atrapada

polo nucleófilo. Con todo, en certos casos específicos suxeríronse roteiros alternativos que implican intermedios de tipo paladaciclobutano (**Esquema 30**).

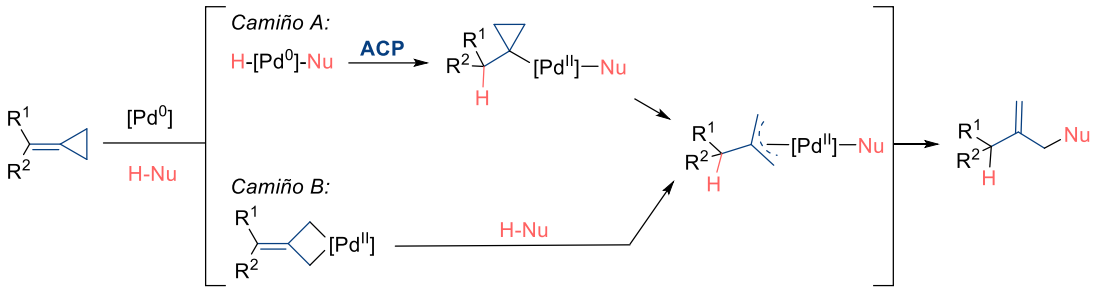

Esquema 30. Posibles mecanismos para hidrofuncionalizacións catalizadas por Pd(0) de ACPs.

A pesar do seu potencial, o alcance dos nucleófilos segue sendo limitado e o uso de reactivos organometálicos, como os ácidos borónicos, aínda permanece inexplorado. Baseándonos en traballos previos sobre a acoplamento cruzado de compostos ACP-carbonilo con ácidos borónicos, propuxémonos desenvolver unha reacción de acoplamento cruzado alílico catalizada por Pd(0) entre ACPs e ácidos borónicos. Este enfoque implica interceptar os intermedios π-alílicos acíclicos resultantes da adición de alcol a ACPs, con nucleófilos de carbono baseados en boro.

O cribado de condicións de reacción revelou que un sistema catalítico Pd(0)/fosforamidita pode promover de forma efectiva a reacción, permitindo o uso de diferentes ACPs e ácidos borónicos de arilo ou alquenilo, para obter alquenos 1,1-disustituidos con alta eficiencia e selectividade (**Esquema 31**). Cabe destacar que a reacción pode realizarse tanto en presenza dunha base como usando un aditivo ácido como o fenol.

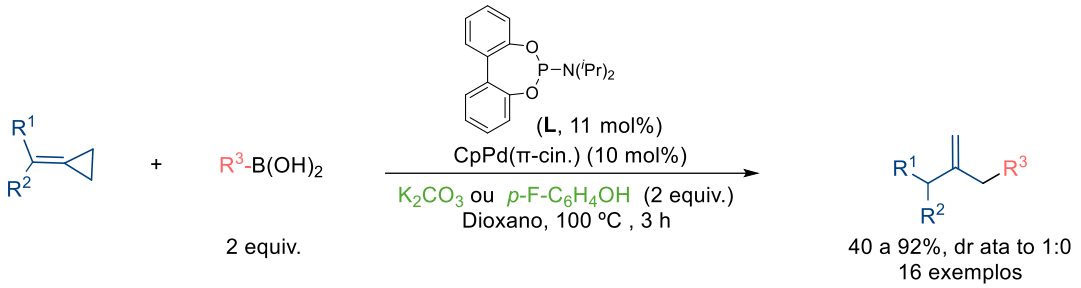

Esquema 31. Rección de acoplamento cruzado alílico entre ACPs e ácidos borónicos.

Realizáronse cálculos DFT para discernir entre os posibles camiños de reacción. Utilizando Pd(0)-$P(OMe)_3$ como catalizador modelo, os resultados indicaron que, independentemente das condicións de reacción (condicións básicas ou ácidas), o camiño que implica a adición oxidante do ACP á especie de Pd(0), seguida da protonación do intermedio alquilideno paladaciclobutano resultante (véxase **Esquema 30**, Camiño B), é enerxeticamente máis favorable que o camiño alternativo de hidropaladación, que transcorre a través de especies de hidruro de paladio (véxase **Esquema 30**, Camiño A).

Cicloadicións (3+2+2) Catalizadas por Pd (0) entre ACPs conectados a Grupos Carbonílicos e Isocianatos

As cicloadicións dipolares entre 1,*n*-dipolos e dipolarófilos constitúen unha ferramenta clave en síntese orgánica, permitindo a construción dunha ampla variedade de esqueletos carbo- e heterocíclicos, incluídos sistemas de aneis de tamaño medio. Aínda que os primeiros estudos centráronse en dipolos 1,3 estables, como azidas ou óxidos de nitrilo, avances recentes ampliaron o campo ao incluír dipolos 1,*n* xerados *in situ*, frecuentemente aproveitando métodos catalíticos mediados por metais de transición. Neste contexto, complexos zwitteriónicos π-alilo de paladio,

xerados a partir de vinilciclopropanos, epóxidos ou carbonatos, demostraron ser especialmente versátiles, participando como dipolos 1,3 en diversas cicloadiciones formais [3+*n*]. Con todo, o desenvolvemento de metodoloxías que utilicen dipolos 1,4 e 1,5 segue estando pouco explorado, con algunhas excepcións destacadas a partir de precursores derivados de carbonatos vinílicos.

Baseándonos nos nosos estudos mecanísticos previos sobre transformacións catalizadas por Pd entre ACPs e carbonilos, que revelaron a formación de intermedios oxapaladacíclicos alílicos, propuxémonos desenvolver novas cicloadicións onde estes intermedios puidesen actuar como dipolos 1,5 formais. En concreto, o noso obxectivo consistía en desenvolver unha cicloadición (3+2+*n*) catalizada por Pd(0) entre ceto-ACPs e un compoñente insaturado externo. Esta estratexia buscaba ampliar o repertorio de anulacións multicompoñente de ACPs, permitindo a síntese directa de heterocicloadutos con enlaces dobres exocíclicos.

Levouse a cabo unha avaliación inicial da reactividade dun ACP unido a un carbonilo empregando un catalizador de Pd(0)/fosforamidita, e unha ampla gama de socios, incluídos alquenos activados, dienos, alenos e substratos heteroinsaturados, como compostos carbonílicos, iminas ou isocianatos. A maioría dos compoñentes non participaron na reacción, o que conduciu á formación de dienos como subprodutos. Con todo, ao utilizar un isocianato arílico como socio observouse unha cicloadición formal (5+2) que proporcionou carbamatos cíclicos fusionados en bo rendemento e con completa diastereoselectividade *syn*.

A optimización das condicións de reacción permitiu o uso de diversos substratos ceto-ACPs e isocianatos arílicos, obténdose as estruturas bicíclicas ou tricíclicas correspondentes, que conteñen unha funcionalidade carbamato, en bos rendementos e con alta diastereoselectividade (**Esquema 32**).

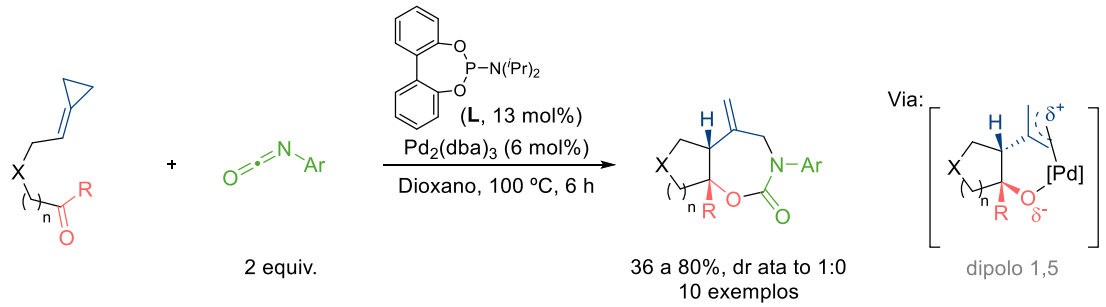

Esquema 32. Cicloadicións (3+2+2) catalizadas por Pd(0) entre ceto-ACPs e isocianatos arílicos.

Estudos preliminares sobre unha transformación asimétrica, empregando catalizadores Pd(0) con fosforamiditas quirais, mostraron unha moderada enantioinducción. Ademais, realizáronse cálculos DFT, os cales apoiaron a xeración *in situ* de dipolos 1,5 (complexos π-alilo de paladio), que reaccionan selectivamente con isocianatos, en lugar de seguir a vía intramolecular de eliminación redutora C-O para dar o cicloaduto (3+2).

1. General Introduction

1.1 Modern Organic Synthesis

Organic synthesis is probably the branch of Chemistry that has contributed more to the scientific and technological progress of our society, particularly in areas such as medicinal chemistry, materials science, and agriculture. By enabling the construction of complex molecular structures, beyond those that can be obtained from nature, synthetic chemistry plays a key role in drug development and facilitates the creation of new products with novel properties.

During the last decades, the focus of organic synthesis has moved from the mere interest in obtaining a specific product to its synthesis in alignment with the principles of green chemistry. Therefore, concepts such as efficiency, sustainability and minimal environmental impact must be now carefully considered. Traditionally, synthetic chemists have used the global yield to measure the success of a chemical synthesis. However, other aspects such as atom economy, which takes into account the fraction of reactants that actually ends up in the final product, are nowadays very important.[2] Accordingly, an *ideal synthesis* should be fast, mild and safe, involving the use of cheap, non-toxic and readily available starting materials and solvents.

In this context, catalytic processes are especially relevant. A catalyst is generally defined as a substance that increases the rate of a chemical reaction without being consumed in the process. The catalyst does not affect the overall ΔG, but it lowers the activation energy of the process, enabling a more selective and efficient reaction, often under mild conditions (**Figure 3**). Consequently, catalytic synthetic methods offer two main advantages over stoichiometric ones. First, since catalysts are regenerated during the reaction, the amount of waste is reduced. Secondly, by decreasing the energy barrier, a catalyst not only accelerates the reaction but can also make possible chemical transformations that do not occur under non-catalyzed conditions.

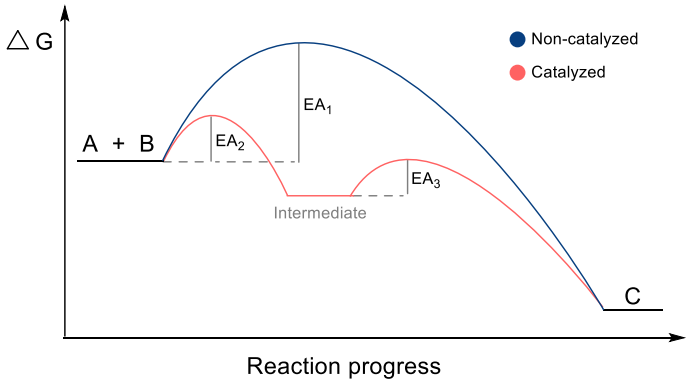

Figure 3. Reaction energy profile using a catalyst (red) or without catalyst (blue).

Homogeneous catalysis, in which the reactants and catalysts are in the same phase, can be divided into three main types depending on the nature of the catalyst: organometallic catalysis (metal complexes bearing organic ligands), organocatalysis (organic molecules), and biocatalysis (enzymes).

1.2 Organometallic Catalysis in Synthesis

Transition metals, with their diverse oxidation potentials and electronegativities, facilitate the feasibility of catalytic cycles. The use of organometallic complexes, in which the metallic center is surrounded by different ancillary ligands is key to modulate the catalytic properties. These catalysts are characterized by the donation and back-donation of electron density between the metal and the

[2] a) Anastas, P. T.; Warner, J. C. *Green chemistry: Theory and practice.* Ed. Oxford university press, **1998**.; b) Erythropel, H. C.; Zimmerman, J. B.; De Winter, T. M.; Petitjean, L.; Melnikov, F.; Lam, C. H.; Lounsbury, A. W.; Mellor, K. E.; Janković, N. Z.; Tu, Q.; Pincus, L. N.; Falinski, M. M.; Shi, W.; Coish, P.; Plata, D. L.; Anastasas, P. T. The Green ChemisTREE: 20 years after taking root with the 12 principles. *Green Chem.* **2018**, *20*, 1929-1961.; c) Wender, P. A. Toward the ideal synthesis and molecular function through synthesis-informed design. *Nat. Prod. Rep.* **2014**, *31*, 433-440.

ligands orbitals, which are key to tune the properties of the metals. By modifying the steric and electronic properties of these ligands, the reactivity of the metal catalyst can be modulated, offering excellent possibilities to promote chemical transformations that could otherwise be challenging or even impossible.[3] Notably, the importance of organometallic catalysis has already been acknowledged with three Nobel prizes in recent decades.[4]

1.2.1 Cross-coupling reactions

The formation of C-C and C-heteroatom bonds is a cornerstone of organic synthesis. In this context, the palladium catalyzed cross-couplings, initially developed by Richard Heck, Ei-ichi Negishi and Akira Suzuki in the early 1970s, are highly valuable transformations.[4c]

Carbon-carbon cross-coupling reactions enable the connection of two different fragments through the creation of a new C-C bond, and typically involve an organic halide (or pseudo halide) as electrophilic partner (**Figure 4**). The type of cross-coupling is determined by the nature of the second partner, which can be an activated alkene (Heck), an alkyne (Sonogashira), an organozinc reagent (Negishi), or an organoboron reagent (Suzuki-Miyaura), among others.

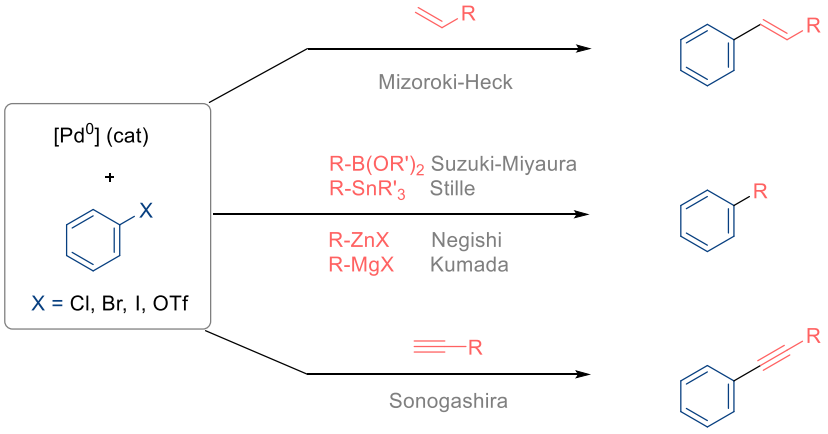

Figure 4. Pd(0)-catalyzed cross-coupling reactions.

Mechanistically, a Pd(0)-catalyzed cross-coupling reaction typically begins with the oxidative addition of an organic halide (or pseudohalide, RX) to the Pd(0) complex, forming a Pd(II) species (**I**, **Scheme 33**). In most processes, this step is followed by a transmetalation with an organometallic reagent generating the intermediate **II** (*left pathway*). Finally, a C-C bond is formed through a reductive elimination, delivering the corresponding product and regenerating the Pd(0) species. In the case of the Heck reaction, after oxidative addition, a *syn*-migratory insertion of the alkene into de Pd-C bond

[3] a) Crabtree, R. H. *The Organometallic Chemistry of the Transition Metals*, 4th ed.; Wiley: Hoboken, **2005**, Chapter 2.; b) Astruc, D. Organometallic Chemistry and Catalysis; Springer-Verlag: Berlin, **2007**.

[4] Related Nobel Prize in Chemistry: a)www.nobelprize.org/prizes/chemistry/2001/summary/; b)www.nobelprize.org/prizes/chemistry/2005/summary/; c) www.nobelprize.org/prizes/chemistry/2010/summary/

occurs, forming the alkylpalladium species **III** (*right pathway*). Finally, a β-hydride elimination and a subsequent reductive elimination complete the cycle, delivering the corresponding product.

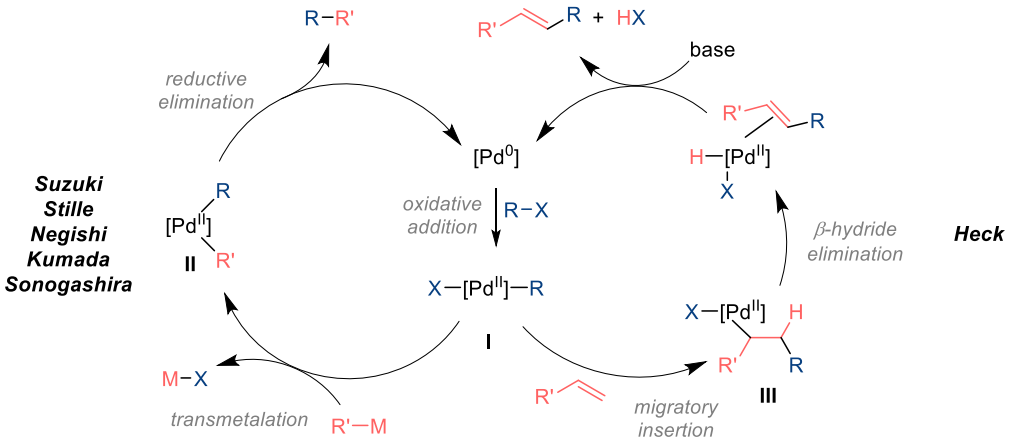

Scheme 33. General mechanism for Pd(0) cross-coupling reactions.

Cross-coupling reactions have found relevant applications in pharmaceutical industry, as exemplified with the Suzuki-Miyaura cross-coupling shown in **Scheme 34**, which is a key step for the Pfizer's preparation of PF-06815345, a PCSK9 protein inhibitor studied for stroke prevention.[5]

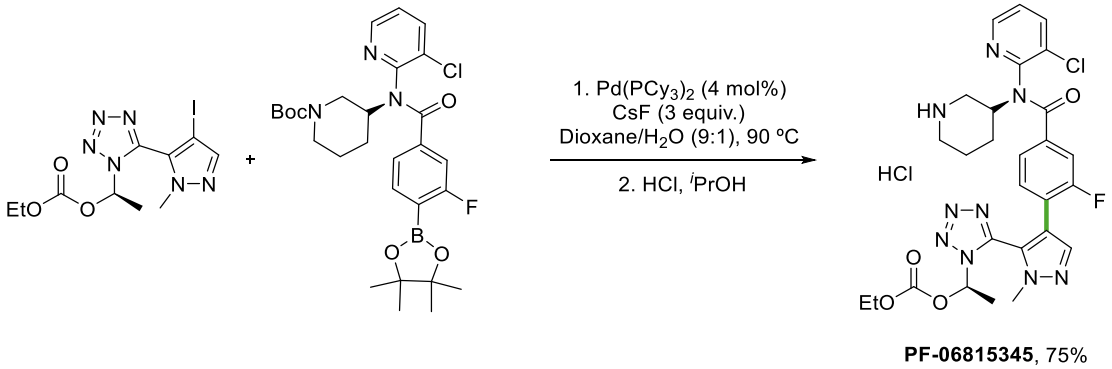

PF-06815345, 75%

Scheme 34. Kilogram-scale Suzuki-Miyaura coupling by Pfizer.

Over the years, new types of cross-coupling reactions have been developed, incorporating new reagents, reaction conditions, and expanding the synthetic applications.[6] A relevant example is the Buchwald-Hartwig amination, which enables C-N bond formation by coupling aryl halides with primary or secondary amines (**Scheme 35**).[7] In fact, this reaction is a key step in many large-scale pharmaceutical and agrochemical processes in industry.[8]

[5] Parmentier, M.; Wagner, M.; Wickendick, R.; Baenziger, M.; Langlois, A.; Gallou, F. A General Kilogram Scale Protocol for Suzuki–Miyaura Cross-Coupling in Water with TPGS-750-M Surfactant. *Org. Process Res. Dev.* **2020**, *24*, 1536–1542.
[6] Campeau, L.; Hazari, N. Cross-Coupling and Related Reactions: Connecting Past Success to the Development of New Reactions for the Future. *Organometallics* **2019**, *38*, 3–35.
[7] Yang, B. H.; Buchwald, S. L. Palladium-Catalyzed Amination of Aryl Halides and Sulfonates. *J. Organomet. Chem.* **1999**, *576*, 125-146.
[8] Dorel, R.; Grugel, C. P.; Haydl, A. M., The Buchwald–Hartwig Amination After 25 Years. *Angew. Chem. Int. Ed.* **2019**, *58*, 17118.

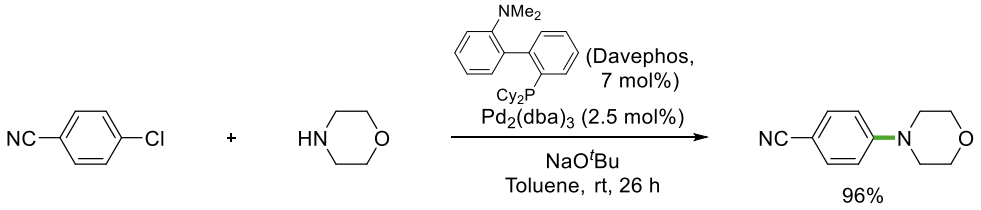

Scheme 35. Example of a Buchwald-Hartwig amination.

1.2.2 Transition metal catalyzed cycloadditions

A common feature of many bioactive organic compounds is the presence of cyclic structural motifs in their core structure, particularly heterocycles. For this reason, cycloaddition reactions have become highly relevant transformations in organic synthesis, as they enable the building of these cyclic frameworks by generating at least two σ bonds and a cycle in a single step. This approach allows a rapid increase in both structural and stereochemical complexity, enabling shorter synthetic routes and promoting atom economy.[9]

A representative example of a classic cycloaddition is the Diels-Alder reaction.[10] This (4+2) pericyclic annulation involves the coupling of a 1,3-diene (4π component) and an olefin (dienophile, 2π component) in a concerted manner, forming a six-membered ring with up to four new stereogenic centers (**Scheme 36**).

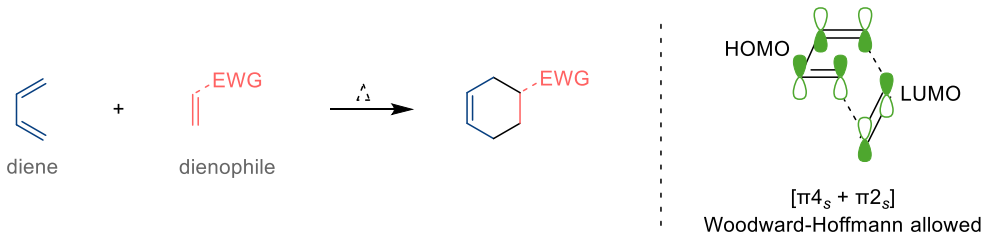

Scheme 36. The Diels-Alder reaction.

Classic cycloadditions, like Diels-Alder, can be generally explained by the Woodward-Hoffmann rules[11] and the Fukui frontier orbital theory.[12] They proceed spontaneously or under heating, whereas the symmetry-forbidden reactions can be induced by other stimuli such as photochemical conditions, radical initiators or the action of other reagents. However, these classic cycloadditions usually require the presence of certain functional groups that activate the substrates, which can restrict their applicability.

For this reason, there is a clear need for the development of new cycloaddition processes for constructing cyclic structures. In this sense, transition metal catalysis provides excellent opportunities to develop new types of formal cycloadditions under mild conditions. Besides, the use of catalysts bearing chiral ligands enables the development of enantioselective variants of these cycloadditions.[13]

A representative example of the potential of transition metal catalyzed (TMC) cycloadditions is the synthesis of the cyclooctatriene (COT), shown in **Scheme 37**. The first synthetic route to this antiaromatic compound was reported by Richard Willstätter and Ernst Waser in 1911,[14] requiring 13 steps with a very low overall yield. In contrast, Reppe's approach in 1948 afforded COT directly from

[9] Kobayashi, S.; Jørgensen, K. A. Cycloaddition reactions in organic synthesis. Wiley-VCH, **2001**.
[10] a) Diels, O.; Alder, K. Synthesen in der hydroaromatischen Reihe. Justus Liebigs Ann. Chem. 1928, 460, 98.; b) Nicolaou, K. C.; Snyder, S. A.; Montagnon, T. The Diels–Alder Reaction in Total Synthesis. *Angew. Chem. Int. Ed.* **2002**, *41*, 1668–1698.
[11] Woodward, R. B.; Hoffmann, R. The Conservation of Orbital Symmetry. *Angew. Chem. Int. Ed.* **1969**, *8*, 781–853.
[12] Inagaki, S.; Fujimoto, H.; Fukui, K. Orbital Interaction in Three Systems. *J. Am. Chem. Soc.* **1976**, *98*, 4693–4701.
[13] Lautens, M.; Klute, W.; Tam, W. Transition Metal-Mediated Cycloaddition Reactions. *Chem. Rev.* **1996**, *96*, 49-92.
[14] Willstätter, R.; Waser, E. Über Cyclo-octatetraen. *Ber. Dtsch. Chem. Ges.* **1911**, *44*, 3423–3430.

acetylene in a single step, with a 90% yield, via a nickel-catalyzed (2+2+2+2) cycloaddition.[15] Notably, this transformation is thermically forbidden by the Woodward-Hoffman rules.

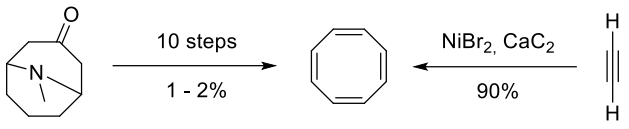

Scheme 37. Classic synthesis and Ni-catalyzed synthesis of cyclooctadiene.

The development of new transition metal catalyzed cycloadditions that could be further applied to the synthesis of natural products has been a long-standing goal in our group (**Scheme 38**). For example, the platinum-catalyzed (4+3) cycloadditions of allene-tethered dienes, developed in the group in 2008,[16] were later applied as key step to the asymmetric synthesis of the antitumoral agent (-)-englerin A.[17]

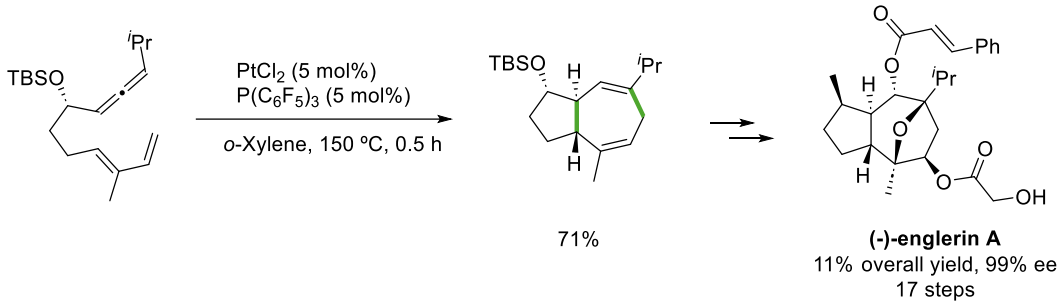

Scheme 38. Platinum-catalyzed (4+3) cycloaddition towards (-)-englerin A.

1.2.3 Asymmetric transition metal catalysis

Chirality plays a critical role in many fields, especially in medicinal chemistry, as different enantiomers of a molecule can exhibit totally different biological activities. Therefore, having efficient access to single enantiomers is of primary relevance.

Transition metal catalysts have proven to be very effective in promoting enantioselective reactions, since the use of chiral ancillary ligands might induce the stereoselective coordination of the metal to the reactants, eventually leading to the preferential formation of one of the two enantiomeric products.

A well-known pioneer example is the rhodium catalyzed asymmetric hydrogenation of alkenes, developed by W. Knowles at Monsanto, which was the first demonstration of the use of asymmetric catalysis in the synthesis of a chiral drug (**Scheme 39**). For its great contribution to the field of asymmetric catalysis, Knowles was awarded the Nobel Prize in Chemistry in 2001, alongside R. Noyori and K. Sharpless, who also made outstanding contributions to this field.[4a]

[15] Reppe, W.; Schlichting, O.; Klager, K.; Toepel, T. Cyclisierende Polymerisation von Acetylen I Über Cyclooctatetraen. *Justus Liebigs Ann. Chem.* **1948**, *560*, 1–92.
[16] Trillo, B.; López, F.; Gulías, M.; Castedo, L.; Mascareñas, J. Platinum-Catalyzed Intramolecular [4C+3C] Cycloaddition between Dienes and Allenes. *Angew. Chem. Int. Ed.* **2008**, *47*, 951-954.
[17] Nelson, R.; Gulías, M.; Mascareñas, J. L.; López, F. Concise, Enantioselective, and Versatile Synthesis of (−)-Englerin A Based on a Platinum-Catalyzed [4C+3C] Cycloaddition of Allenedienes. *Angew. Chem. Int. Ed.* **2016**, *55*, 14359.

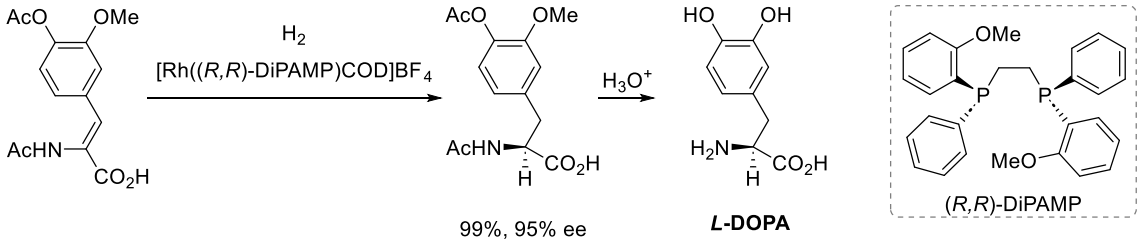

Scheme 39. Monsanto synthesis of *L*-DOPA using a Rh(I)-catalyzed asymmetric hydrogenation.

1.3 Alkylidenecyclopropanes and Transition Metal Catalysis

1.3.1 Alkylidenecyclopropanes (ACPs)

Structural features

Alkylidenecyclopropanes (ACPs) are a group of organic compounds characterized by the presence of a cyclopropyl ring that bears an *exo*-cyclic double bond. The notable reactivity of these compounds is largely attributed to the coordinating abilities of the alkene, together with their high strain energy, which is significantly higher than in other small carbocyclic systems (**Figure 5**).[18]

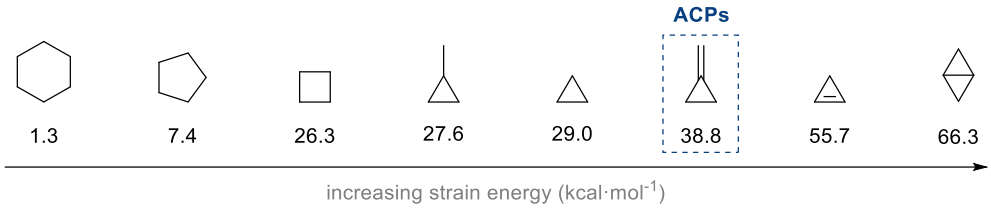

Figure 5. Strain energies of small ring systems.

The simplest member of this family is the methylidenecyclopropane (MCP), which features a terminally unsubstituted alkene. MCP is more strained than cyclopropane due to the presence of the *exo*-cyclic double bond (**Figure 6**). The higher strain is related to the presence of a cyclopropyl sp^2 carbon, which has larger bond angle requirements than a sp^3 counterpart (sp^2, 120º vs sp^3, 109º). The bond angles of an ACP are around 60º. Moreover, the presence of the double bond also causes bond length distortion, further increasing their reactivity.[19] Despite these features, ACPs are generally stable molecules at ambient conditions and are even found in some natural products.

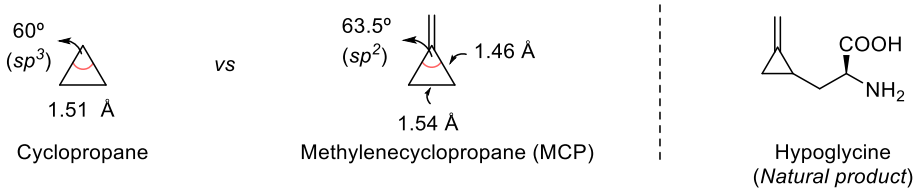

Figure 6. Structural differences between cyclopropane and methylidenecyclopropane (MCP).

Activation of cyclopropyl C-C σ-bonds by metal complexes

The activation of C-C σ-bonds via transition metal reagents is not trivial, since C-C single bonds are thermodynamically very stable, with dissociation energies over 85 kcal·mol^{-1}. In contrast, the M-C bonds formed through the oxidative addition to a metal complex present dissociation energies around 70 kcal·mol^{-1}. From a kinetic perspective, unlike side-on orientation of the π-orbital in C-C double

[18] Souillart, L.; Cramer, N. Catalytic C–C Bond Activations via Oxidative Addition to Transition Metals. *Chem. Rev.* **2015**, *115*, 17, 9410–9464.
[19] Laurie, V. W.; Stigliani, W. M. The Microwave Spectrum, Structure, and Dipole Moment of Methylenecyclopropane. *J. Am. Chem. Soc.* **1970**, *92*, 1485.

bonds, the σ-orbital of C-C bonds is highly directional, being constrained along the bond axis. This factor, along with the steric hindrance around the sp^3 carbons, hinders the approximation of a metal complex (**Figure 7**).[20]

However, the structural properties of cyclopropanes facilitate the C-C bond activation. The formation of a metal complex is thermodynamically favored due to the release of the three-membered ring strain. In addition, the orbitals connecting the carbon atoms are bent outwards from the internuclear axis, facilitating the interaction with the metal orbitals and enhancing the kinetics of the cleavage. These properties of cyclopropanes are even more acute in ACPs and, moreover, the *exo*-double bond can also facilitate the metal-promoted C-C bond cleavage.

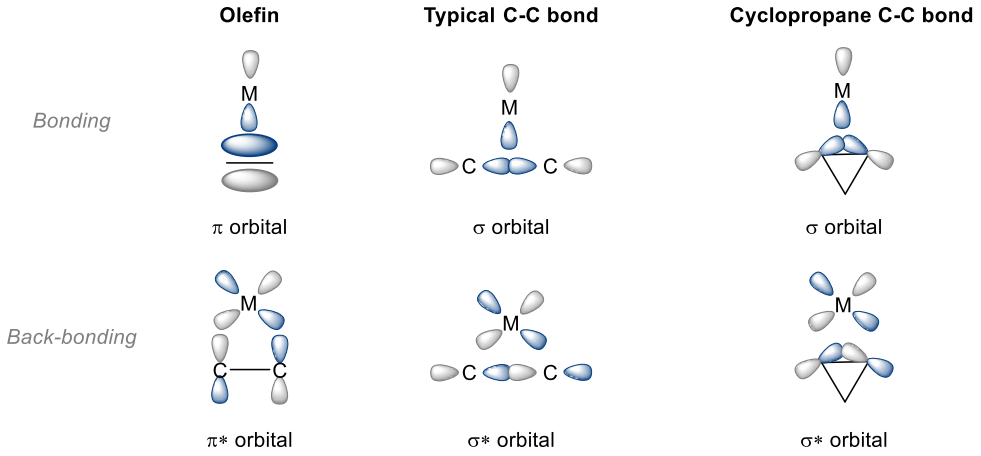

Figure 7. Orbital representation in the activation of C-C double bonds by transition metals.

1.3.2 Reactivity of ACPs

Alkylidenecyclopropanes (ACPs) exhibit a versatile reactivity due to the ring strain of the cyclopropyl ring and the presence of the *exo*-cyclic double bond. They can behave like typical olefins, reacting as 2C synthons in different reactions or, more interestingly, evolve through ring opening, acting as 3C components.[21] In the following sections, we will describe their most significant reactivity modes, focusing on transition metal-catalyzed transformations, which is the topic of this PhD thesis.

Cycloadditions

ACPs can participate as 2C or 3C components in different types of cycloadditions. For instance, in 1989 Nakamura reported a thermal (3+2) cycloaddition between specifically designed methylenecyclopropanes (MCPs) and electron-deficient olefins, to afford cyclopentanes with good regio- and diastereoselectivities (**Scheme 40**).[22] The authors proposed a concerted pathway through

[20] Murakami, M.; Ito, Y. Cleavage of Carbon-Carbon Single Bonds by Transition Metals. In *Activation of Unreactive Bonds and Organic Synthesis*; Murai, S., Ed.; Topics in Organometallic Chemistry, vol 3; Springer: Berlin, Heidelberg, **1999**.

[21] For reviews about ACP reactivity, see: a) Pellissier, H. Recent developments in the reactivity of methylene- and alkylidenecyclopropane derivatives. *Tetrahedron* **2010**, *66*, 8341–8375.; b) Pellissier, H. Recent developments in the synthesis and reactivity of methylene- and alkylidenecyclopropane derivatives. *Tetrahedron* **2014**, *70*, 4991–5031.; c) Souillart, L.; Cramer, N. Catalytic C–C Bond Activations via Oxidative Addition to Transition Metals. *Chem. Rev.* **2015**, *115*, 9410–9464.; d) Fumagalli, G.; Stanton, S.; Bower, J. F. Recent Methodologies That Exploit C–C Single-Bond Cleavage of Strained Ring Systems by Transition Metal Complexes. *Chem. Rev.* **2017**, *117*, 9404–9432.; e) Yu, L.; Shi, M. The Construction of Molecular Complexity from Functionalized Alkylidenecyclopropanes (FACPs). *Chem. Eur. J.* **2019**, *25*, 7591–7606.

[22] Yamago, S.; Nakamura, E. Use of methylenecyclopropanone ketals for cyclopentane synthesis. A new efficient thermal [3 + 2] cycloaddition. *J. Am. Chem. Soc.* **1989**, *111*, 18, 7285–7286.

a trimethylenemethane (TMM) intermediate. The presence of stabilizing substituents (e.g. ketal) is critical for the success of the method.

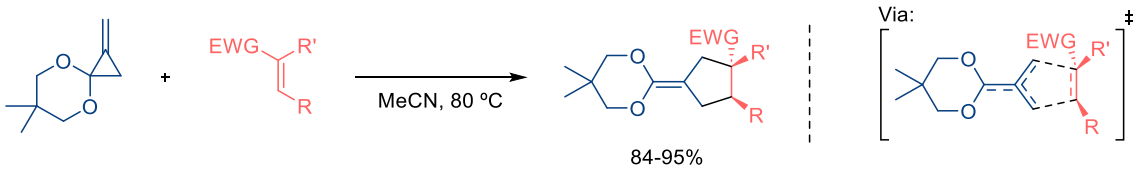

Scheme 40. Thermal (3+2) cycloaddition between MCPs and activated olefins.

Cycloadditions can also be promoted by Lewis acids, as demonstrated by De Meijere and co-workers in their Ag(I)-catalyzed (2+2) cycloaddition of ACPs and imines, which afforded azetidine derivatives in good yields (**Scheme 41**).[23] The high diastereoselectivities in favor of the *syn* cycloadduct were explained by proposing a stepwise mechanism, which involves an equilibrium between intermediate **I** and its more stable conformer **II**. Notably, enol ethers lacking a cyclopropyl ring did not react with tosylimines, suggesting that the cyclopropyl group is key to stabilize the proposed zwitterionic species.[24]

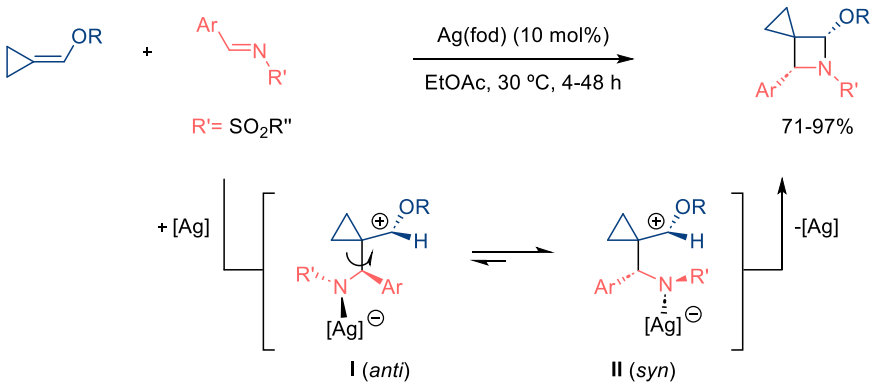

Scheme 41. Silver salt-catalyzed (2+2) cycloaddition between ACPs and imines.

As previously commented, ACPs can participate in a variety of transition metal catalyzed cycloaddition processes. In a pioneering example, Binger demonstrated that palladium catalysts can promote cycloaddition reactions of ACPs through the cleavage of the distal C-C bond of the cyclopropyl ring (**Scheme 42**).[25] Thus, the catalyst derived from $Pd(acac)_2$, $P(^iPr)_3$ and Et_2AlOEt enabled the formal (3+2) cycloaddition between MCP and norbornene, to give the corresponding carbocyclic product in excellent yield. Mechanistically, the reaction was proposed to begin with an oxidative addition of the distal C-C bond, to yield the palladacyclobutane **I**, which evolves to a trimethylmethane (TMM) species **II**. This intermediate would then undergo a migratory insertion of the olefin and a final reductive elimination to afford the cycloadduct.

[23] Nakamura, I.; Nemoto, T.; Yamamoto, Y.; de Meijere, A. Thermally Induced and Silver-Salt-Catalyzed [2+2] Cycloadditions of Imines to (Alkoxymethylene)cyclopropanes. *Angew. Chem. Int. Ed.* **2006**, *45*, 5176–5179.
[24] De Meijere, A. Bonding Properties of Cyclopropane and Their Chemical Consequences. *Angew. Chem. Int. Ed.* **1979**, *18*, 809–826.
[25] Binger, P.; Schuchardt, U. Reaktionen des Methylencyclopropans, IV. Palladium(0)-katalysierte Codimerisierungen des Methylencyclopropans mit Alkenen. *Chem. Ber.* **1980**, *113*, 3334.

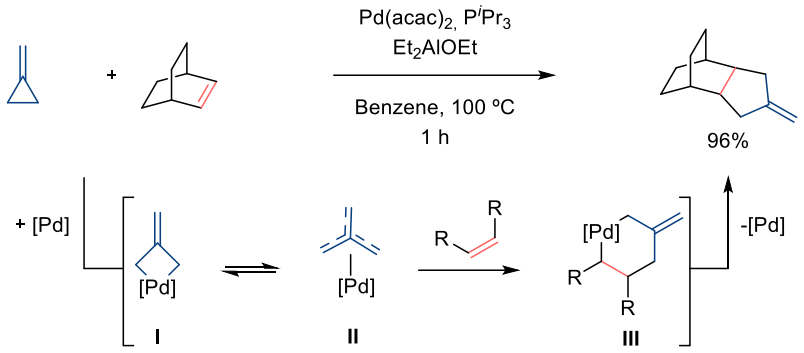

Scheme 42. Pd(0)-catalyzed formal (3+2) cycloaddition between MCPs and strained alkenes.

Early reports of TMC transformations of ACPs were mainly focused on similar intermolecular processes using Pd or Ni catalysts.[21d] The development of intramolecular reactions, which allow to obtain more complex polycyclic structures, was introduced by our group in the early 2000's, through a variety of TMC intramolecular cycloadditions using ACPs tethered to different carbon-based unsaturated partners (alkyne, alkene, diene or allene).[26]

A relevant example is the Pd(0)-catalyzed intramolecular (3+2) cycloaddition between ACPs and alkenes, reported in 2006. Remarkably, the use of a Pd(0)-catalyst bearing a bulky phosphite ligand **L1** was key to enable the selective (3+2) annulation towards the bicyclo[3.3.0]octane systems, which were obtained in good yields and high diastereoselectivities (**Scheme 43**).[26b]

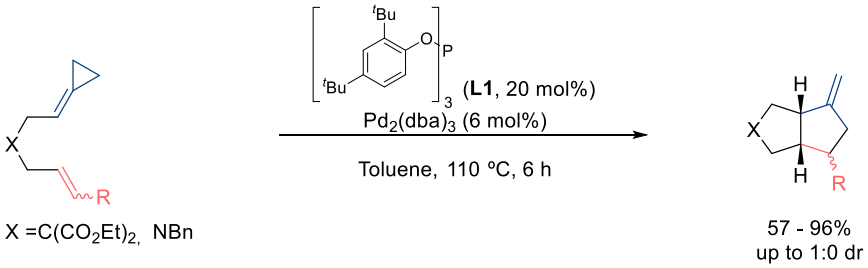

Scheme 43. Pd(0)-catalyzed intramolecular (3+2) cycloaddition between ACPs and alkenes.

In 2012, in collaboration with Cárdenas and García Fandiño, our group proposed different mechanistic paths for these Pd-catalyzed cycloadditions, based on DFT computations.[27] Although the authors examined the influence of electron-deficient and neutral substituents on the alkene partner, the studies were limited to PH_3 as the model ligand due to computational constraints. Consequently, the results should be interpreted with caution, particularly given the small energy differences observed between certain pathways. In all cases, calculations supported the formation of palladacyclobutanes as key intermediates, arising from the initial oxidative addition of the distal C–C

[21d] Fumagalli, G.; Stanton, S.; Bower, J. F. Recent Methodologies That Exploit C–C Single-Bond Cleavage of Strained Ring Systems by Transition Metal Complexes. *Chem. Rev.* **2017**, *117*, 9404–9432.

[26] a) Delgado, A.; Rodríguez J. R.; Castedo, L.; Mascareñas, J. L. Palladium-Catalyzed [3+2] Intramolecular Cycloaddition of Alk-5-ynylidenecyclopropanes: A Rapid, Practical Approach to Bicyclo[3.3.0]octenes. *J. Am. Chem. Soc.* **2003**, *125*, 9282–9283.; b) Gulías, M.; García, R.; Delgado, A.; Castedo, L.; Mascareñas, J.L Palladium-Catalyzed [3 + 2] Intramolecular Cycloaddition of Alk-5-enylidenecyclopropanes. *J. Am. Chem. Soc.* **2006**, *128*, 384–385. c) Gulías, M.; Durán, J.; López, F.; Castedo, L.; Mascareñas, J.L. Palladium-catalyzed [4 + 3] intramolecular cycloaddition of alkylidenecyclopropanes and dienes. *J. Am. Chem. Soc.* **2007**, *129*, 36, 11026–11027.; d) Trillo, B.; Gulías, M.; López, F.; Castedo, L.; Mascareñas, J.L. Palladium-catalyzed intramolecular [3C+2C] cycloaddition of alkylidenecyclopropanes to allenes. *Adv. Synth. Catal.* **2006**, *348*, 2381-2384.

[27] García-Fandiño, R.; Gulías, M.; Mascareñas, J.L.; Cardenas, D. J. Mechanistic study on the palladium-catalyzed (3 + 2) intramolecular cycloaddition of alk-5-enylidenecyclopropanes. *Dalton Trans.* **2012**, *41*, 9468-9481.

bond of the ACP to the Pd(0) complex.[28] **Figure 8** shows the calculated profile with a non-activated alkene as cycloaddition partner.

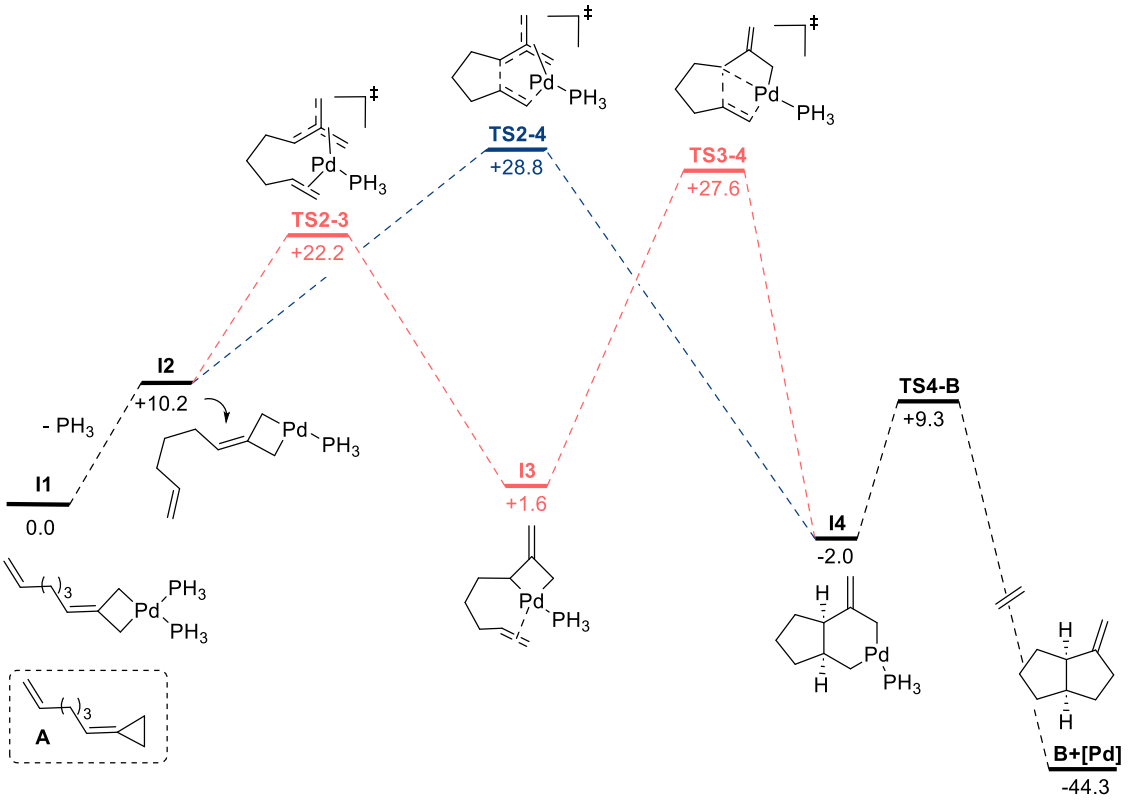

Figure 8. DFT energy profile about Pd-catalyzed (3+2) cycloaddition of ACPs and unactivated alkenes, using Pd(0)-PH_3. [B3LYP/6-31G(d) (LANL2DZ for Pd)//B3LYP/ 6-311+G-(2df,2p) (SDD for Pd)]. Values of ΔG (kcal·mol^{-1}).

The initially generated palladacyclobutane intermediate **I1**, decoordinates one of the PH_3 ligands to generate the intermediate **I2** (ΔG =10.2 kcal·mol^{-1}), which can now evolve through different pathways. One of them (red pathway), consists of its isomerization towards the *exo*-methylene palladacyclobutane **I3** (ΔG = 12.0 kcal·mol^{-1}), followed by a migratory insertion of the tethered alkene, to afford the palladacyclohexane **I4** (ΔG = 26.0 kcal·mol^{-1}). Alternatively, intermediate **I2** can undergo a metalloene rearrangement to directly provide intermediate **I4** (ΔG = 18.6 kcal·mol^{-1}, blue path). The stepwise formation of **I4** (red pathway) seems favored since the initial isomerization involves a lower energy barrier than the metalloenic step (ΔΔG = 6.6 kcal·mol^{-1}). However, the subsequent migratory insertion (**TS3-4**) involves a transition state that is only 1.2 kcal·mol^{-1} less energetic than **TS2-4**. Thus, both pathways seem feasible to generate **I4** and, from this intermediate, the bicyclic product is obtained through an easy reductive elimination (ΔG = 11.3 kcal·mol^{-1}).

Additional studies were conducted with electron-deficient alkenes, revealing that the favored pathway varies depending on the *E* or *Z* stereochemistry of the alkene and the number of ligands coordinated to the metal center.

In summary, the preferred pathway for the formation of cycloadducts from ACPs and C-C unsaturated bonds remains inconclusive, emphasizing the need for further investigations. Moreover, a theoretical study with a more realistic ancillary ligand should also bring new relevant information about these reactions, particularly considering their critical role in the selectivity experimentally observed.

[28] García-Fandiño, R.; Gulías, M.; Castedo, L.; Granja, J. R.; Mascareñas, J. L.; Cárdenas, D. J. Palladium-Catalysed [3+2] Cycloaddition of Alk-5-ynylidenecyclopropanes to Alkynes: A Mechanistic DFT Study. *Chem. Eur. J.* **2008**, *14*, 1, 272–281.

In 2018, our group developed an asymmetric variant of these Pd-catalyzed (3+2) cycloadditions, which represented the first highly enantioselective TMC cycloaddition of ACPs (**Scheme 44**). In particular, employing a catalyst comprising CpPd(π-cin.) and the bulky chiral phosphoramidite **(*S,R,R*)-L2**, derived from VAPOL, the corresponding (3+2) cycloadducts were obtained in good-to-high yields, with excellent diastereoselectivity and enantiomeric ratios of up to 97:3.[29]

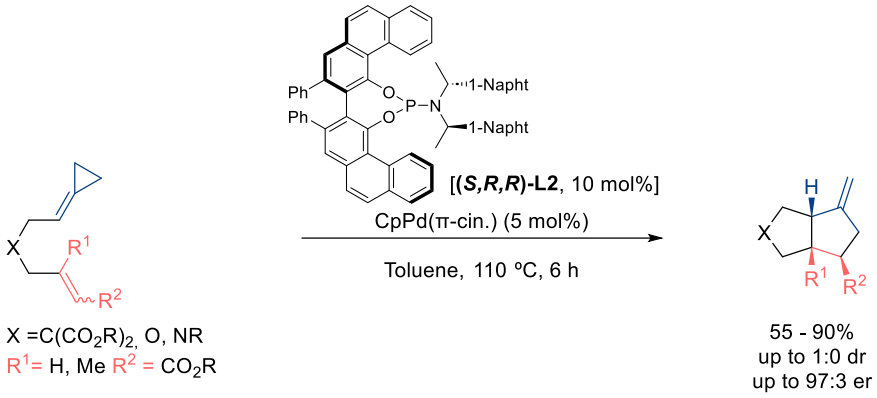

Scheme 44. Asymmetric Pd(0)-catalyzed intramolecular (3+2) cycloaddition of ACP-tethered alkenes.

Remarkably, the same Pd-catalyst also promotes the (4+3) cycloaddition between ACPs and conjugated dienes, providing appealing 5,7-bicyclic systems in an asymmetric fashion (**Scheme 45**).[26c, 29]

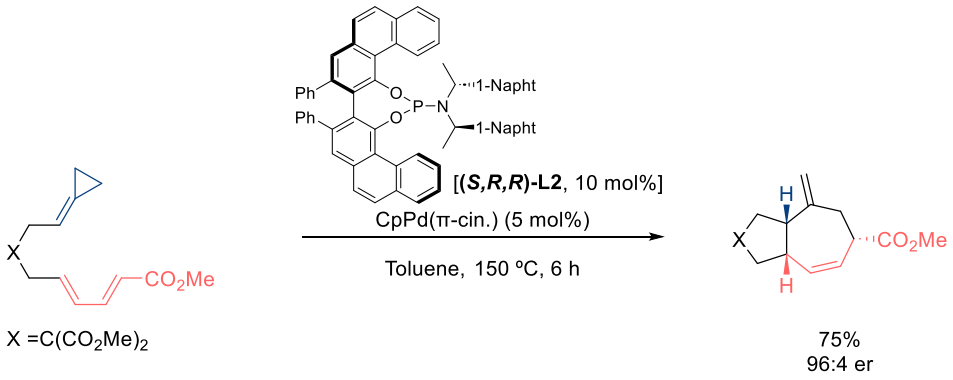

Scheme 45. Asymmetric Pd(0)-catalyzed intramolecular (4+3) cycloaddition between ACPs and dienes.

On the other hand, in 2021 our group reported an asymmetric Co(I)-catalyzed (3+2) cycloaddition between ACPs and alkynes, employing the catalyst *in situ* generated from $CoBr_2$, (*S*)-BINAP and a reducing agent (**Scheme 46**).[30] DFT studies indicated that the mechanism differs from that previously proposed for Pd catalysts. In particular, instead of the standard initial insertion of the cyclopropyl ring to the metal, the ACP evolves via an oxidative cyclometallation toward the cobaltacycle **I**. This species subsequently undergoes a cyclopropyl to π-allyl rearrangement to yield the stable π-allyl cobaltacycle **II**, which was even isolated in a specific case.

[26c] Gulías, M.; Durán, J.; López, F.; Castedo, L.; Mascareñas, J.L. Palladium-catalyzed [4 + 3] intramolecular cycloaddition of alkylidenecyclopropanes and dienes. *J. Am. Chem. Soc.* **2007**, *129*, 36, 11026–11027.
[29] Verdugo, F.; Villarino, L.; Durán, J.; Gulías, M.; Mascareñas, J. L.; López, F. Enantioselective Palladium-Catalyzed [3C + 2C] and [4C + 3C] Intramolecular Cycloadditions of Alkylidenecyclopropanes. *ACS Catal.* **2018**, *8*, 6100-6105.
[30] Da Concepción, E.; Fernández, I.; Mascareñas, J. L.; López, F. Highly Enantioselective Cobalt-Catalyzed (3+2) Cycloadditions of Alkynylidenecyclopropanes. *Angew. Chem. Int. Ed.* **2021**, *60*, 8182–8188.

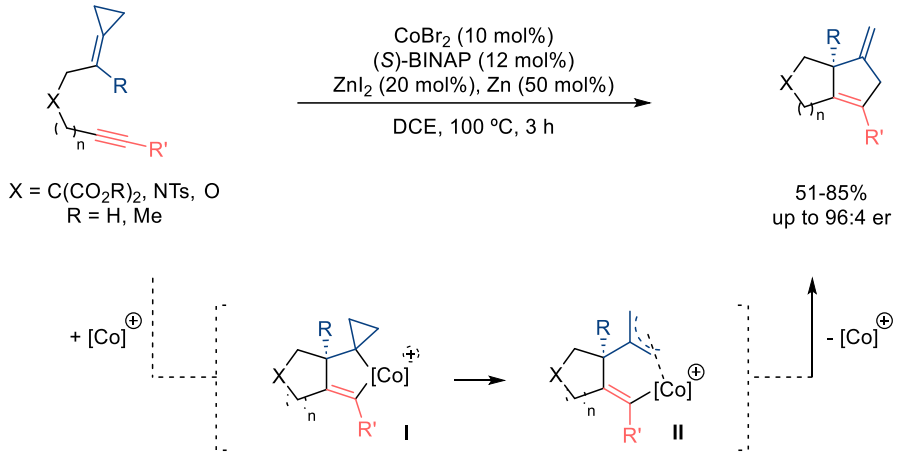

Scheme 46. Asymmetric Co(I)-catalyzed (3+2) cycloaddition between ACPs and alkynes.

ACPs can also participate in multicomponent cycloadditions. In 2010, our group reported a nickel-catalyzed (3+2+2) cycloaddition of alkyne-tethered ACPs and external alkenes, to yield bicyclic systems bearing a seven-membered carbocycle (**Scheme 47**).[31,32] The reaction, which is promoted by $Ni(COD)_2$, was proposed to proceed via a proximal insertion of the Ni(0) complex to the ACP, followed by an intramolecular alkyne migratory insertion. The resulting metallacycle **II** can then interact with an external alkene, yielding after a sequence of migratory insertion and reductive elimination, the corresponding 6,7- fused bicyclic product.

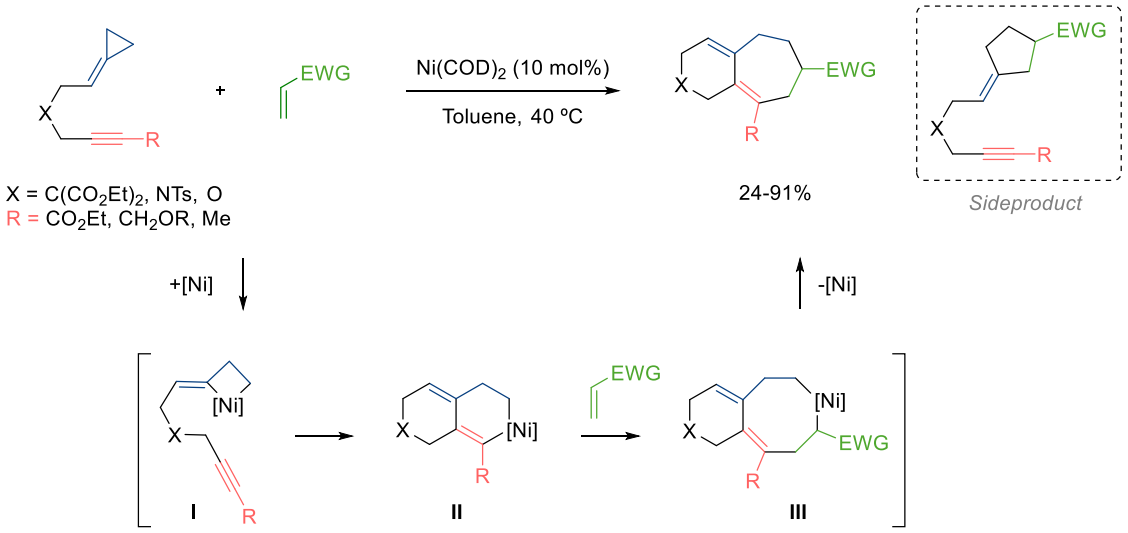

Scheme 47. Ni(0)-catalyzed (3+2+2) cycloaddition between ACP-tethered alkynes and alkenes.

[31] a) Saya, L.; Bhargava, G.; Navarro, M. A.; Gulías, M.; López, F.; Fernández, I.; Castedo, L.; Mascareñas, J. L. Nickel-Catalyzed [3+2+2] Cycloadditions between Alkynylidenecyclopropanes and Activated Alkenes. *Angew. Chem. Int. Ed.* **2010**, 9886–9890.; b) Saya, L.; Fernández, I.; López, F.; Mascareñas, J. L. Nickel-Catalyzed Intramolecular [3 + 2 + 2] Cycloadditions of Alkylidenecyclopropanes. A Straightforward Entry to Fused 6,7,5-Tricyclic Systems. *Org. Lett.* **2014**, *16*, 5008–5011.

[32] For other multicomponent cycloadditions using nickel catalysts, see: a) Saito, S.; Masuda, M.; Komagawa, S. Nickel-Catalyzed Intermolecular [3 + 2 + 2] Cocyclization of Ethyl Cyclopropylideneacetate and Alkynes. *J. Am. Chem. Soc.* **2004**, *126*, 34, 10540–10541.: b) Saito, S.; Maeda, K.; Yamasaki, R.; Kitamura, T.; Nakagawa, M.; Kato, K.; Azumaya, I.; Masu, H. Synthesis of Nine-Membered Carbocycles by the [4+3+2] Cycloaddition Reaction of Ethyl Cyclopropylideneacetate and Dienynes. *Angew. Chem. Int. Ed.* **2010**, *49*, 1830-1833.; c) Komagawa, S.; Wang, C.; Morokuma, K.; Saito, S.; Uchiyama, M., Mechanistic Origin of Chemo- and Regioselectivity of Nickel-Catalyzed [3 + 2 + 2] Cyclization Reaction. *J. Am. Chem. Soc.* **2013**, *135*, 14508–14511.

Rhodium catalysts can also promote multicomponent cycloadditions of ACPs.[33] One of the most recent examples, described by Evans in 2023, consists of an intramolecular (3+2+2) cycloaddition of skipped diene-tethered ACPs (**Scheme 48**).[34] This transformation affords complex tricyclic scaffolds in good yields and with excellent diastereoselectivity. Notably, the synthetic utility of this reaction was shown with the total synthesis of (+)-zizazene from the commercially available (*S*)-(-)-citronellal. Mechanistically, the reaction was proposed to begin with the distal C-C bond activation of the cyclopropyl ring to afford the TMM rhodium complex **I**, which undergoes two consecutive migratory insertions toward the π-allyl intermediate **III**. Finally, a reductive elimination closes the catalytic cycle, affording the corresponding (3+2+2) cycloadduct.

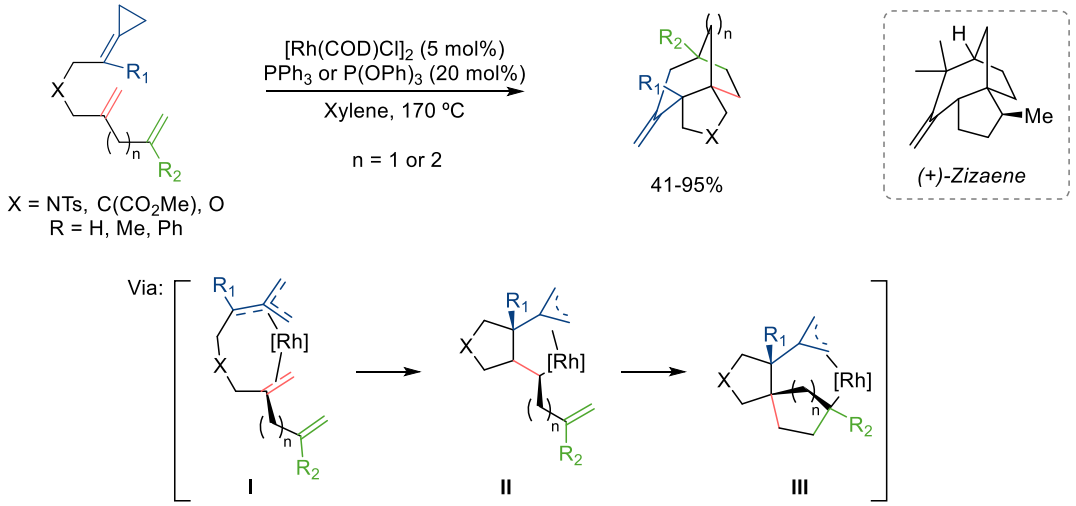

Scheme 48. Rh(I)-catalyzed (3+2+2) cycloaddition of ACPs tethered to a 1, n-dienes (n=1 or 2).

Despite the huge synthetic potential of TMC multicomponent cycloadditions involving ACPs, these transformations remain restricted to the use of carbon-based unsaturated partners. This limitation offers an opportunity to explore new multicomponent transformations involving heteroatom-containing counterparts.

TMC heterocycloaddition reactions of ACPs

As can be deduced from the previous section, the number of TMC cycloadditions between ACPs and different C-C unsaturated bonds, such as alkenes, dienes or alkynes, is significant. However, cycloaddition examples involving heteroatom-based unsaturated partners are extremely scarce.[35]

In 2001, Yamamoto reported a (3+2) intermolecular cycloaddition between ACPs and aldehydes using a palladium catalyst derived from $Pd(PPh_3)_4$ and the phosphine oxide $P(O)Bu_3$ (**Scheme 49**, *left*).[36] Employing a similar Pd(0) catalyst, they also developed a (3+2) intermolecular annulation between ACPs and tosyl imines, to afford interesting pyrrolidine scaffolds (**Scheme 49**, *right*).[37] However, the scope of both transformations is extremely narrow, and the reactions required neat

[33] For Rh-catalysed multicomponent cycloadditions, see: a) Evans, P. A.; Inglesby, P. A., Intermolecular Rhodium-Catalyzed [3 + 2 + 2] Carbocyclization of Alkenylidenecyclopropanes with Activated Alkynes: Regio- and Diastereoselective Construction of cis-Fused Bicycloheptadienes. *J. Am. Chem. Soc.* **2008**, *130*, 12838–12839.; b) Araya, M.; Gulías, M.; Fernández, I.; Bhargava, G.; Castedo, L.; Mascareñas, J. L.; López, F. Rhodium-Catalyzed Intramolecular [3 + 2 + 2] Cycloadditions between Alkylidenecyclopropanes, Alkynes, and Alkenes. *Chem. Eur. J.* **2014**, *20*, 10255–10259.

[34] Zhu, Y.; Zheng, J.; Evans, P. A. Intramolecular Rhodium-Catalyzed [(3+2+2)] Carbocyclization Reactions with Dienylidenecyclopropanes: A Concise and Stereoselective Total Synthesis of the Sesquiterpene (+)-Zizaene. *J. Am. Chem. Soc.* **2023**, *145*, 7, 3833–3838.

[35] Brandi, A.; Cicchi, S.; Cordero, F.M.; Goti, A. Heterocycles from Alkylidenecyclopropanes. *Chem. Rev.* **2003**, *103*, 1213–1270.

[36] Nakamura, I.; Oh, B. H.; Saito, S.; Yamamoto, Y. Novel [3+2] Cycloaddition of Alkylidenecyclopropanes with Aldehydes Catalyzed by Palladium. *Angew. Chem. Int. Ed.* **2001**, *40*, 1298–1300.

[37] Oh, B. H.; Nakamura, I.; Saito, S.; and Yamamoto, Y. Palladium-catalyzed [3+2] cycloaddition of alkylidenecyclopropanes with imines. *Tetrahedron Lett.* **2001**, *42*, 6203-6205.

conditions or a great excess of ACP precursors, which makes the processes less convenient. The authors proposed the π-allyl Pd(II) complex **I** as a key reaction intermediate; nevertheless, since no mechanistic studies were performed, alternative reaction pathways cannot be discarded.

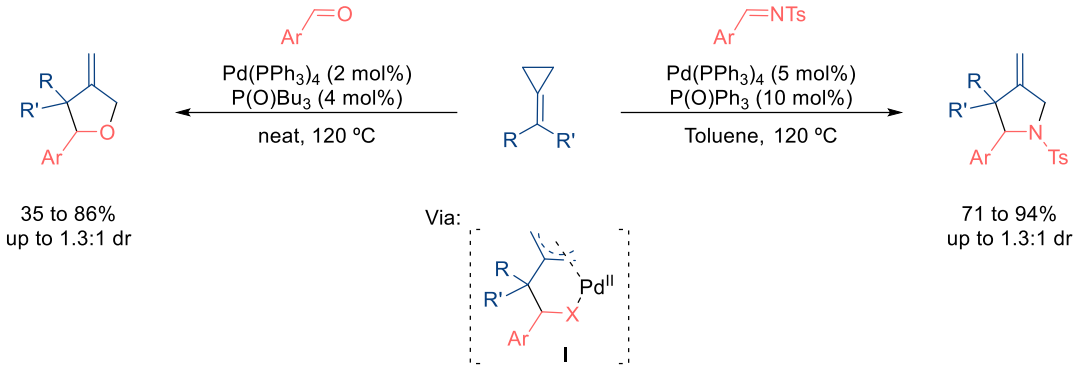

Scheme 49. Pd(0)-catalyzed intermolecular (3+2) heterocycloadditions of ACPs reported by Yamamoto.

Another example was reported by Bhargava's group in 2020, consisting of a Ni(0)-catalyzed (3+2) cycloaddition between bis(alkylidenecyclopropanes) and diazenes, to deliver pyrazole-1,2-dicarboxylates (**Scheme 50**).[38] The reaction, which requires a large excess of diazene as reaction counterparts (DIAD or DEAD, 10 equiv.), usually provides moderate yields and, overall, the scope is very narrow. The process was proposed to begin with an oxidative addition at the proximal C-C bond of the ACP, followed by a migratory insertion and an eventual reductive elimination to give the heterocycle.[39] Curiously, the presence of a second ACP as partner is required for the reaction, obtaining no reactivity when substrates bearing only one ACP are used.

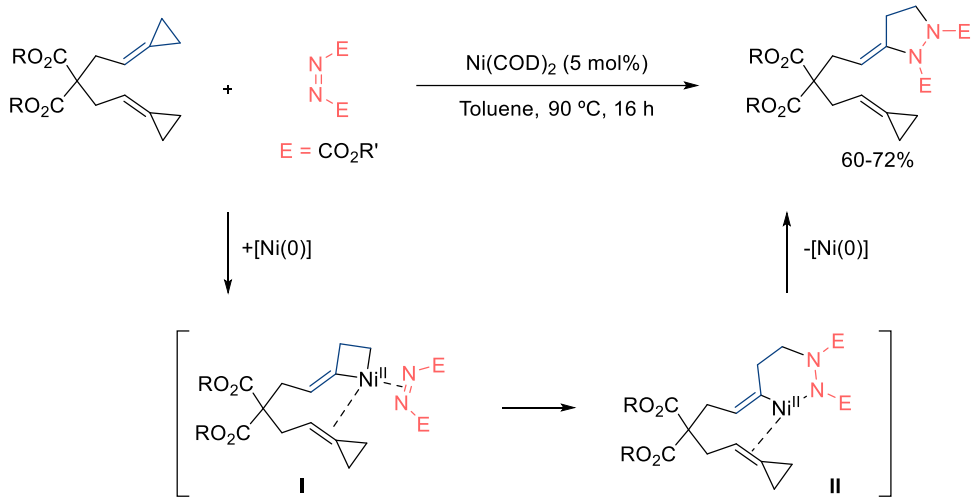

Scheme 50. Nickel(0)-catalyzed (3+2) cycloadditions of bis(alkylidenecyclopropanes) with diazenes.

While examples of intermolecular ACP heterocycloadditions were rare, intramolecular variants remained entirely unexplored at the beginning of this PhD. Given the significant synthetic potential of these transformations, which could generate polyheterocyclic systems in one step, our group tried to fill this gap.

[38] Kuila, B.; Naikoo, R.; Mahajan, D.; Singh, P.; Bhargava, G. Nickel(0)-Catalyzed [3+2] Cycloadditions of Bis(alkylidenecyclopropanes) with Diazenes: A Facile Synthesis of Functionalized Pyrazolidine-1,2-dicarboxylates. *Synlett* **2020**, *31*, 1, 65-68.

[39] a) Saya, L.; Bhargava, G.; Navarro, M. A.; Gulías, M.; López, F.; Fernández, I.; Castedo, L.; Mascareñas, J. L. Nickel-Catalyzed [3+2+2] Cycloadditions between Alkynylidenecyclopropanes and Activated Alkenes. *Angew. Chem. Int. Ed.* **2010**, *49*, 9886–9890.; b) Kuila, B.; Mahajan, D.; Singh, P.; Bhargava, G. Nickel catalyzed [3+2] cycloaddition reaction of bis(methylenecyclopropane) with cyclic and acyclic dienophiles. *Tetrahedron Lett.* **2015**, *56*, 1307–1311.

Thus, Dr. Verdugo made the initial experiments in this area, demonstrating the viability of palladium(0)-catalyzed (3+2) intramolecular cycloadditions between ACPs and carbonyl moieties (**Scheme 51**).[40] Using the Pd catalyst generated *in situ* from $Pd_2(dba)_3$ and Buchwald biaryl ligands, the (3+2) cycloaddition effectively occurs, leading to bicyclic tetrahydrofurans in good-to-excellent yields and high diastereoselectivity. The versatility and broad scope of this reaction, particularly when compared to the original intermolecular reaction of Yamamoto, encouraged us to study, from a computational perspective, the mechanistic details of the process. This research will be summarized in *Section 4.2*.

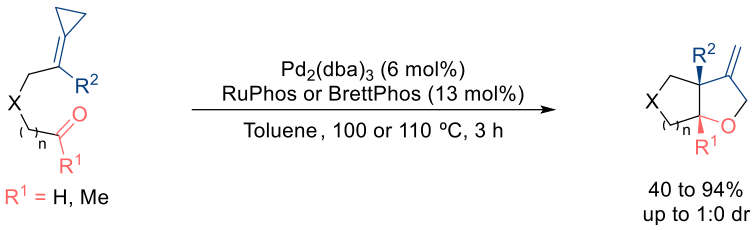

Scheme 51. Palladium(0)-catalyzed intramolecular (3+2) cycloaddition between ACPs and carbonyl moieties.

On the other hand, Dr. Verdugo also initiated the exploration of the Pd(0)-catalyzed intramolecular cycloaddition of ACPs tethered to different C=N partners. Interestingly, his preliminary results showed that the same catalytic system employed for the cycloaddition with carbonyls is also effective for the aza-cycloaddition with oxime ethers. Thus, bicyclic pyrrolidines of type **2** can be obtained in good yield (**Scheme 52**).

Overall, these studies indicated that the use of Pd(0) catalysts bearing Buchwald ligands was crucial for the effective development of the intramolecular (3+2) heterocycloadditions; however, the underlying reasons responsible for such efficiency remained unclear at the moment I started my PhD. Therefore, an important part of my work was focused on further exploring and understanding these heterocycloadditions.

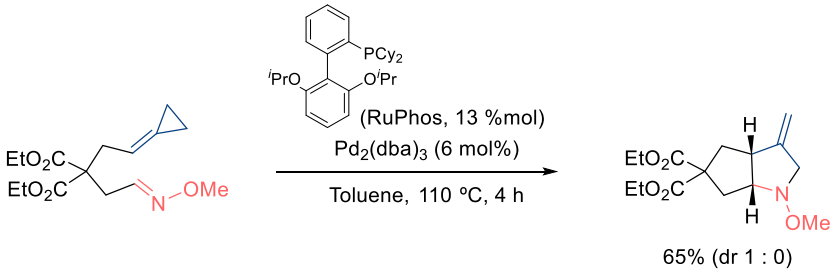

Scheme 52. Palladium(0)-catalyzed (3+2) cycloaddition between ACPs and oxime ether partners.

Cycloisomerizations and rearrangements of ACPs

A variety of metal catalysts have been shown to promote cycloisomerizations or rearrangement processes of ACPs. Gagné reported in 2012 an asymmetric Au(I)-catalyzed Cope rearrangement of ene-alkylidenecyclopropanes to provide chiral vinylcyclopropanes with very good enantioselectivities (**Scheme 53**).[41] The authors proposed that the reaction starts with the coordination of the gold complex to the ACP (**I**), which undergoes a first rearrangement toward the cyclic tertiary carbocation species **II** and, finally, to the vinylcyclopropane product. Notably, similar substrates without the

[40] Verdugo, F.; da Concepción, E.; Rodiño, R.; Calvelo, M.; Mascareñas, J. L.; López, F. Pd-Catalyzed (3 + 2) Heterocycloadditions between Alkylidenecyclopropanes and Carbonyls: Straightforward Assembly of Highly Substituted Tetrahydrofurans. *ACS Catal.* **2020**, *10*, 14, 7710–7718.

[41] Felix, R. J.; Weber, D.; Gutierrez, O.; Tantillo, D. J.; Gagné, M. R. A gold-catalysed enantioselective Cope rearrangement of achiral 1,5-dienes. *Nature Chem.* **2012**, *4*, 405–409.

cyclopropane moiety did not undergo the rearrangement, which suggests that the release of ring strain is crucial.

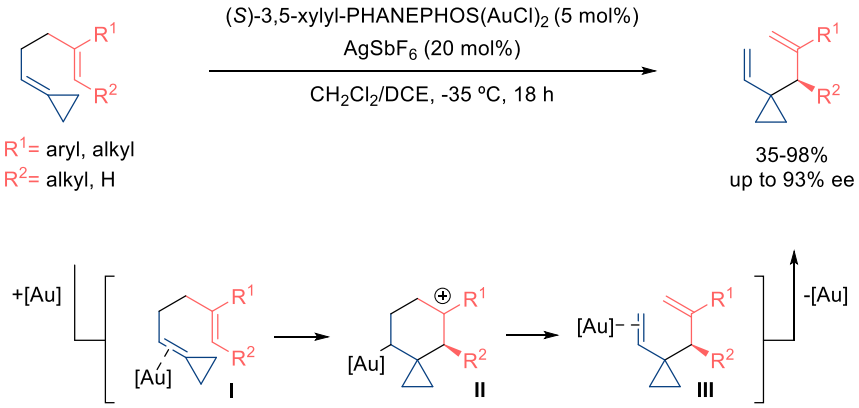

Scheme 53. Asymmetric Au(I)-catalyzed Cope rearrangement of ene-alkylidenecyclopropanes.

Apart from this and other rearrangements, cycloisomerization processes are particularly interesting, enabling the construction of complex cyclic frameworks from linear precursors.[42] This type of reactivity was explored by Evans, in a Rh(I)-catalyzed ene-cycloisomerization of ACPs tethered to alkenes.[43] Employing $Rh(COD)Cl_2/P(O\text{-}p\text{-}Tol)_3$ as catalyst, five-membered rings are generated in excellent yields with complete diastereoselectivity (**Scheme 54**). The reaction was proposed to start with a distal ring opening of the ACP, followed by an isomerization to the rhodacyclobutane **I**. After a regioselective migratory insertion, the resulting complex (**II**) undergoes a β-hydride elimination to afford **III**, and a subsequent reductive elimination provides the observed product.

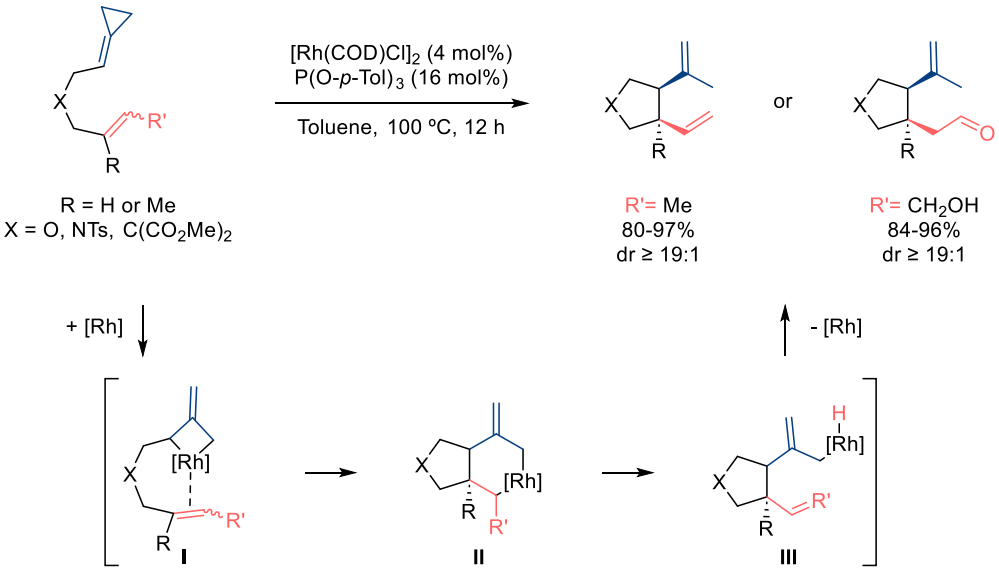

Scheme 54. Rh(I)-catalyzed ene-cycloisomerization of ACPs.

Employing the same catalytic system, Evans also reported an ene-cycloisomerization of ACPs tethered to an allylic sulfide moieties, which yielded the expected cyclic products in good-to-high yields with complete diastereoselectivity (**Scheme 55**).[44] The proposed mechanism resembles the

[42] For reviews on this topic, see: a) Michelet, V.; Toullec, P.; Genêt, J.-P. Cycloisomerization of 1, *n*-enynes: challenging metal-catalyzed rearrangements and mechanistic insights. *Angew. Chem. Int. Ed.* **2008**, *47*, 4268-4315.; b) Yamamoto, Y. Transition-metal-catalyzed cycloisomerizations of α,ω-dienes. *Chem. Rev.* **2012**, *112*, 8, 4736–4769.

[43] Evans, P. A.; Inglesby, P. A. Diastereoselective Rhodium-Catalyzed Ene-Cycloisomerization Reactions of Alkenylidenecyclopropanes: Total Synthesis of (−)-α-Kainic Acid. *J. Am. Chem. Soc.* **2012**, *134*, 8, 3635–3638.

[44] Su, Y.; Inglesby, P.A.; Evans, P.A. Intramolecular thioether migration in the rhodium-catalyzed ene-cycloisomerization of alkenylidenecyclopropanes by a metal-mediated β-sulfide elimination. *Angew. Chem. Int. Ed.* **2018**, *57*, 673.

previous transformation, being the key step a β-sulfide elimination from complex **I**, to generate a metal sulfide intermediate, which subsequently undergoes a C-S reductive elimination to the product.

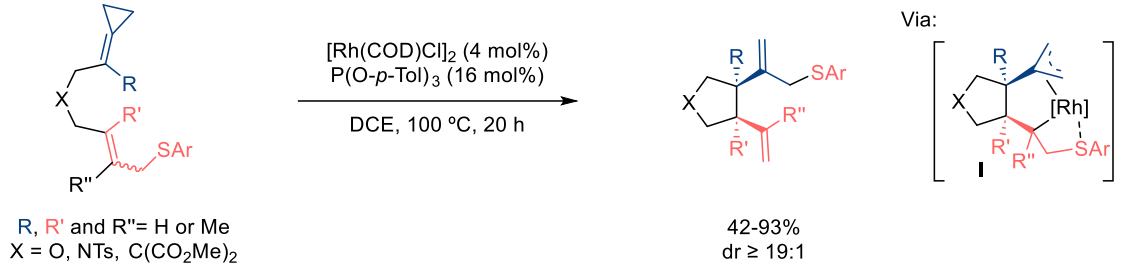

Scheme 55. Rh(I)-catalyzed ene-cycloisomerization of ACPs with intramolecular β-sulfide elimination.

Despite these elegant examples, cycloisomerization processes of ACPs remain largely underexplored, especially tandem processes and multicomponent reactions, as well as related reactions involving heteroatom-containing partners.

Tandem ring-opening/addition reactions

Alkylidenecyclopropanes can undergo ring-opening processes to generate organometallic intermediate species that can be trapped by different nucleophiles, typically leading to allylic and homoallylic compounds. These transformations can be promoted by Lewis or Brønsted acids,[45] and, more commonly, by transition metal catalysts of Ni, Rh or Pd, which offer enhanced selectivity and efficiency.

A pioneering example was reported by Yamamoto in the late 1990s and consists of a palladium (0) catalyzed hydrofunctionalization of ACPs with malonate nucleophiles. The method affords 1,1-disubstituted alkenes in good yields (**Scheme 56**).[46] Mechanistically, the authors suggested the initial formation of a palladium hydride species (**I**), followed by a regioselective hydropalladation of the ACP. The resulting intermediate **II** would then undergo a β-carbon elimination to deliver the π-allyl Pd(II) intermediate **III**. After a reductive elimination, the allylic compound would be eventually released. However, the authors did not support this proposal with further experimental or theoretical studies.

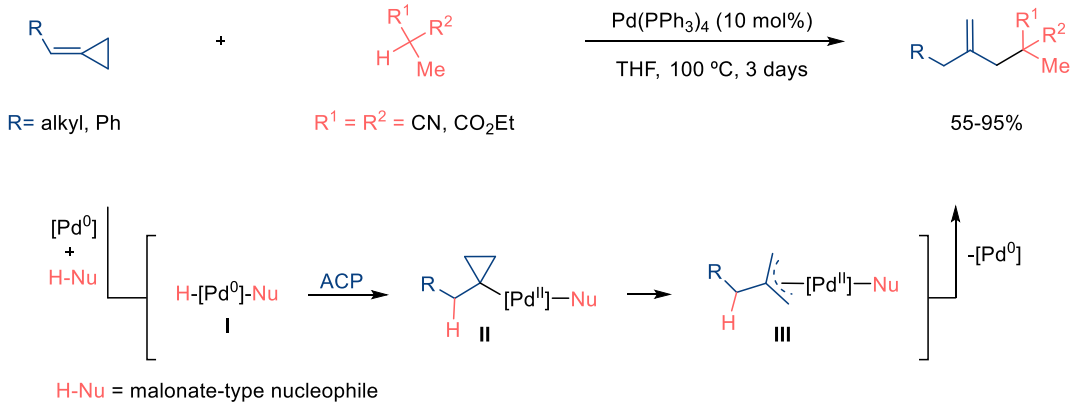

Scheme 56. Pd(0)-catalyzed hydrocarbonation of ACPs with malonate nucleophiles.

In subsequent years, Yamamoto and coworkers exploited this chemistry using different nucleophiles, mostly with heteroatoms. This topic will be covered in more detail in *Section 4.4,* where we explored

[45] For a review on this topic, see: Shao, L.-X.; Shi, M. Lewis and Brønsted Acid Mediated Ring-Opening Reactions of Methylenecyclopropanes and Further Transformation of the Ring-Opened Products. *Curr. Org. Chem.* **2007**, 11, 1135-1153.
[46] Tsukada, N.; Shibuya, A.; Nakamura, I.; Yamamoto, Y. Ring Opening in the Palladium-Catalyzed Hydrocarbonation of Methylenecyclopropanes with Pronucleophiles. *J. Am. Chem. Soc.* **1997**, *119*, 34, 8123–8124.

new types of hydrofunctionalization reactions, together with the computational study of their mechanisms.

The hydrofunctionalization of ACPs can also occur with the opposite regioselectivity to afford 1,3-dienes as products. A recent representative example is the Pd(0)-catalyzed hydrophosphinylation of ACPs reported by Wang and coworkers. The reaction, which ultimately leads to chiral allylic phosphine oxides with high enantioselectivity (**Scheme 57**),[47] was proposed to proceed via a Markovnikov hydropalladation of the ACP to yield intermediate **I**, which undergoes subsequent β-carbo- and β-hydride eliminations to form the diene **III**. The final product would be obtained via a regioselective hydropalladation of the terminal alkene and an eventual C-P reductive elimination. The participation of diene intermediates was corroborated experimentally.

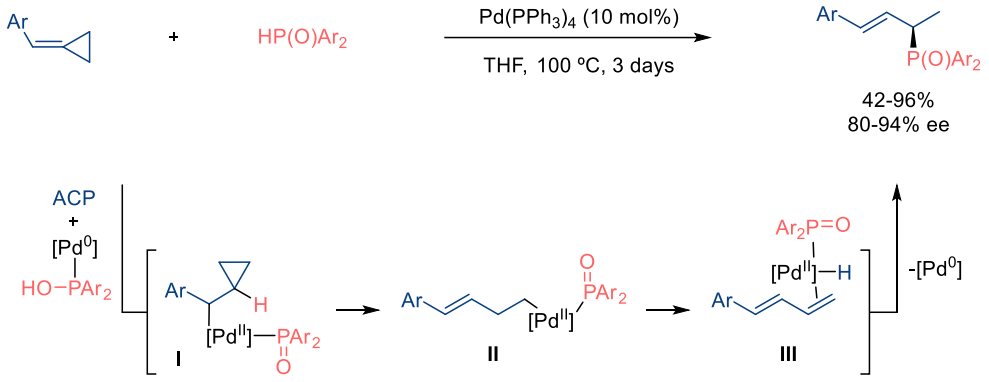

Scheme 57. Pd(0)-catalyzed hydrophosphinylation of ACPs.

Notably, the metalation of ACPs can also generate nucleophilic intermediates capable of reacting with electrophiles. A recent example, consisting of a Cu(I)-catalyzed borocarbonylation of arylidenecyclopropanes was described by Peng in 2022 (**Scheme 58**).[48] In this process, a cooper catalyst derived from IMesCuCl and BINAP, promotes the reaction between the ACP, B_2pin_2 and an acyl chloride to yield γ-boryl-γ,δ-unsaturated carbonyl compounds with complete regio- and diastereoselectivity. Mechanistically, the generated Cu–Bpin species **I**, undergoes regioselective migratory insertion into the ACP leading to intermediate **II**, and eventually to the homoallylic copper **III**, after a β-carboelimination. Then, this cuprate species reacts with the acyl chloride to afford the observed products.

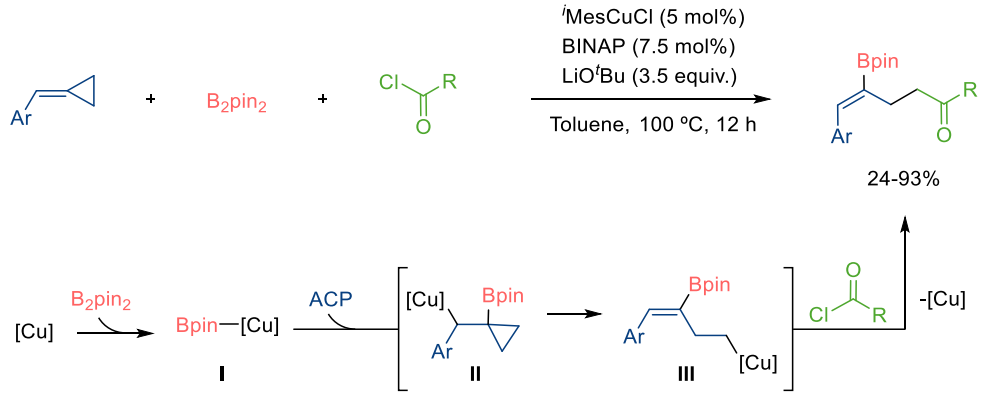

Scheme 58. Cu(I)-catalyzed borocarbonylation of ACPs.

[47] Zhou, J.; Meng, L.; Lin, S.; Cai, B.; Wang, J. Palladium-catalyzed enantio- and regioselective ring-opening hydrophosphinylation of methylenecyclopropanes. *Angew. Chem. Int. Ed.* **2023**, *62*, e202303727.

[48] Yang, L.-M.; Zeng, H.-H.; Liu, X.-L.; Ma, A.-J.; Peng, J.-B. Copper catalyzed borocarbonylation of benzylidenecyclopropanes through selective proximal C–C bond cleavage: synthesis of γ-boryl-γ,δ-unsaturated carbonyl compounds. *Chem. Sci.* **2022**, *13*, 7304-7309.

2. General Objectives

Considering the abovementioned precedents, the limitations of some of the methodologies, and the clear potential for further expanding the metal-catalyzed chemistry of ACPs, we set out the following general objectives for this PhD thesis:

- **Discovery of novel cycloaddition reactions of ACPs with hetero-unsaturated partners and development of a mechanistic rational using computational chemistry**
  Building on the promising experimental results obtained by Dr. Verdugo in ACP heterocycloadditions, we aimed to explore new aza-cycloadditions that lead to functionalized pyrrolidines.
  Computational studies on ACP cycloadditions, particularly those involving heteroatom unsaturated partners, have never been addressed. To fill this gap, DFT mechanistic studies will be performed, in order to elucidate the underlying principles of both oxa- and aza-cycloadditions, as well as the critical role of ancillary metal ligands.

- **Development of tandem cycloisomerization processes of ACPs promoted by metal catalysts**
  Given the potential and limited examples of ACP cycloisomerization reactions, we aim to explore new cycloisomerization processes involving ACPs, to access novel appealing cyclic scaffolds. We also aim to support this work with computational studies.

- **Uncover multicomponent cycloadditions of ACPs involving heteroatom partners**
  Despite the extensive number of metal-promoted cycloadditions involving ACPs, multicomponent reactions, particularly those with hetero-unsaturated partners, remain underexplored. Thus, we aim to uncover new multicomponent cycloaddition reactions with ACPs that lead to interesting medium-sized heterocycles.

3. Methodology

3.1 Materials and Methods

$Pd_2(dba)_3$ (98%) [51364-51-3] was obtained from Sigma-Aldrich. Phosphoramidite ligands are known and were synthesized according to the previously reported procedures.[29] All other ligands, precatalysts, solvents, reaction partners or reagents for the synthesis of precursors were purchased from Sigma-Aldrich, Acros Organics, Alfa Aesar, Fluorochem, TCI or Abcr. Dry solvents were obtained from a solvent purification system (Mbraun, SPS-5) or, eventually, freshly distilled under Ar from an appropriate drying agent before use (1,4-dioxane and toluene were distilled from Na / benzophenone; Et_3N and CH_2Cl_2, from CaH_2).

Reactions were monitored by TLC, GC-MS or NMR analysis of the crude mixture. TLCs were performed on silica gel plates and components were visualized by observation under UV light, or by treating the plates with either *p*-anisaldehyde, ninhydrin, potassium permanganate or cerium nitrate solutions, followed by heating. Regarding GC-MS, we employed the Agilent Tech. 6890N, Network GC System, equipped with the Agilent 190915-433 column and the Agilent 5973 Inert Mass Selective Detector, in Electron Impact or Chemical Ionization Mode (with Methane). NMR spectra of the crude reaction mixtures were recorded on a Varian 300 MHz spectrometer. 1,3,5-Trimethoxybenzene (TMB) was typically employed as an internal standard for quantitative analysis.

Reaction mixtures were stirred using Teflon-coated magnetic stirring bars. Reaction temperatures were maintained using Thermowatch-controlled silicone oil baths. Concentration refers to the removal of volatile solvents via distillation using a Büchi rotary evaporator followed by residual solvent removal under high vacuum. In reactions carried out in sealed tubes, the mixture must be at rt before sealing for safety reasons, to avoid overpressure at high temperatures.

3.2 General Protocol for Catalysis

To a purged Schlenk flask or sealed tube under an argon atmosphere, the palladium precatalyst, ligand and other solid reagents were added. Dry solvent was then introduced to the solid mixture, followed by the addition of liquid reagents via syringe. If necessary, the syringe was flushed with clean, dry solvent to ensure the complete transfer of the reagents.

With all the reaction components in the reaction flask, the mixture was heated to the corresponding temperature. Progress was typically monitored by thin-layer chromatography (TLC); however, gas chromatography-mass spectrometry (GC-MS) or nuclear magnetic resonance (NMR) spectroscopy were occasionally employed. To quench the reaction, the mixture was cooled to room temperature (20-25 °C) and filtered through a short pad of Celite® or Florisil®, using EtOAc for flushing. The crude product was concentrated under reduced pressure and purified by flash column chromatography to isolate the compound of interest.

3.3 Characterization of Compounds

All compounds were characterized using NMR (typically ^1H, ^{13}C and 2D experiments) and mass spectrometry (exact mass measurement).

^1H and ^{13}C NMR spectra were recorded in $CDCl_3$ at 300 MHz or 500MHz (Varian) for substrates and products. Carbon types were determined from DEPT or HSQC-NMR experiments. 2D-NMR experiments (COSY, NOESY, HMBC and HMQC) were conducted, in addition to standard 1D-NMR experiments. The stereochemistry of substrates, products and other compounds was confirmed by nOe experiments, measured at 300 MHz, and reported as follows: H (irradiated)→ H (observed), % enhancement. ^1H NMR spectral data are reported as follows: chemical shift (d ppm),

[29] Verdugo, F.; Villarino, L.; Durán, J.; Gulías, M.; Mascareñas, J. L.; López, F. Enantioselective Palladium-Catalyzed [3C + 2C] and [4C + 3C] Intramolecular Cycloadditions of Alkylidenecyclopropanes. *ACS Catal.* **2018**, *8*, 6100-6105.

multiplicity (s = singlet, d = doublet, t = triplet, q = quartet, quint = quintet, dd = double doublet, td = triple doublet, m = multiplet, br = broad), integration. Data for ^{13}C is reported in terms of chemical shift relative to the residual solvent peak. NMR spectra were analyzed using MestreNova© processing software.[49]

The exact mass of the compounds was acquired using electrospray ionization (ESI) and Atmospheric-pressure chemical ionization (APCI) and were recorded at the CACTUS facility of the USC. Single-crystal X-ray diffraction data were collected for some crystalline compounds using the CACTUS facility of the USC. Structures were solved and refined using standard methods to determine molecular geometry and confirm connectivity. Enantiomeric ratio (er) of the compounds was determined on an Agilent HPLC 1100 Series or a Jasco SFC 4000 series using commercially available chiral columns.

3.4 Computational Details

All DFT calculations have been carried out with the software Gaussian 09.[50] First, the geometries of all complexes and other compounds were optimized using the B3LYP hybrid functional[51], applying D3 version of Grimme's dispersion (GD3)[52] and ultrafine integration grids when specified, together with the standard 6-31G(d) basis set for C, H, B, N, O, F, P and S; and the LANL2DZ basis set for Pd, which includes the relativistic effective core potential (ECP) of Hay and Wadt and employs a split valence (double-zeta) basis set.[53] The possibility of different conformations was considered for all structures. All stationary points were characterized by a frequency analysis performed at the same level used in the geometry optimizations, from which thermal corrections were obtained at 298.15 K. Then, single-point (SP) calculations of the optimized geometries were carried out using different DFT functionals, M06[54] and/or B3LYP hybrid functional with D3 version of Grimme's dispersion (GD3),[51, 52] together with the 6-311++g(d,p) basis set for C, H, B, N, O, F, P and S; and the Stuttgart-Dresden (SDD) ECP for Pd.[55] In this case, a self-consistent reaction field (SCRF) method using the

[49] Willcott, M. R. MestRe Nova. *J. Am. Chem. Soc.* **2009**, *131*, 36, 13180.

[50] M. J. Frisch, G. W. Trucks, H. B. Schlegel, G. E. Scuseria, M. A. Robb, J. R. Cheeseman, G. Scalmani, V. Barone, B. Mennucci, G. A. Petersson, H. Nakatsuji, M. Caricato, X. Li, H. P. Hratchian, A. F. Izmaylov, J. Bloino, G. Zheng, J. L. Sonnenberg, M. Hada, M. Ehara, K. Toyota, R. Fukuda, J. Hasegawa, M. Ishida, T. Nakajima, Y. Honda, O. Kitao, H. Nakai, T. Vreven, J. A. Montgomery, Jr., J. E. Peralta, F. Ogliaro, M. Bearpark, J. J. Heyd, E. Brothers, K. N. Kudin, V. N. Staroverov, T. Keith, R. Kobayashi, J. Normand, K. Raghavachari, A. Rendell, J. C. Burant, S. S. Iyengar, J. Tomasi, M. Cossi, N. Rega, J. M. Millam, M. Klene, J. E. Knox, J. B. Cross, V. Bakken, C. Adamo, J. Jaramillo, R. Gomperts, R. E. Stratmann, O. Yazyev, A. J. Austin, R. Cammi, C. Pomelli, J. W. Ochterski, R. L. Martin, K. Morokuma, V. G. Zakrzewski, G. A. Voth, P. Salvador, J. J. Dannenberg, S. Dapprich, A. D. Daniels, O. Farkas, J. B. Foresman, J. V. Ortiz, J. Cioslowski and D. J. Fox, GAUSSIAN 09 (Revision C.01), Gaussian, Inc., Wallingford CT, **2010**.

[51] a) Becke, A. D. Density-functional exchange-energy approximation with correct asymptotic behaviour. *Phys. Rev. A* **1988**, *38*, 3098. b) Lee, C.; Yang W.; Parr, R. G. Development of the Colle-Salvetti correlation-energy formula into a functional of the electron density. *Phys. Rev. B* **1988**, *37*, 785. c) Becke, A. D. Density-functional thermochemistry. III. The role of exact exchange. *J. Chem. Phys.* **1993**, *98*, 5648. d) Stephens, P. J.; Devlin, F. J.; Chabalowski, C. F.; Frisch, M. J. Ab Initio Calculation of Vibrational Absorption and Circular Dichroism Spectra Using Density Functional Force Fields. *J. Phys. Chem.* **1994**, *98*, 11623. e) Kohn, W.; Becke, A. D.; Parr, R. G. Density Functional Theory of Electronic Structure. *J. Phys. Chem.* **1996**, *100*, 12974.

[52] Grimme, S.; Antony, J.; Ehrlich, S.; Krieg, H. A consistent and accurate ab initio parametrization of density functional dispersion correction (DFT-D) for the 94 elements H-Pu. *J. Chem. Phys.* **2010**, *132*, 154104.

[53] a) Hay, P. J.; Wadt, W. R. Ab initio effective core potentials for molecular calculations. Potentials for the transition metal atoms Sc to Hg. *J. Chem. Phys.* **1985**, *82*, 270. b) Hay, P. J.; Wadt, W. R. Ab initio effective core potentials for molecular calculations. Potentials for main group elements Na to Bi. *J. Chem. Phys.* **1985**, *82*, 284. c) Hay, P. J.; Wadt, W. R. Ab initio effective core potentials for molecular calculations. Potentials for K to Au including the outermost core orbitals. *J. Chem. Phys.* **1985**, *82*, 299.

[54] Zhao, Y.; Truhlar, D. G. The M06 suite of density functionals for main group thermochemistry, thermochemical kinetics, noncovalent interactions, excited states, and transition elements: two new functionals and systematic testing of four M06-class functionals and 12 other functionals. *Theor. Chem. Acc.* **2007**, *120*, 215–241.

[55] Dolg, M.; Wedig, U.; Stoll, H.; Preuss, H. Energy-adjusted ab initio pseudopotentials for the first row transition elements. *J. Chem. Phys.* **1987**, *86*, 866.

SMD model[56] has been employed in order to obtain the solvation-corrected relative free energies, using corresponding solvent.

Gibbs free energies (ΔG) were used for the discussion on the relative stabilities of the considered structures unless otherwise stated. Free energies were calculated using the gas phase standard state concentration (1 atm = 1/24.5 M), by the combination of the thermal correction calculated during geometry optimization and the SP energies. In general, the lowest energy conformer for each calculated stationary point was considered in the discussion of calculated selectivity. Connection between all transition states with their corresponding minima were confirmed performing Intrinsic Reaction Coordinate (IRC) studies.[57]

Natural Bond Orbital (NBO) analysis was conducted using the NBO 7.0 program[58] and Gaussian 9 as an interface. The outcomes were visualized using Multiwfn 3.8.[59]

Regarding the naming of stationary points in the energetic profiles, minima will be generally designated as "**I**" (intermediate), followed by the corresponding number; while transition states will be labeled as "**TS**" (transition state), followed by the numbers of the connected minima. For clarity and convenience, the numbering of stationary points will restart in each chapter.

[56] Marenich, A. V.; Cramer, C. J.; Truhlar, D. G. Universal Solvation Model Based on Solute Electron Density and on a Continuum Model of the Solvent Defined by the Bulk Dielectric Constant and Atomic Surface Tensions. *J. Phys. Chem. B.* **2009**, *113*, 6378.

[57] a) Hratchian, H. P.; Schlegel, H. B. Accurate reaction paths using a Hessian-based predictor–corrector integrator. J. Chem. Phys. **2004**, *120*, 9918–9924.; b) Hratchian, H. P.; Schlegel, H. B. Using Hessian updating to increase the efficiency of a Hessian-based predictor-corrector reaction path following method. *J. Chem. Theory Comput.* **2005**, *1*, 61–69.

[58] Glendening, E. D.; Badenhoop, J. K.; Reed, A. E.; Carpenter, J. E.; Bohmann, J. A.; Morales, C. M.; Karafiloglou, P.; Landis, C. R.; Weinhold, F. Theoretical Chemistry Institute, University of Wisconsin, Madison, **2018**.

[59] a) Lu, T.; Chen, F. Multiwfn: A multifunctional wavefunction analyzer. *J. Comput. Chem.* **2012**, *33*, 580–592.; b) Lu, T. A comprehensive electron wavefunction analysis toolbox for chemists, Multiwfn. *J. Chem. Phys.* **2024**, *161*, 082503.

4. Results and Discussion

4.1 Pd(0)-Catalyzed (3+2) Cycloadditions between ACPs and Imines

Part of the contents of this section have been accepted for publication in:

Rodiño, R.[a]; Verdugo, F.[a]; Mascareñas, J. L.[a]; López, F.[a, b] Palladium-Catalyzed [3+2] Cycloadditions of Alkylidenecyclopropanes to Imines: A Direct Approach to Pyrrolidine Scaffolds *ChemistryEurope* **2025**. Just accepted.

Authors' affiliations:

[a] Centro Singular de Investigación en Química Biolóxica e Materiais Moleculares (CiQUS) and Departamento de Química Orgánica, Universidade de Santiago de Compostela 15782 Santiago de Compostela (Spain).

[b] Misión Biológica de Galicia Consejo Superior de Investigaciones Científicas (CSIC) 36080 Pontevedra (Spain).

4.1.1 Precedents

4.1.1.1 Relevance of pyrrolidine scaffolds

Nitrogen-containing heterocycles are of immense importance in medicinal chemistry, due to their presence in the structural core of a wide range of biologically active molecules.[60] Among these, five-membered heterocycles, particularly saturated systems like pyrrolidines, are highly relevant in drug discovery. These structures offer a higher structural diversity compared to more common aromatic planar compounds, such as pyrroles. In addition, the possibility of exploring the three-dimensional space around their core due to the sp^3 nature of the carbons opens many possibilities in chemistry and medicine (**Figure 9**).[61]

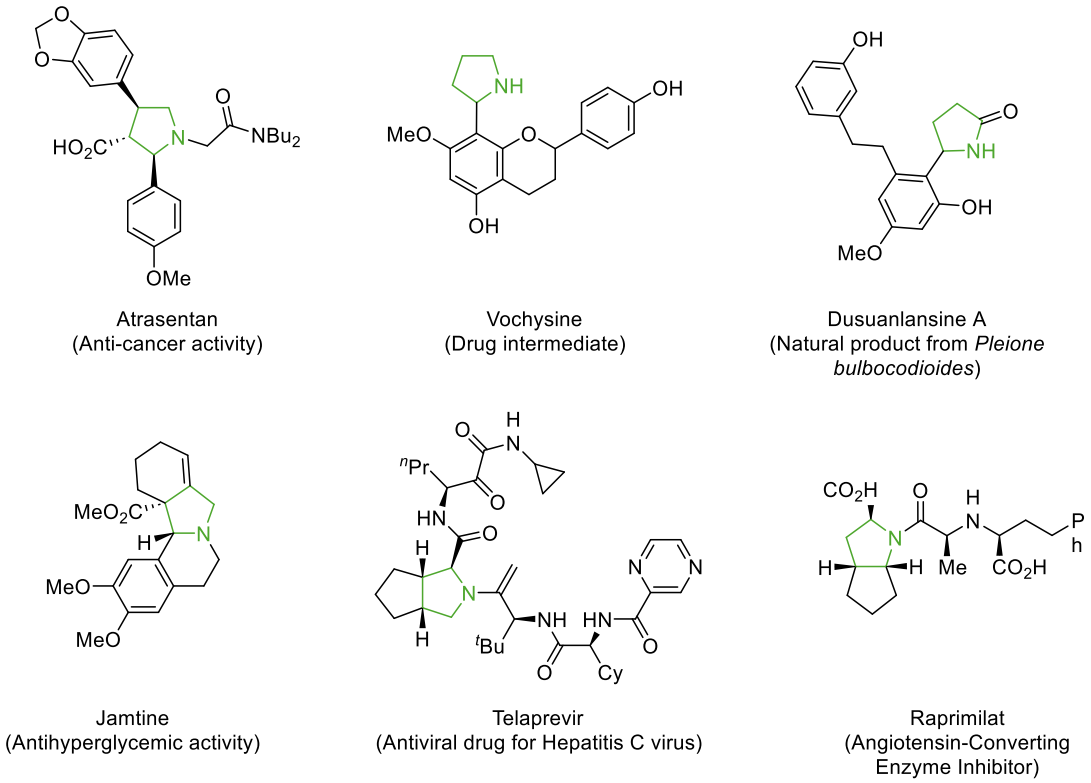

Figure 9. Biologically relevant molecules containing functionalized pyrrolidine scaffolds.

Despite the number of synthetic strategies already available for constructing these scaffolds, many of them involve multistep processes. Therefore, the development of efficient, versatile, direct and practical catalytic approaches to these scaffolds is of primary relevance. In this context, transition-metal catalyzed cycloadditions are particularly valuable because of their ability to create cyclic structures from accessible acyclic precursors, often with high regio- and stereocontrol. The following section summarizes the most relevant precedents in this theme.[62]

[60] a) Pozharskii, A. F.; Soldatenkov, A. T.; Katritzky, A. R. *Heterocycles in Life and Society: An Introduction to Heterocyclic Chemistry, Biochemistry and Applications;* John Wiley & Sons: **2011**.; b) Blakemore, D. C.; Castro, L.; Churcher, I.; Rees, D. C.; Thomas, A. W.; Wilson, D. M.; Wood, A. Organic Synthesis Provides Opportunities to Transform Drug Discovery. *Nat. Chem.* **2018**, *10*, 4, 383-394.; c) Vitaku, E.; Smith, D. T.; Njardarson, J. T. Analysis of the Structural Diversity, Substitution Patterns, and Frequency of Nitrogen Heterocycles among U.S. FDA Approved Pharmaceuticals. *J. Med. Chem.* **2014**, *57*, 10257–10274.

[61] Li Petri, G.; Raimondi, M. V.; Spanò, V.; Holl, R.; Barraja, P.; Montalbano, A. Pyrrolidine in Drug Discovery: A Versatile Scaffold for Novel Biologically Active Compounds. *Top Curr Chem (Z)* **2021**, *379*, 34.

[62] Nakamura, I.; Yamamoto, Y. Transition-Metal-Catalyzed Reactions in Heterocyclic Synthesis. *Chem. Rev.* **2004**, *104*, 5, 2127–2198.

4.1.1.2 TMC azacycloadditions of ACPs and related three-carbon precursors

Palladium-trimethylenemethane (TMM) species

Pd-trimethyenemethane (TMM) intermediates have been proposed to participate as 3C units in a broad variety of (3+n) cycloadditions. Among them, the generation of pyrrolidine systems through their annulation with different imines stands out as one of the most remarkable processes. The initial examples were described by Trost in 1993, using a TMM precursor , *N*-tosylimines as partners and a catalyst based on $Pd(OAc)_2$ and $P(O^iPr)_3$ (**Scheme 59**).[63] The Pd-TMM species **I**, undergoes a 1, 2-addition to the imine, generating the zwitterionic species **II** which evolves to the corresponding pyrrolidine by an intramolecular interception.

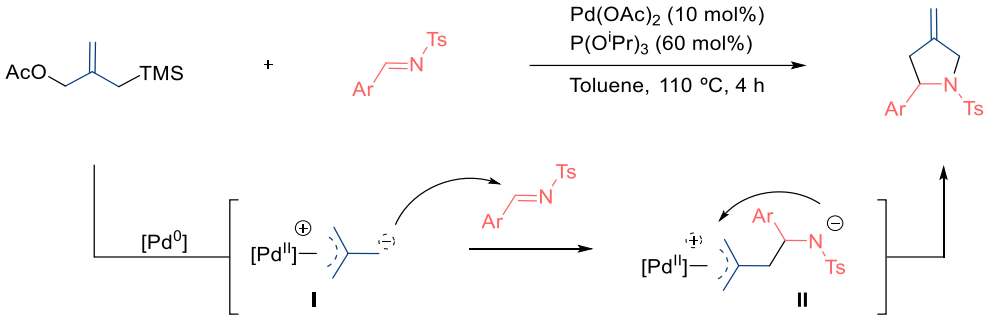

Scheme 59. Pd-catalyzed intermolecular (3+2) between TMM precursors and imines.

In 2007, the same group developed an asymmetric protocol by using the catalyst derived from $CpPd(\eta_3\text{-}C_3H_5)$ and the phosphoramidite ligand **(*R,R,S*)-L3** (**Scheme 60**).[64] Remarkably, both *N*-Boc or *N*-Tosyl imines were suitable partners and chiral pyrrolidines with up to two stereocenters could be generated with excellent diastereo- and enantioselectivities. Moreover, few *N*-Ts ketimines participate in the process, leading to pyrrolidines bearing α-quaternary chiral centers.

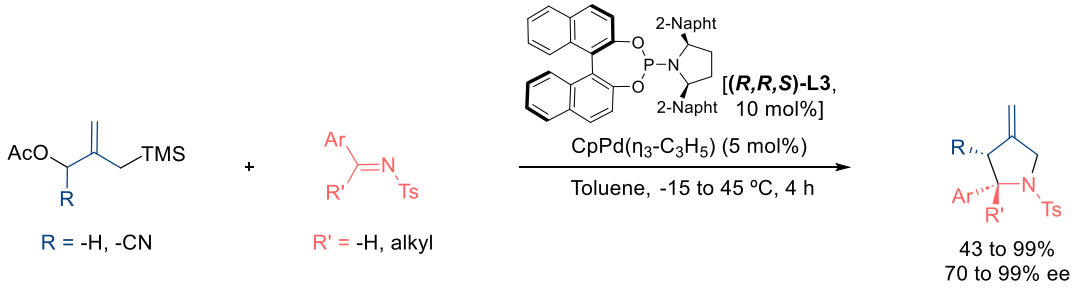

Scheme 60. Asymmetric Pd-catalyzed intermolecular cycloaddition between TMM precursors and imines.

In subsequent years, Trost reported different Pd(0) catalysts derived from $CpPd(\eta^3\text{-}C_3H_5)$ and diamidophosphite ligands, that promote the cycloaddition between aldimines and more sophisticated TMM precursors, bearing alkyl or electron-withdrawing groups, leading to highly substituted pyrrolidines with excellent selectivities (**Scheme 61a**).[65] Other groups further contributed to the field with related examples. Thus, Kim and coworkers reported a Pd-catalyzed (3+2) cycloaddition of

[63] Trost, B.M.; Marrs, C. M. A [3+2] cycloaddition and [4+3] cycloaddition approach to N-heterocycles via palladium-catalyzed TMM reactions with imines. *J. Am. Chem. Soc.* **1993**, *115*, 15, 6636-6645.

[64] a) Trost, B.M.; Silverman, S. M.; Stambuli, J.P. Palladium-Catalyzed Asymmetric [3+2] Cycloaddition of Trimethylenemethane with Imines. *J. Am. Chem. Soc.* **2007**, *129*, 41, 12398–12399.; b) Trost, B.M.; Silverman, S. M. Enantioselective Construction of Pyrrolidines by Palladium-Catalyzed Asymmetric [3 + 2] Cycloaddition of Trimethylenemethane with Imines. *J. Am. Chem. Soc.* **2012**, *134*, 10, 4941–4954.

[65] a) Trost, B.M.; Lam, T. M.; Herbage, M. A. Regio- and Enantioselective Synthesis of Pyrrolidines Bearing a Quaternary Center by Palladium-Catalyzed Asymmetric [3 + 2] Cycloaddition of Trimethylenemethanes. *J. Am. Chem. Soc.* **2013**, *135*, 7, 2459–2461.; b) Trost, B.M.; Wang, Y.; Hung, C.I. Use of α-trifluoromethyl carbanions for palladium-catalysed asymmetric cycloadditions. *Nat. Chem.* **2020**, *12*, 294–301.

TMM precursors and cyclic sulfamate-derived imines, using a Pd(0)-phosphoramidite catalyst (**Scheme 61b**).[66]

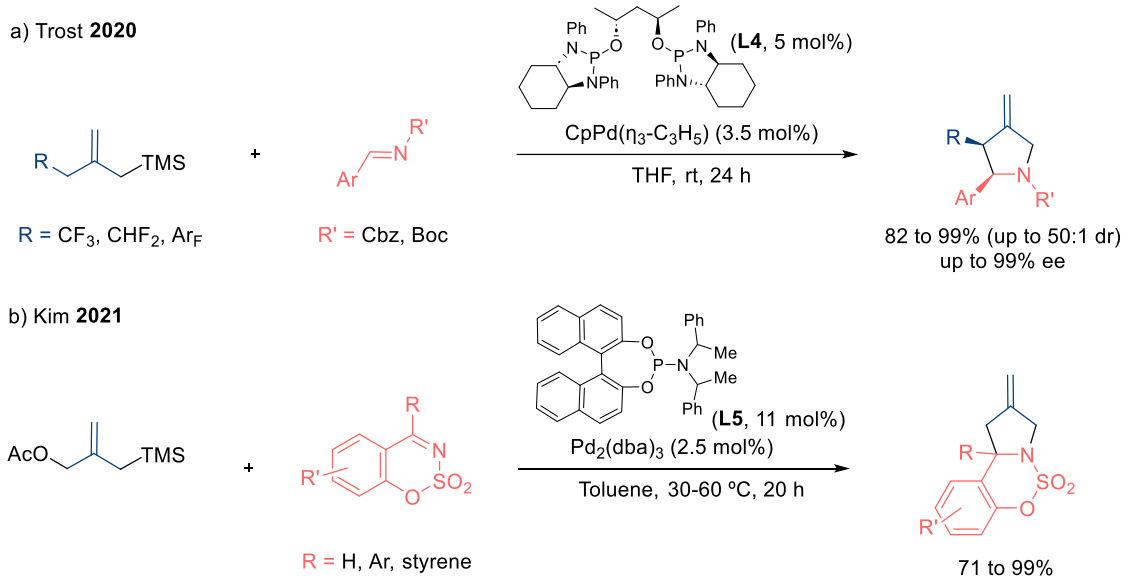

Scheme 61. Pd(0)-catalyzed (3+2) cycloadditions between TMM precursors and imine partners.

Vinyl cyclopropanes

Vinyl cyclopropanes (VCPs) have been used as 3C synthons in several TMC cycloadditions leading to pyrrolidine scaffolds. In 2018, Vitale developed a diastereoselective (3+2) cycloaddition between VCPs and various *N*-sulfonyl aldimines, such as tosylimines and sulfamate-derived imines. This reaction employed a catalyst generated *in situ* from $Pd_2(dba)_3{\cdot}CHCl_3$ and dppe, providing access to functionalized pyrrolidines with excellent yields and diastereoselectivities (**Scheme 62**).[67a] The reaction begins with the insertion of the Pd(0) catalyst into the cyclopropyl ring to form the palladacyclobutane **I**, which undergoes a migratory insertion of the imine towards the π-allyl Pd species **II**. Finally, an intramolecular nucleophilic attack delivers the product.

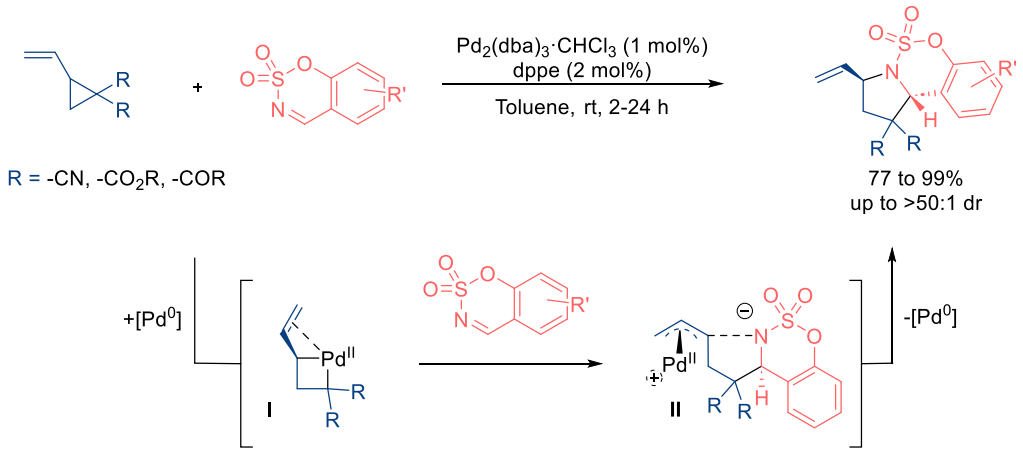

Scheme 62. Pd(0)-catalyzed (3+2) cycloaddition between VCPs and *N*-sulfonyl aldimines.

[66] Choi, S.; Kim, K. D.; Park, J.; Xuan, Z.; Kim, J. H. Pd-catalyzed [3 + 2] cycloaddition of cyclic ketimines and trimethylenemethanes toward *N*-fused pyrrolidines bearing a quaternary carbon. *RSC Adv.* **2021**, *12*, 785–789.

[67] a) Ling, J.; Laugeois, M.; Ratovelomanana-Vidal, V.; Vitale, M. R. Palladium(0)-Catalyzed Diastereoselective (3+2) Cycloadditions of Vinylcyclopropanes with Sulfonyl-Activated Imines. *Synlett* **2018**, *29*, 2288–2292.; b) Wang, Q.; Wang, C.; Shi, W.; Xiao, Y.; Guo, H. Pd-Catalyzed diastereoselective [3 + 2] cycloaddition of vinylcyclopropanes with sulfamate-derived cyclic imines. *Org. Biomol. Chem.* **2018**, *16*, 4881–4887.

One year later, Liu reported an asymmetric (3 + 2) cycloaddition of imines and VCPs bearing a geminal diester group (**Scheme 63**).[68] The catalyst derived from $Pd(dba)_2$ and the chiral phosphoramidite **(*S*)-L6** can promote the annulation with isatin derivatives, whereas the use of **(*S,R,R*)-L7** as ligand enabled the reaction with *N*-sulfonyl aldimines. The transformation generally provides good yields and high enantioselectivities, but modest diastereoselectivities.

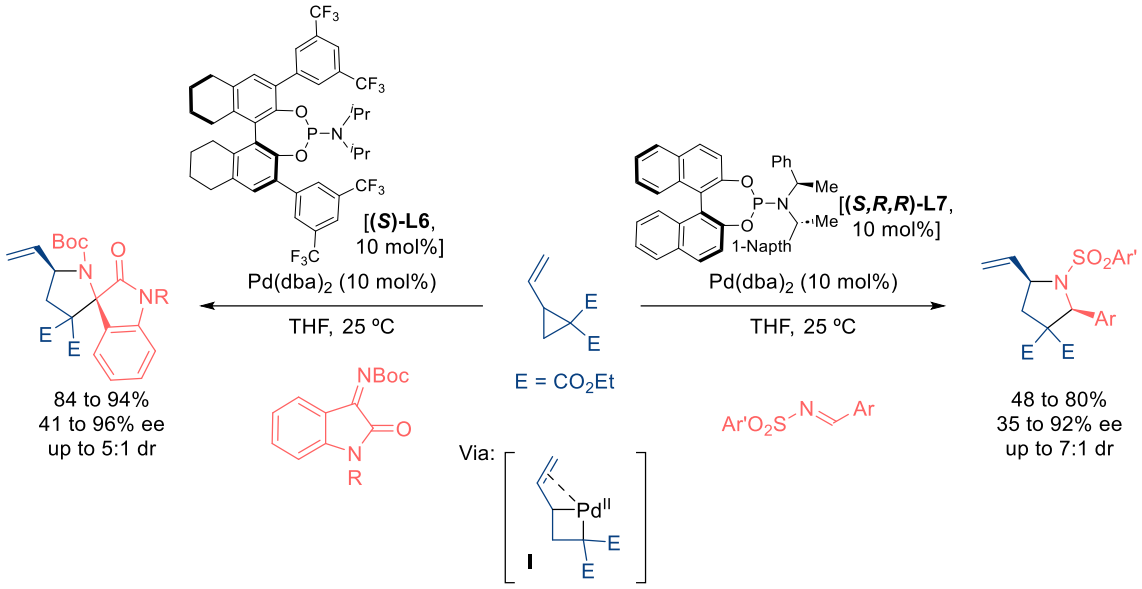

Scheme 63. Asymmetric Pd(0)-catalyzed (3+2) cycloaddition between VCPs and imines.

Vinyl aziridines

Aziridines can be used as nitrogen-containing three-atom partners in TMC cycloadditions to build 5-membered azacycles. In particular, Zhang developed in 2016 a Rh(I)-catalyzed stereoespecific (3+2) cycloaddition between allenes and enantioenriched vinyl aziridines (**Scheme 64**).[69] Curiously, the reaction with monosubstituted allenamides resulted in 3-methylene-pyrrolidines (**Scheme 64**, *left*), while the use of 1,3-disubstituted allenes led to 2-methylene-pyrrolidines (**Scheme 64**, *right*). Both processes afforded chiral pyrrolidines with very good yields and enantioselectivities, but the need of enantioenriched substrates is an important drawback of the method. Mechanistically, the authors proposed an oxidative addition of the aziridine C–N bond to the rhodium catalyst, generating the rhodaazetidine intermediate **I**. A migratory insertion, either through the Rh–C bond (*left side*, allenamides) or the Rh–N bond (*right side*, disubstituted allenes), would lead to the rhodacyclic intermediates **II** and **III**, which eventually deliver the pyrrolidine products after a reductive elimination.

[68] Huang, X.-B.; Li, X.-J.; Li, T.-T.; Chen, B.; Chu, W.-D.; He, L.; Liu, Q.-Z. Palladium-Catalyzed Highly Enantioselective Cycloaddition of Vinyl Cyclopropanes with Imines. *Org. Lett.* **2019**, *21*, 6, 1713-1716.

[69] Lin, T.; Zhu, C.; Zhang, P.; Wang, Y.; Wu, H.; Feng, J.; Zhang, J. Regiodivergent Intermolecular [3+2] Cycloadditions of Vinyl Aziridines and Allenes: Stereospecific Synthesis of Chiral Pyrrolidines. *Angew. Chem. Int. Ed.* **2016**, *55*, 10844–10848.

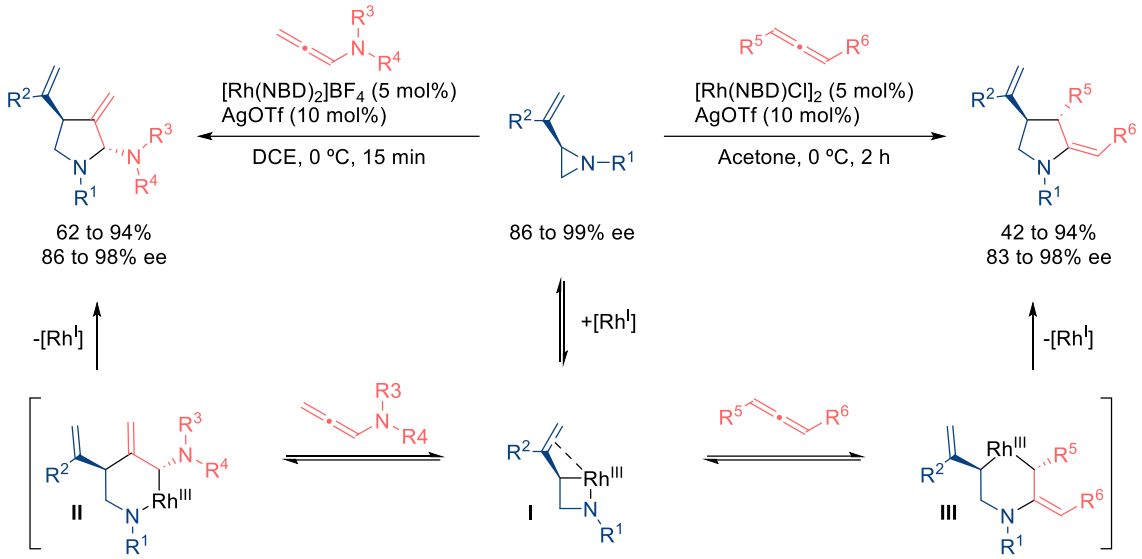

Scheme 64. Rh(I)-catalyzed (3+2) cycloaddition between vinyl aziridines and allenes.

In 2018, Campagne reported a Pd(0) catalyzed (3+2) cycloaddition between vinyl aziridines and sulfamate-derived cyclic imines to give cyclic imidazolidines in good yields and excellent diastereoselectivities (**Scheme 65**, *left*).[70] The reaction was proposed to involve a C-N oxidative addition, followed by a migratory insertion of the imine to generate the π-allyl Pd complex **I.** An eventual interception of this electrophilic species delivers the cycloadduct. In 2018, the same group developed an asymmetric variant using a Pd catalyst comprising the chiral phosphoramidite **(*R*)-L8**, and AcOH as additive (**Scheme 65**, *right).*[71] Both diastereo- and enantioselectivities were highly dependent on the vinyl aziridine substitution.

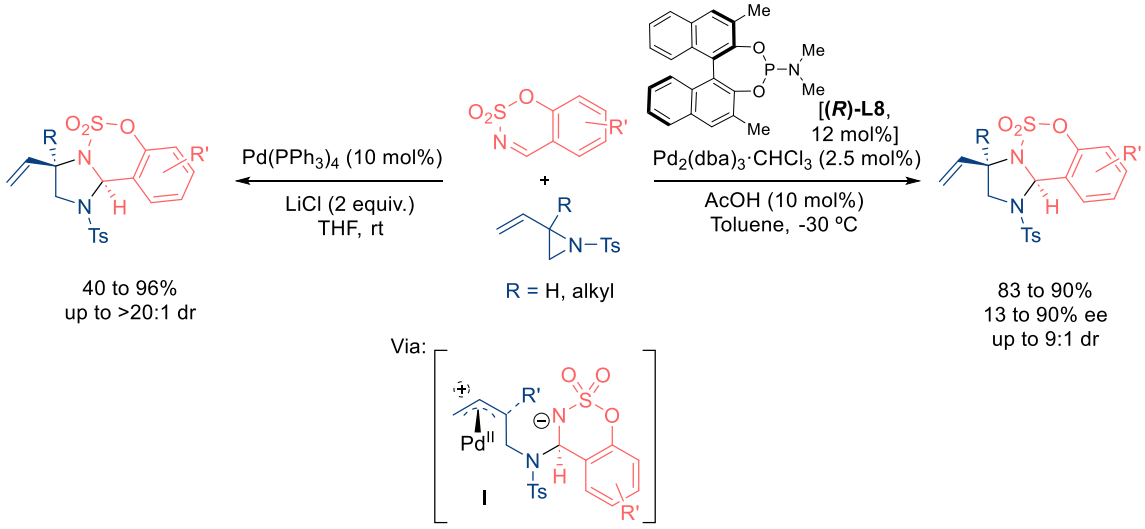

Scheme 65. Pd(0)-catalyzed (3+2) cycloaddition between vinyl aziridines and cyclic derived-sulfamate imines.

Alkylidenecyclopropanes

While most TMC cycloadditions of ACPs so far described lead to carbocycles, ACPs can also participate in TMC cycloadditions to form five-membered heterocyclic adducts. A relevant precedent to this PhD work, briefly mentioned in the *Introduction* (see **Scheme 49**, page 46), is the formal (3+2)

[70] Spielmann, K.; Lee, A. v. d.; de Figueiredo, R. M.; Campagne, J. Diastereoselective Palladium-Catalyzed (3 + 2)-Cycloadditions from Cyclic Imines and Vinyl Aziridines. *Org. Lett.* **2018**, *20*, 1444–1447.

[71] Spielmann, K.; Tosi, E.; Lebrun, A.; Niel, G.; van der Lee, A.; de Figueiredo, R. M.; Campagne, J. Vinyl-aziridines and cyclopropanes in Pd-catalyzed (3+2)-cycloaddition reactions with cyclic *N*-sulfonyl imines. *Tetrahedron* **2018**, *74*, 6497–6511.

cycloaddition between ACPs and *N*-tosyl imines, reported by Yamamoto in 2001 (**Scheme 66**).[37] Using $Pd(PPh_3)_4$ and triphenylphosphine oxide as catalyst, the reaction affords functionalized pyrrolidine scaffolds in good yields. However, the method holds important limitations, such as the need of high temperatures, the use of excess of the ACP, and it has a very limited scope, being restricted to aromatic aldimines and alkyl-disubstituted ACPs. Furthermore, when the ACP precursors contain different substituents, the process exhibits a complete lack of diastereoselectivity. The authors proposed that the reaction proceeds through an initial insertion of the metal at the distal C-C bond of the ACP to give palladacyclobutane **I**. This intermediate undergoes a metalloene rearrangement with the imine, forming the π-allylic intermediate **II**, which is followed by a reductive elimination to give the corresponding heterocycle. However, no mechanistic studies support the proposed pathway, so alternative routes might also be plausible.

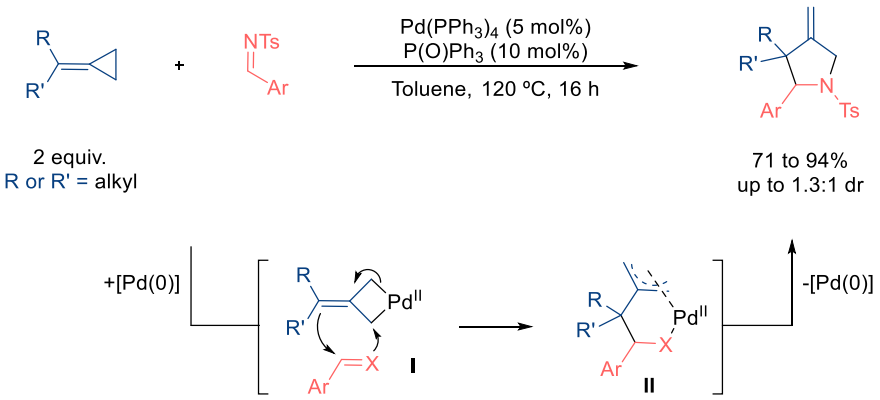

Scheme 66. Pd(0)-Catalyzed intermolecular (3+2) Cycloadditions of ACPs and tosyl aldimines.

In 2004, the same group reported a Pd(0)-catalyzed (3+2) cycloaddition involving disubstituted ACPs with 1,2-diazines (**Scheme 67**).[72] Interestingly, the transformation afforded fused pyrroles, instead of the expected *exo*-methylene cyclic scaffolds. However, the reaction offers a limited scope and requires harsh conditions. The authors suggested an initial insertion of the Pd at the distal C–C bond of the cyclopropane, followed by coordination with the diazine (**I**). Then, a 1,2-addition to the C=N bond would lead to intermediate **II**, which evolves through a reductive elimination to **III**. A final oxidation and aromatization step would yield the 5-azaindolizines, although specific details of the process were not provided.

[37] Oh, B. H.; Nakamura, I.; Saito, S.; and Yamamoto, Y. Palladium-catalyzed [3+2] cycloaddition of alkylidenecyclopropanes with imines. *Tetrahedron Lett.* **2001**, *42*, 6203-6205.

[72] Yamamoto, Y.; Nakamura, I.; Siriwardana, A. I. Synthesis of 5-Azaindolizine Derivatives by the Palladium-Catalyzed Intermolecular Formal [3+2] Cycloaddition of Alkylidenecyclopropanes with 1,2-Diazines. *J. Org. Chem.* **2004**, *69*, 9, 3202–3204.

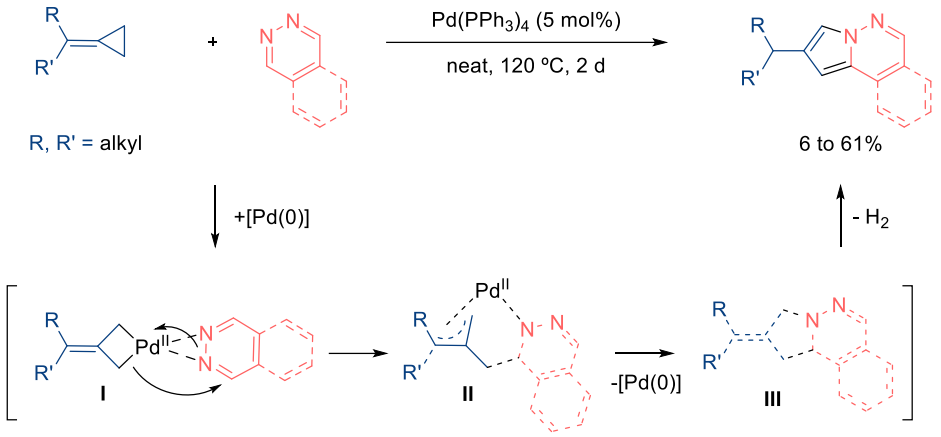

Scheme 67. Pd(0)-catalyzed intermolecular (3+2) cycloadditions of ACPs and 1,2-diazines.

4.1.1.3 Other annulations of ACPs leading to pyrrolidine scaffolds

In addition to TMC cycloadditions with ACPs, other annulation methods that proceed in a stepwise manner can provide five-membered azacycles. An interesting example was reported by Shi in 2006,[73] who used a cationic gold catalyst to promote a formal (4+1) annulation between ACPs and primary tosyl amines (**Scheme 68**). The suggested mechanism starts with the activation of the olefin precursor by the gold catalyst and the subsequent nucleophilic attack of the amine to form intermediate **II**. After protodemetallation, the complex **III** undergoes an intramolecular cyclization to reach **IV**, which protodeaurates to give the pyrrolidine product.

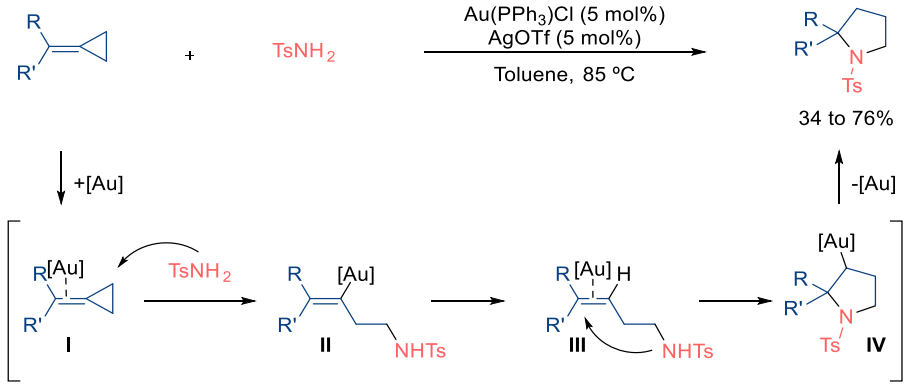

Scheme 68. Au(I)-catalyzed intermolecular (4+1) annulation between ACPs and tosylamides.

In 2011, Wu reported a Cu(I)-catalyzed annulation of alkyne-bearing ACPs and azides, which affords fused indolines (**Scheme 69**).[74] The reaction proceeds under mild conditions, although the scope is very narrow. Mechanistically, a copper-catalyzed click annulation to give species **I** was proposed as first step. Then, the release of N_2 leads to ketimine **II**, which undergoes a 6π-cyclization and an eventual rearrangement, to deliver the indoline. Notably, the metal is only involved in the click transformation and does not participate in the subsequent steps.

[73] Shi, M.; Liu, L.-P.; Tang, J. Gold(I)-Catalyzed Domino Ring-Opening Ring-Closing Hydroamination of Methylenecyclopropanes (MCPs) with Sulfonamides: Facile Preparation of Pyrrolidine Derivatives. *Org. Lett.* **2006**, *8*, 18, 4043–4046.

[74] a) Li, S.; Luo, Y.; Wu, J. An Efficient Approach to Fused Indolines via a Copper(I)-Catalyzed Reaction of Sulfonyl Azide with 2-Ethynylaryl Methylenecyclopropane, *Org. Lett.* **2011**, *13*, 3190–3193.; b) Li, S.; Li, Z.; Wu, J. Synthesis of Benzoindolines via a Copper-Catalyzed Reaction of 1-Bromoethynyl-2-(cyclopropylidenemethyl)arenes with *N*-Allylsulfonamide, *Adv. Synth. Catal.* **2012**, *354*, 3087– 3094.

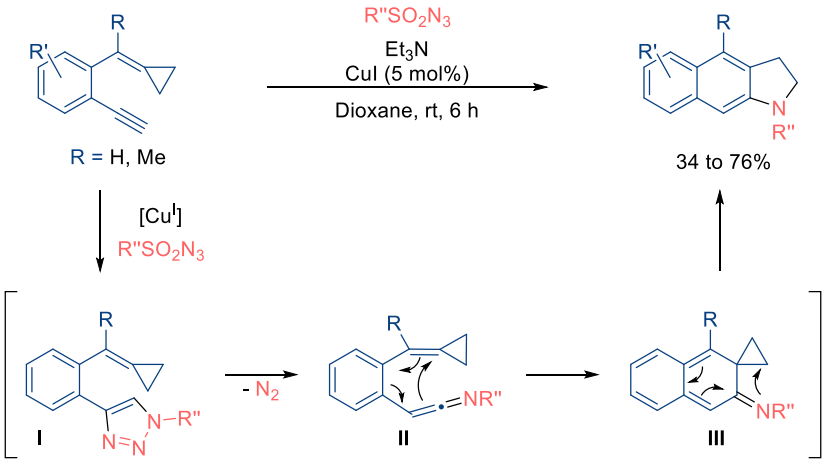

Scheme 69. Cu(I)-catalyzed (3+2) annulation between ACPs and alkynes.

4.1.1.4 Precedents from our group

As mentioned in the *Introduction* (see **Scheme 52**, page 47), our group explored the viability of intramolecular (3+2) cycloadditions of ACPs bearing a tethered oxime ether.

Therefore, Dr. Verdugo discovered that the catalyst generated from $Pd_2(dba)_3$ and the phosphoramidite **L9** afforded the bicyclic pyrrolidine **2a** in 30% yield, along with dienic products **3a** and **4a**, in 9% and 35% yield, respectively (toluene, at 110 ºC for 4h, entry 1, **Table 1**). Notably, the use of the bulky phosphite **L1** provided the cycloadduct **2a** in 60% yield, together with the diene **3a** in 18% yield (entry 2). In addition, the Pd-catalysts featuring RuPhos or ^{t}BuXPhos ligands also afforded the azacycle **2a** in good yields (54% and 65% yield, respectively), together with varying amounts of diene side products **3a** and **4a** (entries 3 and 4).

The influence of the oxime stereochemistry was assessed with the *O*-benzyl ether precursor **1b**, using $Pd_2(dba)_3$/**L1** as catalyst. When using ***E*-1b**, the cycloadduct **2b** was obtained in 62% yield (entry 5). In contrast, the reaction with the *Z* precursor (***Z*-1b**) was less efficient (37% of **2b**, entry 6).

Table 1. Selected screening conditions for the intramolecular Pd-catalyzed (3+2) cycloaddition of ACPs and imine partners.[a]

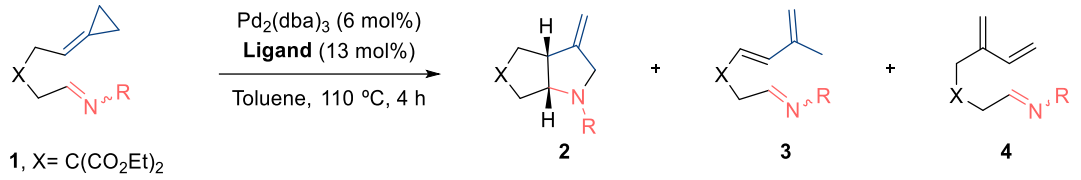

Entry	R	Ligand	**2** (%)	**3** (%)	**4** (%)
1	*E*-OMe, **1a**	**L9**	30	9	35
2	*E*-OMe, **1a**	**L1**	60	18	-
3	*E*-OMe, **1a**	*t*BuXPhos	54	9	10
4	*E*-OMe, **1a**	RuPhos	65	-	35
5	*E*-OBn, **1b**	**L1**	62	28	-
6[b]	*Z*-OBn, **1b**	**L1**	37	9	-

[a] Conditions: **1**, $Pd_2(dba)_3$ (6 mol %), ligand (13 mol %), dry toluene (0.05 M), Ar atmosphere, 110 °C. Conversion of **1** >99%. [b] 75%Conv. of **1**.

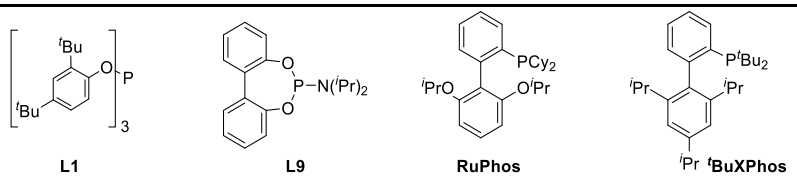

The formation of dienes of type **3** can be explained as shown in **Scheme 70**. The initially formed palladacyclobutane **I** would isomerize to species **II**, which evolves via β-hydride elimination to the palladium hydride complex **III**. Finally, a reductive elimination yields the diene **3**. This type of competitive pathway has been previously described in related ACP cycloadditions;[75] however, to the best of our knowledge, the formation of diene side products of type **4** had never been reported in any type of metal-catalyzed reactions of ACPs.

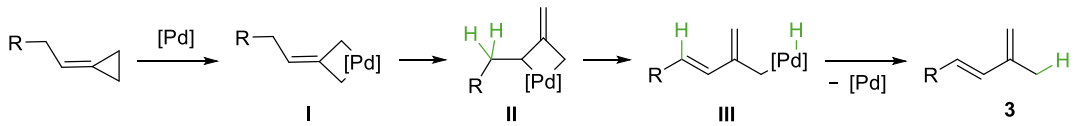

Scheme 70. Formation of diene side products of type **3**.

In addition, Dr. Verdugo preliminary explored an asymmetric version of the above cycloaddition. Using the model substrate **1b**, he found out that the catalyst generated from $Pd_2(dba)_3$ and phosphoramidite ***(S,R,R)*-L2**, provided good results in toluene, using H_2O (5 equiv.) as additive. Thus, *E*-**1b** afforded the cycloadduct **2b** in 85% yield, with an excellent enantioselective ratio (94:6), whereas its *Z*-isomer (*Z*-**1b**) led to **2b** in 60% yield, but with a lower 70:30 er (**Scheme 71**).

[75] a) Gulías, M.; García, R.; Delgado, A.; Castedo, L.; Mascareñas, J. L. Palladium-Catalyzed [3 + 2] Intramolecular Cycloaddition of Alk-5-enylidenecyclopropanes. *J. Am. Chem. Soc.* **2006**, *128*, 2, 384–385.; b) Milner, P. J.; Maimone, T. J.; Su, M.; Chen, J.; Mueller, P.; Buchwald, S. L. Investigating the dearomative rearrangement of biaryl phosphine-ligated Pd(II) complexes. *J. Am. Chem. Soc.* **2012**, *134*, 19922– 19934.

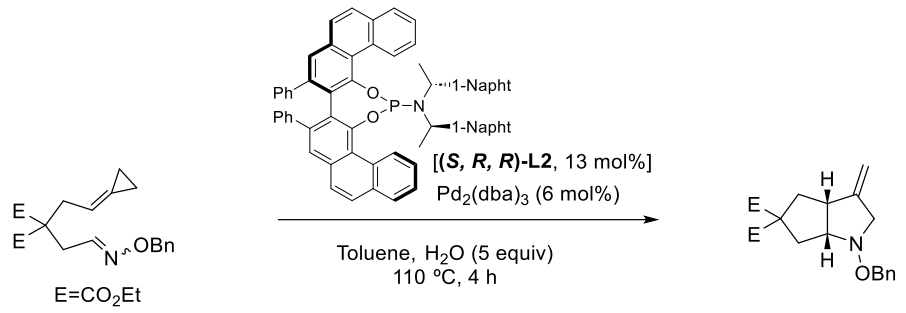

E-**1b**: **2b**, 85% er 94:6

Z-**1b**: **2b**, 60% er 70:30

Scheme 71. Asymmetric conditions for the intramolecular (3+2) cycloaddition of ACPs and oxime ethers.

4.1.2 Objectives

Based on these preliminary results, the first goal of the chapter was to further **develop the Pd-catalyzed intramolecular cycloaddition between ACPs and oxime derivatives**.

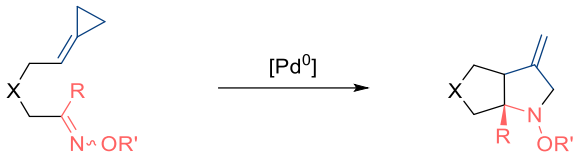

Scheme 72. Pd(0)-catalyzed intramolecular (3+2) cycloaddition of ACPs tethered to oxime ether partners.

Additionally, we aimed to uncover an **intermolecular variant of these (3+2) azacycloadditions** that could show a higher scope and potential than that previously reported by Yamamoto (see **Scheme 66** and **Scheme 67**, page 70).

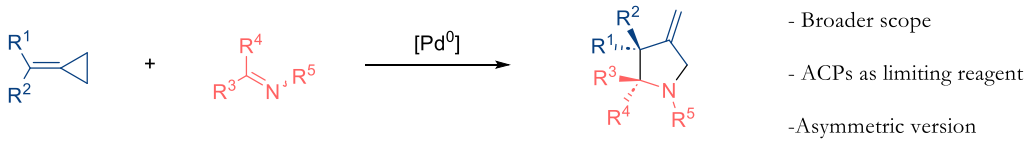

Scheme 73. Goals of Pd(0)-catalyzed intermolecular (3+2) cycloaddition between ACPs and imine partners.

Finally, considering the lack of mechanistic studies on hetero-cycloaddition reactions of ACPs, we also aimed to carry out a DFT computational analysis to **gain mechanistic insights**.

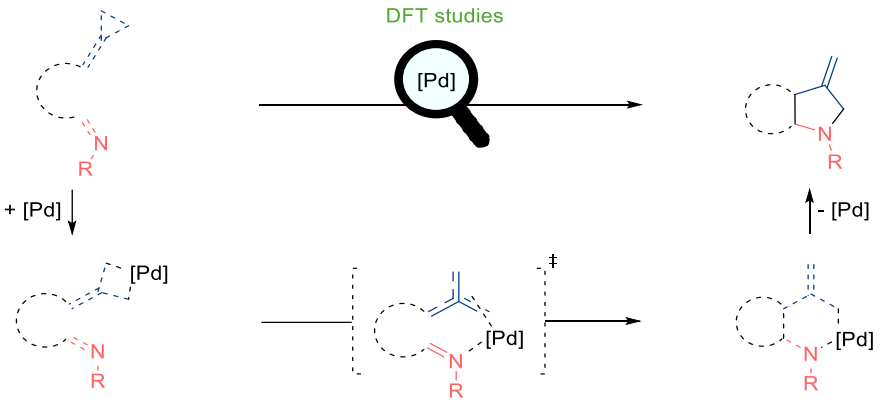

Scheme 74. Mechanistic outline for the Pd(0)-catalyzed (3+2) azacycloadditions.

4.1.3 Intramolecular (3+2) Aza-Cycloadditions

Part of this research was carried out in collaboration with Dr. Verdugo.

First of all, different cycloaddition precursors of type **1** were prepared. Substrates **1a** and **1b** were synthesized following a protocol consisting of an initial Pd-catalyzed allylic substitution between the diester derivative **5** and vinyl tosylate **6**, subsequent acidic treatment to generate the aldehyde **7a**, and a final treatment with the corresponding *O*-alkylhydroxylamine hydrochloride, under basic conditions (**Scheme 75**). Thus, **1a** and **1b** were obtained in good yields and *E:Z* ratios of 2:1. The synthesis of the *O*-Bn aldoxime **1c**, bearing a longer connecting tether between the ACP and the oxime ether, was performed using the same strategy.

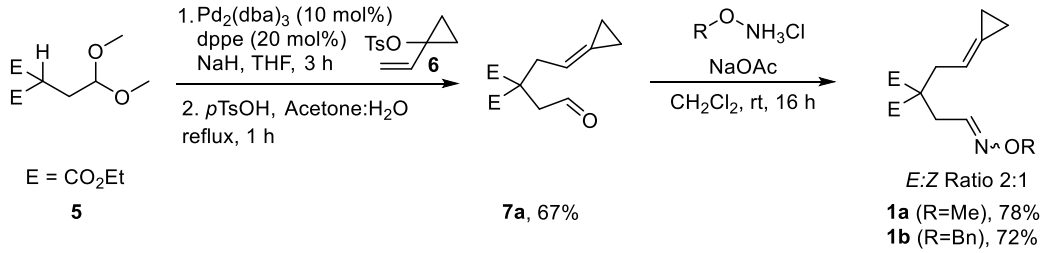

Scheme 75. Synthesis of the aldoxime precursors **1a** and **1b**.

We also prepared the ketoxime ether **1d**, using the ketone **8a** as nucleophile for the first Tsuji-Trost reaction with tosylate **6**. The condensation of intermediate **9a** with the *O*-methylhydroxylaminium salt gave the precursor **1d** as a pure *E* isomer.

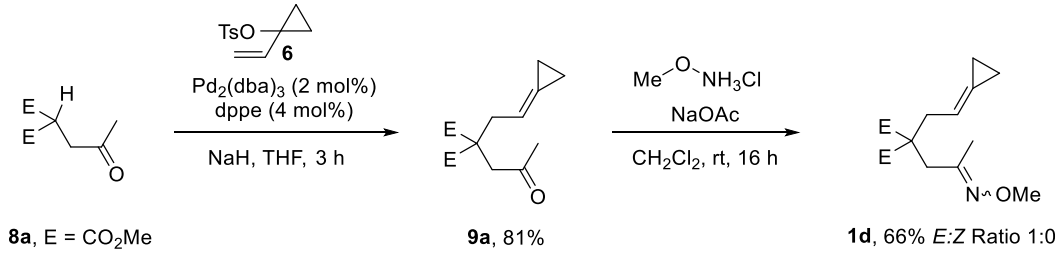

Scheme 76. Synthesis of the ketoxime precursor **1d**.

Precursor **1e** was prepared from ethyleneglycol and tosylate **6** through a related approach, including the oxidation of the intermediate alcohol **10** under Swern conditions (**Scheme 77**). The resulting highly volatile aldehyde was used without further purification in the condensation with *O*-methylhydroxylamine hydrochloride to afford **1e** in 57% yield (*E:Z* ratio 2:1).

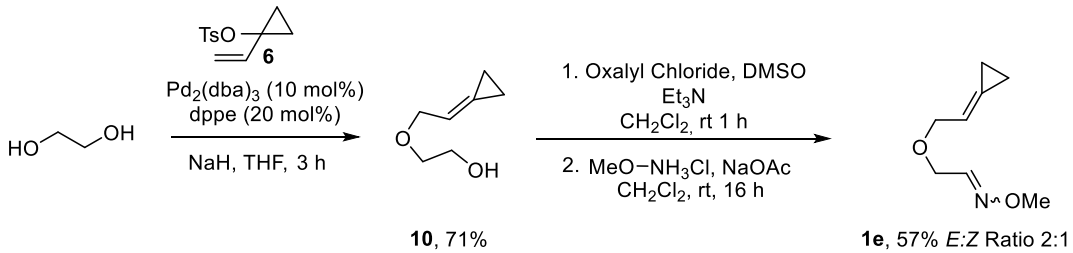

Scheme 77. Synthesis of the oxime precursor **1e**.

The synthesis of a nitrogen-based analogue (**1f**) was carried out from NHTsBoc (**Scheme 78**). After an initial Tsuji-Trost reaction with tosylate **6**, the Boc group was thermally removed to give tosylamine **11**. Next, a second alkylation with 2-bromo-1,1-dimethoxyethane led to the expected acetal, which was hydrolized to give the aldehyde **7b**. A condensation with *O*-methylhydroxylamine hydrochloride yielded the oxime precursor **1f** in 71% yield (*E:Z* ratio 1.3:1).

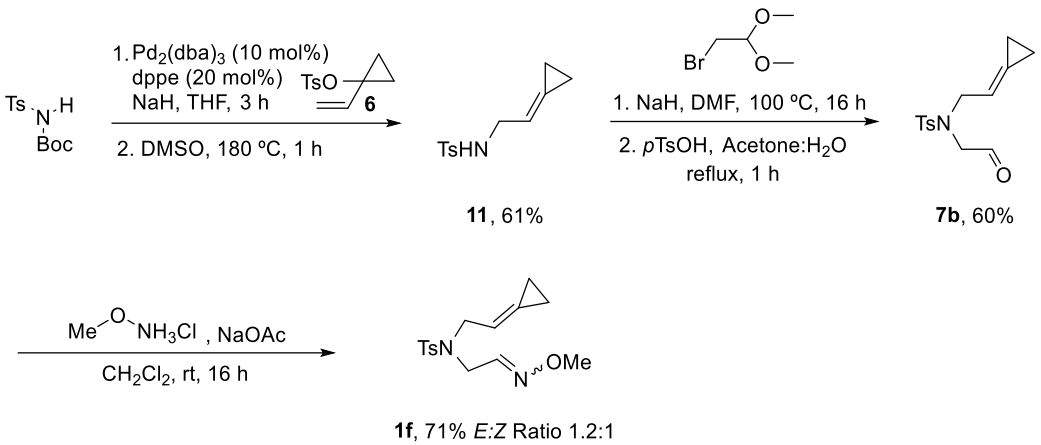

Scheme 78. Synthesis of the oxime precursor **1f**.

4.1.3.1 Pd-catalyzed cycloadditions

With the substrates in hand, we explored the cycloadditions using the catalysts generated from $Pd_2(dba)_3$ and either phosphite **L1** or RuPhos, in toluene under heating (**Table 2**).

The treatment of the ***E*-1a** with $Pd_2(dba)_3$/**L1** at 90 ºC, afforded the bicyclic product **2a** in 47% yield, alongside diene **3a** in 26% yield (entry 1). Employing RuPhos as ligand, instead **L1**, the cyclic compound **2a** was obtained in 65% yield, together with the diene **4a** in 35% yield (reaction temperature 110 ºC, entry 2). Curiously, the best result was obtained when using the *E*:*Z* ratio directly obtained from the condensation (*E*:*Z* = 2:1). Heating this mixture at 90 ºC with the Pd(0) catalyst made from **L1**, the fused pyrrolidine **2a** was isolated in 70% yield, together with the diene **3a** in 28% yield (entry 3).

In addition, the treatment of the *O*-benzyl analogue **1b** (*E*:*Z* = 2:1) with $Pd_2(dba)_3$/**L1** at 90 ºC, provided the bicyclic system **2b** in 69% yield, together with the diene **3b** in 20% yield (entry 4).

Then, precursor **1c**, bearing a longer connecting tether between the reactants, was tested using the Pd(0)-catalyst derived from **L1**, at 110 ºC. The reaction proceeded with high conversion, but we only detected small amounts of diene **3c** (12%, entry 5). Employing RuPhos as ligand, we observed full conversion, but only the diene **4c** was obtained (entry 6). Similarly, reactions of the ketoxime ether **1d** only afforded the dienes **3d** [6%, with Pd(0)-**L1**, entry 7] and **4d** [60%, Pd(0)-RuPhos, entry 8].

On the other hand, reactions of substrate **1e**, containing an oxygenated tether, led to high consumption of the precursors but neither cycloadducts nor diene products were detected (entries 7 and 8). A similar result was observed when the precursor **1f**, which features a nitrogenated tether, was tested with $Pd_2(dba)_3$/**L1** (entry 9), whereas the use of RuPhos as ligand led to the diene **4f** in 35% yield (entry 10).

All these reactions were also explored in different solvents and at lower temperatures but, unfortunately, these conditions generally provided partial conversions of starting materials and only diene products of type **3** and/or **4**. Therefore, we can conclude that the scope of the method is limited to a very narrow range of precursors.

Table 2. Scope of the intramolecular (3+2) cycloaddition using **L1** and RuPhos.[a]

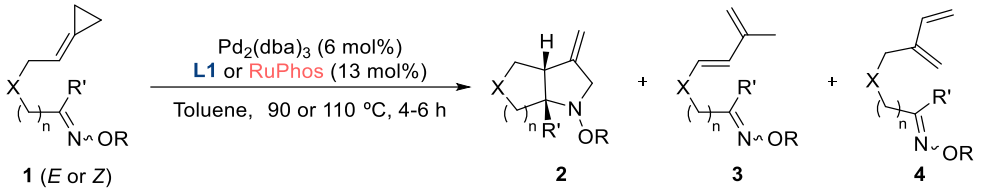

Entry	Substrate	T (°C)	Ligand	Conv. (%)	2 / 3 / 4 (%)
1	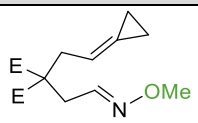	90	**L1**	100	**2a**, 47 / **3a**, 26
2	***E*-1a**	110	RuPhos	100	**2a**, 65 / **4a**, 35
3	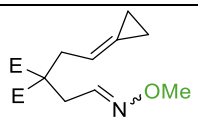	90	**L1**	100	**2a**, 70 / **3a**, 28
	(*E*:*Z* 2:1)-**1a**				
4	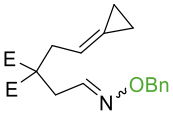	90	**L1**	100	**2b**, 69 / **3b**, 20
	(*E*:*Z* 2:1)-**1b**				
5	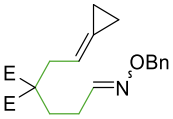	110	**L1**	75	**3c**, 12
6		110	RuPhos	95	**4c**, 95
	(*E*:*Z* 1.1:1)-**1c**				
7	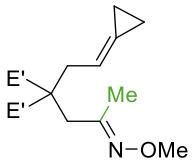	110	**L1**	76	**3d**, 6
8		110	RuPhos	100	**4d**, 60
	(*E*:*Z* 1:0)-**1d**				
9	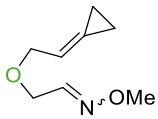	110	**L1**	84	-
10		110	RuPhos	92	-
	(*E*:*Z* 1.1:1)-**1e**				
11	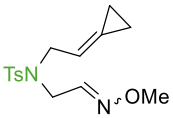	110	**L1**	100	-
12		110	RuPhos	100	**4f**, 35
	(*E*:*Z* 1.1:1)-**1f**				

[a] Conditions: **1**, $Pd_2(dba)_3$ (6 mol %), **L** (13 mol %), dry toluene (0.05 M), Ar atmosphere, T. E = CO_2Et, E' = CO_2Me.

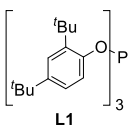

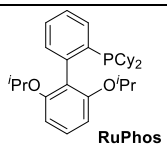

Despite this poor scope, we decided to test asymmetric variants. Therefore we tested the reaction of precursors ***E*-1** using $Pd_2(dba)_3$ (6 mol%) and **(*S,R,R*)-L2** (13 mol%) in refluxing toluene, in presence of 5 equivalents of water as additive (**Table 4**).[76] As mentioned in the *Precedents*, treatment of the *O*-benzyl substrate **1b** under these conditions led to **2b** in 85% yield, and 88% ee (entry 1). Gratifyingly, the use of the *O*-methyl analogue ***E*-1a**, under identical catalytic conditions, provided the product **2a** in 90% yield, and 94% ee (entry 2).

However, we also encountered problems when trying to expand the scope of the asymmetric version. Using $Pd_2(dba)_3$/**(*S,R,R*)-L2** as catalyst, substrates with longer tethers, such as ***E*-1c**; the ketoxime ***E*-1d**, or precursors like ***E*-1e** or ***E*-1f**, which bear alternative connecting chains, resulted in low conversions, and the desired cycloadducts were not observed (entries 3-6). Moreover, reactions conducted at higher temperatures (130 or 150 ºC) only led to a higher consumption of the precursors (**1**), but none of the expected cycloadducts were formed.

Table 3. Scope of the asymmetric (3+2)-cycloaddition between ACPs tethered to oxime ethers.[a]

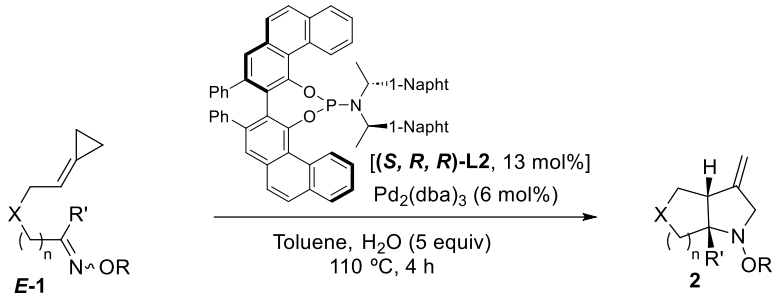

Entry	Substrate		Conv. (%)	2 (%)	ee (%)
1	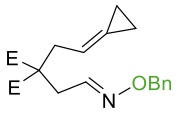	***E*-1b**	100	85	88
2	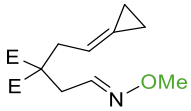	***E*-1a**	100	90	94
3	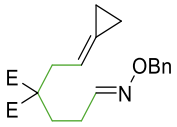	***E*-1c**	20	0	-
4	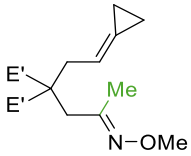	***E*-1d**	10	0	-
5	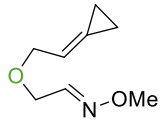	***E*-1e**	15	0	-
6	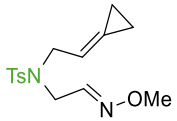	***E*-1f**	25	0	-

[a] Conditions: **1**, $Pd_2(dba)_3$ (6 mol %), **(*S,R,R*)-L2** (13 mol %), dry toluene (0.05 M), Ar atmosphere, 110 ºC. E = CO_2Et, E' = CO_2Me.

[76] The asymmetric scope was mainly explored by Dr. Verdugo.

These results confirm the problems for performing the desired cycloadditions, likely because of the difficulties associated to the migratory insertion of the oxime ether, as in most of the cases we observed dienic by-products as a result of the exclusive reactivity of the ACP moiety, or decomposition of the precursor. To favor the migratory insertion step and promote the formation of cycloadducts of type **2**, we considered the use of Lewis and Brønsted acid additives, to activate the oxime partner. Additionally, we also explored the use of oxime ethers bearing electron-withdrawing groups.

Screening of acidic additives

These assays were carried out with methyl oxime **1a**, using as catalytic system $Pd_2(dba)_3$/**L1**, and heating the mixtures at 80 ºC. Unfortunately, the formation of the desired cycloadduct was not observed. Apparently, the additives deactivated the Pd catalyst, resulting in varying degrees of **1a** consumption (**Table 4**).

Table 4. Screening of Lewis and Brønsted acids using $Pd_2(dba)_3$ and **L1**.[a]

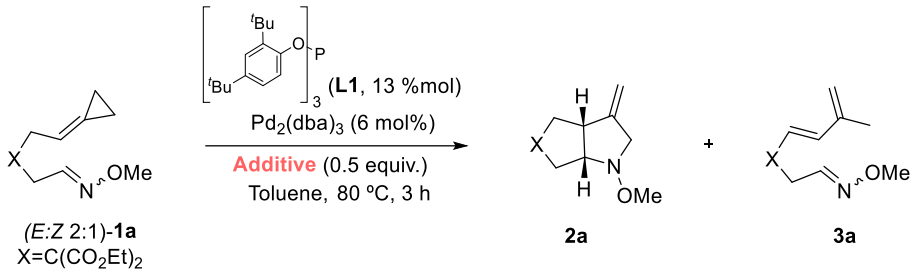

Entry	Additive	Conv. (%)	2a (%)	3a (%)
1	-	75	50	20
2	$NiClO_4 \cdot 6H_2O$	8	-	-
3	$Al(Me)_3$	100	10	-
4	$Cu(OTf)_2$	10	-	-
5	$InCl_3$	15	-	-
6	$Sc(OTf)_3$	26	-	-
7	$B(OMe)_3$	15	-	10
8	Thiourea	45	-	-
9	*p*-TsOH·H_2O	20	<5	<5
10	(*R*)-CPA	12	-	12

[a] Conditions: **1a**, $Pd_2(dba)_3$ (6 mol %), **L1** (13 mol %), dry toluene (0.05 M), Ar atmosphere, 80 °C.

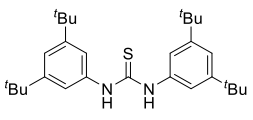

Thiourea

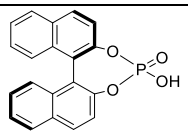

(*R*)-CPA

In addition, the reaction of the oxime ether **1a** was studied using the catalyst generated from $Pd_2(dba)_3$ and RuPhos, at 80 ºC, in presence of various additives (**Table 5**). Disappointedly, we again observed low consumption of **1a** and only small amounts of cycloadduct **2a**.

Table 5. Additives screening using $Pd_2(dba)_3$ and RuPhos.[a]

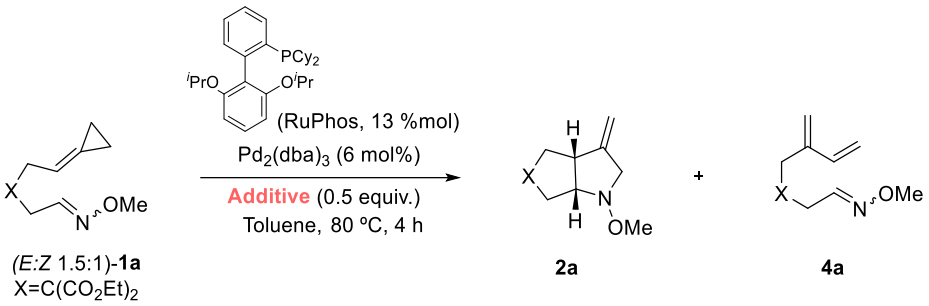

Entry	Additive	Conv. 1a (%)	2a (%)	4a (%)
1	-	26	<5	<5
2	$FeCl_3$	32	-	-
3	DMF	13	<5	<5
4	$NiClO_4 \cdot 6H_2O$	12	-	-
5	DMA	20	<5	<5
6	$Cu(OTf)_2$	22	-	-
7	$InCl_3$	38	-	-
8	$B(OMe)_3$	11	10	-

[a] Conditions: **1a**, $Pd_2(dba)_3$ (6 mol %), RuPhos (13 mol %), dry toluene (0.05 M), Ar atmosphere, 80 °C.

Use of electron deficient oxime ethers

To check whether we could increase the reactivity of the oxime partner, we prepared the acetyl oxime **1g**, and the oxime ethers **1h** and **1i**, bearing a trifluoromethylethyl group ($-CH_2CF_3$). For the synthesis of **1h** and **1i**, we first prepared the *O*-(2,2,2-trifluoroethyl)hydroxylamine hydrochloride **12** (**Scheme 79**).

After the triflation of trifluoroethanol, a reaction with *N*-hydroxyphtalimide provided **13** in 66% yield. A subsequent deprotection with hydrazine, followed by treatment with HCl, afforded the *O*-alkyl hydroxylammonium chloride **12** in 82% yield.

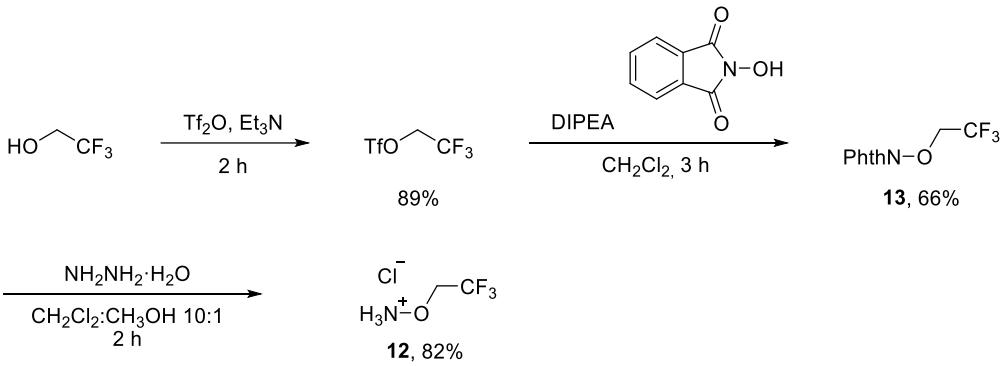

Scheme 79. Synthesis of the electron deficient hydroxylammonium salt **12**.

The oxime precursors **1g**, **1h** and **1i** were prepared following the procedure previously used for the synthesis of **1a** and **1f** (see **Schemes 76** and **78**, page 76 and 77), by condensing the corresponding aldehydes with the hydroxylammonium salts (**Scheme 80**).

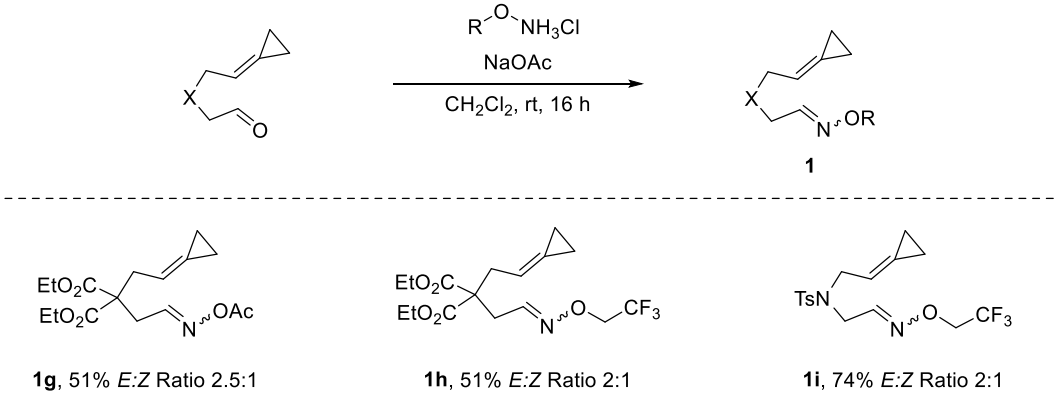

Scheme 80. Synthesis of oxime ether precursors **1g-i**.

The reaction of the *O*-acetyl oxime precursor **1g** with the catalyst generated from $Pd_2(dba)_3$ and **L1,** in toluene at 110 ºC, unexpectedly delivered the nitrile derivative **14g**, as only observed product (20% yield). Its formation can be explained by assuming a favored insertion of the palladium(0) catalyst into the oxime N-O bond, and a subsequent β-hydride elimination to deliver **14g**. Related insertions of low valent metal catalysts in the N-O bonds of oxime esters have been previously reported.[77]

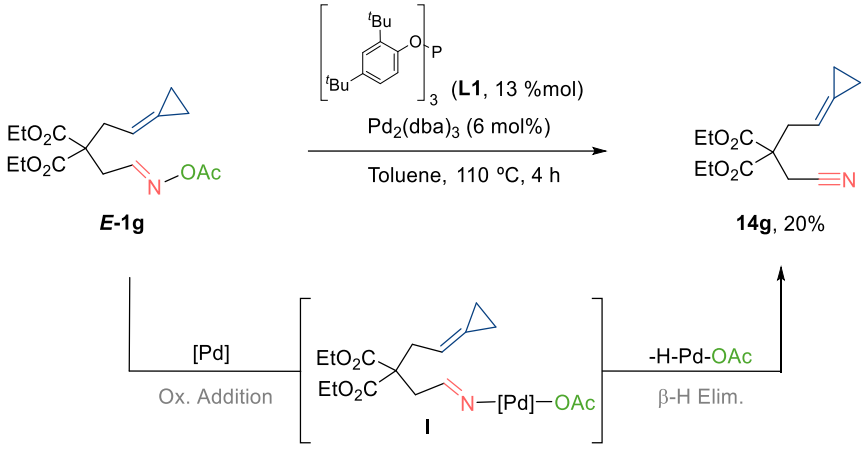

Scheme 81. Pd-catalyzed intramolecular cycloaddition using acetyl oxime ***E*-1g** as substrate.

Next, we evaluated the efficiency of the *O*-CH_2CF_3 oxime ether **1h** (**Table 6**). The reaction of an equimolar *E:Z* mixture of this precursor with the Pd catalyst generated from $Pd_2(dba)_3$ and **L1**, in toluene at 90 ºC, afforded the desired cycloadduct **2h** in 16% yield, together with the side-diene product **3h** (33% yield, entry 1, **Table 6**). Curiously, when using exclusively the *E*-isomer (***E*-1h**) at 90 ºC, the reaction was fully selective towards the diene **3h**, which was isolated in 59% yield (entry 2). Carrying out the same reaction at a higher temperature (110 ºC), increased the yield of **3h**, while the cycloadduct **2h** was formed in a low 10% yield (entry 3). In contrast, using RuPhos as ligand, at 110 ºC, product **2h** was obtained in a moderate 48% yield (entry 4).

[77] a) Kukushkin, V. Y.; Pombeiro, A. J. L. Oxime and oximate metal complexes: unconventional synthesis and reactivity. *Coord. Chem. Rev.* **1999**, *181*, 147.; b) Tan, Y.; Hartwig, J. F. Palladium-Catalyzed Amination of Aromatic C−H Bonds with Oxime Esters. *J. Am. Chem. Soc.* **2010**, *132*, 3676- 3677.; c) Shimbayashi, T.; Okamoto, K.; Ohe, K. C–H Activation Induced by Oxidative Addition of N–O Bonds in Oxime Esters: Formation of Rhodacycles and Cycloaddition with Alkynes. *Organometallics* **2016**, *35*, 2026-2031.

Table 6. Results from precursor **1h**.[a]

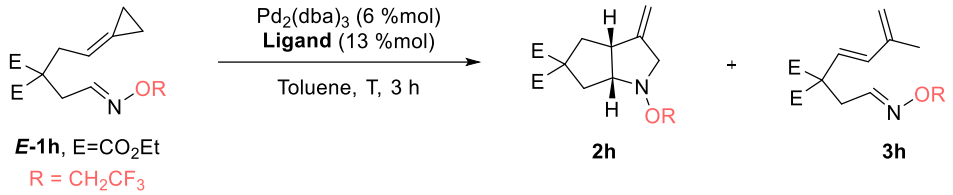

Entry	**1h**, *E:Z* ratio	**T** (ºC)	Ligand	**2h** (%)	**3h** (%)
1[b]	1.1:1	90	**L1**	16	33
2	1:0	90	**L1**	0	59
3	1:0	110	**L1**	10	74
4	1:0	110	RuPhos	48	0

[a] Conditions: **1h**, $Pd_2(dba)_3$ (6 mol %), ligand (13 mol %), dry toluene (0.05 M), Ar atmosphere at indicated temperature. Conversion of **1h** >99%. [b]%Conv. **1h** = 85

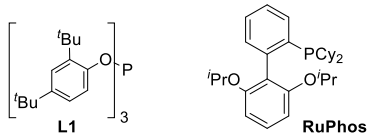

Finally, oxime precursor **1h** was evaluated under asymmetric conditions (**Scheme 82**). Using ***E*-1h**, the catalyst generated from $Pd_2(dba)_3$ and **(*S,R,R*)-L2**, led to the cycloadduct **2h** in 53% yield. In contrast, when using ***Z*-1h**, the yield decreased to 11%. The enantiomeric excesses could not be determined due to the impossibility of separating enantiomers via HPLC or SFC (with chiral columns).

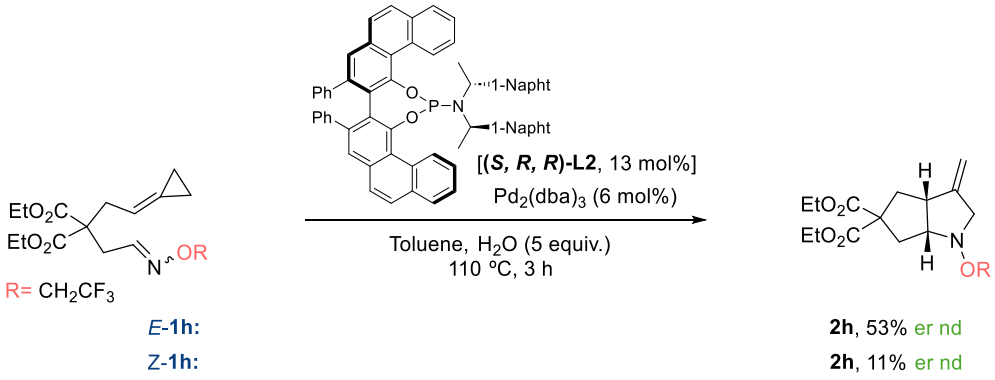

Scheme 82. Treatment of the activated oxime ether **1h** under Pd(0)-**(*S,R,R*)-L2** conditions.

On the other hand, the reactions of **1i** (*E:Z* ratio 1.8:1) with the catalysts generated from $Pd_2(dba)_3$ and **L1** or RuPhos, did not provide any product (entries 1 and 2). Furthermore, the asymmetric conditions [$Pd_2(dba)_3$/**(*S,R,R*)-L2** and 5 equivalents of water] neither afforded the desired product **2i** (entry 3), despite full conversion of **1i**.

Additional studies were performed by varying solvents or adding additives, but we did not observe significant improvements. Therefore, the scope of the asymmetric reaction seems to be also narrow.

Table 7. Results from precursor **1i** under racemic conditions.[a]

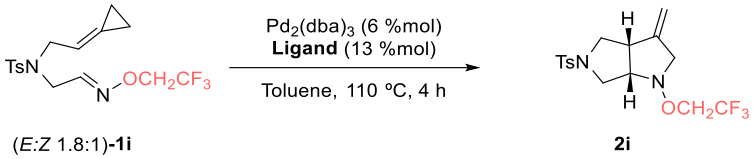

(*E*:*Z* 1.8:1)-**1i** **2i**

Entry	Ligand	Conv. (%)	**2i** (%)
1	**L1**	64	-
2	RuPhos	100	-
3[a]	**(*S,R,R*)-L2**	100	-

[a] Conditions: **1i**, $Pd_2(dba)_3$ (6 mol%), ligand (13 mol%), dry toluene (0.05 M), Ar atmosphere, 110 ºC. [b] 5 equiv. of H_2O as additive.

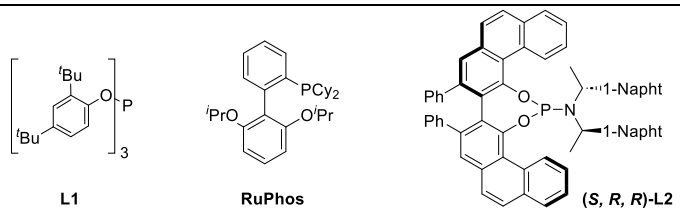

L1 **RuPhos** **(*S, R, R*)-L2**

4.1.3.2 Mechanistic studies

Experiments with deuterated compounds

To obtain a better understanding of the mechanism under the formation of cycloadducts **2** and side products of type **4**, a deuterium labelled precursor, ***E*-d_4-1a**, was prepared with the same protocol as for the non-deuterated analogue **1a** (**Scheme 75**), using a deuterated vinyl tosylate (***d*$_4$-6**).

Treatment of ***E*-d_4-1a** with the Pd(0)/RuPhos catalyst, in refluxing toluene, provided the fused pyrrolidine ***d*$_4$-2a** (57% yield) and the diene ***E*-d_4-4a** in 33% yield (**Scheme 83**, deuterated positions depicted with red dots).

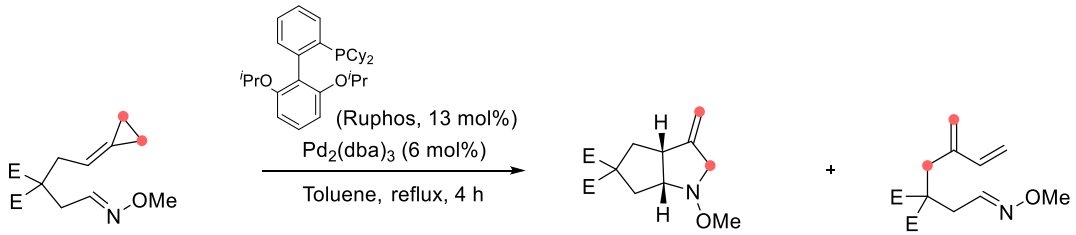

***E*-d_4-1a**, E =CO_2Et ***d*$_4$-2a**, 57% ***E*-d_4-4a**, 33%

Scheme 83. Pd(0)-catalyzed (3+2) cycloaddition using the deuterated precursor ***E*-d_4-1a** (%D>99).

DFT studies

To shed further light on the mechanism behind the formation of products **2** and **4**, we carried out DFT calculations using B3LYP-GD3/6-31G(d) (LANL2DZ for Pd) for the optimization of the stationary points, and B3LYP-GD3/6–311++g(d,p) (SDD for Pd), in toluene, for single point energy optimizations. The precursor *E*-**1j**, similar to ***E*-1a**, was employed as model substrate and *t*BuXPhos, which is experimentally competent (**Table 1**, entry 3), was used as model ligand. **Figure 10** shows the computed energy profile, while key palladium complexes are illustrated in **Figure 11**.

The reaction starts with the coordination of the Pd complex to the distal C-C bond of the cyclopropane (**I1**), followed by an easy oxidative addition to reach palladacyclobutane **I2** (ΔG=3.4

kcal·mol^{-1}). From this intermediate, a slight rotation of the phosphine enables a γ-agostic interaction between a hydrogen atom of the ^{t}Bu group and the Pd [*d*(H–Pd) = 2.7 Å, **Figure 11**], forming the species **I3** (ΔG=0.9 kcal·mol^{-1}). Alternatively, intermediate **I2** can evolve to a T-shaped isomer **I6**, bearing the biaryl moiety of the ligand oriented away from the palladium, therefore lacking any kind of hemilabile interaction. Remarkably, this intermediate is 12.7 kcal·mol^{-1} less stable than **I2**.

From **I3**, the reaction proceeds through a migratory insertion of the C=N bond, via the TMM-like transition state (**TS3-4**, ΔG=10.6 kcal·mol^{-1}), which exhibits C-C bond lengths of 2.42-2.45 Å. This step delivers the square planar σ-allyl Pd-complex **I4**, which holds a secondary interaction between the C-*ipso* of the biaryl phosphine and the metallic center [*d*(C–Pd) = 2.7 Å, **Figure 11**].

The reductive elimination step from intermediate **I4** is elusive, but this species can easily evolve to the isomeric intermediate **I5**, via **TS4-5** (ΔG=3.6 kcal·mol^{-1}). Then, complex **I5**, which holds the N and P atoms *trans* to each other, and exhibits a γ-agostic interaction between the Pd and a H atom of the ^{t}Bu group [*d*(H–Pd) = 2.5 Å, **Figure 11**], can undergo a C-N reductive elimination to afford **2j** (**TS5-2j**, ΔG= 20.0 kcal·mol^{-1}). Thus, the reductive elimination, with a ΔG of 20.0 kcal·mol^{-1}, would be the turnover limiting step.[78]

Despite the formation of palladacyclobutane **I6** was significantly less favored, we also calculated the evolution from this intermediate, to gather more information about the relevance of the subtle interactions between the metal center and the Buchwald ligands. Thus, complex **I6** can also undergo a migratory insertion with an energy barrier of 12.5 kcal·mol^{-1}, just slightly higher than that from I3, through **TS3-4** [ΔΔG= 1.9 kcal·mol^{-1}]. Finally, the resulting square planar complex **I7**, bearing an γ-agostic interaction, suffers a reductive elimination with an energy barrier of 17.4 kcal·mol^{-1}, to give the cycloadduct **2j**. Although the relative energy barrier for the reductive elimination is lower than that from **I5**, via **TS5-2j,** [ΔΔG= 2.6 kcal·mol^{-1}], this alternative pathway via **I6** and **I7** can be fully discarded, as it involves significantly higher energetic stationary points than the route from **I3**.

The energy difference between the two pathways may be attributed to the ligand's ability to provide more stable intermediates throughout the entire reaction profile, by establishing secondary hemilabile interactions with the Pd center.

[78] Kozuch, S.; Shaik, S. How to Conceptualize Catalytic Cycles? The Energetic Span Model. *Acc. Chem. Res.* **2011**, *44*, 101-110.

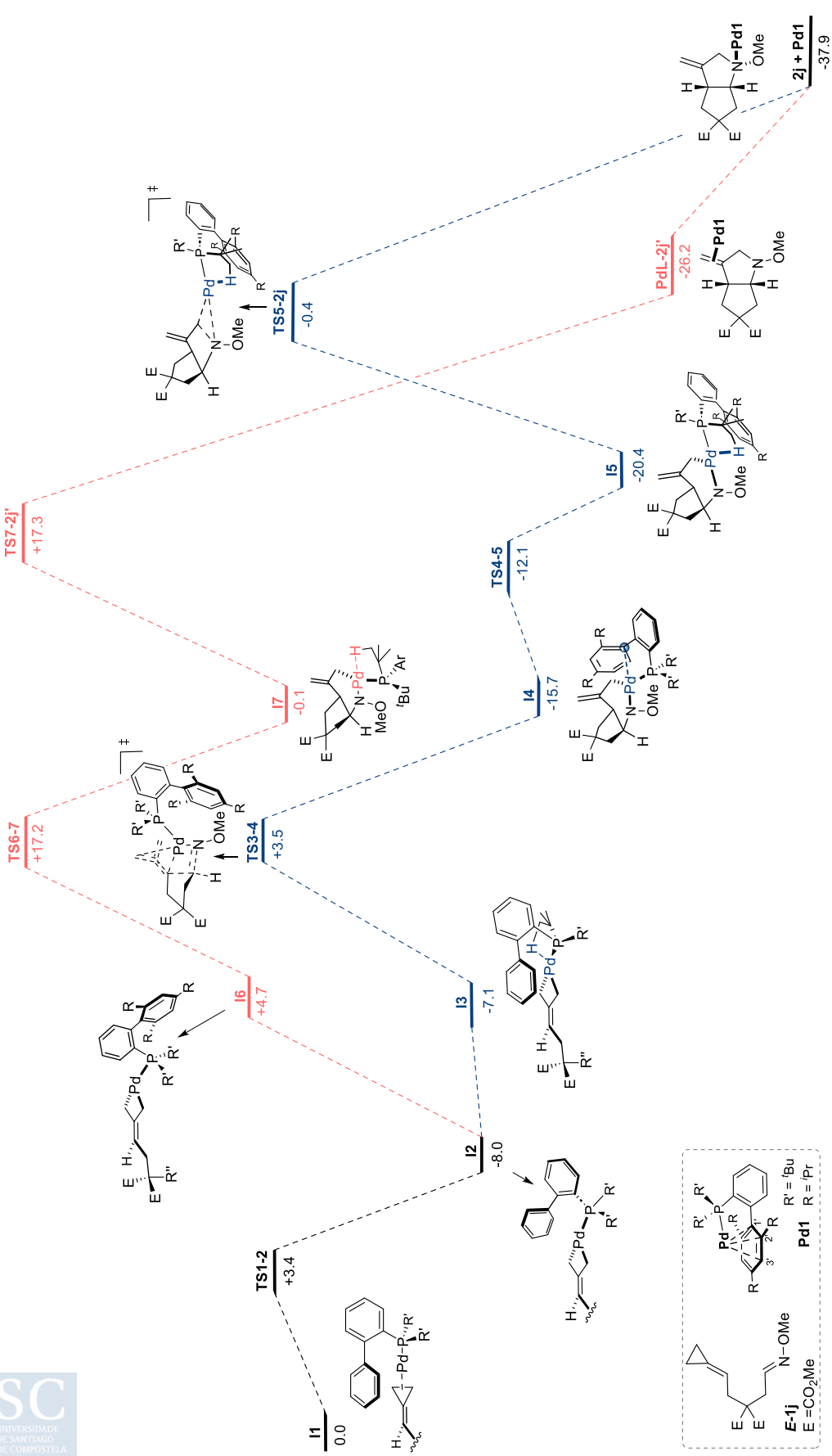

Figure 10. DFT-calculated energy profile ΔG_{solv} (kcal·mol^{-1}) for the (3+2) cycloaddition of **1j** using the Pd(0)-BuXPhos complex (**Pd1**) in toluene, with [B3LYP-GD3/6-31G(d) (LANL2DZ for Pd)//B3LYP-GD3/6–311++g(d,p) (SDD for Pd)].

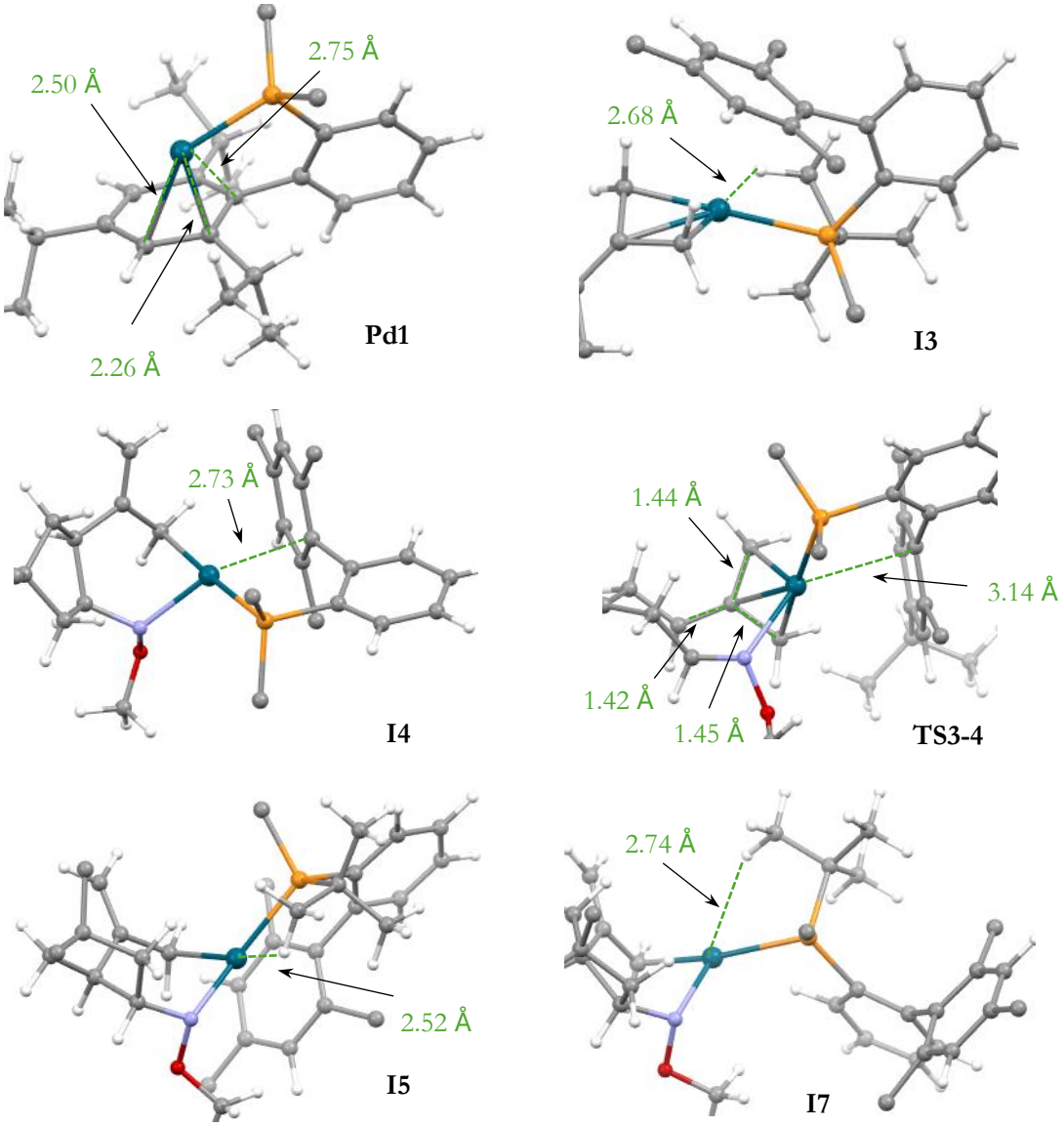

Figure 11. Selected simplified 3D representations of the most relevant structures of **Figure 10**.

To shed more light on the formation of dienes of type **4**, we further explored alternative pathways from intermediate **I2** (**Figure 12**). Thus, we found that this palladacyclobutane could also evolve to a slightly more stable conformer **I8** (ΔG=1.9 kcal·mol^{-1}), bearing a secondary interaction between the Pd and the C*ipso* of the biaryl moiety. This intermediate can undergo a rearrangement (ΔG=12.4 kcal·mol^{-1}) to form a C2-vinyl π-allyl Pd complex (**I-9**), in which the released malonate anion establishes electrostatic interactions with the allyl moiety though the oxygen atoms [*d*(C-O) = 2.6-3.0 Å]. Finally, an eventual trapping of the π-allyl-palladium electrophile with the malonate unit, in a S_N2' manner, would generate the observed diene **4j** (ΔG=4.1 kcal·mol^{-1}).

An alternative route was found from the more energetic palladacyclobutane conformer **I10**, with a different biaryl moiety configuration, lacking secondary interactions. However, this pathway can be discarded due to the higher energy of all its stationary points. Additionally, all attempts to achieve a direct transposition from palladacyclobutanes **I8** or **I10** to the product **4j** were unsuccessful.

The fact that the **TS3-4**, leading to the (3+2) cycloadduct **2j**, is 1.0 kcal·mol^{-1} above **TS8-9**, is consistent with the experimental results shown in **Table 2** (page 78). Indeed, although the cycloaddition of **1a** provides cycloadduct **2a** in 65% yield, together with a 35% of diene **4a**, the small energy gap ($\Delta\Delta G$ = 1.0 kcal·mol^{-1}) qualitatively indicates that both pathways are competitive, so

minor modifications in the reagents (e.g. length of the tether, stereochemistry of the oxime ether, etc.) might severely influence the selectivity, as it is experimentally observed (**Table 2**, page 78).

Notable, the computed route towards diene **4** is in agreement with the deuterium-labeling experiments, as the distribution of the CD_2 moieties fits with the evolution from palladacyclobutane **I8** to diene product **4.** Therefore, this proposal seems to be in good agreement with the experimental results and is coherent with the energetic requirements of the reaction.

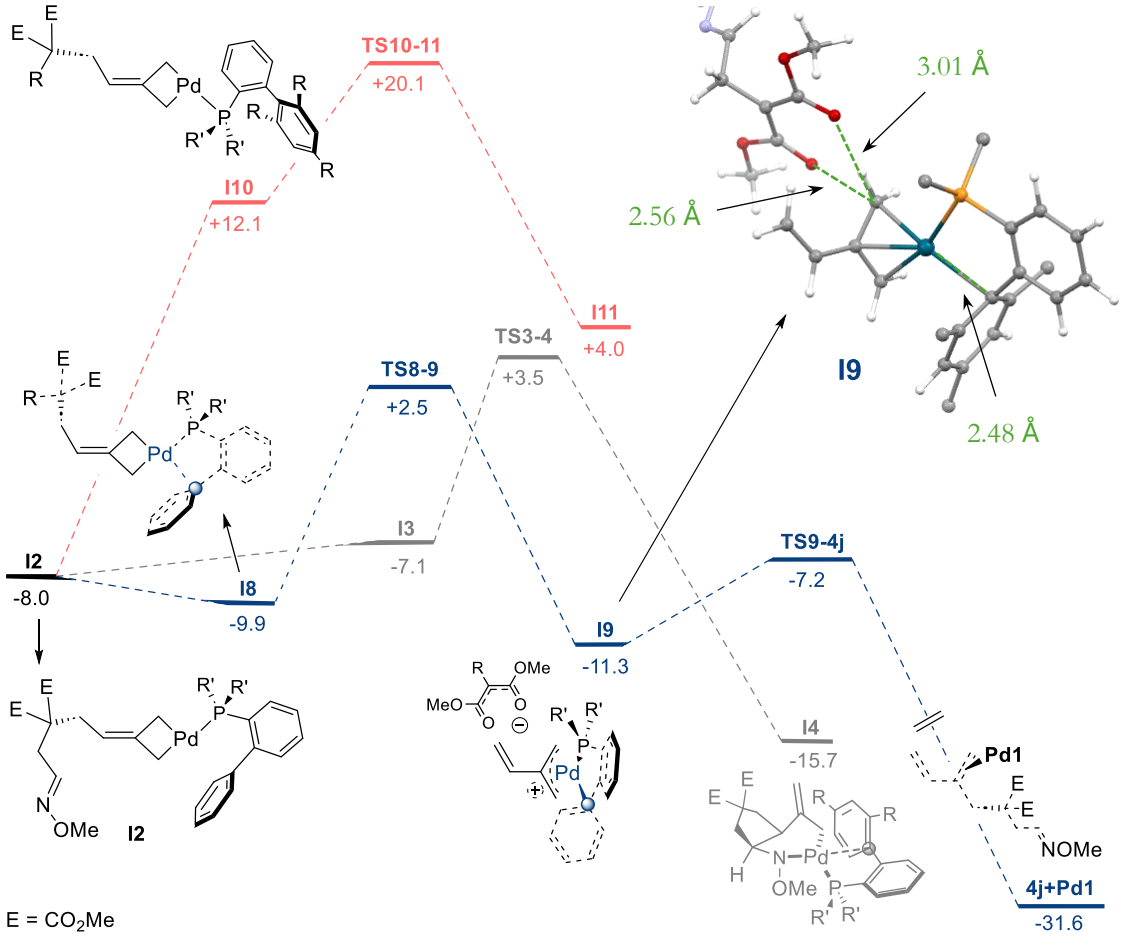

Figure 12. DFT-calculated energy profile ΔG_{solv} (kcal·mol^{-1}) for the formation of diene **4j** from oxime-tethered ACP **1j** using Pd(0)/*t*BuXPhos (**Pd1**) in toluene, with [B3LYP-GD3/6-31G(d) (LANL2DZ for Pd)//B3LYP-GD3/6–311++g(d,p) (SDD for Pd)].

Cross-experiments

To gather more information about the final step of the above-described pathway, the S_N2' interception of the 2-vinyl π-allyl Pd species **I9** by the malonate anion (see **Figure 12**), we conducted a series cross-experiments to see whether this trapping could be achieved by external nucleophiles. In particular, we observed that the *O*-benzyl oxime ether **1c**, when treated with $Pd_2(dba)_3$/RuPhos conditions, afforded the diene **4c** quantitatively (see **Table 2**, page 78).

When **1c** was reacted in presence of an excess of dimethyl malonate and K_2CO_3, the standard diene **4c** was obtained in 49% yield, and no traces of the cross-product diene (**4c'**) were detected (**Scheme 84a**). Besides, treatment of both **1c** and ***E*-d_4-1a** with the catalyst generated from $Pd_2(dba)_3$ and RuPhos afforded **4c** in quantitative yield, along with the cycloadduct ***d_4*-2a** (55% yield) and diene ***E*-d_4-4a**, derived from ***E*-d_4-1a** (36% yield). In any case, cross-products were not observed (**Scheme 84b**), indicating that the putative trapping of the π-allyl species can only be achieved intramolecularly,

within the ionic pair proposed in **I9** (**Figure 12**). These experimental results are in consonance with the low energy barrier calculated for this step, via **TS9-4j**, of 4.1 kcal·mol^{-1}.

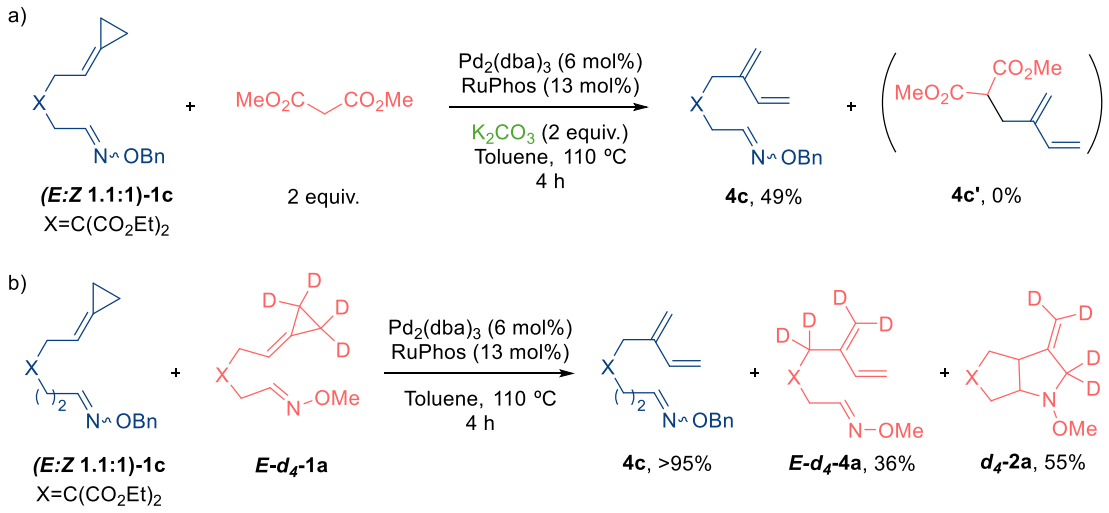

Scheme 84. Cross-experiments related to the diene of type **4** formation.

4.1.4 Intermolecular (3+2) Aza-Cycloadditions

4.1.4.1 Development of the racemic transformation

Reactivity and optimization

For this study, we selected as model ACP the precursor **9b**, bearing a carbonyl tether, which can undergo an intramolecular cycloaddition to yield bicyclic tetrahydrofuran (THF) products (see **Scheme 51**, page 47, *Introduction*). In this way, we could better uncover selective conditions to favor the desired intermolecular cycloaddition with an external imine.

The substrate **9b** was obtained from the Pd-catalyzed reaction between the malonate **8b** and vinyl tosylate **6** (**Scheme 85**).

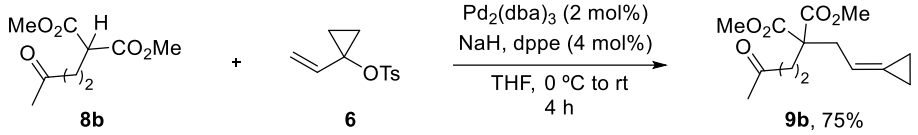

Scheme 85. Synthesis of model ACP precursor **9b**.

As imine partners, we prepared the oxime ether **15a**, the phenyl imine **15b**, the tosyl imine **15c** and the acyl imine **15d**. The first three imines were synthesized using a condensation reaction (**Scheme 86**). The acyl imine **15d** required a first reaction between the aldehyde and the benzamide, followed by basic treatment. In addition, the sulfamate-derived imine **15e** was obtained from *ortho*-hydroxy benzaldehyde and sulfamoyl chloride, *in situ* prepared from formic acid and chlorosulfonyl isocyanate.

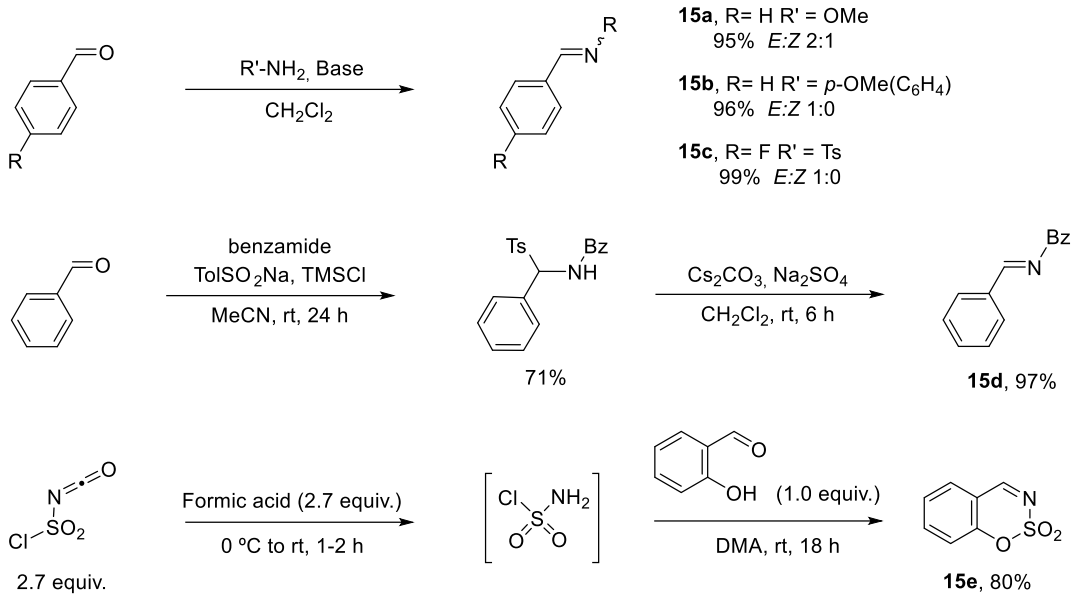

Scheme 86. Synthesis of imine partners **15**.

We initially tested the reaction of oxime ether **15a**, with substrate **9b**, in presence of the catalyst generated *in situ* from $Pd_2(dba)_3$ and ^{t}BuXPhos. The reaction did not afford the desired pyrrolidine **16ba**, but the bicyclic THF cycloadduct **17b** in 95% yield (entry 1). Similarly, the aryl imine **15b** and the benzoyl imine **15d**, did not participate in the process, so **17b** was isolated in excellent yields (entries 2 and 3). Interestingly, when tosyl imine **15c** was used,[37] the pyrrolidine **16bc** was formed in a moderate 47% yield, as a mixture of diastereoisomers (**16bc**:**16bc'** = 3:1), with the major diastereoisomer (**16bc**) featuring the hydrogens in *syn* disposition, according to nOe experiments. However, the intramolecular adduct **17b** was also obtained in 26% yield (entry 4).

Gratifyingly, using the sulfamate-derived cyclic imine **15e**, we exclusively observed the intermolecular cycloadduct **16be** as a mixture of diastereoisomers (91% yield, dr = 1:2.4, entry 5). nOe experiments confirmed that the major diastereoisomer (**16be'**) holds the hydrogens in *anti* disposition. This result is particularly appealing since sulfamate moieties are present in numerous drugs with anticancer, antifungal and antiviral properties, as well as in hormone-enzyme inhibitors.[79]

[37] Oh, B. H.; Nakamura, I.; Saito, S.; and Yamamoto, Y. Palladium-catalyzed [3+2] cycloaddition of alkylidenecyclopropanes with imines. *Tetrahedron Lett.* **2001**, *42*, 6203-6205.

[79] a) Winum, J.-Y.; Scozzafava, A.; Montero, J.-L.; Supuran, C. T. Sulfamates and Their Therapeutic Potential. *Med. Res. Rev.* **2005**, *25,* 186–228.; b) Winum, J.-Y.; Scozzafava, A.; Montero, J.-L.; Supuran, C. T. The Sulfamide Motif in the Design of Enzyme Inhibitors. *Expert Opin. Ther. Pat.* **2006**, *16,* 27–47.; c) Woo, L. W. L.; Purohit, A.; Potter, B. V. L. Development of Steroid Sulfatase Inhibitors. *Mol. Cell. Endocrinol.* **2011**, *340,* 175–185.

Table 8. Viability of a (3+2) intermolecular cycloaddition between **9b** and imine partners **15**.[a]

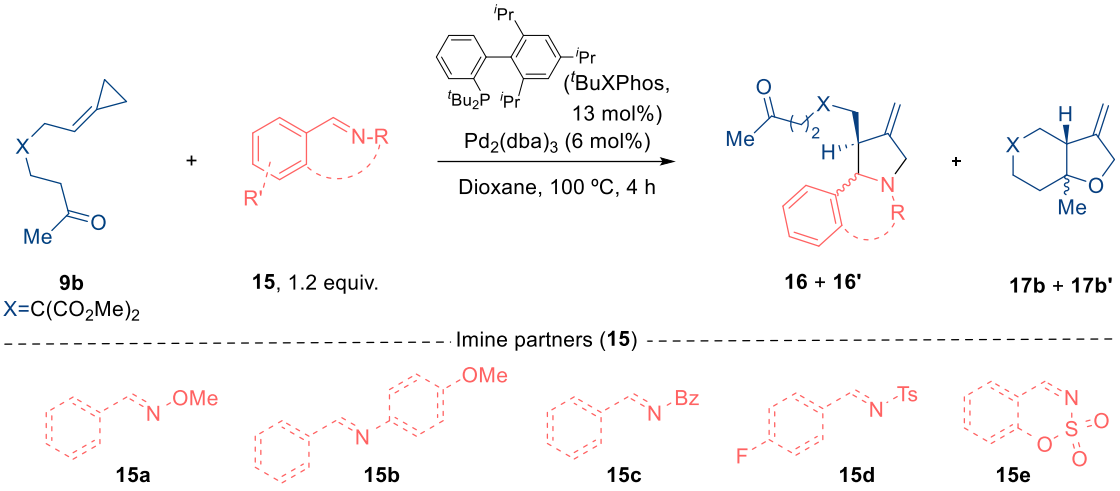

Entry	15	16+16',% (dr)[b]	17b+17b',% (dr)[b]
1	**15a**	-	95 (8:1)
2	**15b**	-	97 (7:1)
3	**15d**	-	85 (6:1)
4[c]	**15c**	**16bc**, 47 (3:1)	26 (4:1)
5	**15e**	**16be**, 91 (1:2.4)	-

[a] Conditions: **9b**, **15** (1.2 equiv.), $Pd_2(dba)_3$ (6 mol %), *t*BuXPhos (13 mol %), dry 1,4-dioxane (0.05 M), Ar atmosphere, 100 °C. [b] Diastereomeric ratio *syn*/*anti* by ^{1}H–NMR of the crude reaction mixture. [c] 1.5 equiv. of **15c**.

To see whether we could further improve the yield and, particularly, the diastereoselectivity of the cycloaddition, we evaluated different ligands, Pd sources and reaction conditions, including variations in solvents and temperature (**Tables 9 - 11**).

The catalyst derived from $Pd_2(dba)_3$ and the bulky phosphite **L1** resulted in partial consumption of **9b**, providing **16be** in a poor 15% yield, as a mixture of diastereoisomers (*syn*:*anti* 1:2.8, entry 1). The use of P(*o*-tolyl)$_3$ raised the yield of **16be** to 29% yield (dr 1:1.4), with minor amounts of dienic product **18b** (entry 2).[80] Using $Pd(PPh_3)_4$ (12 mol%) and $Ph_3P(O)$ (24 mol%),[37] the pyrrolidine **16be** was obtained in a moderate 47% yield (dr 1:1.1), with small amounts of diene **18b** (20%, entry 3). Gratifyingly, phosphoramidite **L9** led to the formation of cycloadduct **16be** in excellent yield (96%, dr = 1.2:1, entry 4). In addition, the reaction with the electron poor phosphine P[3,5-$(CF_3)_2C_6H_3$]$_3$ (**L17**) afforded **16be** in 85% yield (dr 2:1, entry 5). Meanwhile, the use of PPh_3 provided the cycloadduct **16be** in a low 7% yield (dr 1:1, entry 6). On the other hand, Pd-catalysts using bisphosphines, such as dppe, proved inefficient, resulting in full consumption of **9b**, but no products were observed (entry 7)

Catalysts generated from $Pd_2(dba)_3$ and diverse Buchwald ligands, like RuPhos, BrettPhos or *t*BuBrettPhos, resulted in low yields of **16be** (up to 13% yield, entries 8-10). With XPhos, the reaction led to **16be** in 57% yield, but the conversion of **9b** was not complete (entry 11). *t*BuXPhos affords

[37] Oh, B. H.; Nakamura, I.; Saito, S.; and Yamamoto, Y. Palladium-catalyzed [3+2] cycloaddition of alkylidenecyclopropanes with imines. *Tetrahedron Lett.* **2001**, *42*, 6203-6205.

[80] Dienes of type **18** are formed from precursors **9** via the same mechanism as dienes **3**, from precursors of type **1**. See **Scheme 54**, *Precedents*, page 73.

the desired adduct **16be** in 91% yield, providing the best performance among these ligands (dr 1:2.4, entry 12).

Table 9. Ligand screening for (3+2) intermolecular cycloadditions between **9b** and **15e**.[a]

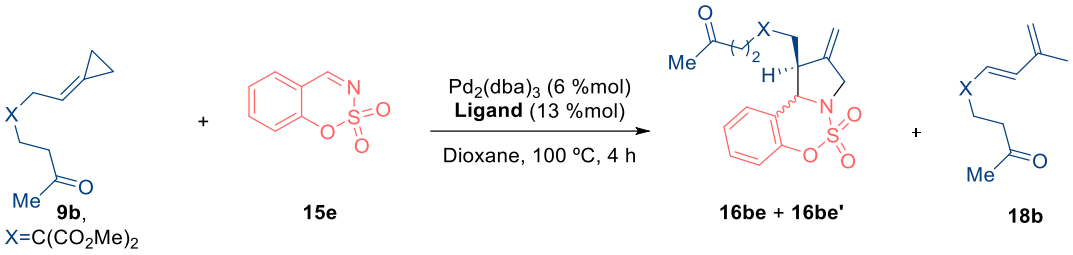

Entry	Ligand	Conv. **9b** (%)	**16be+16be'**,% (dr)[b]	**18b** (%)
1	**L1**	67	15 (1:2.8)	-
2	P(*o*-tolyl)$_3$	35	29 (1:1.4)	5
3[c]	P(O)Ph$_3$	95	46 (1.1:1)	19
4	**L9**	100	96 (1.2:1)	<5
5	**L17**	100	85 (2:1)	15
6	PPh$_3$	67	7 (1:1)	15
7[d]	dppe	>95	-	-
8	RuPhos	100	9 (1:1)	-
9	BrettPhos	16	10 (1:1)	-
10	^{t}BuBrettPhos	17	13 (1:1.6)	-
11	XPhos	65	57 (1:2.4)	-
12	^{t}BuXPhos	100	91 (1:2.4)	-

[a] Conditions: **9b**, **15e** (1.2 equiv.), Pd$_2$(dba)$_3$ (6 mol %), ligand (13 mol %), dry 1,4-dioxane (0.05 M), Ar atmosphere, 100 °C. [b] Diastereomeric ratio *syn*/*anti* by ^{1}H–NMR of the crude reaction mixture. [c] Pd(PPh$_3$)$_4$ (12 mol%)/Ph$_3$P(O) (24 mol%), 120 ºC, 14 h. [d] t = 20 h.

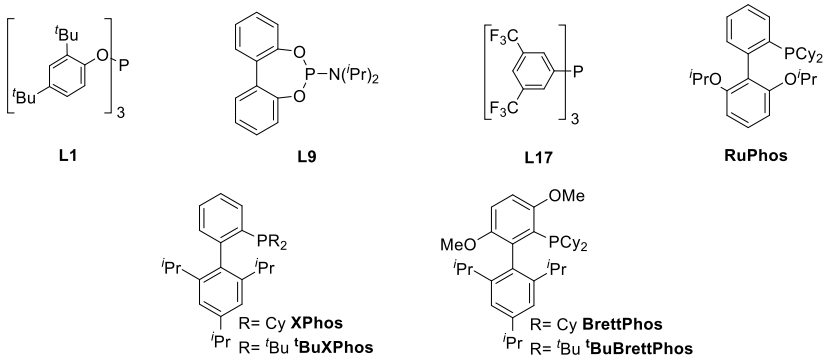

We then evaluated alternative Pd(0) sources using **L9** as ligand (**Table 10**). While Pd$_2$(dba)$_3$ affords the pyrrolidine **16be** in 96% yield (dr 1.2:1, entry 1), the use of Pd[P(*o*-tolyl)$_3$] gave 95% (dr 1:1, entry 2). We also tested Pd[P(*o*-tolyl)$_3$] in absence of **L9**, but we observed a lower conversion of **9b** (entry 3). On the other hand, the use of CpPd(π-cin.) or Pd(PPh$_3$)$_4$ resulted in lower consumptions of **9b**, reduced yields and similar diastereoselectivities (56 and 37% yield, entries 4 and 5). Curiously, with a Pd(0)-*N*-heterocyclic carbene (NHC) complex, the reaction provides the intramolecular oxacycloadduct **17b** in 14% yield, as the only product (entry 6).

Table 10. Precatalyst screening for (3+2) intermolecular cycloadditions between **9b** and **15e**.[a]

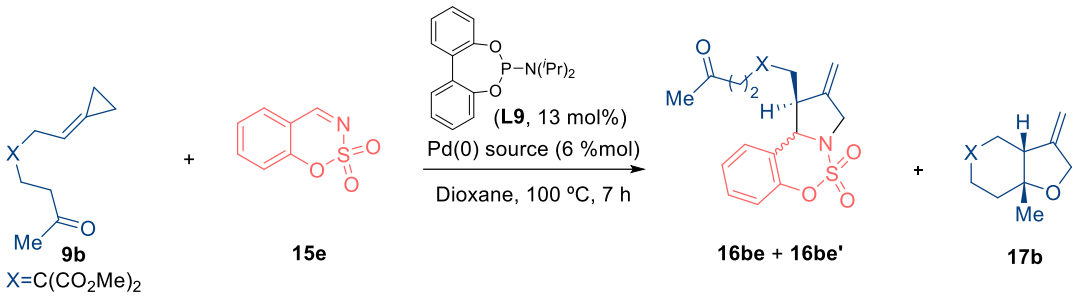

Entry	Pd(0) source	Conv. 9b (%)	16be + 16be' (%)[b]	17b (%)[b]
1[c]	$Pd_2(dba)_3$	100	96 (1.2:1)	-
2	$Pd[P(o\text{-tolyl})_3]_2$	100	95 (1:1)	-
3[d]	$Pd[P(o\text{-tolyl})_3]_2$	61	20 (1.9:1)	-
4	CpPd(π-cin.)	90	59 (1.2:1)	-
5	$Pd(PPh_3)_4$	79	37 (1:1)	-
6	Pd(0) NHC	87	-	14 (10:1)

[a] Conditions: **9b**, **15e** (1.2 equiv.), Pd(0) source (6 mol %), **L9** (13 mol %), solvent (0.05 M), Ar atmosphere, 100 °C, 7 h. [b] Diastereomeric ratio *syn*/*anti* by ^{1}H–NMR of the crude reaction mixture. [c] t = 4 h. [d] Without **L9**, 21 h.

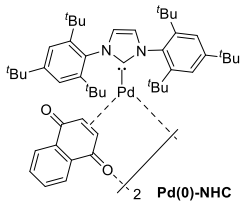

Finally, we performed a solvent screening using $Pd_2(dba)_3$/**L9** as catalyst (**Table 11**). Surprisingly, the reaction tolerates solvents with varying polarity and coordination abilities. For instance, both dioxane and MeCN afforded the cycloadduct **16be** in 96% yield and equal dr's (entries 1 and 2). Similarly, solvents such as toluene, hexane, ^{t}AmOH and 2-MeTHF also performed well, enabling the formation of the pyrrolidine **16be** in very good yields (88-90%, entries 3-6). On the other hand, the use of DCE or DMF led to lower yields, with minor amounts of diene **18b** being formed (entries 7 and 8). From all the solvents tested, only DMSO proved to be incompatible with the transformation (entry 9).

Table 11. Solvent screening for (3+2) intermolecular cycloadditions between **9b** and **15e**.

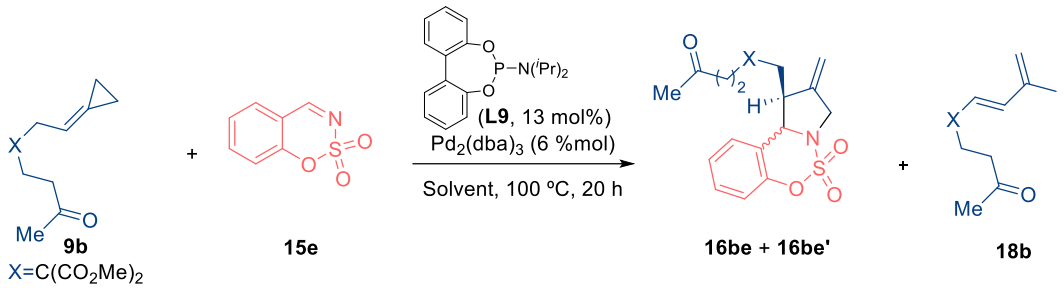

Entry	Ligand	Conv. 9b (%)	16be + 16be' (%)[b]	18b (%)
1[c]	1,4-dioxane	100	96 (1.2:1)	<5
2	MeCN	100	96 (1.2 :1)	-
3	Toluene	100	89 (1.1:1)	11
4	Hexane	100	90 (1:1)	-
5	^{t}AmOH	100	90 (1.1:1)	<5
6	2-MeTHF	100	88 (1:1)	12
7	DCE	86	74 (1.1:1)	12
8	DMF	100	60 (1.1:1)	20
9	DMSO	46	<5	-

[a] Conditions: **9b**, **15e** (1.2 equiv.), $Pd_2(dba)_3$ (6 mol %), **L9** (13 mol %), solvent (0.05 M), Ar atmosphere, 100 °C, 20 h. [b] Diastereomeric ratio *syn*/*anti* by ^{1}H–NMR of the crude reaction mixture. [c] t = 4 h.

Scope with respect to ACP precursors

We next explored the scope of the transformation, using as optimal catalyst the species generated *in situ* from $Pd_2(dba)_3$ (6 mol%) and the phosphoramidite **L9** (13 mol%) at 100 ºC. Acetonitrile was selected as solvent since generally provided faster reactions and cleaner crude mixtures, although 1,4-dioxane also proved to be a suitable alternative in some cases.

Therefore, different ACP precursors were synthesized. The ACPs **9a**, **9c** and **19a** were prepared via a Tsuji-Trost reaction using vinyl tosylate **6** and the corresponding nucleophilic partners (**Scheme 87**).

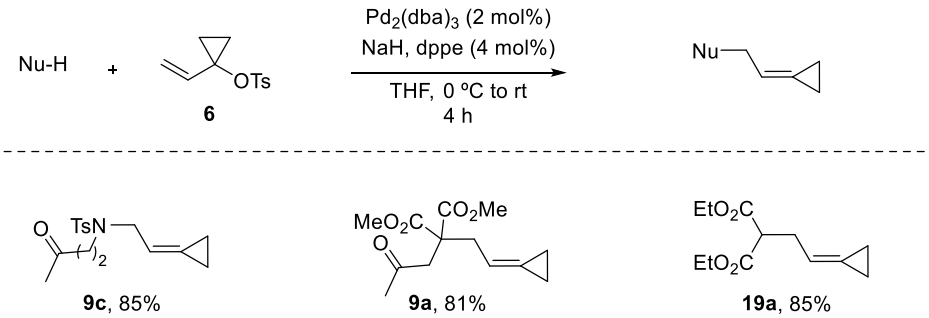

Scheme 87. Synthesis of ACP precursors of type **9** and **19** via Tsugi-Trost reactions.

On the other hand, ACP's **19b**-**19f** were prepared through Wittig reactions of the corresponding carbonyl precursors (**Scheme 88**).

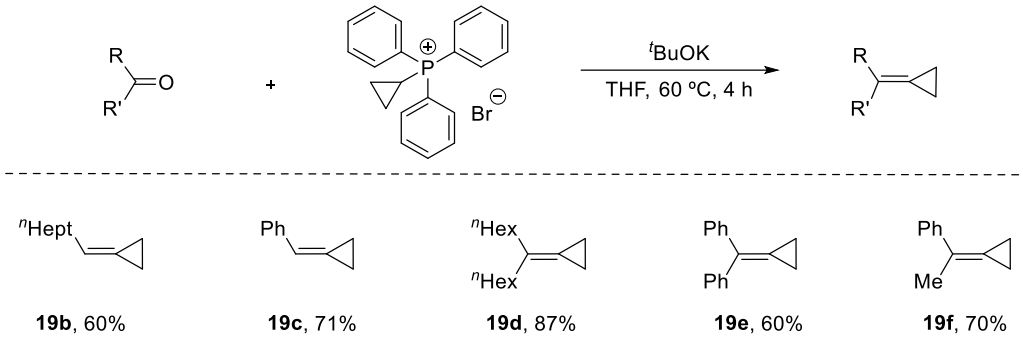

Scheme 88. Synthesis of ACP precursors of type **19** via Wittig reactions.

The ACP precursors **19g** and **19h**, bearing an ester group in the *exo*-methylene moiety, were prepared following the procedure depicted in **Scheme 89**.

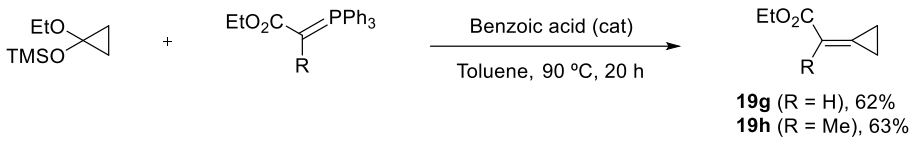

Scheme 89. Synthesis of ACP precursors bearing an ester moiety.

Finally, the ACP **19i**, bearing an amide moiety, was synthetized from the alcohol precursor **20**, which was converted into an amine derivative (**21**) via Mitsunobu reaction, and further monoprotected with a nosyl group (**Scheme 90**).

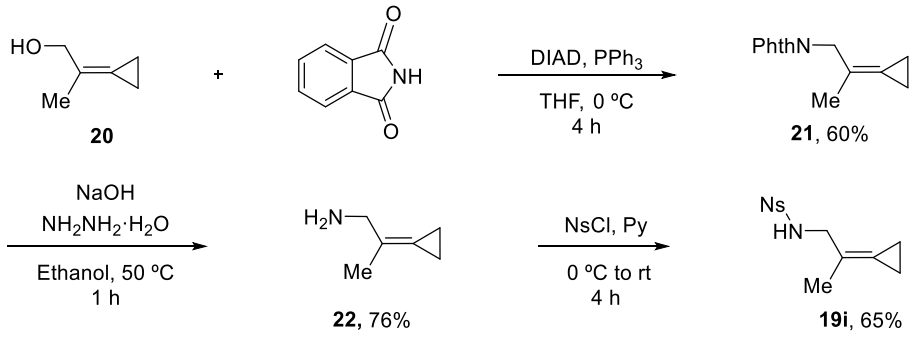

Scheme 90. Synthesis of ACP precursor **19i**.

With the ACP precursors in hand, we evaluated their corresponding cycloadditions with the model imine **15e** (**Scheme 91**). Monosubstituted ACPs with tethered carbonyl groups, such as **9c** and **9a**, that could undergo competing intramolecular cycloadditions, also exhibited complete preference for the intermolecular reaction with the imine, yielding pyrrolidines **16ce** and **16ae** in 51% and 68% yield, respectively.

The substrate **19a**, which holds a malonate moiety, afforded the pyrrolidine **23ae** in 80% yield.[81] Simpler ACP precursors, bearing aliphatic or aromatic moieties instead of the malonate unit, were also suitable partners, leading to the corresponding cycloadducts in good yields (**23be**: 90% and **23ce**: 52% yield, respectively). The ACP **19g**, featuring a carboxy ester at the alkene, reacted faster (t=2 h for full conversion), providing the corresponding cycloadduct in 63% yield, as a single diastereoisomer that holds the hydrogen atoms in *anti*-disposition.

[81] For clarity and consistency with the following sections of the manuscript, ACPs precursors tethered to ketone moieties are labeled as **9**, while the substrates without carbonyl moieties are named **19**. Consequently, the corresponding intermolecular (3+2) cycloadducts between ACPs and imine partners, are named as **16** (from ACPs **9**) and **23** (from ACPs **19**).

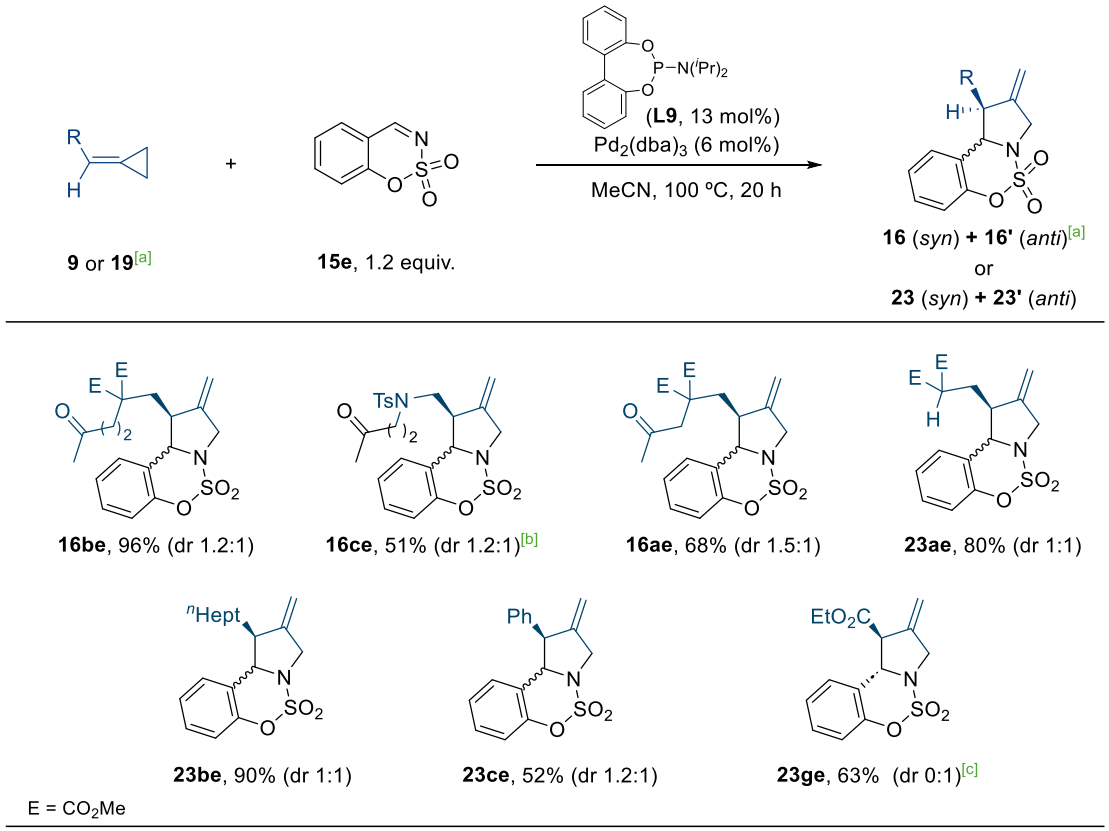

[a]See footnote 81. [b]Using 1,4-dioxane instead MeCN. [c]*t* = 2h.

Scheme 91. Scope for (3+2) intermolecular cycloaddition between monosubstituted ACPs (**9** or **19**) and **15e**.

Importantly, the methodology also supports the use of 1,1-disubstituted ACPs (**Scheme 92**). The symmetric ACP **19d**, bearing *n*-hexyl chains, participated in the cycloaddition to give the fused pyrrolidine **23de** in quantitative yield. Meanwhile, diphenyl substituted ACP **19e** afforded the corresponding product, **23ee**, in 58% yield. Its structure was further confirmed by X-ray diffraction analysis. On the other hand, the asymmetrically substituted ACPs **19f** and **19h** led to the corresponding compounds, **23fe** and **23he**, in excellent yields as mixtures of diastereoisomers (90 and 97%, respectively). Gratifyingly, the presence of a nosylamide, like in ACP **19i**, was well-tolerated, so that the pyrrolidine adduct **23ie** was obtained in 68% yield. Its structure was also confirmed by X-ray diffraction analysis.

[81]For clarity and consistency with the following sections of the manuscript, ACPs precursors tethered to ketone moieties are labeled as **9**, while the substrates without carbonyl moieties are named **19**. Consequently, the corresponding intermolecular (3+2) cycloadducts between ACPs and imine partners, are named as **16** (from ACPs **9**) and **23** (from ACPs **19**).

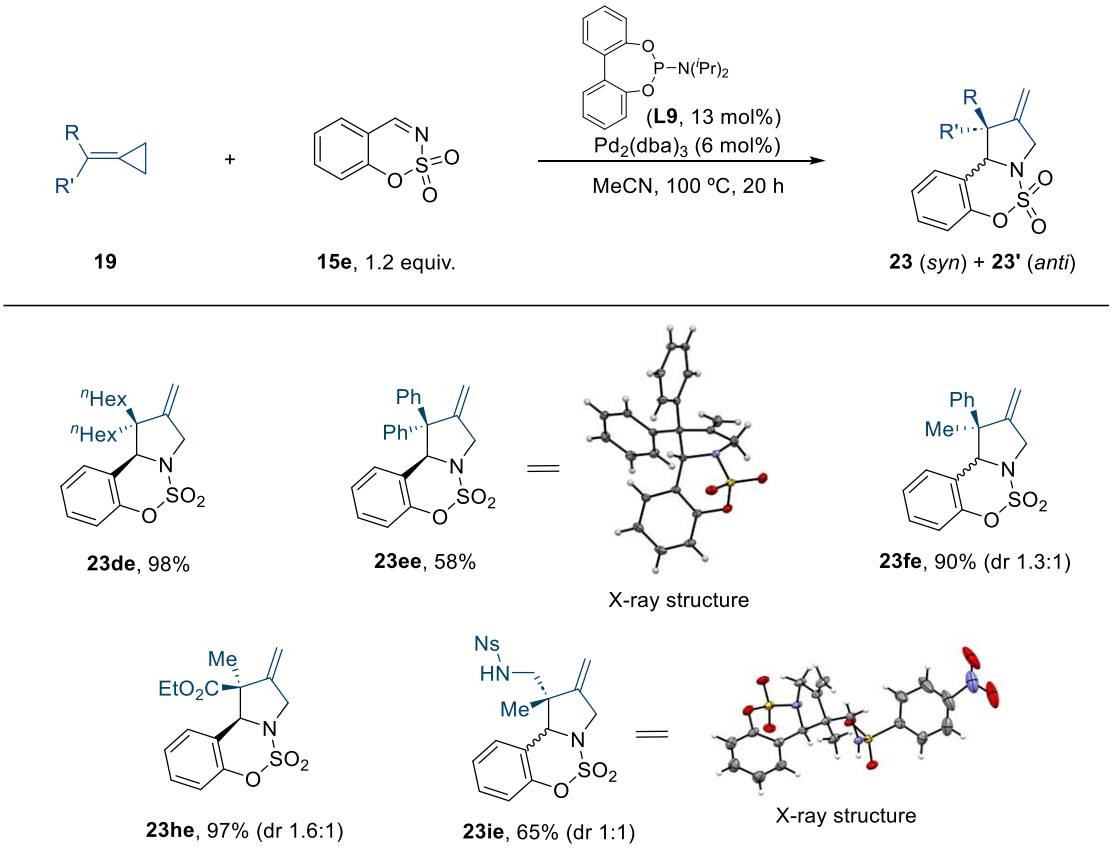

Scheme 92. Scope for (3+2) intermolecular cycloaddition between disubstituted ACPs of type **19** and **15e**.

Scope with respect to the aldimine partners

A variety of sulfamate-derived cyclic imines of type **15** were prepared according to the protocol used for **15e**, using *in situ* generated sulfamoyl chloride and the corresponding *o*-hydroxy benzaldehydes.

As shown in **Scheme 93**, the cycloaddition showed excellent tolerance for sulfamate-derived imines with larger aromatic rings, providing the expected fused pyrrolidines **16bf**, **16gf** and **23dg** in almost quantitative yields. On the other hand, the cycloadduct **16bh** was obtained in 58% yield. The structures of **16bh** and **16bh'** could be further confirmed by X-ray diffraction analysis.

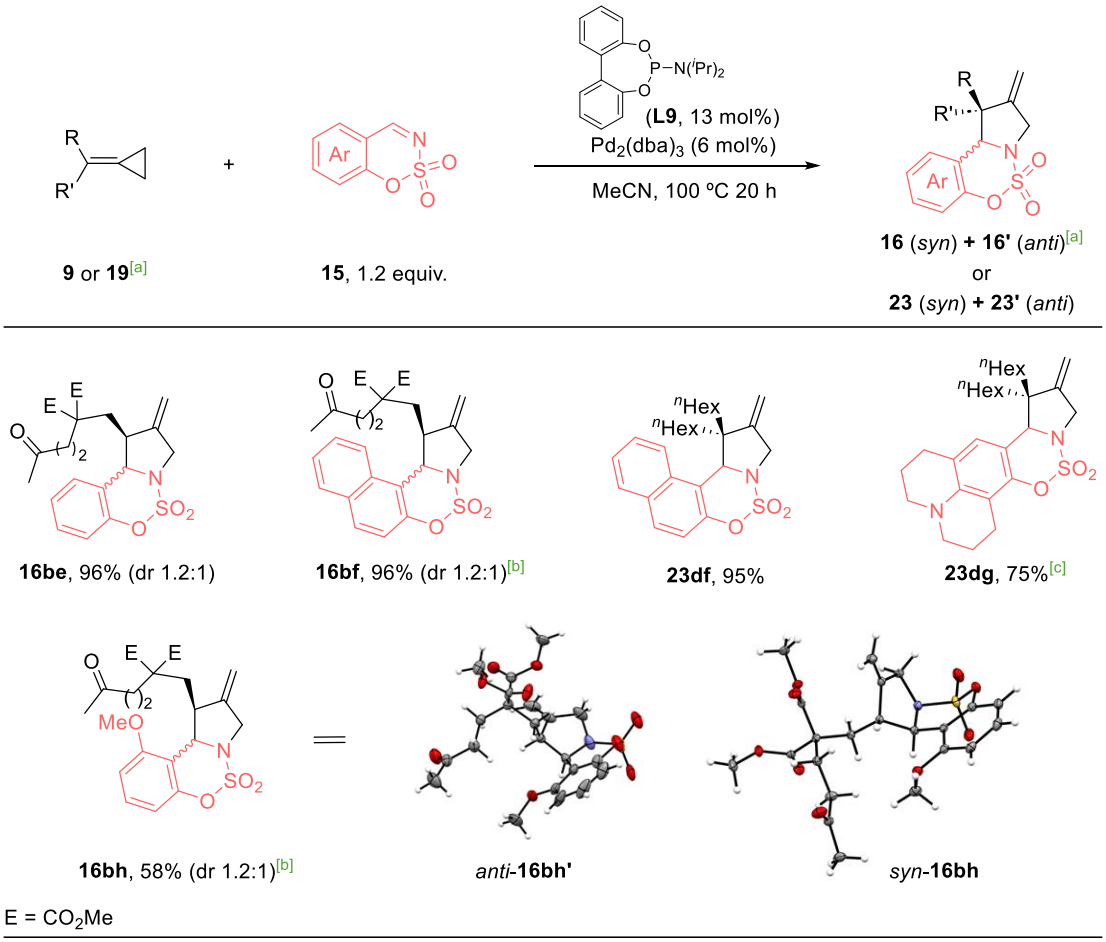

[a]See footnote 81. [b]Using 1,4-dioxane instead MeCN. [c]*t*=48 h.

Scheme 93. Scope for (3+2) intermolecular cycloaddition between ACPs (**9** or **19**) and sulfamate-derived imines **15**.

To check whether other cyclic *Z*-sulfonyl imines could also be suitable partners, we prepared the imine **15i** from bromobenzenesulfonamide, via a Suzuki coupling followed by an acid-promoted condensation (**Scheme 94**).

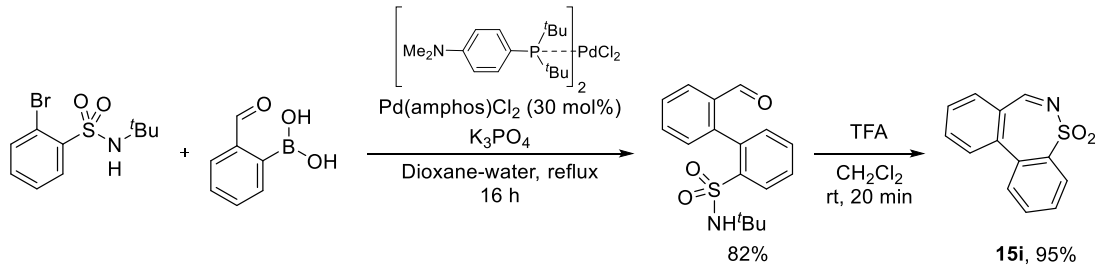

Scheme 94. Synthesis of *Z* cyclic sulfonyl imine **15i**.

Gratifyingly, under $Pd_2(dba)_3$/**L9** catalytic conditions, this imine participated in the cycloadditions with different ACP precursors, leading to the corresponding pyrrolidines **23di**, **23fi**, **23hi** and **23gi'** in yields varying from 55 to 95% (**Scheme 95**). Notably, the product **23gi'**, derived from the ACP

[81]For clarity and consistency with the following sections of the manuscript, ACPs precursors tethered to ketone moieties are labeled as **9**, while the substrates without carbonyl moieties are named **19**. Consequently, the corresponding intermolecular (3+2) cycloadducts between ACPs and imine partners, are named as **16** (from ACPs **9**) and **23** (from ACPs **19**).

19g, was obtained as the only diastereoisomer, bearing the hydrogen atoms of the stereocenters in *anti*-configuration (60% yield).

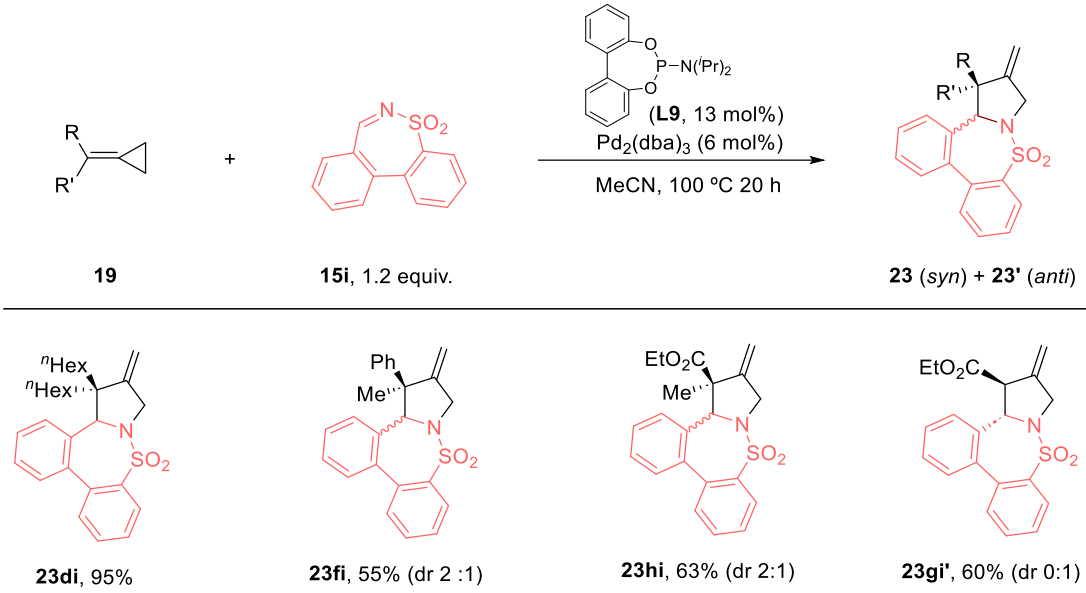

Scheme 95. Scope for (3+2) intermolecular cycloaddition between ACPs and cyclic *Z*-tosyl imine **15i**.

Pleasingly, the use of acyclic *E*-tosyl imines like **15c** is also possible, employing the Pd(0)-catalyst containing the phosphoramidite **L9** in acetonitrile (**Scheme 96**). The reaction tolerates different aromatic *N*-tosyl imines, with various functional groups in the aromatic ring (e.g. fluorine, nitro, ester, aldehyde or methoxy groups), giving the corresponding cycloadducts **16** or **23** in good to excellent yields (70-99%). Moreover, a *N*-benzoyl imine such as **15d** also afforded the desired cycloadduct, **23dd**, in 90% yield. Notably, in these reactions of *E* imines, the use of **L9** as ligand and MeCN as solvent was crucial, as other conditions led to significantly lower yields and/or the formation of side products.

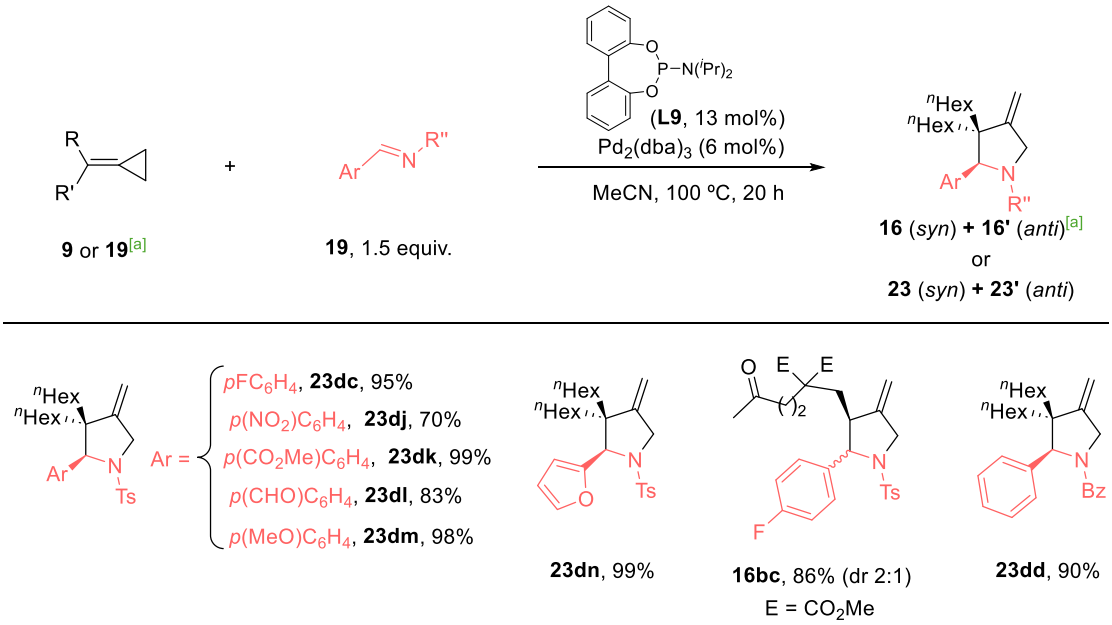

[a]See footnote 81.

Scheme 96. Scope for (3+2) intermolecular cycloaddition between ACPs and acyclic *E*-imines **15**.

Ketimine partners

The use of ketimines as imine partners, instead of aldimines, would allow the formation of interesting pyrrolidines bearing up to two quaternary carbon centers. For this purpose, we prepared the sulfamate-derived ketimine **15o**, just like previous sulfamate-derived imines. Unfortunately, treatment of the ACP **9b** and ketimine **15o** with the catalyst generated from $Pd_2(dba)_3$ and **L9**, in dioxane at 100 ºC, only led to small amounts of the intramolecular cycloadduct **17b**, despite full consumption of **9b** (entry 1, **Table 12**). Using *t*BuXPhos instead of **L9**, the intramolecular adduct **17b** was obtained in 60% yield (entry 2). With the electron poor phosphine **L17**, which had provided an excellent performance in the intermolecular cycloaddition of **9b** (see **Table 9**, page 92), we observed partial consumption of **9b**, but the desired azacycloadduct was not detected (entry 3).

[81]For clarity and consistency with the following sections of the manuscript, ACPs precursors tethered to ketone moieties are labeled as **9**, while the substrates without carbonyl moieties are named **19**. Consequently, the corresponding intermolecular (3+2) cycloadducts between ACPs and imine partners, are named as **16** (from ACPs **9**) and **23** (from ACPs **19**).

Table 12. Evaluation of methyl ketimine **15o** with **9b** for Pd(0)-catalyzed (3+2)-cycloadditions.[a]

Entry	Ligand	Conv. 9b (%)	16ar+16ar' (%)	17b,% (dr)[b]
1	**L9**	100	-	<5
2	*t*BuXPhos	100	-	60 (10:1)
3	**L17**	65	-	-

[a] Conditions: **9b**, **15o** (1.2 equiv.), $Pd_2(dba)_3$ (6 mol%), ligand (13 mol%), dry dioxane (0.05 M), Ar atmosphere, 100 °C, 4 h. [b] Diastereomeric ratio *syn*/*anti* by ^{1}H–NMR of the crude reaction mixture.

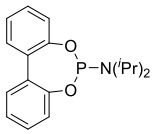

L9

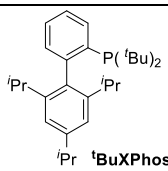

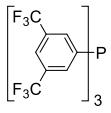

L17

On these bases, we hypothesized that more activated ketimines, bearing electron-withdrawing groups such as CF_3 or CO_2Et could afford the desired heterocyclic products. The synthesis of these substrates followed the same protocols previously used for sulfamate-derived imine **15o**.

Gratifyingly, the reaction of ACP **19d** with the trifluoromethyl ketimine **15p**, using $Pd_2(dba)_3$/**L9** as catalyst, afforded the desired (3+2) cycloadduct **23dp**, bearing a trifluoromethyl group at the ring fusion, in 60% yield (**Scheme 97**). Furthermore, ketimine **15p** also participates in the cycloaddition of different ACP precursors, leading to the corresponding pyrrolidine products **23** in good yields, but poor diastereoselectivities (61-70%, dr up to 1.7:1). Note that the incorporation of trifluoromethyl groups in bioactive molecules is highly relevant from a drug development perspective.[83]

[83] Purser, S.; Moore, P. R.; Swallow, S.; Gouverneur, V. Fluorine in medicinal chemistry. *Chem. Soc. Rev.* **2008**, *37*, 320−330.

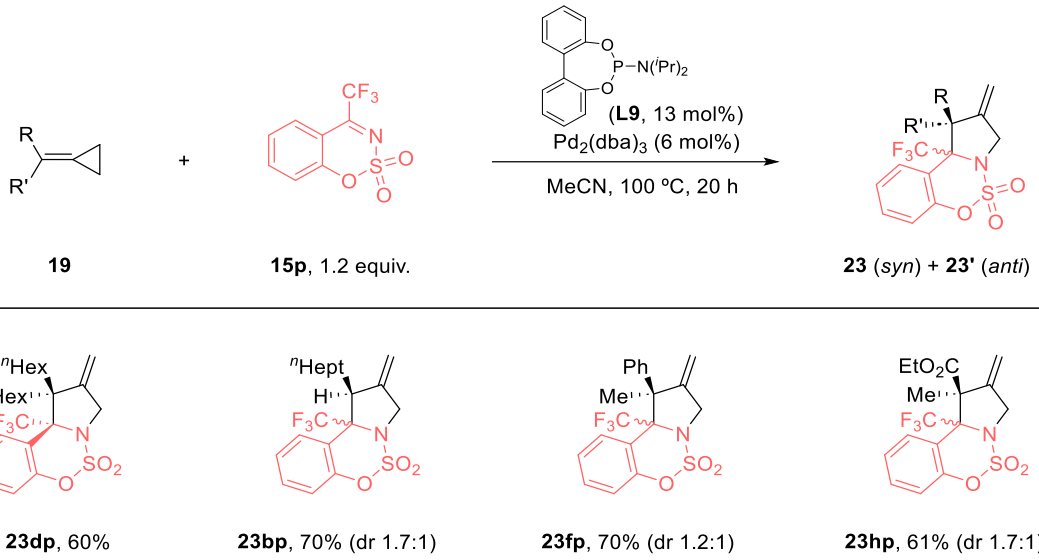

Scheme 97. Scope for (3+2) intermolecular cycloaddition between ACPs and trifluoromethyl ketimines **15p**.

We next examined ketimine **15q**, bearing an ester group, and **15r**, bearing a phenyl ring. The reaction between the imine **15q** and the ACP **19b** afforded the pyrrolidine **23bq** in good yield (70%, **Scheme 98**). Meanwhile, the use of the disubstituted ACP **19d** also led to the desired pyrrolidine (**23dq**), but in a lower yield (43%). Similarly, the reaction between the phenyl ketimine **7r** and the ACP **19b** yielded the product **23br** in a good 82% yield, but when using the disubstituted ACP **19d**, the efficiency of the reaction was significantly affected (10% yield, after 20 h).

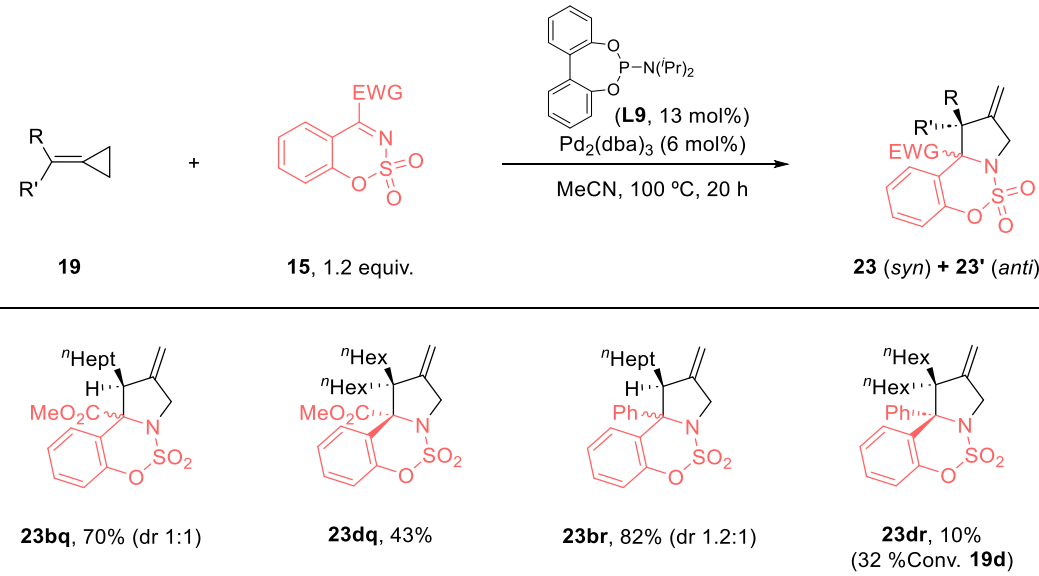

Scheme 98. Scope for (3+2) intermolecular cycloaddition between ACPs and ketimines **15q** and **15r**.

α, β-Unsaturated imines

We also analyzed the reactivity of α, β-unsaturated tosyl imines such as **15s** and **15t**. These compounds were prepared from benzofuranone and indanone via an aldol condensation with benzaldehyde, followed by a second condensation with tosyl amide to yield the imine (**Scheme 99**).

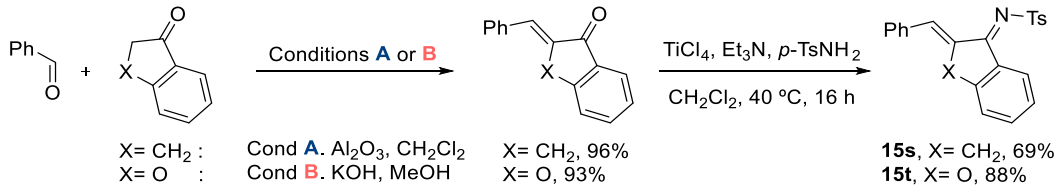

Scheme 99. Synthesis of α, β-unsaturated tosyl imines **15s** and **15t**.

In a preliminary screening, we found that only the highly reactive ACP **19g**, bearing a carboxy ester unit, was able to participate in the cycloaddition with these α, β-unsaturated imines. However, to our surprise, employing the catalyst generated from $Pd_2(dba)_3$/**L9** in MeCN at 70 ºC, the reaction of **19g** with imines **15s** or **15t** did not yield the desired (3+2) adducts, but the corresponding (4+3) derivatives **24gs** and **24gt**, in moderate yields (46 and 37% yield, respectively) and variable diastereoselectivity (dr = 1:0 and 4:1, **Scheme 100**). This is a particularly interesting transformation that will be further studied in the future, to uncover a new direct route to hydrogenated azepines.

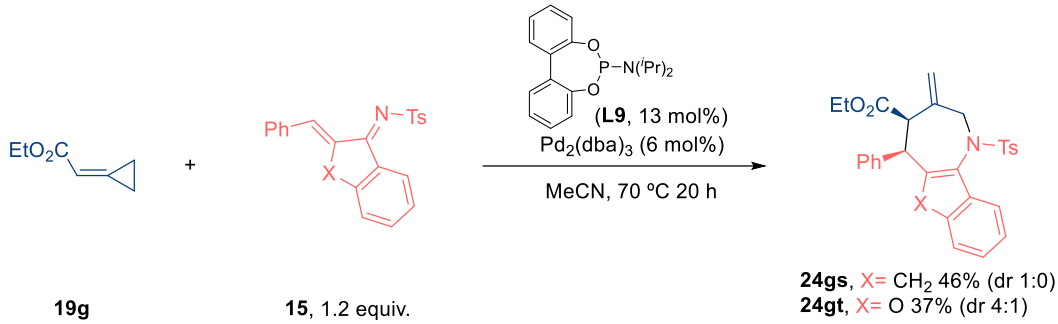

Scheme 100. Formal (4+3) intermolecular cycloaddition between ACP **19g** and α, β-unsaturated tosyl imines **15**.

Curiously, when a related α, β-unsaturated sulfamate imine like **15u** was tested, under otherwise identical conditions, neither the seven-membered ring nor the pyrrolidine cycloadduct were formed (**Scheme 101**). Instead, the reaction afforded the cyclopentane **25gu**, resulting from a (3+2) cycloaddition with the alkene (58% yield as a 3.5:1 mixture of diastereomers). A similar reactivity had been previously reported between vinyl cyclopropanes and α, β-unsaturated imines.[84] Further studies will be performed, varying the Pd(0)-catalyst and/or reaction conditions.[85]

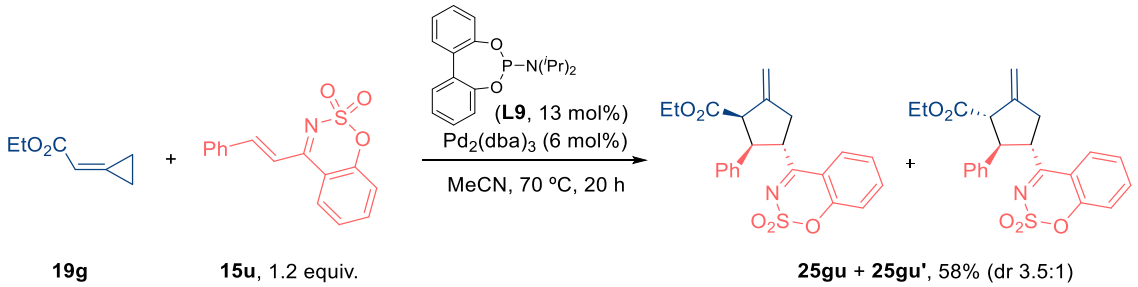

Scheme 101. (3+2) cycloaddition between ACP **19g** and α, β-unsaturated sulfamate-derived imines **15u**.

[84] a) Lin, Y.; Wang, Q.; Wu, Y.; Wang, C.; Jia, H.; Zhang, C.; Huang, J.; Guo, H. Pd-Catalyzed [3 + 2] Cycloaddition of Vinylcyclopropanes with 1-Azadienes: Synthesis of 4-Cyclopentylbenzo[*e*][1,2,3]oxathiazine 2,2-Dioxides. *RSC Adv.* **2018**, *8*, 40798–40803.; b) Qing, Z.; Chen, B.; Huang, X.-B.; Zeng, Y.-L.; Chu, W.-D.; He, L.; Liu, Q.-Z. Palladium-Catalyzed Diastereo- and Enantioselective Formal [3 + 2] Cycloaddition of Vinyl Cyclopropanes with Cyclic 1-Azadienes. *Org. Chem. Front.* **2019**, *6*, 1891–1894.

[85] Other α, β-unsaturated imines, such as tosyl imines derived of *trans*-cinnamaldehyde, did not participate in the cycloaddition.

4.1.4.2 Derivatization of the pyrrolidine cycloadducts

The synthetic potential of the fused pyrrolidines was preliminary analyzed with the model cycloadduct **23de** (**Scheme 102**). This adduct can be easily converted into the free pyrrolidine scaffold **26de** in 78% yield using $LiAlH_4$ at 70 ºC. Moreover, treatment of **23de** with $RuCl_3/NaIO_4$ afforded the 3-pyrrolidinone **27de**, in 65% yield. Alternatively, the *exo*-cyclic double bond can also be reduced with high selectivity under Pd/C conditions, forming **28de** in 58% yield (*syn*/*anti* 4.8:1). Remarkably, the reaction of **23de** with *t*BuOK in DMSO at 70 ºC, not only resulted in the cleavage of the carbamate moiety, but also in a subsequent oxidation, providing the *3H* pyrrole **29de** in 71% yield**.** Worth to note, *3H* pyrroles are the core of several bioactive molecules with antitumoral and antimicrobial properties.[86]

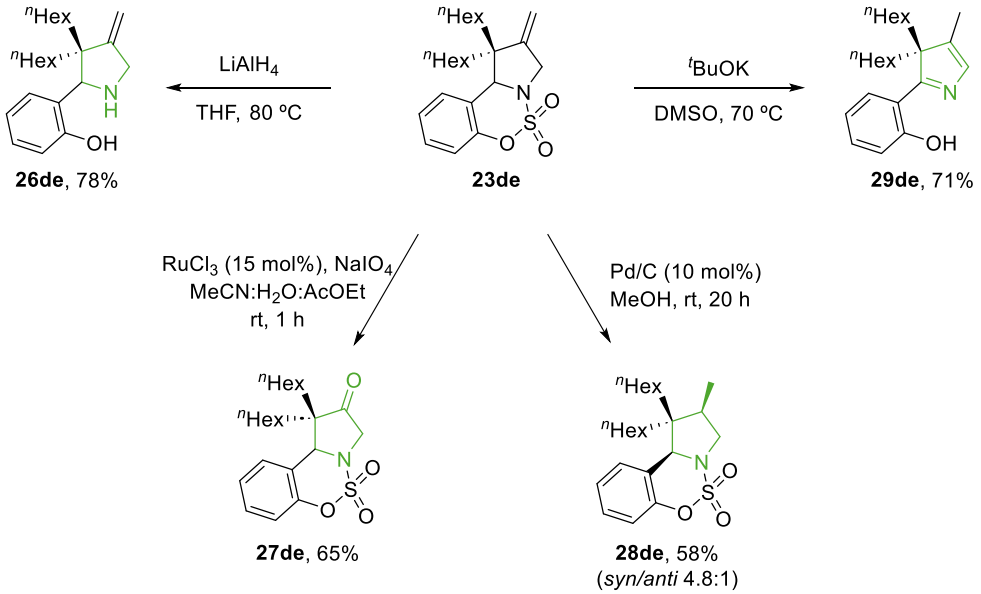

Scheme 102. Synthetic derivatization of the fused pyrrolidine product **23de**.

4.1.4.3 Studies on asymmetric transformations

We evaluated the viability of an enantioselective variant using ACP **9b** and imine **15e** as model substrates. Thus, the catalyst generated from $Pd_2(dba)_3$ (6 mol%) and the (*S*)-BINOL-derived phosphoramidite **(*S,R,R*)-L5** (13 mol%) in dioxane at 100 ºC afforded the pyrrolidine product **16be** in quantitative yield as an equimolar mixture of diastereoisomers (**Table 13**, entry 1). The pyrrolidine **16be** (*syn*) was obtained with 48% ee, while **16be'** (*anti*) was formed with 22% ee. Additionally, we tested the diastereomeric ligand **(*R,R,R*)-L5**, which led to the pyrrolidines **16be** and **16be'** in 77% yield. The ee of **16be** was 26% whereas that of **16be'** turned out to be of 61% (entry 2).

[86] a) Cirrincione. G.; Almerico, A.M.; Grimaudo, S.; Diana P.; Mingoia, F.; Barraja, P.; Misuraca, F. 3-Diazopyrroles. Part 6. Mutagenic activity of 3-diazopyrroles in Streptomyces coelicolor A3(2) during various phases of growth. *Farmaco*, **1996**, *51*, 49-52.; b) Cirrincione. G.; Almerico, A.M.; Dattolo, G.; Aiello, E.; Diana P.; Misuraca, F. 3-Diazopyrroles. Part 5. Antibacterial activity of 3-diazo-2-phenylpyrroles. *Farmaco*, **1992**, *47*, 1555-1562.; c) Padmavathi, V.; Lakshmi, T.R.; Mahesh, K.; Padmaja, A. Synthesis and Biological Activity of a New Class of Sulfone-Linked Pyrrolylpyrazoles and Pyrrolylisoxazoles from Methyl-3-aryl-2-(*E*-arylethenesulfonyl)acrylate. *Chem. Pharm. Bull.* **2009**, *57*, 1200-1205.

Table 13. Initial asymmetric approach to the (3+2) intermolecular cycloadditions.

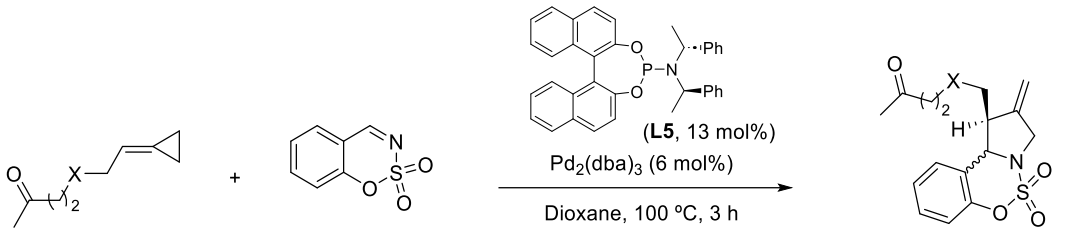

9b, X=C(CO_2Me)$_2$ **15e**, 1.2 equiv. **16be** : **16be'** (*syn:anti*)

Entry	Ligand	16be+16be',% (dr)	16be (% ee)	16be' (% ee)
1	**(S,R,R)-L5**	99 (1:1)	48	22
2	***(R,R,R)*-L5**	77 (1:1)	26	61

We next performed a brief screening of solvents, using the Pd-catalyst involving ***(S,R,R)*-L5** (**Table 14**). Different solvents allowed to obtain the cycloadduct **16be** in very good yields (78 – 99%, entries 1-5). However, the ee's were lower than those achieved using dioxane as solvent (entry 1).

Table 14. Solvent screening using the Pd-catalyst with ***(S,R,R)*-L5** as ligand.[a]

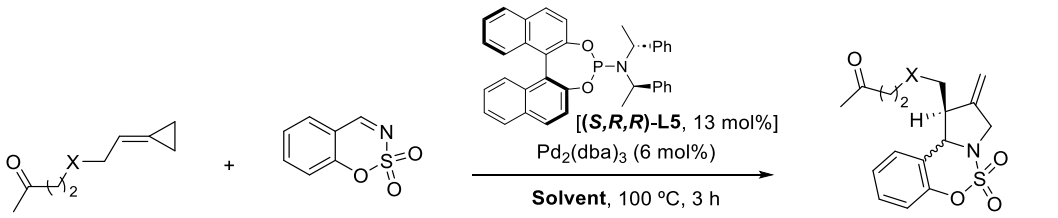

9b, X=C(CO_2Me)$_2$ **15e**, 1.2 equiv. **16be** (*syn*) **: 16be'** (*anti*) 1:1

Entry	Solvent	16be + 16be' (%)	16be (% ee)	16be' (% ee)
1	1,4-dioxane	>95	48	22
2	2-Me THF	78	45	9
3	^{t}AmOH	90	32	4
4	Hexane	>95	25	10
5	MeCN	>95	-6	-10

[a] Conditions: **9b**, **15e** (1.2 equiv.), $Pd_2(dba)_3$ (6 mol%), ***(S,R,R)*-L5** (13 mol%), dry solvent (0.05 M), Ar atmosphere, 100 °C, 3 h.

We also conducted a brief screening of precatalysts with ***(S,R,R)*-L5** as ligand (**Table 15**). The use of CpPd(π-cin.) afforded the cycloadduct **16be** in 53% overall yield and almost identical ee's (**16be**: 49% ee and **16be'**: 21% ee, entry 2). Both $Pd(dba)_2$ and $Pd_2(dba)_3{\cdot}CHCl_3$ provided **16be** quantitatively, with very similar ee's (entries 3 and 4). Notably, performing the model reaction with a lower catalyst loading (entry 5) resulted in incomplete conversion and lower enantioselectivities (**16be**: 38% ee and **16be'**: 12% ee, entry 5).

Table 15. Pd(0) source screening with **(*S,R,R*)-L5** as ligand.[a]

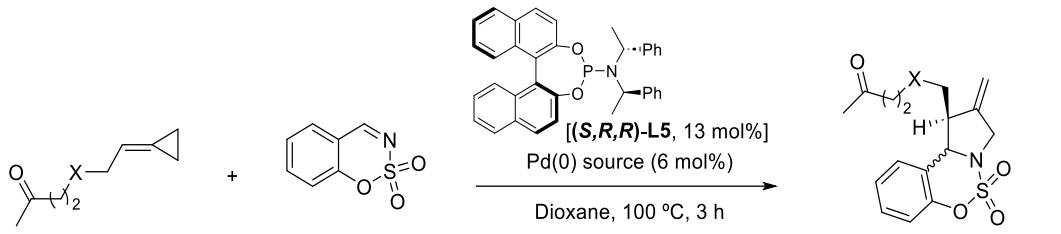

9b, X=C(CO_2Me)$_2$ **15e**, 1.2 equiv. **16be** (*syn*) **: 16be'** (*anti*) 1:1

Entry	Pd(0) source	Conv. **9b** (%)	**16be**+**16be'** (%)	**16be** (% ee)	**16be'** (% ee)
1	$Pd_2(dba)_3$	100	>95	48	22
2	CpPd(π-cin.)	96	53	49	21
3	$Pd(dba)_2$	100	>95	51	14
4	$Pd_2(dba)_3$·$CHCl_3$	100	>95	48	14
5[b]	$Pd_2(dba)_3$	85	68	38	12

[a] Conditions: **9b**, $Pd_2(dba)_3$ (6 mol %), ligand (13 mol %), dry toluene (0.05 M), Ar atmosphere, 110 °C. Conversion of **9b** >99%. [b] 75%Conv. of **9b**. [b] $Pd_2(dba)_3$ (3 mol%) and **(*S,R,R*)-L5** (7 mol%).

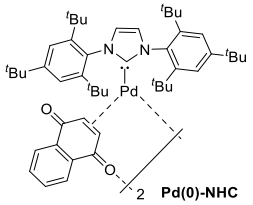

Finally, we explored different chiral phosphoramidites, instead of **(*S,R,R*)-L5**, under optimal conditions, using $Pd_2(dba)_3$ (6 mol%) in dioxane at 100 ºC. The main results are presented on **Table 16**.

Using the biphenol-derived phosphoramidite **(*S,S*)-L10**, the diastereomeric cycloadducts were obtained in quantitative yield but both with moderate ee's (**16be**: 44% ee and **16be'**: 35% ee). The use of the BINOL derivative **(*R,R,R*)-L11**, bearing a 1-(naphthalen-1-yl)ethyl)amine, led to the an excellent global yield, and moderate enantioselectivities of both **16be'** (-64% ee) and **16be** (-40% ee). Other ligands like **(*R,R,R*)-L12** and **(*R,R,R*)-L13**, as well as those featuring aryl groups at the 3,3'-positions of the BINOL [e.g. **(*S,R,R*)-L14** or **(*R,R,R*)-L15**], afforded the desired cycloadducts in very good yield, but poor enantioinductions. Regarding VANOL derivatives, the use of **(*S,R,R*)-L16** afforded the pyrrolidine **16be** in 81% yield, with moderate enantioselectivities (**16be**: -49% ee and **16be'**: -58% ee).

The best result was obtained with the VANOL derivative **(*S,R,R*)-L2**, bearing a bulkier amine moiety, which provided the desired pyrrolidines in quantitative yield, with remarkable enantioselectivites (**16be**: 77% ee and **16be'**: -78% ee).

Table 16. Selection of the ligand screening for (3+2) intermolecular cycloadditions.

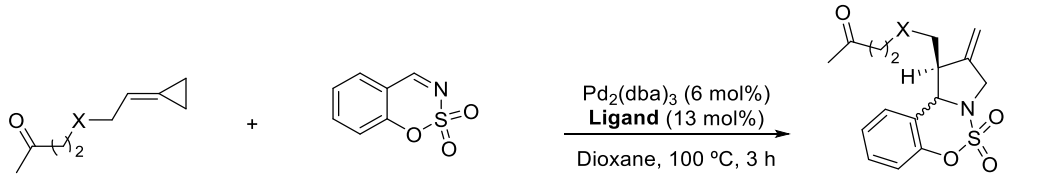

9b, X=C(CO_2Me)$_2$ + **15e**, 1.2 equiv. → **16be** (*syn*) : **16be'** (*anti*) 1:1

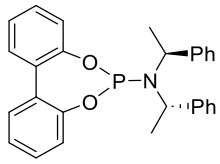

(***S, S***) **- L10**, 99%
44% ee 35% ee

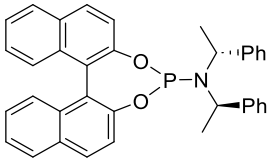

(***S, R, R***) **- L7**, 99% -48% ee 22% ee
(***R, R, R***) **- L7**, 77% -26% ee -61% ee

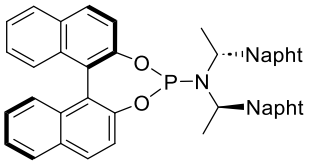

1-Napht: (***R, R, R***) **- L11**, 99%
-40% ee -64% ee
2-Napht (***R, R, R***) **- L12**, 84%
35% ee 48% ee[b]

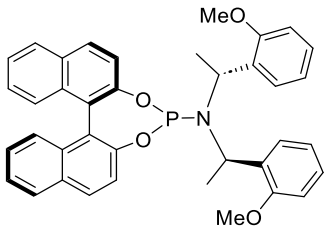

(***R, R, R***) **- L13**, 99%
34% ee 37% ee

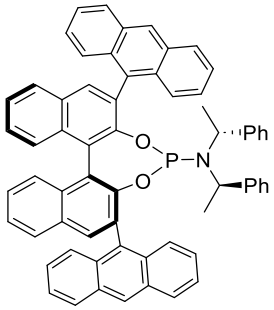

(***S, R, R***) **- L14**, 78%
17% ee -43% ee

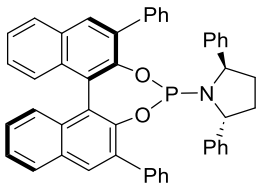

(***R, R, R***) **- L15**, 83%
64% ee 7% ee

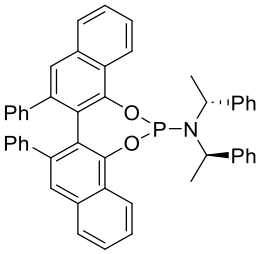

(***R,R,R***)**-L16**, 82% -29% ee 68% ee
(***S,R,R***)**-L16**, 81% -49% ee -58% ee

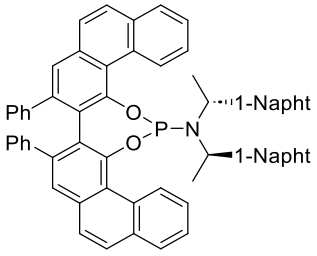

(***S,R,R***)**-L2**, 83% 77% ee -78% ee
(***R,R,R***)**-L2**, 99% 67% ee 72% ee

[a] Conditions: **9b**, **15e** (1.2 equiv.), $Pd_2(dba)_3$ (6 mol%), ligand (13 mol%), in 1,4-dioxane was heated under Ar at 100 ºC. Conversion **9b** > 99%, as determined by ^{1}H–NMR of the crude reaction mixture. Yield determined by NMR with internal standard. Diastereomeric ratio by ^{1}H–NMR of the crude reaction mixture. **16be**:**16be'** dr = 1:1, unless otherwise noted. Negative ee values imply that the minor enantiomer elutes first. [b] dr = 1.4:1.

Scope of the intermolecular asymmetric transformation

The scope of the asymmetric transformation was explored using ligand **(*R,R,R*)-L11**, instead of **(*R,R,R*)-L2,** as it is less expensive and easier to prepare, while its performance in the model reaction (see **Table 16**, page 107) is more or less similar than that of **L2** (**Scheme 103**).[81]

Treatment of ACP **9b** and imine **15e** with the catalyst derived from $Pd_2(dba)_3$ and **(*R,R,R*)-L11** provided the corresponding pyrrolidine isomers in overall quantitative yield. Unfortunately, the ee of **16be** was only of 40% whereas that of **16be'** was of 64%. The cycloaddition of precursor **9b** and the cyclic imine **15h** promoted by this Pd(0)-catalyst, led to the cycloadducts in a good 83% yield, but poor enantioselectivities (**16bh**: 28% ee and **16bh'**: 50% ee). With other monosubstituted ACP precursors, such as **19b** or **19g**, the reaction afforded the pyrrolidines **23** in good to excellent yields but again, with poor enantioselectivities, below 40% ee.

In addition, the performance $Pd_2(dba)_3$/**(*R,R,R*)-L11** was also tested in the cycloadditions between the ACP **19d** and different imine counterparts; but again, the corresponding products were obtained with modest enantioselectivities.

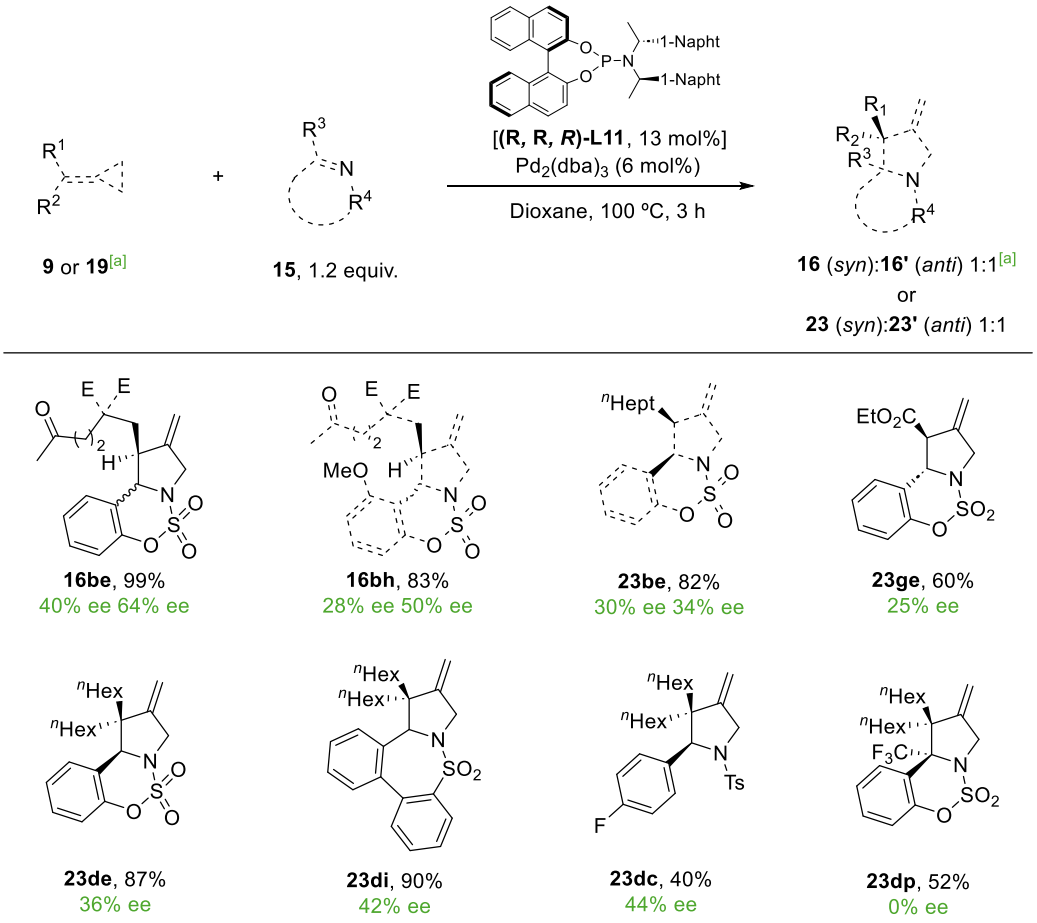

Enantiomeric excess (ee) presented as absolute values. E = CO_2Et

[a]See footnote 81.

Scheme 103. Scope for (3+2) intermolecular cycloaddition using $Pd_2(dba)_3$/**(*R,R,R*)-L11**.

[81] For clarity and consistency with the following sections of the manuscript, ACPs precursors tethered to ketone moieties are labeled as **9**, while the substrates without carbonyl moieties are named **19**. Consequently, the corresponding intermolecular (3+2) cycloadducts between ACPs and imine partners, are named as **16** (from ACPs **9**) and **23** (from ACPs **19**).

4.1.4.4 DFT mechanistic studies

To shed light on the mechanism of these intermolecular (3+2) cycloadditions, we performed a DFT computational analysis. As model substrates, we selected the dihexyl ACP **19d** and the sulfamate-derived imine **15e**, while the Pd(0)-catalyst featuring the phosphoramidite **L9** was used as model catalyst. As in the intramolecular variant, we employed the B3LYP-GD3/6-31G(d) (LANL2DZ for Pd) level of theory for the optimization of stationary points, and B3LYP-GD3/6-311++G(d,p) (SDD for Pd) for the single-point energy calculations, using acetonitrile as solvent. The calculated energy profile is shown in **Figure 13** and the key stationary points are depicted in **Figure 14**.

In analogy to the intramolecular transformation, the reaction starts with the coordination of the Pd(0)-catalyst to the distal C-C bond of the cyclopropane (**I12**), and evolves through an oxidative addition toward the palladacyclobutane **I13** (ΔG=4.3 kcal·mol^{-1}, **Figure 13**). Notably, this Pd complex exhibits an agostic interaction with a hydrogen atom of one of the isopropyl groups of the ligand [*d*(H–Pd) = 2.5 Å, **Figure 14**].

After coordination of the imine **15e** to **I13**, a migratory insertion, via **TS14-15**, leads to **I15** (see **Figure 14**). Remarkably, the associated energy barrier, of only 1.9 kcal·mol^{-1}, is significantly lower than that observed for the intramolecular cycloaddition (7.9 vs 10.6 kcal·mol^{-1}, **TS14-15** vs **TS3-4**). Then, the π-allyl azapalladacycle **I15**, can easily evolve to the more stable σ-allyl species **I16**, featuring a Pd-H γ-agostic interaction with the isopropyl moiety of **L9** [*d*(H–Pd) = 2.5 Å, **Figure 14**].

Intermediate **I16** can evolve through a reductive elimination (**TS16-23de**) toward the product, with an energy barrier of 30.6 kcal·mol^{-1}. However, its evolution towards the square planar species **I17**, with the coordination of a sulfonamide oxygen to Pd [*d*(O–Pd) = 2.5 Å, **Figure 14**], enables a more accessible reductive elimination path (**TS17-23de**, ΔG=20.0 kcal·mol^{-1}). This new transition state, **TS15-23de**, involves a π-allyl Pd complex; whereas **TS14-23de** holds a σ-allyl conformation (**Figure 14**). Therefore, the reductive elimination via **TS15-23de** would be the turnover determining step of the intermolecular process.

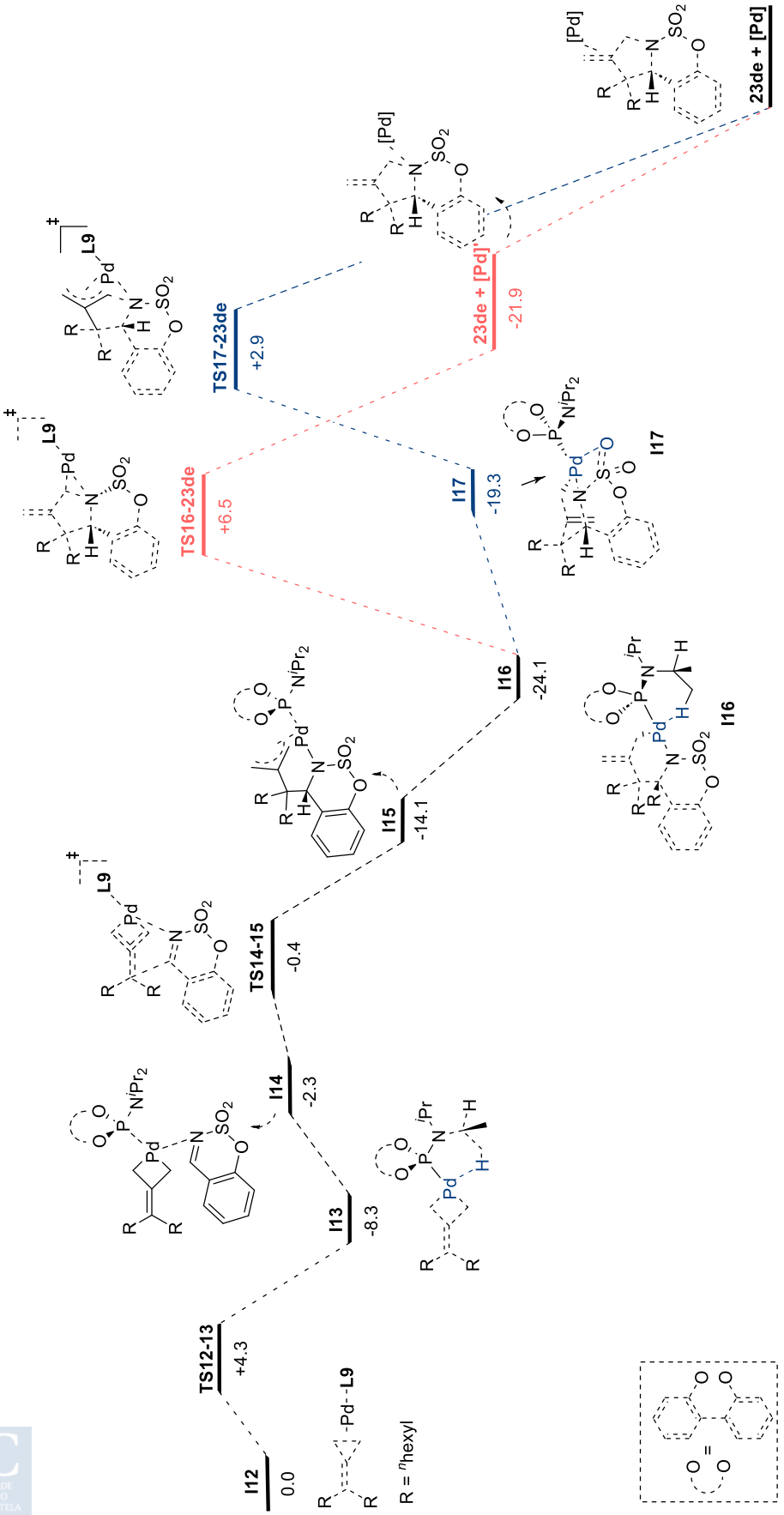

Figure 13. DFT-calculated energy profile ΔG_{solv} (kcal·mol^{-1}) for the intermolecular (3+2) cycloaddition between **19d** and **15e** using Pd(0)-**L9** in acetonitrile, with [B3LYP-GD3/6-31G(d) (LANL2DZ for Pd)//B3LYP-GD3/6–311++g(d,p) (SDD for Pd)].

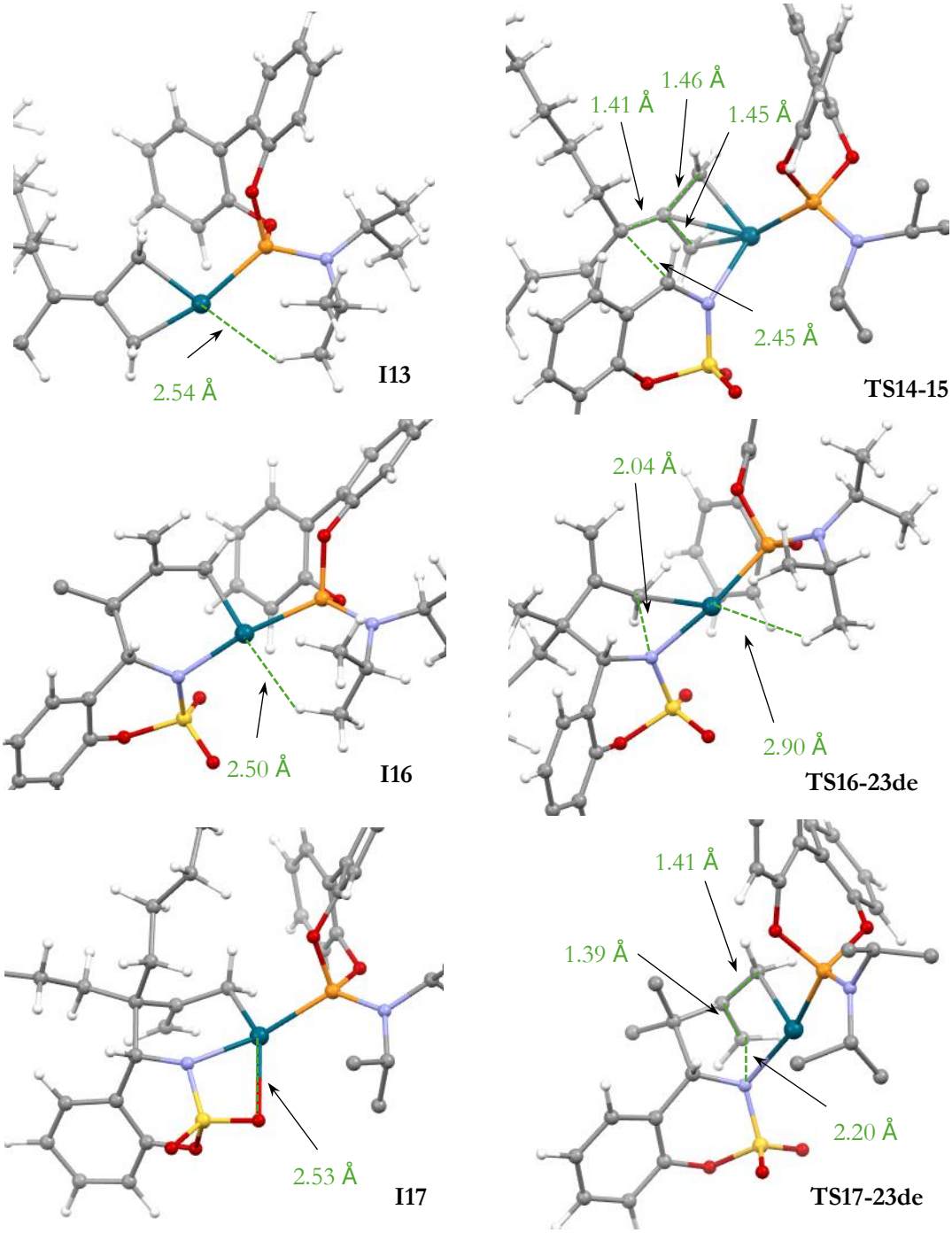

Figure 14. Selected simplified 3D representations of the most relevant structures of **Figure 13**.

Analysis of the chemoselectivity of the migratory insertion using carbonyl-tethered precursors like 9b

We also performed a preliminary computational analysis of the chemoselectivity in the reaction between the carbonyl-tethered ACP **9b** and the cyclic sulfamate-derived imine **15e**, using Pd(0)/*t*BuXPhos (**Pd1)** as model catalyst. Experimentally we observed the pyrrolidine **16be** instead of the bicyclic fused intramolecular oxaadduct **17b** (see **Table 9**, entry 5, page 92). Given that these cycloadditions are not under thermodynamic control, and assuming that both C-heteroatom reductive eliminations may involve similar energy barriers, we focused our attention on the migratory insertion steps.

As model substrates, we employed carbonyl-tethered ACP **9d**, which is very similar to the experimentally used substrate **9b** without the malonate functionality in the tether, and the sulfamate-derived cyclic imine **15e** (**Figure 15**).

The study began from the palladacyclobutane **I18**, which bears the carbonyl chain extended and a secondary interaction between the C*ipso* of the biaryl and the metallic center. A conformational folding of the chain in **I18**, affords **I19**, which has the carbonyl moiety appropriately located for a subsequent intramolecular migratory insertion. This transition state, **TS19-20**, entails a 19.9 kcal·mol^{-1} energy barrier from **I18**, and leads to the π-allyl intermediate **I20**.

Alternatively, the approximation of the imine **15e** to **I18** leads to the more stable intermediate, **I21**, which easily undergoes an intermolecular migratory insertion of the imine, via a TMM-like transition state (**TS21-22**), to give the π-allyl intermediate **I22**. Remarkably, the energy penalty for this step is only of 2.0 kcal·mol^{-1} from **I21**, much less energetic than the intramolecular migratory insertion over the carbonyl [ΔΔG(**TS19-20–TS21-22**)=17.9 kcal·mol^{-1}].

These results are in consonance with the experimental results obtained with the catalyst generated from $Pd_2(dba)_3$ and *t*BuXPhos, which shows electivity towards the external imine, to give the intermolecular (3+2) cycloaddition (**Table 9**, entry 11, page 92).

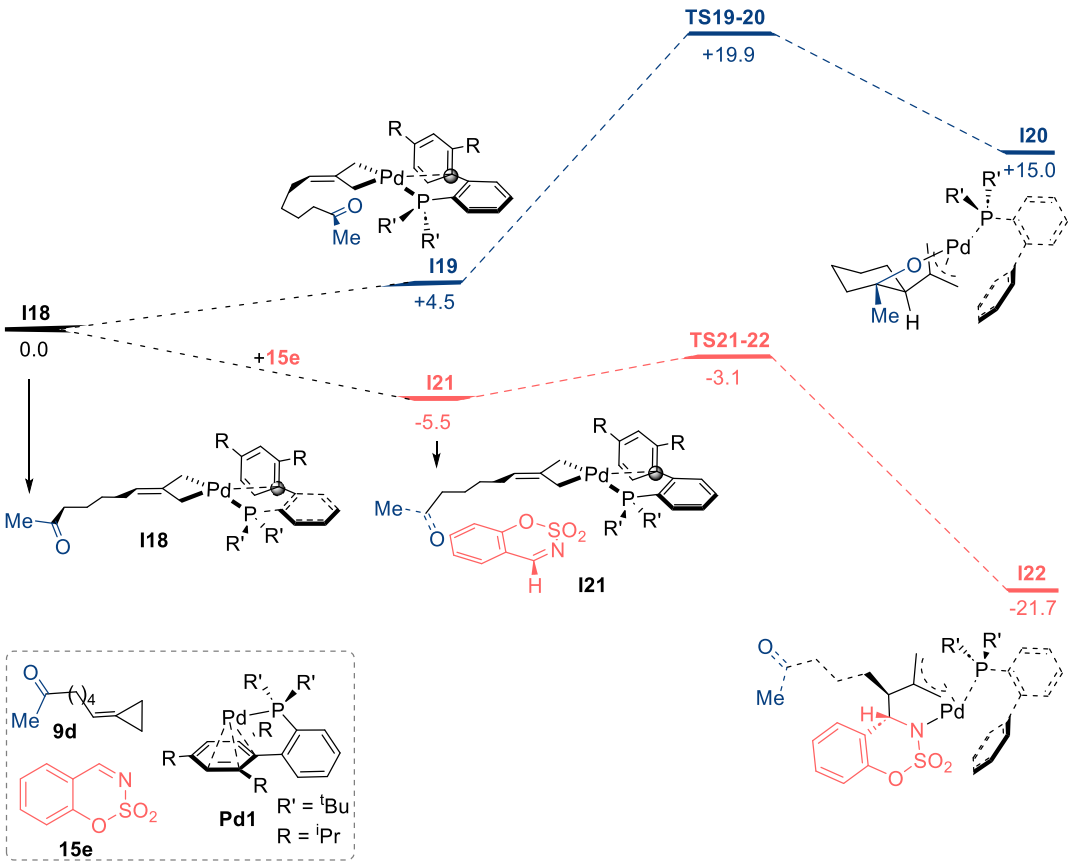

Figure 15. Study of the migratory insertion for the carbonyl-tethered ACP **9d** and imine **15e** using Pd(0)/*t*BuXPhos (**Pd1**), in 1,4-dioxane [ΔG_{solv} (kcal·mol^{-1})]. [B3LYP-GD3/6-31G(d) (LANL2DZ for Pd)//B3LYP-GD3/6–311++g(d,p) (SDD for Pd)].

4.1.5 Conclusions

In summary, we have developed new inter- and intramolecular Pd(0)-catalyzed (3+2) cycloadditions between ACPs and C=N partners, enabling the synthesis of a variety of pyrrolidines and pyrrolidine-fused polycyclic systems, featuring β-*exo*-methylene moieties.

Regarding the intramolecular transformation, the cycloaddition of ACPs tethered to oxime ethers proved to be highly sensitive to structural features of the substrates, providing the desired cycloadducts **2** only when precursors bearing a diester moiety at the tether were used, whereas dienic by-products **3** and **4** were obtained in many of the cases. The limited scope was attributed to difficulties in the C=N migratory insertion of the oxime ether, but efforts to enhance reactivity using acidic additives and electron-poor imines proved unsuccessful.

Mechanistic DFT studies using Pd(0)-*t*BuXPhos as model catalyst, confirmed that these cycloadditions occur via an initial insertion of the Pd complex into the distal C–C bond of the ACP, followed by a metalloene rearrangement and a final reductive elimination. We also identified a novel stepwise path leading to dienes **4**, a pathway that energetically competes with the cycloaddition ($\Delta\Delta G$ = 1.0 kcal·mol^{-1}). These theoretical results are in qualitative agreement with experimental data, which shows that diene **4** is the major product in many cases with these Pd(0) catalysts.

Remarkably, the computations showed the importance of secondary hemilabile interactions between the Pd center and the Buchwald ligand, as well as the relevance of the ligand conformation in stabilizing reaction intermediates.

Regarding the intermolecular variant, the catalyst generated from $Pd_2(dba)_3$ and **L9** facilitates the (3+2) cycloaddition between ACPs and sulfonyl imines. A range of cyclic and acyclic imines, including ketimines, participate in the process, leading to functionalized pyrrolidines in high yields. Additionally, studies on the enantioselective version enabled to find out that **(*S,R,R*)-L2** is the ligand that so far provides the highest enantioselectivity, of 78% ee.

Finally, DFT computations with the Pd(0)-**L9** catalyst supported a palladaene process for the cycloaddition, similar to that of the intramolecular transformation, and underscored again the importance of hemilabile interactions between the Pd center and specific atoms of the bulky ancillary ligand.

4.2 A DFT Mechanistic Study of Pd(0)-Catalyzed (3+2) Cycloadditions between ACPs and Carbonyls

Part of the contents of this section are published in:

Verdugo, F.[a]; da Concepción, E.[a]; Rodiño, R.[a]; Calvelo, M.[a]; Mascareñas, J. L.[a]; López, F.[a, b] Pd-Catalyzed (3 + 2) Heterocycloadditions between Alkylidenecyclopropanes and Carbonyls: Straightforward Assembly of Highly Substituted Tetrahydrofurans. *ACS Catal.* **2020**, *10*, 14, 7710–7718. DOI: 10.1021/acscatal.0c01827

Authors' affiliations:

[a] Centro Singular de Investigación en Química Biolóxica e Materiais Moleculares (CiQUS) and Departamento de Química Orgánica, Universidade de Santiago de Compostela 15782 Santiago de Compostela (Spain).

[b] Misión Biológica de Galicia Consejo Superior de Investigaciones Científicas (CSIC) 36080 Pontevedra (Spain).

4.2.1 Precedents

As mentioned in the *Introduction*, ACPs can participate in numerous transition metal-mediated cycloadditions as 3C synthons. However, examples of their cycloadditions with carbonyl compounds are scarce. Indeed, the only precedent is the work of Yamamoto in 2001, describing a TMC (3+2) cycloaddition between ACPs and aromatic aldehydes, but the scope is very limited and the reaction requires neat conditions (**Scheme 49**).[36]

Considering these scarce precedents, and the lack of intramolecular variants of these cycloadditions with carbonyl partners, our group explored these processes at the first stages of my PhD. During the optimization with model substrates like the aldehyde **7a** or the methyl ketone **9e** (**Table 17**), Dr. Verdugo found that bulky phosphites, phosphoramidites or phosphine oxides, typically used for promoting Pd-catalyzed (3+2) cycloadditions between ACPs and carbon-based unsaturated partners, failed to give the cycloadducts in good yields (entries 1-3). However, Pd(0) complexes equipped with Buchwald's biaryl phosphines, which had been traditionally used for Pd-mediated C-N and C-O cross-couplings,[87] were excellent catalysts for promoting these (3+2) cycloadditions (entries 4 and 5). For aldehydes, the optimal conditions involved a catalyst derived from $Pd_2(dba)_3$ and BrettPhos, in toluene at 100 ºC; whereas for ketones, the use of RuPhos, instead of BrettPhos, provided better results, at 110 ºC.

Table 17. Screening conditions for the intramolecular Pd-catalyzed (3+2) cycloaddition of ACPs and aldehydes or ketones.

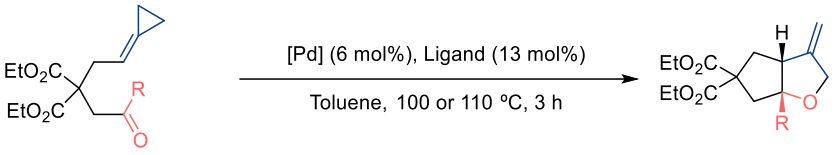

7a, R = H
9e, R = Me

30a, R = H
17e, R = Me

Entry	7/9, R	T (ºC)	[Pd]	Ligand	Yield 30 / 17 (%)
1	**7a**, H	100	$Pd_2(dba)_3$	L1	-
2	**7a**, H	100	$Pd_2(dba)_3$	L2	**30a**, 20
3	**7a**, H	100	$Pd(PPh_3)_4$	$P(O)Bu_3$	**30a**, 20
4	**7a**, H	100	$Pd_2(dba)_3$	RuPhos	**30a**, 45
5	**7a**, H	100	$Pd_2(dba)_3$	*t*BuXPhos	**30a**, 74
6	**7a**, H	100	$Pd_2(dba)_3$	BrettPhos	**30a**, 75
7	**7a**, H	100	$Pd_2(dba)_3$	XPhos	**30a**, 71
8	**9e**, Me	110	$Pd_2(dba)_3$	BrettPhos	**17e**, 65
9	**9e**, Me	110	$Pd_2(dba)_3$	*t*BuXPhos	**17e**, 80
10	**9e**, Me	110	$Pd_2(dba)_3$	RuPhos	**17e**, 90

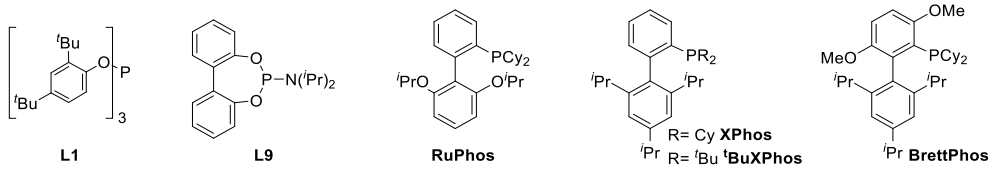

[36] Nakamura, I.; Oh, B. H.; Saito, S.; Yamamoto, Y. Novel [3+2] Cycloaddition of Alkylidenecyclopropanes with Aldehydes Catalyzed by Palladium. *Angew. Chem. Int. Ed.* **2001**, *40*, 1298–1300.
[87] Ingoglia, B. T.; Wagen, C. C.; Buchwald, S.L. Biaryl monophosphine ligands in palladium-catalyzed C–N coupling: An updated User's guide. *Tetrahedron* **2019**, *75*, 32, 4199-4211.

The transformation, studied by Dr. Verdugo, proved to be highly versatile, leading to appealing *exo*-methylene 5,5- and 6,5-fused oxabicyclic adducts (15 examples), in high yields and with excellent diastereoselectivities (**Scheme 104**).[40]

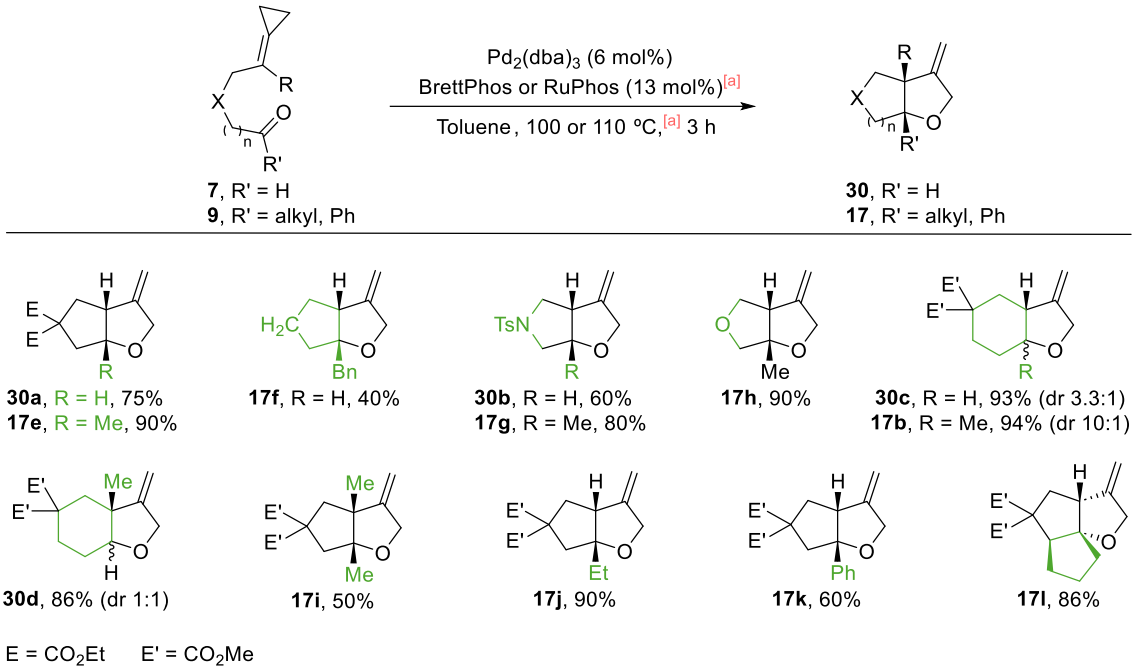

[a]BrettPhos (100 ºC) for aldehydes **7**, RuPhos (110 ºC) for ketones **9**

Scheme 104. Pd-catalyzed intramolecular cycloaddition between ACPs and carbonyls (selected examples).

Considering the broad scope of the intramolecular processes, Dr. da Concepción explored the viability of intermolecular variants. These studies revealed that the above catalysts are not efficient when carbonyl partners such as benzaldehyde or acetophenone. However, the use of trifluoromethyl ketones allowed the reaction to occur efficiently. In particular, when ACP **19j** and trifluoroacetophenone (**31a**) were refluxed in toluene, in the presence of $Pd_2(dba)_3$ and a Buchwald ligand, like XPhos, BrettPhos or *t*BuXPhos, the desired cycloadducts were obtained in excellent yields (**Table 18**). Remarkably, the method leads to β-methylene THFs (10 examples) with excellent yields, and modest diastereoselectivities.

[40] Verdugo, F.; da Concepción, E.; Rodiño, R.; Calvelo, M.; Mascareñas, J. L.; López, F. Pd-Catalyzed (3 + 2) Heterocycloadditions between Alkylidenecyclopropanes and Carbonyls: Straightforward Assembly of Highly Substituted Tetrahydrofurans. *ACS Catal.* **2020**, *10*, 14, 7710–7718.

Table 18. Screening conditions for the intermolecular Pd-catalyzed (3+2) cycloaddition of ACPs and trifluoromethylated ketones.

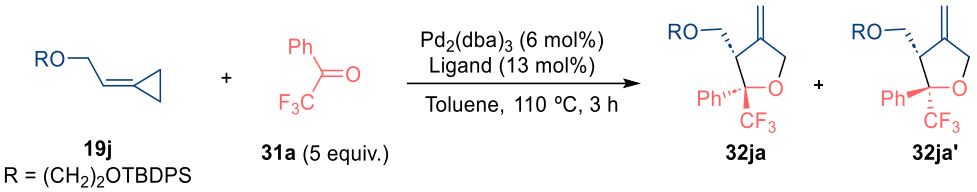

19j
R = $(CH_2)_2OTBDPS$

31a (5 equiv.)

32ja

32ja'

Entry	Ligand	Yield (%)	32ja:32ja'
1	XPhos	81	1.5:1
2	BrettPhos	82	1.4:1
3	^{t}BuXPhos	87	1.6:1
4	RuPhos	96	1.4:1

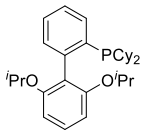

RuPhos

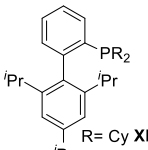

R= Cy **XPhos**
R= ^{t}Bu **^{t}BuXPhos**

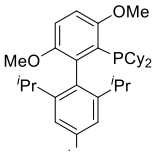

BrettPhos

4.2.2 Objectives

The above transformation between ACPs and carbonyl moieties was only found efficient and general when Buchwald ligands like *t*BuXphos or RuPhos were used.

With my experience in DFT calculations, we aimed to use this type of studies to uncover mechanistic insights into the heterocycloadditions described in **Scheme 105**, and to understand the role of the ligands.

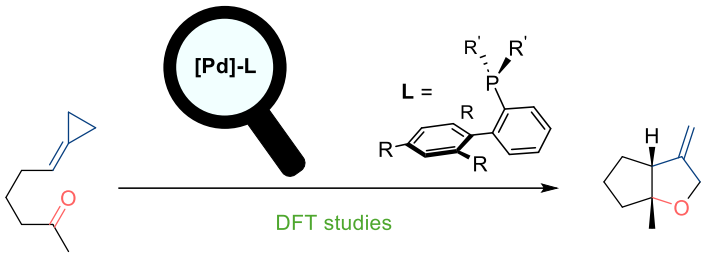

Scheme 105. DFT studies with experimentally relevant ligands.

4.2.3 Analysis of the Intramolecular Oxacycloaddition

4.2.3.1 Initial hypothesis

Considering prior mechanistic information gathered for the Pd-catalyzed (3 + 2) cycloadditions,[27, 88] we hypothesized that the current annulations with carbonyls might proceed by an initial insertion of the Pd(0) complex into the distal C–C bond of the cyclopropyl ring, to yield a palladacyclobutane intermediate of type **A** (**Figure 16**). This species might then undergo a rearrangement to its *exo*-methylene isomer of type **B**, prior to carbonyl coordination and migratory insertion to yield an oxapalladacycle of type **C** (**Figure 16**, route a). Alternatively, species **A** could engage in a metallo–ene process to directly afford species **C** (**Figure 16**, route b), which would eventually provide the product through a C–O reductive elimination. The precise role of the biaryl ligand, facilitating the overall process, was unclear at this stage.

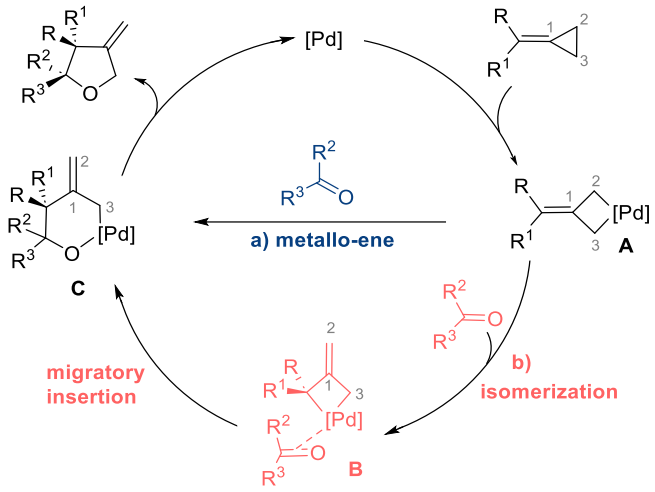

Figure 16. Initial mechanistic hypothesis based on prior work.

To discern between these two mechanistic alternatives, we performed a DFT analysis of the intramolecular cycloaddition of **9m** (**Figures 17** and **18**), which is very similar to the experimentally used substrate **9f**, but lacks the diester group in the connecting tether (see **Scheme 104**, *Precedents*, page 118). Related precursors lacking the diester also undergo the cycloaddition reaction,[30] so it can be considered a valid model.

In a first approach, we chose PH_3 as model ligand to explore the proposed reaction pathways saving computation time while keeping the rough electronic properties of the system. We then conducted the same studies using ^{t}BuXPhos, as model Buchwald ligand, as it provides optimal results in all types of reactions (with aldehydes, ketones and in intermolecular cases) (see **Table 17**, entries 5 and 9; **Table 18**, entry 3). In all cases, we employed the B3LYP/6-31G(d) (LANL2DZ for Pd) level of theory, for the optimization of the stationary points, and M06/6–311++g(d,p) (SDD for Pd), in toluene, for the single-point energy calculations.

[27] García-Fandiño, R.; Gulías, M.; Mascareñas, J.L.; Cardenas, D. J. Mechanistic study on the palladium-catalyzed (3 + 2) intramolecular cycloaddition of alk-5-enylidenecyclopropanes. *Dalton Trans.* **2012**, *41*, 9468-9481.

[88] Araya, M.; Gulías, M.; Fernández, I.; Bhargava, G.; Castedo, L.; Mascareñas, J. L.; López, F. Rhodium-catalyzed intramolecular [3+2+2] cycloadditions between alkylidenecyclopropanes, alkynes, and alkenes. *Chem. Eur. J.* **2014**, *20*, 10255– 10259.

[30] Da Concepción, E.; Fernández, I.; Mascareñas, J. L.; López, F. Highly Enantioselective Cobalt-Catalyzed (3+2) Cycloadditions of Alkynylidenecyclopropanes. *Angew. Chem. Int. Ed.* **2021**, *60*, 8182–8188.

4.2.3.2 Studies using PH_3 as model ligand

In consonance with previous studies, the reaction starts with an oxidative addition of the distal C-C bond of the ACP to the palladium catalyst, to reach the palladacyclobutane **I2** (**Figure 17**, ΔG=18.0 kcal·mol^{-1}, from **9m+PdL$_2$**).[89]

From intermediate **I3**, which already holds the carbonyl moiety in an appropriate orientation for the migratory insertion, a metalloene process might occur via **TS3-5**, in which the palladium is unsymmetrically coordinated to the four carbon atoms of the TMM unit. Besides this route, which generates the π-allyl Pd intermediate **I5**, we also located the isomerization of **I3** to the *exo*-methylene palladacyclobutane **I4** (ΔG=16.4 kcal·mol^{-1}). However, the transition state for this step lies 2.3 kcal·mol^{-1} above that of the metalloene process and, more importantly, the subsequent migratory insertion, via **TS4-5**, is significantly more costly (ΔG=29.4 kcal·mol^{-1}), making this pathway very unlikely. These results contrast with previous calculations on cycloadditions between ACPs and unsubstituted alkenes, in which the energy difference between these two types of TS' was minimal, but against the metalloene process (see **Figure 8**, *General Introduction*, page 42).[27]

The reductive elimination from π-allyl intermediate **I5** provides smoothly **17m'** with an energy barrier of 9.9 kcal·mol^{-1}. We also found alternative pathways which could be competitive. In particular, **I5** can also tautomerize to a slightly less stable σ–bound oxa–palladacyclic T-shaped intermediate **I6** (O and P are *cis* to each other).[90] All attempts to obtain a TS for the reductive elimination process from **I6** failed; however, we found that this intermediate can easily evolve to its *trans* derivative **I7**, which can undergo the reductive elimination (**TS7-17m**) with an energy barrier of 21.2 kcal·mol^{-1}.

[89] For additional steps involving two PH_3 ligands attached to the palladium, see **Figure A1** (*Appendix*, page 328).

[27] García-Fandiño, R.; Gulías, M.; Mascareñas, J.L.; Cardenas, D. J. Mechanistic study on the palladium-catalyzed (3 + 2) intramolecular cycloaddition of alk-5-enylidenecyclopropanes. *Dalton Trans.* **2012**, *41*, 9468-9481.

[90] During the studies of the analog cycloadditions between ACPs and alkenes, π-allyl palladacyclic species like **I5** could not be located computationally, so only σ–complexes of type **I4** were found. Indeed, the analog metalloene transition state directly leads to a σ-allyl–Pd intermediate of type **I4**. See reference 27: García-Fandiño, R.; Gulías, M.; Mascareñas, J.L.; Cardenas, D. J. Mechanistic study on the palladium-catalyzed (3 + 2) intramolecular cycloaddition of alk-5-enylidenecyclopropanes. *Dalton Trans.* **2012**, *41*, 9468-9481.

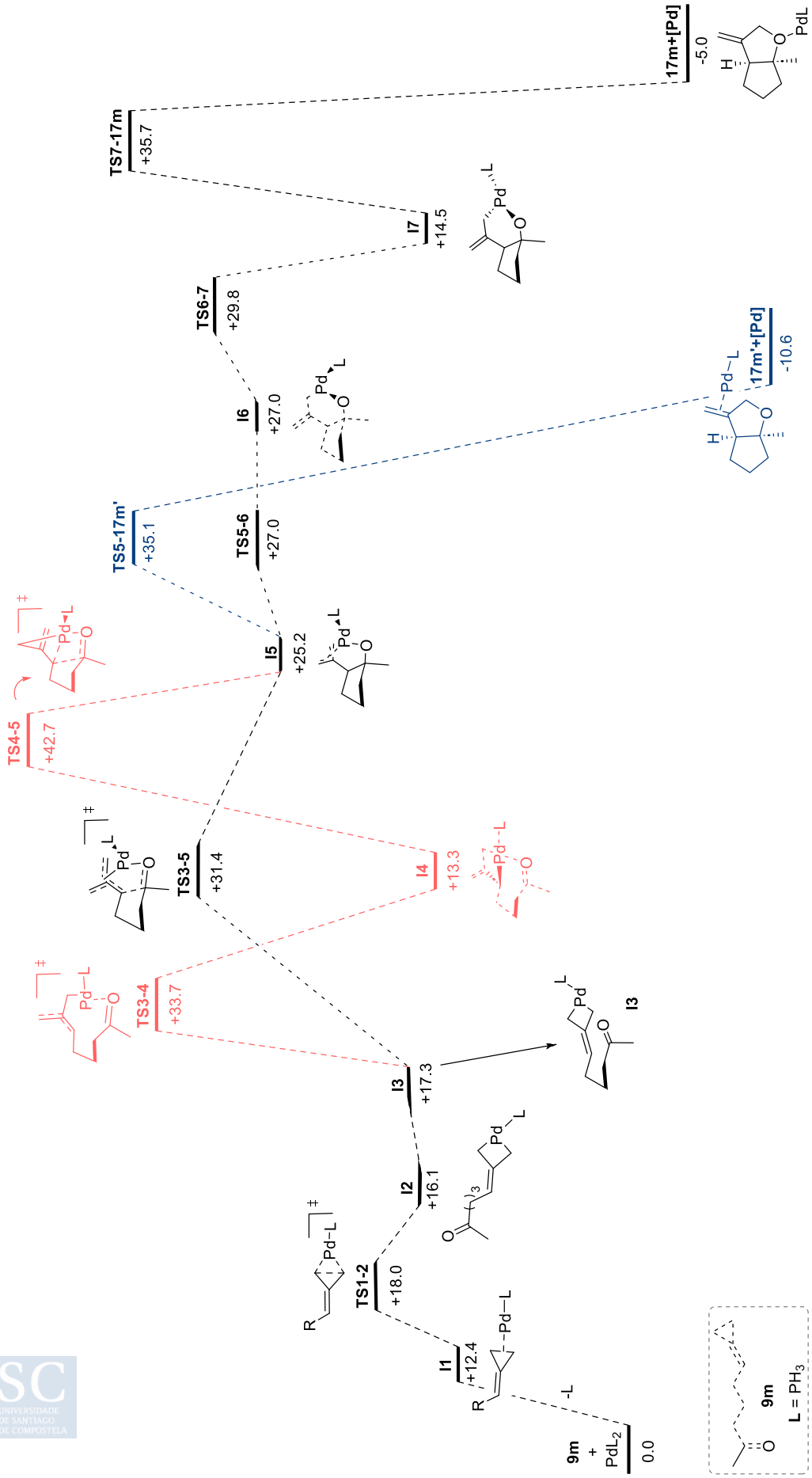

Figure 17. DFT-calculated energy profile ΔG_{solv} (kcal·mol^{-1}) for the cycloaddition of **9m** in toluene. [B3LYP/6-31G(d) (LANL2DZ for Pd)//M06/6–311++g(d,p) (SDD for Pd)].

4.2.3.3 Computational analysis using ^{t}BuXPhos as ancillary ligand

Having studied the overall pathway with PH_3 as ligand, we next explored the energy surface with ^{t}BuXPhos, using as reference the stationary points located with PH_3. Therefore, we performed a detailed DFT analysis of the intramolecular cycloaddition using the Pd(0)-^{t}BuXPhos complex (**Pd1**) as model catalyst (**Table 17**, entry 8, 80% yield). In consonance with previous reports on related Pd-complexes of Buchwald biaryl phosphines,[91] the *in silico* analysis of **Pd1** revealed the bidentate while hemilabile character of the ligand, which coordinates the Pd through the phosphorus and its *ortho*-aryl ring (in particular through C2' and C3', **Figures 18** and **19**).

Upon coordination of the alkylidenecyclopropane moiety through its distal C–C bond (**I8**), the hemilabile Pd–arene interaction is partially loosened, but the aryl ring remains blocking one side of the ACP–Pd complex, almost perpendicular to the Pd plane [*d*(Pd–C1) = 3.21 Å]. The stabilization provided by such Pd(0) interaction is significant, since the energetically closest intermediate lacking this interaction, **I13**, turned out to be >10 kcal·mol^{-1} less stable than **I8** (**Figure 18**).

From intermediate **I8**, the oxidative addition of the ACP takes place through a very accessible activation barrier (**TS8-9**, ΔG = 6.0 kcal·mol^{-1}), to yield the palladacyclobutane species **I9**, a square planar (distorted) intermediate wherein the *ipso* carbon of the biaryl group (C1') occupies the fourth coordination site [*d*(C1'–Pd) = 2.7 Å].[92] This Pd–C*ipso* interaction seems essential for the stability of this palladacyclobutane. Indeed, alternative square planar complexes bearing a γ-agostic interaction with the ^{t}Bu group of the phosphine (**I14**) or related three-coordinate T-shaped isomers lacking any kind of hemilabile interactions (**I14'**)[93] were found to be more than 18 kcal·mol^{-1} less stable than **I9**. In consonance with the high stability of **I9**, the oxidative addition step via **TS8-9** is exergonic by 5.9 kcal·mol^{-1} (from **9m+Pd1**).

These results contrast with those resulting from the use of PH_3 as the model phosphine ligand, as in that case the oxidative addition step was endergonic by 16.1 kcal·mol^{-1} from **9m+PdL$_2$** (**TS1-2**, ΔG=5.6 kcal·mol^{-1}, see **Figure 17**).

From the palladacyclobutane intermediate **I9**, the migratory insertion of the methyl ketone, through a palladaene pathway (route b) was found to involve an energy barrier of 16.0 kcal·mol^{-1} (via **TS9–10**).[94] The resulting σ-allyl oxapalladacycle intermediate **I10** is a square planar complex that holds the oxygen and the phosphorus *cis* to each other. The Pd–C1' interaction, which is now *trans* to the oxygen, has been strengthened, as judged by the shorter Pd–C1' distance (2.61 Å, **I10** vs 2.71 Å, **I9**).

An alternative path, based on a stepwise process involving an initial isomerization to the *exo*-methylene palladacycle of type **B** (see **Figure 16**, page 121) and a subsequent migratory insertion of the carbonyl moiety, could not be located from **I9**; however, this pathway is feasible from the isomeric metallacyclobutane species **I14** (via **I15**), which features a weak Pd–H γ-agostic interaction. Curiously, the generated oxapalladacycle **I16** features a π-allyl ligand (engaging the three carbons of the former

[91] a) Melvin, P. R.; Nova, A.; Balcells, D.; Hazari, N.; Tilset, M. DFT investigation of Suzuki-Miyaura reactions with aryl sulfamates using a dialkylbiarylphosphine-ligated palladium catalyst. *Organometallics* **2017**, *36*, 3664– 3675.; b) Ikawa, T.; Barder, T. E.; Biscoe, M. R.; Buchwald, S. L. Pd-catalyzed amidations of aryl chlorides using monodentate biaryl phosphine ligands: a kinetic, computational, and synthetic investigation. *J. Am. Chem. Soc.* **2007**, *129*, 13001– 13007.; c) Barder, T. E.; Biscoe, M. R.; Buchwald, S. L. Structural insights into active catalyst structures and oxidative addition to (biaryl)phosphine–palladium complexes via density functional theory and experimental studies. *Organometallics* **2007**, *26*, 2183– 2192.

[92] a) Milner, P. J.; Maimone, T. J.; Su, M.; Chen, J.; Mueller, P.; Buchwald, S. L. Investigating the dearomative rearrangement of biaryl phosphine-ligated Pd(II) complexes. *J. Am. Chem. Soc.* **2012**, *134*, 19922– 19934.; b) We also located the isomer of **I9** in which the alkyl chain of the alkene and the P atom are in *anti*-disposition (**I9^{anti}**, **Figure A2,** *Appendix*, page 329).

[93] **I14'**, lacking any Pd-H interaction, is not included in **Figure 17**. Its relative energy is 15 kcal·mol^{-1}.

[94] The evolution of **I9** towards **I10** involves an additional step, from **I9** to **I9'**, which was omitted in the **Figure 17** for clarity. It involves a conformational change consisting of the folding of the carbonyl chain to enable the subsequent palladaene step (**TS9-10**). The relative energy of **I9'** is -2.5 kcal·mol^{-1}.

cyclopropane), a type of intermediate that was not computationally located from palladacyclobutane intermediate **I9**.[95] From π-allyl intermediate **I16**, the reductive elimination was found through an energy barrier of 13.8 kcal·mol^{-1} to give the cycloadduct **17m'**.

All attempts to locate a reductive elimination step from γ-allyl intermediate **I10** were not successful. However, this step was again located from an isomeric *trans* intermediate (**I12**, O and P are *trans* to each other). This complex exhibits a weak γ-agostic interaction between the Pd and a hydrogen atom of a *t*butyl group.[96] The energy value of the reductive elimination, 21.6 kcal·mol^{-1} (via **TS12-17m**), is similar to that calculated for analogous step using PH_3 as ligand [ΔG(**TS12-17m** –**TS7-17m**) < 1 kcal·mol^{-1}]. Therefore, it fits with the heating requirements of the reaction and suggests that it is the turnover limiting step.

Overall, the significant energy differences between the paths starting from **I8** and **I13**, allow to propose the former as the most favorable route. Remarkably, when considering PH_3 as model ligand, instead of *t*BuXPhos, the energy difference among the different routes were much shorter, in consonance with a relevant role for the ligand (**Figure 17** vs **Figure 18**).

[95] As we mentioned in **Figure 16**, this type of π-allyl palladacyclic species was not located in any of the (3 + 2) cycloadditions between ACPs and alkenes, for which a σ-complex of type **C** was found. See reference 27: García-Fandiño, R.; Gulías, M.; Mascareñas, J.L.; Cardenas, D. J. Mechanistic study on the palladium-catalyzed (3 + 2) intramolecular cycloaddition of alk-5-enylidenecyclopropanes. *Dalton Trans.* **2012**, *41*, 9468-9481.

[96] For selected examples on related γ-agostic interactions in Pd(II) complexes, see: a) Stambuli, J. P.; Incarvito, C. D.; Buhl, M.; Hartwig, J. F. Synthesis, structure, theoretical studies, and ligand exchange reactions of monomeric, T-shaped arylpalladium(II) halide complexes with an additional, weak agostic interaction. *J. Am. Chem. Soc.* **2004**, *126*, 1184– 1194.; b) Walter, M. D.; White, P. S.; Brookhart, M. Synthesis, structure and computational studies of a cationic T-shaped Pd-complex. *New J. Chem.* **2013**, *37*, 1128– 1133.

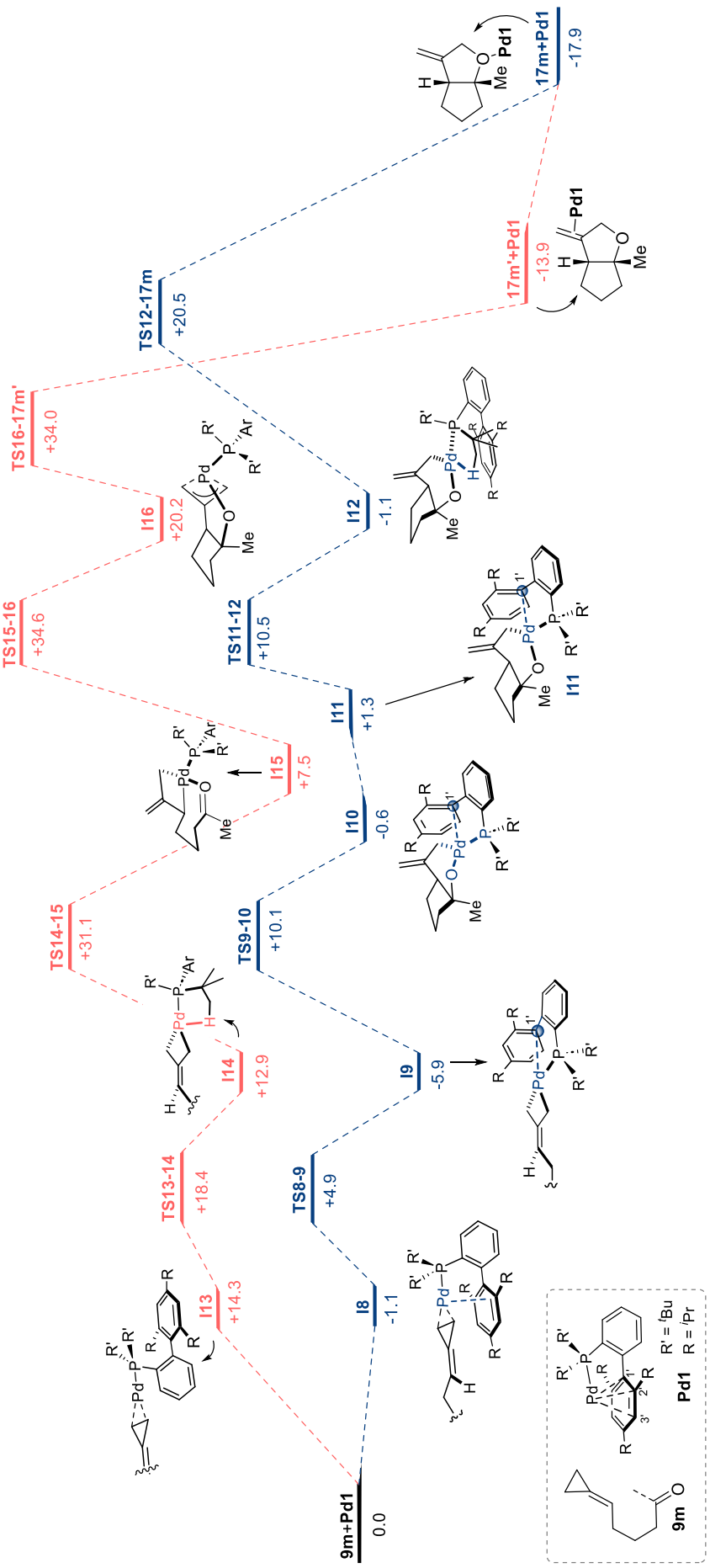

Figure 18. DFT-calculated energy profile ΔG_{solv} (kcal·mol^{-1}) for the (3+2) cycloaddition of **9m** using Pd-BuXPhos (**Pd1**), in toluene. [B3LYP/6-31G(d) (LANL2DZ for Pd)//M06/6–311++g(d,p) (SDD for Pd)]. Some steps were simplified to a better understanding. See **Figure A3** (*Appendix*, page 326) for the complete energy profile.

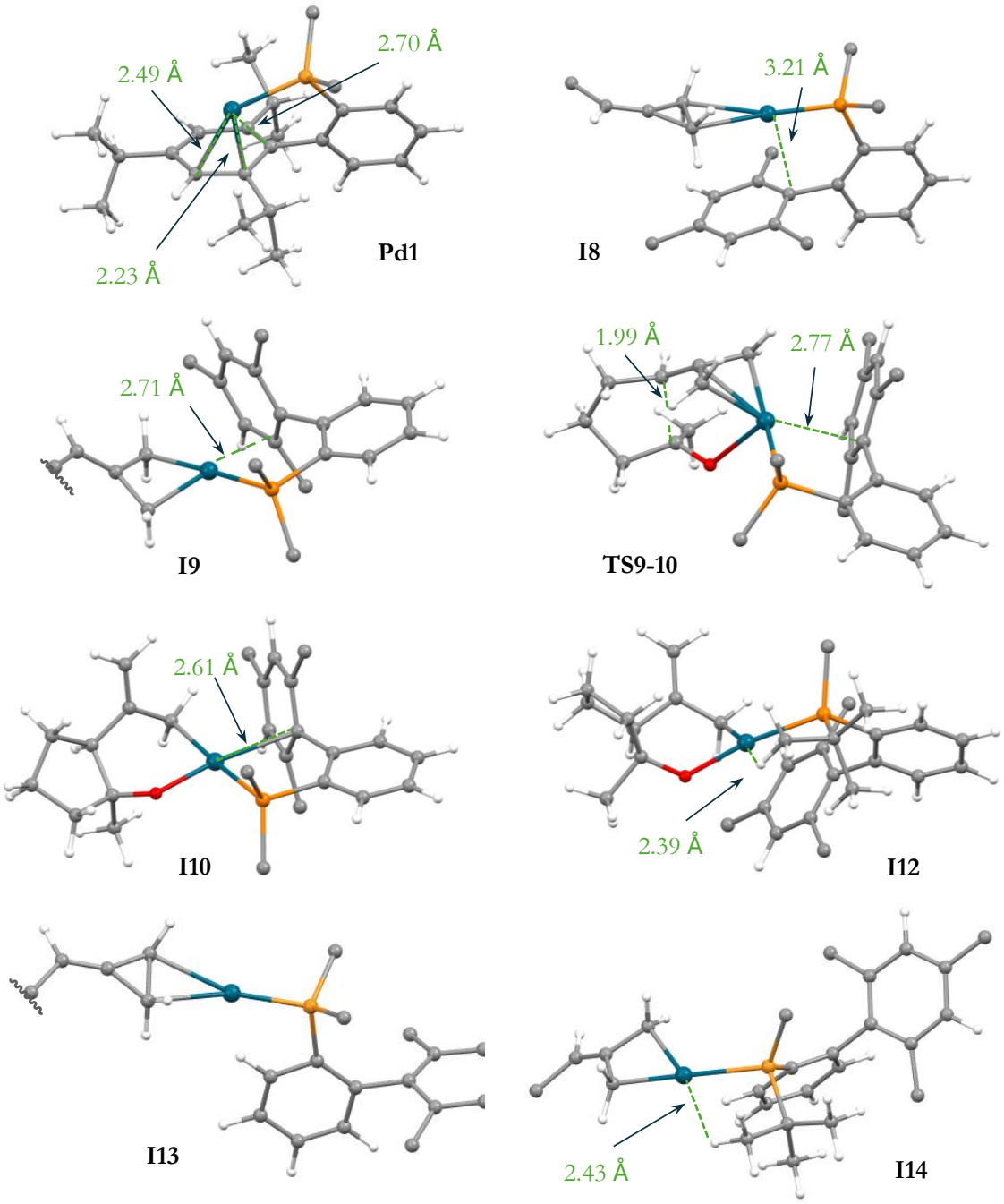

Figure 19. Selected simplified 3D representations of the most relevant structures of **Figure 18**.

In addition to the above-described reductive elimination pathway from the σ-allyl oxapalladacycle **I10** via **I11** and **I12** (**Figure 18**), we identified other alternative routes (**Figure 20**). **I10** and its energetically related rotamer **I17**, can evolve towards their O-P *trans* isomers (**I19** and **I18**, respectively), each featuring a Pd-H γ-agostic interaction, and eventually undergo energetically feasible reductive eliminations, with barriers comparable to those from **I12** (ΔG's 21.6 vs 23.1 and 23.9 kcal·mol^{-1}, **Figure 20**, *right*, blue pathways). Additionally, we also located the isomer **I20**, with a Pd-C_{ipso} hemilabile interaction, which might also evolve through a reductive elimination to **17m** (ΔG=24.1 kcal·mol^{-1}, **Figure 20**, *left*, green pathway). In contrast, the reductive elimination could not be located from **I21**, a T-shape isomer of **I10** that lacks any hemilabile interaction (red pathway).

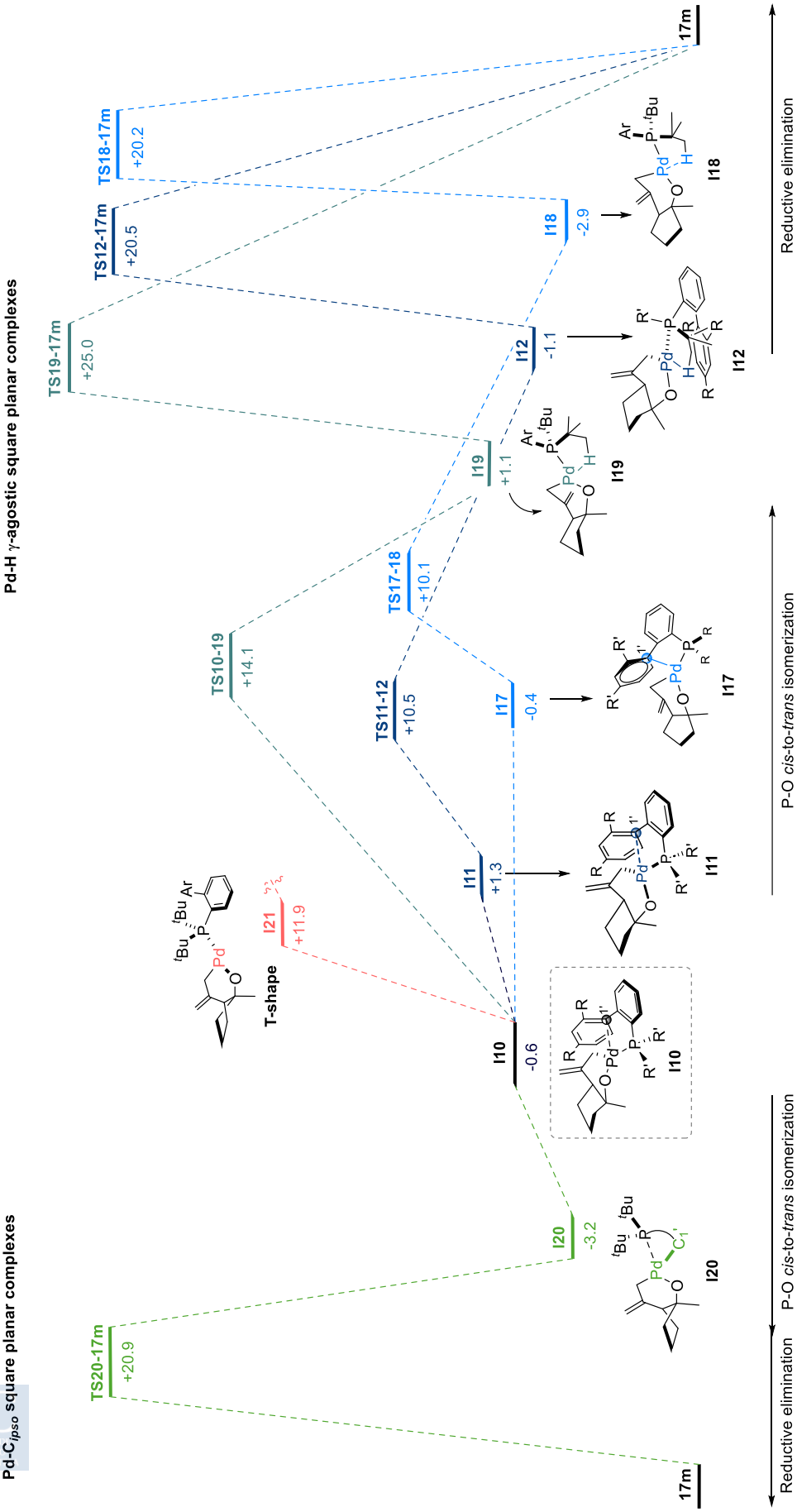

Figure 20. Alternative conformers of the oxa-palladacyclic intermediates of type **I10**, their respective P-O *trans* isomers and the subsequent reductive eliminations. ΔG_{solv} (kcal·mol^{-1}). [B3LYP/6-31G(d) (LANL2DZ for Pd)//M06/6–311++g(d,p) (SDD for Pd) in toluene].

In conclusion, our DFT calculations suggest that the use of bulky biaryl ligands such as *t*BuXphos, is instrumental to facilitate the oxidative addition of the cyclopropane as well as the migratory insertion of the carbonyl moiety through a metalloene process (**Figure 16**, route b). Indeed, this type of ligands seems to favor the whole process when compared with regular monodentate phosphines, through secondary hemilabile interactions with the metallic center that low down the energies of both intermediates and transitions states. This is well exemplified in the **Figure 18**, where the orientation of the secondary aryl of the ligand (inward or outward) enables or disables secondary interactions between the palladium and the aryl moiety, stabilizing the stationary points to varying degrees and, ultimately, leading to two routes (red and blue, **Figure 18**) with significant differences in energy.

Analysis of the diastereoselectivity of the cycloaddition

We also performed a preliminary analysis of the diastereoselectivity of the process. 5,5-Fused and 6,5-fused bicyclic systems can be either *cis* or *trans* regarding the ring fusion. Since these cycloadditions are not under thermodynamic control, and the reductive eliminations might be energetically similar in both cases, we focused our attention on the migratory insertion steps (**Figure 21** and **22**).

Figure 21 shows the migratory insertion involved in the formation of 5,5-bicyclic systems for **9m**. Starting from palladacyclobutane intermediates (**I9'** and **I9'*trans***), the migratory insertion to provide the *trans* palladacycle (**I10*trans***) involves an energy barrier of 26.6 kcal·mol^{-1}. Meanwhile, the migratory insertion to give the *cis* fusion intermediate (**I10**) proceeds through a 12.6 kcal·mol^{-1} barrier. The higher energy barrier of the **TS9-10*trans*** ($\Delta\Delta G$=13.6 kcal·mol^{-1}) might be explained by the quasi-planar conformation adopted by the connecting tether in the transition structure and the smaller stabilizing Pd-C*ipso* interaction (2.77 Å vs 3.00 Å). These results are in consonance with the experimental results, since the *cis*-fused 5,5-bicycles are obtained with total diastereoselectivity.

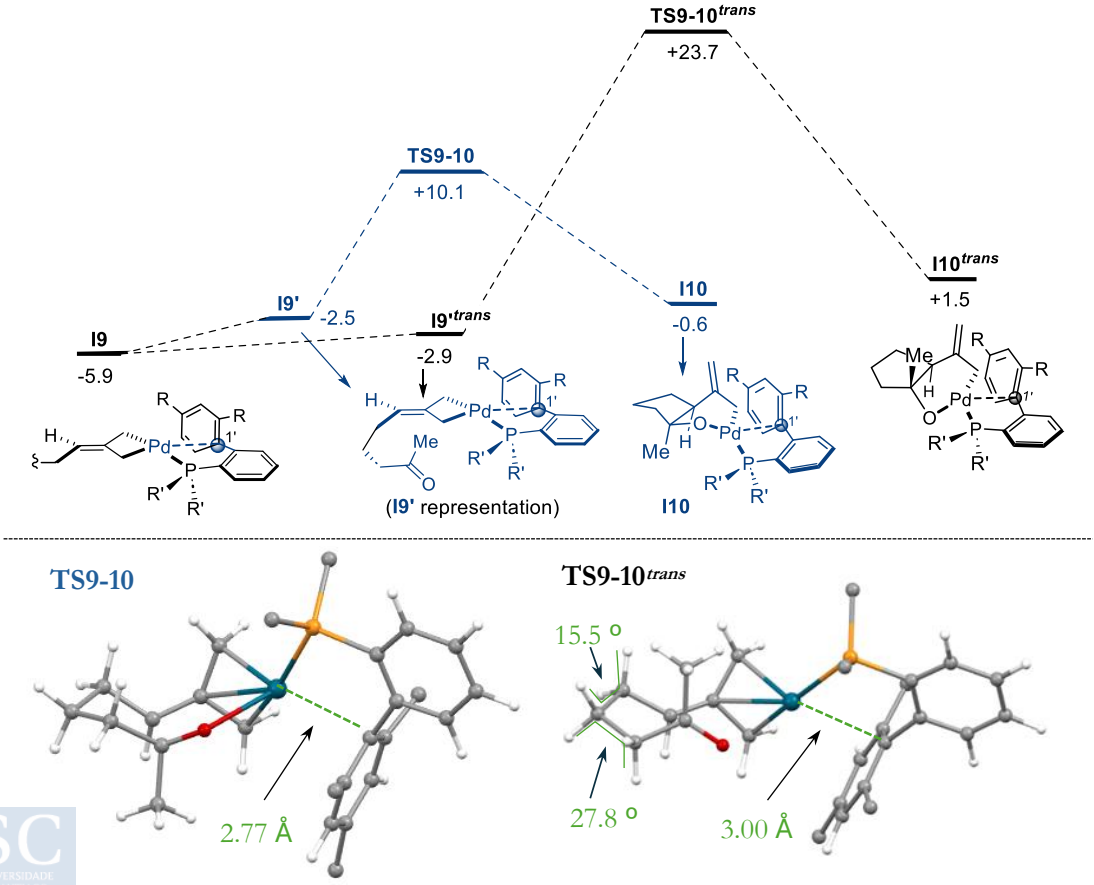

Figure 21. Stereoselectivity in the migratory insertion towards 5,5-bicyclic systems. ΔG_{solv} (kcal·mol^{-1}). [B3LYP/6-31G(d) (LANL2DZ for Pd)//M06/6–311++g(d,p) (SDD for Pd)].

We also analyzed the diastereoselectivity in processes leading to 6,5-bicycles. The methyl ketone **9d** and the aldehyde **7e** were selected as model substrates (**Figure 22**, A and B).

Regarding the methyl ketone **9d** (*left* side), the palladacyclobutane species **I22**^{trans} undergoes a migratory insertion to provide the *trans* fused palladacycle **I23**^{trans}, with an energy barrier of 22.9 kcal·mol^{-1}. Meanwhile, the migratory insertion to give the *cis* fusion (**I22**^{cis}) has a lower energy barrier, of 15.2 kcal·mol^{-1}. Notably, this difference ($\Delta\Delta G$=7.7 kcal·mol^{-1}) is smaller than that observed for the formation of 5,5-bicycles ($\Delta\Delta G$=13.6 kcal·mol^{-1}, **Figure 21**). This is qualitatively consistent with the experimental results, since the 6,5-bicyclic product **17b** is obtained with slightly lower diastereoselectivity (*cis:trans* ratio= 10:1) whereas the 5,5-counterpart **17e**, is exclusively *cis* (see **Scheme 104**, *Precedents*, page 118).

Furthermore, the computed barriers for the aldehyde precursor **7e** (**Figure 22**, *right*) show an even smaller difference ($\Delta\Delta G$=4.7kcal·mol^{-1}), which qualitatively aligns with the lower diastereoselectivity observed for the 6,5-bicyclic product **30c** (*cis:trans* ratio = 3.3:1, see **Scheme 104**, *Precedents*, page 118).

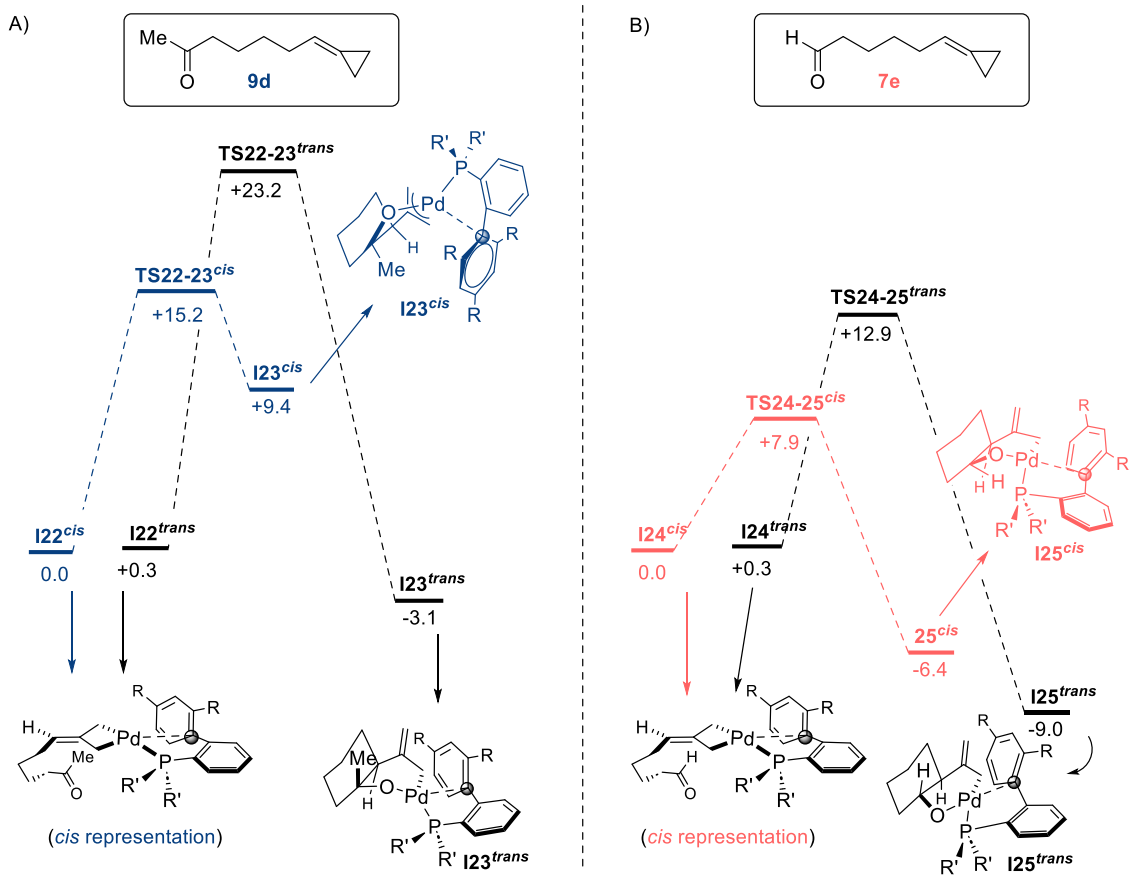

Figure 22. Analysis of the migratory insertion related to 6,5-bicyclic systems for **9d** (*left*) and **7e** (*right*) using Pd(0)-ᵗBuXPhos (**Pd1**), in toluene. ΔG_{solv} (kcal·mol^{-1}). [B3LYP/6-31G(d) (LANL2DZ for Pd)//M06/6–311++g(d,p) (SDD for Pd)].-

4.2.4 Analysis of the Intermolecular Oxacycloaddition

Regarding the intermolecular variants of the cycloadditions, we aimed to shed some light on the critical relevance of the CF_3 substituents in the ketone partner, which seemed mandatory for the success of the reactions. Therefore, we performed DFT calculations using as model ACP **19k**, which is similar to the experimentally used substrate **19j** (see **Table 18**, *Precedents*, page 119). Trifluoroacetophenone (**31a**) and acetophenone (**31b**) were used as carbonyl partners. Based on the

previous results, only the metalloene pathway, to yield oxapalladacyclic intermediates of type **C**, was explored (**Figure 16**, route a, page 121).

4.2.4.1 Study using PH_3 as model ligand

Initially, computations were conducted with PH_3 as ligand, focusing exclusively on the pathways leading to the experimentally observed major diastereoisomer (**Figure 23**). The black pathway shows the reaction profile of the ACP **19k** with trifluoroacetophenone, whereas the blue one displays the analogous profile with acetophenone.

The former starts with the palladacyclobutane intermediate **I26**, which suffers a migratory insertion to reach the π-allyl **I27**, with an accessible energy barrier of 7.2 kcal·mol^{-1}. Finally, the cycloadduct **32ka** is obtained through a reductive elimination (ΔG=8.8 kcal·mol^{-1}).

The blue pathway begins with the analogue palladacyclobutane intermediate **I28**, bearing the methyl ketone **31b** coordinated to the metallic center through the carbonyl oxygen. The subsequent migratory insertion involves a much higher energy barrier (ΔΔG=17.9 kcal·mol^{-1}) while the final reductive elimination is energetically very similar, with an energy penalty of 8.9 kcal·mol^{-1}.

Therefore, the CF_3 moiety stabilizes all the stationary points, resulting in a significant difference between the two systems. The most pronounced effect is observed in the migratory insertion, in which the use of the trifluoromethyl ketone reduces the energy cost by almost 18 kcal·mol^{-1}.

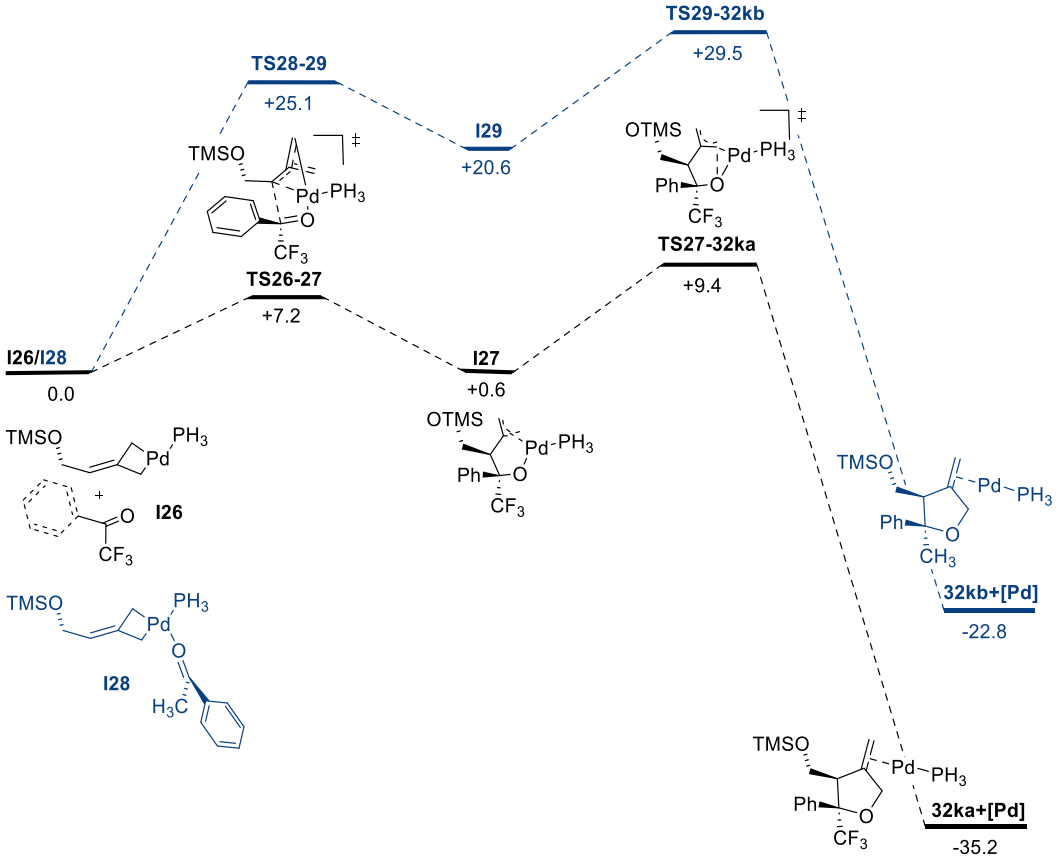

Figure 23. DFT-calculated energy profile ΔG_{solv} (kcal·mol^{-1}) for the (3+2) cycloaddition of **19k** with trifluoroacetophenone **31a** (black route) and acetophenone **31b** (blue route) using Pd(0)-PH_3, in toluene. [B3LYP/6-31G(d) (LANL2DZ for Pd)//M06/6–311++g(d,p) (SDD for Pd)].

4.2.4.2 Study using *t*BuXPhos as model ligand

Based on the above results with PH_3, DFT computations were conducted using *t*BuXPhos as ligand, which is experimentally competent (**Table 18**, entry 3, 87% yield, dr 1.6:1). Thus, the Pd(0)-*t*BuXPhos complex (**Pd1**) was used as model catalyst.

Figure 24 illustrates the route involving the ACP substrate **19k** and the fluorinated partner **31a**. As shown in intramolecular studies, Buchwald ligands give access to different pathways depending on the biaryl disposition. Starting from **I30**, where *ipso* carbon C1' is coordinated to the metallic center, **I31** is reached through a metalloene migratory insertion with an energy barrier of 8.6 kcal·mol^{-1}, similar to that calculated for PH_3 ($\Delta\Delta G$=1.4 kcal·mol^{-1}). The alternative square planar complex **I32**, is much less stable (ΔG=19.2 kcal·mol^{-1}), although it can proceed through an accessible barrier to **I33** (ΔG=4.5 kcal·mol^{-1}). We could not locate a direct reductive elimination from this complex, but it can easily evolve to **I34**, from which a reductive elimination is possible, but was found to be highly demanding (ΔG=30.9 kcal·mol^{-1}).

On the contrary, the analog reductive elimination from the σ-allyl Pd intermediate **I31** is accessible (ΔG=22.4 kcal·mol^{-1}). Notably, this barrier is significantly higher than that observed when using PH_3 as ligand, which highlights the importance of performing the study with realistic models. In any case, the barrier fits with the heating requirements of the reaction and suggests that the reductive elimination is the turnover limiting step, similar to the intramolecular reaction. Like in the intramolecular profiles (**Figure 18**, page 126), *t*BuXPhos provides more stable pathways by enabling secondary hemilabile interactions with the metallic center, stabilizing both intermediates and transitions structures.

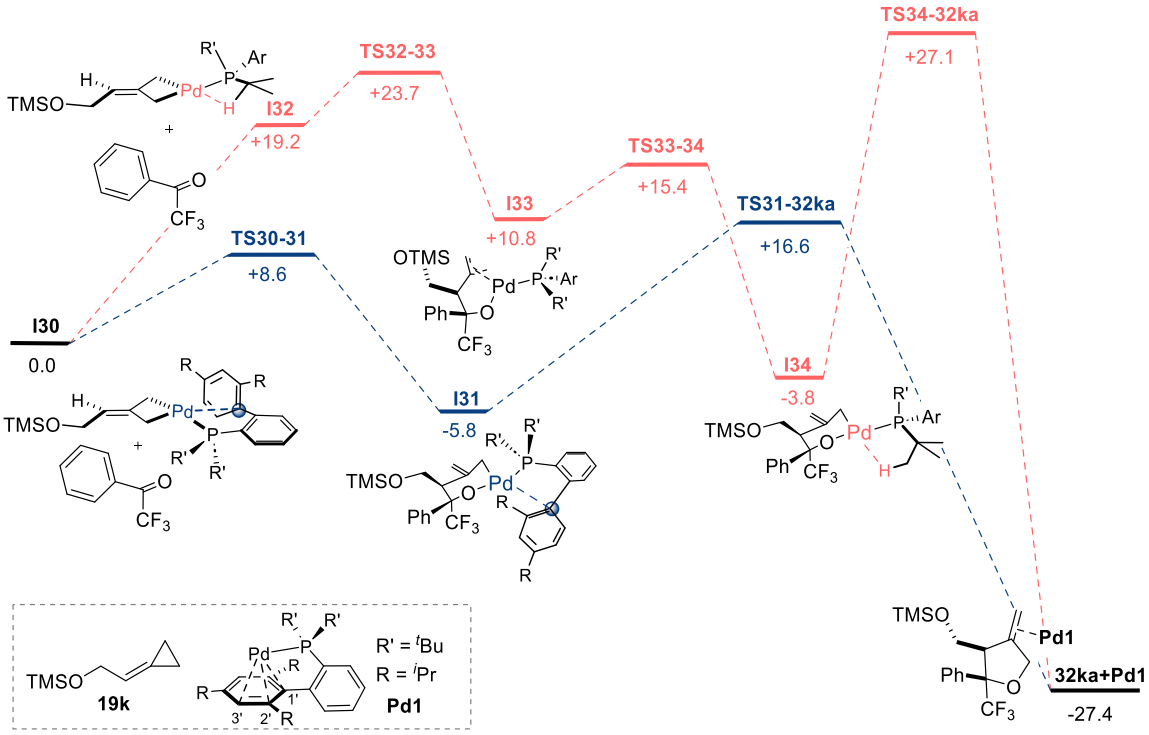

Figure 24. DFT-calculated profile ΔG_{solv} (kcal·mol^{-1}) for the cycloaddition between **19k** and **31a** using Pd(0)-*t*BuXPhos (**Pd1**), in toluene. [B3LYP/6-31G(d) (LANL2DZ for Pd)//M06/6–311++g(d,p) (SDD for Pd)].

In parallel, preliminary DFT studies were also performed using acetophenone instead trifluoroacetophenone as partner (**Figure 25**). The profile starts from palladacyclobutane **I35**, containing a hemilabile coordination of the C*ipso* to the Pd center. The subsequent metalloene step

to π-allyl **I36** has an energy barrier that doubles that calculated for trifluoracetophenone (ΔG=16.1 kcal·mol^{-1}).[97] From **I36**, the reductive elimination takes place to give the corresponding cycloadduct **32kb** with a short energy barrier.

Interestingly, despite these energy values seem accessible, the cycloadducts derived from the methyl ketone **31b** and ACP precursors similar to **19k**, were never observed experimentally. This suggests the existence of alternative side pathways, more favorable than the migratory insertion, which could explain the complete conversion of the starting materials into a complex mixture of products, when acetophenone is used.

To conclude, the role of the fluorine atoms (CF_3) appears to be twofold: not only facilitating the migratory insertion, but also hampering potentially competitive processes, such as β-hydride eliminations and others.

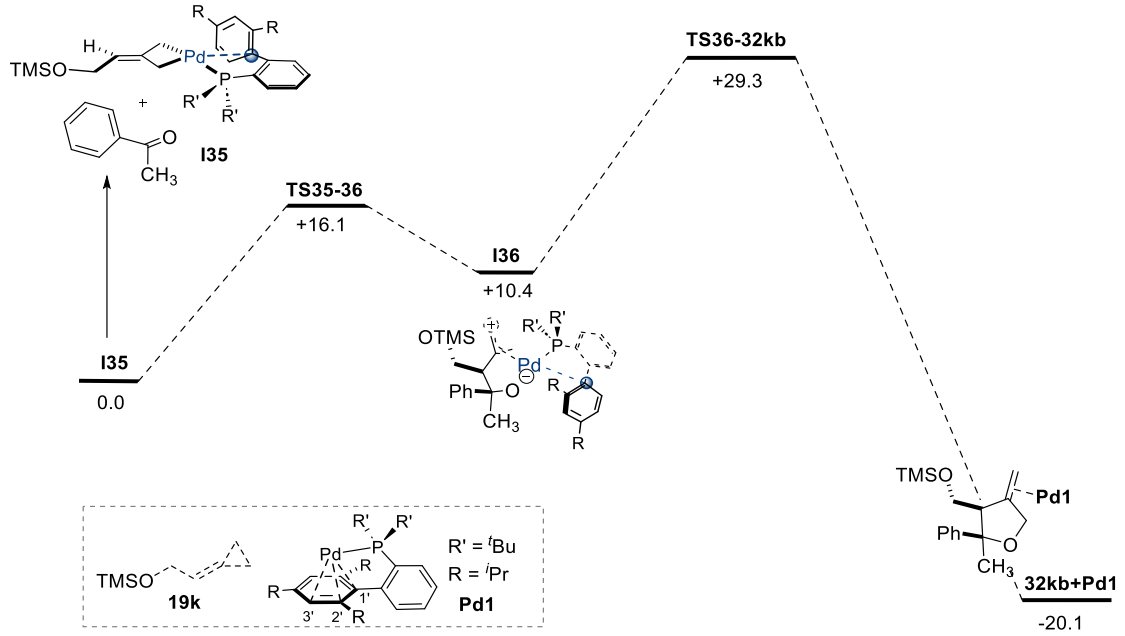

Figure 25. DFT-calculated energy profile ΔG_{solv} (kcal·mol^{-1}) for the (3+2) cycloaddition of **19k** and methyl ketone **31b** using Pd(0)-ᵗBuXPhos (**Pd1**), in toluene. [B3LYP/6-31G(d) (LANL2DZ for Pd)//M06/6–311++g(d,p) (SDD for Pd)].

[97] **Figure A4** shows the pathway from an alternative square planar complex bearing a γ-agostic interaction (**I39**).

4.2.5 Conclusions

In summary, we have computationally explored the reaction pathways for the Pd(0)-catalyzed (3+2) cycloadditions between ACPs and carbonyl partners, both intra- and intermolecularly. For comparative purposes, we employed a simple Pd(0)-PH_3 model and the more realistic Pd(0)-*t*BuXPhos system.

Regarding the intramolecular transformation, we have evaluated the most plausible pathways based on the precedents: a metalloene process (path A) and an isomerization/migratory insertion sequence (path B). Studies with Pd(0)-PH_3 suggested that the metalloene pathway is energetically preferred. These conclusions were much more clear when using Pd(0)-*t*BuXPhos as catalytic system.

Overall, the use of Buchwald ligands seems crucial for the heterocycloaddition, enabling hemilabile interactions between the palladium center and specific atoms of the ligand (Pd-H and Pd-C_{ipso} of the biaryl), which stabilize the metal complexes. The "inward" biaryl conformation of *t*BuXPhos was particularly important, facilitating these interactions and favoring a less energetic overall reaction pathway. Additional studies on migratory insertion and reductive elimination steps confirmed the importance of these secondary metal-ligand interactions in stabilizing key intermediates.

For the intermolecular cycloaddition, we examined the metalloene proposal using acetophenone and 2,2,2-trifluoroacetophenone as carbonyl partners, both with Pd(0)-PH_3 and Pd(0)-*t*BuXPhos. Remarkably, the fluorinated carbonyl partner significantly facilitates the migratory insertion with both catalysts. In addition, the studies with Pd(0)-*t*BuXPhos suggested that these catalysts could play a role in favoring the cycloaddition path, suppressing side reactions. They also reinforced the importance of the hemilabile interactions between the Buchwald ligand and the metal center, and the relevance of the "inward" ligand conformation in enabling lower energy profiles.

4.3. Pd(0)-Catalyzed Tandem Cycloisomerization/ Allylic Substitution Reactions of ACPs tethered to Carbonyl and Imine partners

Part of the contents of this section are published in:

Rodiño, R.[a]; Verdugo, F.[a]; Calvelo, M.[a]; Mascareñas, J. L.[a]; López, F.[a, b] Palladium-Catalyzed Tandem Cycloisomerization/Cross-Coupling of Carbonyl- and Imine-Tethered Alkylidenecyclopropanes. *Angew. Chem. Int. Ed.* **2022**, *61*, e20220229. DOI: 10.1002/anie.202202295

Authors' affiliations:

[a] Centro Singular de Investigación en Química Biolóxica e Materiais Moleculares (CiQUS) and Departamento de Química Orgánica, Universidade de Santiago de Compostela 15782 Santiago de Compostela (Spain).

[b] Misión Biológica de Galicia Consejo Superior de Investigaciones Científicas (CSIC) 36080 Pontevedra (Spain).

4.3.1 Precedents

4.3.1.1 TMC reactions involving Pd(II) π-allyl intermediates

Metal-catalyzed allylic substitutions are fundamental processes in organic synthesis, allowing the efficient formation of C−C, C−N, and C−O bonds.[98] These transformations proceed through π-allyl metal complexes, that are easily obtained from allylic systems with leaving groups (OAc, OCO_2R, Cl …) in presence of metal complexes, although they can also be generated from other substrates like vinyl epoxides, dienes and others. Among the different metals that have been used for generating these reactive intermediates (e.g. Pd, Rh, Ir, Ru), palladium stands out due to its versatility and wide scope.[99] Indeed, palladium π-allyl species can act as electrophiles with a myriad of nucleophiles (malonates, amines, alkoxides…) and pronucleophiles, to create new allylic systems bearing carbon-carbon or carbon-heteroatom bonds. These nucleophiles are usually soft, and generated from conjugated bases of low pKa's, to warrant easy deprotonations.

The general mechanism of this reactivity is represented in **Figure 26**. It starts with the coordination of the Pd(0) catalyst to the double bond, followed by an oxidative addition to afford a π allyl Pd(II) complex **II**, with release of the leaving group. This intermediate can suffer a direct nucleophilic addition (out-sphere attack), usually through the face opposed to the palladium, to give complex **IV**. Alternatively, the coordination of the nucleophile to the metal, prior to the nucleophilic addition, is also possible, leading to an inner-sphere pathway, that gives **IV**.

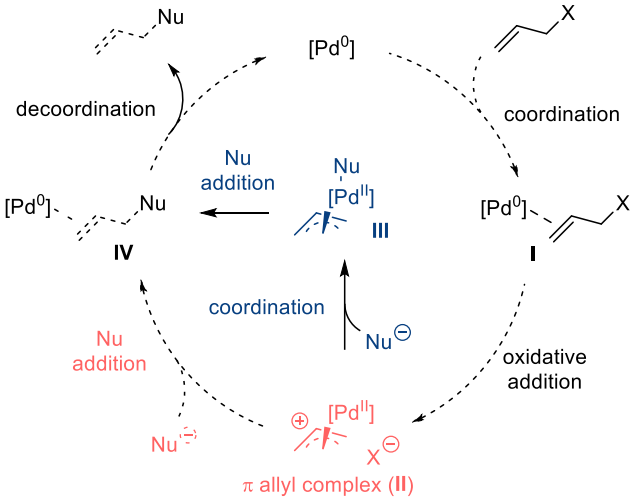

Figure 26. General mechanism for π-allyl Pd(II) complexes.

This reactivity can also be exploited using organometallic reagents as nucleophiles, for instance, organozinc or organoboron reagents, which allow the generation of allyl cross-coupling products, which are very useful in organic synthesis. The more common strategy is based on the use of allylic acetates as palladium π-allyl precursors.[100] For instance, in 2008 Sawamura reported a reaction

[98] a) Trost, B. M.; Van Vranken, D. L. Asymmetric transition metal-catalyzed allylic alkylations. *Chem. Rev.* **1996**, *96*, 395−422.; b) Trost, B. M.; Crawley, M. L. Asymmetric transition-metal-catalyzed allylic alkylations: Applications in total synthesis. *Chem. Rev.* **2003**, *103*, 2921−2943. c) Pàmies, O.; Margalef, J.; Cañellas, S.; James, J.; Judge, E.; Guiry, P. J.; Moberg, C.; Bäckvall, J.-E.; Pfaltz, A.; Pericàs, M. A.; Diéguez, M. Recent Advances in Enantioselective Pd-Catalyzed Allylic Substitution: From Design to Applications. *Chem. Rev.* **2021**, *121*, 8, 4373–4505.

[99] a) Tsuji, J. The Tsuji–Trost Reaction and Related Carbon–Carbon Bond Formation Reactions: Overview of the Palladium–Catalyzed Carbon–Carbon Bond Formation via π-Allylpalladium and Propargylpalladium Intermediates; In *Handbook of Organopalladium Chemistry for Organic Synthesis;* Negishi, E., Ed.; Wiley, **2002**, 1669–1687; b) Trost, B. M.; Crawley, M. L. Asymmetric Transition-Metal-Catalyzed Allylic Alkylations: Applications in Total Synthesis. *Chem. Rev.* **2003**, *103*, 2921–2943.

[100] a) Ohmiya, H.; Makida, Y.; Tanaka, T.; Sawamura, M. Palladium-Catalyzed γ-Selective and Stereospecific Allyl−Aryl Coupling between Allylic Acetates and Arylboronic Acids. *J. Am. Chem. Soc.* **2008**, *51*, 17276–17277.; b) Li, C.; Xing, J.;

between chiral allylic acetates and boronic acids, using the catalyst derived from $Pd(OAc)_2$, $AgSbF_6$ and 1,10-phenanthroline, to provide different arylated products with an excellent α-to-γ chirality transfer (**Scheme 106**).[101] The active catalyst **I** evolves through a transmetalation step to reach species **II**. After coordination of the allylic precursor, the complex **III** suffers a regioselective migratory insertion to give intermediate **IV**, and eventually the product.

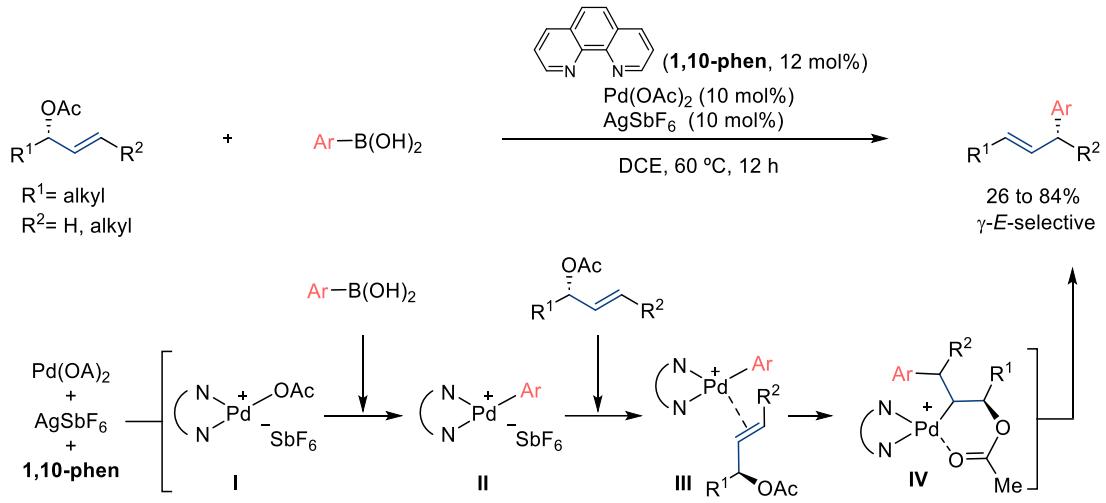

Scheme 106. Pd(0) catalyzed allyl-aryl coupling between allyl acetates and boronic acids using the bidentate neutral phenanthroline as ligand.

Another example, reported by Fernandes and coworkers in 2016, involves the reaction between γ-vinyl lactones and aryl boronic acids using $Pd(OAc)_2$/TMEDA as catalyst, to afford arylated allylic products (**Scheme 107**).[102] In these cases, the initially generated π-allyl Pd complex of type **I** reacts with the boronic acid through a transmetalation step to give the Pd(II) intermediate **II**. After a reductive elimination, the monoarylated allylic alcohol is released.

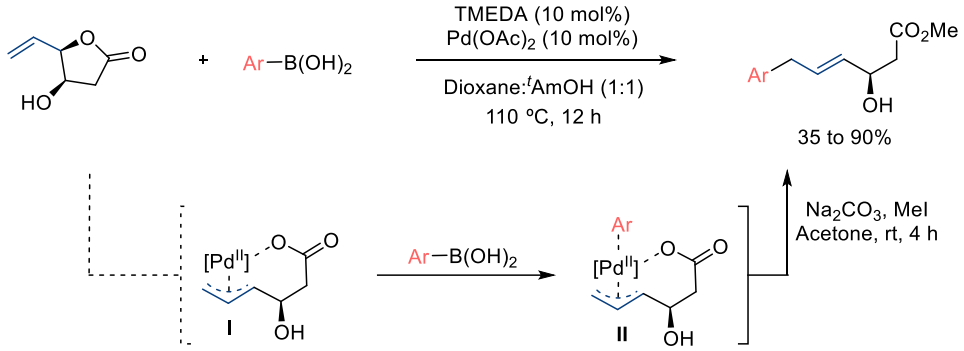

Scheme 107. Pd(0) catalyzed cross-coupling of γ-vinyl-lactones.

The reactive π-allyl Pd species can also be obtained from alternative precursors, such as dienes, as demonstrated by Sigman in 2009 (**Scheme 108**).[103] Thus, the Pd(II) catalyzed hydroarylation of dienes with boronic esters proceeds through the formation of a catalytically active Pd hydride, that regioselectively hydrometalates the diene to yield the key π-allyl Pd species **I**. A subsequent

Zhao, J.; Huynh, P.; Zhang, W.; Jiang, P; Zhang, Y. J. Pd-Catalyzed Regioselective and Stereospecific Suzuki–Miyaura Coupling of Allylic Carbonates with Arylboronic Acids. *Org. Lett.* **2012**, *14*, 390–393.

[101] Ohmiya, H.; Makida, Y.; Li, D.; Tanabe, M.; Sawamura, M. Palladium-Catalyzed γ-Selective and Stereospecific Allyl−Aryl Coupling between Acyclic Allylic Esters and Arylboronic Acids. *J. Am. Chem. Soc.* **2010**, *132*, 2, 879–889.

[102] Nallasivam, J. L.; Fernandes, R. A. Pd-Catalyzed Site-Selective Mono-allylic Substitution and Bis-arylation by Directed Allylic C–H Activation: Synthesis of anti-γ-(Aryl,Styryl)-β-hydroxy Acids and Highly Substituted Tetrahydrofurans. *J. Am. Chem. Soc.* **2016**, *138*, 13238–13245.

[103] Liao, L.; Sigman, M. S. Palladium-Catalyzed Hydroarylation of 1,3-Dienes with Boronic Esters via Reductive Formation of π-Allyl Palladium Intermediates under Oxidative Conditions. *J. Am. Chem. Soc.* **2010**, *132*, 10209–10211.

transmetalation with the boronic ester leads to species **II**, that eventually affords the branched products after reductive elimination.

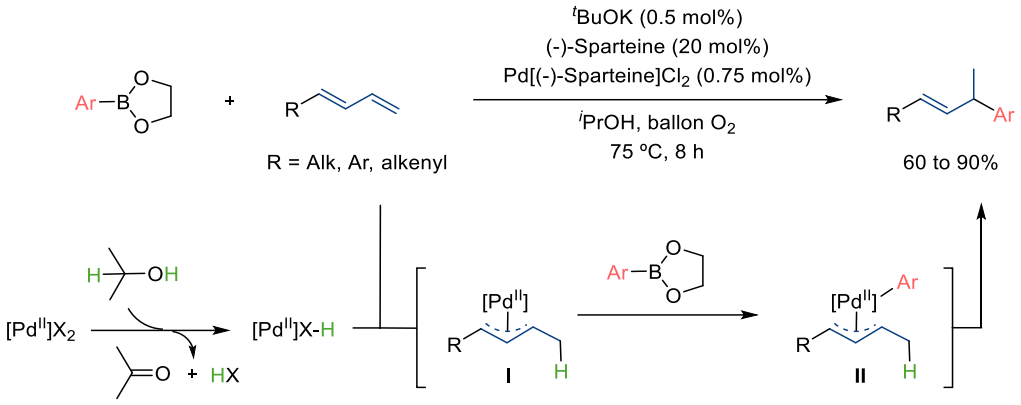

Scheme 108. Pd(0) catalyzed hydroarylation of dienes.

4.3.1.2 Tandem processes involving ACPs and related strained systems entailing π-allyl intermediates

ACPs and other 3C-membered strained rings can be cleaved to give π-allyl metal intermediates, which can be further trapped with appropriate nucleophiles. However, such examples remain scarce. One notable case, reported by Hyland in 2015, consists of a Pd(0) catalyzed ring-opening/cross-coupling of vinyl cyclopropanes (VCPs) with boronic acids, to afford linear and branched allylic products with high diastereoselectivity (**Scheme 109**).[104] The reaction starts with the *in situ* generation of Pd(0) nanoparticles from $Pd(OAc)_2$ and boronic acid. Then, an oxidative addition of the vinylcyclopropane gives the π-allyl Pd complex **I**, which transmetalates to intermediate **II**. Finally, a reductive elimination releases the cross-coupled products, regenerating the active catalyst.

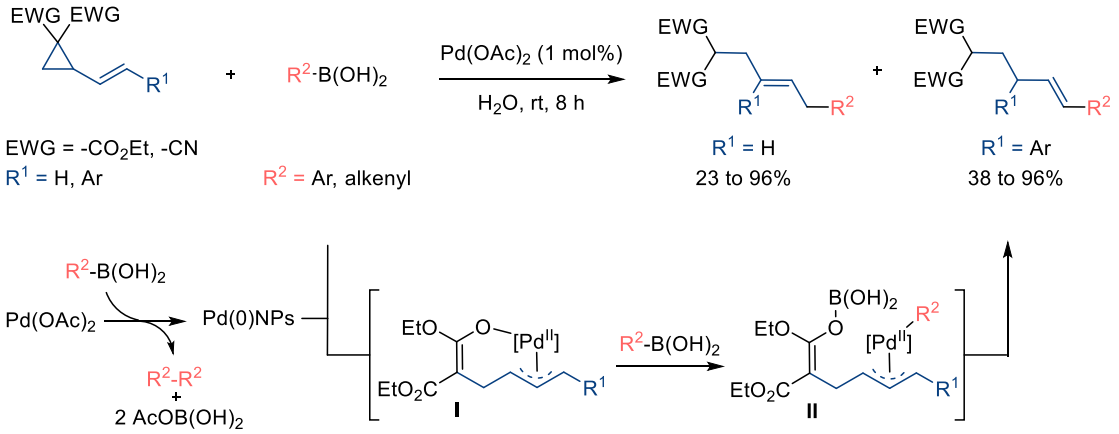

Scheme 109. Pd(0) catalyzed VCP ring-opening/Suzuki-type coupling process.

Another example, reported by Rousseaux in 2020, involves a nickel(0) catalyzed ring opening/ cross coupling reaction between arylcyclopropyl tosylates and boronic acids, to produce 2-arylated allyl derivatives with moderate yields (**Scheme 110**).[105] Interestingly, the boronic acid has a dual role in the transformation, enabling the ring-opening to give a π-allyl Ni(II) intermediate **I**, and participating in the subsequent cross-coupling process.

[104] Yin, J.; Hyland, C. J. T. Ring-Opening of Vinylcyclopropane-1,1-dicarboxylates by Boronic Acids under Ligandless Palladium Catalysis in Neat Water. *J. Org. Chem.* **2015**, *80*, 6529–6536.
[105] Mills, L. Reginald; Monteith, J. J.; Rousseaux, S. A. L. Boronic acid-mediated ring-opening and Ni-catalyzed arylation of 1-arylcyclopropyl tosylates.*Chem. Commun.* **2020**, *56*, 12538-12541.

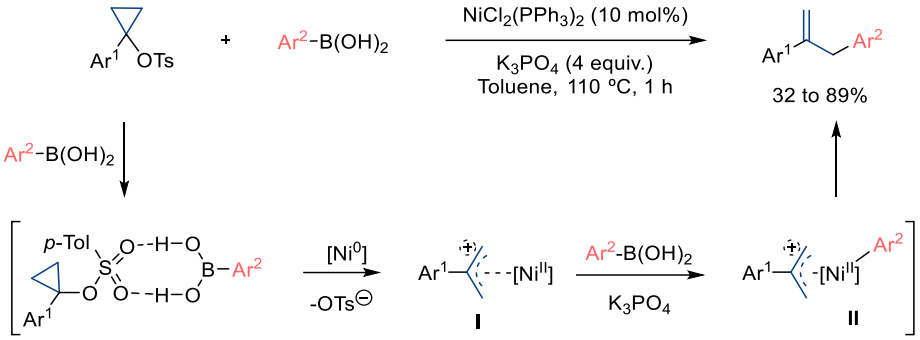

Scheme 110. Ni(0) catalyzed ring-opening/Suzuki-type coupling process involving arylcyclopropyl tosylate.

Shi and coworkers reported a rhodium(I) promoted cycloisomerization/ allylic substitution tandem processes between vinilydenecyclopropanes (VDCP) tethered to carbonyls and alkynes. The reaction provides functionalized 6-membered rings bearing a new chiral center, with enantioselectivities above 93% (**Scheme 111**).[106] The catalyst generated from $[Rh(COD)_2]_2$, $AgNTf_2$ and (*R*)-SDP reacts with the ACP to give a rhodacyclobutane intermediate **I**, which undergoes a migratory insertion of the ketone to deliver a π-allyl Rh(III) species (**II**). After transmetalation with an *in situ* generated silver alkynylide, and a reductive elimination, the coupling product is obtained.

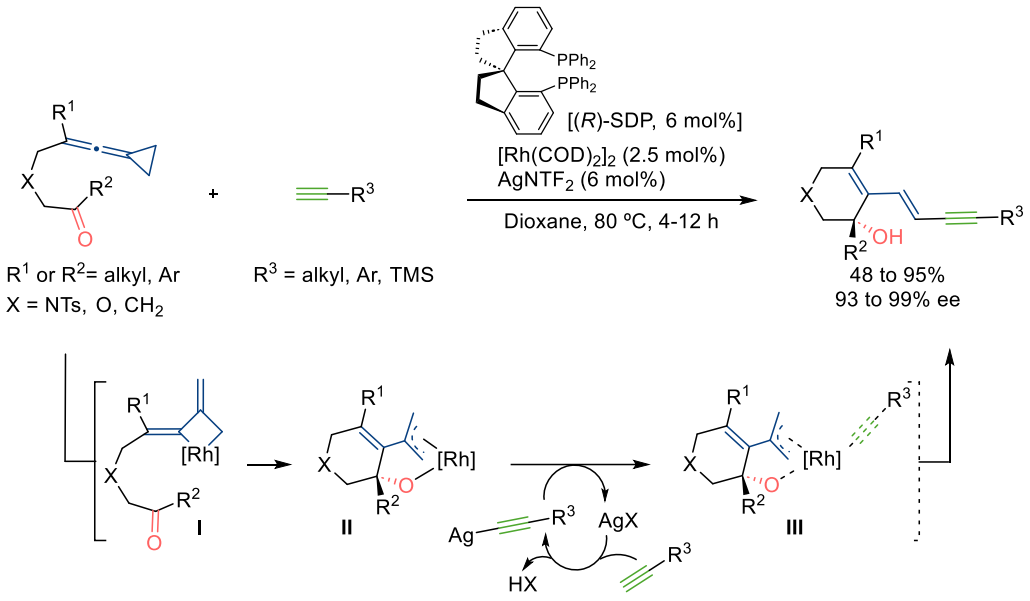

Scheme 111. Rh(I) /Ag(I) catalyzed cycloisomerization / cross coupling tandem reaction involving VDCPs.

Shi *et al.* extended this Rh(I)-catalyzed methodology to other nucleophiles, such as indoles[107] and 1,3-dicarbonyls[108], instead of the silver alkynylide (**Scheme 112**). However, the scope of these transformations is more limited, and the use of a N-Ts group at the linker between the carbonyl and the VDCP is mandatory. Unlike the previous transformation with alkynes, these nucleophiles are proposed to perform an outer-sphere nucleophilic attack to the π-allyl Rh(III) intermediate of type **I**.

[106] Yang, S.; Rui, K. H.; Tang, X.Y.; Xu, Q.; Shi, M. Rhodium/Silver Synergistic Catalysis in Highly Enantioselective Cycloisomerization/Cross Coupling of Keto-Vinylidenecyclopropanes with Terminal Alkynes *J. Am. Chem. Soc.* **2017**, *139*, 16, 5957–5964.

[107] Yang, S.; Li, Q.; Xu, C.; Xu, Q.; Shi, M. Rhodium-catalyzed asymmetric hydroamination and hydroindolation of keto-vinylidenecyclopropanes. *Chem. Sci.* **2018**, *9*, 5074–5081.

[108] Xu, C.; Ning, C.; Yang, S.; Wei, Y.; Shi, M. Rhodium-Catalyzed Asymmetric Cycloisomerization of 1,3-Diketones with Keto-Vinylidenecyclopropanes: Synthesis of Enantiomerically Enriched Cyclic β-Amino Alcohols. *Adv. Synth. Catal.* **2021**, *363*, 1727–1732.

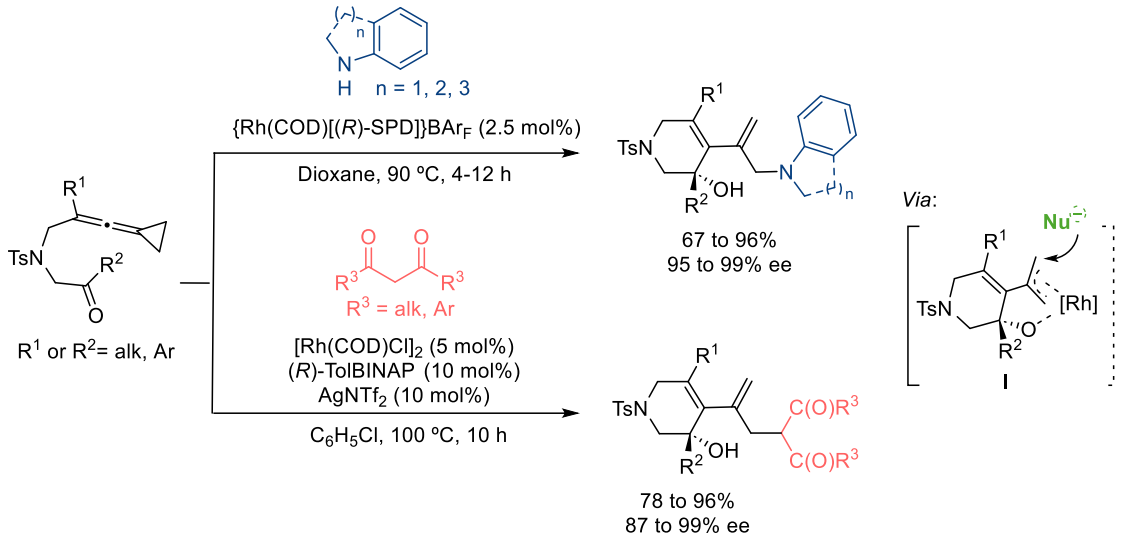

Scheme 112. Rh(I) catalyzed cycloisomerization/ amination or alkylation tandem reaction of VDCPs.

Regarding the use of ACPs in this type of chemistry, in our group, Dr. Verdugo explored the possibility of intercepting π-allyl Pd species of type **C**, that were computationally proposed in Pd-catalyzed (3+2) cycloadditions between ACPs and carbonyls (see **Figures 16** and **18**, *Section 4.2*, pages 121 and 126),[109] with a suitable boron-based nucleophile to get access to functionalized 1,2-disubstituted cyclic alcohols (**Scheme 113**).[110] Note that related, but acyclic, π-allyl Pd(II) complexes of type **C**, featuring coordination to both oxygen and carbon atoms to the palladium, have been postulated as intermediates in Suzuki cross-couplings.[111]

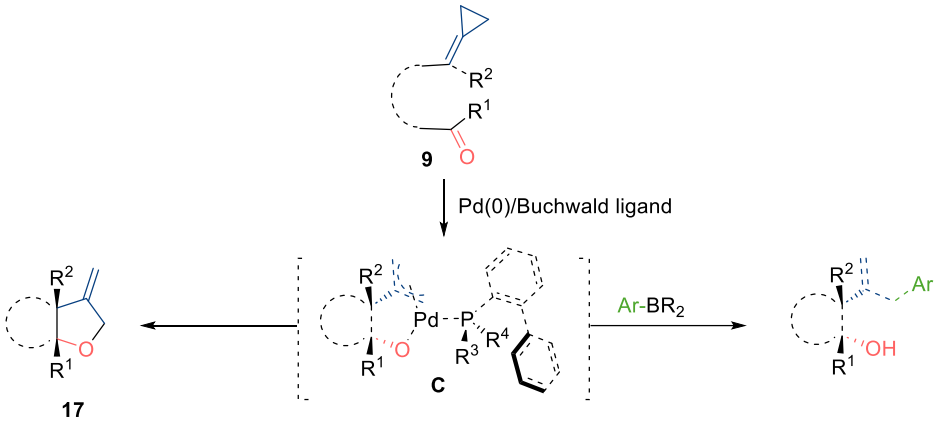

Scheme 113. Interception of the computationally described Pd(II) π-allyl intermediate of type **C** with organoboron reagents.

[109] This transformation is further discussed in *Section 4.2* and reference 40: Verdugo, F.; da Concepción, E.; Rodiño, R.; Calvelo, M.; Mascareñas, J. L.; López, F. Pd-Catalyzed (3 + 2) Heterocycloadditions between Alkylidenecyclopropanes and Carbonyls: Straightforward Assembly of Highly Substituted Tetrahydrofurans. *ACS Catal.* **2020**, *10*, 14, 7710–7718.

[110] Verdugo, F.; Rodiño, R.; Calvelo, M.; Mascareñas, J. L.; López, F. Palladium-Catalyzed Tandem Cycloisomerization/Cross-Coupling of Carbonyl- and Imine-Tethered Alkylidenecyclopropanes. *Angew. Chem. Int. Ed.* **2022**, *61*, e20220229.

[111] For selected mechanistic studies on Suzuki couplings, see: a) Ortuño, M. A.; Lledós, A.; Maseras, F.; Ujaque, G. The Transmetalation Process in Suzuki–Miyaura Reactions: Calculations Indicate Lower Barrier via Boronate Intermediate. *ChemCatChem* **2014**, *6*, 3132–3138.; b) Carrow, B. P.; Hartwig, J. F. Distinguishing Between Pathways for Transmetalation in Suzuki−Miyaura Reactions. *J. Am. Chem. Soc.* **2011**, *133*, 2116–2119.; c) Braga, A. A. C.; Morgon, N. H.; Ujaque, G.; Maseras, F. Computational characterization of the role of the base in the Suzuki-Miyaura cross-coupling reaction. *J. Am. Chem. Soc.* **2005**, *127*, 9298–9307.; d) Melvin, P. R.; Nova, A.; Balcells, D.; Hazari, N.; Tilset, M. DFT Investigation of Suzuki–Miyaura Reactions with Aryl Sulfamates Using a Dialkylbiarylphosphine-Ligated Palladium Catalyst. *Organometallics* **2017**, *36*, 3664–3675.

As shown in **Table 19**, treatment of the ACP-ketone **9a** and 4-methoxyphenylboronic acid (**33a**) with the catalyst derived from $Pd_2(dba)_3$ and RuPhos or *t*BuXPhos (standard cycloaddition conditions), led to the (3+2) cycloadduct **17a** as the only product (entries 1 and 2). In contrast, using PPh_3 as ligand, which is not able to establish secondary interactions with the metallic center, switches the selectivity to give the desired *syn*-cyclopentanol **34aa**, but with a low 15% conversion (entry 3). Gratifyingly, using more electron deficient ligands, such as the phosphoramidite **L9**, phosphite **L1** and phosphine **L17**, allowed higher yields of **34aa**, above 90%, with complete diastereoselectivity (entries 4-6). Importantly, Dr. Verdugo found that when using more challenging boronic acids, such as the alkenyl derivative **33b**, the addition of an external base (e.g. K_3PO_4) is required to achieve full conversions, likely by favoring the transmetalation step (entries 7 and 8).

Table 19. Optimization of the tandem reaction between keto-ACP **9a** and boronic acids **33a** and **33b**.[a]

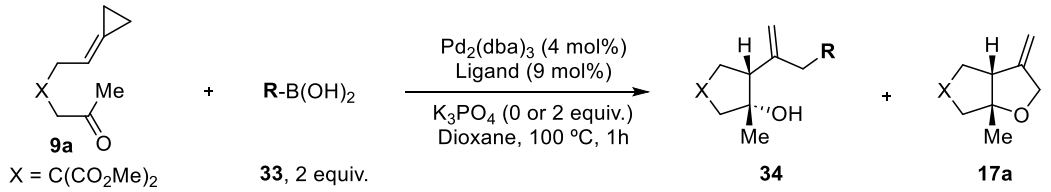

Entry	Ligand	33	Base (equiv.)	34 (%)[b]	17a (%)[b]
1	RuPhos	**33a**	-	-	90
2	*t*BuXPhos	**33a**	-	-	64
3	PPh_3	**33a**	-	**34aa**, 0 (15)	-
4	**L9**	**33a**	-	**34aa**, 90	-
5	**L1**	**33a**	-	**34aa**, 90	-
6	**L17**	**33a**	-	**34aa**, 94	-
7[c]	**L17**	**33b**	-	**34ab**, 40 (60)	-
8	**L17**	**33b**	K_3PO_4 (2)	**34ab**, 95	-

[a] Conditions: **9a**, boronic acid (**33**, 2 equiv.), base (0–2 equiv.), $Pd_2(dba)_3$ (4 mol%), ligand (9 mol%), dry 1,4-dioxane (0.05 M), Ar atmosphere, 100 °C. [b] Determined by NMR with an internal standard. Values of conversion are shown under parenthesis. [c] t = 3 h.

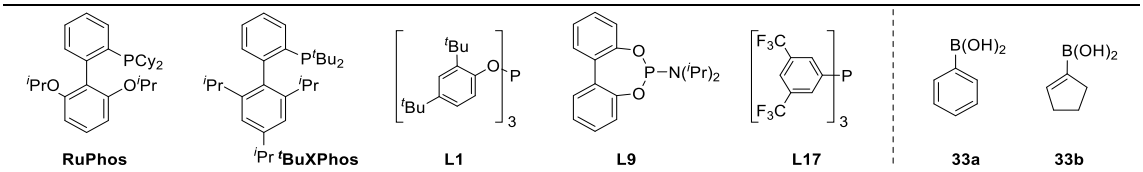

The scope of the transformation was explored by Dr. Verdugo under optimal conditions, comprising $Pd_2(dba)_3$ (4 mol%) and phosphine **L17** (9 mol%), in the presence of K_3PO_4 (2 equiv.) under refluxing dioxane (**Scheme 114**). The reaction works with arylboronic acids bearing a variety of functional groups in the aryl moiety, affording the corresponding cyclopentanols in good to excellent yields (66-96%, **34aa-34af**). Notably, the precursor **9l**, bearing a cyclopentanone moiety, led to the bicyclo[3.3.0]octanol derivative **34la** in 90% yield and with complete diastereoselectivity. Likewise, aryl ketone **9k** provided the product **34ka** in 53% yield (dr 2:1).

The use of alkenylboronic acids led to products like **34ag** and **34ab** in excellent yields (95% and 88%). Curiously, when using an alkylboron species, such as *n*butylboronic acid, the lactone **35a'** was observed as the only product (70%). Its formation was explained by assuming a preferred β-hydride elimination, after the transmetalation of the alkylboron reagent. Thus, the generated π-allyl Pd(II) hydride species would evolve through a C-H reductive elimination and, eventually, an intramolecular transesterification to deliver the product **35a'**.

Finally, substrates containing different connecting tethers between the ACP and the carbonyl moiety (-CH_2-, -NTs-, -O-) were also viable, providing the corresponding products in good to excellent yields (50–93%). The use of substrates with longer connecting tethers, such as **9i**, allowed the obtention of the cyclohexanol **34ba'** in 70% yield, with complete diastereoselectivity.

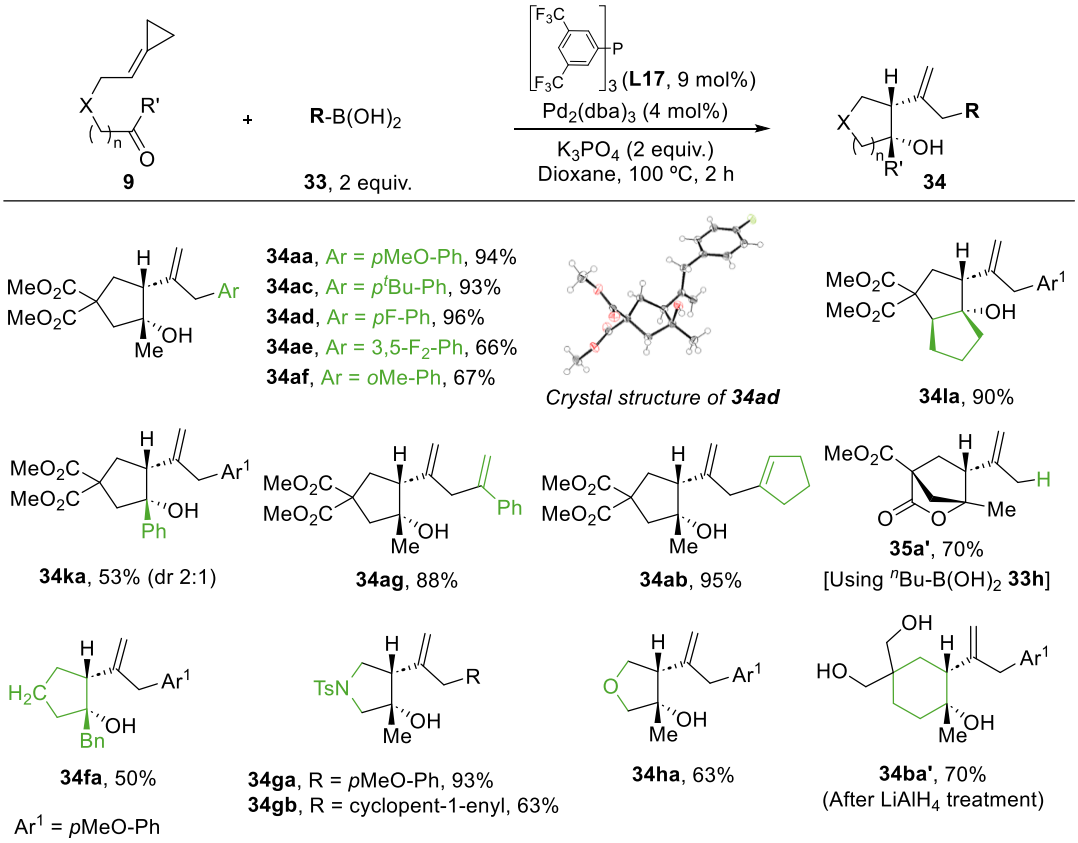

Scheme 114. Scope of the tandem cycloisomerization/ cross coupling between ACPs and boronic acids.

Preliminary work by Dr. Verdugo also showed that this methodology could be extended to other nucleophiles, in addition to organoboron reagents (**Scheme 115**). Using the same catalytic system, dimethyl malonate reacts with ACP **9a** to give **37aa'** in 90% yield, with complete *syn* selectivity. Interestingly, by using K_2CO_3 instead K_3PO_4, the initially expected cyclopentanol **37aa** was obtained in 89% yield. Control experiments suggested that the lactone **37aa'** results from an intramolecular transesterification of the initially formed alcohol **37aa**.[112]

[112] Product **37aa** can lactonize to **37aa'** in presence of K_3PO_4 under refluxing dioxane (40% yield, 3 h).

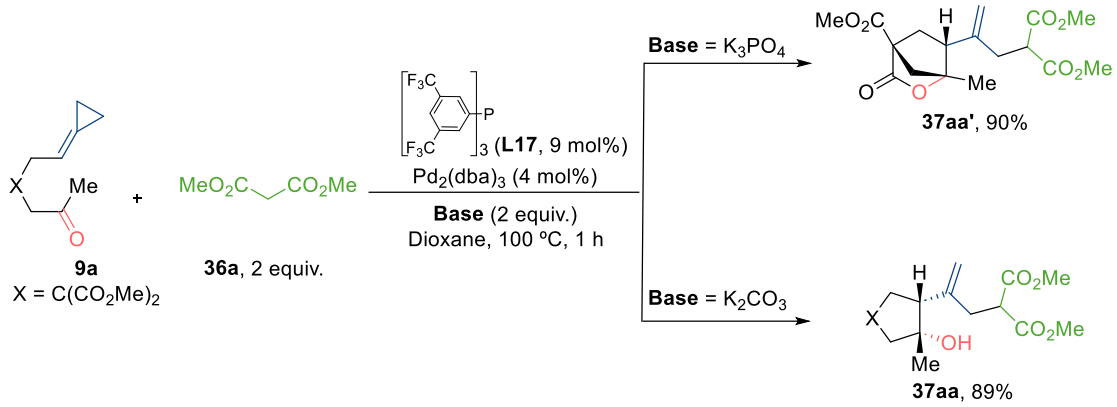

Scheme 115. Tandem cycloisomerization/malonate addition reactions.

Despite these findings, the feasibility of the reaction and its potential extension to other nucleophiles was uncertain. Likewise, the mechanism underlying the divergent pathways remained unclear. Moreover, the possibility of using ACPs tethered to imines, instead of carbonyl moieties, which would enable the synthesis of functionalized cyclic amines, had neither been assessed.

4.3.2 Objectives

Based on these precedents, we set out the following objectives:

- **Extend the cycloisomerization/cross-coupling reaction to other nucleophiles**, like 1,3-dicarbonyls and phenols.
- **Develop analog tandem processes using ACPs tethered to imines**, instead to carbonyl moieties.
- **Obtain mechanistic insights using DFT** computational studies.

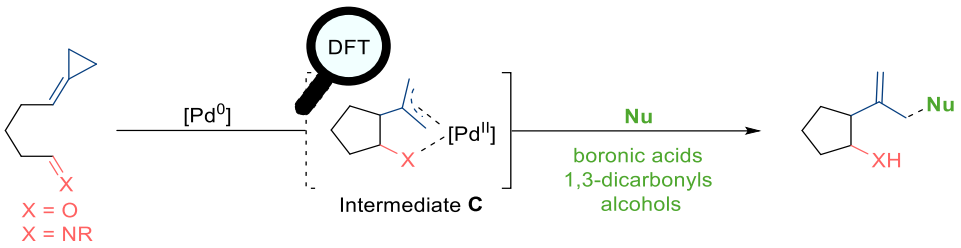

Scheme 116. Study of the cycloisomerization/ allylic substitution tandem processes.

4.3.3 Tandem Cycloisomerization/Nucleophilic Addition of ACPs, using 1,3-Dicarbonyls as Nucleophiles

Preliminary results indicated that dimethyl malonate can also trap intermediates of type **C**, generated from keto-ACPs **9** with a Pd/**L17** catalyst (see **Scheme 115**, *Precedents*, page 144), although the reaction needs further analysis.

Therefore, we prepared other precursors of type **9** following the same strategy used for **9a**, consisting of a Tsuji-Trost reaction between the corresponding nucleophile and the vinyl tosylate **6**. Precursor **9f**, bearing an aliphatic tether between the ACP and the carbonyl group, was synthetized through a Wittig reaction from the corresponding aldehyde, followed by a nucleophilic addition of BnMgBr to its Weinreb amide (**Scheme 117**).

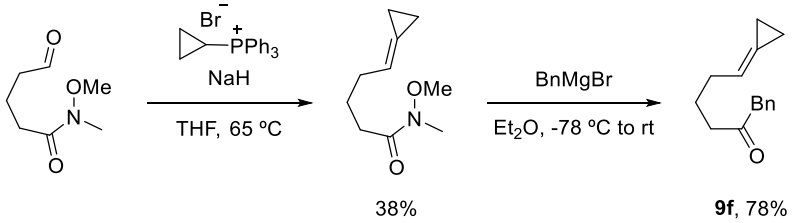

Scheme 117. Synthesis of the precursor **9f**.

With the substrates in hand, we explored the scope of the reaction using the catalyst derived from $Pd_2(dba)_3$ (4 mol%) and the electron-poor phosphine **L17** (9 mol%), and 2 equivalents of K_3PO_4 as base, in refluxing dioxane (**Scheme 118**). Under these conditions, the reaction between carbonyl-tethered ACP **9a** and dimethyl malonate (**36a**) provided lactone **37aa'** in 90% yield. As aforementioned, the intramolecular transesterification can be avoided by using K_2CO_3 instead K_3PO_4, delivering the cyclopentanol **37aa** in 89%. Substrate **9l**, bearing a cyclopentanone moiety, afforded the bicyclic product **37la** in 90% yield (dr 5:1).

The tandem process tolerates different tethers between ACP and the carbonyl partner, such as an aliphatic chain (product **37fa**, 74%) or an ether moiety (product **37ha**, 55%). The use of a longer connecting tether afforded the lactonized product **37ba'** in an excellent 90% yield (dr 1:1). Finally, other monoalkylated malonates and other 1,3-dicarbonyl compounds, such as ethyl acEtOAcetate, also proved to be suitable nucleophiles, enabling the synthesis of products like **37ab'**, **37ac'** or **37ad'** in moderate to good yields.

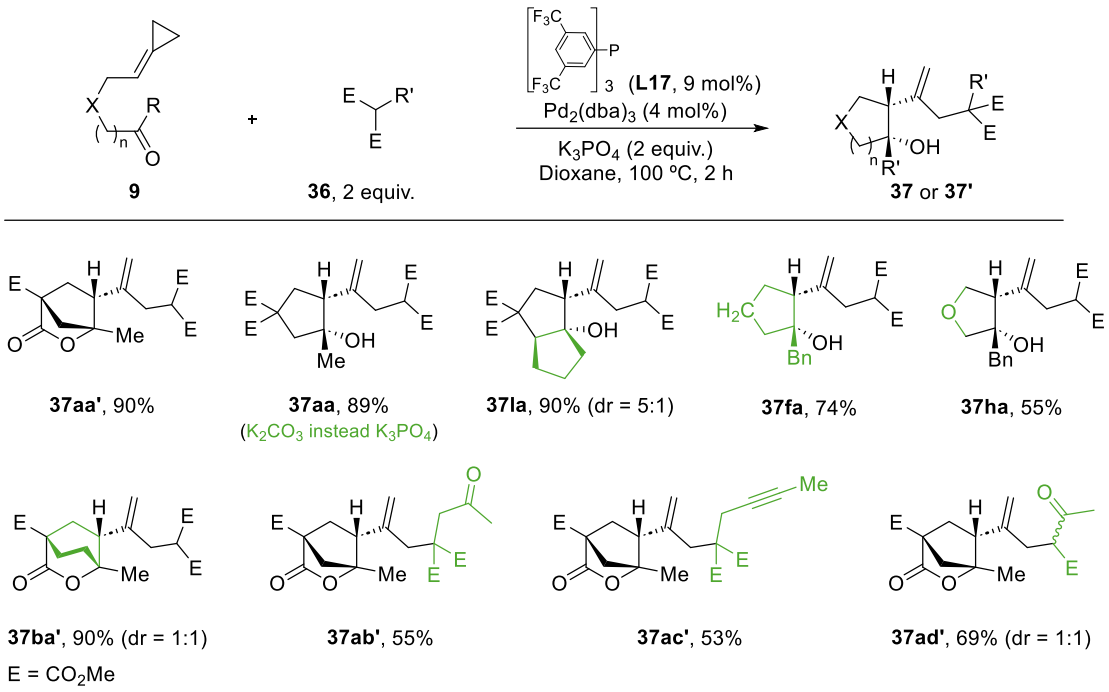

Scheme 118. Scope of the tandem cycloisomerization/ allylic substitution reaction between keto-ACPs **9** and 1,3-dicarbonyl reagents **36**.

4.3.4 Tandem Cycloisomerization/Nucleophilic Addition of ACPs using Alcohols as Nucleophiles

4.3.4.1 Optimization

In collaboration with Dr. Verdugo, we also examined the ability of phenols to intercept allylic intermediates of type **C**. The initial results are presented in **Table 20**.

The reaction involving the catalyst generated *in situ* from $Pd_2(dba)_3$ and the bulky phosphite **L1** led to almost full recovery of the starting material; however, traces of the desired product **39aa** were also observed (entry 1). The use of the electron-poor phosphine **L17** or the phosphoramidite **L9**, instead of **L1**, led to higher conversions, although yields were not significantly higher (15% and 17% of **39aa**, entries 2 and 3). Besides, the use of K_3PO_4 with **L1** as ligand, aiming to enhance the reactivity of the phenol, only led to traces of the product, despite the high consumption of **9a** (entry 4). Similar results were observed when the reaction was carried out employing **L9** or **L17** in the presence of K_3PO_4 (entries 5 and 6).

Table 20. Viability of a tandem process between phenol and keto-ACP **9a**.[a]

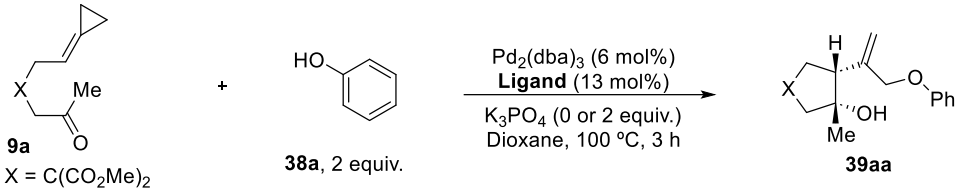

Entry	Ligand	K_3PO_4 (x equiv.)	Conv. **9a** (%)[b]	**39aa** (%)[b]
1	**L1**	-	<5	<5
2	**L17**	-	60	15
3	**L9**	-	20	17
4	**L1**	2	60	<5
5	**L17**	2	100	20
6	**L9**	2	50	10

[a] Conditions: **9a**, phenol (2 equiv.), K_3PO_4 (x equiv.), $Pd_2(dba)_3$ (6 mol%), ligand (13 mol%), dry 1,4-dioxane (0.05 M), Ar atmosphere, 100 ºC, 3 h. [b] Determined by NMR with an internal standard.

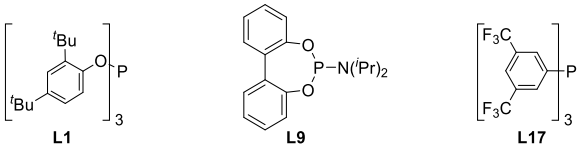

At this point, we decided to study the effect of water in the reaction (**Table 9**). The addition of 10 equivalents of water, using **L1** or **L17** as ligands, did not affect significatively the formation of product **39aa** (entries 1 and 2). However, when using phosphoramidite **L9**, the yield of the cyclopentanol (**39aa**) raised up to a 50% (entry 3). Further variations in the amounts of water did not lead to any additional improvements (entries 4 and 5). Although the exact role of water is unknown, we hypothesize that small amounts of water might enhance the overall homogeneity of the mixture, or help to establish key interactions within the metal complex.

Table 21. Effect of water in the tandem process with phenol and keto-ACP **9a**.[a]

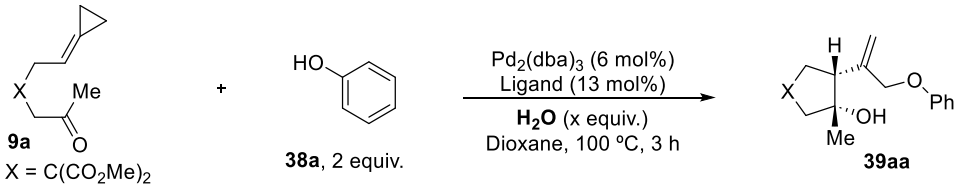

Entry	Ligand	H_2O (x equiv.)	Conv. **9a** (%)[b]	**39aa** (%)[b]
1	**L1**	H_2O (10)	<5	<5
2	**L17**	H_2O (10)	100	20
3	**L9**	H_2O (10)	100	50
4	**L9**	H_2O (20)	100	50
5	**L9**	H_2O (5)	60	36

[a] Conditions: **9a**, phenol (**38a**, 2 equiv.), H_2O (x equiv.), $Pd_2(dba)_3$ (6 mol%), ligand (13 mol%), dry 1,4-dioxane (0.05 M), Ar atmosphere, 100 ºC, 3 h. [b] Determined by NMR with an internal standard.

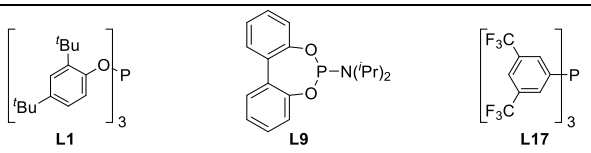

Finally, the effect of the temperature in the tandem process was investigated (**Table 22**). Intriguingly, when the reaction was conducted at higher temperatures, such as 130 ºC, the formal (3+2) cycloadduct **17a** was exclusively obtained (75% yield). Interestingly, the use of the same reaction conditions in the absence of phenol (**38a**), afforded only traces of **17a**, which confirms that the phenol plays a role in the formation of the cycloadduct **17a** (entry 3). When the reaction was carried out at 80 ºC, the allylic compound **39aa** was obtained in 70% yield as the only detected product (entry 3).

Table 22. Effect of the temperature in the tandem process with phenol and keto-ACP **9a**.[a]

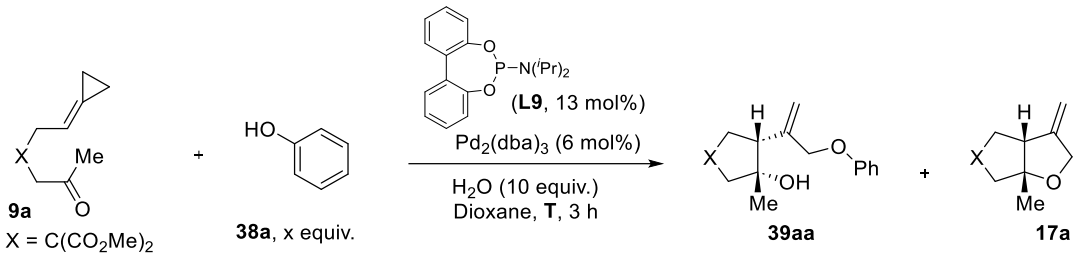

Entry	**38a** (x equiv.)	**T** (ºC)	**39aa** (%)[b]	**17a** (%) [b]
1	2	100	50	<5
2	2	130	<5	75
3	0	130	-	<5
4	2	80	70	<5

[a] Conditions: **9a**, phenol (**38a**, 2 equiv.), H_2O (10 equiv.), $Pd_2(dba)_3$ (6 mol%), **L9** (13 mol%), dry 1,4-dioxane (0.05 M), Ar atmosphere, 3 h. [b] Determined by NMR with an internal standard.

To try to rationalize the formation of **17a**, product **39aa** was treated under the optimal catalytic conditions [$Pd_2(dba)_3$ and **L9**] at 130 ºC, and the bicyclic product **17a** was obtained in 70% yield (**Scheme 119**). This result confirms that **39aa** is formed at 80 ºC but, at higher temperatures, it evolves to the THF derivative **17a**. This transformation might occur through an oxidative addition of the allylic C-O bond to the Pd(0) complex, followed by an intramolecular nucleophilic attack by the hydroxy group to the Pd-allyl moiety.

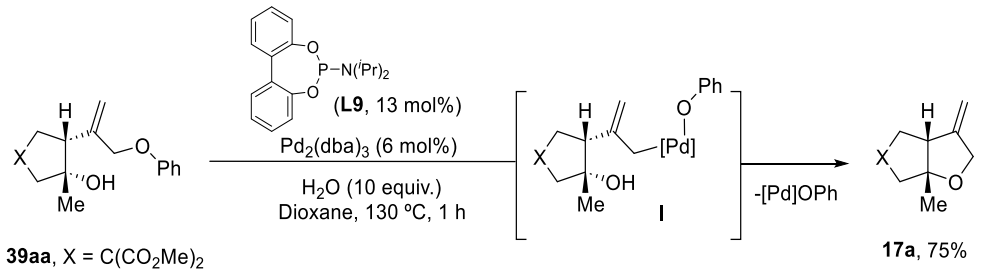

Scheme 119. Control experiment for the formation of **17a** at high temperature.

4.3.4.2 Scope of the transformation

Using as optimal conditions $Pd_2(dba)_3$ (6 mol%), **L9** (13 mol%) and 10 equivalents of water, in dioxane at 80 ºC, we explored briefly the scope of the reaction with different alcohols (**Scheme 120**). The transformation can be performed using different aromatic alcohols, providing the expected products in good yields and complete diastereoselectivity (**39ac**-**39ac**). The use of benzyl alcohol led to the lactone **35a'** (45% yield), which incorporates a hydrogen atom at the allylic position. However, the use of an electron deficient benzyl alcohol, such as pentafluorobenzyl alcohol, inhibits this side pathway, leading to the cyclopentanol **39ad** in 80% yield, as a single diastereoisomer.

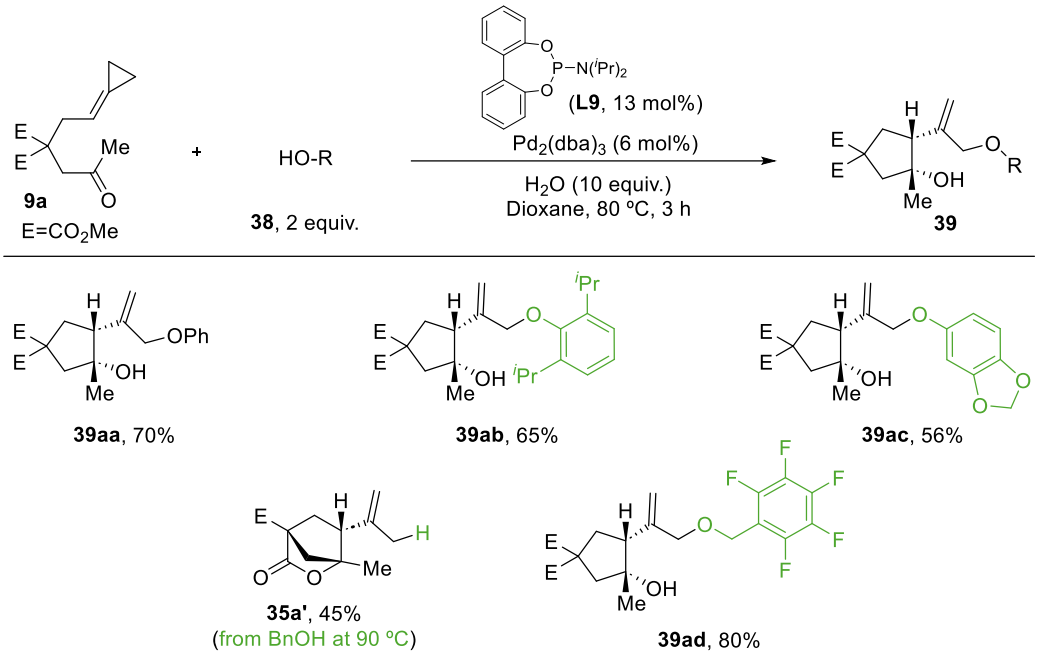

Scheme 120. Scope of the tandem cycloisomerization/ allylic substitution reaction between keto-ACPs **9** and alcohols **38**.

The formation of product **35a'** can be explained assuming that the π-allyl intermediate **I** (type **C**), bearing the benzyloxy group coordinated to the metallic center, evolves through a β-hydride elimination to the palladium hydride intermediate **II** and benzaldehyde (**Scheme 121**). Product **35a'** would be obtained after C-H reductive elimination and intramolecular transesterification.

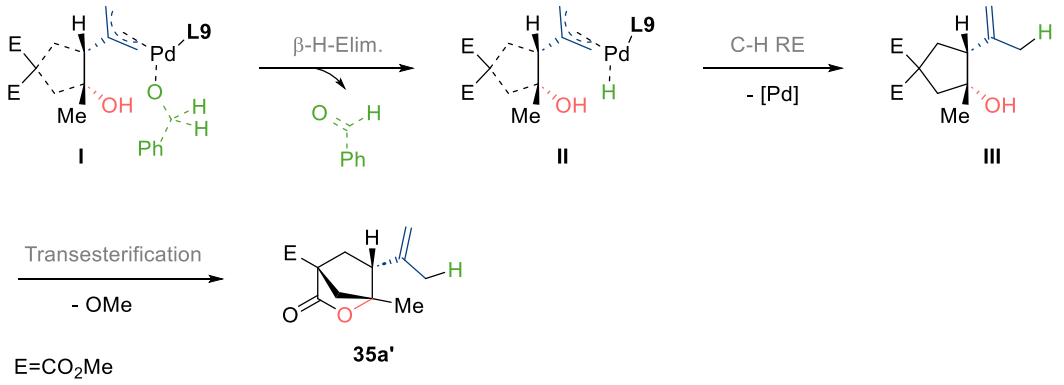

Scheme 121. Mechanistic explanation for the formation of lactone **35a'**.

4.3.5 Tandem Cycloisomerization/Allylic Substitution Reactions of Imine-tethered ACPs

4.3.5.1 Tandem cycloisomerization/cross couplings using boronic acids

Reactivity and optimization

To test the viability of the process, we prepared three types of imine precursors, either bearing an oxime ether (**1d** and **1k**) or a sulfinyl imine (**40a**). The synthesis of the former was previously indicated in *Section 4.1*, via condensation of the appropriate carbonyl precursors (see **Scheme 33**, page 35). On the other hand, the sulfinyl imine **40a** was obtained from the corresponding aldehyde **30e** and sulfinylamine, using tris(2,2,2-trifluoroethyl)borate as dehydrating agent (**Scheme 122**). The product **40a** was obtained in 93% yield as a single isomer (*E*).

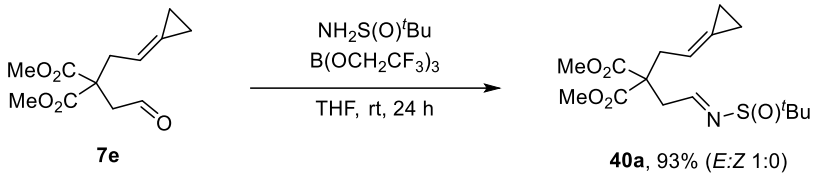

Scheme 122. Synthesis of sulfinyl imine **40a**.

We first evaluated the reactivity of ketoxime **1d** under conditions previously shown successful for the tandem process with carbonyls, namely $Pd_2(dba)_3$ (6 mol%), an electron-poor phosphine ligand (13 mol%) and K_3PO_4 (2 equiv.), under refluxing dioxane (**Table 23**). Disappointingly, the reaction using phosphoramidite **L9** afforded a very low yield of the desired product, **41da**,[113] and small amounts of diene **3d** (10%).[114] The use of **L1** provided exclusively diene **3d** in a 10% yield, whereas with **L17** we obtained **41da**, but in a poor 10% yield.

Table 23. Tandem reaction with the ketoxime-ACP **1d** using different ligands.[a]

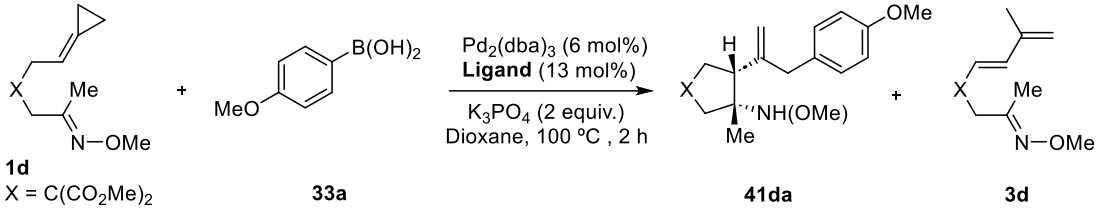

Entry	Ligand	**41da** (%)[b]	**3d** (%)[b]
1	**L9**	6	8
2	**L1**	-	10
3	**L17**	10	7

[a] Conditions: **1d**, boronic acid (**33a**, 2 equiv.), base (2 equiv.), $Pd_2(dba)_3$ (6 mol%), ligand (13 mol%), dry 1,4-dioxane (0.05 M), Ar atmosphere, 100 °C, 2h. [b] Determined by NMR with an internal standard.

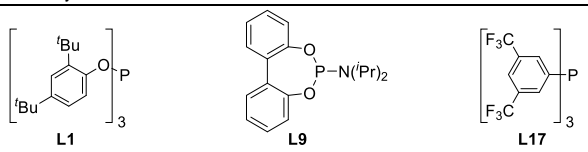

On the other hand, the reaction promoted by $Pd_2(dba)_3$/**L9** using the aldoxime precursor **1k** (*E:Z* = 3:7), led to full consumption of **1k**, but the expected adduct, **41ka**, was not observed in the crude mixture (entry 1, **Table 24**). The use of **L17** as ligand provided similar results (entry 2).

Gratifyingly, the reaction with phosphite **L1** afforded the cross-coupling product **41ka** in a 37% yield with total *syn* selectivity. However, the diene **3k**, resulting from side β-H elimination processes, was also observed in 28% yield (entry 3). To check the influence of the *E*/*Z* geometry of the oxime ether, we tried different samples of **1k** with diverse *E:Z* ratios. Unfortunately, the *E* isomer just led to traces of the desired product, **41ka**, together with the diene **3k** (26% yield, entry 5), a result that diminishes the synthetic potential of these oxime precursors.

[113] Product **41ka** was identified by homology to **42aa** NMR signals in the reaction crude.
[114] For a detailed mechanism of the formation of these dienes, see **Figure 11**, *Section 4.1*, page 87.

Table 24. Evaluation of the aldoxime-ACP **1k** in tandem processes.[a]

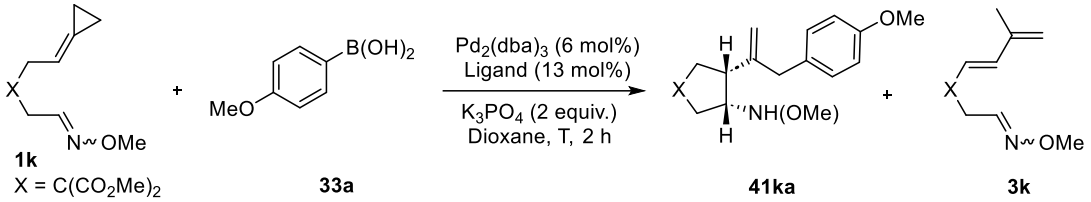

Entry	E:Z ratio (1k)	T(ºC)	Ligand	41ka (%)[b]	3k (%)[b]
1	3:7	100	**L9**	-	-
2	3:7	100	**L17**	(53)	-
3	3:7	100	**L1**	37	28
4	1.5:1	100	**L1**	24	40
5	1:0	100	**L1**	5	26

[a] Conditions: **1k**, boronic acid (**33a**, 2 equiv.), base (2 equiv.), $Pd_2(dba)_3$ (6 mol%), ligand (13 mol%), dry dioxane (0.05 M), Ar atmosphere, 2 h. [b] Determined by NMR with an internal standard. Values of conversion are shown under parenthesis unless conversion>99%.

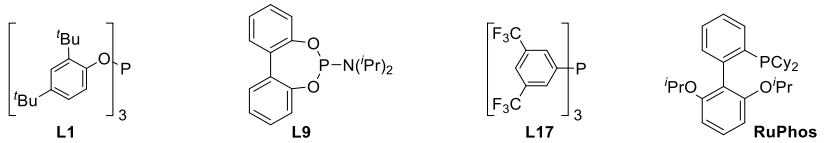

Considering these results, we focused on the reactivity of the sulfinyl imine **40a** (**Table 25**). The catalyst generated from $Pd_2(dba)_3$ and either RuPhos or $P(C_6F_5)_3$ as ligand, provided a complex mixture of products (entries 1 and 2). However, the use of phosphoramidite **L9** allowed to obtain the desired cycloadduct, **42aa**, with total *syn* selectivity in 52% yield (entry 3). A similar result was obtained when using the electron-poor phosphine **L17** (53% yield, entry 4). Notably, a Pd(0)-catalyst featuring the bulky phosphite **L1** afforded the cyclopentamine **42aa** in a higher 80% yield (entry 5).

Table 25. Evaluation of the sulfinylimine-ACP **40a** in tandem processes with different ligands.[a]

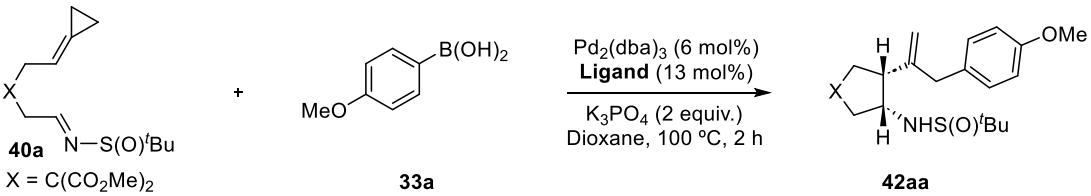

Entry	Ligand	Conv. 40a (%)[b]	42aa (%)[b]
1	RuPhos	100	-
2	$P(C_6F_5)_3$	70	-
3	**L9**	100	52
4	**L17**	100	53
5	**L1**	100	80

[a] Conditions: **40a**, boronic acid (**33a**, 2 equiv.), base (2 equiv.), $Pd_2(dba)_3$ (6 mol%), ligand (13 mol%), dry dioxane (0.05 M), Ar atmosphere, 2 h. [b] Determined by NMR with an internal standard.

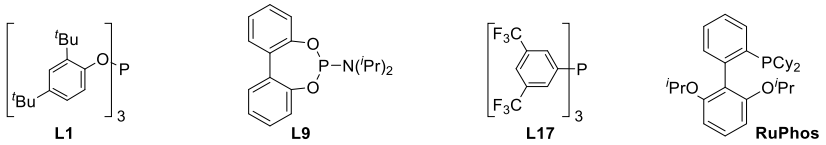

Worth to mention, product **42aa** consists of a 1:1 mixture of diastereoisomers, because of the presence of the chiral sulfinamide. However, they can be separated by chromatography or transformed into the common sulfonyl derivative (**43aa**) by treatment with *m*CPBA (**Scheme 123**).

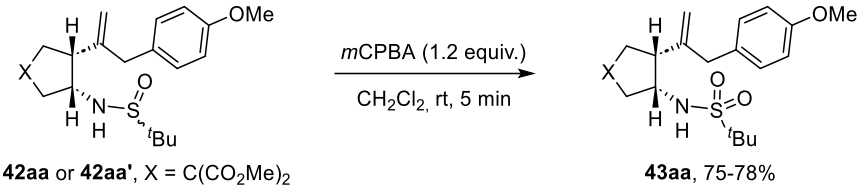

Scheme 123. Conversion of **42aa** and **42aa'** into **43aa** by oxidation of the sulfoxide center.

We also evaluated the effect of different bases (**Table 26**). Interestingly, bases such as Cs_2CO_3, K_2CO_3, KOH or NaOAc, also allowed the formation of product **42aa** in excellent yields, between 85% and 95% (entries 2-5), although a similar yield was obtained without base (94% yield, entry 6). These results align with those obtained using the ACP precursor **9a**, which contains a carbonyl moiety and required an external base only when challenging boronic acids were used (see **Table 19**, *Precedents*, page 142).

Table 26. Influence of the base in the tandem process with sulfinylimine-ACP **40a**.[a]

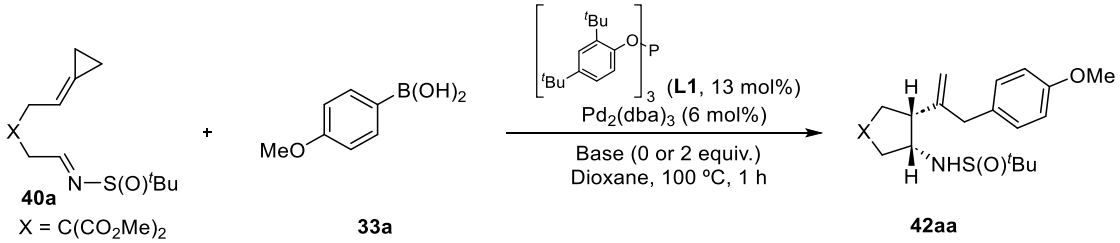

Entry	Base (2 equiv.)	42aa (%)[b]
1	K_3PO_4	80
2	Cs_2CO_3	86
3	K_2CO_3	94
4	KOH	95
5	NaOAc	95
6	-	94

[a] Conditions: **40a**, boronic acid (**33a**, 2 equiv.), base (0 or 2 equiv.), $Pd_2(dba)_3$ (6 mol%), **L1** (13 mol%), dry 1,4-dioxane (0.05 M), Ar atmosphere, 1h. [b] Determined by NMR with an internal standard. Conversion > 99%

Using different solvents like 1,4-dioxane, ^{t}AmOH, heptane or 2-methyl THF led to similar yields. We also performed a brief analysis of the influence of the temperature, observing that the reactions provided similar results in a range of temperatures from 70 to 115 ºC, with the formation of the cyclopentylamine **42aa** in all cases.

In conclusion, to ensure full conversions, we established as optimal reaction conditions the use of $Pd_2(dba)_3$ (6 mol%) and phosphite **L1** (13 mol%), in dioxane, at 100 ºC for 2 hours.

Scope of the transformation

With the optimal conditions in hand, we analyzed the scope of the method (**Scheme 124**). The imine partners were obtained from the corresponding aldehydes **7**, as indicated for the preparation of **40a**.

We started testing the reactivity of **40a** with different boronic acids (**33**). The reaction tolerates *para*-substituted arylboronic acids bearing either electron-donating groups, such as *p*-OMe or *p*-^{t}Bu (**42aa**

and **42ac**, respectively), or electron-withdrawing ones, such as *p*-F (**42ad**), with yields above 90%. Gratifyingly, the reaction works with naphthyl and *ortho*-tolyl boronic acids, affording good to excellent yields (**42ai**, 76% and **42af**, 99%). However, it seems sensitive to steric hindrance, as demonstrated by the low consumption of **40a** when the mesitylene-2-boronic acid (**33j**) was used as partner (42 %Conv. **40a**).

Alkenyl boronic acids, such the cyclopentenyl derivative **33b**, are much less efficient (**42ab**, 19% yield) and, not unexpectedly, alkyl boronic acids led to complex mixtures of products. The use of a 2-pyridine boronic acid provided the product in a poor yield (**42ak**, 13%), likely due to catalyst poisoning by coordination of the palladium to the nitrogen atom. In addition, the reaction employing the electron poorer imine **40b**, containing a sulfonyl group instead the sulfinyl moiety, provided the product **42ba** in a low 20% yield. Finally, a precursor with a NTs group at the connecting tether between the ACP and the imine moiety afforded the corresponding product, **42ca**, in 66% yield.

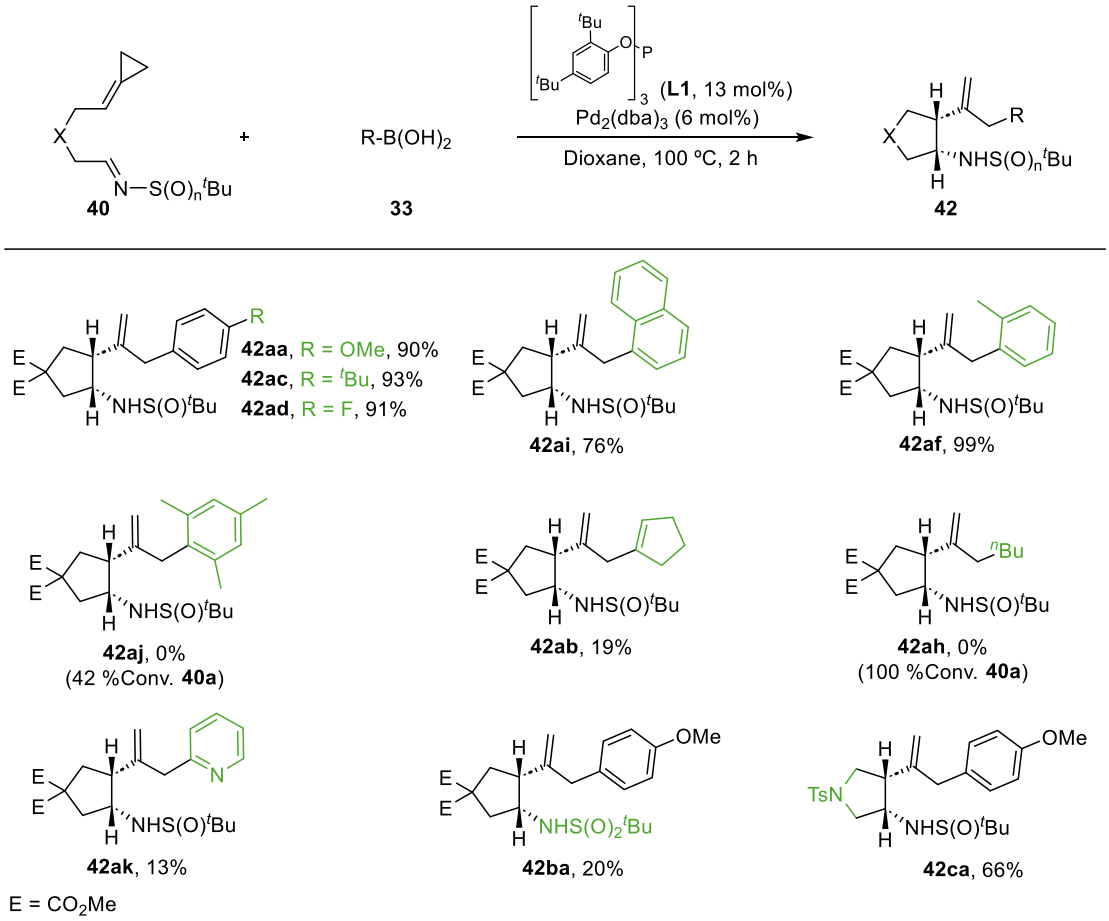

Scheme 124. Scope of the tandem cycloisomerization/ cross-coupling reaction between imine-ACPs **40** and boronic acids **33**.

Additional experiments were carried out with some substrates at lower temperatures or increasing the reaction times, but no improvements in the reactivity were observed. The use of an external base (K_3PO_4) neither increased the efficiency of these processes.

4.3.5.2 Tandem cycloisomerization/nucleophilic additions using 1,3-dicarbonyl partners

To see whether the ACP-tethered imines could also be coupled to other nucleophiles, we tried the reaction of **40a** and dimethyl malonate, using the optimal conditions comprising $Pd_2(dba)_3$ (6 mol%) and **L1** (13 mol%), in the presence of K_3PO_4 (2 equiv.). Unfortunately, the product **44aa** was not observed (**Table 27**, entry 1). The use of other ligands, such as **L9** or **L17**, did not bring any

improvement (entries 2 and 3). In all cases, high consumptions of ACP **40a** were observed, leading to complex mixtures of products.

Table 27. Evaluation of sulfinylimine-ACP **40a** in tandem process with dimethyl malonate.[a]

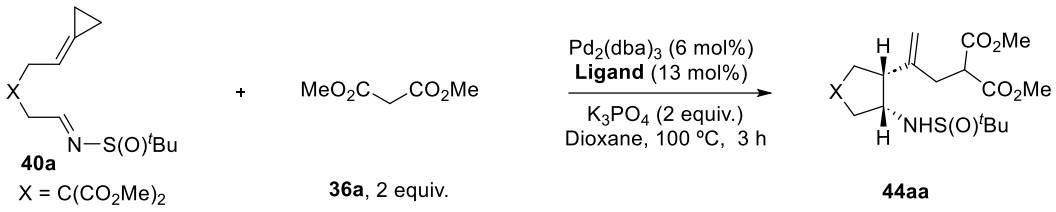

Entry	Ligand	Conv. **40a** (%)[b]	**44aa** (%)
1	**L1**	72	-
2	**L17**	91	-
3	**L9**	90	-

[a] Conditions: **40a**, dimethyl malonate (**36a**, 2 equiv.), K_3PO_4 (2 equiv.), $Pd_2(dba)_3$ (6 mol%), ligand (13 mol%), dry 1,4-dioxane (0.05 M), Ar atmosphere, 100 ºC, 3 h. [b] Determined by NMR with an internal standard.

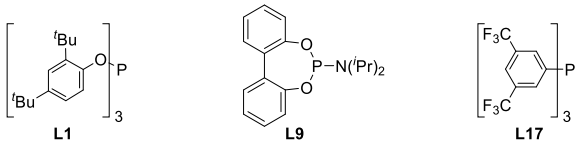

The oxime ether precursor **1k** was also tested (**Scheme 125**). Despite the complete consumption of the substrate, cross-coupling products were not detected and only the diene **4k** could be isolated in low yield.

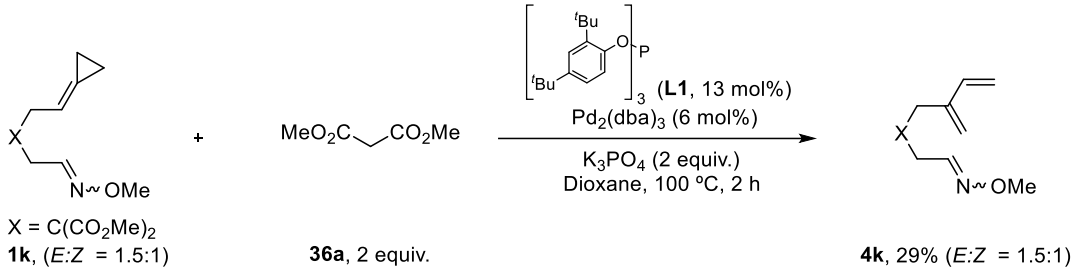

Scheme 125. Evaluation of aldoxime-ACP **1k** in tandem process with dimethyl malonate.

4.3.6 DFT Mechanistic Studies

To gain mechanistic insights on these cycloisomerization/ cross-coupling processes and to find out the factors behind the suppression of the (3+2) cycloaddition pathway, we performed a detailed DFT analysis of the transformations using the B3LYP/6-31G(d) (LANL2DZ for Pd) level of theory for the optimization of stationary points and M06/6–311++g(d,p) (SDD for Pd), in 1,4-dioxane, for single-point energy calculations.

4.3.6.1 Tandem cycloisomerization/ Suzuki-like coupling between ACP-tethered carbonyls and boronic acids

This reaction was studied using the boronic acid **33a**, *p*(MeO)C_6H_4−$B(OH)_2$, and the keto-ACP **9m**, a precursor closely related to the experimentally used substrates **9a** and **9f** (see **Scheme 114**, page 143). Initially, our model catalytic species was a Pd(0) complex bearing one $P(OMe)_3$ ligand (**Figure**

27), which should mimic the behavior of the Pd catalysts bearing electron-deficient ligands like **L1**, **L9** or **L17**.[115]

The **Figure 27** starts with the palladacyclobutane **I1**,[116] which undergoes a migratory insertion of the carbonyl moiety, via **TS1-2** (ΔG=10.8 kcal·mol^{-1}), delivering the π-allyl intermediate **I2**, analogue to the proposed intermediate **C** (see **Scheme 113**, page 141). However, a coordination of the boronic acid to the carbonyl oxygen of **I1**, via hydrogen bonding, leads to a more stable palladacyclobutane, **I3**, from which the migratory insertion occurs with a lower energy barrier of 7.2 kcal·mol^{-1} (**TS3-4**). The resulting π-allyl oxapalladacycle **I4**, is similar to **I2**, but more stable by ~10 kcal·mol^{-1}. We could not identify alternative σ-allyl Pd species, previously located for (3+2) cycloadditions promoted with Pd(0)-*t*BuXPhos (see *Sections* 4.1 and 4.2). From oxapalladacycle **I4**, we can obtain the (3+2) cycloadduct (**17m**) through a reductive elimination with an energy barrier of 14.7 kcal·mol^{-1} (via **TS4-17m**).

However, we located a significatively more favored pathway via **TS4-5** ($\Delta\Delta G$=3.1 kcal·mol^{-1}), which delivers the aryl boronate **I5**.[117] A π-allyl to σ-allyl isomerization via **TS5-6** delivers a new intermediate (**I6**), which undergoes a conformational change to coordinate the aryl group to the Pd center (**I7**). This enables the transmetalation process to occur with a very accessible energy barrier of 5.5 kcal·mol^{-1} (overall barrier of 8.3 kcal·mol^{-1} from **I6**) to form the σ-allyl Pd(II) complex **I8**. A *cis-trans* isomerization provides **I9**, a σ-allyl species with the proper ligand spatial arrangement for the following C-C reductive elimination (**TS9-34ma**, ΔG= 11.1 kcal·mol^{-1}).

Alternatively, the σ-allyl oxapalladacycle **I8** can undergo a σ-allyl to π-allyl isomerization to provide the very stable complex **I10** (**TS8-10**, ΔG=3.7 kcal·mol^{-1}).[118] From **I10**, a reductive elimination entails an energy barrier of 18.2 kcal·mol^{-1}.

Both reductive eliminations, from **I8** and **I10**, are compatible with the temperature required for the reaction, and lead to the cross-coupling product **34ma**, which after further protonation, would provide the experimentally isolated cyclic alcohol. Probably, the precise structure and electronic properties of the ancillary ligand play a crucial role in determining which of these pathways prevails.

[115] Complementary profiles with additional steps (**Figure A5** and **Figure A6**) or different model catalysts [**Figure A7**, Pd(0)-**L17**; and **Figure A8**, Pd(0)-PMe_3] can be found in the *Appendix*.

[116] The initial oxidative addition is computed in **Figure A5** (ΔG= 6.9 kcal·mol^{-1}, *Appendix*, page 333). For previous mechanistic studies on Pd-promoted ACP cycloadditions, covering this first oxidative addition step, see *Section* 4.2 and/or reference 40: Verdugo, F.; da Concepción, E.; Rodiño, R.; Calvelo, M.; Mascareñas, J. L.; López, F. Pd-Catalyzed (3 + 2) Heterocycloadditions between Alkylidenecyclopropanes and Carbonyls: Straightforward Assembly of Highly Substituted Tetrahydrofurans. *ACS Catal.* **2020**, *10*, 14, 7710–7718.

[117] Two alternative pathways that deliver the (3+2) cycloadduct **17m** were found, from **I5** and **I6** respectively, but both were significantly less favorable than the transmetalation pathway through **I6** ($\Delta\Delta G$=4.3 and 5.8 kcal·mol^{-1}, see **Figure A6**, *Appendix,* page 334).

[118] An alternative transmetalation process was found from **I5** to provide **I10** (ΔG= 6.9 kcal·mol^{-1}, **Figure A5**, *Appendix*, page 333).

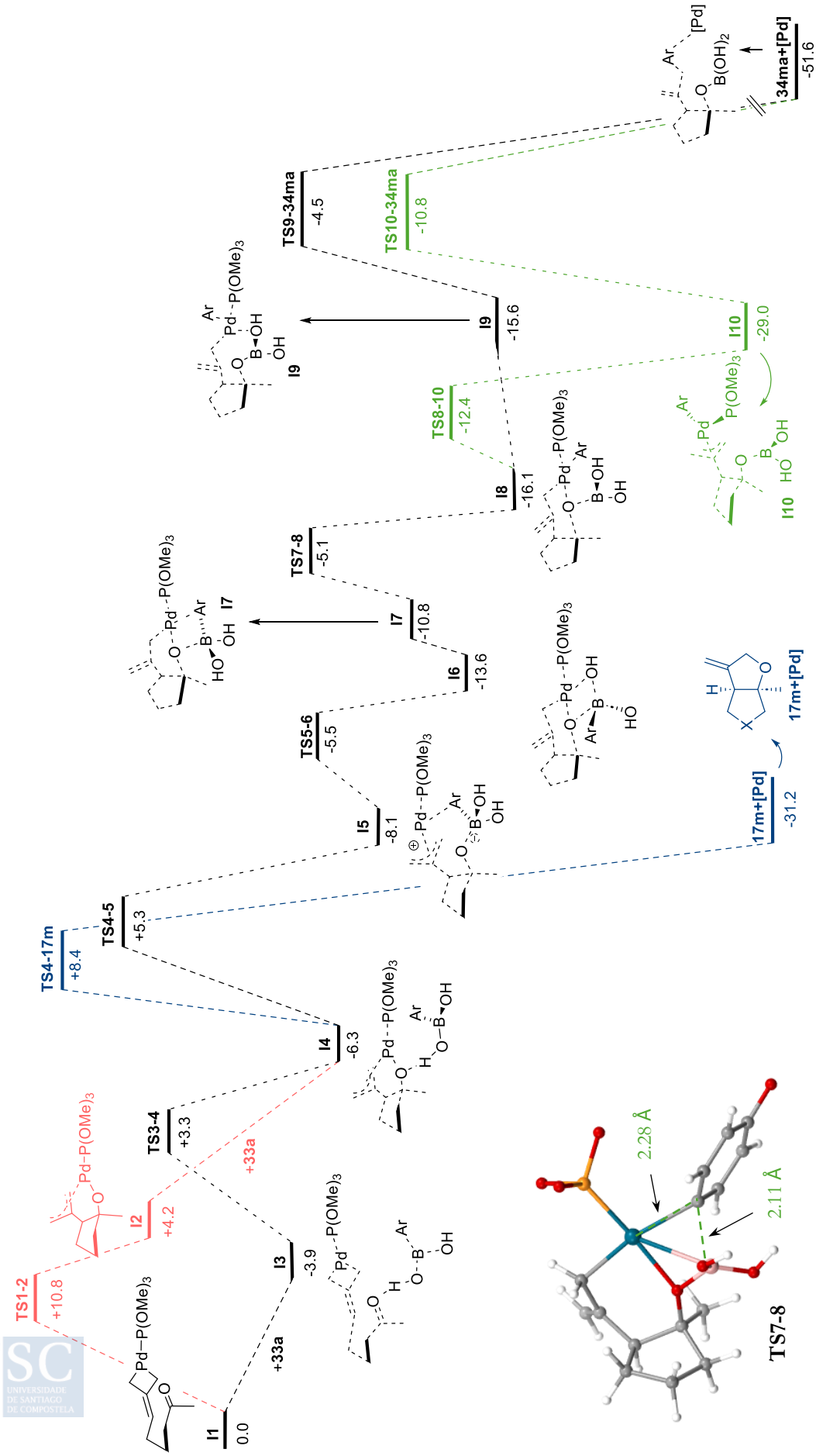

Figure 27. DFT-calculated energy profile ΔG_{solv} (kcal·mol^{-1}) for the tandem process between **9m** and boronic acid **33a** using Pd(0)-P(OMe)$_3$, in 1,4-dioxane. [B3LYP/6-31G(d) (LANL2DZ for Pd)//M06/6–311++g(d,p) (SDD for Pd)]. Ar=*p*(MeO)C$_6$H$_4$.

We then analyzed the profile of the reaction from intermediates of type **I2**, using the Buchwald ligand ^{t}BuXPhos, instead of P(OMe)$_3$. By using this ligand, the (3+2) adduct is experimentally observed, so we wondered whether a computational analysis would replicate this trend.

As depicted in **Figure 28**, intermediate **I13** (analog of **I2**) can undergo a reductive elimination through a 21.6 kcal·mol^{-1} energy barrier to give the (3+2)-cycloadduct **17m**. Alternatively, the oxygen of **I11** can coordinate the boronic acid through a hydrogen bond. Contrary to the situation shown in **Figure 27**, where this coordination stabilized **I3** in almost 11 kcal·mol^{-1}, in this case there is a destabilization by 8.7 kcal·mol^{-1}, forming **I12**.

From this intermediate, the formation of the boronate **I13** proceeds with an energy barrier of 5.0 kcal·mol^{-1}. After an isomerization to orientate the aryl group towards the metal center, the transmetalation occurs through **TS14-15**, to give the π-allyl complex **I15**. Finally, the cross-coupling product **34ma** is formed through a reductive elimination (ΔG=22.8 kcal·mol^{-1}).

Remarkably, the transition state **TS14-15**, that leads to the allylic product **34ma**, is 1.2 kcal·mol^{-1} above **TS11-17m**, which delivers the cycloadduct **17m**. These outcomes qualitatively align with the experimental results, which show that catalysts featuring Buchwald ligands exclusively provide the (3+2) cycloadducts, despite the presence of boronic acids in the reaction media.

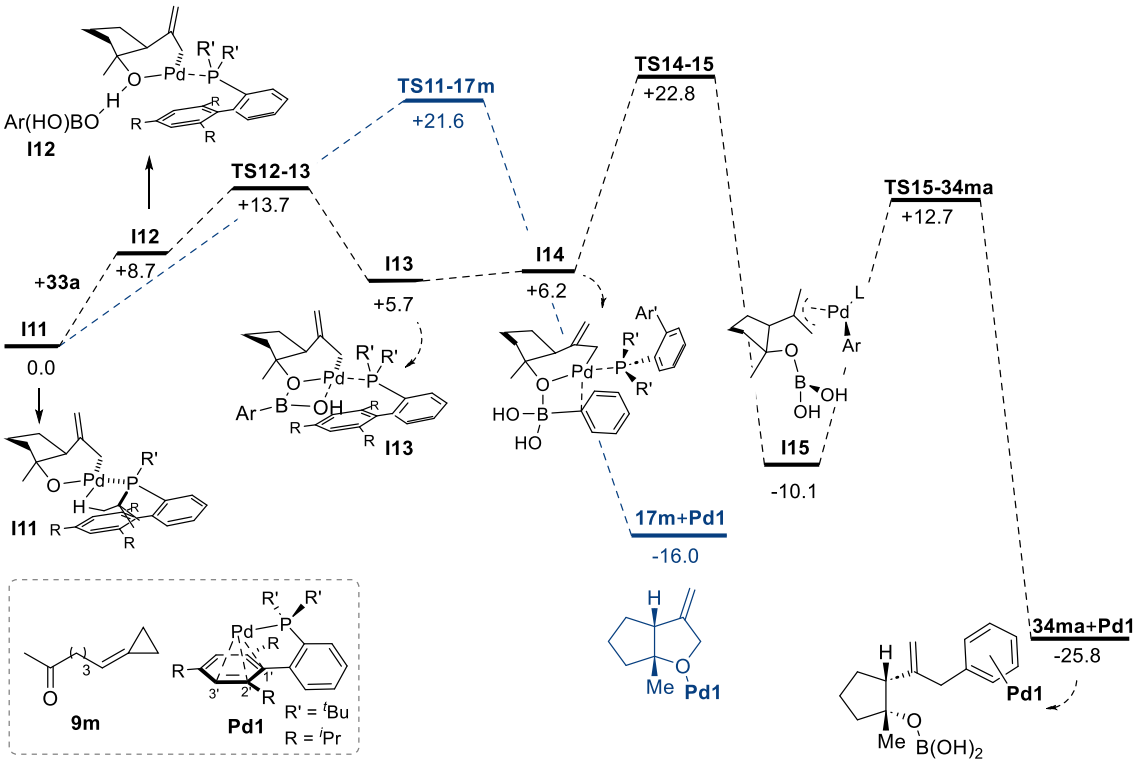

Figure 28. DFT-calculated energy profile ΔG_{solv} (kcal·mol^{-1}) for the tandem process between **9m** and boronic acid **33a** using Pd-^{t}BuXPhos (**Pd1**), in toluene. [B3LYP/6-31G(d) (LANL2DZ for Pd)//M06/6–311++g(d,p) (SDD for Pd)]. [Ar=*p*(MeO)C$_6$H$_4$].

Moreover, we also explored the tandem process between keto-ACPs **9m** and the aryl boronic acid **33a** using monophosphines **L17** and PMe$_3$ as ligands (**Figure A7** and **Figure A8**, respectively, *Appendix*). Collectively, all these results highlight that the π-acidic character of the monodentate ligand plays a crucial role in the formation of the cycloisomerization/cross-coupling products, since these acidic ligands lower the energy barriers of key steps such as the transmetalation and reductive elimination.

4.3.6.2 Tandem processes between ACP-tethered carbonyls and 1,3-dicarbonyl nucleophiles

To analyze these processes, we employed as model substrates the keto-ACP **9m**, and the malonate anion of **36a'**. A Pd(0) complex with one $P(OMe)_3$ ligand was employed as model catalyst (**Figure 29**).

The process starts from the key π-allyl oxapalladacycle **I2**, which is obtained from **I1** (see **Figure 27**, page 157). Then, the out-sphere attack of the malonate ion (**36a'**) to **I2** occurs through an accessible barrier of 7.9 kcal·mol^{-1}, affording the alkylated product **37ma** (**Figure 29**). Alternatively, **I2** could also reach the (3+2) cycloadduct **17m** through a reductive elimination with a barrier of 9.5 kcal·mol^{-1}. This step is 1.6 kcal·mol^{-1} more energetic than the out-sphere nucleophilic attack, which is in qualitative agreement with the experimental results, as only the cyclopentanols of type **37** are observed.

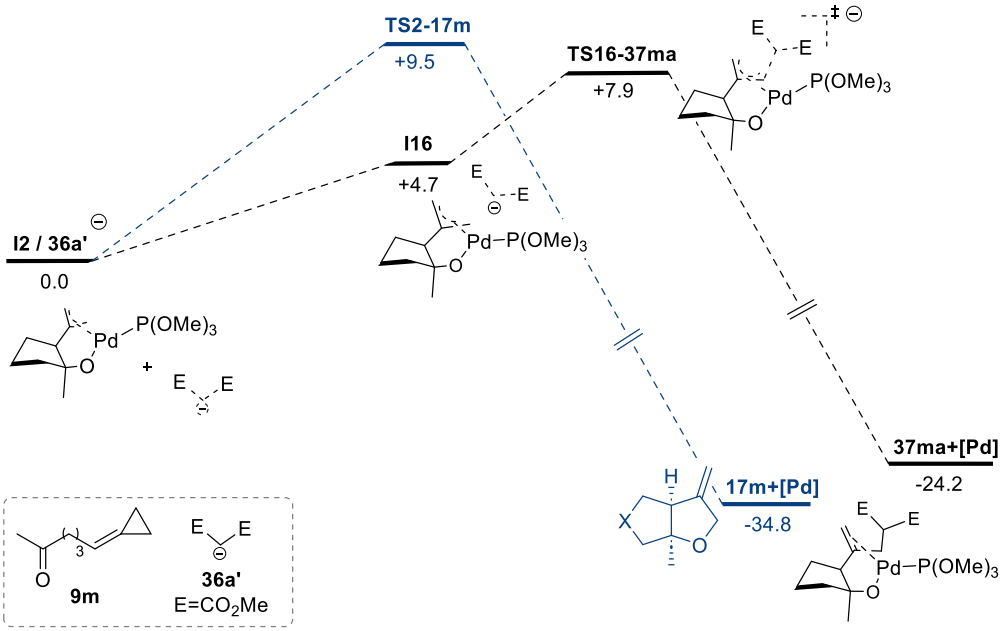

Figure 29. Energy profile for the evolution of **I2** in the presence of anion **36a'**, in 1,4-dioxane. ΔG_{solv} (kcal·mol^{-1}). [B3LYP/6-31G(d) (LANL2DZ for Pd)//M06/6–311++g(d,p) (SDD for Pd)].

4.3.6.3 Tandem processes between ACPs tethered to imine partners and boronic acids

We also performed preliminary computations with the *N*-sulfinyl imine **40d**, a precursor closely related to the experimentally tested substrate **40a**. The results of the key carbometallation step are summarized in **Figures 30** and **31**.

Figure 30, using (*S*)-sulfinyl imine **40d**, starts from the palladacyclobutane **I17**, which undergoes a migratory insertion to the palladium π-allyl species **I18** (ΔG=11.6 kcal·mol^{-1}). Curiously, coordination of the boronic acid to either the oxygen (blue path) or nitrogen atom (red path) of the imine led to a destabilization of the palladacyclobutane **I17**, affording **I19** and **I21**. However, these interactions favor eventually easier migratory insertions, with overall energy barriers of 8.8 and 10.5 (respectively via **TS19-20** and **TS21-22**).

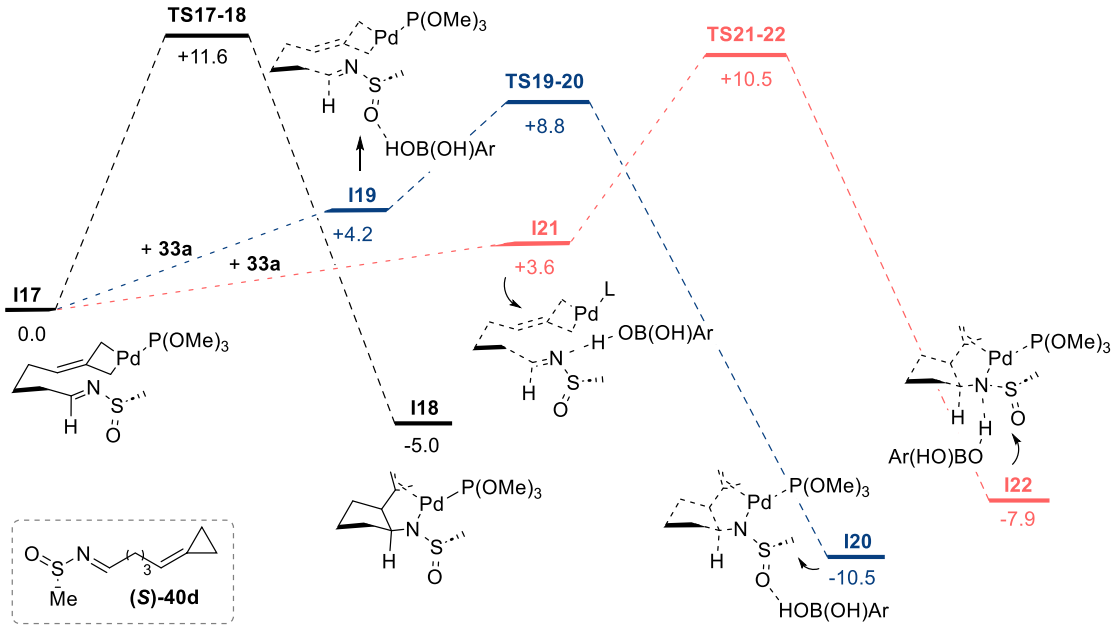

Figure 30. Energy profile ΔG_{solv} (kcal·mol^{-1}) for carbometallation step from for **(*S*)-40d**, in 1,4-dioxane. [B3LYP/6-31G(d) (LANL2DZ for Pd)//M06/6–311++g(d,p) (SDD for Pd)]. Ar=*p*(MeO)C_6H_4.

Figure 31 shows the analog migratory insertion step for the (*R*)-sulfinyl imine **40d**. Again, the coordination of the boronic acid to the sulfinyl imine, both through de nitrogen or oxygen atom, causes a destabilization of palladacyclobutane **I23**. In this case, this energy penalty is sufficient to favor the migratory insertion without coordination (via **TS23-24**) by 1.4 and 5.0 kcal·mol^{-1}, respectively.

In conclusion, the presence of a chiral center at the sulfur atom of these precursors opens diastereoisomeric pathways that might have different behaviors, as demonstrated in the migratory insertion, where the activation of the imine by hydrogen bonding with the boron reagent is only favorable from **(*S*)-40d**.

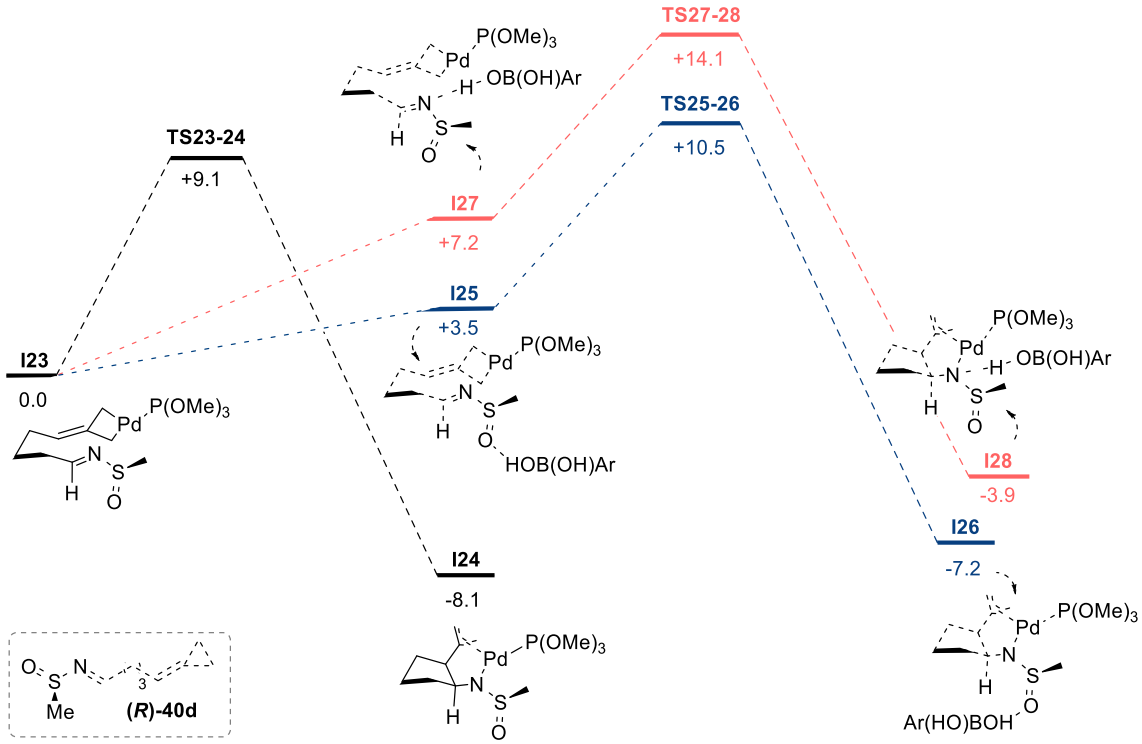

Figure 31. Energy profile ΔG_{solv} (kcal·mol^{-1}) for the carbometallation step for **(*R*)-40d**, in 1,4-dioxane. [B3LYP/6-31G(d) (LANL2DZ for Pd)//M06/6–311++g(d,p) (SDD for Pd)]. Ar=*p*(MeO)C_6H_4.

Besides, we explored the transmetalation step for **(*S*)-40d**. From the σ allyl intermediate **I29** (**Figure 32**, path A), the transmetalated intermediate **I30** is formed via a 3.8 kcal·mol^{-1} energy barrier. On the other hand, the π allyl species **I31** is more energetic than the σ allyl complex **I29** (ΔG=7.3 kcal·mol^{-1}), and transmetalates through an energy barrier of 5.0 kcal·mol^{-1} to form the very stable π allyl intermediate **I32** (**Figure 32**, path B). Therefore, the transmetalation step seems to proceed preferentially through σ allyl species.

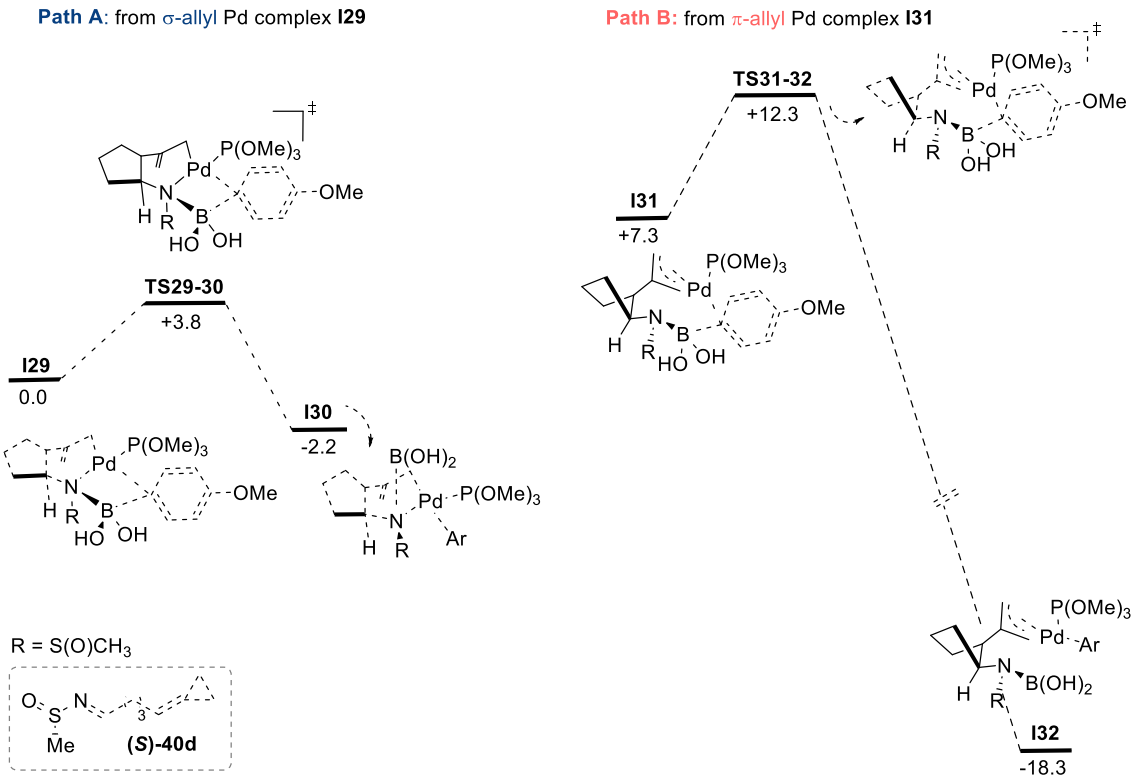

Figure 32. Energy profile ΔG_{solv} (kcal·mol^{-1}) for the transmetalation step for **(*S*)-40d**, in 1,4-dioxane. [B3LYP/6-31G(d) (LANL2DZ for Pd)//M06/6–311++g(d,p) (SDD for Pd)]. Ar=*p*(MeO)C_6H_4.

In conclusion, the overall process follows the same steps as for the carbonyl precursor **9m**. The main difference lies in the migratory insertion of the imine double bond [ΔG=8.8 kcal ·mol^{-1} for **(*S*)-40d** and ΔG=9.1 kcal ·mol^{-1} for **(*R*)-40d**], which is slightly more demanding than that of the methyl ketone **9m** (ΔG=7.2 kcal ·mol^{-1}, **Figure 27**, page 157). In addition, the chirality of the sulfur atom leads to different carbometallation pathways, where the coordination of the boronic acid provides a less energetic step only with the **(*S*)-**isomer.

4.3.7 Conclusions

In summary, we have developed novel Pd(0)-catalyzed tandem cycloisomerization/allylic substitution reactions through the nucleophilic interception of Pd(II) allylic intermediates of type **C**, *in situ* generated from ACPs tethered to carbonyl or imine partners.

The reaction between ACP-tethered carbonyls and a variety of 1,3-dicarbonyl nucleophiles, promoted by the catalyst generated from $Pd_2(dba)_3$ and the electron poor phosphine **L17**, provided the expected cyclic alcohols in good-to-excellent yields and high *syn* selectivity for most cases. Furthermore, the use of the phosphoramidite **L9**, instead **L17**, allowed the use of alcohols as coupling partners, providing the corresponding products with ether allylic functionalities in good yields.

DFT computations demonstrated that the characteristics of the ancillary ligand can modulate the results of the Pd(0)-catalyzed reactions of these ACPs-tethered carbonyl systems. Using Pd(0)-$P(OMe)_3$ as model catalyst, the studies demonstrated that the allyl oxapalladacyclic species **C** preferentially evolves through transmetalation with the boronic acid rather than the competitive C–O reductive elimination to give the cycloadduct. In contrast, the use of Pd(0)-*t*BuXPhos favored the formation of σ-allyl oxapalladacyclic intermediates that eventually evolve to the (3+2) cycloaddition products.

Similarly, calculations with Pd(0)-$P(OMe)_3$ revealed that the out-of-sphere attack of a dimethyl malonate on intermediate **C** is energetically preferred over the potentially competitive C-O reductive elimination. These findings align with experimental results, since electron-poor monophosphines favor the formation of tandem products, whereas Buchwald ligands promote (3+2) intramolecular cycloadducts.

Additionally, we developed a tandem cycloisomerization/cross-coupling process of ACPs tethered to sulfinyl imines, and aryl boronic acids, using $Pd_2(dba)_3$/ **L1** as catalyst. Although with a narrower scope than the analogue process with carbonyls, these transformations provided the expected cyclopentamines in good-to-excellent yields and complete *syn* selectivity.

A preliminary DFT analysis of these reactions with ACP-tethered imines and boronic acids, indicated that the transformation follows a similar mechanistic pathway than the analogue reaction with keto-ACPs.

4.4. Pd(0)-Catalyzed Cross-Coupling between ACPs and Boronic Acids

This section is published in:

Rodiño, R.[a]; Mardones, F.[b]; Paredes, K.[b]; Jiménez, C. A.[b]; Nelson, R.; Mascareñas, J. L.[a]; López, F.[a, d]; Verdugo, F.[b] Palladium-Catalyzed Cross-Coupling between Alkylidenecyclopropanes and Boronic Acids. *Adv. Synth. Catal.* **2024**, 366, 5144. DOI: 10.1002/adsc.202400657

Authors' affiliations:

[a] Centro Singular de Investigación en Química Biolóxica e Materiais Moleculares (CiQUS) and Departamento de Química Orgánica, Universidade de Santiago de Compostela 15782 Santiago de Compostela (Spain).

[b] Departamento de Química Orgánica, Facultad de Ciencias Químicas, Universidad de Concepción, Concepción, 4070371 Chile

[c] Departamento de Química, Facultad de Ciencias, Universidad Católica del Norte, Avda. Angamos 0610, Antofagasta, 1270709 Chile

[d] Misión Biológica de Galicia Consejo Superior de Investigaciones Científicas (CSIC) 36080 Pontevedra (Spain).

4.4.1 Pd(0)-Catalyzed Hydrofunctionalization Reactions of ACPs

The transition metal catalyzed hydrofunctionalization of ACPs is an efficient tool to synthesize 1,1-difunctionalized alkenes. Under Pd(0) conditions, in the presence of certain pronucleophiles, ACPs can undergo ring-opening reactions to form π-allyl intermediates of type **A**, which can evolve to a broad range of products (**Figure 33**).[119] This method, initially developed in the late nineties (see **Scheme 56**, *Introduction*, page 49), has been applied to various hydrogen-containing nucleophiles like alcohols, amines or amides. Its use with carbon-based nucleophiles is underexplored and limited to malonates or electron-rich heteroaromatics.

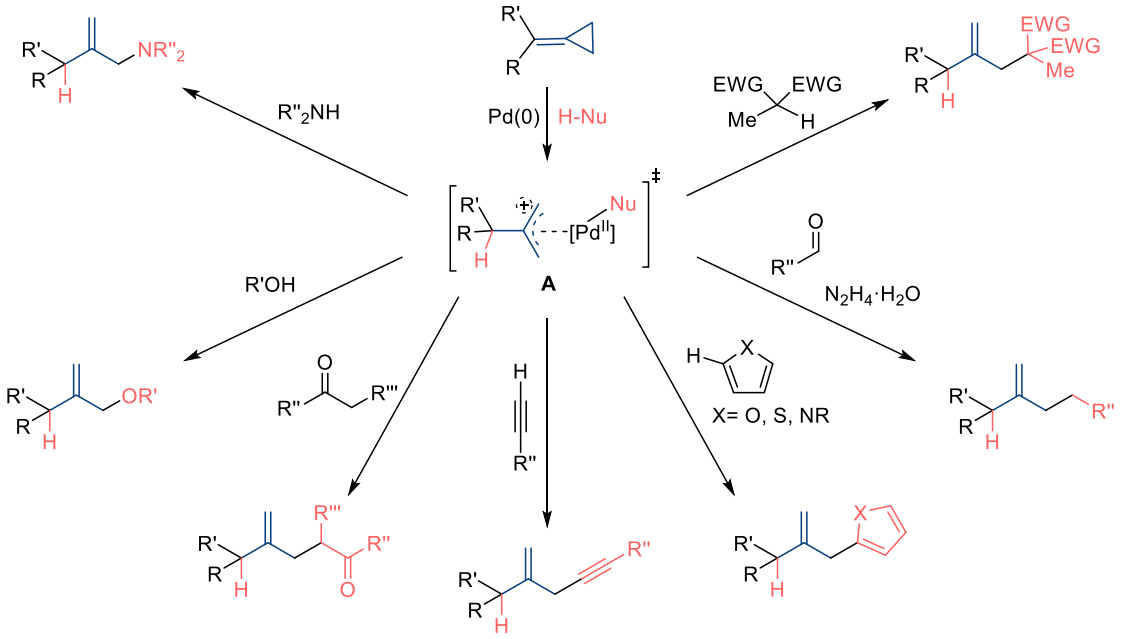

Figure 33. Pd(0)-catalyzed hydrofuncionalization of ACPs.

From a mechanistic point of view, these processes were generally proposed to involve the formation of an initial palladium hydride species of type **B**, followed by a regioselective hydropalladation of the ACP affording the σ-cyclopropyl complex **C**, which eventually evolves through a β-carbon elimination to a key π-allyl Pd(II) intermediate **A** (**Scheme 126**, path A). As an alternative, a path involving palladacyclobutane intermediates like **D** has also been suggested in few specific cases (path B).[119c, 119e-g, 119i] Nonetheless, the mechanistic experimental data is very scarce and not conclusive, whereas computational studies have never been reported.

[119] a) Tsukada, N.; Shibuya, A.; Nakamura, I.; Yamamoto, Y. Ring Opening in the Palladium-Catalyzed Hydrocarbonation of Methylenecyclopropanes with Pronucleophiles. *J. Am. Chem. Soc.* **1997**, *119*, 34, 8123–8124.; b) Tsukada, N.; Shibuya, A.; Nakamura, I.; Kitahara, H.; Yamamoto, Y. Inter- and Intramolecular Palladium-Catalyzed Hydrocarbonation of Methylenecyclopropanes with Carbon Pronucleophiles. *Tetrahedron* **1999**, *55*, 30, 8833–8844.; c) Nakamura, I.; Saito, S.; Yamamoto, Y. Hydrofurylation of Alkylidenecyclopropanes Catalyzed by Palladium. *J. Am. Chem. Soc.* **2000**, *122*, 11, 2661–2662.; d) Camacho, D. H.; Nakamura, I.; Saito, S.; Yamamoto, Y. Palladium-Catalyzed Addition of Alcohol Pronucleophiles to Alkylidenecyclopropanes. J. Org. Chem. **2001**, *66*, 1, 270–275.; e) Nakamura, I.; Siriwardana, A. I.; Saito, S.; Yamamoto, Y. Addition of Heteroaromatics to Alkylidenecyclopropanes Catalyzed by Palladium. *J. Org. Chem.* **2002**, *67*, 10, 3445–3449.; f) Camacho, D. H.; Nakamura, I.; Oh, B. H.; Saito, S.; Yamamoto, Y. Palladium-catalyzed addition of ketones to alkylidenecyclopropanes. *Tetrahedron* **2002**, *43*, 16, 2903-2907.; g) Siriwardana, A. I.; Kamada, M.; Nakamura, I.; Yamamoto, Y. Palladium-Catalyzed Addition of Nitrogen Pronucleophiles to Alkylidenecyclopropanes. *J. Org. Chem.* **2005**, *70*, 15, 5932–5937.; h) Villarino, L.; López, F.; Castedo, L.; Mascareñas, J. Palladium-Catalyzed Hydroalkynylation of Alkylidenecyclopropanes. *Chemistry – A European Journal* **2009**, *15*, 13308–13312.; i) Yao, J.; Chen, Z.; Yu, L.; Lv, L.; Cao, D.; Li, C.-J. Palladium-catalyzed hydroalkylation of methylenecyclopropanes with simple hydrazones. *Chem. Sci.* **2020**, *11*, 10759-10763.

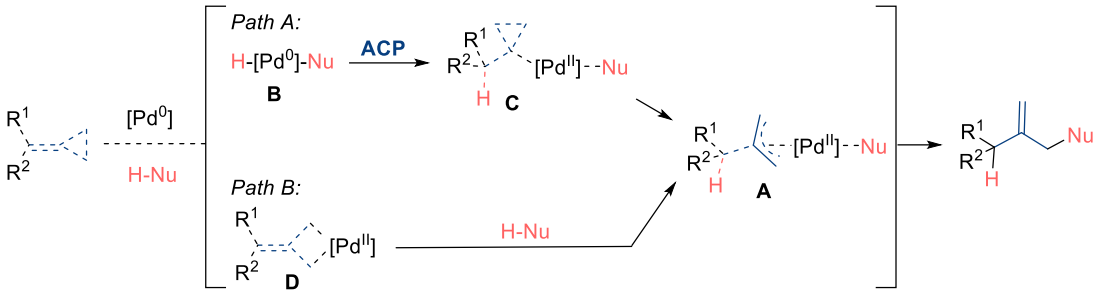

Scheme 126. Possible mechanisms for Pd(0)-catalyzed hydrofuncionalizations of ACPs.

Regardless the type of mechanism, the interception of the resulting π-allyl Pd species is limited to a restricted range of nucleophiles (**Figure 33**), and the use of organometallic reagents, like organoboronic acids [HNu = $ArB(OH)_2$], which could drastically increase the synthetic versatility of these transformations, has never been addressed.

4.4.2 Objectives

In the previous section, we demonstrated that the reactions of ACP-carbonyls like **9** with boronic acids proceed via π-allyl oxapalladacycles, which undergo a transmetalation step with the boronic acid (**Scheme 127**).

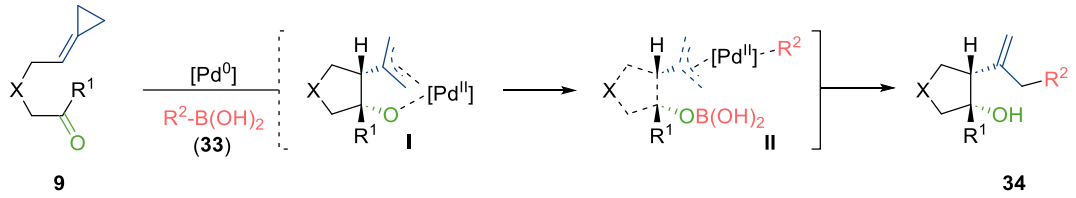

Scheme 127. Pd(0)-catalyzed tandem cycloisomerization/ cross coupling process.

Considering the aforementioned hydrofuncionalization precedents, we reasoned that it would be possible to develop an intermolecular cross-coupling reaction between ACPs and boronic acids, assuming that acyclic π-allyl intermediates of type **A**, resulting from the addition of alcohols, could be intercepted by a boron-based nucleophile (**Scheme 128**).

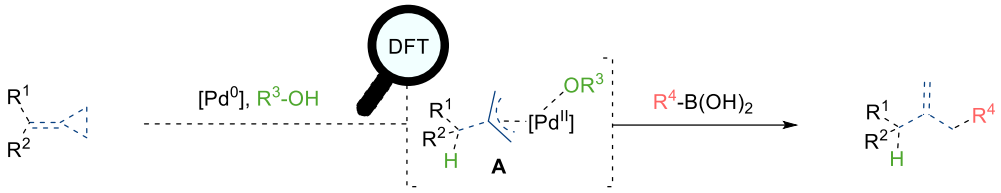

Scheme 128. Pd(0) hydrofunctionalization of ACPs with boronic acids.

On these bases, we set as objective the **development of a Pd-catalyzed allylic cross-coupling between ACPs and boron-based organometallic reagents**. The approach would be synthetically relevant, since the obtained 1,1-disubstituted alkenes are often challenging to synthesize by other methods, whereas alternative allylic Suzuki couplings with allyl bromides are scarce.

Additionally, we planned to **explore the reaction mechanism using computational methods**.

4.4.3 Results and Discussion

The experimental work was carried out in collaboration with Dr. Verdugo.

4.4.3.1 Optimization

We first explored the reaction between ACP **19b** and phenyl boronic acid, under the catalytic conditions developed for the cycloisomerization/cross-coupling reactions [$Pd_2(dba)_3$ / **L1**, **L2** or **L3** (ratio Pd:L 1:1.1) in refluxing dioxane]. We employed phenol as additive (**38a**, 2 equiv.), aiming to favor the formation of alkoxide Pd species of type **A** (**Scheme 128**, *Objectives*), which could enable the subsequent transmetalation of the boronic acid.

The reaction in presence of $Pd_2(dba)_3$ and phosphine **L17** provided full consumption of the ACP **19b**, but we only observed a complex mixture of products (**Table 28**, entry 1). Gratifyingly, when using the phosphite **L1**, we observed the desired coupling product **45bl** in 40% yield (entry 2), and traces of the subproduct **45bl'** (detected in the crude mixture). The reaction with phosphoramidite **L9** provided a slightly higher yield (**45bl**, 50%) after 6 h of reaction (entry 3). As expected, the use of more electron-rich phosphines, such as PPh_3 or RuPhos, led to complex mixtures of products (entries 4 and 5). Notably, by switching the Pd(0) source from $Pd_2(dba)_3$ to CpPd(π-cin.), the arylated product **45bl** could be obtained in 80% yield, after just 3 h (entry 6). Under the same conditions, but using *p*-fluorophenol as additive (**38e**), the product **45bl** was obtained in a slightly higher yield (85%, entry 7).

As expected, a control experiment in the absence of boronic acid, afforded the allylic phenoxide product **46ba** in 55% yield (entry 8).[119d] This result suggests the formation of the putative alkoxide Pd species **A**, which, in the absence of boronic acid, would proceed via a C-O reductive elimination to deliver **46ba**.

However, to our surprise, when the reaction was carried out in the absence of phenol (**38a**), we observed that the product **45bl** was still formed, although in a somewhat lower yield (60%, entry 9). Interestingly, the yield could be enhanced by using KOH or K_2CO_3 (2 equiv.) instead of phenol, obtaining the product **45bl** in 85% and 90% yield, respectively (entries 10 and 11). Contrary, using the preformed phenyl boronate $[PhB(OH)_3]^-$ as nucleophilic partner, the desired product **45bl** was not detected in the reaction crude mixture (entry 12), what is an interesting result from a mechanistic perspective.

[119d] Camacho, D. H.; Nakamura, I.; Saito, S.; Yamamoto, Y. Palladium-Catalyzed Addition of Alcohol Pronucleophiles to Alkylidenecyclopropanes. J. Org. Chem. **2001**, *66*, 1, 270–275.

Table 28. Optimization of the catalytic conditions for the allylic cross-coupling process.[a]

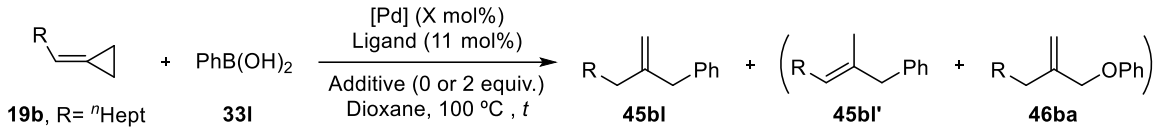

19b, R= ^{n}Hept | **33l** | **45bl** | **45bl'** | **46ba**

Entry	**Pd** (x mol%)	**Ligand**	**Additive** (2 equiv.)	**t**/h	**45bl** (%)[b]	**46ba** (%)
1	$Pd_2(dba)_3$ (5)	**L17**	**38a**, PhOH	6	<5	-
2	$Pd_2(dba)_3$ (5)	**L1**	**38a**, PhOH	8	40	-
3	$Pd_2(dba)_3$ (5)	**L9**	**38a**, PhOH	6	50	-
4	$Pd_2(dba)_3$ (5)	PPh_3	**38a**, PhOH	6	-	-
5	$Pd_2(dba)_3$ (5)	**RuPhos**	**38a**, PhOH	6	-	-
6	CpPd(π-cin.) (10)	**L9**	**38a**, PhOH	3	80	-
7	CpPd(π-cin.) (10)	**L9**	**38e**, *p*-F(C_6H_4)OH	3	85	-
8[c]	CpPd(π-cin.) (10)	**L9**	**38a**, PhOH	3	-	55
9	CpPd(π-cin.) (10)	**L9**	-	3	60	-
10	CpPd(π-cin.) (10)	**L9**	KOH	3	85	-
11	CpPd(π-cin.) (10)	**L9**	K_2CO_3	3	90	-
12[d]	CpPd(π-cin.) (10)	**L9**	-	3	-	.

[a] Conditions: **19b**, boronic acid (**33l**, 2 equiv.), additive (0 or 2 equiv.), [Pd] (x mol%), ligand (11 mol%), dry 1,4-dioxane (0.1 M), Ar atmosphere, 100 °C. %Conv. **19b** > 99. [b] Traces (< 5%) of **45bl'** were detected in the crude (^{1}H-NMR). [c] Without boronic acid. [d] Carried out with preformed $[PhB(OH)_3]K$, previously prepared from $PhB(OH)_2$ and KOH.

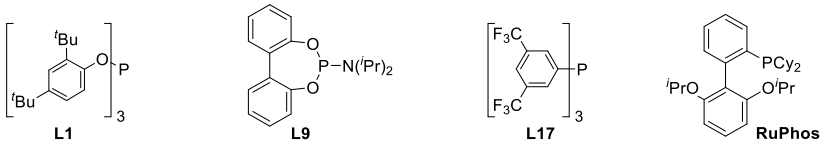

4.4.3.2 Scope of the transformation

To evaluate the scope, we established as optimal conditions the use of CpPd(π-cin.) (10 mol%) and phosphoramidite **L9** (11 mol%) as catalyst, together with K_2CO_3 (2 equiv.), in refluxing dioxane.

We initially evaluated different boronic acids with the model ACP **19b**. As can be seen in **Scheme 129**, the reaction works with electron-rich boronic acids, such as *p*-OMe-phenylboronic acid, affording the product **45ba** and its regioisomer **45ba'** in 92% yield, in a ratio (rr) 5:1. The formation of isomer **45ba'** can be minimized by using *p*-fluorophenol as additive, instead K_2CO_3 (70% yield, **45ba:45ba'** ratio >15:1).

The reaction can be used for the synthesis of other products, like benzodioxole derivative **45bm**, which was formed in an excellent 90% yield, while the *ortho*-tolyl derivatives **45bf** and **45b'** were isolated in 50% yield (rr = 5.3:1). In this case, the use of *p*-fluorophenol enhanced both the ratio (up to >12:1) and the overall yield of **45bf** (71%).

The method tolerates boronic acids exhibiting larger aromatic rings, such as 1-naphthalene (**45bi**, 55% yield), and electron-deficient boronic acids, like *p*-fluorophenylboronic acid. In this case, the corresponding products (**45bd** and **45bd'**) were obtained in an excellent 90% yield (6:1 ratio) under

basic conditions. Meanwhile, when *p*-fluorophenol was used as additive, **45bd** was isolated as an only isomer in 60% yield.

The transformation is not restricted to aromatic boronic acids, so products derived from alkenyl boronic acids, such as **45bb** and **45bb'** (80%, rr = 5:1), and **45bj** and **45bj'** (85%, rr = 5:1), could also be generated. Moreover, heteroaromatic boronic acids, such as 3-pyridinylboronic acid (**33k**), are also compatible, providing the corresponding allylic product, **45bk**, in 40% yield. As expected, alkylboronic acids were not suitable reactants, as β-hydride elimination processes might compete. This was demonstrated in the reaction between **19b** and ^{n}Bu-B(OH)$_2$ (**33h**), which resulted in traces of the product **45bh**.

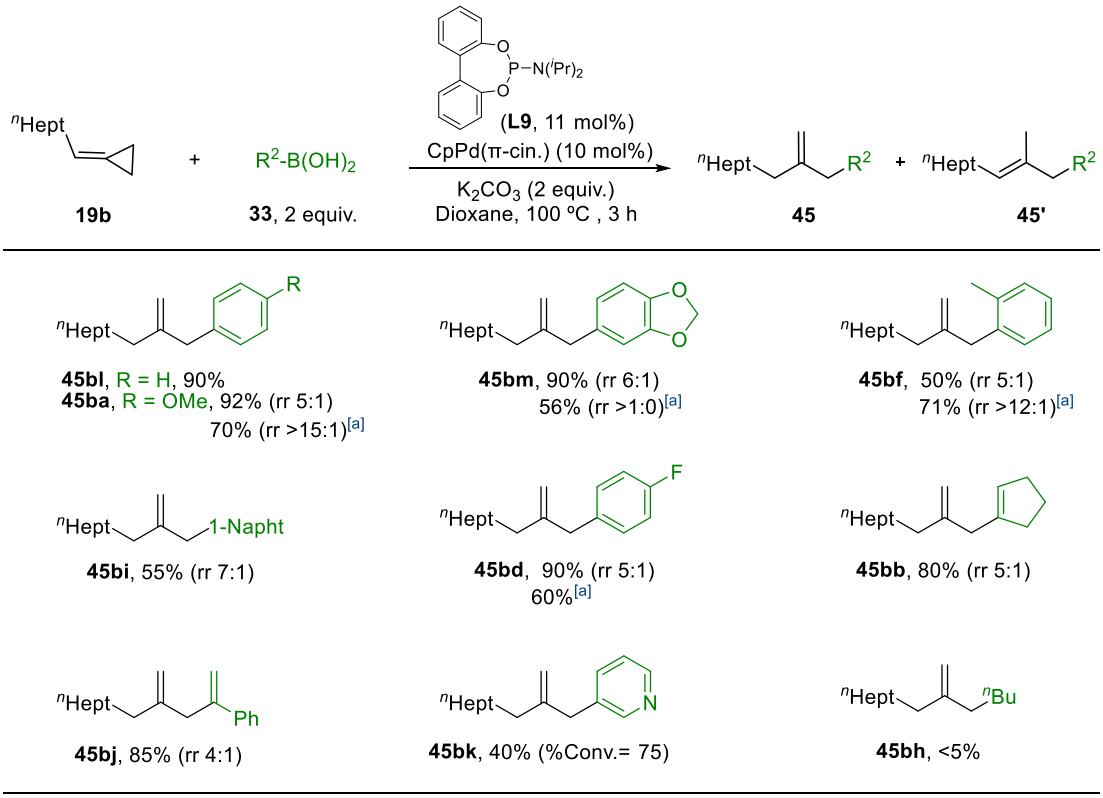

[a]Using *p*-F-C$_6$H$_4$OH (**38e**, 2 equiv.) instead K$_2$CO$_3$
rr = regioisomeric ratio

Scheme 129. Scope of the allylic cross-coupling reaction between model ACPs **19b** and boronic acids.

We next evaluated different monosubstituted ACPs (**Scheme 130**). The reaction with substrate **19l**, containing a *gem*-diester group, provided the product **45la** in a poor 35% yield, together with a complex mixture of side products. The reaction was also tested using *p*-fluorophenol, instead of the base and, in this case, the product **45la** was isolated in 88% yield as unique isomer. Under the same conditions, the product **47na**, containing a ketone, was obtained in 85% yield. Additionally, ACP **19g**, bearing a carboxy ester directly attached to the alkene, provided the adduct **45gl** in a moderate 40% yield, at 60 °C.

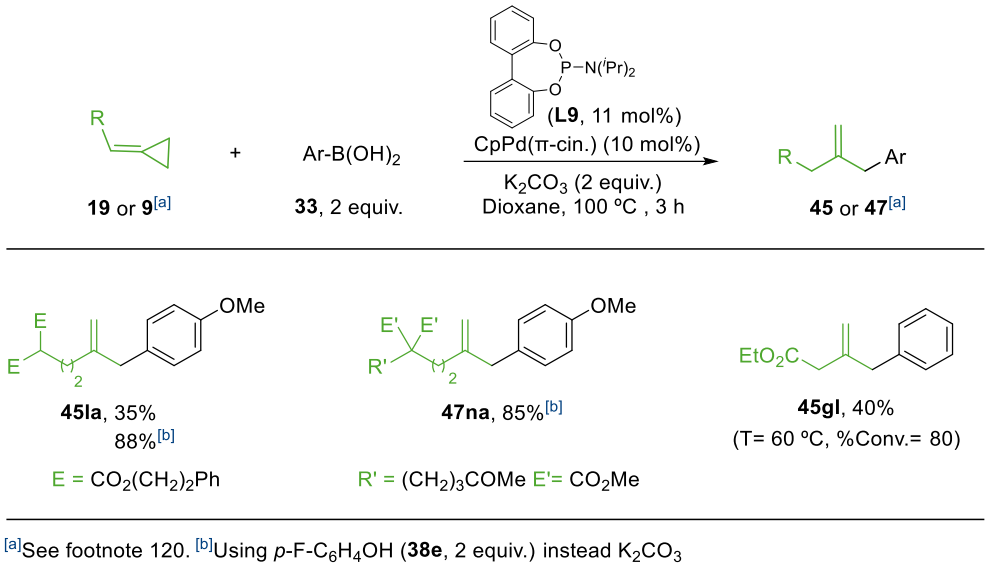

[a]See footnote 120. [b]Using *p*-F-C_6H_4OH (**38e**, 2 equiv.) instead K_2CO_3

Scheme 130. Scope of the allylic cross-coupling reaction using different monosubstituted ACPs **19** or **9**.[120]

The method also works with 1,1-disubstituted ACPs (**Scheme 131**), which were prepared through Wittig reactions from the corresponding ketones. Symmetric substrates like **19d** and **19e** led to the corresponding products, **45dl** and **45el**+**45el'**, in 85% and 83% yield, respectively. Meanwhile, the non-symmetric ACP **19m**, containing a pentyl and an ethyl group, afforded the corresponding products (**45ma** and **45ma'**) in 71% yield in a 7:1 ratio. Likewise, the ACP **19f**, containing a phenyl and a methyl group, provided the products **45fa** and **45fa'** in excellent yield (92%, rr= 10:1).

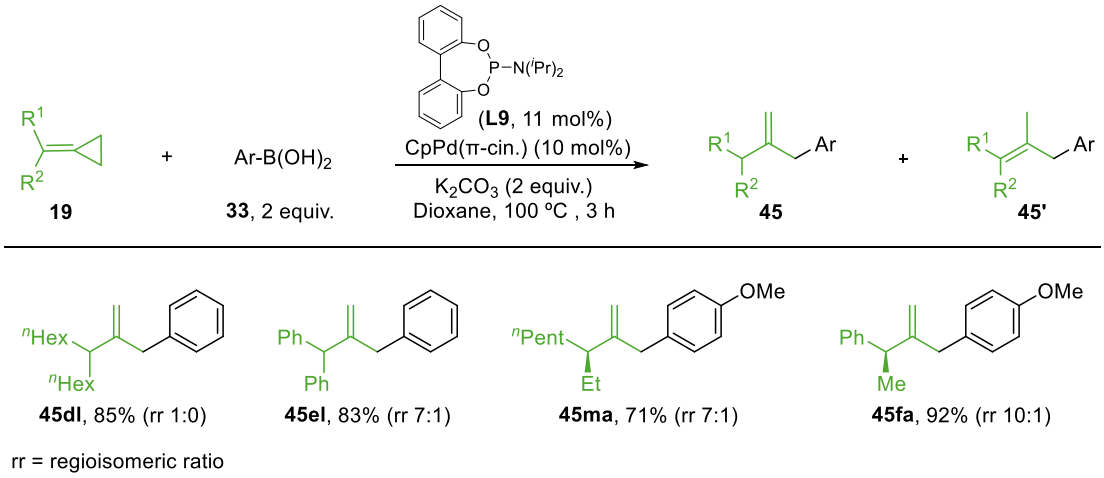

Scheme 131. Scope of the allylic cross-coupling reaction between disubstituted ACPs **19** and boronic acids **33**.

4.4.4 Mechanistic Studies

4.4.4.1 Experimental studies

To gain insight into the reaction mechanism, the deuterated phenylboronic acid ***d*-33l** was prepared from triphenylboroxine using deuterated water, observing a 74% of deuteration (**Scheme 135**).

[120] For clarity and consistency with the different sections of the manuscript, ACPs precursors tethered to ketone moieties are labeled as **9**, while the substrates without carbonyl moieties are named **19**. Consequently, the products from ACPs **9** are named as **45**, while product from ACPs **19** are named as **47**.

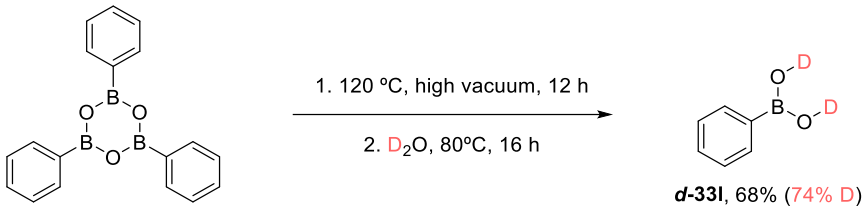

Scheme 132. Synthesis of the deuterated phenyl boronic acid ***d*-33l**.

The reaction between ACP **19b** and the deuterated phenyl boronic acid ***d*-33l**, using $Pd_2(dba)_3$ and phosphoramidite **L9**, in absence of additives, afforded the allylic product ***d*-45bl** in 50% yield, with a 70% of deuteration, and the subproduct ***d*-45bl'** in 14% (**Scheme 137**).[121] This result suggests that boronic acids are behind the formation of the proposed π-allyl Pd intermediate **A**, but cannot determine which is the precise pathway (see **Scheme 126**, *Precedents*, page 168).

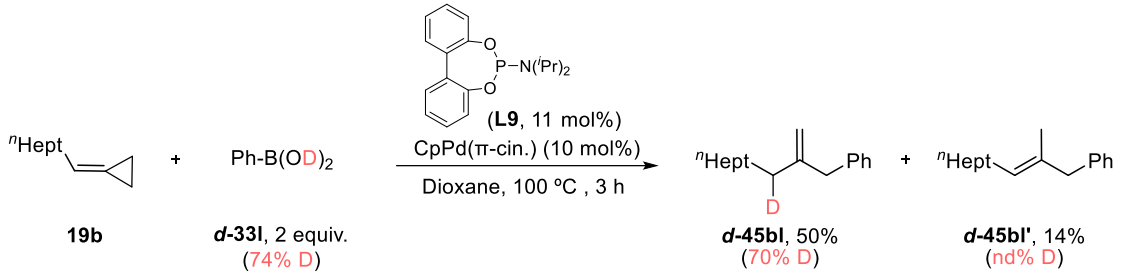

Scheme 133. Pd-catalyzed cross-coupling reaction between ACP **19b** and deuterated boronic acid ***d*-33l**.

On the other hand, we confirmed that the product **46ba**, generated from the Pd-catalyzed cross-coupling between ACP **19b** and phenol (**Table 28**, entry 8, page 171), reacts with phenyl boronic acid, using CpPd(π-cin.)/**L9** in refluxing dioxane, to afford the cross-coupling product **45bl** in 95% yield (**Scheme 134**). This result suggests that the proposed π-allyl Pd alkoxide intermediate (**A**) can be regenerated from **46ba** after an initial C-O oxidative addition, eventually affording the cross-coupling product **45bl**.

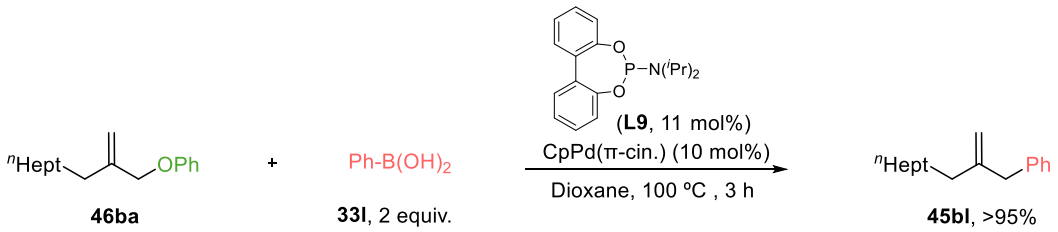

Scheme 134. Treatment of product **46ba** under $Pd_2(dba)_3$/**L9** conditions in presence of phenyl boronic acid.

4.4.4.2 DFT studies

DFT studies were performed to shed light on the mechanism of these processes, both using basic conditions and with phenol as additive. The ACP **19b** and phenyl boronic acid were selected as model reagents, together with a Pd(0)-$P(OPh)_3$ complex, which should mimic the behavior of the experimentally used catalysts with **L1** and **L9** as ligands. We employed B3LYP/6-31G(d) (LANL2DZ for Pd) for the optimization of the stationary points, and B3LYP-GD3/6–311++g(d,p) (SDD for Pd) in 1,4-dioxane for the energy calculations of the resulting single points.

Study of the cross-coupling process under standard basic conditions

Firstly, we analyzed the formation of the π-allyl intermediate **A** through a hydropalladation step (**Scheme 126**, path A, page 168). The route begins with the Pd(0) catalyst coordinated to the boronic

[121] The deuteration percent of subproduct ***d*-45bl'** could not be determined due to its small proportion, and being inseparable of ***d*-45bl** by employed purification methods.

acid (**I1**, **Figure 34**). This species evolves via oxidative addition of the OH bond to the Pd(0) center, (ΔG = 27.7 kcal·mol^{-1}), to deliver the palladium hydride species **I2**. Then, a coordination of the C-C double bond of the ACP (**I3**) enables a regioselective hydropalladation of this alkene (**TS3-4**, ΔG=4.2 kcal·mol^{-1}), which gives rise to the cyclopropyl intermediate **I4**. A subsequent β-carbon elimination in **I5** proceeds with a relatively high energy barrier of 27.3 kcal·mol^{-1} and, curiously, delivers a σ-allyl Pd complex **I6**, rather than the initially expected π-allyl counterpart. This π-allyl isomer of type **A** (**I7**) was obtained from **I6**, through an isomerization step; however, it proved to be less stable than its σ-allyl counterpart.

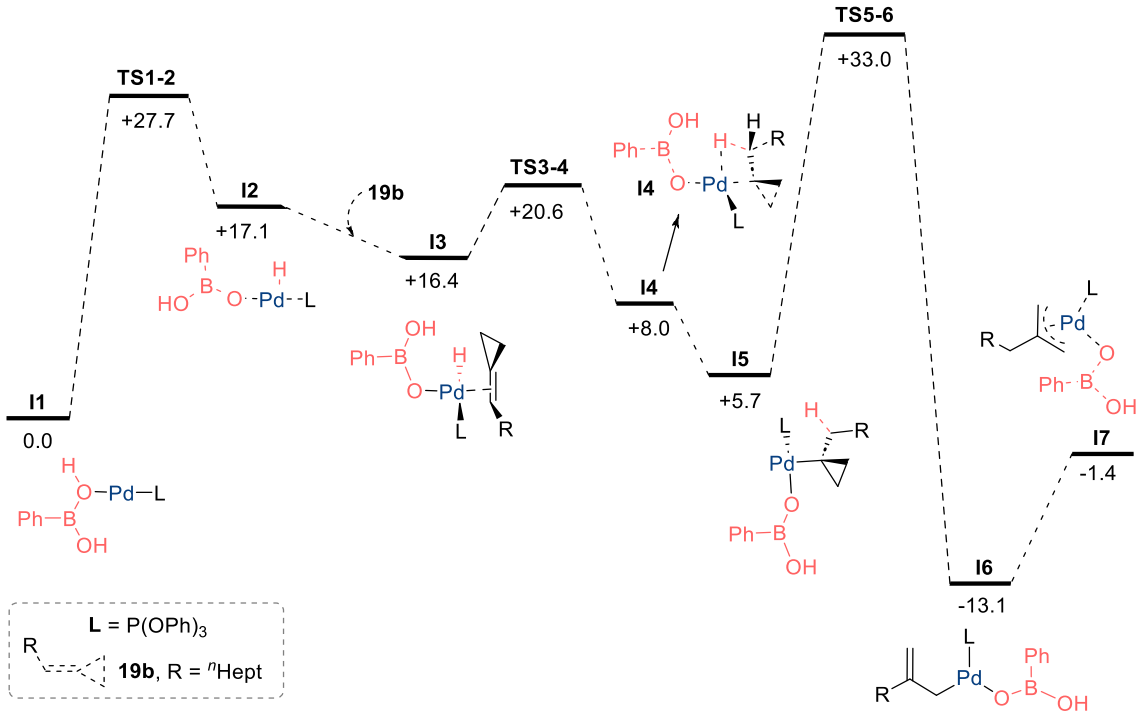

Figure 34. Energy profile ΔG_{solv} (kcal·mol^{-1}) for the formation of π-allyl intermediate **I7**, by a hydropalladation process, using **19b**, phenyl boronic acid and Pd(0)-P(OPh)$_3$, in 1,4-dioxane. [B3LYP/6-31G(d) (LANL2DZ for Pd)//B3LYP-GD3/6–311++g(d,p) (SDD for Pd)].

Although compatible with the general heating requirements of the transformation, the energy barriers of the oxidative addition and β-carbon elimination steps are considerably high (>27 kcal·mol^{-1}). Therefore, we evaluate the alternative pathway involving palladacyclobutane intermediates of type **D** (**Scheme 126**, path B, page 168).

The route starts with the Pd(0)-P(OPh)$_3$ complex coordinated to the distal bond of the ACP (**I8**, **Figure 35**). This species evolves through an accessible oxidative addition (**TS8-9**, ΔG=5.8 kcal·mol^{-1}) to form the T-shaped palladacyclobutane **I9**, which can be stabilized by the boronic acid coordination (ΔG=1.9 kcal·mol^{-1}). Upon a slight decoordination of the boronic acid from the Pd center (ΔG=4.9 kcal·mol^{-1}), the resulting species, **I11**, undergoes a protonation of the γ-carbon of the palladacyclobutane (**TS11-7**, ΔG=11.8 kcal·mol^{-1}), leading to the π-allyl Pd species **I7** (type **A**). This intermediate holds the boronate anion coordinated to the metallic center.

Interestingly, an NBO analysis of the HOMO of **TS11-7** shows interactions between the γ-carbon of the ACP and the acidic hydrogen atom of the boronic acid, as well as between the Pd center and the oxygen atom that releases this hydrogen (**Figure 36**).

Therefore, from these computational studies, we can conclude that the formation of the π allyl intermediate **I7**, is significantly more favorable from palladacyclobutane species **I11** (**Scheme 126**, path B, page 168, and **Figure 34**), rather than through the hydropalladation route (**Scheme 126**, path A, ΔΔG = 18.5 kcal·mol^{-1}, and **Figure 35**). Further analysis from this intermediate revealed that **I7**

can be stabilized by the addition of a hydroxy anion to the boron center to provide the σ-allyl Pd intermediate **I12**, [122] which mimics the basic experimental conditions. Then, a transmetalation step would afford the σ-allyl intermediate **I14**, with an overall energy barrier of 6.7 kcal·mol^{-1}. Finally, **I14** undergoes an almost barrierless isomerization to its π-allyl isomer **I15**, followed by a reductive elimination (**TS15-45bl**, ΔG = 20.0 kcal·mol^{-1}), to deliver the product **45bl**. The reductive elimination would be the turnover limiting step.[78]

Worth to mention, an analog route from **I9** involving the boronate reagent $PhB(OH)_3^-$ instead of the boronic acid was also computed, although the corresponding γ-protonation step exhibited a significantly higher energy barrier (ΔΔG = 10.1 kcal·mol^{-1}, **Figure A9**, *Appendix*, page 333). These results are in consonance with the low performance observed when the reaction was conducted with a the preformed boronate reagent $PhB(OH)_3^-$ (see **Table 28**, entry 12, page 171).

[122] Equilibrium between neutral boronic acids and anionic boronate species are commonly established in basic media. For more information, see: a) Carrow, B. P.; Hartwig, J. F. Distinguishing Between Pathways for Transmetalation in Suzuki-Miyaura Reactions. *J. Am. Chem. Soc.* **2011**, *133*, 2116-2119.; b) Thomas, A. A.; Denmark, S. E. Pre-Transmetalation Intermediates in the Suzuki-Miyaura Reaction Revealed: The Missing Link. *Science* **2016**, *352*, 329–332.

[78] Kozuch, S.; Shaik, S. How to Conceptualize Catalytic Cycles? The Energetic Span Model. *Acc. Chem. Res.* **2011**, *44*, 101-110.

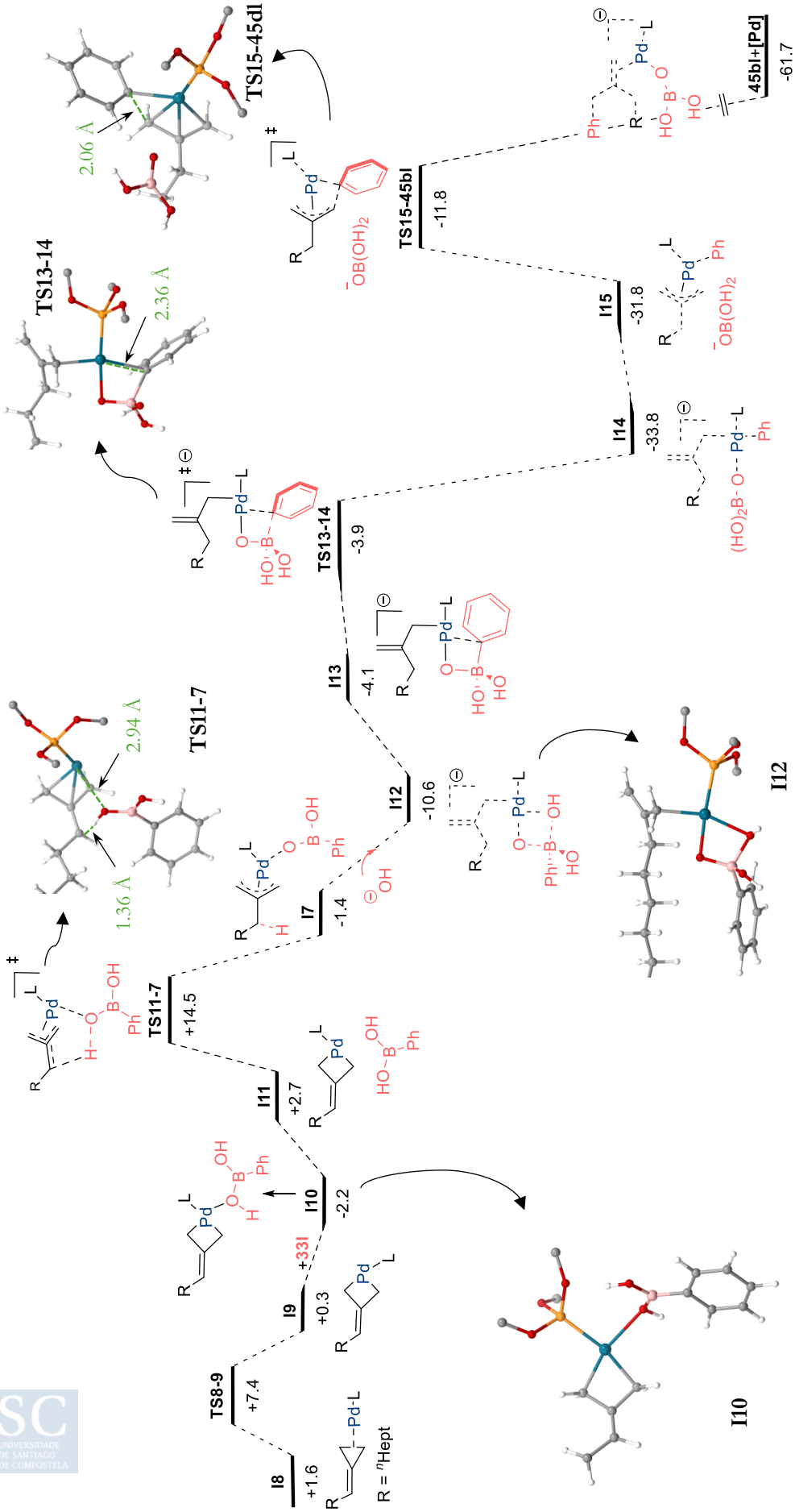

Figure 35. Energy profile ΔG_{solv} (kcal·mol^{-1}) for the model reaction involving **19b**, phenyl boronic acid (**33l**), trihydroxy(phenyl)borate and Pd(0)-P(OPh)$_3$, in 1,4-dioxane. [B3LYP/6-31G(d) (LANL2DZ for Pd)//B3LYP-GD3/6–311++g(d,p) (SDD for Pd)].

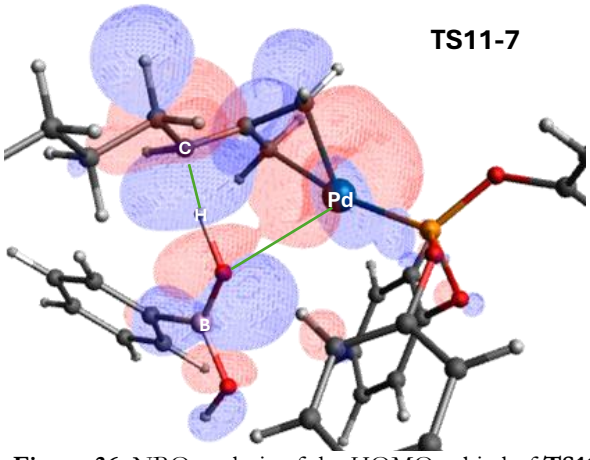

Figure 36. NBO analysis of the HOMO orbital of **TS11-7**.

Study of the cross-coupling process using phenol as additive

As deduced from **Table 28** (entries 6 and 7, page 171), the reaction can also proceed without base, when phenol (or *p*-fluorophenol) is used as additive. Therefore, the energy profile was computationally reanalyzed using PhOH (**Figure 37**).

Accordingly, we found that the initial palladacyclobutane **I16** can react with phenol to give the π allyl complex **I17** (**TS16-17**, ΔG = 10.8 kcal·mol^{-1}).[123] From **I17**, the coordination of $PhB(OH)_2$ (**I18**) and subsequent formation of a mixed-boronate species coordinated to the Pd center (**I19**), enables a transmetalation step with an energy barrier of 17.8 kcal·mol^{-1} (**TS19-20**). Remarkably, the energy barrier of this step is significatively higher than that calculated when using a base (**TS19-20** vs **TS13-14**; ΔΔG = 11.1 kcal·mol^{-1}).

Nonetheless, the overall barrier is still feasible, so that after transmetalation, the resulting σ-allyl Pd intermediate (**I20**) can evolve directly to product **45bl** via a reductive elimination (ΔG= 20.2 kcal·mol^{-1}). Alternatively, its tautomerization to its more stable π-allyl isomer (**I21**), enables a new reductive elimination toward **45bl**, with a very similar barrier (ΔG = 20.5 kcal·mol^{-1}). Overall, this route seems feasible and is quite similar to the one previously calculated under basic conditions (**Figure 35**). However, the transmetalation step is considerably more favorable with base (ΔΔG = 11.1 kcal·mol^{-1}), which is consistent with the higher yields achieved under these conditions.

[123] An alternative pathway based on hydropalladation to reach **I17** was calculated using PhOH, instead of $PhB(OH)_2$. It resulted in energy barriers of 26.1 and 29.3 kcal·mol^{-1}, respectively for the initial O-H oxidative addition and for the β-carboelimination step (**Figure A10**, *Appendix*, page 333). Thus, the route is less favored than the one showed in **Figure 37**.

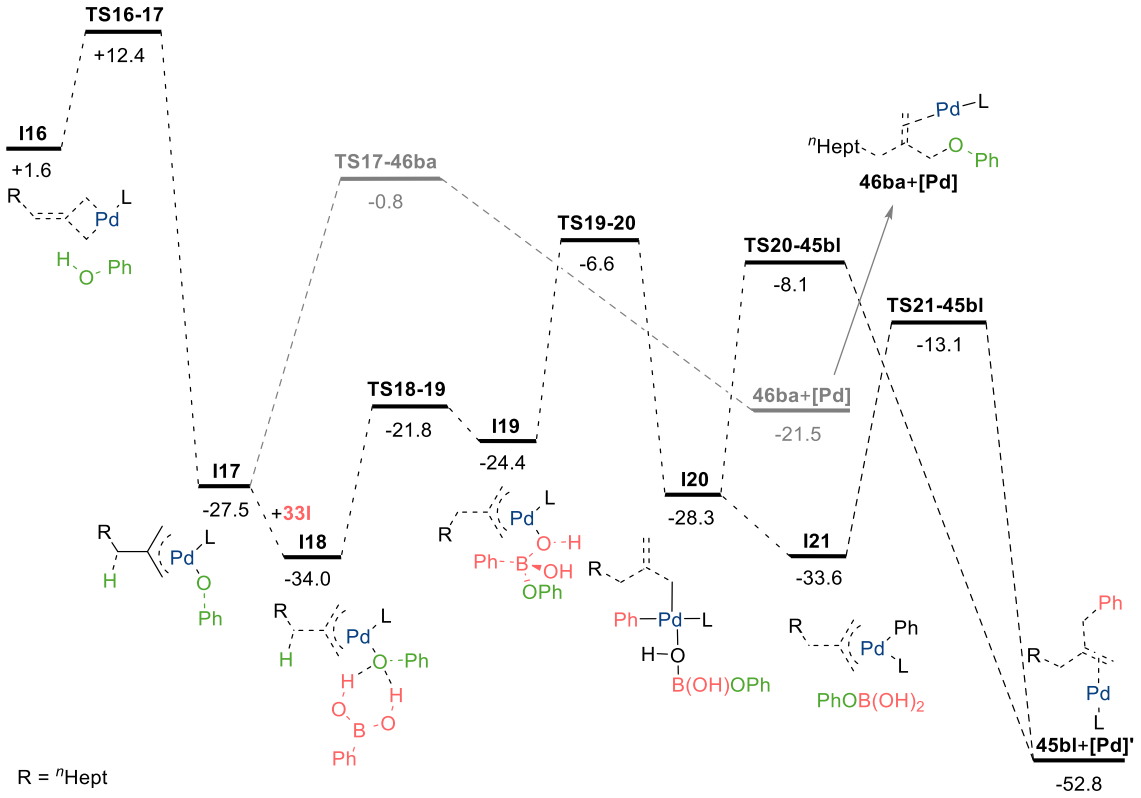

Figure 37. Energy profile ΔG_{solv} (kcal·mol^{-1}) for the model reaction involving **19b**, phenyl boronic acid (**33l**), phenol and Pd(0)-P(OPh)$_3$, in 1,4-dioxane. [B3LYP/6-31G(d) (LANL2DZ for Pd)//B3LYP-GD3/6–311++g(d,p) (SDD for Pd)]. See also **Figure A11** (*Appendix*, page 334) for a complete energy profile.

In addition, computations confirmed that intermediate **I17** can also evolve to product **46ba** in the absence of boronic acid (**TS17-46ba**, ΔG = 26.7 kcal·mol^{-1}, **Figure 37**). Worth to note, product **46ba** was not experimentally detected in the presence of boronic acids under catalytic conditions, which is in full agreement with its reversible formation shown in this energy profile (see **Scheme 134**, page 174).

4.4.5 Conclusions

In conclusion, we have developed the first transition-metal-catalyzed allylic cross-coupling between ACPs and boronic acids. Using a Pd(0)/phosphoramidite catalyst, various alkylidenecyclopropanes and aryl- or alkenyl boronic acids can be employed, to yield 1,1-disubstituted alkenes with high efficiency and good selectivity. Notably, the reaction can be conducted either in the presence of base or with a phenol additive.

DFT computations helped us to discern between two possible reaction pathways. Using Pd(0)-$P(OMe)_3$ as a model catalyst, the pathway involving an oxidative addition of the ACP to the Pd(0) species, followed by protonation of the resulting alkylidenepalladacyclobutane turned out to be more favorable than the alternative hydropalladation route.

4.5. Pd(0)-Catalyzed (3+2+2) Cycloaddition between ACPs tethered to Carbonyl Moieties and Isocyanates

Part of the contents of this section are published in:

Rodiño, R.[a]; Calvelo, M.[a]; Mascareñas, J. L.[a]; López, F.[a, b] Palladium-Catalyzed [3+2+2] Cycloaddition Between Carbonyl-Tethered Alkylidenecyclopropanes and Isocyanates. *Helv. Chim. Acta* **2025**, e202500011. DOI: 10.1002/hlca.202500011

Authors' affiliations:

[a] Centro Singular de Investigación en Química Biolóxica e Materiais Moleculares (CiQUS) and Departamento de Química Orgánica, Universidade de Santiago de Compostela 15782 Santiago de Compostela (Spain).

[b] Misión Biológica de Galicia Consejo Superior de Investigaciones Científicas (CSIC) 36080 Pontevedra (Spain).

4.5.1 Precedents

Dipolar cycloadditions between 1,*n*-dipoles and unsaturated partners (dipolarophiles) are a cornerstone in classical and contemporaneous organic synthesis, providing access to a wide range of structurally diverse carbo- and heterocyclic frameworks. These transformations are particularly relevant for the construction of complex cyclic scaffolds, such as fused- and bridged-ring systems, as well as medium-sized rings (7 to 11-membered rings), which are a common core in many natural products and drugs.[124]

These reactions originally employed relatively stable 1,3-dipoles, such as azides, carbonyl ylides or nitrile oxides, which undergo dipolar cycloadditions via a concerted mechanism following the Woodward–Hoffmann rules.[125] However, the field has further evolved to include newly designed 1,*n*-dipolar species, often non-conjugated, which are generated *in situ* from stable neutral precursors, generally using catalytic methods.

Many types of reactive dipolar intermediates have been explored,[126] being especially relevant the transformations involving zwitterionic π-allyl palladium complexes.[127] This type of palladium intermediates can be generated *in situ* from vinylcyclopropanes, epoxides, aziridines or carbonates, as well as from alkylidene lactones, among others (**Figure 38**). They usually participate as 1,3- dipoles in [3+*n*] formal cycloadditions. Notably, the number of methods wherein these intermediates participate as 1,4- or 1,5-dipoles, providing access to seven-membered rings, is much more limited.

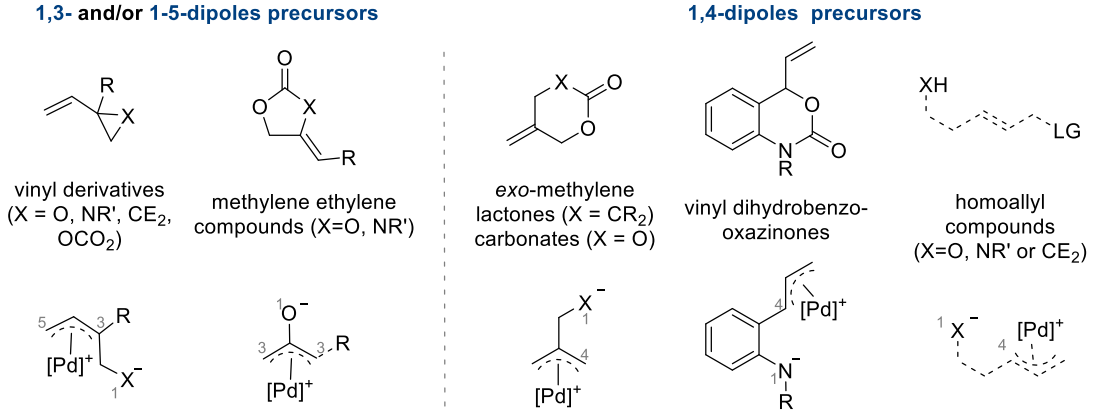

Figure 38. Representative precursors of 1,*n*- π-allyl Pd dipoles for cycloaddition reactions.

1,*n*-Dipoles bearing an *O*-centered anion can provide rapid and practical access to carbo- or oxacyclic products from simple precursors.[128] A representative example is the regioselective Pd(0)-catalyzed cycloaddition reported by Zi in 2021, in which methylene ethylene carbonates (MECs) serve as π-oxyallyl 1,3-dipole precursors, reacting with dienes to give five-or seven-membered carbocycles (**Scheme 135**).[129] Using a catalytic system involving CpPd(π-cin.) and the phosphine **L18**,

[124] Yao, T.; Li, J.; Jiang, C.; Zhao, C. Recent advances for the catalytic asymmetric construction of medium-sized rings. *Chem Catalysis* **2022**, *2*, 2929–2964.
[125] a) Huisgen, R. 1,3-Dipolar Cycloadditions. Past and Future. *Angew. Chem. Int. Ed.* **1963**, *2*, 565-598.; b) Breugst, M.; Reissig, H.-U. The Huisgen Reaction: Milestones of the 1,3-Dipolar Cycloaddition. *Angew. Chem. Int. Ed.* **2020**, *59,* 12293–12307.
[126] De, N.; Yoo, E.-J. Recent Advances in the Catalytic Cycloaddition of 1, *n*-Dipoles. *ACS Catal.* **2018**, *8*, 48–58.
[127] a) Du, J.; Li, Y.; Ding, C. Recent advances of Pd-π-allyl zwitterions in cycloaddition reactions. *Chinese Chemical Letters* **2023**, *34*, 108401.; b) Niu, B.; Wei, Y.; Shi, M. Recent advances in annulation reactions based on zwitterionic π-allyl palladium and propargyl palladium complexes. *Org. Chem. Front.* **2021**, *8*, 3475–3501.
[128] Example of another relevant π-oxyallyl 1,3-dipole precursor: Trost, B.M.; Huang, Z.; Murhade, G.M. Catalytic palladium-oxyallyl cycloaddition. *Science* **2018**, *362*, 564-568.
[129] Chai, W.; Zhou, Q.; Ai, W.; Zheng, Y.; Qin, T.; Xu, X.; Zi, W. Lewis-acid-promoted ligand-controlled regiodivergent cycloaddition of Pd-oxyallyl with 1,3-dienes: reaction development and origins of selectivities. *J. Am. Chem. Soc.* **2021**, *143*, 3595–3603.

cyclopentanones were obtained in good yields and high regioselectivity. However, a Pd(0)-catalyst containing **L19** led to formal (4+3) cycloadducts. The authors proposed an initial decarboxylative ring-opening of the carbonate forming the dipolar species **I**. After coordinating the diene, the complex **I** undergoes migratory insertion, leading to the π-allyl Pd(II) species **II**. Depending on the ligand employed, different reductive eliminations occur, affording either the seven- or the five-membered carbocycle.

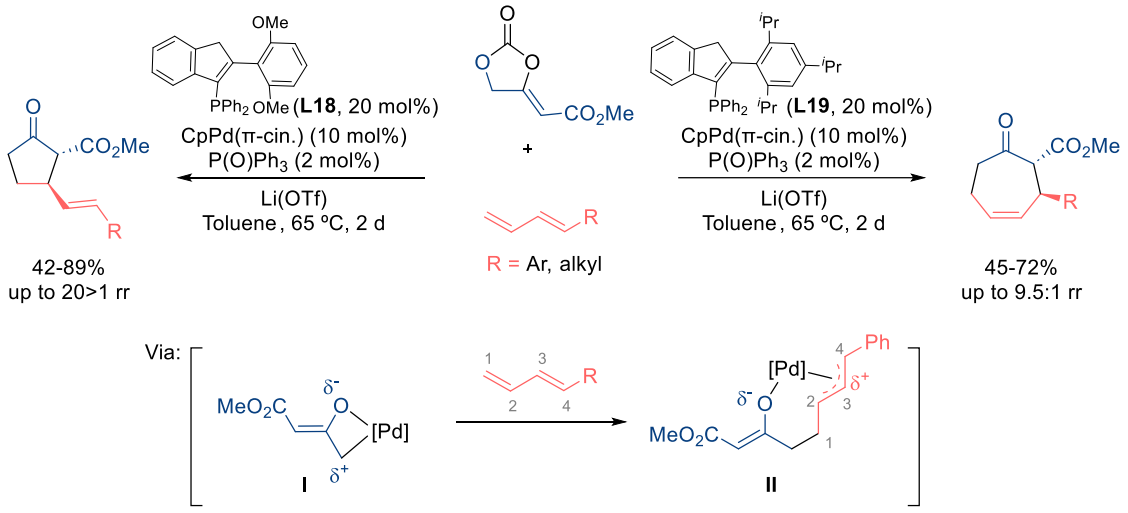

Scheme 135. Pd(0)-catalyzed (3+2) and (4+3) cycloadditions between MECs and diene partners.

In 2019, Xiao reported a Pd(0)-catalyzed (5+2) cycloaddition using vinylethylene carbonates (VECs) as 1,5-dipoles precursors and *in situ* photogenerated ketenes as 2C partners. The reaction provides seven-membered lactones bearing a quaternary stereocenter, with high enantioselectivity (**Scheme 136**).[130] Mechanistically, the ring-opening of the vinyl carbonate generates the zwitterionic Pd complex **I**, which reacts with the generated ketene through its central carbon. The resulting π-allyl species **II** undergoes a regioselective reductive elimination forming the seven-membered lactone.

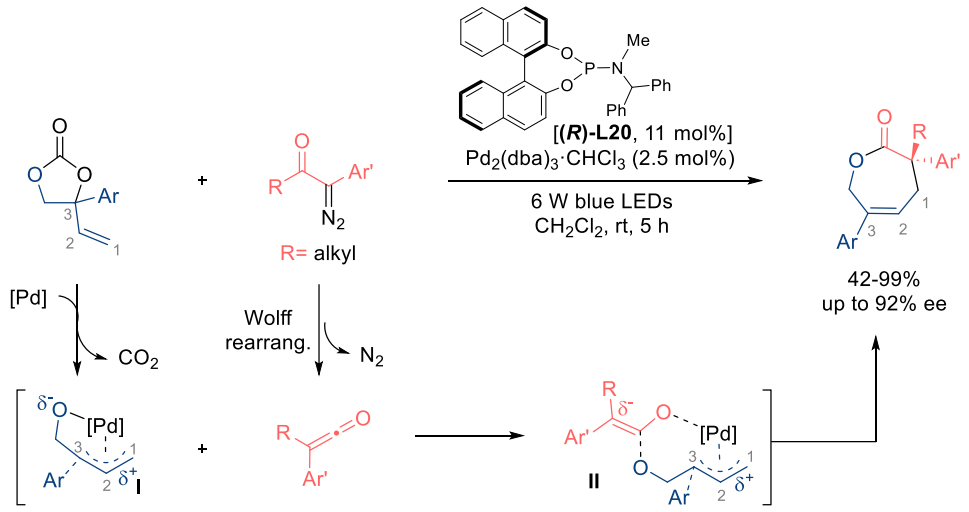

Scheme 136. Pd(0)-catalyzed (5+2) cycloaddition between vinyl carbonates and *in situ* photogenerated ketenes.

Feng reported in 2024 a formal Pd(0)-catalyzed (4+3) cycloaddition of 2-alkylidenetrimethylene carbonates (ADTMCs) and oxo-bicyclobutanes, leveraging π-oxyallyl palladium 1,4-dipoles to yield

[130] Wei, Y.; Liu, S.; Li, M.-M.; Li, Y.; Lan, Y.; Lu, L.-Q.; Xiao, W.-J. Enantioselective trapping of Pd-containing 1,5-dipoles by photogenerated ketenes: access to 7-membered lactones bearing chiral quaternary stereocenters. *J. Am. Chem. Soc.* **2019**, *141*, 1, 133–137.

2-oxabicyclo[4.1.1]octane frameworks (**Scheme 138**).[131] The reaction proceeds via a decarboxylative ring-opening of the ADTMC, generating a transient 1,4-dipole that reacts with the bicyclobutane to form the π-allyl complex **I**. A subsequent reductive elimination delivers the cycloadduct.

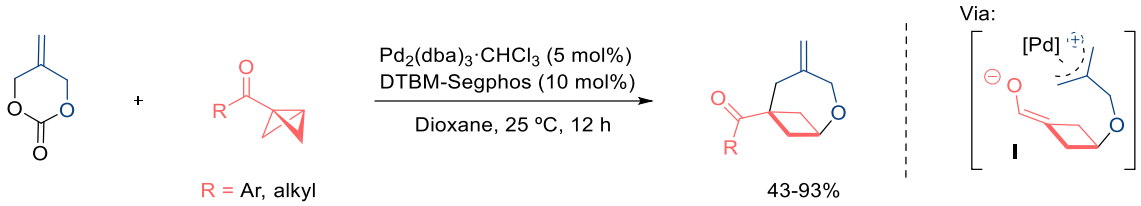

Scheme 137. Pd(0)-catalyzed (4+3) cycloaddition between ADTMCs and oxo-bicyclobutanes.

[131] Gao, X.-Y., Tang, L., Zhang, X., Feng, J.-J. Palladium-catalyzed decarboxylative (4 + 3) cycloadditions of bicyclobutanes with 2-alkylidenetrimethylene carbonates for the synthesis of 2-oxabicyclo[4.1.1]octanes. *Chem. Sci.* **2024**, *15*, 13942–13948.

4.5.2 Objectives

Our mechanistic studies on Pd-catalyzed transformation involving ACPs and carbonyls, revealed the formation of π-allyl oxapalladacyclic species **A** and **B**, which can evolve via reductive elimination to (3+2) cycloadducts (**Scheme 139**, *left*), or undergo a transmetalation/reductive elimination process toward cross-coupling products (**Scheme 139**, *right*), depending on the palladium catalyst.[132]

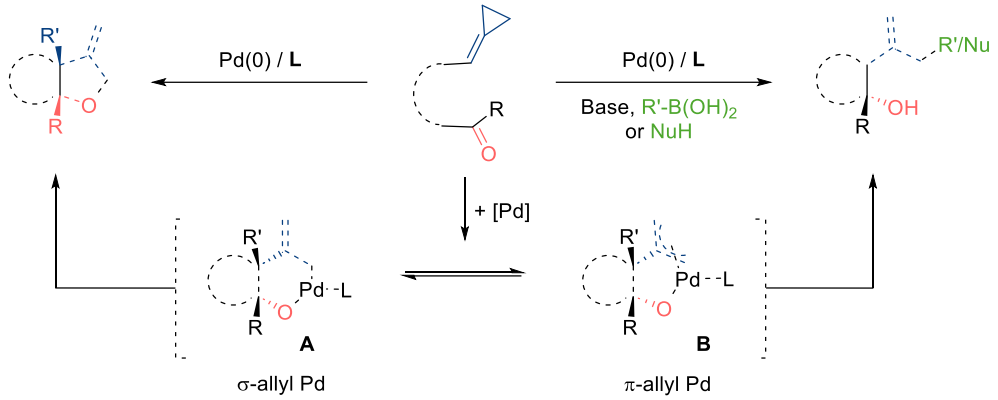

Scheme 138. Pd(0)-catalyzed cycloisomerization/ allylic substitution reactions of ACPs tethered to carbonyls.

We envisioned that, under appropriate catalytic conditions, intermediates of type **B** could behave as π-allyl 1,5-dipoles, and undergo formal annulation reactions with external unsaturated partners. Therefore, we set as objective the **development of Pd formal (3+2+2) catalyzed cycloadditions between ACP-tethered carbonyls and diverse two-atom unsaturated components** (**Scheme 140**). This would provide direct access to interesting oxacyclic cycloadducts bearing an *exo*-cyclic double bond.

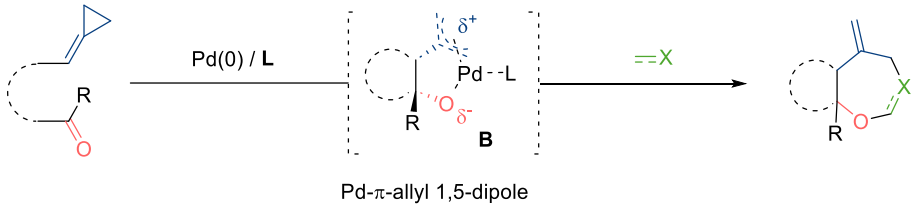

Scheme 139. Pd(0)-catalyzed (3+2+2) cycloaddition between ACP-tethered carbonyls and 2-atom unsaturated partners.

As cycloaddition partners, we will test activated alkenes, dienes or allenes, but also **hetero-unsaturated partners**, such as carbonyl compounds, imines and isocyanates, which have been much less explored in multicomponent cycloadditions with ACPs.

[132] These transformations are further discussed in Sections 4.1 and 4.2. See also the following references 40 and 110: a) Verdugo, F.; da Concepción, E.; Rodiño, R.; Calvelo, M.; Mascareñas, J. L.; López, F. Pd-Catalyzed (3 + 2) Heterocycloadditions between Alkylidenecyclopropanes and Carbonyls: Straightforward Assembly of Highly Substituted Tetrahydrofurans. *ACS Catal.* **2020**, *10*, 14, 7710–7718.; b) Verdugo, F.; Rodiño, R.; Calvelo, M.; Mascareñas, J. L.; López, F. Palladium-Catalyzed Tandem Cycloisomerization/Cross-Coupling of Carbonyl- and Imine-Tethered Alkylidenecyclopropanes. *Angew. Chem. Int. Ed.* **2022**, *61*, e20220229.

4.5.3 Experimental Results

4.5.3.1 Study of the reactivity of the 1,5- dipolar intermediate

We preliminary explored the reactivity of the keto-ACP **9b** with different partners. Based on the conditions developed for the tandem cycloisomerization process, we employed the catalyst generated from $Pd_2(dba)_3$ and phosphoramidite **L9**, using an excess of the cycloaddition partner. **Scheme 141** summarizes the results obtained.

The use of carbonyl partners **31a** and **31c**, led to small amounts of the intramolecular cycloadduct **17b**, and diene **18b**, derived from a β-elimination process. When using activated alkenes, only the diene **18b** was formed in varying yields. When testing dienes **48d** and **48e**, the intramolecular cycloadduct **17b** was obtained in good yields (63-80%). On the other hand, the use of an α,β-unsaturated imine (**15s**) led to small amounts of diene **18b**. Overall, the desired cycloadducts of type **50ba** were not obtained.

With isonitriles and sulfur ylides, we did not observe any new product and, in the presence of ketenes (**48h**), we fully recovered **9b**. However, the use of the isocyanate **49a** led to the formal (5+2) cycloadduct **50ba**, which was isolated in a good 76% yield with complete diastereoselectivity.

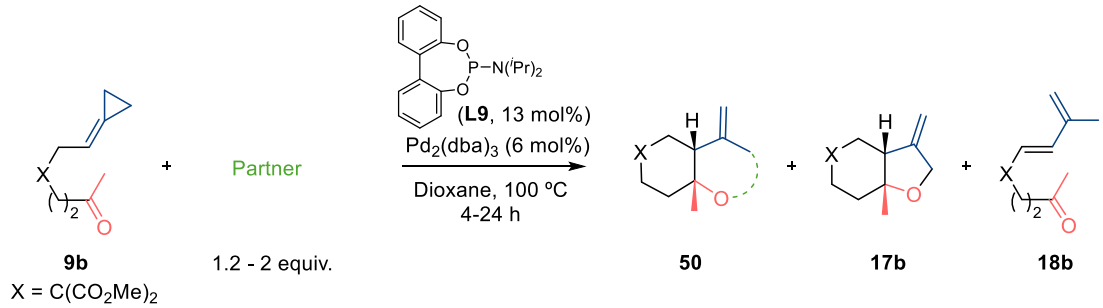

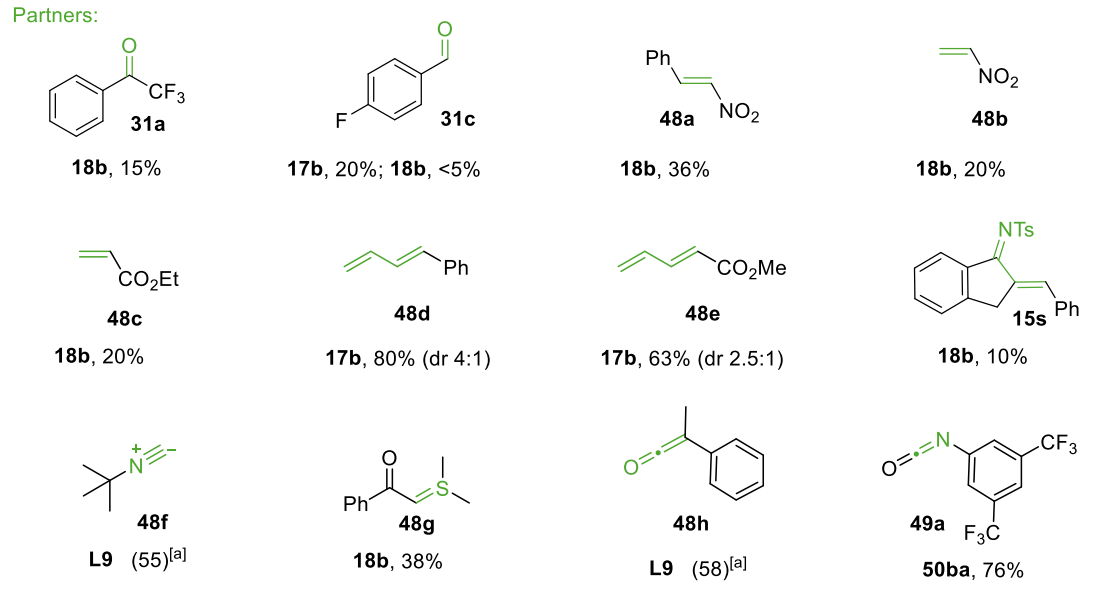

[a]Conv. (%) of **9b** between brackets. Otherwise %Conv.>99

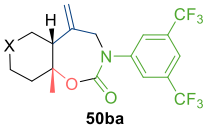

Scheme 140. Study of reactivity for the *in situ* generated 1,5-dipole with different dipolarophiles.

Among nitrogen heterocycles, seven-membered ring carbamates are relatively under-represented despite their notable biological activities.[133] Thus, our method could provide a rapid access to this type of appealing bicyclic products.

4.5.3.2 Formal (3+2+2) cycloaddition between ACPs tethered to carbonyls and isocyanates

Racemic studies

With this preliminary result in hand, we performed a ligand screening (**Table 29**). In contrast to the previous result with **L9** (entry 1), the use of other phosphines, such as **L17** or PPh_3, provided **50ba** in poorer yields (12 and 14%, respectively), being the diene **18b** the major product (21 and 28%, entries 2 and 3). The phosphite **L1** led to the diene **18b** in 11% yield (entry 4). The catalyst generated from $Pd_2(dba)_3$ and *t*BuXPhos afforded the (3+2) cycloadduct **17b** in 35% yield, while diene **18b** was also observed in 12% (entry 5). In addition, bisphosphine ligands proved to be ineffective, leading to the recovery of **9b** (entries 6-8).

Using $Pd_2(dba)_3$/**L9** as optimal catalyst, we tried several temperatures and solvents (entries 9 – 12), concluding that 100 ºC is required for full conversion, but different solvents, such as toluene, hexane, or DCE, afford the (3+2+2) cycloadduct **50ba** in similar yields to dioxane (72-80%, entries 10-12).

[133] a) Green, L.; Guba, W.; Jaeschke, G.; Jolidon, S.; Lindemann, L.; Ricci, A.; Rueher, D.; Stadler, H.; Vieira, E. Arylethynyl Derivatives. U.S. Pat. Appl., US20110251169A1, **2011**.; b) Claremon, D. A.; Zhuang, L.; Tice, C. M.; Singh, S. B.; Ye, Y.; Zhao, W.; Leftheris, K. 1,3-Oxazepan-2-One and 1,3-Diazepan-2-One Inhibitors of 11ß-Hydroxysteroid Dehydrogenase 1. U.S. Pat. Appl. US20100041637A1, **2010**.; c) Hino, T.; Yamada, Y.; Shigenari, T.; Mametsuka, K. Haloalkylsulfonanilide Derivative or Salt Thereof, Herbicide Comprising the Derivative as Active Ingredient, and Use of the Herbicide. PCT Int. Appl. WO2008059948A1, **2008**.; d) Madera, A. M.; Stabler, R. S.; Weikert, R. J. Substituted 1-Aminoalkyl-Lactams and Their Use as Muscarinic Receptor Antagonists. PCT Int. Appl. WO2001090082A1, **2001**.

Table 29. Ligand screening for the (3+2+2) cycloaddition between keto-ACP **9b** and isocyanate **49a**.[a]

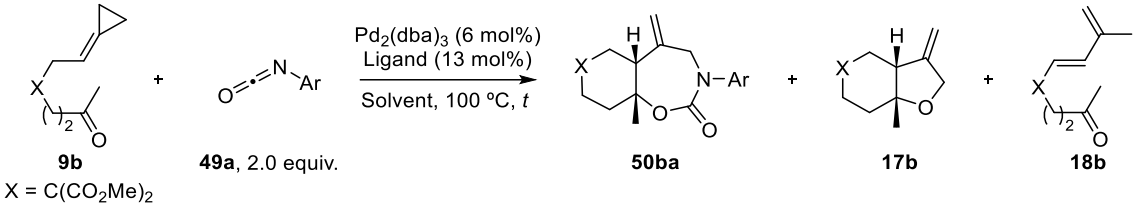

Entry	Ligand	Solvent	Conv. 9b (%)	t / h	50ba (%)[b]	17b/18b (%)[b]
1	**L9**	dioxane	100	4	76	-
2	**L17**	dioxane	100	24	14	**18b**, 21
3	PPh_3	dioxane	46	20	12	**18b**, 28
4	**L1**	dioxane	38	17	-	**18b**, 11
5	*t*BuXPhos	dioxane	100	3	12	**17b**, 35
6	dFppe	dioxane	14	17	-	-
7	BTFM-Garphos	dioxane	13	17	-	-
8	Walphos	dioxane	11	17	-	-
9[c]	**L9**	dioxane	71	14	40	-
10	**L9**	toluene	100	20	72	-
11	**L9**	hexane	100	3	80	-
12	**L9**	DCE	100	2	75	-

[a] Conditions: **9b**, isocyanate (**49a**, 2 equiv.), $Pd_2(dba)_3$ (6 mol%), ligand (13 mol%), dry solvent (0.05 M), Ar atmosphere, 100 °C. Ar = 3,5-bis(trifluoromethyl)benzene. [b] Determined by NMR with an internal standard. [c] T = 80 ºC.

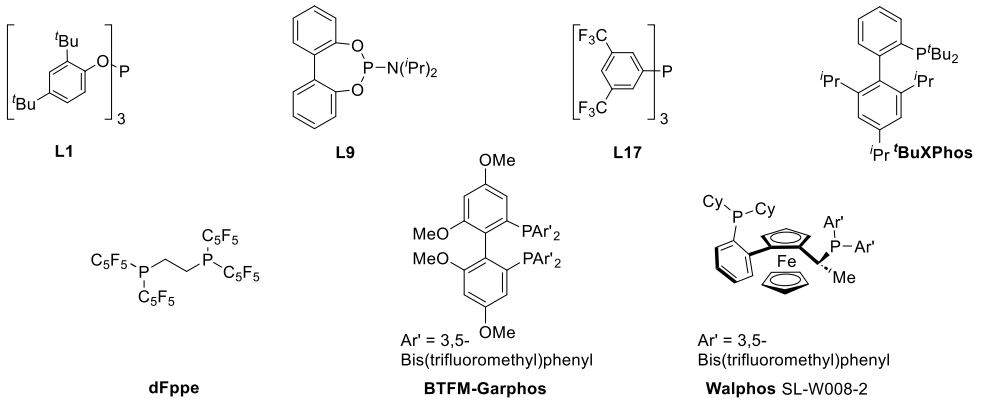

Reaction scope

Using as optimal conditions $Pd_2(dba)_3$ (6 mol%) and phosphoramidite **L9** (13 mol%) in refluxing dioxane at 100ºC, we analyzed the scope of the above formal (3+2+2) cycloaddition (**Scheme 142**).

First, we evaluated different keto-ACPs of type **9**, using isocyanate **49a** as partner. As previously indicated, the precursor **9b**, bearing a diester at the tether, afforded the cycloadduct **50ba** in 76% yield. Its structure was further confirmed by X-ray diffraction analysis. A precursor bearing an NTs group at the linker (**9c**), afforded the desired product **50ca** in 36% yield. Meanwhile, the use of a shorter tether between the ACP and the ketone (**9a**) afforded the 5,7-bicyclic product **50aa** in a good 78% yield, in this case as a 7:1 mixture of *cis*:*trans* isomers at the ring fusion.

On the other hand, the cyclopentanone derivative **9l** reacted to afford the tricyclic carbamate **50la** in a moderate 41% yield, as a 2:1 mixture of diastereoisomers. In contrast, the use of a phenyl ketone (**9p**) was detrimental, so that the (3+2) intramolecular cycloadduct **17p** was obtained in 28% (dr 13:1). In addition, with substrate **9o**, bearing the ACP moiety disubstituted in the *exo*-cyclic alkene, we obtained the diene **51o**, derived from a rearrangement, in 60% yield.[134]

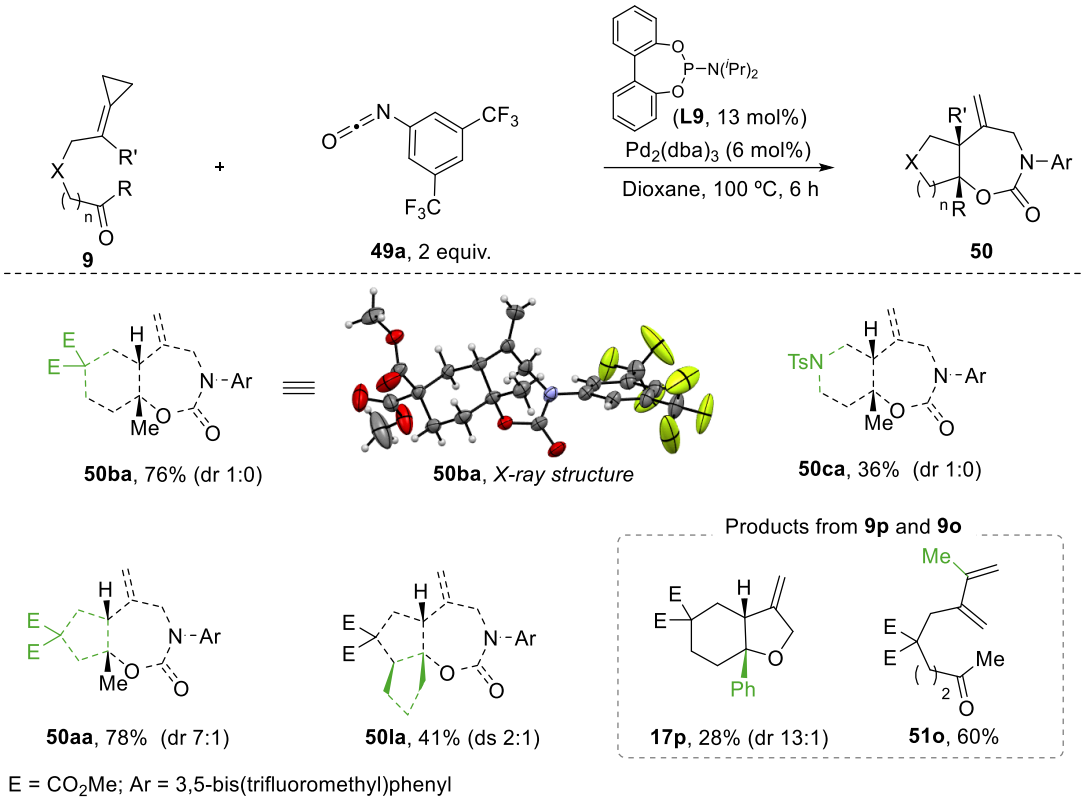

Scheme 141. Scope of the (3+2+2) cycloaddition between keto-ACPs **9** and isocyanate **49a**.

The reaction is not limited to the use of 3,5-bistrifluoromethyl phenyl isocyanate (**49a**). The cycloaddition of phenyl isocyanate (**49b**) with ACP **9b** afforded the (3+2+2) cycloadduct **50bb** in 55% yield as a 4:1 mixture of diastereoisomers (**Scheme 143**). The reaction between the precursor **9a** and phenyl isocyanate **49b** provided **50ab** in 75% (dr 5:1).

Other aryl isocyanates bearing electron withdrawing substituents at the aromatic ring are also suitable partners, affording the expected carbamate bicycles in good yields (**50bc** – **50bf**, 45 – 65% yield). Non-aromatic isocyanates, such as *N*-benzyl or *N*-acyl isocyanates, did not participate in the reaction, leading to complex mixtures of products.

[134] For more information about the formation diene product **51o**, closely related with products of type **4**, see *Section 4.1*.

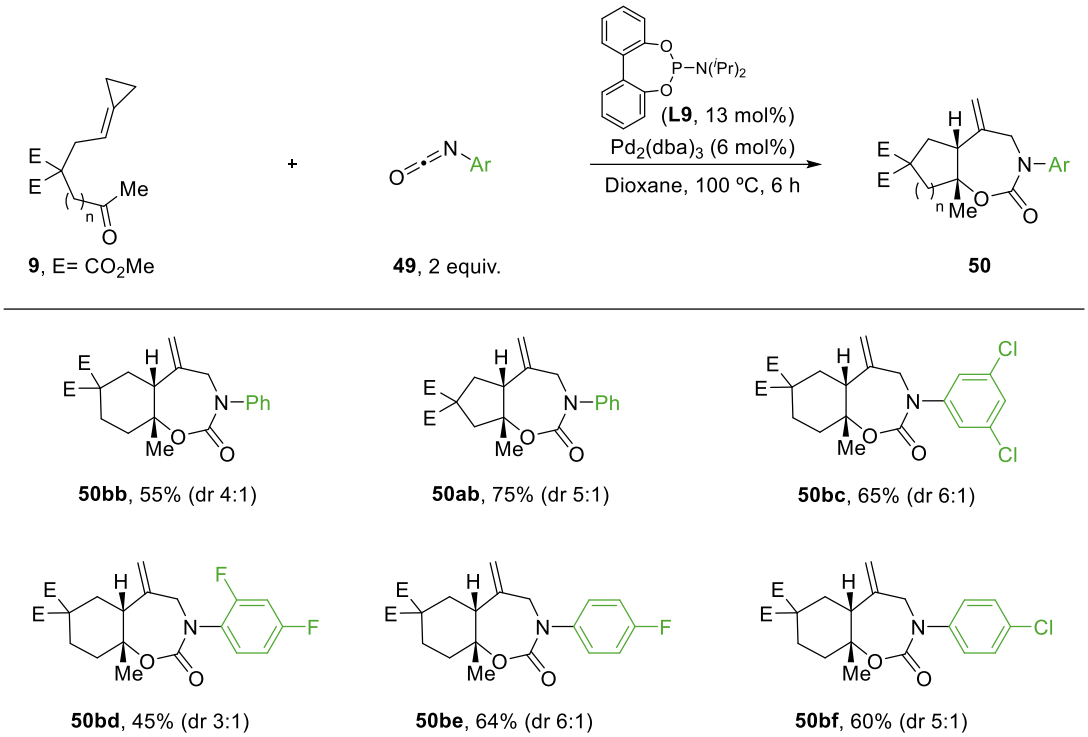

Scheme 142. Scope of the (3+2+2) cycloaddition between ACP precursors **9** and different isocyanates **49**.

Finally, we evaluated additional ACP precursors tethered to different unsaturated moieties (**Scheme 144**). Thus, aldehyde **7c** resulted in a complex mixture of products; while the trifluoromethyl ketone **9q** afforded diene **3q**, derived from a β-hydride elimination, in 29% yield. On the other hand, the ketoxime **1l** and sulfinyl imine **40e** did not lead to the desired cycloadduct.

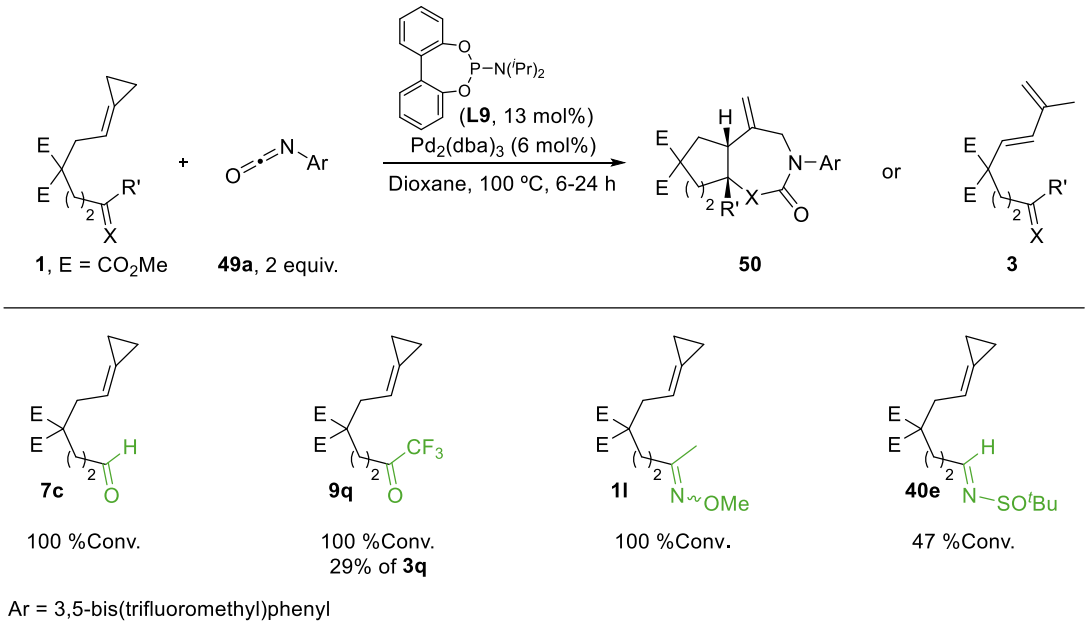

Scheme 143. Evaluation of ACP precursors tethered to different unsaturated components.

Cleavage of the carbamate moiety

The treatment of the seven-membered cycloadduct **50ba** with H_2SO_4 at room temperature promoted the carbamate cleavage and, presumably, dehydration of the resulting alcohol, yielding product **52ba** in 40% yield (**Scheme 145**).

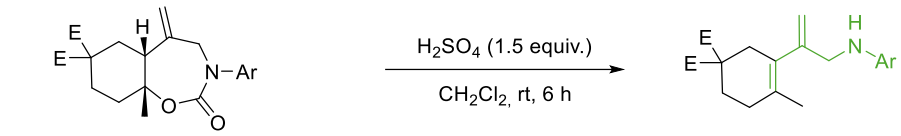

50ba, E = CO_2Me
Ar = 3,5-bis(trifluoromethyl)phenyl

52ba, 40%

Scheme 144. Synthetic derivatization of the cycloadduct **50ba**.

4.5.3.3 Preliminary asymmetric tests

We explored the viability of an asymmetric version of this (3+2+2) cycloaddition using **9b** and **49b** as model substrates. First, we performed a ligand screening of different chiral phosphoramidites. The main results are presented on **Table 30**.

The **(*S*)-Carreira's ligand** afforded the cycloadduct **50ba** in 15% yield with a poor 5% of enantioinduction. The use of the BINOL derivatives **(*S,R,R*)-L5** and **(*R,R,R*)-L5** provided **50ba** in good yields and slightly better enantioselectivity (10 and 14% ee, respectively). On the other hand, the H_8–BINOL-derivative **(*S,R,R*)-L21** led to the product in 65% yield, with only 6% ee. The Pd(0)-catalyst derived from the BINOL phosphoramidite **(*R,R,R*)-L12**, bearing a 1-(naphthalen-1-yl)ethyl)amine, led to the product in 75% yield and 30% ee. We also tested the analogue **(*R,R,R*)-L13**, bearing a 1-(naphthalen-2-yl)ethyl)amine, but led to lower yields and enantioinductions.

Additionally, we tested the chiral Pd(0)-catalyst with the VAPOL derivative **(*S,R,R*)-L2**, which afforded the cycloadduct **50ba** with 20% ee. The tetrahydroquinoline-derived ligand **(*R,S*)-L22**, yielded the bicyclic product **50ba** in moderate yield, with 24% ee; while the spirocyclic phosphoramidite **(*R,R,R*)-L23** provided **50ba** in excellent yield, but 18% ee. Finally, the use of (*R*)-BriPhos also led to the seven-membered ring **50ba** in good yields, but in an almost racemic fashion (2% ee).

Table 30. Selection of the ligand screening for (3+2+2) cycloadditions.[a]

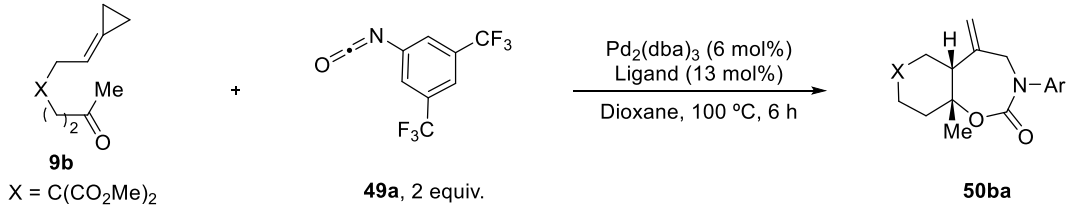

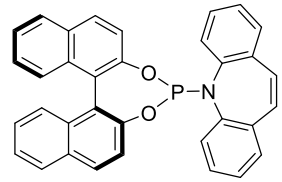

(*S*) - Carreira's Ligand
15% -5% ee

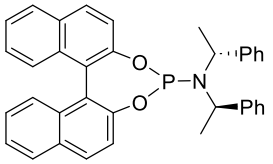

(*S, R, R*) - L5, 70% 10% ee
(*R, R, R*) - L5, 57% 14% ee

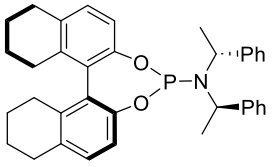

(*S, R, R*) - L21, 65% 6% ee

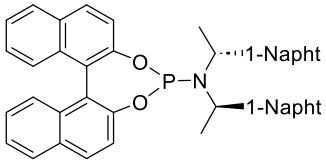

(*S R, R*) - L12, 90% 22% ee
(*R, R, R*) - L12, 75% 30% ee

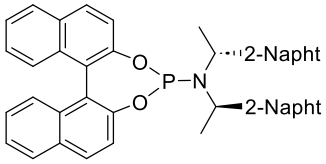

(*R, R, R*) - L13, 45% 3% ee

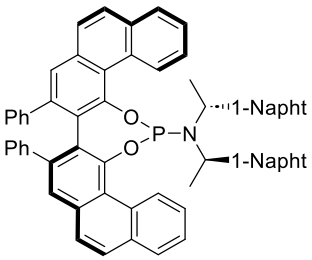

(*S,R,R)*-L2, 72% 20% ee

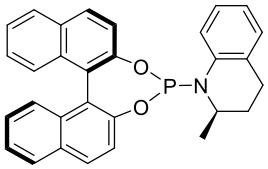

(*R, S*) - L22, 50% -24% ee

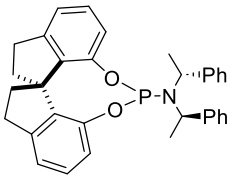

(*R, R, R*) - L23, 90% 18% ee

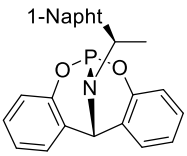

(*R*)-BriPhos, 65% -2% ee

[a] Conditions: **9b**, **49a** (1.2 equiv.), $Pd_2(dba)_3$ (6 mol%), **L** (13 mol%), in 1,4-dioxane was heated under Ar at 100 ºC. Conversion > 99%, as determined by ^{1}H–NMR of the crude reaction mixture, unless otherwise value of conversion under parenthesis. Yield determined by NMR with internal standard. Negative values in "ee" imply that the peak area of the enantiomer that elute later is higher. Ar = 3,5-bis(trifluoromethyl)phenyl.

We also performed a brief solvent screening using the Pd-catalyst involving **(*R,R,R*)-L5**, but none of the solvents checked provided good enantioselectivities (**Table 31**). Therefore, we can conclude that, although Pd(0)/phosphoramidite complexes seem to be excellent catalysts to promote the (3+2+2) cycloaddition between keto-ACPs and isocyanates, their ability to induce asymmetry is very limited.

Table 31. Screening of solvents for (3+2+2) cycloadditions using **(*R,R,R*)-L5** as ligand.

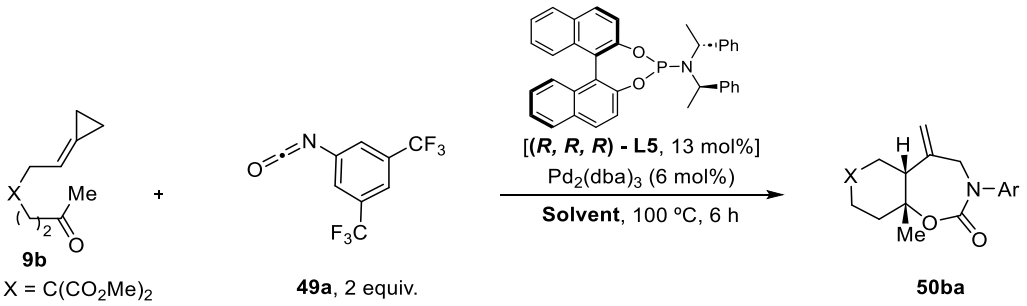

Entry	Solvent	Conv. **9b** (%)	Yield **50ba** (%)	**5bba** (% ee)
1	1,4-dioxane	100	75	30
2	Hexane	100	55	12
3	Toluene	100	68	13
4	DCE	100	45	7
5	Trifluorotoluene	84	15	4

Ar = 3,5-bis(trifluoromethyl)phenyl

4.5.4 DFT Mechanistic Studies

To shed light on the mechanism of these (3+2+2) cycloadditions we performed DFT computations. As model substrates, we selected the ACP precursor **9d**, which is very similar to the experimentally used substrate **9b**, and the isocyanate **49a**. We employed the phosphoramidite **L9** as ligand, the B3LYP/6-31G(d) (LANL2DZ for Pd) level of theory for the optimization of stationary points, and M06/6-311++G(d,p) (SDD for Pd) in 1,4-dioxane for the single-point energy calculations.

The **Figure 39** starts with the palladacyclobutane **I1**, which exhibits an agostic interaction between the palladium and a hydrogen atom of one of the isopropyl groups of the ligand [*d*(H–Pd) = 2.3 Å].[135] This intermediate undergoes a migratory insertion of the carbonyl moiety with an energy barrier of 20.8 kcal·mol^{-1} (**TS1-2**) to reach the π-allyl palladium complex **I2**, which can evolve to a much more stable σ-allyl intermediate **I3** (ΔG=23.0 kcal·mol^{-1}). Although this σ-allyl species might yield the intramolecular (3+2) cycloadduct **17d** via **TS3-17d** (ΔG=23.1 kcal·mol^{-1}), its interaction with the isocyanate moiety leads to a more stable regioisomeric intermediate (**I4**, ΔG=11.5 kcal·mol^{-1}), from which new favorable pathways were eventually located.[136]

The oxapalladacycle **I4** could easily evolve to **I5**, which holds the nitrogen atom of the isocyanate close to the Pd center [*d*(N-Pd) = 2.7 Å]. Then, an oxygen attack to the central carbon of the isocyanate unit via **TS5-6** (ΔG=6.5 kcal·mol^{-1} from **I4**), leads to the oxaazapalladacyclic species **I6** (see **Figure 40** for 3D structures). All attempts to find a C-N reductive elimination from **I6** were unsuccessful, but this step is possible from the related π-allyl Pd complex **I7**, 2.5 kcal·mol^{-1} less stable, which yields the seven-membered bicycle **50da** through an overall energy barrier of 26.0 kcal·mol^{-1} from **I6** (**TS7-50da**). This energy penalty fits with the heating requirements of the reaction and suggests that it is the turnover limiting step.

We also found an alternative migratory insertion of the isocyanate from complex **I4** via **TS4-8** (ΔG=9.6 kcal·mol^{-1}), delivering the σ-allyl oxapalladacyclic species **I8**. However, this step entails a

[135] For see the initial oxidative addition of the distal C-C of the ACP to the Pd(0) complex (**TS10-11**, ΔG=17.1 kcal·mol^{-1}), and other additional steps, see **Figure A12** (*Appendix*, page 340).

[136] Intermediate **I2** can also undergo a reductive elimination (**TS2-17d**) to give the (3+2) cycloadduct **17d** (ΔG=12.6 kcal·mol^{-1}). However, the evolution from **I2** to **I3** seems more feasible. See **Figure A12** (*Appendix*, page 340).

significantly higher energy penalty regarding **TS5-6** ($\Delta\Delta G$=3.1 kcal·mol^{-1}), and the resulting intermediate (**I8**) is substantially less stable than **I6** ($\Delta\Delta G$=17.8 kcal·mol^{-1}). Moreover, its progression toward the 6,7-bicycle **50da**, although feasible, involves a more energetic reductive elimination step via **TS9-50da**. Therefore, the overall evolution via **TS5-6** and **TS7-50da** is favored.

The absence of the (3+2) cycloadducts of type **17** under reaction conditions can be explained by the evolution of intermediate **I2** to the σ-allyl complexes of type **I3**, which react rapidly with the isocyanate, instead of undergoing the less favored C-O reductive elimination, to further deliver the (3+2+2) cycloadducts of type **50** as only products.

Calculations in previous sections demonstrated that biaryl Buchwald ligands, such as ^{t}BuXPhos, facilitate subtle hemilabile interactions between the Pd center and specific atoms of this type of ligands, enabling the reductive elimination from complexes like **I3**, to yield the (3+2) cycloadducts of type **17**. However, this pathway is inhibited when phosphoramidite ligand **L9** is used, as in this case.

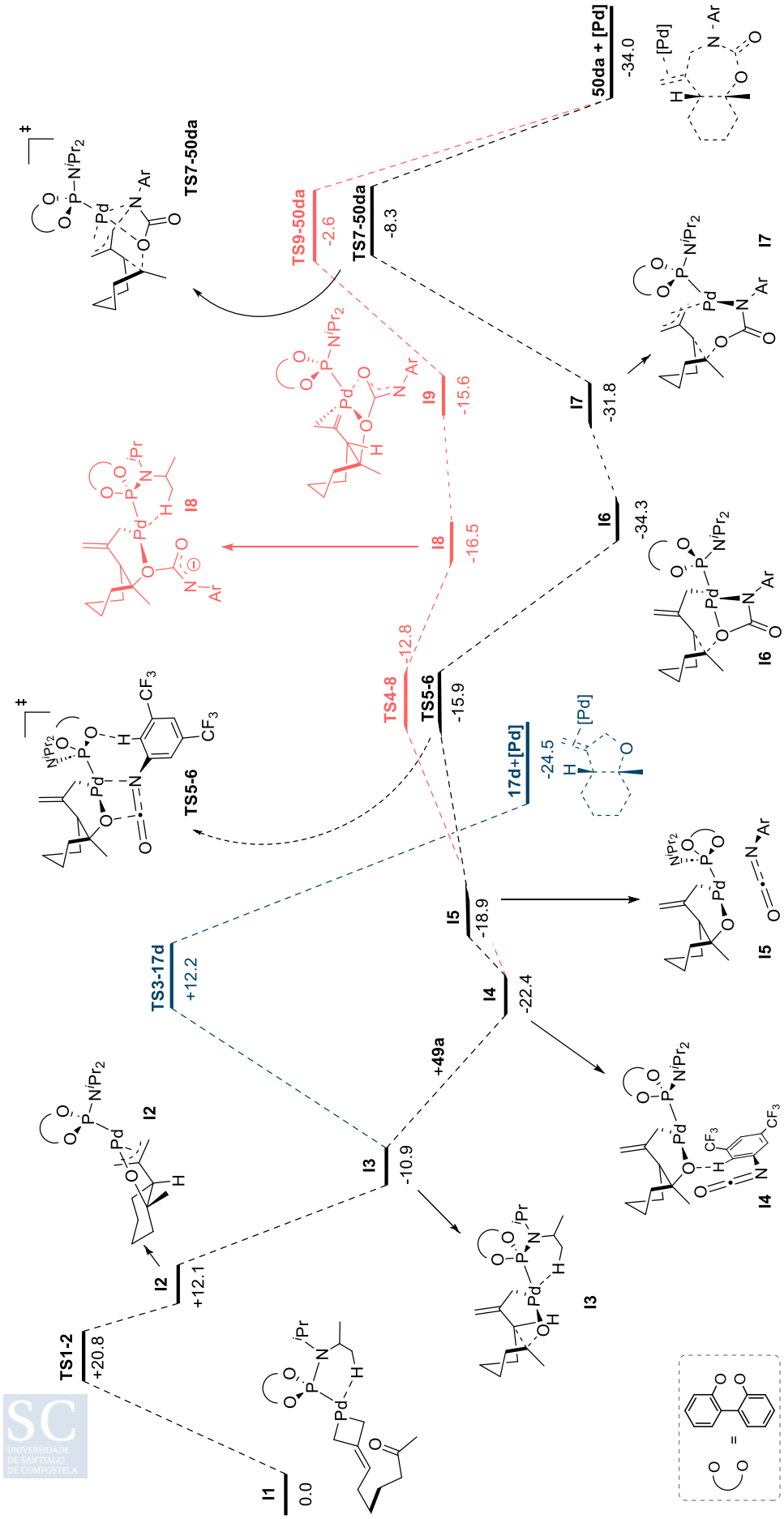

Figure 39. DFT-calculated energy profile ΔG_{sdv} (kcal·mol^{-1}) for the (3+2+2) cycloaddition of **9d** and **49a** using Pd(0)-**L9**, in 1,4-dioxane. [B3LYP/6-31G(d) (LANL2DZ for Pd)//M06/6–311++g(d,p) (SDD for Pd)]. Ar = 3,5-bis(trifluoromethyl)phenyl.

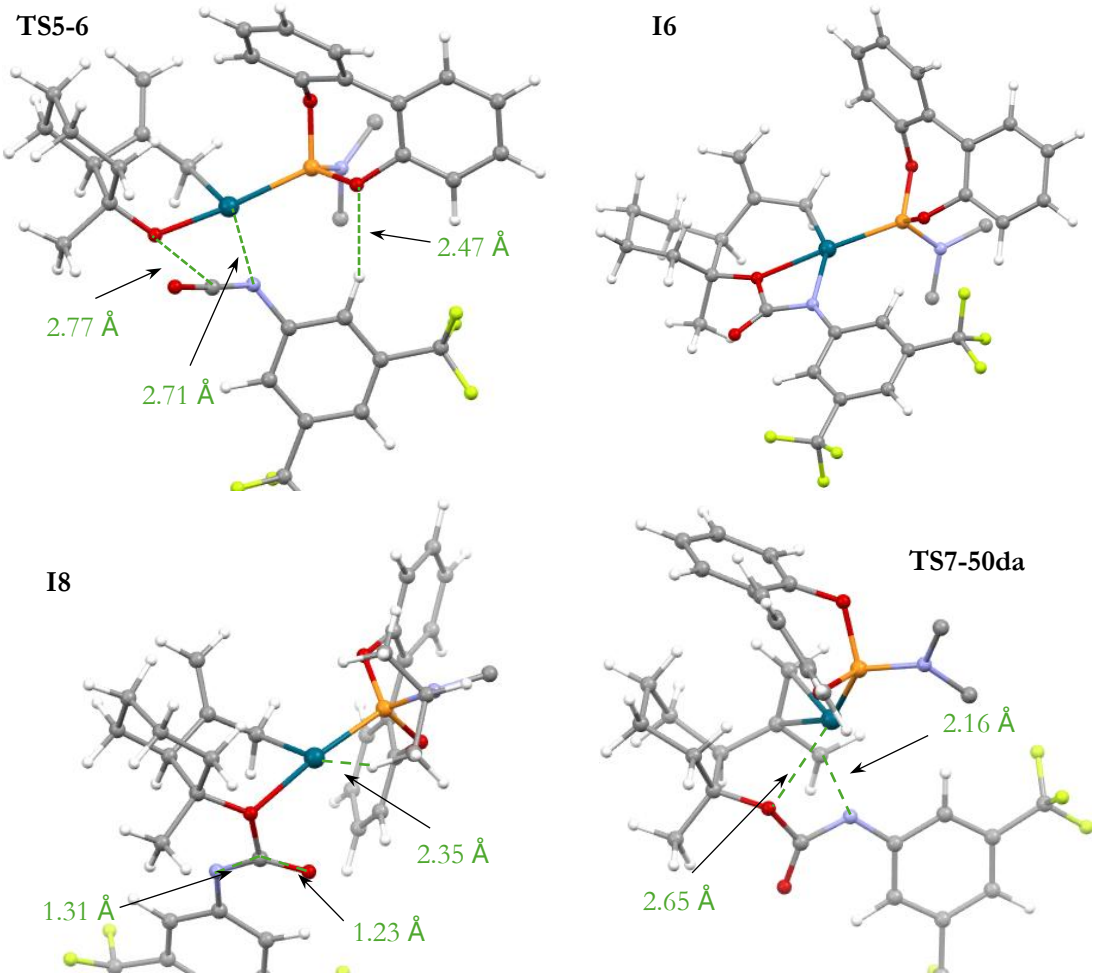

Figure 40. Selected simplified 3D representations of the most relevant structures of **Figure 39**.

4.5.5 Conclusions

In summary, we have developed a formal Pd(0)-catalyzed (3+2+2) heterocycloaddition between ACPs tethered to carbonyl moieties and aryl isocyanates to access to complex bicyclic or tricyclic structures, containing a carbamate functionality, in good yields and high diastereoselectivity. Notably, the transformation involves the *in situ* formation of a palladium π-allyl 1,5-dipole, which under the appropriate catalytic system, can react selectively with an isocyanate partner, instead of following the intramolecular C-O reductive elimination pathway to give a (3+2) cycloadduct. These results are supported by DFT computations. In addition, a preliminary asymmetric transformation is being carried out.

5. General Conclusions

Through this doctoral thesis, we have explored different reactive modes of alkylidenecyclopropanes (ACPs) under Pd(0)-catalysis.

In the first part, we developed Pd-catalyzed (3+2) heterocycloadditions between ACPs and unsaturated partners, uncovering new synthetic approaches to functionalized five-membered heterocycles. *Section 4.1* describes the use of ACPs and imine partners to synthesize functionalized pyrrolidines; while *Section 4.2* is centered on mechanistic computational studies of the cycloadditions between ACPs and carbonyl counterparts. These studies revealed the critical role of secondary hemilabile interactions between the Pd center and the ligand, underscoring the importance of selecting an appropriate catalytic system for promoting these (3+2) heterocycloadditions.

In *Section 4.3*, we successfully developed Pd(0)-catalyzed tandem cycloisomerization/allylic substitution reactions. Using Pd(0)-catalysts with electron-poor monophosphines, Pd(II)-allylic intermediates generated from precursors bearing an ACP tethered to a carbonyl moiety were intercepted by various nucleophiles (boronic acids, 1,3-dicarbonyls or alcohols) to yield functionalized cyclic alcohols. A related catalytic system also enabled the synthesis of cyclic cyclopentamines from ACPs tethered to imine moieties and boronic acids as coupling partners. DFT computations revealed how electron-poor phosphines favor the tandem processes, whereas Buchwald ligands promote the intramolecular (3+2) cycloaddition. Furthermore, in *Section 4.4* we developed the first transition-metal-catalyzed allylic cross-coupling between ACPs and boronic acids, yielding 1,1-disubstituted alkenes. DFT computations revealed the importance of palladacyclobutane species as key intermediates.

In *Section 4.5*, we explored a formal Pd(0)-catalyzed (3+2+2) cycloaddition of ACPs tethered to carbonyl moieties with aryl isocyanates, leading to carbamate polycyclic structures. This transformation involves a palladium π-allyl 1,5-dipole, which selectively reacts with isocyanates instead of undergoing C-O reductive elimination, as corroborated by DFT studies.

In conclusion, this thesis underscores the versatility of Pd(0)-catalyzed transformations involving ACPs, particularly for the synthesis of heterocycles. It highlights the importance of studying reaction intermediates to uncover novel reactivity modes and emphasizes the pivotal role of selecting appropriate catalytic systems to direct reaction pathways.

6. Experimental Procedures and Characterization of Compounds

This section details the synthesis of starting materials and products, along with the characterization of the unreported compounds. The compounds are listed numerically, not strictly following their order of appearance in *Results and Discussion.*

Diethyl 2-(2-cyclopropylideneethyl)-2-(2-(methoxyimino)ethyl)malonate (**1a**)[137]

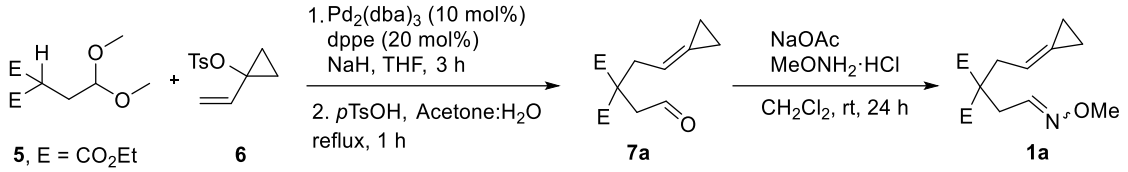

In a round bottom flask, a solution of $Pd_2(dba)_3$ (111 mg, 121 μmol, 0.1 equiv.), 1,2-bis(diphenylphosphino)ethane (96.3 mg, 242 μmol, 0.2 equiv.) and 1-vinylcyclopropyl tosylate (**6**, 3.74 g, 15.7 mmol, 1.3 equiv.) in dry THF (20 mL) was stirred at rt for 15 min.

In a separate round bottom flask, a solution of diethyl 2-(2, 2-dimethoxyethyl) malonate (**5**, 3.00 g, 12.1 mmol, 1.0 equiv.) in dry THF (25 mL) was added to a suspension of NaH (530 mg, 13.3 mmol, 1.1 equiv., 60% in mineral oil) in dry THF (100 mL), at 0 °C and the mixture was stirred for 30 min at rt. Then, the solution of vinyl tosylate (**6**) was added dropwise *via cannula*. The resulting mixture was stirred for 3 h, poured into water and extracted with Et_2O (3x60 mL). The organic layers were dried, filtered and concentrated to give a crude oily residue that was purified by flash chromatography (10% EtOAc/Hexane) to yield the intermediate acetal diethyl 2-(2-cyclopropylideneethyl)-2-(2,2-dimethoxyethyl)malonate as a colourless oil (2.66 g, 8.50 mmol, 70% yield).

Next, *p*-toluenesulfonic acid (323 mg, 1.70 mmol, 0.2 equiv.) was added to a solution of the acetal intermediate (2.66 g, 8.50 mmol, 1.0 equiv.) in H_2O:acetone 1:1 (85 mL), and the mixture was stirred under reflux for 1 h. The acetone was removed under reduced pressure and the product was extracted with Et_2O (3x40 mL). The combined organic layers were dried, filtered and concentrated. The product **7a** was isolated by flash chromatography (10% EtOAc/Hexane) as a colourless oil (2.20 g, 8.10 mmol, 95% yield). Spectroscopic data of **7a** agrees with that reported in the literature.[26c] **^{1}H NMR** (300 MHz, $CDCl_3$) δ (ppm) 9.70 (s, 1H), 5.63 (m, 1H), 4.22 (q, *J* = 7.25, 4H), 3.09 – 2.39 (m, 4H), 1.35 – 1.21 (t, *J* = 7.17 Hz, 6H), 1.03 (dd, *J* = 26.9, 7.7 Hz, 4H).

In a round-bottom flask, the aldehyde **7a** (1.30 g, 15.3 mmol, 1.0 equiv.) was added dropwise over a suspension of NaOAc (2.50 g, 30.5 mmol, 2.0 equiv.) in CH_2Cl_2 (30 mL) at rt. After 5 minutes, methoxyamine hydrochloride (3.67 g, 15.3 mmol, 1.0 equiv.) was added in one portion and the mixture was stirred for 16 h. The reaction was quenched with $NaHCO_{3(sat)}$ (50 mL), and the aqueous phase was extracted with Et_2O (3x20 mL). The combined organic layers were dried, filtered, concentrated and the resulting residue was purified by flash chromatography (5% EtOAc/ Hexane) to afford diethyl 2-(2-cyclopropylideneethyl) -2-(2-(methoxyimino)ethyl)malonate, **1a**, as a pale-yellow oil (3.54 g, 11.9 mmol, 78% yield, *E*:*Z* ratio 2:1).

- *E*:*Z* mixture 2:1. **^{1}H NMR** (300 MHz, $CDCl_3$) δ (ppm) 7.69 (t, *J* = 6.4 Hz, 0.67H), 7.06 (t, *J* = 5.3 Hz, 0.33H), 6.04 – 5.90 (m, 1H), 4.66 – 4.46 (m, 4H), 4.20 (s, 1H), 4.15 (s, 2H), 3.22 (d, *J* = 5.3 Hz, 0.67H), 3.17 (d, *J* = 7.4 Hz, 2H), 3.08 (d, *J* = 6.4 Hz, 1.33H), 1.62 (t, *J* = 7.1 Hz, 6H), 1.50 – 1.28 (m, 4H). **^{13}C NMR** (75 MHz, $CDCl_3$) δ (ppm) 170.7 (C), 146.9 (CH), 146.8 (CH), 127.6 (C), 127.4 (C), 111.6 (CH), 111.5 (CH), 61.8 (CH_3), 61.8 (CH_3), 61.7 (CH_2), 61.6 (CH_2), 61.5 (CH_3), 61.5 (CH_3), 56.1 (C), 56.0 (C), 36.4 (CH_2), 36.1 (CH_2), 32.9 (CH_2), 29.1 (CH_2), 14.2 (CH_3), 3.1 (CH_2), 2.0 (CH_2). **HRMS** (ESI-TOF): m/z calculated for $C_{15}H_{24}NO_5^+$ $[M + H]^+$: m/z 298.1649, found 298.1651.

[137] nOe experiments were performed to establish the *E*/*Z* isomerism, but they were not conclusive. The ratio of isomers has been calculated by NMR, assuming that *E* is the major because it is thermodynamically more stable.

[26c] Gulías, M.; Durán, J.; López, F.; Castedo, L.; Mascareñas, J.L. Palladium-catalyzed [4 + 3] intramolecular cycloaddition of alkylidenecyclopropanes and dienes. *J. Am. Chem. Soc.* **2007**, *129*, 36, 11026–11027.

- *E* isomer. **^{1}H NMR** (300 MHz, C_6D_6) δ (ppm) 7.69 (t, *J* = 6.4 Hz, 1H), 6.02 – 5.78 (m, 1H), 4.20 – 3.90 (m, 4H), 3.79 (s, 3H), 3.17 (d, *J* = 7.5 Hz, 2H), 3.04 (d, *J* = 6.4 Hz, 2H), 1.24 – 0.77 (m, 10H). **^{13}C NMR** (75 MHz, C_6D_6) δ (ppm) 170.4 (C), 146.6 (CH), 127.3 (C), 112.2 (CH), 61.4 (CH_2), 61.3 (CH_3), 57.2 (C), 36.5 (CH_2), 33.4 (CH_2), 14. (CH_3), 3.1 (CH_2), 2.1 (CH_2). **HRMS** (ESI-TOF): m/z calculated for $C_{15}H_{24}NO_5^+$ $[M + H]^+$: m/z 298.1649, found 298.1651.

Diethyl 2-(2-(cyclopropylidene-d$_4$)ethyl)-2-(2-(methoxyimino)ethyl) malonate (**d$_4$-1a**)

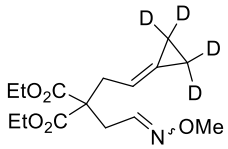

(*E:Z* 2:1)-d$_4$-1a

Compound **d$_4$-1a** was prepared following the procedure employed for the synthesis of precursor **1a**, using **d$_4$-7a** as starting material. Purification by flash chromatography (5% EtOAc/ Hexane) afforded to **d$_4$-1a** in 72% yield as a yellowish oil (*E:Z* ratio 2:1).

- *E* isomer. **^{1}H NMR** (500 MHz, CD_3OD) δ (ppm) 7.36 (t, *J* = 6.4 Hz, 1H), 5.68 (t, *J* = 7.4 Hz, 1H), 4.23 (t, *J* = 7.1 Hz, 4H), 3.81 (s, 3H), 2.82 (d, *J* = 7.5 Hz, 2H), 2.72 (d, *J* = 6.4 Hz, 2H), 1.30 (t, *J* = 7.1 Hz, 6H). **^{2}H NMR** (77 MHz, CD_3OD) δ 1.15 (m, 4H). **^{13}C NMR** (126 MHz, CD_3OD) δ (ppm) 171.7 (C), 148.0 (CH), 128.2 (C), 112.7 (CH), 62.7 (CH_2), 61.7 (CH_3), 58.0 (C), 36.8 (CH_2), 33.7 (CH_2), 14.4 (CH_3), 3.3-1.0 (m, CD_2). **HRMS** (ESI-TOF): m/z, calculated for $C_{15}H_{20}D_4NO_5^+$ $[M+H]^+$: m/z 302.1900; found 302.1899.

- *Z* isomer (NMR data deduced from a *E:Z* mixture = 1:9). **^{1}H NMR** (500 MHz, CD_3OD) δ (ppm) 6.72 (t, *J* = 5.3 Hz, 1H), 5.66 (t, *J* = 7.4 Hz, 1H), 4.23 (q, *J* = 7.1, 1.2 Hz, 4H), 3.86 (s, 3H), 2.86 (d, *J* = 5.4 Hz, 2H), 2.82 (d, *J* = 7.4 Hz, 2H), 1.29 (t, *J* = 7.1 Hz, 6H). **^{2}H NMR** (77 MHz, CD_3OD) δ (ppm) 0.96 (d, *J* = 5.8 Hz, 4H). **^{13}C NMR** (126 MHz, CD_3OD) δ (ppm) 171.8 (C), 148.0 (CH), 128.30 (C), 112.7 (CH), 62.8 (CH_2), 62.1 (CH_3), 57.2 (C), 37.2 (CH_2), 29.9 (CH_2), 14.4 (CH_3), 2.9-1.3 (m, CD_2). **HRMS** (ESI-TOF): m/z, calculated for $C_{15}H_{20}D_4NO_5^+$ $[M+H]^+$: m/z 302.1900; found 302.1899.

Diethyl 2-(2-((benzyloxy)imino)ethyl)-2-(2-cyclopropylideneethyl)malonate (**1b**)

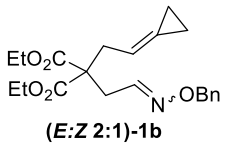

(*E:Z* 2:1)-1b

Compound **1b** was prepared following the procedure employed for the synthesis of precursor **1a**, using benzoxyamine hydrochloride as starting material. Purification by flash chromatography (5% EtOAc/ Hexane) afforded to **1a** as a yellowish oil in 72% (*E:Z* ratio 2:1). NMR data of both *E* and *Z* isomers can be easily deduced from the NMR data of two different fractions, with 10:1 and 1:6 E: Z ratios, respectively.

- *E* isomer (NMR data deduced from a *E:Z* mixture = 10:1). **^{1}H NMR** (300 MHz, $CDCl_3$) δ 7.36 (t, *J* = 6.4 Hz, 1H), 7.29 – 7.18 (m, 5H), 5.58 – 5.48 (m, 1H), 4.96 (s, 2H), 4.07 (q, *J* = 7.1 Hz, 4H), 2.73 (dt, *J* = 7.4, 1.2 Hz, 2H), 2.66 (d, *J* = 6.4 Hz, 2H), 1.15 (t, *J* = 7.1 Hz, 6H), 1.04 – 0.85 (m, 4H). **^{13}C NMR** (75 MHz, $CDCl_3$) δ 170.5 (C), 147.5 (CH), 137.7 (C), 128.5 (CH), 128.3 (CH), 127.9 (CH), 127. (C), 111.5 (CH), 75.8 (CH_2), 61.6 (CH_2), 56.8 (C), 36.0 (CH_2), 32.9 (CH_2), 14.1 (CH_3), 3.1 (CH_2), 2.0 (CH_2). **HMRS** (ESI-TOF): m/z calculated for $C_{22}H_{27}NO_5^+$ $[M + H]^+$: m/z 374.1967, found 374.1966.

- *Z* isomer (NMR data deduced from a *E:Z* mixture = 1:5.7). **^{1}H NMR** (300 MHz, $CDCl_3$) δ 7.29 – 7.18 (m, 5H), 6.68 (t, *J* = 5.2 Hz, 1H), 5.60 – 5.48 (m, 1H), 5.02 (s, 2H), 4.14 – 4.02 (m, 4H), 2.87 (d, *J* = 5.2 Hz, 2H), 2.74 (dt, *J* = 7.4, 1.3 Hz, 2H), 1.16 (t, *J* = 7.2 Hz, 6H), 1.03 – 0.84 (m, 4H). **^{13}C NMR** (75 MHz, $CDCl_3$) δ 170.7 (C), 147.5 (CH), 137.9 (C), 128.4 (CH), 128.1 (CH), 127.4 (C), 127.3 (C), 111.5 (CH), 76.0 (CH_2), 61.7 (CH_2), 55.9 (C), 36.3 (CH_2), 29.3 (CH_2), 14.1 (CH_3), 3.1 (CH_2), 2.0 (CH_2).

Diethyl 2-(3-((benzyloxy)imino)propyl)-2-(2-cyclopropylideneethyl)malonate (**1c**)

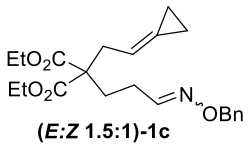

(*E*:*Z* 1.5:1)-1c

Compound **1c** was prepared following the procedure employed for the synthesis of precursor **1a**, using benzoxyamine hydrochloride as starting material and the corresponding aldehyde. Purification by flash chromatography (5% EtOAc/ Hexane) afforded to **1c**, which was isolated as a colourless oil in 90% yield (*E*:*Z* ratio 1.5:1). **^{1}H NMR** (300 MHz, CD_2Cl_2) δ 7.44 – 7.21 (m, 5.6H), 6.62 (t, *J* = 5.3 Hz, 0.4H), 5.66 – 5.53 (m, 1H), 5.07 (s, 0.8H), 5.01 (s, 1.2H), 4.25 – 4.06 (m, 4H), 2.78 (dq, *J* = 7.4, 1.2 Hz, 2H), 2.36 – 2.22 (m, 1H), 2.18 – 2.08 (m, 1H), 2.07 – 1.95 (m, 2H), 1.32 – 1.14 (m, 6H), 1.14 – 0.91 (m, 4H). **^{13}C NMR** (75 MHz, CD_2Cl_2) δ 171.5 (C), 151.4 (CH), 150.7 (CH), 138.9 (C), 138.6 (C), 128.9 (CH), 128.7 (CH), 128.5 (CH), 128.3 (CH), 128.2 (CH), 127.1 (C), 127.0 (C), 112.4 (CH), 76.3 (CH_2), 76.0 (CH_2), 61.9 (CH_2), 57.7 (C), 57.6 (C), 35.5 (CH_2), 35.3 (CH_2), 29.6 (CH_2), 29.2 (CH_2), 25.3 (CH_2), 21.5 (CH_2), 14.4 (CH_3), 3.3 (CH_2), 2.3 (CH_2), 2.3 (CH_2). **HRMS (ESI-TOF):** m/z calculated for $C_{22}H_{30}NO_5$ $[M + H]^+$: m/z 388.2124, found 388.2119.

Dimethyl (*E*)-2-(2-cyclopropylideneethyl)-2-(2-(methoxyimino)propyl)malonate (***E*-1d**)

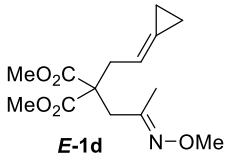

***E*-1d**

Compound ***E*-1d** was prepared following the procedure employed for the synthesis of precursor **1a**, using ketone **9a** as starting material. Purification by flash chromatography (5% EtOAc/ Hexane) afforded to ***E*-1d**, which was isolated as a yellowish oil in 66% yield (*E*:*Z* ratio 1:0). **^{1}H NMR** (300 MHz, $CDCl_3$) δ (ppm) 5.62 – 5.24 (m, 1H), 3.59 (s, 3H), 3.52 (s, 6H), 2.71 (d, *J* = 7.5 Hz, 2H), 2.62 (s, 2H), 1.57 (s, 3H), 1.03 – 0.60 (m, 4H). **^{13}C NMR** (75 MHz, CD_3OD) δ (ppm) 170.9 (C), 152.3 (C), 126.2 (C), 111.9 (CH), 61.0 (CH_3), 56.3 (C), 52.1 (CH_3), 37.6 (CH_2), 34.9 (CH_2), 14.8 (CH_3), 2.6 (CH_2), 1.4 (CH_2). **HRMS** (ESI-TOF): m/z calculated for $C_{14}H_{22}NO_5^+$ $[M+H]^+$: m/z 284.1492, found 284.1490.

2-(2-Cyclopropylideneethoxy)acetaldehyde *O*-methyl oxime (**1e**)

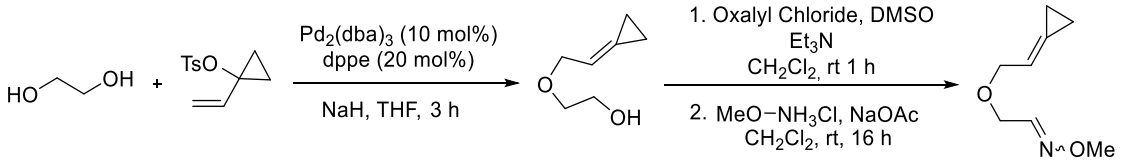

6 **10** **1e**

In a round bottom flask, a solution of $Pd_2(dba)_3$ (740 mg, 805 μmol, 0.1 equiv.), 1,2-bis(diphenylphosphino)ethane (640 mg, 1.60 mmol, 0.2 equiv.) and 1-vinylcyclopropyl tosylate **6** (1.92 g, 8.10 mmol, 1.0 equiv.) in dry THF (29 mL) was stirred at rt for 15 min.

In a separate round bottom flask, ethylene glycol (901 μL, 16.1 mmol, 2.0 equiv.) was added carefully to a suspension of NaH (644 mg, 16.1 mmol, 2.0 equiv., 60% in mineral oil) in dry THF (10 mL), at 0 °C and the mixture was stirred for 30 min at rt. Then, the solution of vinyl tosylate (**6**) was added dropwise *via cannula*. The resulting mixture was stirred for 3 h, poured into water and extracted with Et_2O (3x50 mL). The organic layers were dried, filtered and concentrated to give a crude oily residue that was purified by flash chromatography (5-10% EtOAc/Hexane) to yield the 2-(2-cyclopropylideneethoxy)ethan-1-ol **10** as an uncolored oil (731 mg, 5.70 mmol, 71% yield). Spectroscopic data of **10** agrees with that reported in the literature.[29] **^{1}H NMR** (300 MHz, $CDCl_3$) δ (ppm) 6.07 – 5.82 (m, 1H), 4.16 (d, *J* = 6.7, 1.2 Hz, 2H), 3.79 – 3.65 (m, 2H), 3.64 – 3.40 (m, 4H), 1.96 – 1.67 (br s, 1H), 1.19 – 1.02 (m, 4H).

At -78 ºC, DMSO (1.00 mL, 14.1 mmol, 2.4 equiv.) in CH_2Cl_2 (7 mL) was added dropwise over a solution of oxalyl chloride (1.00 mL, 12.0 mmol, 2.0 equiv.) in CH_2Cl_2 (20 mL). After 10 minutes, a solution of the alcohol **10** (0.74 g, 6.0 mmol, 1.0 equiv.) in CH_2Cl_2 (7 mL) added by slow addition

[29] Verdugo, F.; Villarino, L.; Durán, J.; Gulías, M.; Mascareñas, J. L.; López, F. Enantioselective Palladium-Catalyzed [3C + 2C] and [4C + 3C] Intramolecular Cycloadditions of Alkylidenecyclopropanes. *ACS Catal.* **2018**, *8*, 6100-6105.

over the mixture. After 30 minutes, Et_3N (2.20 mL, 15.8 mmol, 2.8 equiv.) was added. After stirring for 30 minutes, the reaction was allowed to warm to rt and quenched with brine (40 mL). Then, extractions were carried out with CH_2Cl_2 (3x30 mL), and the organic layers were washed with H_2O (20 mL), dried, filtered and partially evaporated to 10-15 mL. To this solution, NaOAc (2.50 g, 30.5 mmol, 2.0 equiv.) was added at rt. After 5 minutes of stirring, methoxyamine hydrochloride (752 mg, 9.00 mmol, 1.0 equiv.) was added in one portion and the mixture was stirred for 16 h. The reaction was quenched with $NaHCO_{3(sat)}$ (10 mL), and the aqueous phase was extracted with Et_2O (3x5 mL). The combined organic layers were dried, filtered, concentrated and the resulting residue was purified by flash chromatography (5% EtOAc/ Hexane) to afford 2-(2-cyclopropylideneethoxy)acetaldehyde *O*-methyl oxime, **1e**, as a pale-yellow oil (528 mg, 3.40 mmol, 57% yield, *E:Z* ratio 1.5:1). **^{1}H NMR** (300 MHz, $CDCl_3$) δ (ppm) 7.44 (t, *J* = 5.7 Hz, 0.6H), 6.84 (t, *J* = 3.7 Hz, 0.4H), 5.92 (m, 1H), 4.25 (d, *J* = 3.7 Hz, 0.8H), 4.14 (m, 2H), 4.07 (d, *J* = 5.7 Hz, 1.2H), 3.86 (s, 1.8H), 3.86 (s, 1.2H), 1.18 – 1.01 (m, 4H). **^{13}C NMR** (75 MHz, $CDCl_3$) δ (ppm) 150.3 (CH), 147.1 (CH), 127.7 (C), 114.1 (CH), 114.0 (CH), 71.1 (CH_2), 70.5 (CH_2), 66.3 (CH_2), 63.9 (CH_2), 61.9 (CH_3), 61.5 (CH_3), 2.2 (CH_2), 1.7 (CH_2), 1.7 (CH_2). **HRMS** (ESI-TOF): m/z calculated for $C_8H_{14}NO_2^+$ $[M+H]^+$: m/z 156.1019, found 156.1020.

***N*-(2-cyclopropylideneethyl)-*N*-(2-(methoxyimino)ethyl)-4-methylbenzenesulfonamide** (**1f**)

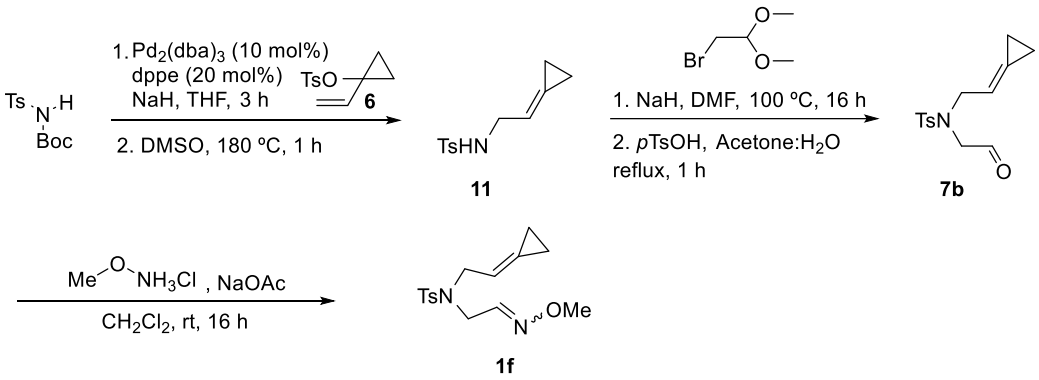

In a round bottom flask, a solution of $Pd_2(dba)_3$ (772 mg, 840 μmol, 0.1 equiv.), 1,2-bis(diphenylphosphino)ethane (680 mg, 1.70 mmol, 0.2 equiv.) and 1-vinylcyclopropyl tosylate **6** (2.00 g, 8.40 mmol, 1.0 equiv.) in dry THF (29 mL) was stirred at rt for 15 min.

In a separate round bottom flask, a solution of *tert*-butyl tosylcarbamate (3.40 g, 12.6 mmol, 1.5 equiv.) in dry THF (20 mL) was added carefully to a suspension of NaH (504 mg, 12.6 mmol, 1.5 equiv., 60% in mineral oil) in dry THF (47 mL), at 0 °C and the mixture was stirred for 30 min at rt. Then, the solution of vinyl tosylate (**6**) was added dropwise *via cannula*. The resulting mixture was stirred for 3 h, poured into water and extracted with Et_2O (3x50 mL). The organic layers were dried, filtered and concentrated to give a crude oily residue that was purified by flash chromatography (20-40% EtOAc/Hexane) to yield the *tert*-butyl (2-cyclopropylideneethyl)(tosyl)carbamate as a white solid (2.10 g, 6.30 mmol, 75% yield). Spectroscopic data this product agrees with that reported in the literature.[29] **^{1}H NMR** (300 MHz, $CDCl_3$) δ 6.07 – 5.82 (m, 1H), 4.16 (d, *J* = 6.7, 1.2 Hz, 2H), 3.79 – 3.65 (m, 2H), 3.64 – 3.40 (m, 4H), 1.96 – 1.67 (br s, 1H), 1.19 – 1.02 (m, 4H). For removing the Boc group, a solution of *tert*-butyl (2-cyclopropylideneethyl)(tosyl)carbamate in DMSO (38 mL) was heated in a sealed tube at 180 ºC for 1 h. After cooling down to rt, the mixture was poured over a H_2O:$NaCl_{(aq)}$ 10:1 solution (330 mL), and extracted with Et_2O (3x50 mL). The organic layers were dried, filtered and concentrated to give a crude oily residue that was purified by flash chromatography (40% EtOAc/Hexane) to yield the *tert*-butyl (2-cyclopropylideneethyl)(tosyl)carbamate **11** as a yellow solid (1.20 g, 5.10 mmol, 81% yield). Spectroscopic data the **11** product agrees with that reported in

[29] Verdugo, F.; Villarino, L.; Durán, J.; Gulías, M.; Mascareñas, J. L.; López, F. Enantioselective Palladium-Catalyzed [3C + 2C] and [4C + 3C] Intramolecular Cycloadditions of Alkylidenecyclopropanes. *ACS Catal.* **2018**, *8*, 6100-6105.

the literature.[29] **^{1}H NMR** (300 MHz, CDCl3) δ (ppm) 7.75 (d, *J* = 8.0 Hz, 2H), 7.29 (d, *J* = 8.0 Hz, 2H), 5.74 – 5.59 (m, 1H), 4.91 (t, *J* = 6.1 Hz, 1H), 3.70 (t, *J* = 5.9 Hz, 1H), 2.42 (s, 3H), 0.98 (s, 4H).

In a round bottom flask, the monosubstituted amine **11** (1.00 g, 4.21 mmol, 1.0 equiv.) was added in one portion to a suspension of NaH (185 mg, 4.64 mmol, 1.1 equiv., 60% in mineral oil) in dry DMF (17 mL), at 0 °C and the mixture was stirred for 30 min at rt. Then, 2-bromo-1,1-dimethoxyethane (1.50 mL, 12.6 mmol, 3.0 equiv.) was added dropwise to the mixture. After 16 h at 100 ºC, the reaction was quenched with NH_4Cl_{sat} (200 mL) and extracted with Et_2O (3x30 mL). The organic layers were dried, filtered and concentrated to give a crude oily residue that was purified by flash chromatography (50% EtOAc/Hexane) to give the desired acetal as a pale-yellow solid (1.00 g, 3.15 mmol, 75% yield). Spectroscopic data the *N*-(2- cyclopropylideneethyl)-*N*-(2,2-dimethoxyethyl)-4-methylbenzenesulfonamide agrees with that reported in the literature.[40] **^{1}H NMR** (300 MHz, $CDCl_3$) δ (ppm) 7.67 (d, *J* = 6.9 Hz, 2H), 7.25 (d, *J* = 7.5 Hz, 2H), 5.49 (tq, *J* = 6.6, 2.0 Hz, 1H), 4.47 (t, *J* = 5.4 Hz, 1H), 4.01 (d, *J* = 6.8 Hz, 2H), 3.31 (s, 6H), 3.17 (d, *J* = 5.4 Hz, 2H), 2.36 (s, 3H), 1.04 – 0.81 (m, 4H).

The acetal *N*-(2- cyclopropylideneethyl)-*N*-(2,2-dimethoxyethyl)-4-methylbenzenesulfonamide (250 mg, 768 μmol, 1.0 equiv.) and *p*-toluenesulfonic acid monohydrate (438 mg, 2.31 mmol, 3.0 equiv.) were dissolved in acetone/water (1:1, 7.6 mL). The resulting mixture was refluxed for 1 h and cooled to rt. The acetone was removed under reduced pressure and the aqueous solution was extracted with Et_2O. The resulting organic phase was dried and evaporated under reduced pressure and the crude was purified by flash chromatography (10% EtOAc/ Hexane) to afford the aldehyde *N*-(2-cyclopropylideneethyl)-4-methyl-*N*-(2- oxoethyl)benzenesulfonamide, **7b**, as a pale-yellow solid (172 mg, 614 mmol, 80% yield). Spectroscopic data of **7b** agrees with that reported in the literature.[40] **^{1}H NMR** (300 MHz, $CDCl_3$) δ (ppm) 9.55 (t, *J* = 1.7 Hz, 1H), 7.71 (d, *J* = 8.3 Hz, 2H), 7.35 (d, *J* = 8.4 Hz, 2H), 5.75 – 5.55 (m, 1H), 3.93 (d, *J* = 7.2 Hz, 2H), 3.71 (s, 2H), 2.45 (s, 3H), 1.18 – 0.82 (m, 4H). The aldehyde **7b** (172 mg, 618 μmol, 1.0 equiv.) was reacted with methoxyamine hydrochloride (51.6 g, 618 μmol, 1.0 equiv.) following the abovementioned procedure for the synthesis of the oxime ether **1a**, providing after flash chromatography (10% EtOAc/ Hexane) to afford *N*-(2-cyclopropylideneethyl)-*N*-(2-(methoxyimino)ethyl)-4-methylbenzenesulfonamide, **1f**, as a colourless oil (135 mg, 439 μmol, 71% yield, *E:Z* ratio 1.2:1). **^{1}H NMR** (300 MHz, $CDCl_3$) δ (ppm) 7.67 (d, J = 7.4 Hz, 2H), 7.34 – 7.23 (m, 2H), 7.13 (t, J = 6.0 Hz, 0.55H), 6.58 (t, J = 4.2 Hz, 0.45H), 5.70 – 5.49 (m, 1H), 3.94 (d, J = 4.2 Hz, 0.9H), 3.89 (dd, J = 6.9, 1.2 Hz, 2H), 3.82 (d, J = 6.0 Hz, 1.1H), 3.77 (s, 1.35H), 3.72 (s, 1.65H), 2.39 (s, 3H), 1.11 – 0.87 (m, 4H).**^{13}C NMR** (75 MHz, $CDCl_3$) δ (ppm) 148.3 (CH), 145.7 (CH), 143.6 (C), 143.5 (C), 136.8 (C), 136.2 (C), 129.8 (CH), 129.7 (CH), 129.0 (C), 128.5 (C), 127.1 (CH), 112.0 (CH), 111.8 (CH), 61.9 (CH_3), 61.5 (CH_3), 50.5 (CH_2), 49.2 (CH_2), 45.7 (CH_2), 42.8 (CH_2), 21.4 (CH_3), 2.6 (CH_2), 2.5 (CH_2), 1.8 (CH_2), 1.6 (CH_2). **HRMS** (ESI-TOF): m/z calculated for $C_{15}H_{21}N_2O_3S$ $[M + H]^+$: m/z 309.1273, found 309.1270.

Diethyl 2-(2-(acetoxyimino)ethyl)-2-(2-cyclopropylideneethyl)malonate (**1g**)

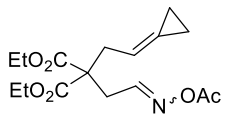

(*E:Z* 2.3:1)-1g

Compound **1g** was prepared following the procedure employed for the synthesis of precursor **1a**, using *O*-acetylhydroxylammonium chloride and aldehyde **7a** as starting materials. Purification by flash chromatography (5% EtOAc/ Hexane) afforded to **1g** as a yellowish oil in 51% yield (*E:Z* ratio 2.3:1). **^{1}H NMR** (300 MHz, $CDCl_3$) δ (ppm) 7.78 (t, *J* = 6.4 Hz, 0.7H), 7.22 (t, *J* = 4.7 Hz, 0.3H), 5.67 – 5.56 (m, 1H), 4.28 – 4.12 (m, 4H), 2.95 (d, *J* = 5.2 Hz, 1H), 2.88 – 2.79 (m, 3H), 2.17 (s, 1H), 2.12 (s, 2H), 1.26 (t, *J* = 7.1 Hz, 6H), 1.14 – 0.92 (m, 4H). **^{13}C NMR** (75 MHz, $CDCl_3$) δ (ppm) 169.0 (C), 169.0 (C), 167.2 (C), 155.3 (CH), 155.2 (CH), 153.5 (CH), 126.9 (CH), 126.8 (CH), 110.0 (CH), 109.9 (CH), 60. (CH_2), 60.9 (CH_2), 55.5 (C), 55.4 (C), 54.5 (C), 51.6 (CH), 35.6 (CH_2), 35.4 (CH_2), 31.9 (CH_2), 29.2 (CH_2), 18.4 (CH_3), 18.3 (CH_3), 12.9 (CH_3), 2.0 (CH_2), 1.9 (CH_2), 0.9

[40] Verdugo, F.; da Concepción, E.; Rodiño, R.; Calvelo, M.; Mascareñas, J. L.; López, F. Pd-Catalyzed (3 + 2) Heterocycloadditions between Alkylidenecyclopropanes and Carbonyls: Straightforward Assembly of Highly Substituted Tetrahydrofurans. *ACS Catal.* **2020**, *10*, 14, 7710–7718.

(CH_2), 0.8 (CH_2). **HRMS** (ESI-TOF): m/z calculated for $C_{16}H_{24}NO_6$ $[M+H]^+$: m/z 326.1604, found 326.1599.

Diethyl 2-(2-cyclopropylideneethyl)-2-(2-((2,2,2-trifluoroethoxy) imino)ethyl)malonate (**1h**)

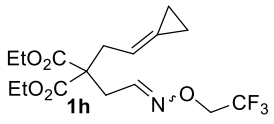

Compound **1h** was prepared following the procedure employed for the synthesis of precursor **1a**, using amine hydrochloride **12** and aldehyde **7a** as starting materials. Purification by flash chromatography (5% EtOAc/ Hexane) afforded to **1h** as a yellowish oil in 51% yield (*E:Z* ratio 2:1), allowing the separation of both isomers.

- *E* isomer. **^{1}H NMR** (300 MHz, CD_3OD) δ (ppm) 7.50 (t, *J* = 6.4 Hz, 1H), 5.74 – 5.55 (m, 1H), 4.45 (q, *J* = 8.8 Hz, 2H), 4.20 (q, *J* = 7.0 Hz, 4H), 2.81 (d, *J* = 7.6 Hz, 2H), 2.72 (d, *J* = 6.4 Hz, 2H), 1.26 (t, *J* = 7.1 Hz, 6H), 1.15 – 0.93 (m, 4H). **^{13}C NMR** (75 MHz, CD_3OD) δ (ppm) 171.6 (C), 150.7 (CH), 128.5 (C), 125.3 (q, *J* = 279.7 Hz, C), 112.4 (CH), 71.6 (q, *J* = 33.7, CH_2), 62.7 (CH_2), 57.9 (C), 36.8 (CH_2), 33.5 (CH_2), 14.4 (CH_3), 3.3 (CH_2), 2.4 (CH_2). **^{19}F NMR** (282 MHz, CD_3OD) δ (ppm) -72.0 (t, *J* = 8.8 Hz). **HRMS** (ESI-TOF): m/z calculated for $C_{16}H_{23}F_3NO_5^+$ $[M+H]^+$: m/z 366.1528, found 366.1522.

- *Z* isomer. **^{1}H NMR** (300 MHz, CD_3OD) δ (ppm) 6.85 (t, *J* = 5.3 Hz, 1H), 5.76 – 5.52 (m, 1H), 4.52 (q, *J* = 8.8 Hz, 2H), 4.22 (q, *J* = 7.1 Hz, 4H), 2.89 (d, *J* = 5.3 Hz, 2H), 2.82 (d, *J* = 7.5 Hz, 2H), 1.27 (t, *J* = 7.1 Hz, 6H), 1.19 – 0.90 (m, 4H). **^{13}C NMR** (75 MHz, CD_3OD) δ (ppm) 171.7 (C), 150.6 (CH), 128.7 (C), 125.3 (q, *J* = 279.5 Hz, C), 112.4 (CH), 71.6 (q, *J* = 33.7 Hz, CH_2), 62.9 (CH_2), 57.0 (C), 37.2 (CH_2), 30.1 (CH_2), 14.3 (CH_3), 3.3 (CH_2), 2.4 (CH_2). **^{19}F NMR** (282 MHz, CD_3OD) δ (ppm) -72.3 (t, *J* = 8.8 Hz). **HRMS** (ESI-TOF): m/z calculated for $C_{16}H_{23}F_3NO_5^+$ $[M+H]^+$: m/z 366.1528, found 366.1522.

***N*-(2-cyclopropylideneethyl)-4-methyl-*N*-(2-((2,2,2-trifluoroethoxy)imino)ethyl)benzene-sulfonamide** (**1i**)

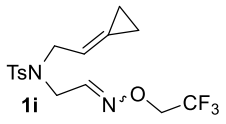

Compound **1i** was prepared following the procedure employed for the synthesis of precursor **1a**, using amine hydrochloride **12** and aldehyde **7b** as starting materials. Purification by flash chromatography (5% EtOAc/ Hexane) afforded to **1i** as a pale-yellow oil in 74% yield (*E:Z* ratio 1.9:1). **^{1}H NMR** (300 MHz, CD_3OD) δ (ppm) 7.76 – 7.68 (m, 2H), 7.48 – 7.36 (m, 2H), 7.32 (t, *J* = 5.7 Hz, 0.65H), 6.79 (t, *J* = 4.1 Hz, 0.35H), 5.71 – 5.52 (m, 1H), 4.49 (q, *J* = 8.8 Hz, 0.7H), 4.40 (q, *J* = 8.8 Hz, 1.3H), 4.00 (d, *J* = 4.1 Hz, 0.7H), 3.94 (d, *J* = 7.0 Hz, 2H), 3.89 (d, *J* = 5.7 Hz, 1.3H) 2.54-2.35 (m, 3H), 1.17 – 0.90 (m, 4H). **^{13}C NMR** (75 MHz, CD_3OD) δ (ppm) 152.6 (CH), 150.0 (CH), 145.5 (C), 145.3 (C), 138.1 (C), 137.4 (C), 131.1 (CH), 130.9 (CH), 130.5 (C), 129.9 (C), 128.4 (CH), 125.2 (q, *J* = 279.4 Hz, C), 113.1 (CH), 112.9 (CH), 71.9 (q, *J* = 33.8 Hz, CH_2), 71.5 (q, *J* = 33.8 Hz, CH_2), 51.7 (CH_2), 50.4 (CH_2), 46.3 (CH_2), 43.9 (CH_2), 21.5 (CH_3), 21.5 (CH_3), 2.9 (CH_2), 2.8 (CH_2), 2.3 (CH_2), 2.2 (CH_2). **^{19}F NMR** (282 MHz, CD_3OD) δ (ppm) -72.00 (t, *J* = 9.3 Hz, 3.9F), -72.29 (t, *J* = 9.3 Hz, 2.1F). **HRMS** (ESI-TOF): m/z calculated for $C_{16}H_{20}F_3N_2O_3S^+$ $[M+H]^+$: m/z 377.1141, found 377.1139.

Dimethyl 2-(2-cyclopropylideneethyl)-2-(2-(methoxyimino)ethyl)malonate (**1k**)

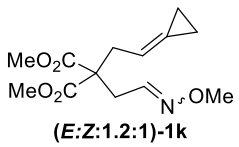

(*E:Z*:1.2:1)-1k

Compound **1k** was prepared following the procedure employed for the synthesis of precursor **1a**, using amine hydrochloride **12** and aldehyde **7e** as starting materials. Purification by flash chromatography (5% EtOAc/ Hexane) affordedto **1k** as a pale-yellow oil in 80% yield (*E:Z* ratio 1.2:1).

- *E* isomer. **^{1}H NMR** (300 MHz, CD_3OD) δ (ppm) 7.32 (t, *J* = 6.4 Hz, 1H), 5.67 – 5.55 (m, 1H), 3.77 (s, 3H), 3.73 (s, 6H), 2.79 (dd, *J* = 7.4, 1.6 Hz, 2H), 2.70 (d, *J* = 6.4 Hz, 2H), 1.23 – 1.02 (m, 4H). **^{13}C NMR** (75 MHz, CD_3OD) δ (ppm) 172.1 (C), 147.7 (CH), 128.6, (C) 112.4 (CH), 61.8 (CH_3), 58.1 (C), 53.1 (CH_3), 36.8 (CH_2), 33.7 (CH_2), 3.3 (CH_2), 2.4 (CH_2).

- E:Z mixture 1:2.3. **^{1}H NMR** (300 MHz, CD_3OD) δ (ppm) 7.30 (t, *J* = 6.4 Hz, 0.3H), 6.67 (t, *J* = 5.4 Hz, 0.7H), 5.68 – 5.53 (m, 1H), 3.82 (s, 2.1H), 3.75 (s, 0.9H), 3.75 (br. s, 6H), 2.83 (d, *J* = 5.4 Hz, 1.4H), 2.80 – 2.74 (m, 2H), 2.68 (d, *J* = 6.4 Hz, 0.6H), 1.16 – 0.95 (m, 4H). **^{13}C NMR** (75 MHz, CD_3OD) δ (ppm) 172.3 (C), 172.1 (C), 147.9 (CH), 147.7 (CH), 128.7 (C), 128.6 (C), 112.4 (CH), 112.3 (CH), 62.1 (CH_3), 61.7 (CH_3), 58.1 (C), 57.3 (C), 53.2 (CH_3), 53.1 (CH_3), 37.2 (CH_2), 36.8 (CH_2), 33.7 (CH_2), 29.9 (CH_2), 3.3 (CH_2), 2.4 (CH_2), 2.3 (CH_2).

- *Z* isomer (NMR data deduced from a *E:Z* mixture = 1:2.3). **^{1}H NMR** (300 MHz, CD_3OD) δ (ppm) 6.67 (t, *J* = 5.4 Hz, 1H), 5.68 – 5.53 (m, 1H), 3.82 (s, 3H), 3.75 (s, 6H), 2.83 (d, *J* = 5.4 Hz, 2H), 2.80 – 2.74 (m, 2H), 1.16 – 0.95 (m, 4H). **^{13}C NMR** (75 MHz, CD_3OD) δ (ppm) 172.3 (C), 147.9 (CH), 128.7 (C), 112.4 (CH), 62.1 (CH_3), 57.3 (C), 53.2 (CH_3), 37.2 (CH_2), 29.9 (CH_2), 3.3 (CH_2), 2.3 (CH_2).

Dimethyl 2-(3-((benzyloxy)imino)propyl)-2-(2-cyclopropylideneethyl)malonate (**1l**)

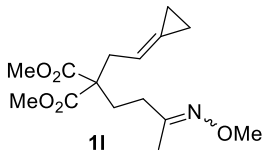

1l

Compound **1l** was prepared following the procedure employed for the synthesis of precursor **1a**, from the corresponding starting materials. Purification by flash chromatography (5% EtOAc/ Hexane) afforded **1l** as a pale-yellow oil in 84% yield (*E:Z* ratio 1:0). **^{1}H NMR** (300 MHz, $CDCl_3$) δ (ppm) 5.66 – 5.54 (m, 1H), 3.80 (s, 2H), 3.77 (s, 1H), 3.73 – 3.62 (m, 6H), 2.81 (d, *J* = 7.4 Hz, 2H), 2.26 – 1.98 (m, 4H), 1.82 (s, 1H), 1.78 (s, 2H), 1.13 – 0.93 (m, 4H). **^{13}C NMR** (75 MHz, $CDCl_3$) δ (ppm) 171.7 (C), 171.6 (C), 156.9 (C), 156.4 (C), 126.7 (C), 126.7 (C), 111.9 (CH), 111.8 (CH), 61.2 (CH_3), 61.2 (CH_3), 57.6 (C), 57.5 (C), 52.5 (CH_3), 35.4 (CH_2), 35.0 (CH_2), 30.9 (CH_2), 29.3 (CH_2), 28.1 (CH_2), 24.3 (CH_2), 19.8 (CH_3), 14.0 (CH_3), 3.0 (CH_2), 1.9 (CH_2), 1.9 (CH_2).

Diethyl (3*aR*,6*aR*)-1-methoxy-3-methylenehexahydrocyclopenta[*b*]pyrrole-5,5(1*H*)-dicarboxylate (**2a**)

***E*-1a** **2a**, 65% ***E*-4a**, 35%

Prepared following general procedure for catalytic reactions (see *Methodology*, page 57), using $Pd_2(dba)_3$ (7.40 mg, 8.10 µmol, 6 mol%), RuPhos (12.6 mg, 27.0 µmol, 20 mol%) and ***E*-1a** (40.0 mg, 135 µmol, 1.0 equiv.) in freshly distilled toluene (1.1 mL). The reaction crude was purified by flash chromatography (5% EtOAc/Hexane) to afford **12a** as a colourless oil (26.0 mg, 88.0 µmol, 65% yield). **^{1}H NMR** (300 MHz, $CDCl_3$) δ (ppm) 5.00 (s, 1H), 4.93 (s, 1H), 4.31 – 4.04 (m, 4H), 3.85 (d, *J* = 14.2 Hz, 1H), 3.70 (dt, *J* = 10.4, 5.7 Hz, 1H), 3.53 (s, 3H), 3.43 (d, *J* = 13.5 Hz, 1H), 3.16 (q, *J* = 7.9 Hz, 1H), 2.56 – 2.38 (m, 3H), 2.31 (dd, *J* = 13.5, 6.8 Hz, 1H), 1.24 (t, *J* = 7.1 Hz, 6H). **^{13}C NMR** (75 MHz, $CDCl_3$) δ (ppm) 172.2 (C), 171.3 (C), 149.5 (C), 107.6 (CH_2), 72.9 (CH), 61.7 (CH_2), 61.5 (CH_2), 61.0 (CH), 60.8 (CH_2), 45.0 (CH_3), 40.2 (CH_2), 38.8 (CH_2), 14.2 (CH_3), 14.1 (CH_3). **HRMS** (ESI-TOF): m/z calculated for $C_{15}H_{24}NO_5^+$ [M + H]$^+$: m/z 298.1654, found 298.1646. Stereochemistry of **2a** was determined by nOe experiments.

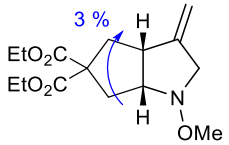

Figure 41. Significant nOe's observed for **2a**.

Enantioselectivity was determined by chiral HPLC analysis on Chiralpak OZ-H at rt, (Hexane:iPrOH = 98:2, 1 mL/min).

Racemic sample:

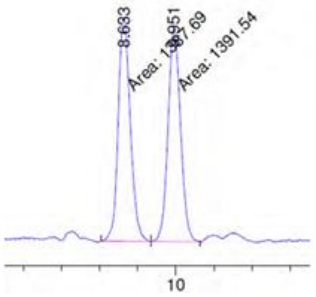

Signal 1: DAD1 A, Sig=220,8 Ref=360,100

Peak #	RetTime [min]	Type	Width [min]	Area [mAU*s]	Height [mAU]	Area %
1	8.633	MF	0.3641	1387.69446	63.52994	49.9308
2	9.951	FM	0.3830	1391.54285	60.55071	50.0692
Totals :				2779.23730	124.08065	

Using **(*S,R,R*)-L2** as ligand (from ***E*-1a**, 97.0:3.0 er, 90% yield):

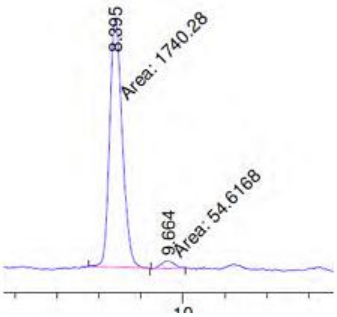

Signal 1: DAD1 A, Sig=220,8 Ref=360,100

Peak #	RetTime [min]	Type	Width [min]	Area [mAU*s]	Height [mAU]	Area %
1	8.395	MM	0.3468	1740.27795	83.62944	96.9571
2	9.664	MM	0.3699	54.61684	2.46096	3.0429
Totals :				1794.89479	86.09040	

Diethyl 1-methoxy-3-(methylene-*d*$_2$) hexahydrocyclopenta[*b*]pyrrole-5,5(1*H*)-dicarboxylate-2,2-*d*$_2$ (d$_4$-2a)

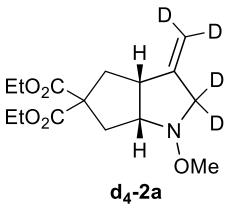

d$_4$-2a

Prepared following the procedure employed for the synthesis of the cycloadduct **2a**, using ***E*-d$_4$-1a** as starting material. Purification by flash chromatography (5% EtOAc/ Hexane) afforded to **d$_4$-2a** as a colourless oil in 57% yield. **^{1}H NMR** (300 MHz, $CDCl_3$) δ (ppm) 4.27 – 4.05 (m, 4H), 3.75 – 3.65 (m, 1H), 3.52 (s, 3H), 3.20 – 3.09 (m, 1H), 2.53 – 2.23 (m, 4H), 1.28 – 1.20 (m, 6H). **^{2}H NMR** (46 MHz, $CDCl_3$) δ (ppm) 5.25 – 4.77 (m, 2H), 3.98 – 3.65 (m, 1H), 3.60 – 3.19 (m, 1H). **^{13}C NMR** (75 MHz, $CDCl_3$) δ (ppm) 172.2 (C), 171.4 (C), 149.3 (C), 72.9 (CH), 61.7 (CH_2), 61.5 (CH_2), 61.0 (CH), 44.9 (CH_3), 40.24(CH_2), 38.8 (CH_2), 14.2 (CH_3), 14.1 (CH_3). **HRMS** (ESI-TOF): m/z calculated for $C_{15}H_{20}D_4NO_5^+$ $[M+H]^+$: m/z 302.1900, found 302.1902.

Diethyl (3*aR*,6*aR*)-1-benzoxy-3-methylenehexahydrocyclopenta[*b*]pyrrole-5,5(1*H*)-dicarboxylate (2b)

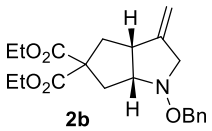

2b

Prepared following the procedure employed for the synthesis of the cycloadduct **2a**, using **(*E:Z* 2:1)-1b** as starting material. Reaction carried out at 90 ºC. Purification by flash chromatography (5% EtOAc/ Hexane) afforded to **2b** as a yellowish oil in 69% yield. **^{1}H NMR** (300 MHz, $CDCl_3$) δ (ppm) 7.43 – 7.24 (m, 5H), 4.96 (d, *J* = 2.2 Hz, 1H), 4.91 (d, *J* = 2.2 Hz, 1H), 4.80 – 4.58 (m, 2H), 4.27 – 4.04 (m, 4H), 3.83 – 3.65 (m, 2H), 3.46 (dt, *J* = 13.5, 2.4 Hz, 1H), 3.15 (q, *J* = 8.4 Hz, 1H), 2.55 – 2.20 (m, 4H), 1.31 – 1.18 (m, 6H). **^{13}C NMR** (75 MHz, $CDCl_3$) δ (ppm) 172.2 (C), 171.4 (C), 149.3 (C), 138.0 (C), 128.7 (CH), 128.4 (CH), 127.9 (CH), 107.4 (CH_2), 76.0 (CH_2), 73.1 (CH), 61.7 (CH_2), 61.6 (CH_2), 61.6 (C), 61.5 (CH_2), 45.0 (CH), 40.2 (CH_2), 38.7 (CH_2), 14.2 (CH_3), 14.1 (CH_3). **HMRS** (ESI-TOF): m/z calculated for $C_{21}H_{27}NO_5^+$ $[M + H]^+$: m/z 374.1967, found 374.1958. Stereochemistry of **2b** was determined by nOe experiments.

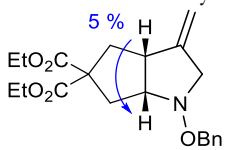

Figure 42. Significant nOe's observed for **2b**.

Enantioselectivity was determined by chiral HPLC analysis on Chiralpak IE-3 at rt, (Hexane:iPrOH = 98:2, 0.5 mL/min), by comparison with an independently prepared racemic sample (see below).

Racemic sample:

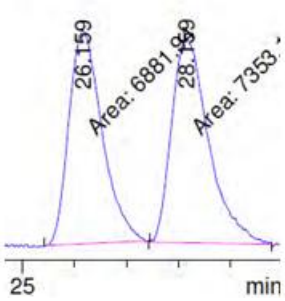

Signal 3: DAD1 C, Sig=210,8 Ref=360,100

Peak #	RetTime [min]	Type	Width [min]	Area [mAU*s]	Height [mAU]	Area %
1	26.159	MM	0.7410	6881.93848	154.79091	48.3449
2	28.159	MM	0.8265	7353.16162	148.28255	51.6551
Totals :				1.42351e4	303.07346	

Using **(*S,R,R*)-L2** as ligand (from ***E*-1b**, 94.3:5.7 er, 85% yield):

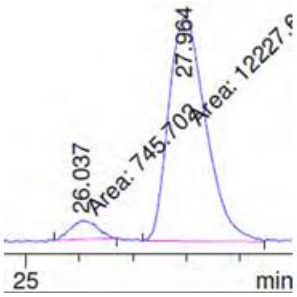

Signal 3: DAD1 C, Sig=210,8 Ref=360,100

Peak #	RetTime [min]	Type	Width [min]	Area [mAU*s]	Height [mAU]	Area %
1	26.037	MM	0.5831	745.70197	21.31582	5.7480
2	27.964	MM	0.8087	1.22276e4	252.00256	94.2520
Totals :				1.29733e4	273.31839	

Diethyl 3-methylene-1-(2,2,2-trifluoroethoxy)hexahydrocyclopenta[*b*]pyrrole-5,5 (1*H*)-dicarboxylate (**2h**)

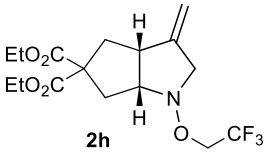

2h

Prepared following the procedure employed for the synthesis of the cycloadduct **2a**, using ***E*-1h** as precursor at 100 °C. Purification by flash chromatography (5% EtOAc/ Hexane) afforded to **2h** as a colourless oil in 54% yield. **^{1}H NMR** (300 MHz, $CDCl_3$) δ (ppm) 5.01 (s, 1H), 4.94 (s, 1H), 4.27 – 4.01 (m, 6H), 3.89 (d, *J* = 13.6 Hz, 1H), 3.82 – 3.71 (m, 1H), 3.53 (dt, *J* = 13.7, 2.5 Hz, 1H), 3.18 (q, *J* = 8.3 Hz, 1H), 2.56 – 2.25 (m, 4H), 1.30 – 1.18 (m, 6H). **^{13}C NMR** (75 MHz, $CDCl_3$) δ (ppm) 172.1 (C), 171.4 (C), 148.4 (C), 123.9 (q, *J* = 280.3 Hz, C), 108.0 (CH_2), 73.6 (CH),71.3 (q, *J* = 33.0 Hz, CH_2), 61.8 (CH_2), 61.6 (CH_2), 61.3 (C), 44.9 (CH), 40.2 (CH_2), 38.5 (CH_2), 29.9 (CH_2), 14.2 (CH_3), 14.1 (CH_3). **^{19}F NMR** (282 MHz, $CDCl_3$) δ (ppm) -74.38 (t, *J* = 9.3 Hz). **HRMS** (ESI-TOF): m/z calculated for $C_{16}H_{23}F_3NO_5^+$ [M + H]$^+$: m/z 366.1523, found 366.1522. Stereochemistry of **2h** was deduced by comparison with analogue products.

Diethyl 2-(2-(methoxyimino)ethyl)-2-(3-methylbuta-1,3-dien-1-yl)malonate (**3a**)

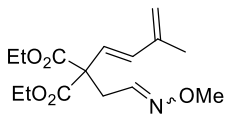

(E:Z 2 :1)-**3a**

Prepared following the procedure employed for the synthesis of the cycloadduct **2a**, using phosphite **L1** as ligand and **(*E:Z* 2:1)-1a** as precursor. Purification by flash chromatography (3% EtOAc/ Hexane) afforded to **3a** as a colourless oil in 28% yield (*E*:*Z* ratio 2:1). **^{1}H NMR** (300 MHz, CD_3OD) δ (ppm) 7.30 (t, *J* = 6.2 Hz, 0.67H), 6.60 (t, *J* = 5.3 Hz, 0.33H), 6.30 (d, *J* = 16.4 Hz, 0.67H), 6.27 (d, *J* = 16.4 Hz, 0.33H), 6.11 (d, *J* = 16.5 Hz, 0.67H), 6.09 (d, *J* = 16.4 Hz, 0.33H), 5.11 – 5.07 (m, 1H), 5.06 – 5.02 (m, 1H), 4.30 – 4.14 (m, 4H), 3.87 (s, 1H), 3.77 (s, 2H), 3.07 (d, *J* = 5.3 Hz, 0.66H), 2.92 (d, *J* = 6.3 Hz, 1.34H), 1.89 (s, 3H), 1.28 (t, *J* = 7.1 Hz, 6H). **^{13}C NMR** (75 MHz,CD_3OD) δ (ppm) 171.0 (C), 170.9 (C), 147.6 (CH), 147.6 (CH), 142.5 (C), 142.5 (C), 136.2 (CH), 136.1 (CH), 126.7 (CH), 126.5 (CH), 118.8 (CH_2), 118.6 (CH_2), 63.1 (CH_2), 63.0 (CH_2), 62.1 (CH_3), 61.8 (CH_3), 59.5 (C), 58.7 (C), 36.2 (CH_2), 31.6 (CH_2), 18.5 (CH_3), 14.3 (CH_3), 14.3 (CH_3). **HRMS** (ESI-TOF): m/z calculated for $C_{15}H_{24}NO_5^+$ [M + H]$^+$: m/z 298.1649, found 298.1647.

Diethyl 2-((*E*)-3-methylbuta-1,3-dien-1-yl)-2-((*E*)-2-((2,2,2-trifluoroethoxy)imino) ethyl)malonate (**3h**)

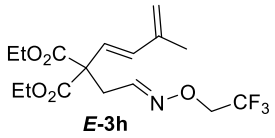

***E*-3h**

Prepared following the procedure employed for the synthesis of the cycloadduct **2a**, using phosphite **L1** as ligand and ***E*-1h** as precursor. Purification by flash chromatography (3% EtOAc/ Hexane) afforded to **3h** as a colourless oil in 74% yield. **^{1}H NMR** (300 MHz, $CDCl_3$) δ (ppm) 7.44 (t, *J* = 6.2 Hz, 1H), 6.36 – 5.98 (m, 2H), 5.05 (s, 1H), 4.99 (s, 1H), 4.33 (q, *J* = 8.6 Hz, 2H), 4.22 (q, *J* = 7.2 Hz, 4H), 2.95 (d, *J* = 6.2 Hz, 2H), 1.87 (s, 3H), 1.26 (t, *J* = 7.1 Hz, 6H). **^{13}C NMR** (75 MHz, $CDCl_3$) δ (ppm) 169.6 (C), 149.3 (CH), 141.3 (C), 135.3 (CH), 125.1 (CH), 123.8 (q, *J* = 280.3 Hz, C), 118.4 (CH_2), 70.7 (q, *J* = 34.0 Hz, CH_2), 62.1 (CH_2), 58.0 (C), 35.2 (CH_2), 18.5 (CH_3), 14.1 (CH_3). **^{19}F NMR** (282 MHz, $CDCl_3$) δ -74.46 (t, *J* = 9.2 Hz). **HRMS** (ESI-TOF): m/z calculated for $C_{16}H_{23}F_3NO_5^+$ $[M + H]^+$: m/z calculated for 366.1523, found 366.1525.

Diethyl 2-(2-(methoxyimino)ethyl)-2-(2-methylenebut-3-en-1-yl)malonate (**4a**)

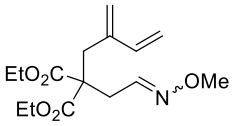

(E:Z 1:2.3)-**4a**

Prepared following the procedure employed for the synthesis of the cycloadduct **2a**, using ***E*-1a** as precursor. NMR crude showed **4a** in *E*:*Z* ratio 1:0. Purification by flash chromatography (5% EtOAc/ Hexane) afforded to **4a** as a colourless oil in 35% yield (*E*:*Z* ratio 1:2.3). **^{1}H NMR** (300 MHz, $CDCl_3$) δ (ppm) 7.33 (t, *J* = 6.2 Hz, 0.3H), 6.68 (t, *J* = 5.2 Hz, 0.7H), 6.29 (dd, *J* = 17.5, 11.0 Hz, 1H), 5.26 (d, *J* = 17.5 Hz, 0.3H), 5.24 (d, *J* = 17.9 Hz, 0.7H), 5.20 (s, 1H), 5.04 (d, *J* = 11.0 Hz, 1H), 5.04 (s, 0.3H), 4.97 (s, 0.7H), 4.26 – 4.05 (m, 4H), 3.85 (s, 2.1H), 3.79 (s, 0.9H), 2.92 – 2.91 (m,0.6H), 2.90 (s, 1.4H), 2.87 (d, *J* = 5.2 Hz, 1.4H), 2.73 (d, *J* = 6.2 Hz, 0.6H) , 1.25 (t, *J* = 7.1 Hz, 6H). **^{13}C NMR** (75 MHz, $CDCl_3$) δ (ppm) 170.6 (C), 170.5 (C), 147.1 (C), 146.9 (C), 141.1 (C), 140.9 (C), 139.0 (CH), 138.9 (CH), 120.0 (CH_2), 114.3 (CH_2), 61.9 (CH_2), 61.8 (CH_2), 61.7 (CH_3), 61.6 (CH_3), 56.6 (C), 55.7 (C), 34.4 (CH_2), 34.0 (CH_2), 32.9 (CH_2), 29.3 (CH_2), 14.1 (CH_3). **HRMS** (ESI-TOF): m/z calculated for $C_{15}H_{24}NO_5^+$ $[M + H]^+$: m/z 298.1649, found 298.1647.

Diethyl 2-(2-(methoxyimino)ethyl)-2-(2-(methylene-*d*$_2$)but-3-en-1-yl-1,1-*d*$_2$)malonate (**d$_4$-4a**)

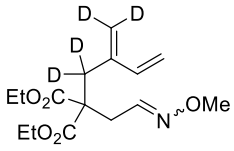

d$_4$-4a
(E:Z 4:1)

Prepared following the procedure employed for the synthesis of the cycloadduct **2a**, using ***E*-d$_4$-1a** as starting material. Compound **d$_4$-4a** was isolated as a colourless oil in 33% yield, *E*:*Z* ratio 1:0. Purification by flash chromatography (3% EtOAc/ Hexane). Characterized as a *E*:*Z* mixture 4:1. **^{1}H NMR** (500 MHz, CD_3OD) δ (ppm) 7.33 (t, *J* = 6.2 Hz, 0.8H), 6.69 (t, *J* = 5.2 Hz, 0.2H), 6.35 (dd, *J* = 17.6, 11.0 Hz, 0.8H), 6.35 (dd, *J* = 17.6, 11.0 Hz, 0.2H), 5.27 (dd, *J* = 17.6, 0.9 Hz, 0.8H), 5.25 (dd, *J* = 17.6, 0.9 Hz, 0.2H), 5.06 (dd, *J* = 10.9, 0.9 Hz, 0.8H), 5.06 (dd, *J* = 11.0, 0.9 Hz, 0.2H), 4.24 – 4.09 (m, 4H), 3.84 (s, 0.5H), 3.77 (s, 2.5H), 2.83 (d, *J* = 5.2 Hz, 0.4H), 2.70 (d, *J* = 6.2 Hz, 1.6H), 1.26 (t, *J* = 7.2 Hz, 1.2H), 1.26 (t, *J* = 7.1 Hz, 4.8H). **^{2}H NMR** (77 MHz, CD_3OD) δ (ppm) 5.21 (s, 1H), 5.12 – 4.98 (m, 1H), 2.94 – 2.78 (m, 2H). **^{13}C NMR** (126 MHz, CD_3OD) δ (ppm) 171.8 (C), 171.7 (C) 148.1 (CH), 148.0 (CH), 142.5 (C), 142.3 (C), 140.2 (CH), 140.1 (CH), 114.6 (CH_2), 114.6 (CH_2), 62.9 (CH_2), 62.8 (CH_2), 62.1 (CH_3), 61.8 (CH_3), 57.7 (C), 56.7 (C), 33. (CH_2), 30.8 (CH_2), 14.3 (CH_3). **HRMS** (ESI-TOF): m/z calculated for $C_{15}H_{20}D_4NO_5^+$ $[M+H]^+$: m/z 302.1900, found 302.1900.

Dimethyl (*E*)-2-(2-(methoxyimino)propyl)-2-(2-methylenebut-3-en-1-il)malonate (***E*-4d**)

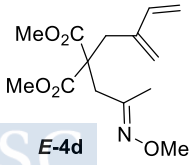

***E*-4d**

Prepared following the procedure employed for the synthesis of the cycloadduct **2a**, using ***E*-1d** as starting material. Purification by flash chromatography (3% EtOAc/ Hexane) afforded to ***E*-4d** as a colourless oil in 60% yield. **^{1}H NMR** (300 MHz, $CDCl_3$) δ (ppm) 6.29 (dd, *J* = 17.8, 10.9 Hz, 1H), 5.23 – 5.13 (m, 2H), 5.00 (d, *J* = 11.0 Hz, 1H), 4.92 (s, 1H), 3.78 (s, 3H), 3.68 (s, 6H), 3.11 (d, *J* = 0.9 Hz, 2H), 2.80 (s, 2H), 1.74 (s, 3H). **^{13}C NMR** (75 MHz, $CDCl_3$) δ (ppm) 171.3(C), 152.9 (CH), 142.1 (C), 139.2 (C), 119.6 (CH_2), 113.9 (CH_2), 61.6 (CH_3), 55.9 (C), 52.6 (CH_3), 37.4 (CH_2), 32.7 (CH_2), 29.8

(CH_2), 15.4 (CH_3). **HRMS** (ESI-TOF): m/z calculated for $C_{14}H_{22}NO_5^+$ $[M+H]^+$: m/z 284.1492, found 284.1491.

Diethyl 2-(2-(cyclopropylidene-d_4)ethyl)-2-(2-oxoethyl)malonate (**d_4-7a**)

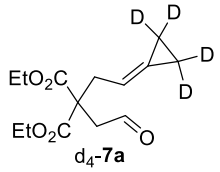

Compound **d_4-7a** was prepared following the procedure employed for the synthesis of intermediate **7a**, using vinyl tosylate **d_4-6** as substrate. Purification by flash chromatography (20-30% EtOAc/ Hexane) afforded to **d_4-7a** in 83% yield as a colourless oil. **^{1}H NMR** (300 MHz, $CDCl_3$) δ (ppm) 9.66 (s, 1H), 5.60 (t, *J* = 7.5 Hz, 1H), 4.18 (q, *J* = 7.1 Hz, 4H), 2.88 – 2.82 (m, 4H), 1.23 (t, *J* = 7.1 Hz, 6H). **^{2}H NMR** (46 MHz, $CDCl_3$) δ (ppm) 1.02 (m, 4H). **^{13}C NMR** (75 MHz, $CDCl_3$) δ (ppm) 199.2 (CH), 170.3 (C), 127.7 (C), 111.9 (CH), 61.9 (CH_2), 55.1 (C), 46.3 (CH_2), 36.7 (CH_2), 14.1 (CH_3). **HRMS** (ESI-TOF): m/z calculated for $C_{14}H_{16}D_4NaO_5^+$ $[M+Na]^+$: m/z 295.1454; found 295.1449.

Dimethyl 2-(2-cyclopropylideneethyl)-2-(3-oxopropyl)malonate (**7c**)

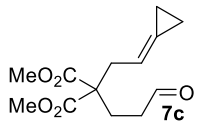

Compound **7c** was prepared following the procedure employed for the synthesis of intermediate **7a**, using dimethyl 2-(3,3-dimethoxypropyl)malonate as substrate. After liquid-liquid extraction, no chromatography column was needed. Compound **7c** was obtained in 90% yield as a colourless oil. **^{1}H NMR** (300 MHz, $CDCl_3$) δ (ppm) 9.67 (t, *J* = 1.3 Hz, 1H), 5.64 – 5.40 (m, 1H), 3.67 (s, 6H), 2.74 (dd, *J* = 7.4, 1.3 Hz, 2H), 2.43 (ddd, *J* = 8.5, 7.5, 1.3 Hz, 2H), 2.14 (dd, *J* = 8.8, 6.8 Hz, 2H), 1.27 – 0.81 (m, 4H). **^{13}C NMR** (75 MHz, $CDCl_3$) δ (ppm) 201.0 (C), 171.6 (C), 127.1 (C), 111.7 (CH), 57.1 (C), 52.6 (CH_3), 39.4 (CH_2), 36.2 (CH_2), 25.2 (CH_2), 3.1 (CH_2), 2.0 (CH_2).

Dimethyl 2-(2-cyclopropylideneethyl)-2-(2-oxopropyl)malonate (**9a**)

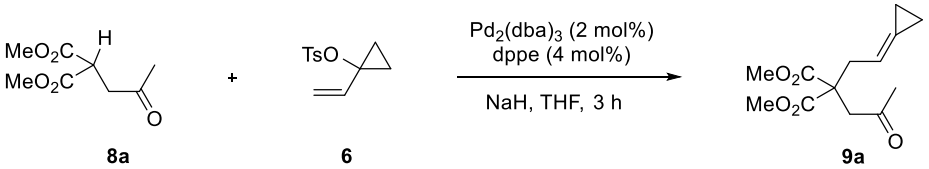

In a round bottom flask, a solution of $Pd_2(dba)_3$ (222 mg, 224 μmol, 0.02 equiv.), 1,2-bis(diphenylphosphino)ethane (193 mg, 484 μmol, 0.04 equiv.) and 1-vinylcyclopropyl tosylate **6** (3.74 g, 15.7 mmol, 1.3 equiv.) in dry THF (20 mL) was stirred at rt for 15 min.

In a separate round bottom flask, a solution of dimethyl 2-(2, 2-dimethoxyethyl)malonate **8a** (3.00 g, 12.1 mmol, 1.0 equiv.) in dry THF (25 mL) was added carefully to a suspension of NaH (532 mg, 13.3 mmol, 1.1 equiv., 60% in mineral oil) in dry THF (100 mL), at 0 °C and the mixture was stirred for 30 min at rt. Then, the solution of vinyl tosylate (**6**) was added dropwise *via cannula*. The resulting mixture was stirred for 3 h, poured into water and extracted with Et_2O (3x60 mL). The organic layers were dried, filtered and concentrated to give a crude oily residue that was purified by flash chromatography (10% EtOAc/Hexane), to yield the dimethyl 2-(2-cyclopropylideneethyl)-2-(2-oxopropyl)malonate, **9a**, as a pale-yellow oil (2.20 g, 8.50 mmol, 70% yield). **^{1}H NMR** (300 MHz, $CDCl_3$) δ (ppm) 5.72 – 5.44 (m, 1H), 3.73 (s, 6H), 3.10 (s, 2H), 3.00 – 2.70 (m, 2H), 2.11 (s, 3H), 0.97 – 0.84 (m, 2H). **^{13}C NMR** (75 MHz, $CDCl_3$) δ (ppm) 205.2 (C), 171.1 (C), 127.1 (C), 112.3 (CH), 55.5 (C), 52.8 (CH_3), 46.0 (CH_2), 36.1 (CH_2), 30.3 (CH_3), 3.1 (CH_2), 1.9 (CH_2). **HRMS** (ESI-TOF): m/z calculated for $C_{13}H_{18}NaO_5^+$ $[M+Na]^+$: m/z 277.1052, found 277.1047.

Dimethyl 2-(2-cyclopropylideneethyl)-2-(3-oxobutyl)malonate (**9b**)

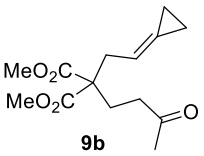

Compound **9b** was prepared following the procedure employed for the synthesis of compound **9a**, using dimethyl 2-(3-oxobutyl)malonate as substrate. Isolated as a white solid in 75% yield. Purification by flash chromatography (20-40% EtOAc/ Hexane). Spectroscopic data of **9b** agrees with that reported in the literature.[40] **^{1}H NMR** (300 MHz, $CDCl_3$) δ (ppm) **^{1}H NMR** (300 MHz, $CDCl_3$) δ (ppm) 5.57 – 5.45 (m, 1H), 3.65 – 3.60 (m, 6H), 2.69 (d, J = 7.5 Hz, 2H), 2.44 – 2.33 (m, 2H), 2.10 – 2.01 (m, 5H), 1.04 – 0.86 (m, 4H).

***N*-(2-Cyclopropylideneethyl)-4-methyl-*N*-(3-oxobutyl)benzenesulfonamide** (**9c**)

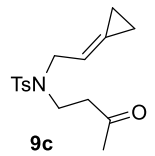

Compound **9c** was prepared following the procedure employed for the synthesis of precursor **9a**, using 4-methyl-*N*-(3-oxobutyl) benzenesulfonamide as starting material. Isolated as a white solid in 85% yield. Purification by flash chromatography (10-20% EtOAc/ Hexane).**^{1}H NMR** (300 MHz, $CDCl_3$) δ (ppm) 7.66 (d, *J* = 7.8 Hz, 2H), 7.27 (d, *J* = 7.9 Hz, 2H), 5.61 – 5.40 (m, 1H), 3.89 (d, *J* = 6.8 Hz, 2H), 3.29 (t, *J* = 7.4 Hz, 2H), 2.76 (t, *J* = 7.4 Hz, 2H), 2.40 (s, 3H), 2.10 (s, 3H), 1.33 – 0.79 (m, 4H). **^{13}C NMR** (75 MHz, $CDCl_3$) δ (ppm) 206.8 (C), 143.2 (C), 136.6 (C), 129.6 (CH), 127.7 (C), 127.1 (CH), 112.7 (CH), 50.3 (CH_2), 43.5 (CH_2), 42.2 (CH_2), 30.2 (CH_3), 21.4 (CH_3), 2.5 (CH_2), 1.7 (CH_2). **HRMS** (ESI-TOF): m/z calculated for $C_{16}H_{22}NO_3S^+$ $[M+H]^+$: m/z 308.1315, found 308.1316.

Compounds 9e-9l: Substrates **9e-9l** are known compounds and were synthesized following reported procedures.[40]

Dimethyl 2-(2-cyclopropylideneethyl)-2-(4-oxopentyl)malonate (**9n**)

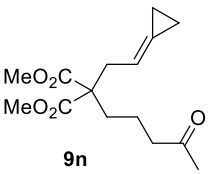

Compound **9n** was prepared following the procedure employed for the synthesis of precursor **9a**, using dimethyl 2-(4-oxopentyl)malonate as starting material. Isolated as a pale-yellow oil in 48% yield. Purification by flash chromatography (10-20% EtOAc/ Hexane). **^{1}H-NMR** (300 MHz, $CDCl_3$) δ (ppm) 5.59 – 5.46 (m, 1H), 3.65 (s, 6H), 2.74 (d, J = 7.4 Hz, 2H), 2.36 (t, J = 7.1 Hz, 2H), 2.06 (s, 3H), 1.84 – 1.75 (m, 2H), 1.61 – 1.34 (m, 2H), 1.06 – 0.87 (m, 3H). **^{13}C-NMR** (75 MHz, $CDCl_3$) δ (ppm) 207.9 (C), 171.6 (C), 126.2 (C), 111.7 (CH), 57.6 (C), 52.2 (CH_3), 43.4 (CH_2), 34.9 (CH_2), 31.7 (CH_2), 29.7 (CH_3), 18.2 (CH_2), 2.8 (CH_2), 1.6 (CH_2). **HRMS** (ESI-TOF): m/z calculated for $C_{15}H_{23}O_5$ $[M+H]^+$: m/z 283.1540, found 283.1538.

Dimethyl 2-(2-cyclopropylidenepropyl)-2-(3-oxobutyl)malonate (**9o**)

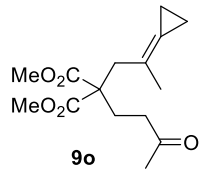

Compound **9o** was prepared following the procedure employed for the synthesis of precursor **9a**, using (2-cyclopropylidenepropoxy)benzene instead vinyl tosylated **6**, and dimethyl 2-(3-oxobutyl)malonate as starting material. Isolated as a pale-yellow oil in 48% yield. Purification by flash chromatography (10-20% EtOAc/ Hexane). **^{1}H NMR** (300 MHz, $CDCl_3$) δ (ppm) 3.70 (s, 3H), 3.69 (s, 3H), 2.84 (s, 2H), 2.41 (t, *J* = 7.5 Hz, 2H), 2.25 – 1.91 (m, 5H), 1.68 (s, 3H), 1.10 – 0.89 (m, 4H). **^{13}C NMR** (75 MHz, $CDCl_3$) δ (ppm) 207.2 (C), 172.0 (C), 121.7 (C), 119.1 (C), 56.4 (C), 52.4 (CH_3), 40.3 (CH_2), 38.9 (CH_2), 29.8 (CH_3), 26.5 (CH_2), 21.2 (CH_3), 3.6 (CH_2), 2.7 (CH_2). **HRMS** (ESI-TOF): m/z calculated for $C_{15}H_{23}O_5^+$ $[M+H]^+$: m/z 283.1540, found 283.1543.

Dimethyl 2-(2-cyclopropylideneethyl)-2-(3-oxo-3-phenylpropyl)malonate (**9p**)

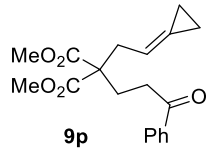

Compound **9p** was prepared following the procedure employed for the synthesis of precursor **9a**, using dimethyl 2-(3-oxo-3-phenylpropyl)malonate as starting material. Isolated as a pale-yellow oil in 26% yield. Purification by flash chromatography (10-20% EtOAc/ Hexane). **^{1}H NMR** (300 MHz, $CDCl_3$) δ (ppm) 7.95 – 7.89 (m, 2H), 7.59 – 7.52 (m, 1H), 7.44 (dd, *J* = 8.2, 6.8 Hz, 2H), 5.73 – 5.55 (m, 1H), 3.71 (s, 6H), 3.05 – 2.92 (m, 2H), 2.85 (dt, *J* = 7.4, 1.3 Hz, 2H), 2.31 (dd, *J* = 8.8, 6.8 Hz, 2H), 1.22 – 0.89 (m, 4H). **^{13}C NMR** (75 MHz, $CDCl_3$) δ (ppm) 199.0 (C), 171.8 (C), 136.9

[40] Verdugo, F.; da Concepción, E.; Rodiño, R.; Calvelo, M.; Mascareñas, J.L.; López, F. Pd–Catalyzed (3 + 2) Heterocycloadditions between Alkylidenecyclopropanes and Carbonyls: Straightforward Assembly of Highly Substituted Tetrahydrofurans. *ACS. Catal.* **2020**, *10*, 7710–7718.

(C), 133.2 (CH), 128.7 (CH), 128.1 (CH), 126.9 (C), 111.9 (CH), 57.3 (C), 52.5 (CH_3), 36.5 (CH_2), 33.9 (CH_2), 27.4 (CH_2), 3.1 (CH_2), 1.9 (CH_2). **HRMS** (ESI-TOF): m/z calculated for $C_{19}H_{23}O_5^+$ $[M+H]^+$: m/z 331.1540, found 331.1539.

Dimethyl 2-(2-cyclopropylideneethyl)-2-(4,4,4-trifluoro-3-oxobutyl)malonate (**9q**)

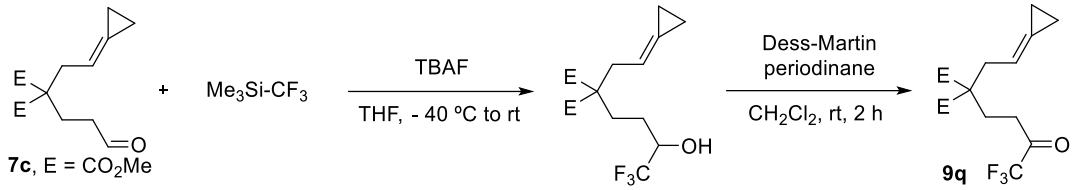

Trifluorotrimethylsilane (190 µL, 1.30 mmol, 2.2 equiv.) was added dropwise to a solution of aldehyde **7c** (150.0 mg, 590 µmol, 1.0 equiv.) in THF (2.0 mL) at -40 ºC. Then TBAF (29.0 µL, 29.0 µmol, 0.05 equiv.) was added dropwise and the mixture was stirred at rt for 4 h. After quenching HCl (2 N), the biphasic mixture was stirred until full conversion of the silyl ether was observed by TLC. The mixture was extracted with Et_2O (3x1 mL), dried and concentrated to afford an oily residue, that was dissolved in CH_2Cl_2 (10.0 mL) and added by syringe over a solution of Dess-Martin periodinane (265 mg, 630 µmol, 1.1 equiv.) in CH_2Cl_2 (5.0 mL). After stirring for 2 h, the reaction was quenched by addition of $NaHCO_{3\,(sat)}$ (5 mL) and $Na_2S_2O_{3\,(sat)}$ (5 mL). After stirring for another 15 min, the layers were separated, and the aqueous layer was extracted with CH_2Cl_2 (3x5 mL). The combined organic extracts were dried over $MgSO_4$, filtered, and concentrated. The residue was purified by column chromatography (15% EtOAc/Hexane), to yield the dimethyl 2-(2-cyclopropylideneethyl)-2-(4,4,4-trifluoro-3-oxobutyl)malonate **9q** as a pale-yellow oil (139 mg, 430 µmol, 72% yield). **^{1}H NMR** (300 MHz, $CDCl_3$) δ (ppm) 5.71 – 5.50 (m, 1H), 3.72 (s, 6H), 2.81 (t, J = 7.7 Hz, 4H), 2.20 (t, J = 7.5 Hz, 2H), 1.17 – 0.91 (m, 4H). **^{13}C NMR** (75 MHz, $CDCl_3$) δ (ppm) 190.7 (q, *J* = 35.1 Hz, C), 171.3 (C), 127.5 (C), 115.6 (q, *J* = 291.8 Hz, C), 111.5 (CH), 56.7 (C), 52.7 (CH_3), 36.6 (CH_2), 32.1 (CH_2), 25.6 (CH_2), 3.1 (CH_2), 1.9 (CH_2). **HRMS** (ESI-TOF): m/z calculated for $C_{14}H_{18}F_3O_5^+$ $[M+H]^+$: m/z 323.1101, found 323.1105.

***O*-(2, 2, 2-Trifluoroethyl)hydroxylammonium chloride** (**12**)[138, 139]

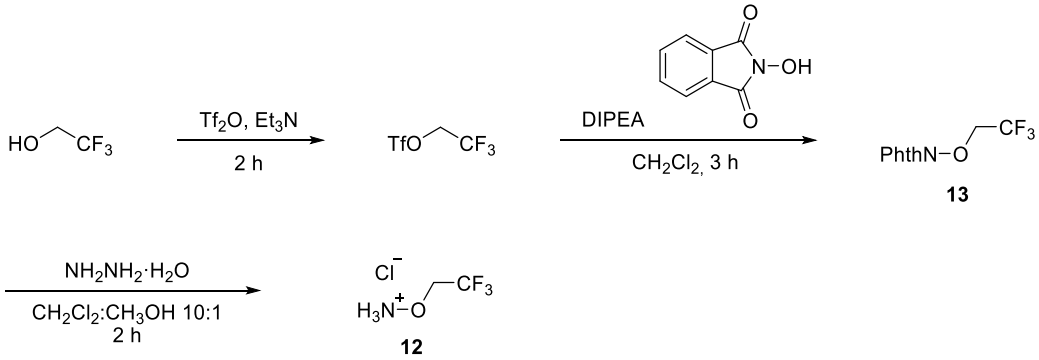

In a round-bottom flask, trifluoroethanol (1.50 mL, 20.0 mmol, 1.0 equiv.) was added dropwise over triflic anhydride (3.40 mL, 20.0 mmol, 1.0 equiv.). Subsequently, Et_3N (2.80 mL, 20.0 mmol, 1.0 equiv.) was added and the reaction was stirred at rt for 2 h, monitoring its progress by GC-MS. The triflated trifluoroethanol was purified by short path distillation under vacuum at -78 °C (4.12 g, 17.8 mmol, 89% yield).[138]

DIPEA (6.80 mL, 39.0 µmol, 2.0 equiv.) was added over a solution of *N*-hydroxyphthalimide (3.10 g, 19.0 mmol, 1.1 equiv.) in dry CH_2Cl_2 (22 mL). After stirring for 5 min, the triflate (4.10 g, 17.8 mmol, 1.0 equiv.) was added, and the mixture was stirred for 2 h (followed by GC-MS). Ice water (50 mL) was added and CH_2Cl_2 (2x30 mL) was used for extractions. The combined organic layers were dried, filtered and concentrated. The resulting crystals were finally washed with ice water and hexane.

[138] Nguyen, T. B.; Martel, A.; Dhal, R.; Dujardin, G. N-(β,β-Difluorovinyl)oxazolidin-2-ones: First Synthesis and Application in [3+2]- and [4+2]-Cycloaddition-Type Reactions. *Synlett*, **2009**, *15*, 2492-2496.

The product **13** was afforded as a white solid (2.90 g, 11.7 mmol, 66% yield). In the final step, hydrazine (591 μL, 12.2 mmol, 2.0 equiv., 65% w/w) was added dropwise over a solution of the phthalimide derivative **13** (1.50 g, 6.10 mmol, 1.0 equiv.) in CH_2Cl_2 (32.2 mL) and MeOH (3.2 mL). The resulting mixture was stirred for 2 h, filtered and washed with $NaHCO_3$ (35 mL). The hydroxylamine was extracted from the aqueous layer with CH_2Cl_2 (2x30 mL). The combined organic layers were dried, filtered and concentrated. HCl(c) in Et_2O (1 mL) and EtOH (8 mL), were added dropwise to the remaining residue, and the solvent was removed under reduced pressure. The resulting solid was washed with Et_2O, to yield **12** as white crystals (756 mg, 5.00 mmol, 82% yield). Spectroscopic data of **12** agrees with that reported in the literature.[139] **^{1}H NMR** (300 MHz, DMSO-d_6) δ (ppm) 7.83 (m, 2H), 4.53 (br. s, 3H). **^{19}F NMR** (282 MHz, DMSO-d_6) δ (ppm) -67.32 (t, J = 8.9 Hz).

Compounds 15a-15d: Imines **15a**[140], **15b**[141], **15c**[142], **15d**[143] are known compounds and were synthesized following their corresponding reported procedures.

Benzo[*e*][1,2,3]oxathiazine 2,2-dioxide (**15e**)[144]

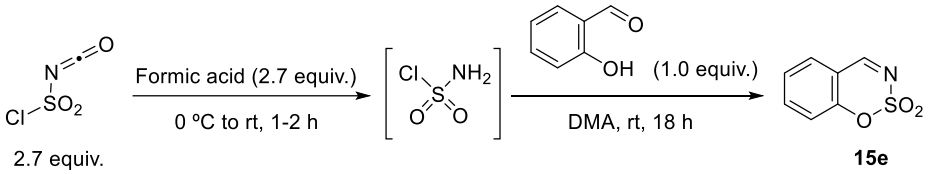

In a dry Schlenk tube under Ar, formic acid (1.10 mL, 28.0 mmol, 2.7 equiv.) was added dropwise to neat chlorosulfonyl isocyanate (2.40 mL, 28.0 mmol, 2.7 equiv.) at 0 °C, with vigorous stirring. Rapid gas evolution and an increase in solution viscosity were observed during the addition process. The viscous suspension was stirred at rt until gas evolution ceased (1-2 h). The resulting white solid was used in the following step immediately, assuming full conversion.

A solution of this freshly prepared sulfamoyl chloride dissolved in dry DMA (20 mL) was carefully added in small portions to a solution of salicylaldehyde (920 mg, 7.35 mmol, 1.0 equiv.) in dry DMA (44 mL), at rt. The mixture was stirred for 18 h under argon, carefully quenched with water (64 mL) and extracted with CH_2Cl_2 (3x 30 mL). The combined organic layers were washed with $NaHCO_{3(sat)}$ (50 mL), dried and concentrated under vacuum. The product was isolated by flash chromatography (a mixture of 15% EtOAc/ 2% CH_2Cl_2 / Hexane was used to remove the remaining DMA; then a mixture of 40% EtOAc/ Hexane to elute the product) to yield **15e** as a white solid (1.10 g, 5.90 mmol, 80% yield). Spectroscopic data of **15e** agrees with that reported in the literature. **^{1}H NMR** (300 MHz, $CDCl_3$) δ (ppm) 8.67 (s, 1H), 7.83 – 7.71 (m, 1H), 7.68 (dd, J = 7.9, 1.7 Hz, 1H), 7.43 (t, J = 7.6 Hz, 1H), 7.31 (d, J = 8.4 Hz, 1H).

---

[139] Ishikawa, T.; Kamiyama, K.; Matsunaga, N.; Tawada, H.; Iizawa, Y.; Okonogi, K.; Miyake, A. Studies on Anti-MRSA Parenteral Cephalosporins II. Synthesis and Antibacterial Activity of 7β-[2-(5-Amino-1, 2, 4-thiadiazol-3-yl)-2(Z)-alkoxyiminoacetamido]-3-(substituted imidazo[1, 2-b]pyridazinium-1-yl)methyl-3-cephem-4-carboxylates and Related Compounds. *J Antibiot.*, **2000**, *53*, 10, 1071-1085.

[140] Pilgrim, B.S.; Gatland, A.E.; Esteves; C.H.A., McTernan, C.T.; Jones, G.R.; Tatton, M.R.; Procopiou, P.A.; Donohoe, T.J. Palladium-catalyzed enolate arylation as a key C–C bond-forming reaction for the synthesis of isoquinolines. *Org. Biomol. Chem.* **2016**, *14*, 1065-1090.

[141] Mayerhofer, V.J.; Lippolis, M.; Teskey, C.J. Dual-Catalysed Intermolecular Reductive Coupling of Dienes and Ketones. *Angew. Chem. Int. Ed.* **2024**, *63*, e202314870.

[142] Morales, S.; Guijarro, F. G.; Garcia Ruano, J. L.; Cid, M. B. A General Aminocatalytic Method for the Synthesis of Aldimines. *J. Am. Chem. Soc.* **2014**, *136*, 1082-1089.

[143] Cowen, B.J.; Saunders, L.B.; Miller, S.J. Pyridylalanine (Pal)-Peptide Catalyzed Enantioselective Allenoate Additions to N-Acyl Imines. *J. Am. Chem. Soc.* **2009**, *131*, 6105–6107.

[144] Wang, C.; Li, Y.; Wu, Y.; Wang, Q.; Shi, W.; Yuan, C.; Zhou, L.; Xiao, Y.; Guo, H.; Enantioselective Construction of Tetrahydroquinazoline Motifs *via* Palladium-Catalyzed [4 + 2] Cycloaddition of Vinyl Benzoxazinones with Sulfamate-Derived Cyclic Imines. *Org. Lett.* **2018**, *20*, 10, 2880–2883.

Compound 15f: Imine **15f** is a known compound and was synthesized following reported procedures.[145]

2,3,6,7-Tetrahydro-1*H*,5*H*-[1,2,3] oxathiazino[6,5-*f*] pyrido[3,2,1-*ij*] quinoline 11,11-dioxide (**15g**)

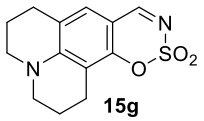

15g

Compound **15g** was prepared following the procedure employed for the synthesis of precursor **15e**, using 8-hydroxy-2,3,6,7-tetrahydro-1*H*,5*H*-pyrido[3,2,1-*ij*]quinoline-9-carbaldehyde as starting material. Compound **15g** was isolated as a yellow solid in 51% yield, following the flash chromatography conditions used for compound **15e**. **^{1}H NMR** (300 MHz, $CDCl_3$) δ (ppm) 8.11 (s, 1H), 6.92 (s, 1H), 3.36 (dt, *J* = 6.9, 4.3 Hz, 4H), 2.73 (dt, *J* = 13.6, 6.4 Hz, 4H), 2.21 – 1.65 (m, 4H). **^{13}C NMR** (75 MHz, $CDCl_3$): δ (ppm) 165.2 (CH), 152.4 (C), 150.6 (C), 128.8 (CH), 118.4 (C), 107.9 (C), 104.7 (C), 50.6 (CH_2), 50.1 (CH_2), 27.2 (CH_2), 20.9 (CH_2), 19.9 (CH_2), 19.6 (CH_2). **HRMS** (APCI-TOF): m/z calculated for $C_{13}H_{15}N_2O_3S^+$ $[M + H]^+$: m/z 279.0799, found 279.0799.

Compounds 15h-15u: Imines **15h**[145], **15i**[146], **15j**[142], **15k**[142], **15l**[147], **15m**[142], **15n**[148], **15o**[149], **15p**[150], **15q**[151], **15r**[149], **15s**[152], **15t**[152], **15u**[153] are known compounds and were synthesized following reported procedures.

Dimethyl 2-((2-methylene-5,5-dioxido-1,2,3,10*b*-tetrahydrobenzo[*e*]pyrrolo[1,2-*c*][1,2,3]oxathiazin-1-yl)methyl)-2-(3-oxobutyl)malonate (**16be+16be'**)

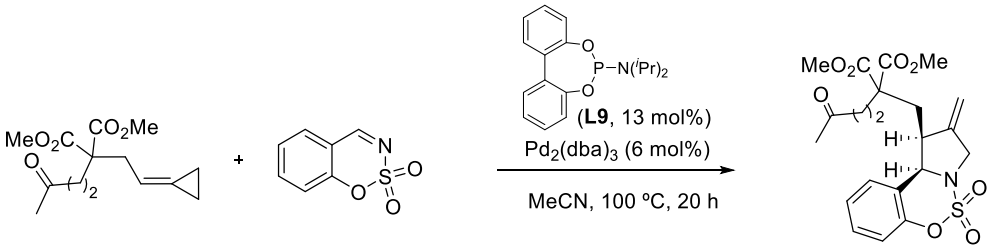

9b **15e** **16be + 16be'**

Prepared following general procedure for catalytic reactions (see *Methodology*, page 57), using $Pd_2(dba)_3$ (4.40 mg, 4.80 μmol, 6 mol%), phosphoramidite **L9** (3.30 mg, 10.4 μmol, 13 mol%), ACP precursor **9b** (21.5 mg, 80.0 μmol, 1.0 equiv.) and imine **15e** (17.6 mg, 96.0 μmol, 1.2 equiv.) in dry acetonitrile (1.6 mL). The reaction crude was purified by flash chromatography (25-40% EtOAc/Hexane) to afford dimethyl 2-((2-methylene-5,5-dioxido-1,2,3,10*b*-tetrahydrobenzo[*e*]pyrrolo[1,2-

145 De Munck, L.; Vila, C.; Munoz, M. C.; Pedro, J. R. Catalytic Enantioselective Aza-Reformatsky Reaction with Cyclic Imines. *Chem. Eur. J.* **2016**, *22*, 49, 17590-17594.

146 Zhou, Y. G.; Li, Y.; Meng, F. J.; Shi, L.; Zhao, Z. G. Synthesis of chiral seven-membered cyclic sulfonamides through palladium-catalyzed arylation of cyclic imines. *Org. Chem. Front.* **2019**, *6*, 1572-1576.

147 Hasaninejad, A.; Zare, A.; Sharghi, H.; Shekouhy, M. P2O5/SiO2 an efficient, green and heterogeneous catalytic System for the solvent-free synthesis of *N*-sulfonyl imines. *ARKIVOC,* **2008***, 11*, 64–74.

148 Padwa, A.; Harris, J. M. A Flexible Approach toward Trisubstituted Piperidines and Indolizidines: Synthesis of 6-epi-Indolizidine 223A. *Org. Chem.* **2003**, *68*, 11, 4371–4381.

149 Wang, Y.-Q.; Yu, C.-B.; Wang, D.-W.; Wang, X.-B.; Zhou, Y.-G. Enantioselective Synthesis of Cyclic Sulfamidates via Pd-Catalyzed Hydrogenation. *Org. Lett.* **2008**, *10*, 10, 2071–2074.

150 Du Bois, J.; Brodsky, B. H.; Oxaziridine-Mediated Catalytic Hydroxylation of Unactivated 3° C-H Bonds Using Hydrogen Peroxide. *JACS* **2005**, *127*, 44, 15391-15393.

151 Quan, M.; Yang, G.; Xie, F. Grideny, I-D-; Zhang, W. Pd(II)-catalyzed asymmetric addition of arylboronic acids to cyclic *N*-sulfonyl ketimine esters and a DFT study of its mechanism. *Org. Chem. Front.*, **2015**, *2*, 398-402.

152 Trost, B. M.; Zuo, Z. Highly regio-, diastereo-, and enantioselective synthesis of tetrahydroazepines and benzo[*b*]oxepines through palladium-catalyzed [4+3] cycloaddition reactions, *Angew. Chem. Int. Ed.* **2020**, *59*, 1243.

153 Gao, X., Zhu, D., Jiang, F., Liao, J., Wang, W., Wu, Y., Zheng, L., Guo, H., Palladium-catalyzed stereoselective (3+2) cycloaddition of vinylethylene carbonates with cyclic N-sulfonyl ketimines, *Org. Biomol. Chem.*, **2021**, *19*, 4877–4881.

75a Gulías, M.; García, R.; Delgado, A.; Castedo, L.; Mascareñas, J. L. Palladium-Catalyzed [3 + 2] Intramolecular Cycloaddition of Alk-5-enylidenecyclopropanes. *J. Am. Chem. Soc.* **2006**, *128*, 2, 384–385.

d][1,2,3]oxathiazin-1-yl)methyl)-2-(3-oxobutyl)malonate (**16be+16be'**) as a pale-yellow solid (39.8 mg, 76.0 μmol, 96%, dr 1.2:1).

Dimethyl 2-(((1*S*,10*bR*)-2-methylene-5,5-dioxido-1,2,3,10*b*-tetrahydrobenzo[*e*]pyrrolo[1,2-*c*][1,2,3]oxathiazin-1-yl)methyl)-2-(3-oxobutyl)malonate (**16be**)

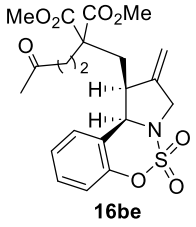

16be

Compound **16be'** was isolated from the mixture as a white solid in 52% yield. **^{1}H NMR** (500 MHz, $CDCl_3$) δ (ppm) 7.35 (td, *J* = 7.9, 1.2 Hz, 1H), 7.24 (td, *J* = 7.6, 1.2 Hz, 1H), 7.13 – 7.05 (m, 2H), 5.17 – 5.07 (m, 2H), 5.00 (d, *J* = 5.6 Hz, 1H), 4.25 (d, *J* = 12.5 Hz, 1H), 4.02 (d, *J* = 12.5 Hz, 1H), 3.65 (s, 3H), 3.63 (s, 3H), 3.25 – 3.13 (m, 1H), 2.50 – 2.33 (m, 1H), 2.31 – 2.21 (m, 1H), 2.20 – 2.12 (m, 1H), 2.10 (s, 3H), 2.07 – 1.99 (m, 1H), 1.95 (dd, *J* = 14.9, 11.3 Hz, 1H), 1.67 (dd, *J* = 14.9, 3.0 Hz, 1H). **^{13}C NMR** (126 MHz, $CDCl_3$) δ (ppm) 206.7 (C), 171.1 (C), 171.0 (C), 151.5 (C), 142.5 (C) 129.7 (CH), 127.2 (CH), 125.8 (CH), 120.2 (C), 119.5 (CH), 111.8 (CH_2), 66.2 (CH), 55.4 (C), 52.5 (CH_3), 52.1 (CH_3), 51.7 (CH_2), 45.0 (CH), 38.5 (CH_2), 30.6 (CH_2), 30.0 (CH_3), 27.2 (CH_2). **HRMS** (APCI-TOF): m/z calculated for $C_{21}H_{26}NO_8S^+$ [M + H]$^+$ m/z 452.1374, found 452.1373. Stereochemistry of **16be** was determined by nOe experiments.

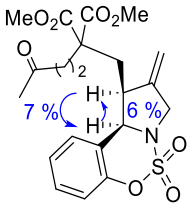

Figure 43. Significant nOe's observed for **16be**.

Enantioselectivity was determined by chiral SFC analysis on Lux i-Cellulose-5 at 40 ºC, (CO_2:MeOH = 70:30, 1 mL/min, λ=220 nm).

Racemic sample:

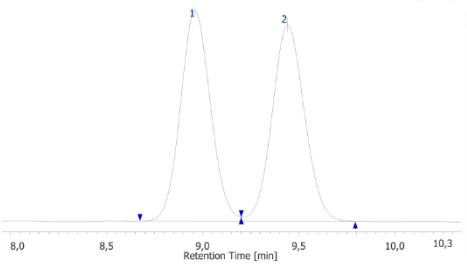

tR [min]	Area [μV·sec]	Height [μV]	Area%	Height%	Quantity	NTP
8.960	2446638	225405	49.816	51.741	N/A	15679
9.440	2464724	210240	50.184	48.259	N/A	14959

Using **(*S,R,R*)-L2** as ligand (88.3:11.7 er, 42% yield):

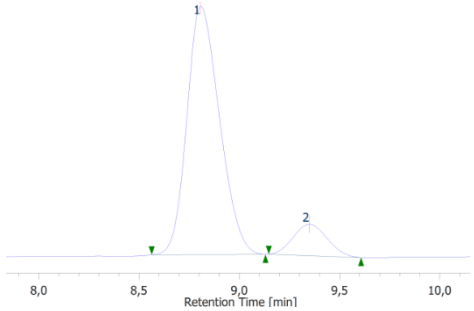

tR [min]	Area [μV·sec]	Height [μV]	Area%	Height%	Quantity	NTP
8.807	9558122	844535	88.288	88.755	N/A	13847
9.350	1267959	107004	11.712	11.245	N/A	13591

Dimethyl 2-(((1*S*,10*bS*)-2-methylene-5,5-dioxido-1,2,3,10*b*-tetrahydrobenzo[*e*]pyrrolo [1,2-*c*][1,2,3]oxathiazin-1-yl)methyl)-2-(3-oxobutyl)malonate (**16be'**)

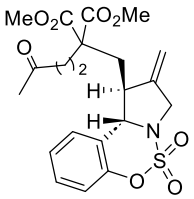

16be'

Compound **16be'** was isolated from the mixture as a white solid in 44% yield. **^{1}H NMR** (500 MHz, $CDCl_3$) δ (ppm) 7.33 – 7.27 (m, 1H), 7.25 – 7.18 (m, 2H), 6.97 (dd, *J* = 8.3, 1.0 Hz, 1H), 4.99 (s, 1H), 4.93 (s, 1H), 4.85 (s, 1H), 4.20 – 4.12 (m, 1H), 3.94 – 3.85 (m, 1H), 3.77 (s, 3H), 3.74 (s, 3H), 3.22 (t, *J* = 6.1 Hz, 1H), 2.58 – 2.48 (m, 2H), 2.37 (dd, *J* = 14.9, 7.3 Hz, 1H), 2.31 (t, *J* = 7.6 Hz, 2H), 2.22 (dd, *J* = 14.9, 5.2 Hz, 1H), 2.17 (s, 3H). **^{13}C NMR** (126 MHz, $CDCl_3$) δ (ppm) 206.7 (C), 171.4 (C), 171.2 (C), 151.0 (C), 145.4 (C), 129.7 (CH), 127.1 (CH), 125.9 (CH), 119.8 (C), 118.6 (CH), 110.6 (CH_2), 69.0 (CH) 56.4 (C), 52.7 (CH_3), 52.6 (CH_3), 51.9 (CH_2), 48.0 (CH), 38.8 (CH_2), 38.6 (CH_2), 30.1 (CH_3), 27.7 (CH_2). **HRMS** (APCI-TOF): m/z calculated for $C_{21}H_{26}NO_8S^+$ $[M + H]^+$: m/z 452.1374, found 452.1373. Stereochemistry of **16be'** was determined by nOe experiments.

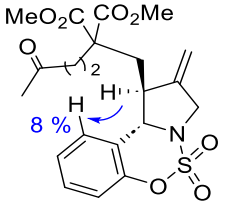

Figure 44. Significant nOe's observed for **16be'**.

Enantioselectivity was determined by chiral SFC analysis on Lux i-Cellulose-5 at 40 ºC, (CO_2:MeOH = 70:30, 1 mL/min, λ=254 nm).

Racemic sample (SFC)**:**

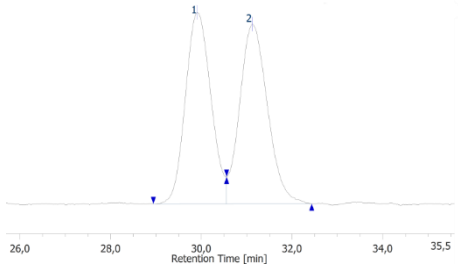

tR [min]	Area [μV·sec]	Height [μV]	Area%	Height%	Quantity	NTP
29.907	1095046	28059	49.419	51.601	N/A	13096
31.117	1120785	26318	50.581	48.399	N/A	12368

Using **(*S,R,R*)-L2** as ligand (10.8:89.2 er, 41% yield):

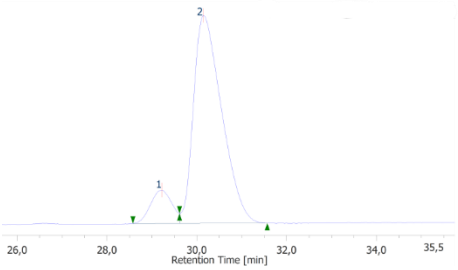

tR [min]	Area [μV·sec]	Height [μV]	Area%	Height%	Quantity	NTP
29.223	2798228	85372	10.769	13.824	N/A	16035
30.137	23184744	532180	89.231	86.176	N/A	10758

Cycloaddition between 9a and 15e: Isomers **16ae** and **16ae'** are obtained in 68% combined yield and can be easily separated by column chromatography (25% EtOAc/Hexane for **16ae'**, 40% EtOAc/Hexane for **16ae**).

Diethyl 2-(((1*S*,10*bR*)-2-methylene-5,5-dioxido-1,2,3,10*b*-tetrahydrobenzo[*e*]pyrrolo [1,2-*c*][1,2,3]oxathiazin-1-yl)methyl)-2-(2-oxopropyl)malonate (**16ae**)

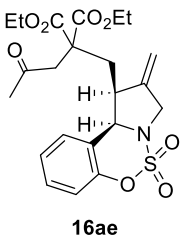

16ae

41% yield as a yellow oil. **^{1}H NMR** (500 MHz, C_6D_6) δ (ppm) 6.99 (d, *J* = 7.7 Hz, 1H), 6.79 (td, *J* = 7.4, 1.5 Hz, 1H), 6.73 – 6.69 (m, 1H), 6.67 (dd, *J* = 8.3, 1.5 Hz, 1H), 4.94 (d, *J* = 5.9 Hz, 1H), 4.89 – 4.83 (m, 1H), 4.62 – 4.56 (m, 1H), 4.23 – 4.11 (m, 1H), 4.00 – 3.87 (m, 1H), 3.87 – 3.71 (m, 4H), 3.25 – 3.13 (m, 1H), 2.92 (d, *J* = 18.1 Hz, 1H), 2.82 (d, *J* = 18.1 Hz, 1H), 2.41 (dd, *J* = 15.0, 3.6 Hz, 1H), 2.15 (dd, *J* = 15.0, 10.1 Hz, 1H), 1.56 (s, 3H), 0.87 (t, *J* = 7.1 Hz, 3H), 0.83 (t, *J* = 7.1 Hz, 3H). **^{13}C NMR** (126 MHz, C_6D_6) δ (ppm) δ 203.7 (C), 170.4 (C), 170.1 (C), 152.2 (C), 143.9 (C), 129.6 (CH), 128.0 (CH), 125.5 (CH), 120.7 (C), 119.4 (CH), 110.6 (CH_2), 66.5 (CH), 61.6 (CH_2), 61.4 (CH_2), 54.6 (C), 52.1 (CH_2), 46.8 (CH_2), 45.5 (CH), 30.2 (CH_2), 29.8 (CH_3), 13.8 (CH_3), 13.8 (CH_3). **HRMS** (APCI-TOF): m/z calculated for $C_{22}H_{28}NO_8S^+$ $[M + H]^+$ m/z 466.1530, found 466.1530. Stereochemistry of **16ae** was determined by nOe experiments.

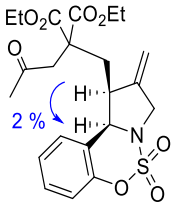

Figure 45. Significant nOe's observed for **16ae**.

Diethyl 2-(((1*S*,10*bS*)-2-methylene-5,5-dioxido-1,2,3,10*b*-tetrahydrobenzo[*e*]pyrrolo [1,2-*c*][1,2,3]oxathiazin-1-yl)methyl)-2-(2-oxopropyl)malonate (**16ae'**)

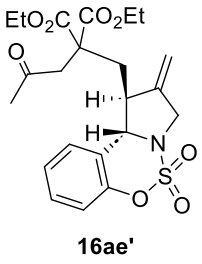

16ae'

27% yield as a yellow oil. **^{1}H NMR** (500 MHz, C_6D_6) δ (ppm) 7.38 (dt, *J* = 7.6, 1.3 Hz, 1H), 6.77 (td, *J* = 7.5, 1.4 Hz, 1H), 6.72 (td, *J* = 7.6, 1.7 Hz, 1H), 6.65 (dd, *J* = 8.2, 1.4 Hz, 1H), 5.09 (s, 1H), 4.97 – 4.82 (m, 1H), 4.42 (s, 1H), 4.03 – 3.96 (m, 3H), 3.93 – 3.85 (m, 2H), 3.78 – 3.72 (m, 1H), 3.64 (t, *J* = 6.2 Hz, 1H), 2.99 (d, *J* = 18.1 Hz, 1H), 2.89 (d, *J* = 18.1 Hz, 1H), 2.46 (d, *J* = 1.3 Hz, 1H), 2.45 (d, *J* = 3.5 Hz, 1H), 1.63 (s, 3H), 1.01 – 0.88 (m, 6H). **^{13}C NMR** (126 MHz, C_6D_6) δ (ppm) 203.7 (C), 170.4 (C), 170.1 (C), 152.2 (C), 143.9 (C), 129.6 (CH), 127.9 (CH), 125.5 (CH), 120.7 (C), 119.4 (CH), 110.6 (CH_2), 66.5 (CH), 61.6 (CH_2), 61.4 (CH_2), 54.6 (C), 52.1 (CH_2), 46.8 (CH_2), 45.5 (CH), 30.2 (CH_2), 29.8 (CH_3), 13.8 (CH_3), 13.8 (CH_3). **HRMS** (APCI-TOF): m/z calculated for $C_{22}H_{28}NO_8S^+$ $[M + H]^+$ m/z 466.1530, found 466.1530. Stereochemistry of **16ae'** was determined by nOe experiments.

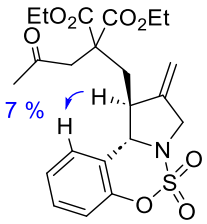

Figure 46. Significant nOe's observed for **16ae'**.

Cycloaddition between 9b and 15c: Prepared following the procedure employed for the synthesis of the cycloadduct **16be**. **16bc** and **16bc'** are obtained in 86% combined yield. **16bc** could be independently isolated by column chromatography (25% EtOAc/Hexane)

Dimethyl 2-(((2*R*,3*S*)-2-(4-fluorophenyl)-4-methylene-1-tosylpyrrolidin-3-yl)methyl)-2-(3-oxobutyl)malonate (**16bc**)

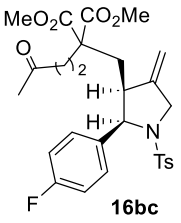

16bc

57% yield as a yellowish oil. **^{1}H NMR** (300 MHz, $CDCl_3$) δ (ppm) 7.41 (d, *J* = 8.2 Hz, 2H), 7.14 (d, *J* = 7.9 Hz, 2H), 7.02 – 6.94 (m, 2H), 6.87 (t, *J* = 8.6 Hz, 2H), 5.13 (s, 1H), 4.99 (d, *J* = 8.2 Hz, 1H), 4.92 (s, 1H), 4.20 (d, *J* = 13.1 Hz, 1H), 3.97 (d, *J* = 14.0 Hz, 1H), 3.69 (s, 3H), 3.62 (s, 3H), 2.76 – 2.65 (m, 1H), 2.37 (s, 3H), 2.34 – 2.18 (m, 2H), 2.06 (s, 3H), 1.99 (t, *J* = 7.6 Hz, 2H), 1.78 – 1.68 (m, 1H), 1.54 – 1.49 (m, 1H). **^{13}C NMR** (75 MHz, $CDCl_3$) δ (ppm) 206.5 (C), 171.4 (C), 171.3 (C), 162.4 (d, *J* = 246.8 Hz, C), 147.3 (C), 143.2 (C), 135.5 (C), 134.4 (d, *J* = 3.43 Hz, C), 130.0 (d, *J* = 8.03 Hz, CH), 129.4 (CH), 127.1 (CH), 115.2 (d, *J* = 21.4 Hz, CH), 107.0 (CH_2), 66.0 (CH), 56.7 (C), 52.6 (CH_3), 52.5 (CH_3), 51.6 (CH_2), 44.0 (CH), 38.7 (CH_2), 31.0 (CH_2), 29.8 (CH_3), 28.3 (CH_2), 21.4 (CH_3). **^{19}F NMR** (282 MHz, $CDCl_3$) δ (ppm) -114.3 (s). **HRMS** (APCI-TOF): m/z calculated for $C_{28}H_{33}FNO_7S^+$ $[M + H]^+$: m/z 546.1956, found 546.1953. Stereochemistry of **16bc** was determined by nOe experiments.

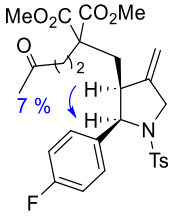

Figure 47. Significant nOe's observed for **16bc**.

Dimethyl 2-((2-(4-fluorophenyl)- 4-methylene- 1-tosylpyrrolidin- 3-yl)methyl)-2-(3-oxobutyl)malonate (**16bc** + **16bc'**)

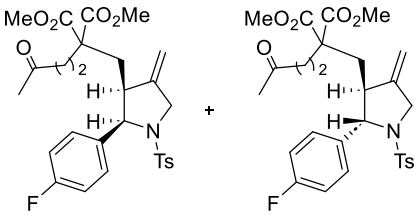

16bc : 16bc' 2.8 : 1

16bc:**16bc'** 2.8:1 ratio. Yellowish oil. **^{1}H NMR** (500 MHz, $CDCl_3$) δ (ppm) 7.54 (d, *J* = 8.3 Hz, 0.52H), 7.40 (d, *J* = 8.3 Hz, 1.48H), 7.22 (d, *J* = 8.0 Hz, 0.52H), 7.14 (d, *J* = 7.8 Hz, 1.48H), 7.12 – 7.08 (m, 0.52H), 7.01 – 6.96 (m, 1.48H), 6.94 – 6.84 (m, 2H), 5.12 (s, 0.74H), 5.02 (s, 0.26H), 4.99 (d, *J* = 8.3 Hz, 0.74H), 4.92 (s, 0.74H), 4.89 (m, 0.26H), 4.57 – 4.54 (m, 0.26H), 4.25 – 4.17 (m, 0.74H), 4.17 – 4.12 (m, 0.26H), 4.00 – 3.92 (m, 1H), 3.69 (s, 2.22H), 3.67 (s, 0.78H), 3.64 (s, 0.78H), 3.62 (s, 2.22H), 2.74 – 2.67 (m, 0.74H), 2.56 (t, *J* = 6.6 Hz, 0.26H), 2.39 (s, 0.78H), 2.36 (s, 2.22H), 2.34 – 2.17 (m, 2H), 2.09 (s, 0.78H), 2.05 (s, 2.22H), 2.02 – 1.95 (m, 2H), 1.88 – 1.81 (m, 0.26H), 1.79 – 1.68 (m, 1H), 1.57 – 1.47 (m, 0.74H). **^{13}C NMR** (126 MHz, $CDCl_3$) δ (ppm) 206.6 (C), 171.4 (C), 171.2 (C), 171.2 (C), 171.1 (C), 162.3 (d, *J* = 246.9 Hz, C), 162.1 (d, *J* = 246.0 Hz), 147.2 (C), 145.9 (C), 143.6 (C), 143.2 (C), 137.1 (d, *J* = 3.2 Hz), 135.4 (C), 135.4 (C), 134.4 (d, *J* = 3.3 Hz), 130.0 (d, *J* = 7.9 Hz), 129.5 (m, CH), 129.3 (CH), 128.1 (CH), 128.0 (CH), 127.2 (CH), 127.1 (CH), 115.20 (d, *J* = 21.4 Hz), 115.16 (d, *J* = 21.4 Hz), 110.4 (CH_2), 107.0 (CH_2), 68.8 (CH), 66.0 (CH), 56.6 (C), 55.9 (C), 52.6 (CH_3), 52.5 (CH_3), 52.5 (CH_3), 52.3 (CH_3), 51.5 (CH_2), 51.3 (CH_2), 49.6 (CH), 43.9 (CH), 38.6 (CH_2), 38.5 (CH_2), 37.6 (CH_2), 30.9 (CH_2), 29.9 (CH_3), 29.8 (CH_3), 28.2 (CH_2), 27.4 (CH_2), 26.7 (CH_2), 21.4 (CH_3), 21.4 (CH_3). **^{19}F NMR** (282 MHz, $CDCl_3$) δ (ppm) -114.3 (s, 2.8F), -115.1 (s, 1.0F). **HRMS** (APCI-TOF): m/z calculated for $C_{28}H_{33}FNO_7S^+$ $[M + H]^+$:m/z 546.1956, found 546.1953. Stereochemistry of **16bc'** was determined by comparison with **16bc** and with its analogue **16be'**.

Cycloaddition between 9b and 15f: Prepared following the procedure employed for the synthesis of the cycloadduct **16be**, using 1,4-dioxane as solvent. Isomers **16bf** and **16bf'** are obtained in 96% combined yield can be easily separated by column chromatography (25% EtOAc/Hexane for **16bf'**, 40% EtOAc/Hexane for **16bf**)

Dimethyl 2-(((1*S*,12*cR*)-2-methylene-5,5-dioxido-1,2,3,12*c*-tetrahydronaphtho[1,2-*e*]pyrrolo[1,2-*c*][1,2,3]oxathiazin-1-yl)methyl)-2-(3-oxobutyl)malonate (**16bf**)

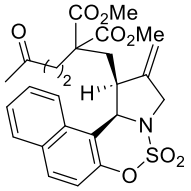

16bf

52% yield as a colourless oil. **^{1}H NMR** (500 MHz, $CDCl_3$) δ (ppm) 7.96 – 7.86 (m, 2H), 7.74 (d, *J* = 8.4 Hz, 1H), 7.59 (t, *J* = 7.3 Hz, 1H), 7.54 (t, *J* = 7.5 Hz, 1H), 7.27 (d, *J* = 6.9 Hz, 1H), 5.66 (d, *J* = 5.7 Hz, 1H), 5.23 (s, 1H), 5.20 (s, 1H), 4.41 (d, *J* = 11.8 Hz, 1H), 4.07 (d, *J* = 11.8 Hz, 1H), 3.57 (s, 3H), 3.47 (s, 3H), 3.42 – 3.35 (m, 1H), 2.24 – 2.09 (m, 1H), 1.95 (dd, *J* = 14.9, 12.7 Hz, 1H), 1.90 – 1.85 (m, 1H), 1.84 (s, 3H), 1.66 – 1.41 (m, 1H), 1.05 (dd, *J* = 15.0, 2.6 Hz, 1H). **^{13}C NMR** (126 MHz, $CDCl_3$) δ (ppm) 206.2 (C), 170.8 (C), 170.7 (C), 149.8 (C), 142.1 (C), 131.4 (C), 131.1 (CH), 130.0 (C), 129.6 (CH), 127.9 (CH), 126.1 (CH), 121.8 (CH), 119.1 (CH), 114.2 (C), 112.8 (CH_2), 64.8 (CH), 54.6 (C), 52.5 (CH_3), 52.4 (CH_2), 51.9 (CH_3), 44.6 (CH), 37.6 (CH_2), 29.8 (CH_3), 29.3 (CH_2), 25.5 (CH_2). **HRMS** (APCI-TOF): m/z calculated for $C_{25}H_{28}NO_8S^+$ $[M + H]^+$: m/z 502.1530, found 502.1533. Stereochemistry of **16bf** was determined by analogy with that of **16be**.

Dimethyl 2-(((1*S*,12*cS*)-2-methylene-5,5-dioxido-1,2,3,12*c*-tetrahydronaphtho[1,2-*e*]pyrrolo[1,2-*c*][1,2,3]oxathiazin-1-yl)methyl)-2-(3-oxobutyl)malonate (**16bf'**)

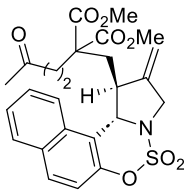

16bf'

44% yield as a colourless oil. **^{1}H NMR** (500 MHz, $CDCl_3$) δ (ppm) 7.86 (d, *J* = 8.2 Hz, 1H), 7.78 (d, *J* = 8.9 Hz, 1H), 7.66 – 7.57 (m, 2H), 7.55 – 7.46 (m, 1H), 7.10 (d, *J* = 8.9 Hz, 1H), 5.37 (s, 1H), 4.89 (s, 1H), 4.73 (s, 1H), 4.38 – 4.23 (m, 1H), 4.20 – 4.09 (m, 1H), 3.74 (s, 3H), 3.68 (s, 3H), 3.37 (dd, *J* = 11.8, 3.5 Hz, 1H), 2.70 (dd, *J* = 14.7, 11.8 Hz, 1H), 2.66 – 2.44 (m, 3H), 2.43 – 2.34 (m, 1H), 2.24 – 2.18 (m, 1H), 2.17 (s, 3H). **^{13}C NMR** (126 MHz, $CDCl_3$) δ (ppm) 206.5 (C), 171.1 (C), 170.9 (C), 149.2 (C), 141.8 (C), 131.6 (C), 130.7 (CH), 130.2 (C), 129.4 (CH), 127.3 (CH), 125.7 (CH), 122.9 (CH), 118.4 (CH), 114.5 (C), 112.6 (CH_2), 70.5 (CH), 55.8 (C), 53.2 (CH_2), 52.7 (CH_3), 52.2 (CH_3), 48.9 (CH), 38.8 (CH_2), 36.6 (CH_2), 30.0 (CH_3), 27.5 (CH_2). **HRMS** (APCI-TOF): m/z calculated for $C_{25}H_{28}NO_8S^+$ $[M + H]^+$: m/z 502.1530, found 502.1533. Stereochemistry of **16bf'** was determined by analogy with that of **16be'**.

Cycloaddition between 9b and 15h: Prepared following the procedure employed for the synthesis of the cycloadduct **16be**, using 1,4-dioxane as solvent. Isomers **16bh** and **16bh'** are obtained in 58% combined yield and can be easily separated by column chromatography (25% EtOAc/Hexane for **16bh'**, 40% EtOAc/Hexane for **16bh**).

Dimethyl 2-(((1*S*,10*bR*)-10-methoxy-2-methylene- 5,5-dioxido- 1,2,3,10*b*-tetrahydrobenzo[*e*] pyrrolo [1,2-*c*][1,2,3] oxathiazin-1-yl)methyl)-2- (3-oxobutyl)malonate (**16bh**)

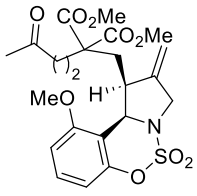

16bh

32% yield, colourless solid. **^{1}H NMR** (500 MHz, $CDCl_3$) δ (ppm) 7.25 (t, *J* = 8.4 Hz, 1H), 6.68 (t, *J* = 8.4 Hz, 2H), 5.06 (d, *J* = 7.4 Hz, 2H), 4.99 (d, *J* = 5.6 Hz, 1H), 4.18 (d, *J* = 11.8 Hz, 1H), 3.89 (d, *J* = 11.8 Hz, 1H), 3.80 (s, 3H), 3.55 (s, 3H), 3.53 (s, 3H), 3.30 – 3.17 (m, 1H), 2.40 – 2.29 (m, 1H), 2.28 – 2.20 (m, 1H), 2.14 – 2.05 (m, 1H), 2.03 (s, 3H), 1.94 – 1.76 (m, 2H), 1.37 – 1.25 (m, 1H). **^{13}C NMR** (126 MHz, $CDCl_3$) δ (ppm) 207.0 (C), 171.3 (C), 171.1 (C), 156.5 (C), 152.2 (C), 142.7 (C), 130.4 (CH), 112.4 (CH_2), 112.1 (CH), 109.9 (C), 107.6 (CH), 63.8 (CH), 56.1 (CH_3), 55.2 (C), 52.6 (CH_3), 52.0 (CH_3), 51.9 (CH_2), 43.6 (CH), 38.6 (CH_2), 31.3 (CH_2), 30.1 (CH_3), 26.9 (CH_2). **HRMS** (APCI-TOF): m/z calculated for $C_{22}H_{28}NO_9S^+$ $[M + H]^+$:m/z 502.1530, found 502.1533. Structure of **16bh** was confirmed by X-ray analysis.

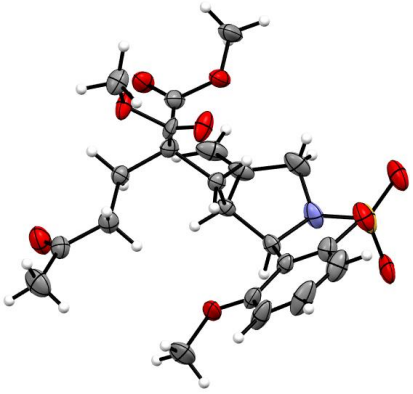

Figure 48. Crystal structure of **16bh** (**CCDC** 2401937).

Dimethyl 2-(((1*S*,10*bS*)-10-methoxy- 2-methylene- 5,5-dioxido- 1,2,3,10*b*-tetrahydrobenzo[e] pyrrolo[1,2-*c*][1,2,3] oxathiazin-1-yl)methyl)-2- (3-oxobutyl)malonate (**16bh'**)

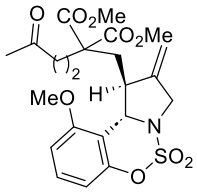

16bh'

26% yield, colourless solid. **^{1}H NMR** (500 MHz, $CDCl_3$) δ (ppm) 7.23 (t, *J* = 8.4 Hz, 1H), 6.70 (dd, *J* = 8.4, 1.0 Hz, 1H), 6.61 (dd, *J* = 8.4, 1.0 Hz, 1H), 4.89 (s, 1H), 4.85 (s, 1H), 4.84 (s, 1H), 4.17 (d, *J* = 14.6 Hz, 1H), 4.03 (d, *J* = 14.6 Hz, 1H), 3.88 (s, 3H), 3.74 (s, 3H), 3.67 (s, 3H), 3.40 – 3.31 (m, 1H), 2.64 – 2.34 (m, 5H), 2.23 (s, 1H), 2.17 (s, 3H). **^{13}C NMR** (126 MHz, $CDCl_3$) δ (ppm) 207.1 (C), 171.5 (C), 171.2 (C), 157.2 (C), 152.1 (C), 144.2 (C), 129.9 (CH), 111.4 (CH), 110.9 (CH_2), 110.0 (C), 107.8 (CH), 68.7 (CH), 56.0 (C), 56.0 (CH_3), 52.9 (CH_2), 52.8 (CH_3), 52.3 (CH_3), 46.4 (CH), 38.9 (CH_2), 37.1 (CH_2), 30.2 (CH_3), 26.7 (CH_2). **HRMS** (APCI-TOF): m/z calculated for $C_{22}H_{28}NO_9S^+$ $[M + H]^+$: m/z 502.1530, found 502.1533. Structure of **16bh'** was confirmed by X-ray analysis.

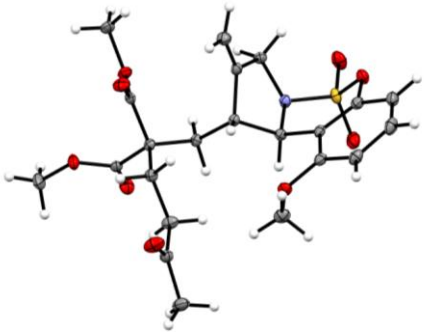

Figure 49. Crystal structure of **16bh'** (**CCDC** 2401925).

Cycloaddition between 9c and 15e: Prepared following the procedure employed for the synthesis of the cycloadduct **16be**, using 1,4-dioxane as solvent. Isomers **16ce** and **16ce'** are obtained in 51% combined yield and can be easily separated by column chromatography (25% EtOAc/Hexane for **16ce'**, 40% EtOAc/Hexane for **16ce**).

4-Methyl- *N*-(((1*R*,10*bR*)-2-methylene- 5,5-dioxido-1,2,3,10*b*- tetrahydrobenzo[*e*] pyrrolo[1,2-*c*][1,2,3]oxathiazin-1-yl)methyl)-*N*-(3-oxobutyl)benzenesulfonamide (**16ce**)

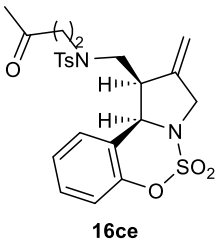

16ce

28% yield as a yellowish oil. **^{1}H NMR** (500 MHz, $CDCl_3$) δ (ppm) 7.56 (d, *J* = 8.1 Hz, 2H), 7.41 – 7.33 (m, 1H), 7.33 – 7.28 (m, 2H), 7.28 – 7.21 (m, 2H), 7.07 (d, *J* = 8.2 Hz, 1H), 5.27 (s, 1H), 5.21 (s, 1H), 5.01 (d, *J* = 5.8 Hz, 1H), 4.34 – 4.21 (m, 1H), 4.17 – 4.02 (m, 1H), 3.67 – 3.57 (m, 1H), 3.42 – 3.30 (m, 1H), 3.22 – 3.08 (m, 1H), 2.97 (dd, *J* = 14.6, 4.1 Hz, 1H), 2.80 – 2.73 (m, 1H), 2.72 – 2.65 (m, 1H), 2.62 – 2.55 (m, 1H), 2.41 (s, 3H), 2.08 (s, 3H). **^{13}C NMR** (126 MHz, $CDCl_3$) δ (ppm) 206.5 (C), 151.1 (C), 144.1 (C), 141.5 (C), 135.3 (C), 129.9 (CH), 129.9 (CH), 127.6 (CH), 127.6 (CH), 125.9 (CH), 119.7 (C), 119.3 (CH), 113.0 (CH_2), 64.8 (CH), 51.2 (CH_2), 48.7 (CH_2), 47.7 (CH) , 44.9 (CH_2), 43.0 (CH_2), 30.4 (CH_3) , 21.6 (CH_3). **HRMS** (APCI-TOF): m/z calculated for $C_{23}H_{27}N_2O_6S_2^+$ [M + H]$^+$: m/z 491.1305, found 491.1307. Stereochemistry of **16ce** was determined by nOe experiments.

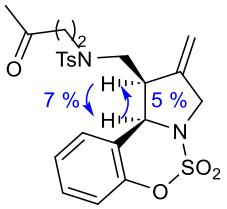

Figure 50. Significant nOe's observed for **16ce**.

4-Methyl-*N*-(((1*R*,10*bS*)-2-methylene-5,5-dioxido-1,2,3,10*b*-tetrahydrobenzo[*e*] pyrrolo[1,2-*c*][1,2,3]oxathiazin-1-yl)methyl)-*N*-(3-oxobutyl)benzenesulfonamide (16ce')

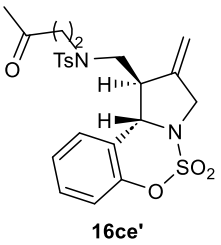

16ce'

23% yield as a yellowish oil. **^{1}H NMR** (500 MHz, $CDCl_3$) δ (ppm) 7.75 (d, *J* = 8.2 Hz, 2H), 7.40 – 7.34 (m, 3H), 7.34 – 7.29 (m, 1H), 7.24 (td, *J* = 7.5, 1.2 Hz, 1H), 7.01 (dd, *J* = 8.3, 1.2 Hz, 1H), 5.26 (s, 1H), 5.10 – 5.07 (m, 1H), 5.06 – 5.02 (m, 1H), 4.22 – 4.09 (m, 1H), 4.03 – 3.90 (m, 1H), 3.79 – 3.61 (m, 2H), 3.22 – 3.11 (m, 2H), 3.12 – 3.00 (m, 1H), 2.90 (td, *J* = 7.4, 4.8 Hz, 2H), 2.46 (s, 3H), 2.17 (s, 3H).**^{13}C NMR** (126 MHz, $CDCl_3$) δ (ppm) 206.5 (C), 150.9 (C), 144.2 (C), 142.4 (C), 134.3 (C), 130.0 (CH), 129.6 (CH), 127.6 (CH), 127.4 (CH), 126.0 (CH), 119.7 (C), 118.5 (CH), 111.6 (CH_2), 65.5 (CH), 52.7 (CH_2), 52.4 (CH_2), 52.0 (CH), 45.5 (CH_2), 42.8 (CH_2), 30.2 (CH_3), 21.6 (CH_3). **HRMS** (APCI-TOF): m/z calculated for $C_{23}H_{27}N_2O_6S_2^+$ [M + H]$^+$: m/z 491.1305, found 491.1307. Stereochemistry of **16ce'** was determined by nOe experiments.

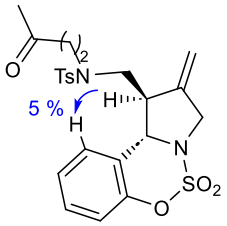

Figure 51. Significant nOe's observed for **16ce'**.

Dimethyl (*E*)-2-(3-methylbuta-1,3-dien-1-yl)-2-(3-oxobutyl)malonate (18b)

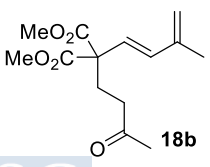

18b

Obtained following the procedure employed for the synthesis of the cycloadduct **16be**, using $P[(3,5\text{-}CF_3)_2C_6H_3]_3$ (**L17**) as ligand and 1,4-dioxane as solvent. Purification by flash chromatography (3-5% EtOAc/Hexane) afforded to **18b** as a yellow oil in 15% yield. **^{1}H NMR** (300 MHz, $CDCl_3$) δ (ppm) 6.18 (d, *J* = 16.4 Hz, 1H), 6.02 (d, *J* = 16.4 Hz, 1H), 5.03 (s, 1H), 4.98 (s, 1H), 3.73 (s, 6H), 2.47 – 2.36 (m, 2H), 2.37 – 2.23 (m, 2H), 2.10 (s, 3H), 1.86 (s, 3H). **^{13}C NMR** (75 MHz, $CDCl_3$) δ (ppm) 207.1 (C), 170.8 (C), 141.1 (C), 134.7 (CH), 125.5 (CH), 118.1 (CH_2), 58.6 (C), 52.8 (CH_3), 38.7

(CH_2), 28.9 (CH_2), 18.3 (CH_3). **HRMS** (APCI-TOF): m/z calculated for $C_{14}H_{21}O_5^+$ $[M + H]^+$: m/z 269.1384, found 269.1376.

Compounds 19a-19h: Substrates **19a**[75a], **19b**[154], **19c**[155], **19d**[156], **19e**[157], **19f**[158], **19g**[159] and **19h**[160] are known compounds and were synthesized following reported procedures.

***N*-(2-cyclopropylidenepropyl)-4-nitrobenzenesulfonamide** (**19i**)

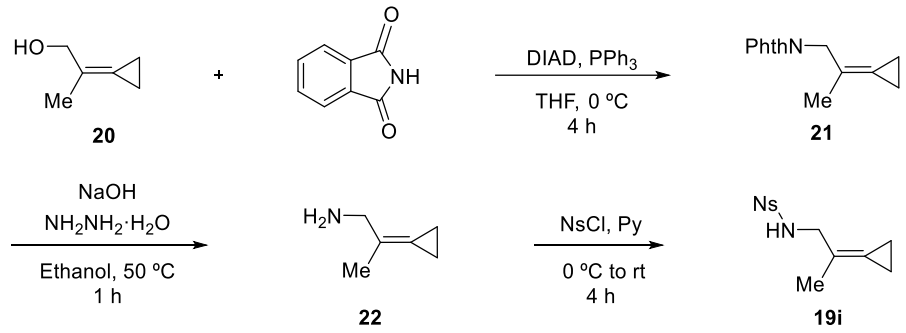

DIAD (5.50 mL, 28.1 mmol, 1.2 equiv.) was slowly added to a solution of triphenyl phosphine (7.40 g, 28.1 mmol, 1.2 equiv.), phthalimide (3.40 g, 23.4 mmol, 1.0 equiv.) and 2-cyclopropylidenepropan-1-ol **20** (2.30 g, 23.4 mmol, 1.0 equiv.) in THF (29 mL) at 0 ºC. The mixture was stirred at 0 ºC for 3 h, quenched with water (30 mL) and extracted with CH_2Cl_2 (2x30 mL). The combined organic layers were dried, filtered and concentrated to yield a crude residue that was purified by flash chromatography (20% EtOAc/ Hexane) to give **21** as a pale-yellow solid (3.20 g, 14.1 mmol, 60% yield).

To a solution of phthalimide **21** (1.60 g, 7.04 mmol, 1.0 equiv.) in ethanol (28 mL), hydrazine (680 µL, 14.1 mmol, 2.0 equiv.) was added and the mixture was stirred at 50 ºC for 1 h. Then, the reaction was quenched with HCl (c) until all the precipitate was formed, which was removed by filtration. The resulting solution was dried, filtered and concentrated. The crude residue was used without further purification in the next step (**22**, 522 mg, 5.37 mmol, 76% yield).

Nosyl chloride (847 mg, 3.70 mmol, 1.2 equiv.) was added to a solution of 2-cyclopropylidenepropan-1-amine **22** (300 mg, 3.10 mmol, 1.0 equiv.) in pyridine (3.10 mL, 39.5 mmol, 12.5 equiv.) at 0 ºC. After stirring for 1 h at 0 ºC, the reaction was kept at rt for 4 h. Then, the reaction was quenched with water (3 mL) and HCl 1M (until neutral pH) and extracted with Et_2O (3x3 mL). The organic phases were dried, filtered and concentrated to give a crude residue that was purified by flash chromatography (10-20% Et_2O/Hexane) to yield *N*-(2-cyclopropylidenepropyl)-4-nitrobenzenesulfonamide **19i** (663 mg, 2.00 mmol, 65% yield) as a pale-orange solid. **^{1}H NMR** (300 MHz, $CDCl_3$) δ (ppm) 8.35 (d, *J* = 8.8 Hz, 2H), 8.04 (d, *J* = 8.8 Hz, 2H), 4.90 – 4.66 (m, 1H), 3.75 (d, *J* = 5.9 Hz, 2H), 1.74 (s, 3H), 1.21 – 0.87 (m, 4H). **^{13}C NMR** (75 MHz, $CDCl_3$) δ (ppm) 150.1 (C),

[75a] Gulías, M.; García, R.; Delgado, A.; Castedo, L.; Mascareñas, J. L. Palladium-Catalyzed [3 + 2] Intramolecular Cycloaddition of Alk-5-enylidenecyclopropanes. *J. Am. Chem. Soc.* **2006**, *128*, 2, 384–385.

[154] Anderson, T. E.; Woerpel, K. A. Strain-Promoted Oxidation of Methylenecyclopropane Derivatives using *N*-Hydroxyphthalimide and Molecular Oxygen in the Dark. *Org. Lett.* **2020**, *22*, 14, 5690-5694.

[155] Lopez, M. M.; Jamey, N.; Pinet, A.; Figadere, B.; Ferrie, L. Oxidative Ring Expansion of Cyclobutanols: Access to Functionalized 1,2-Dioxanes. *Org. Lett.* **2021**, *23*, 5, 1626-1631.

[156] Utimoto, K.; Tamaru, M.; Sisido, K. Preparation and reaction of cyclopropyltriphenylphosphonium salt. *Tetrahedron* **1973**, *29*, 1169.

[157] Siriwardana, A. I.; Nakamura, I.; Yamamoto, Y. Addition of water to arylidenecyclopropanes: a highly efficient method for the preparation of gem-aryl disubstituted homoallylic alcohols. *Tetrahedron Lett.* **2003**, *44*, 24, 4547-4550.

[158] Jiao. M.; Fang, X. Cobalt-Catalyzed Hydrocyanation of Methylenecyclopropanes to Homoallylic Nitriles. *Org. Lett.* **2022**, 24, 48, 8890-8894.

[159] Kim, S. and Chung., Y. K. Rhodium-Catalyzed Carbonylative [3 + 2 + 1] Cycloaddition of Alkyne-Tethered Alkylidenecyclopropanes to Phenols in the Presence of Carbon Monoxide. *Org. Lett.* **2014**, *16*, 17, 4352–4355.

[160] Zhang, X.Y.; Ning, C.; Mao, B.; Wei, Y.; Shi, M. A visible-light mediated ring opening reaction of alkylidenecyclopropanes for the generation of homopropargyl radicals. *Chem. Sci.* **2021**, *12*, 9088-9095.

146.3 (C), 128.4 (CH), 124.4 (CH), 120.6 (C), 119.1 (C), 48.8 (CH_2), 18.7 (CH_3), 3.0 (CH_2), 1.5 (CH_2). **HRMS** (APCI-TOF): m/z calculated for $C_{12}H_{15}N_2O_4S^+$ $[M + H]^+$: m/z 283.07047, found 283.07048.

Cycloaddition between 19a and 15e: Prepared following the procedure employed for the synthesis of the cycloadduct **16be**. Isomers **23ae** and **23ae'** are obtained in 80% combined yield and can be easily separated by column chromatography (9% EtOAc/Hexane).

Diethyl 2-(((1*S*,10*bR*)-2-methylene-5,5-dioxido-1,2,3,10*b*-tetrahydrobenzo[*e*]pyrrolo [1,2-*c*][1,2,3]oxathiazin-1-yl)methyl)malonate (**23ae**)

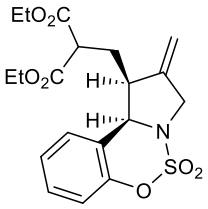

23ae

40% yield as a colourless oil. **^{1}H NMR** (500 MHz, $CDCl_3$) δ (ppm) 7.37 – 7.31 (m, 1H), 7.29 – 7.22 (m, 1H), 7.16 (d, *J* = 7.6 Hz, 1H), 7.08 (d, *J* = 8.2 Hz, 1H), 5.21 (s, 1H), 5.13 (s, 1H), 5.06 (d, *J* = 5.9 Hz, 1H), 4.32 – 4.21 (m, 3H), 4.17 – 4.11 (m, 2H), 4.11 – 4.05 (m, 1H), 3.56 – 3.37 (m, 1H), 3.16 – 3.03 (m, 1H), 2.01 – 1.87 (m, 1H), 1.75 – 1.58 (m, 1H), 1.30 (t, *J* = 7.1 Hz, 3H), 1.22 (t, *J* = 7.1 Hz, 3H). **^{13}C NMR** (126 MHz, $CDCl_3$) δ (ppm) 168.9 (C), 168.9 (C), 151.3 (C), 142.8 (C), 129.6 (CH), 127.3 (CH), 125.9 (CH), 119.8 (C), 119.2 (CH), 111.5 (CH_2), 65.5 (CH), 61.7 (CH_2), 61.7 (CH_2), 51.3 (CH_2), 49.2 (CH), 46.4 (CH), 26.7 (CH_2), 14.1 (CH_3), 14.0 (CH_3). **HRMS** (APCI-TOF): m/z calculated for $C_{19}H_{23}NO_7S^+$ $[M + H]^+$: m/z 410.1268, found 410.1266. Stereochemistry of **23ae** was determined by NOESY experiments.

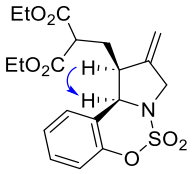

Figure 52. Significant nOe's observed for **23ae**.

Diethyl 2-(((1*S*,10*bR*)-2-methylene-5,5-dioxido-1,2,3,10*b*-tetrahydrobenzo[*e*]pyrrolo [1,2-*c*][1,2,3]oxathiazin-1-yl)methyl)malonate (**23ae'**)

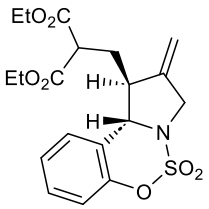

23ae'

40% yield as a colourless oil. **^{1}H NMR** (500 MHz, $CDCl_3$) δ (ppm) 7.30 (t, *J* = 7.7 Hz, 1H), 7.20 (t, *J* = 7.6 Hz, 1H), 7.15 (d, *J* = 7.6 Hz, 1H), 7.00 (dd, *J* = 8.3, 1.1 Hz, 1H), 5.04 (s, 1H), 5.02 (s, 1H), 5.01 (s, 1H), 4.34 – 4.24 (m, 4H), 4.23 – 4.17 (m, 1H), 4.01 – 3.92 (m, 1H), 3.54 (t, *J* = 7.6 Hz, 1H), 3.13 (t, *J* = 7.8 Hz, 1H), 2.59 – 2.35 (m, 1H), 2.33 – 2.17 (m, 1H), 1.31 (t, *J* = 7.1 Hz, 6H). **^{13}C NMR** (126 MHz, $CDCl_3$) δ (ppm) 168.9 (C), 168.8 (C), 150.9 (C), 143.9 (C), 129.7 (CH), 126.9 (CH), 125.8 (CH), 120.0 (C), 118.8 (CH), 111.2 (CH_2), 68.3 (CH), 61.9 (CH_2), 61.8 (CH_2), 52.3 (CH_2), 49.9 (CH), 49.7 (CH), 32.8 (CH_2), 14.1 (CH_3), 14.1 (CH_3). **HRMS** (APCI-TOF): m/z calculated for $C_{19}H_{23}NO_7S^+$ $[M + H]^+$: m/z 410.1268, found 410.1266. Stereochemistry of **23ae'** was determined by comparation with **23ae**.

Cycloaddition between 19b and 15e: Prepared following the procedure employed for the synthesis of the cycloadduct **16be**. Isomers **23be** and **23be'** are obtained in 90% combined yield and can be easily separated by column chromatography (1.5-2% EtOAc/Hexane).

(1*S*,10*bS*)-1-Heptyl-2-methylene-1,2,3,10*b*-tetrahydrobenzo[*e*]pyrrolo[1,2-*c*][1,2,3] oxathiazine 5,5-dioxide (**23be**)

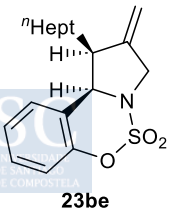

23be

4 5% yield as a colourless oil. **^{1}H NMR** (500 MHz, $CDCl_3$) δ (ppm) 7.31 (td, *J* = 7.9, 1.6 Hz, 1H), 7.20 (td, *J* = 7.6, 1.3 Hz, 1H), 7.16 – 7.09 (m, 1H), 7.05 (dd, *J* = 8.3, 1.2 Hz, 1H), 5.13 (d, *J* = 6.2 Hz, 1H), 5.07 (s, 1H), 5.01 (s, 1H), 4.19 (d, *J* = 13.3 Hz, 1H), 4.10 (d, *J* = 13.3 Hz, 1H), 3.12 – 2.93 (m, 1H), 1.40 – 1.16 (m, 12H), 0.87 (t, *J* = 7.0 Hz, 3H).**^{13}C NMR** (126 MHz, $CDCl_3$) δ (ppm) 151.6 (C), 144.2 (C), 129.4 (CH), 127.6 (CH), 125.5 (CH), 120.5 (C), 119.4 (CH), 109.2 (CH_2), 65.7 (CH), 52.7 (CH_2), 49.3 (CH), 31.9 (CH_2), 29.5 (CH_2), 29.3 (CH_2), 27.3 (CH_2), 27.3 (CH_2),

22.7 (CH_2), 14.2 (CH_3). **HRMS** (APCI-TOF): m/z calculated for $C_{18}H_{26}NO_3S^+$ $[M + H]^+$: m/z 336.1628, found 336.1627. Stereochemistry of **23be** was determined by nOe experiments.

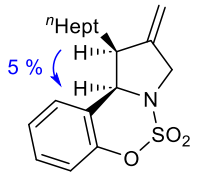

Figure 53. Significant nOe's observed for **23be**.

(1*S*,10*bS*)-1-Heptyl-2-methylene-1,2,3,10*b*-tetrahydrobenzo[*e*]pyrrolo[1,2-*c*][1,2,3]oxathiazine 5,5-dioxide (**23be'**)

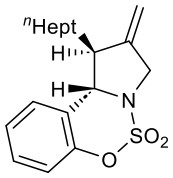

23be'

45% yield as a colourless oil. **^{1}H NMR** (500 MHz, $CDCl_3$) δ (ppm) 7.29 (td, *J* = 7.8, 1.7 Hz, 1H), 7.20 (td, *J* = 7.5, 1.3 Hz, 1H), 7.15 – 7.11 (m, 1H), 7.00 (dd, *J* = 8.2, 1.2 Hz, 1H), 5.01 (s, 1H), 4.98 (d, *J* = 7.4 Hz, 1H), 4.18 (dd, *J* = 14.5, 1.8 Hz, 1H), 3.97 (dt, *J* = 14.4, 2.4 Hz, 1H), 2.98 (t, *J* = 7.4 Hz, 1H), 1.82 – 1.72 (m, 1H), 1.70 – 1.59 (m, 1H), 1.50 (dq, *J* = 10.2, 3.7 Hz, 2H), 1.43 – 1.28 (m, 8H), 0.91 (t, *J* = 6.8 Hz, 3H). **^{13}C NMR** (126 MHz, $CDCl_3$) δ (ppm) 151.1 (C), 145.8 (C), 129.5 (CH), 127.1 (CH), 125.8 (CH), 121.2 (C), 118.9 (CH), 109.4 (CH_2), 68.3 (CH), 53.0 (CH_2), 52.8 (CH), 35.0 (CH_2), 32.0 (CH_2), 29.6 (CH_2), 29.4 (CH_2), 27.8 (CH_2), 22.8 (CH_2), 14.2 (CH_3). **HRMS** (APCI-TOF): m/z calculated for $C_{18}H_{26}NO_3S^+$ $[M + H]^+$:m/z 336.1628, found 336.1627. Stereochemistry of **23be'** was determined by nOe experiments.

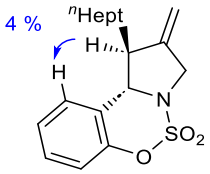

Figure 54. Significant nOe's observed for **23be'**.

1-Heptyl-2-methylene-10*b*-(trifluoromethyl)-1,2,3,10*b*-tetrahydrobenzo[*e*]pyrrolo[1,2-*c*][1,2,3]oxathiazine 5,5-dioxide (**23bp+23bp'**)

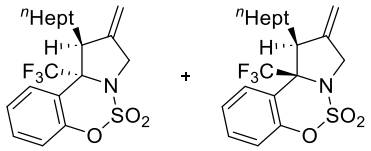

23bp:**23bp'** 1.5:1

Prepared following the procedure employed for the synthesis of **16be**, using ACP **19b** and imine **15p** as starting materials. Isolated by column chromatography (1-2% EtOAc/Hexane) as a yellowish oil in 70% yield (dr 1.7:1). Characterized as a **23bp**:**23bp'** mixture 1.5:1. **^{1}H NMR** (500 MHz, $CDCl_3$) δ (ppm) 7.54 (d, *J* = 8.0 Hz, 0.6H), 7.48 – 7.39 (m, 1.4H), 7.35 – 7.27 (m, 1H), 7.17 (dd, *J* = 8.3, 1.3 Hz, 0.4H), 7.13 (dd, *J* = 8.2, 1.3 Hz, 0.6H), 5.27 – 5.17 (m, 0.4H), 5.17 – 5.10 (m, 0.4H), 5.10 – 5.04 (m, 0.6H), 5.04 – 4.95 (m, 0.6H), 4.49 – 4.41 (m, 0.4H), 4.37 – 4.27 (m, 1.2H), 4.26 – 4.17 (m, 0.4H), 3.11 (dd, *J* = 11.6, 4.2 Hz, 0.4H), 2.88 (d, *J* = 11.2 Hz, 0.6H), 2.09 – 1.94 (m, 1H), 1.81 – 1.64 (m, 1H), 1.53 – 1.44 (m, 1H), 1.39 – 1.20 (m, 9H), 1.20 – 1.10 (m, 2H), 0.88 (t, *J* = 7.0 Hz, 1.8H), 0.84 (d, *J* = 7.2 Hz, 1.2H). **^{13}C NMR** (126 MHz, $CDCl_3$) δ (ppm) 151.0 (C), 150.4 (C), 141.7 (C), 141.2 (C), 131.1 (CH), 131.0 (CH), 127.9 (CH, m), 127.9 (CH), 126.4 (CH), 126.4 (CH), 126.3 (CH), 123.8 (C, q, *J*=288.9 Hz), 123.1 (C, q, *J*=287.3 Hz), 120.1(C), 120.0 (CH), 120.0 (CH), 118.1 (C), 110.5 (CH_2), 109.3 (CH_2), 74.8 (C, q, *J*=29.2 Hz), 69.1 (C, q, *J*=30.0 Hz), 56.3 (CH), 55.3 (CH_2), 53.8 (CH_2), 50.9 (CH), 31.7 (CH_2), 31.6 (CH_2), 29.4 (CH_2), 29.0 (CH_2), 28.9 (CH_2), 28.8 (CH_2), 28.3 (CH_2), 26.3 (CH_2), 26.1 (CH_2), 22.6 (CH_2), 22.5 (CH_2), 14.1 (CH_3), 14.0 (CH_3). **^{19}F NMR** (282 MHz, $CDCl_3$) δ (ppm) -66.9 (s, 1.5F), -73.2 (s, 1.0F). **HRMS** (APCI-TOF): m/z calculated for $C_{19}H_{25}F_3NO_3S^+$ $[M + H]^+$:m/z 404.1502, found 404.1501. Stereochemistry of **23bp** and **23bp'** was deduced by comparison with analogue products.

Cycloaddition between 19b and 15q: Prepared following the procedure employed for the synthesis of the cycloadduct **16be**. Isomers **23bq** and **23bq'** are obtained in 70% combined yield (dr 1:1) and can be easily separated by column chromatography (1.5-2% EtOAc/Hexane).

Methyl (1*S*,10*bS*)-1-heptyl-2-methylene-2,3-dihydrobenzo[*e*]pyrrolo[1,2-*c*][1,2,3] oxathiazine-10*b*(1*H*)-carboxylate 5,5-dioxide (**23bq**)

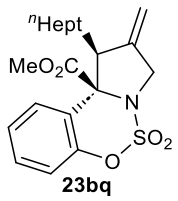

23bq

35% yield as a colourless oil. **^{1}H NMR** (500 MHz, $CDCl_3$) δ (ppm) 7.64 (dd, *J* = 8.0, 1.6 Hz, 1H), 7.33 (td, *J* = 7.8, 1.7 Hz, 1H), 7.29 – 7.18 (m, 1H), 6.97 (dd, *J* = 8.2, 1.3 Hz, 1H), 4.96 (s, 1H), 4.86 (d, *J* = 1.7 Hz, 1H), 4.41 – 4.28 (m, 1H), 4.10 (d, *J* = 14.3 Hz, 1H), 3.82 (s, 3H), 3.05 (dd, *J* = 10.8, 4.1 Hz, 1H), 1.70 – 1.58 (m, 1H), 1.55 – 1.42 (m, 1H), 1.34 – 1.21 (m, 10H), 0.89 (t, *J* = 6.8 Hz, 3H). **^{13}C NMR** (126 MHz, $CDCl_3$) δ (ppm) 169.2 (C), 150.6 (C), 142.3 (C), 130.6 (CH), 130.2 (CH), 125.3 (CH), 120.9 (C), 118.6 (CH), 111.0 (CH_2), 78.0 (C), 59.0 (CH_3), 53.7 (CH_2), 53.0 (CH), 31.9 (CH_2), 30.2 (CH_2), 29.5 (CH_2), 29.3 (CH_2), 27.2 (CH_2), 22.8 (CH_2), 14.2 (CH_3). **HRMS** (APCI-TOF): m/z calculated for $C_{20}H_{28}NO_5S^+$ $[M + H]^+$: m/z 394.1683, found 394.1686. Stereochemistry of **23bq** was determined by nOe experiments.

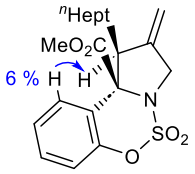

Figure 55. Significant nOe's observed for **23bq**.

Methyl (1*R*,10*bS*)-1-heptyl-2-methylene-2,3-dihydrobenzo[*e*]pyrrolo[1,2-*c*][1,2,3] oxathiazine-10*b*(1*H*)-carboxylate 5,5-dioxide (**23bq'**)

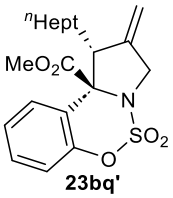

23bq'

35% yield as a colourless oil. Data extracted from a 1:10 mixture. **^{1}H NMR** (500 MHz, $CDCl_3$) δ (ppm) 7 7.41 (dd, *J* = 8.0, 1.6 Hz, 1H), 7.26 (ddd, *J* = 8.4, 7.4, 1.7 Hz, 1H), 7.13 (td, *J* = 7.7, 1.4 Hz, 1H), 6.96 (dd, *J* = 8.3, 1.3 Hz, 1H), 4.99 (d, *J* = 1.6 Hz, 1H), 4.92 (s, 1H), 4.25 – 4.13 (m, 2H), 3.69 (s, 3H), 3.19 (t, *J* = 7.1 Hz, 1H), 1.12 – 1.03 (m, 12H), 0.75 (t, *J* = 7.1 Hz, 3H). It contains silicon grease. **^{13}C NMR** (126 MHz, $CDCl_3$) δ (ppm) 171.1 (C), 151.1 (C), 142.5 (C), 130.3 (CH), 129.4 (CH), 125.4 (CH), 119.4 (CH), 118.9 (C), 110.3 (CH_2), 76.4 (C), 55.1 (CH_3), 53.7 (CH), 53.1 (CH_2), 31.8 (CH_2), 29.4 (CH_2), 29.2 (CH_2), 27.8 (CH_2), 26.7 (CH_2), 22.7 (CH_2), 14.2 (CH_3). **HRMS** (APCI-TOF): m/z calculated for $C_{20}H_{28}NO_5S^+$ $[M + H]^+$: m/z 394.1683, found 394.1686. Stereochemistry of **23bq'** was determined by comparison with **23bq**.

Cycloaddition between 19b and 15r: Prepared following the procedure employed for the synthesis of the cycloadduct **16be**. Isomers **23br** and **23br'** are obtained in 82% combined yield (dr 1.2:1) and can be easily separated by column chromatography (1.5% EtOAc/Hexane).

(1*R*,10*bR*)-1-Heptyl-2-methylene-10*b*-phenyl-1,2,3,10*b*-tetrahydrobenzo[*e*]pyrrolo[1,2-*c*] [1,2,3]oxathiazine 5,5-dioxide (**23br**)

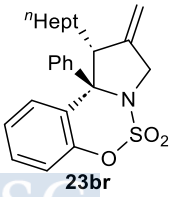

23br

45% yield as a colourless oil. **^{1}H NMR** (500 MHz, $CDCl_3$) δ (ppm) 7.36 (dd, *J* = 7.7, 1.7 Hz, 1H), 7.24 (ddd, *J* = 7.6, 6.1, 1.8 Hz, 3H), 7.20 – 7.16 (m, 1H), 7.16 – 7.11 (m, 3H), 6.95 (dd, *J* = 8.1, 1.4 Hz, 1H), 4.90 (d, *J* = 1.8 Hz, 1H), 4.82 (d, *J* = 1.8 Hz, 1H), 4.33 – 4.16 (m, 1H), 4.06 – 3.92 (m, 1H), 2.95 (dd, *J* = 10.3, 3.3 Hz, 1H), 1.30 – 1.19 (m, 2H), 1.08 – 1.00 (m, 10H), 0.71 (t, *J* = 7.1 Hz, 3H). **^{13}C NMR** (126 MHz, $CDCl_3$) δ (ppm) 150.4 (C), 144.4 (C), 138.5 (C), 129.8 (CH), 128.4 (CH), 128.0 (CH), 128.0 (CH), 127.7 (CH), 126.5 (C), 125.2 (CH), 119.8 (CH), 109.0 (CH_2), 78.0 (C), 57.3 (CH), 54.3 (CH_2), 31.9 (CH_2), 30.2 (CH_2), 29.6 (CH_2), 29.3 (CH_2), 28.1 (CH_2), 22.7 (CH_2), 14.2 (CH_3).

HRMS (APCI-TOF): m/z calculated for $C_{24}H_{30}NO_3S^+$ [M + H]$^+$: m/z 412.1941, found 412.1941. Stereochemistry of **23br** was determined by comparison with **23br'**.

(1*S*,10*bR*)-1-Heptyl-2-methylene-10*b*-phenyl-1,2,3,10*b*-tetrahydrobenzo[*e*]pyrrolo[1,2-*c*][1,2,3]oxathiazine 5,5-dioxide (**23br'**)

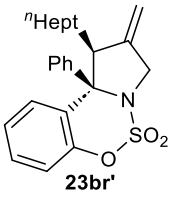

23br'

37% yield as a colourless oil. **^{1}H NMR** (500 MHz, $CDCl_3$) δ (ppm) 7.36 (dd, *J* = 7.7, 1.7 Hz, 1H), 7.24 (ddd, *J* = 7.6, 6.1, 1.8 Hz, 3H), 7.20 – 7.16 (m, 1H), 7.16 – 7.11 (m, 3H), 6.95 (dd, *J* = 8.1, 1.4 Hz, 1H), 4.90 (d, *J* = 1.8 Hz, 1H), 4.82 (d, *J* = 1.8 Hz, 1H), 4.33 – 4.16 (m, 1H), 4.06 – 3.92 (m, 1H), 2.95 (dd, *J* = 10.3, 3.3 Hz, 1H), 1.30 – 1.19 (m, 2H), 1.08 – 1.00 (m, 10H), 0.71 (t, *J* = 7.1 Hz, 3H). **^{13}C NMR** (126 MHz, $CDCl_3$) δ (ppm) 150.4 (C), 144.4 (C), 138.5 (C), 129.8 (CH), 128.4 (CH), 128.0 (CH), 128.0 (CH), 127.7 (CH), 126.5 (C), 125.2 (CH), 119.8 (CH), 109.0 (CH_2), 78.0 (C), 57.3 (CH), 54.3 (CH_2), 31.9 (CH_2), 30.2 (CH_2), 29.6 (CH_2), 29.3 (CH_2), 28.1 (CH_2), 22.7 (CH_2), 14.2 (CH_3). **HRMS** (APCI-TOF): m/z calculated for $C_{24}H_{30}NO_3S^+$ [M + H]$^+$: m/z 412.1941, found 412.1941. Stereochemistry of **23br'** was determined by nOe experiments.

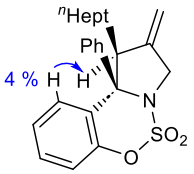

Figure 56. Significant nOe's observed for **23br'**.

Cycloaddition between 19c and 15e: Prepared following the procedure employed for the synthesis of the cycloadduct **16be**. Isomers **23ce** and **23ce'** are obtained in 52% combined yield. **23ce** could be independently isolated by column chromatography (1.5% EtOAc/Hexane).

2-Methylene-1-phenyl-1,2,3,10*b*-tetrahydrobenzo[*e*]pyrrolo[1,2-*c*][1,2,3]oxathiazine 5,5-dioxide (**23ce**)

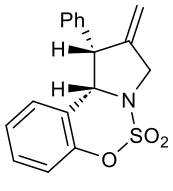

23ce

Yellowish oil. **^{1}H NMR** (500 MHz, $CDCl_3$) δ (ppm) 7.55 – 7.24 (m, 7H), 7.22 (td, *J* = 7.4, 1.2 Hz, 1H), 7.05 (dd, *J* = 8.3, 1.1 Hz ,1H), 5.31(d, J = 2.8 Hz, 1H), 5.16 (q, *J* = 2.1 Hz, 1H), 4.89 (q, *J* = 2.1 Hz, 1H), 4.34 (d, *J* = 15.4 Hz, 1H), 4.28 – 4.15 (m, 2H). **^{13}C NMR** (126 MHz, $CDCl_3$) δ (ppm) 150.5 (C), 145.7 (C), 141.3 (C), 129.7 (CH), 129.3 (CH), 127.8 (CH), 127.8 (CH), 127.1 (CH), 126.0 (CH), 121.8 (C), 119.2 (CH), 111.5 (CH_2), 70.2 (CH), 58.3 (CH), 54.0 (CH_2). It contains hexane. **HRMS** (APCI-TOF): m/z calculated for $C_{17}H_{16}NO_3S^+$ [M + H]$^+$: m/z 314.0845, found 314.0845. Stereochemistry of **23ce** was determined by the comparation of coupling constants of ring fusion hydrogens of **23ce** and **23ce'**.

2-Methylene-1-phenyl-1,2,3,10*b*-tetrahydrobenzo[*e*]pyrrolo[1,2-*c*][1,2,3]oxathiazine 5,5-dioxide (**23ce+23ce'**)

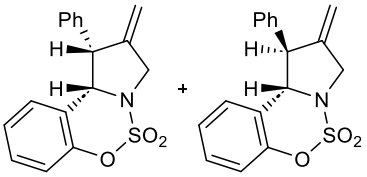

23ce+23ce' 2 : 1

Mixture of **23ce+23ce'** (2:1 ratio). Yellowish oil. **^{1}H NMR** (500 MHz, $CDCl_3$) δ (ppm) 7.55 – 7.37 (m, 3H), 7.36 – 7.30 (m, 1.33H), 7.29 – 7.24 (m, 1.33H), 7.22 (td, *J* = 7.4, 1.2 Hz, 0.66H), 7.20 (dd, *J* = 7.9, 2.1 Hz, 0.66H), 7.14 (dq, *J* = 7.2, 0.9 Hz, 0.33H), 7.08 (dd, *J* = 7.5, 2.1 Hz, 0.66H), 7.05 (dd, *J* = 8.3, 1.1 Hz, 0.66H), 6.97 (dd, *J* = 8.3, 1.2 Hz, 0.33H), 6.74 (td, *J* = 7.6, 1.2 Hz, 0.33H), 5.99 (d, *J* = 7.8 Hz, 0.33H), 5.37 (d, *J* = 7.9 Hz, 0.33H), 5.31 (d, *J* = 2.8 Hz, 0.66H), 5.21 (q, *J* = 2.4 Hz, 0.33H), 5.16 (q, *J* = 2.1 Hz, 0.66H), 4.98 (q, *J* = 2.5 Hz, 0.33H), 4.89 (q, *J* = 2.1 Hz, 0.66H), 4.66 – 4.59 (m, 0.33H), 4.39 – 4.37 (m, 0.66H), 4.34 (d, *J* = 15.4, 0.66H), 4.28 – 4.15 (m, 1.33H). **^{13}C NMR** (126 MHz, $CDCl_3$) δ (ppm) 151.4 (C), 150.5 (C), 145.7 (C), 144.8 (C), 141.3 (C), 136.4 (C), 130.9 (CH), 129.7 (CH), 129.5 (CH), 129.3 (CH), 129.2 (CH), 128.6 (CH), 128.1

(CH), 127.8 (CH), 127.8 (CH), 127.1 (CH), 126.0 (CH), 124.3 (CH), 121.8 (C), 119.1 (CH), 118.9 (C), 118.8 (CH), 111.5 (CH_2), 110.4 (CH_2), 70.2 (CH), 67.0 (CH), 58.2 (CH), 55.3 (CH), 54.0 (CH_2), 53.9 (CH_2). **HRMS** (APCI-TOF): m/z calculated for $C_{17}H_{16}NO_3S^+$ [M + H]$^+$: m/z 314.0845, found 314.0845. Stereochemistry of **23ce'** was determined by comparison with other analogs.

2-(4-Fluorophenyl)-3,3-dihexyl-4-methylene-1-tosylpyrrolidine (**23dc**)

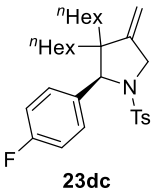

23dc

Prepared following the procedure employed for the synthesis of the cycloadduct **16be**, using ACP **19d** and imine **15c** as starting materials. Isolated by column chromatography (0.5% EtOAc/Hexane) as a yellowish oil in 95% yield. **^{1}H NMR** (500 MHz, $CDCl_3$) δ (ppm) 7.38 (d, *J* = 8.3 Hz, 2H), 7.12 (d, *J* = 8.1 Hz, 2H), 7.03 – 6.98 (m, 2H), 6.84 (t, *J* = 8.7 Hz, 2H), 5.12 (s, 1H), 4.82 (s, 1H), 4.55 (s, 1H), 4.19 (dt, *J* = 13.5, 2.3 Hz, 1H), 4.01 (d, *J* = 13.5 Hz, 1H), 2.36 (s, 3H), 1.50 – 1.32 (m, 2H), 1.30 – 1.20 (m, 3H), 1.20 – 0.90 (m, 14H), 0.87 (t, *J* = 7.2 Hz, 3H), 0.77 (t, *J* = 7.3 Hz, 3H), 0.65 – 0.52 (m, 1H). **^{13}C NMR** (126 MHz, $CDCl_3$) δ (ppm) 162.2 (d, *J* = 245.8 Hz, C), 149.6 (C), 143.1 (C), 135.9 (C), 135.8 (m, C) 129.7 (m, CH), 129.3 (CH), 127.2 (CH), 114.8 (d, *J* = 21.6 Hz, CH), 108.3 (CH_2), 72.8 (CH), 53.0 (C), 52.0 (CH_2), 35.0 (CH_2), 31.8 (CH_2), 31.4 (CH_2), 29.7 (CH_2), 29.6 (CH_2), 29.4 (CH_2), 23.3 (CH_2), 23.3 (CH_2), 22.8 (CH_2), 22.5 (CH_2), 21.5 (CH_3), 14.2 (CH_3), 14.1 (CH_3). **^{19}F NMR** (282 MHz, $CDCl_3$) δ (ppm) -115.3 (s). **HRMS** (APCI-TOF): m/z calculated for $C_{30}H_{42}FNO_2S^+$ [M + H]$^+$: m/z 500.2993, found 500.2996.

(3,3-Dihexyl-4-methylene-2-phenylpyrrolidin-1-yl)(phenyl)methanone (**23dd**)

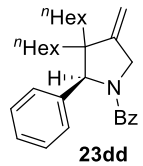

23dd

Prepared following the procedure employed for the synthesis of the cycloadduct **16be**, using ACP **19d** and imine **15d** as starting materials. Isolated by column chromatography (1-2% EtOAc/Hexane) as a colourless oil in 90% yield. **^{1}H NMR** (300 MHz, $CDCl_3$) δ (ppm) 7.65 – 7.20 (m, 7H), 7.10 (d, *J* = 7.5 Hz, 1.5H), 6.86 (d, *J* = 6.9 Hz, 1.5H), 5.34 (s, 1H), 5.17 (s, 0.26H), 5.12 – 4.90 (m, 1H), 4.76 (d, *J* = 16.8 Hz, 0.74H), 4.55 – 4.38 (m, 1.74H), 4.28 (d, *J* = 14.9 Hz, 0.26H), 1.68 (td, *J* = 11.8, 5.8 Hz, 1H), 1.59 – 0.93 (m, 21H), 0.84 (t, *J* = 7.1 Hz, 3H), 0.60 (t, *J* = 12.9 Hz, 1H). **^{13}C NMR** (75 MHz, $CDCl_3$) δ (ppm) 171.6 (C), 150.9 (C), 149.2 (C), 140.6 (C), 137.1 (C), 129.8 (CH), 129.4 (CH), 128.4 (CH), 128.1 (CH), 128.1 (CH), 127.6 (CH), 127.5 (CH), 127.3 (CH), 126.9 (CH), 126.8 (CH), 108.3 (CH_2), 107.5 (CH_2), 74.1 (CH), 70.4 (CH), 54.5 (CH_2), 53.6 (C), 51.6 (CH_2), 36.1 (CH_2), 35.8 (CH_2), 31.9 (CH_2), 31.4 (CH_2), 30.1 (CH_2), 29.8 (CH_2), 29.7 (CH_2), 29.6 (CH_2), 23.7 (CH_2), 23.5 (CH_2), 22.8 (CH_2), 22.5 (CH_2), 14.2 (CH_3), 14.0 (CH_3). **HRMS** (APCI-TOF): m/z calculated for $C_{30}H_{42}NO^+$ [M + H]$^+$: m/z 432.3261, found 432.3260.

1,1-Dihexyl- 2-methylene- 1,2,3,10*b*- tetrahydrobenzo [*e*]pyrrolo[1,2-*c*] [1,2,3] oxathiazine 5,5-dioxide (**23de**)

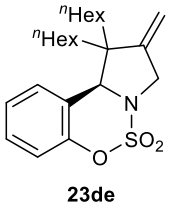

23de

Prepared following the procedure employed for the synthesis of the cycloadduct **16be**, using ACP **19d** and imine **15e** as starting materials. Isolated by column chromatography (0.5-1.5% EtOAc/Hexane) as a colourless oil in 98% yield. **^{1}H NMR** (500 MHz, $CDCl_3$) δ (ppm) 7.36 – 7.29 (m, 1H), 7.22 (td, *J* = 7.6, 1.3 Hz, 1H), 7.11 (dt, *J* = 7.6, 1.2 Hz, 1H), 7.07 (dd, *J* = 8.2, 1.2 Hz, 1H), 5.26 – 5.17 (m, 1H), 4.98 (s, 1H), 4.90 – 4.84 (m, 1H), 4.35 – 4.24 (m, 1H), 4.11 – 4.04 (m, 1H), 1.92 – 1.76 (m, 1H), 1.72 – 1.57 (m, 1H), 1.50 – 1.23 (m, 10H), 1.21 – 1.13 (m, 2H), 1.12 – 0.95 (m, 6H), 0.97 – 0.88 (m, 3H), 0.81 (t, *J* = 7.2 Hz, 3H). **^{13}C NMR** (126 MHz, $CDCl_3$) δ (ppm) 151.5 (C), 145.6 (C), 129.3 (CH), 126.8 (CH), 125.6 (CH), 121.7 (C), 119.5 (CH), 108. (CH_2), 67.3 (CH), 54.0 (C), 53.5 (CH_2), 35.2 (CH_2), 34.0 (CH_2), 31.9 (CH_2), 31.8 (CH_2), 30.2 (CH_2), 29.7 (CH_2), 23.9 (CH_2), 23.7 (CH_2), 22.8 (CH_2), 22.6 (CH_2), 14.2 (CH_3), 14.1 (CH_3). **HRMS** (APCI-TOF): m/z calculated for $C_{23}H_{36}NO_3S^+$ [M + H]$^+$: m/z 406.2410, found 406.2419.

1,1-Dihexyl-2-methylene-1,2,3,12*c*-tetrahydronaphtho[1,2-*e*]pyrrolo[1,2-*c*][1,2,3] oxathiazine 5,5-dioxide (**23df**)

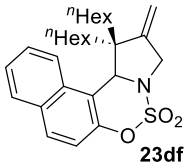

23df

Prepared following the procedure employed for the synthesis of the cycloadduct **16be**, using ACP **19d** and imine **15f** as starting materials. Isolated by column chromatography (1-2% EtOAc/Hexane) as a colourless oil in 95% yield. **^{1}H NMR** (500 MHz, $CDCl_3$) δ (ppm) 7.86 (dd, *J* = 7.5, 1.9 Hz, 1H), 7.84 – 7.79 (m, 2H), 7.57 – 7.48 (m, 2H), 7.19 (d, *J* = 8.9 Hz, 1H), 5.83 (s, 1H), 5.28 (s, 1H), 4.87 (s, 1H), 4.49 – 4.36 (m, 1H), 4.29 – 4.08 (m, 1H), 1.82 – 1.65 (m, 2H), 1.65 – 1.57 (m, 2H), 1.46 – 1.33 (m, 6H), 1.21 – 1.11 (m, 1H), 1.10 – 1.00 (m, 2H), 0.98 – 0.92 (m, 3H), 0.92 – 0.67 (m, 9H), 0.65 – 0.50 (m, 1H). **^{13}C NMR** (126 MHz, $CDCl_3$) δ (ppm) 150.2 (C), 146.0 (C), 131.7 (C), 131.3 (C), 130.4 (CH), 129.1 (CH), 126.7 (CH), 125.7 (CH), 123.4 (CH), 118.9 (CH), 117.0 (C), 108.3 (CH_2), 67.1 (CH), 55.4 (C), 55.4 (CH_2), 36.2 (CH_2), 35.0 (CH_2), 31.7 (CH_2), 31.5 (CH_2), 29.9 (CH_2), 29.4 (CH_2), 23.6 (CH_2), 23.6 (CH_2), 22.7 (CH_2), 22.4 (CH_2), 14.1 (CH_3), 13.9 (CH_3). **HRMS** (APCI-TOF): m/z calculated for $C_{27}H_{38}NO_3S^+$ $[M + H]^+$: m/z 456.2567, found 456.2565.

1,1-Dihexyl-2-methylene- 1,2,3,8,9,12,13,14*b*- octahydro- 7*H*,11*H*-pyrido [3,2,1-*ij*] pyrrolo[1',2':3,4][1,2,3]oxathiazino[6,5-*f*]quinoline 5,5-dioxide (**23dg**)

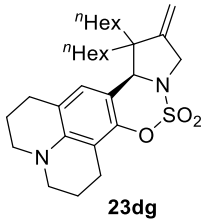

23dg

Prepared following the procedure employed for the synthesis of the cycloadduct **16be**, using ACP **19d** and imine **15g** as starting materials. Reaction carried out for 48 h. Isolated by column chromatography (1.5-2% EtOAc/Hexane) as a red oil in 75% yield. **^{1}H NMR** (500 MHz, $CDCl_3$) δ (ppm) 6.47 (s, 1H), 5.17 (s, 1H), 4.85 (s, 1H), 4.80 (s, 1H), 4.43 – 4.16 (m, 1H), 4.15 – 3.94 (m, 1H), 3.36 – 2.99 (m, 4H), 2.86 – 2.47 (m, 4H), 2.23 – 1.85 (m, 4H), 1.85 – 1.69 (m, 1H), 1.68 – 1.50 (m, 1H), 1.48 – 0.99 (m, 18H), 0.98 – 0.90 (m, 3H), 0.86 (t, *J* = 6.8 Hz, 3H). **^{13}C NMR** (126 MHz, $CDCl_3$) δ (ppm) 147.7 (C), 146.4 (C), 143.3 (C), 123.9 (CH), 118.3 (C), 110.9 (C), 107.7 (CH_2), 107.0 (C), 67.5 (CH), 53.7 (C), 53.3 (CH_2), 49.7 (CH_2), 49.2 (CH_2), 34.2 (CH_2), 33.6 (CH_2), 31.8 (CH_2), 31.7 (CH_2), 30.0 (CH_2), 29.7 (CH_2), 27.5 (CH_2), 23.7 (CH_2), 23.5 (CH_2), 22.6 (CH_2), 22.6 (CH_2), 21.8 (CH_2), 21.0 (CH_2), 20.7 (CH_2), 14.0 (CH_3). **HRMS** (APCI-TOF): m/z calculated for $C_{29}H_{45}N_2O_3S^+$ $[M + H]^+$:m/z 501.3145, found 501.3145.

5,5-Dihexyl-6- methylene-4*b*,5,6,7- tetrahydrodibenzo [*d*,*f*]pyrrolo[1,2-*b*][1,2] thiazepine 9,9-dioxide (**23di**)

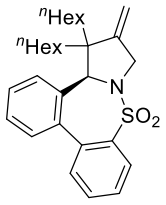

23di

Prepared following the procedure employed for the synthesis of the cycloadduct **16be**, using ACP **19d** and imine **15i** as starting materials. The crude mixture was washed with $NaBH_4$ to eliminate the dba from $Pd_2(dba)_3$ and extracted with Et_2O. After concentrating the organic phases, the crude residue was purified by column chromatography (2% EtOAc/Hexane) to yield **23di** as a colourless oil in 95% yield. **^{1}H NMR** (500 MHz, $CDCl_3$) δ (ppm) 7.92 (dd, *J* = 7.8, 1.4 Hz, 1H), 7.60 (td, *J* = 7.6, 1.4 Hz, 1H), 7.52 (dd, *J* = 7.7, 1.2 Hz, 1H), 7.48 – 7.43 (m, 1H), 7.42 – 7.33 (m, 3H), 7.20 – 7.11 (m, 1H), 5.16 – 5.08 (m, 1H), 5.03 (s, 1H), 4.76 – 4.68 (m, 1H), 4.08 – 3.94 (m, 1H), 3.81 – 3.70 (m, 1H), 1.61 – 1.47 (m, 1H), 1.42 – 1.04 (m, 12H), 0.91 (t, *J* = 6.8 Hz, 3H), 0.89 – 0.81 (m, 4H), 0.78 (t, *J* = 7.4 Hz, 3H), 0.74 – 0.65 (m, 1H), 0.58 (d, *J* = 4.7 Hz, 1H), 0.45 – 0.35 (m, 1H). **^{13}C NMR** (126 MHz, $CDCl_3$) δ (ppm) 144.5 (C), 139.2 (C), 138.8 (C), 137.1 (C), 134.3 (C), 131.9 (CH), 131.5 (CH), 130.7 (CH), 129.5 (CH), 127.5 (CH),127.5 (CH), 127.4 (CH), 125.7 (CH), 107.4 (CH_2), 71.5 (CH), 53.4 (C), 51.6 (CH_2), 32.7 (CH_2), 30.7 (CH_2), 30.3 (CH_2), 29.6 (CH_2), 29.2 (CH_2), 28.3 (CH_2), 22.4 (CH_2), 21.7 (CH_2), 21.6 (CH_2), 21.6 (CH_2), 21.5 (CH_2), 13.1 (CH_3), 13.0 (CH_3). **HRMS** (APCI-TOF): m/z calculated for $C_{29}H_{40}NO_2S^+$ $[M + H]^+$: m/z 466.2774, found 466.2771.

3,3-Dihexyl-4-methylene-2-(4-nitrophenyl)-1-tosylpyrrolidine (**23dj**)

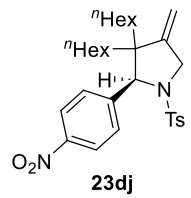

23dj

Prepared following the procedure employed for the synthesis of the cycloadduct **16be**, using ACP **19d** and imine **15j** as starting materials. Isolated by column chromatography (5% EtOAc/Hexane) as a yellowish oil in 70% yield. **^{1}H NMR** (500 MHz, $CDCl_3$) δ (ppm) 8.06 (d, *J* = 8.9 Hz, 2H), 7.49 (d, *J* = 8.2 Hz, 2H), 7.27 (d, *J* = 8.2 Hz, 2H), 7.18 (d, *J* = 8.0 Hz, 2H), 5.21 (s, 1H), 4.87 (s, 1H), 4.62 (s, 1H), 4.32 – 4.15 (m, 1H), 4.15 – 3.95 (m, 1H), 2.39 (s, 3H), 1.47 – 1.37 (m, 2H), 1.30 – 1.22 (m, 2H), 1.21 – 0.92 (m, 15H), 0.89 (t, *J* = 7.3 Hz, 3H), 0.78 (t, *J* = 7.3 Hz, 3H), 0.60 – 0.45 (m, 1H). **^{13}C NMR** (126 MHz, $CDCl_3$) δ (ppm) 148.7 (C), 147.7 (C), 147.3 (C), 143.7 (C), 135.4 (C), 129.6 (CH), 128.9 (CH), 127.2 (CH), 123.3 (CH), 109.1 (CH_2), 72.4 (CH), 53.4 (C), 52.2 (CH_2), 34.9 (CH_2), 31.7 (CH_2), 31.4 (CH_2), 29.6 (CH_2), 29.5 (CH_2), 29.5 (CH_2), 23.5 (CH_2), 23.2 (CH_2), 22.8 (CH_2), 22.5 (CH_2), 21.5 (CH_3), 14.2 (CH_3), 14.0 (CH_3). **HRMS** (APCI-TOF): m/z calculated for $C_{30}H_{43}N_2O_4S^+$ $[M + H]^+$: m/z 527.2938, found 527.2936.

Methyl 4-(3,3-dihexyl-4-methylene-1-tosylpyrrolidin-2-yl)benzoate (**23dk**)

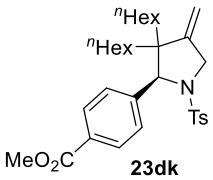

23dk

Prepared following the procedure employed for the synthesis of the cycloadduct **16be**, using ACP **19d** and imine **15k** as starting materials. Isolated by column chromatography (7% EtOAc/Hexane) as a colourless oil in 99% yield. **^{1}H NMR** (500 MHz, $CDCl_3$) δ (ppm) 7.82 (d, *J* = 8.0 Hz, 2H), 7.40 (d, *J* = 8.1 Hz, 2H), 7.14 – 7.05 (m, 4H), 5.14 (s, 1H), 4.81 (s, 1H), 4.59 (s, 1H), 4.21 (d, *J* = 13.5 Hz, 1H), 4.06 (d, *J* = 13.4 Hz, 1H), 3.90 (s, 3H), 2.34 (s, 3H), 1.48 – 1.31 (m, 2H), 1.28 – 1.19 (m, 3H), 1.18 – 0.90 (m, 14H), 0.87 (t, *J* = 7.3 Hz, 3H), 0.75 (t, *J* = 7.3 Hz, 3H), 0.52 (td, *J* = 13.3, 2.8 Hz, 1H). **^{13}C NMR** (126 MHz, $CDCl_3$) δ (ppm) 166.8 (C), 149.1 (C), 145.0 (C), 143.1 (C), 135.5 (C), 129.2 (CH), 129.2 (CH), 128.0 (CH), 127.0 (CH), 108.4 (CH_2), 72.8 (CH), 53.1 (C), 52.0 (CH_2), 52.0 (CH_3), 34.8 (CH_2), 31.6 (CH_2), 31.2 (CH_2), 29.5 (CH_2), 29.4 (CH_2), 29.2 (CH_2), 23.3 (CH_2), 23.1 (CH_2), 22.6 (CH_2), 22.3 (CH_2), 21.3 (CH3), 14.0 (CH_3), 13.9 (CH_3). **HRMS** (APCI-TOF): m/z calculated for $C_{32}H_{46}NO_4S^+$ $[M + H]^+$: m/z 540.3142, found 540.3141.

4-(3,3-Dihexyl-4-methylene-1-tosylpyrrolidin-2-yl)benzaldehyde (**23dl**)

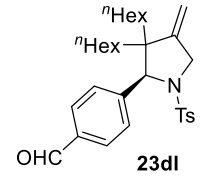

23dl

Prepared following the procedure employed for the synthesis of the cycloadduct **16be**, using ACP **19d** and imine **15l** as starting materials. Isolated by column chromatography (20% EtOAc/Hexane) as a colourless oil in 83% yield. **^{1}H NMR** (500 MHz, $CDCl_3$) δ (ppm) 9.97 (s, 1H), 7.69 (d, *J* = 7.9 Hz, 2H), 7.43 (d, *J* = 8.1 Hz, 2H), 7.23 (d, *J* = 7.7 Hz, 2H), 7.12 (d, *J* = 8.0 Hz, 2H), 5.16 (d, *J* = 1.7 Hz, 1H), 4.83 (d, *J* = 2.0 Hz, 1H), 4.59 (s, 1H), 4.28 – 4.15 (m, 1H), 4.13 – 3.94 (m, 1H), 2.34 (s, 3H), 1.49 – 1.31 (m, 2H), 1.32 – 1.20 (m, 3H), 1.19 – 0.90 (m, 14H), 0.87 (t, *J* = 7.3 Hz, 3H), 0.74 (t, *J* = 7.3 Hz, 3H), 0.58 – 0.44 (m, 1H). **^{13}C NMR** (126 MHz, $CDCl_3$) δ (ppm) 191.8 (CH), 148.9 (C), 146.9 (C), 143.2 (C), 135.5 (C), 135.4 (C), 129.3 (CH), 129.3 (CH), 128.7 (CH), 127.0 (CH), 108.6 (CH_2), 72.8 (CH), 53.2 (C), 52.1 (CH_2), 34.8 (CH_2), 31.5 (CH_2), 31.2 (CH_2), 29.5 (CH_2), 29.4 (CH_2), 29.3 (CH_2), 23.3 (CH_2), 23.1 (CH_2), 22.6 (CH_2), 22.3 (CH_2), 21.4 (CH_3), 13.4 (CH_3) 13.9 (CH_3). **HRMS** (APCI-TOF): m/z calculated for $C_{31}H_{44}NO_3S^+$ $[M + H]^+$: m/z 510.3036, found 510.3038.

3,3-Dihexyl-2-(4-methoxyphenyl)-4-methylene-1-tosylpyrrolidine (**23dm**)

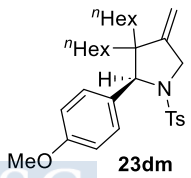

23dm

Prepared following the procedure employed for the synthesis of the cycloadduct **16be**, using ACP **19d** and imine **15m** as starting materials. Purified by column chromatography (3% EtOAc/Hexane) as a colourless oil in 98% yield. **^{1}H NMR** (300 MHz, $CDCl_3$) δ (ppm) 7.36 (d, *J* = 8.2 Hz, 2H), 7.09 (d, *J* = 8.0 Hz, 2H), 6.93 (d, *J* = 8.2 Hz, 2H), 6.66 (d, *J* = 8.4 Hz, 2H), 5.10 (s, 1H), 4.80 (s, 1H), 4.53 (s, 1H), 4.29 – 4.12 (m, 1H), 3.99 (d, *J* = 13.4 Hz, 1H), 3.76 (s, 3H), 2.34 (s, 3H), 1.53 – 0.93 (m, 19H), 0.87 (t, *J* = 7.1 Hz, 3H), 0.77 (t, *J* = 7.2 Hz, 3H), 0.62 (t, *J* = 12.3 Hz, 1H). **^{13}C NMR** (75 MHz, $CDCl_3$) δ (ppm) 158.8 (C), 149.9 (C), 142.5 (C), 136.0 (C), 131.9 (C), 129.2 (CH), 129.0 (CH) 127.1 (CH), 113.2 (CH), 107.7 (CH_2), 72.9 (CH), 55.2 (CH_3), 52.9 (C), 51.8 (CH_2), 34.9 (CH_2),

31.6 (CH_2), 31.3 (CH_2), 29.6 (CH_2), 29.5 (CH_2), 29.3 (CH_2), 23.2 (CH_2), 23.2 (CH_2), 22.6 (CH_2), 22.4 (CH_2), 21.4 (CH_3), 14.0 (CH_3), 13.9 (CH_3). **HRMS** (APCI-TOF): m/z calculated for $C_{31}H_{46}NO_3S^+$ $[M + H]^+$: m/z 512.3193, found 512.3191.

2-(Furan-2-yl)-3,3-dihexyl-4-methylene-1-tosylpyrrolidine (**23dn**)

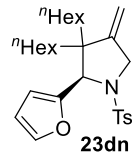

23dn

Prepared following the procedure employed for the synthesis of the cycloadduct **16be**, using ACP **19d** and imine **15n** as starting materials. Purified by column chromatography (1.5-2% EtOAc/Hexane) as a colourless oil in 99% yield. **^{1}H NMR** (500 MHz, $CDCl_3$) δ (ppm) 7.39 (d, *J* = 8.1 Hz, 2H), 7.13 (d, *J* = 8.0 Hz, 2H), 7.03 (d, *J* = 1.8 Hz, 1H), 6.17 (dd, *J* = 3.3, 1.8 Hz, 1H), 6.10 (d, *J* = 3.2 Hz, 1H), 5.01 (s, 1H), 4.75 (s, 1H), 4.72 (s, 1H), 4.19 (d, *J* = 13.2 Hz, 1H), 3.95 (d, *J* = 13.2 Hz, 1H), 2.35 (s, 3H), 1.55 – 1.40 (m, 2H), 1.35 – 1.01 (m, 16H), 0.99 – 0.90 (m, 1H), 0.88 (t, *J* = 7.2 Hz, 3H), 0.82 (t, *J* = 7.2 Hz, 3H), 0.60 – 0.47 (m, 1H). **^{13}C NMR** (126 MHz, $CDCl_3$) δ (ppm) 152.6 (C), 149.6 (C), 142.6 (C), 141.5 (CH), 135.7 (C), 129.2 (CH), 127.0 (CH), 109.7 (CH), 108.6 (CH), 106.9 (CH_2), 66.3 (CH), 53.1 (C), 51.3 (CH_2), 34.6 (CH_2), 31.7 (CH_2), 31.4 (CH_2), 29.8 (CH_2), 29.8 (CH_2), 29.4 (CH_2), 23.8 (CH_2), 23.3 (CH_2), 22.6 (CH_2), 22.5 (CH_2), 21.4 (CH_3), 14.0 (CH_3), 14.0 (CH_3). **HRMS** (APCI-TOF): m/z calculated for $C_{28}H_{42}NO_3S^+$ $[M + H]^+$: m/z 472.2880, found 472.2880.

1,1-Dihexyl-2-methylene-10*b*-(trifluoromethyl)-1,2,3,10*b*-tetrahydrobenzo[*e*]pyrrolo [1,2-*c*][1,2,3]oxathiazine 5,5-dioxide (**23dp**)

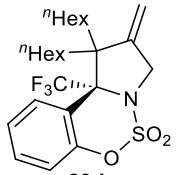

23dp

Prepared following the procedure employed for the synthesis of the cycloadduct **16be**, using ACP **19d** and imine **15p** as starting materials. Isolated by column chromatography (0.5% EtOAc/Hexane) as a yellowish oil in 60% yield. **^{1}H NMR** (500 MHz, $CDCl_3$) δ (ppm) 7.67 (d, *J* = 8.1 Hz, 1H), 7.43 – 7.34 (m, 1H), 7.26 – 7.21 (m, 1H), 7.07 (dd, *J* = 8.1, 1.4 Hz, 1H), 5.11 (s, 1H), 4.97 (s, 1H), 4.45 – 4.36 (m, 1H), 4.19 – 4.04 (m, 1H), 1.79 – 1.69 (m, 2H), 1.32 – 0.77 (m, 22H), 0.74 (t, *J* = 7.2 Hz, 2H). **^{13}C NMR** (126 MHz, $CDCl_3$) δ (ppm) 151.8 (C), 146.0 (C), 131.3 (CH), 128.3 (CH, m), 126.1 (CH), 125.1 (C, q, *J*=288.8 Hz), 120.5 (CH), 118.7 (C), 108.7 (CH_2), 79.6 (C, q, *J*=26.9 Hz), 56.8 (C), 55.0 (CH_2), 31.7 (CH_2), 31.7 (CH_2), 31.1 (CH_2), 30.8 (CH_2), 30.8 (CH_2), 29.5 (CH_2), 24.0 (CH_2), 23.2 (CH_2), 22.8 (CH_2), 22.6 (CH_2), 14.2 (CH_3), 14.1 (CH_3). **^{19}F NMR** (282 MHz, $CDCl_3$) δ (ppm) -68.5 (s). **HRMS** (APCI-TOF): m/z calculated for $C_{24}H_{35}F_3NO_3S^+$ $[M + H]^+$:m/z 474.2284, found 474.2281.

Methyl 1,1-dihexyl-2-methylene-2,3-dihydrobenzo[*e*]pyrrolo[1,2-*c*][1,2,3]oxathiazine-10*b*(1*H*)-carboxylate 5,5-dioxide (**23dq**)

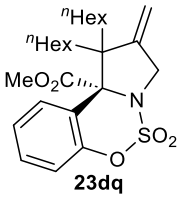

23dq

Prepared following the procedure employed for the synthesis of the cycloadduct **16be**, using ACP **19d** and imine **15q** as starting materials. Isolated by column chromatography (1.5-2% EtOAc/Hexane) as a colourless oil in 43% yield. **^{1}H NMR** (300 MHz, $CDCl_3$) δ (ppm) 7.78 (dd, *J* = 8.1, 1.7 Hz, 1H), 7.37 (td, *J* = 7.8, 1.7 Hz, 1H), 7.26 (td, *J* = 7.6, 1.5 Hz, 1H), 7.03 (dd, *J* = 8.2, 1.5 Hz, 1H), 5.17 (s, 1H), 4.92 (s, 1H), 4.53 – 4.27 (m, 2H), 3.76 (s, 3H), 1.90 – 1.62 (m, 2H), 1.51 – 1.01 (m, 18H), 0.98 – 0.87 (m, 3H), 0.83 (t, *J* = 7.0 Hz, 3H). **^{13}C NMR** (75 MHz, $CDCl_3$) δ (ppm) 170.9 (C), 151.2 (C), 146.0 (C), 131.0 (CH), 130.0 (CH), 124.4 (CH), 119.7 (C), 119.1 (CH), 108.8 (CH_2), 78.4 (C), 59.0 (C), 53.4 (CH_2), 52.9 (CH_3), 35.1 (CH_2), 33.2 (CH_2), 31.8 (CH_2), 31.7 (CH_2), 30.7 (CH_2), 29.7 (CH_2), 24.0 (CH_2), 23.8 (CH_2), 22.8 (CH_2), 22.6 (CH_2), 14.2 (CH_3), 14.1 (CH_3). **HRMS** (APCI-TOF): m/z calculated for $C_{25}H_{38}NO_5S^+$ $[M + H]^+$:m/z 464.2465, found 464.2462.

2-Methylene- 1,1-diphenyl- 1,2,3,10*b*- tetrahydrobenzo[*e*]pyrrolo [1,2-*c*][1,2,3] oxathiazine 5,5-dioxide (**23ee**)

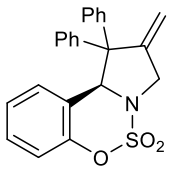

23ee

Prepared following the procedure employed for the synthesis of the cycloadduct **16be**, using ACP **19e** and imine **15e** as starting materials. Purified by column chromatography (0.5% EtOAc/Hexane) as a colourless solid in 58% yield. **^{1}H NMR** (500 MHz, $CDCl_3$) δ (ppm) 7.56 – 7.45 (m, 2H), 7.45 – 7.38 (m, 2H), 7.36 (d, *J* = 7.2 Hz, 1H), 7.25 – 7.17 (m, 2H), 7.16 – 7.10 (m, 2H), 6.96 (dd, *J* = 8.3, 1.2 Hz, 1H), 6.93 – 6.82 (m, 2H), 6.76 (td, *J* = 7.6, 1.3 Hz, 1H), 6.07 (d, *J* = 7.8 Hz, 1H), 5.85 (s, 1H), 5.38 (t, *J* = 2.1 Hz, 1H), 5.04 (t, *J* = 2.4 Hz, 1H), 4.50 (dt, *J* = 14.4, 2.2 Hz, 1H), 4.26 (dt, *J* = 14.4, 2.3 Hz, 1H). **^{13}C NMR** (126 MHz, $CDCl_3$) δ (ppm) 151.4 (C), 148.8 (C), 142.2 (C), 139.0 (C), 131.4 (CH), 129.3 (CH), 129.0 (CH), 128.8 (CH), 128.5 (CH) 127.5 (CH), 127.5 (CH), 127.5 (CH), 124.4 (CH), 119.9 (C), 119.0 (CH), 112.2 (CH_2), 70.8 (CH), 65.4 (C), 53.2 (CH_2). **HRMS** (APCI-TOF): m/z calculated for $C_{23}H_{20}NO_3S^+$ [M + H]$^+$: m/z 390.1157, found 390.1158. The structure of **23ee** was confirmed by X-ray analysis.

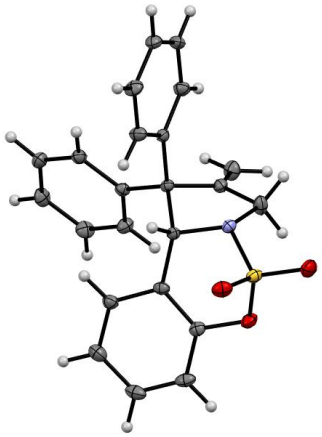

Figure 57. Crystal structure of **23ee** (**CCDC** 2401946).

Cycloaddition between 19f and 15e: Prepared following the procedure employed for the synthesis of the cycloadduct **16be**. Isomers **23fe** and **23fe'** are obtained in 90% combined yield. **23fe'** could be independently isolated by column chromatography (0.5-1.5% EtOAc/Hexane).

(1*S*,10*bR*)-1-Methyl-2-methylene-1-phenyl-1,2,3,10*b*-tetrahydrobenzo[*e*]pyrrolo[1,2-*c*][1,2,3] oxathiazine 5,5-dioxide (**23fe**)

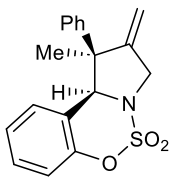

23fe

NMR data extracted from a **23fe:23fe'** mixture 1:1.7. Yellowish oil. **^{1}H NMR** (500 MHz, $CDCl_3$) δ (ppm) 7.19 – 7.09 (m, 4H), 7.07 – 7.01 (m, 2H), 6.89 (dd, *J* = 8.2, 1.2 Hz, 1H), 6.79 (td, *J* = 7.6, 1.3 Hz, 1H), 6.24 (dt, *J* = 7.8, 1.2 Hz, 1H), 5.21 (t, *J* = 2.2 Hz, 1H), 5.01 – 4.90 (m, 2H), 4.62 – 4.54 (m, 1H), 4.48 – 4.40 (m, 1H), 1.90 (s, 3H). **^{13}C NMR** (126 MHz, $CDCl_3$) δ (ppm) 151.8 (C), 151.0 (C), 141.0 (C), 129.2 (CH), 128.8 (CH), 127.9 (CH), 127.4 (CH), 126.7 (CH), 124.6 (CH), 120.2 (C), 118.9 (CH), 109.5 (CH_2), 74.2 (CH), 56.1 (C), 54.5 (CH_2), 28.0 (CH_3). **HRMS** (APCI-TOF): m/z calculated for $C_{18}H_{18}NO_3S^+$ [M + H]$^+$: m/z 328.1002, found 328.1001. Stereochemistry of **23fe** was determined by comparison with that of **23fe'**.

(1*S*,10*bS*)-1-Methyl-2-methylene-1-phenyl-1,2,3,10*b*-tetrahydrobenzo[*e*]pyrrolo[1,2-*c*][1,2,3] oxathiazine 5,5-dioxide (**23fe'**)

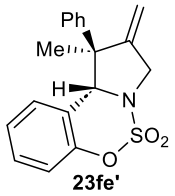

23fe'

^{1}H NMR (500 MHz, $CDCl_3$) δ (ppm) 7.46 – 7.39 (m, 4H), 7.37 – 7.33 (m, 1H), 7.30 – 7.27 (m, 1H), 7.06 (dd, *J* = 8.3, 1.2 Hz, 1H), 6.99 (td, *J* = 7.6, 1.2 Hz, 1H), 6.47 (dt, *J* = 7.8, 1.1 Hz, 1H), 5.29 (s, 1H), 5.16 (t, *J* = 2.0 Hz, 1H), 4.67 (t, *J* = 2.2 Hz, 1H), 4.63 – 4.45 (m, 1H), 4.40 – 4.24 (m, 1H), 1.27 (s, 3H). **^{13}C NMR** (126 MHz, $CDCl_3$) δ (ppm) 151.7 (C), 151.3 (C), 142.2 (C), 129.5 (CH), 128.9 (CH), 128.3 (CH), 127.7 (CH), 126.7 (CH), 125.4 (CH), 120.8 (C), 119.3 (CH), 110.1 (CH_2), 72.9 (CH), 55.5 (C), 53.1 (CH_2), 21.4 (CH_3). **HRMS** (APCI-TOF): m/z calculated for $C_{18}H_{18}NO_3S^+$ [M + H]$^+$: m/z 328.1002, found 328.1001. Stereochemistry of **23fe'** was determined by nOe experiments.

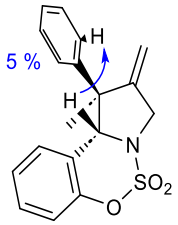

Figure 58. Significant nOe's observed for **23fe'**.

Cycloaddition between 19f and 15i: Prepared following the procedure employed for the synthesis of the cycloadduct **16be**. Isomers **23fi** and **23fi'** are obtained in 55% combined yield and can be easily separated by column chromatography (5-7% EtOAc/Hexane).

(4*bR*,5*R*)-5-Methyl-6-methylene-5-phenyl-4*b*,5,6,7-tetrahydrodibenzo[*d,f*]pyrrolo[1,2-*b*][1,2]thiazepine 9,9-dioxide (**23fi**)

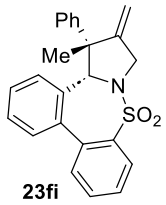

23fi

37% yield, white solid. **^{1}H NMR** (500 MHz, $CDCl_3$) δ (ppm) 7.70 (dd, *J* = 7.5, 1.6 Hz, 1H), 7.51 – 7.34 (m, 3H), 7.18 – 7.05 (m, 3H), 6.99 – 6.84 (m, 1H), 6.72 (dd, *J* = 8.4, 7.3 Hz, 2H), 6.43 (dd, *J* = 7.5, 1.4 Hz, 1H), 6.27 – 6.09 (m, 2H), 5.37 (t, *J* = 2.0 Hz, 1H), 5.13 (t, *J* = 2.3 Hz, 1H), 4.91 (s, 1H), 4.45 – 4.22 (m, 2H), 1.48 (s, 3H).**^{13}C NMR** (126 MHz, $CDCl_3$) δ (ppm) 151.0 (C), 141.7 (C), 141.1 (C), 138.1 (C), 137.6 (C), 134.5 (C), 132.6 (CH), 132.1 (CH), 131.0 (CH), 130.9 (CH), 129.0 (CH), 128.4 (CH), 127.7 (CH), 127.7 (CH), 127.5 (CH), 127.5 (CH), 126.4 (CH), 125.9 (CH), 125.2 (CH), 110.5 (CH_2), 78.3 (CH), 54.8 (CH_2), 54.6 (C), 26.1 (CH_3). **HRMS** (APCI-TOF): m/z calculated for $C_{24}H_{22}NO_2S^+$ [M + H]$^+$: m/z 388.1366, found 388.1367. Stereochemistry of **23fi** was determined by analogy with that of **23fe**.

(4*bS*,5*R*)-5-Methyl-6-methylene-5-phenyl-4*b*,5,6,7-tetrahydrodibenzo[*d,f*]pyrrolo[1,2-*b*][1,2]thiazepine 9,9-dioxide (**23fi'**)

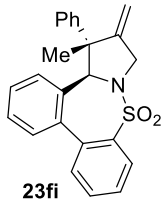

23fi

18% yield, white solid. **^{1}H NMR** (500 MHz, $CDCl_3$) δ (ppm) 7.70 (dd, *J* = 7.5, 1.6 Hz, 1H), 7.51 – 7.34 (m, 3H), 7.18 – 7.05 (m, 3H), 6.99 – 6.84 (m, 1H), 6.72 (dd, *J* = 8.4, 7.3 Hz, 2H), 6.43 (dd, *J* = 7.5, 1.4 Hz, 1H), 6.27 – 6.09 (m, 2H), 5.37 (t, *J* = 2.0 Hz, 1H), 5.13 (t, *J* = 2.3 Hz, 1H), 4.91 (s, 1H), 4.45 – 4.22 (m, 2H), 1.48 (s, 3H).**^{13}C NMR** (126 MHz, $CDCl_3$) δ (ppm) 152.1 (C), 141.9 (C), 139.4 (C), 139.3 (C), 138.3 (C), 134.1 (C), 133.2 (CH), 132.5 (CH), 132.0 (CH), 130.1 (CH), 128.4 (CH), 128.4 (CH), 128.1 (CH), 128.1 (CH), 127.1 (CH), 126.9 (CH), 126.7 (CH), 109.3 (CH_2), 78.9 (CH), 56.7 (C), 52.8 (CH_2), 21.4 (CH_3). **HRMS** (APCI-TOF): m/z calculated for $C_{24}H_{22}NO_2S^+$ [M + H]$^+$: m/z 388.1366, found 388.1367. Stereochemistry of **23fi'** was determined by analogy with that of **23fe'**.

Cycloaddition between 19f and 15p: Prepared following the procedure employed for the synthesis of the cycloadduct **16be**. Isomers **23fp** and **23fp'** are obtained in 70% combined yield (dr 1.2:1).

1-Methyl-2-methylene-1-phenyl-10*b*-(trifluoromethyl)-1,2,3,10*b*-tetrahydrobenzo[*e*]pyrrolo[1,2-*c*][1,2,3]oxathiazine 5,5-dioxide (**23fp** +**23fp'**)

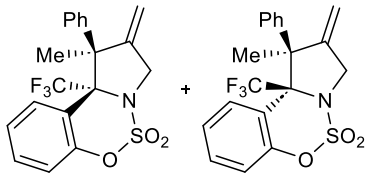

23fp:23fp' 1:1

Characterized as a **23fp :23fp'** mixture (1:1 ratio). **^{1}H NMR** (500 MHz, $CDCl_3$) δ (ppm) 7.69 (dd, *J* = 6.0, 3.7 Hz, 0.5H), 7.54 – 7.46 (m, 1H), 7.44 – 7.38 (m, 2H), 7.25 – 7.18 (m, 2H), 7.10 (d, *J* = 8.1 Hz, 0.5H), 7.04 – 6.93 (m, 1.5H), 6.83 – 6.78 (m, 1H), 6.64 – 6.59 (m, 0.5H), 5.34 (s, 0.5H), 5.28 (s, 0.5H), 5.19 – 5.13 (m, 0.5H), 5.13 (d, *J* = 14.7 Hz, 0.5H), 5.04 – 5.00 (m, 0.5H), 4.91 (d, *J* = 14.2 Hz, 0.5H), 4.62 (d, *J* = 14.7 Hz, 0.5H), 4.57 (d, *J* = 14.2 Hz, 0.5H), 1.88 (q, *J* = 2.5 Hz, 1.5H), 1.24 (s, 1.5H). **^{13}C NMR** (126 MHz, $CDCl_3$) δ (ppm) 151.1 (C), 150.2 (C), 149.9 (C), 147.9 (C), 141.4 (C), 135.6 (C), 131.3 (CH), 130.9 (CH), 128.3 (CH), 127.9 (CH), 127.5 (CH), 127.1 (CH), 127.0 (m, CH), 126.0 (CH), 125.9 (m, CH), 125.8 (CH), 125.3 (q, *J* = 290.9 Hz, C), 124.7 (q, *J* = 288.8 Hz), 119.9 (CH), 119.7 (CH), 118.5 (C), 118.2 (C), 108.8 (CH_2), 108.7 (CH_2), 78.7 (m, C), 58.7 (C), 58.6 (C), 56.9 (CH_2), 54.1 (CH_2), 26.1 (CH_3), 21.8 (m, CH_3). **^{19}F NMR** (282 MHz, $CDCl_3$) δ (ppm) -67.0 (s). **HRMS** (APCI-TOF): m/z calculated for $C_{19}H_{17}F_3NO_3S^+$ [M + H]$^+$: m/z 396.0876, found 396.0882. Stereochemistry of **23fp** and **23fp'** was deducted by comparison with analogue products.

Ethyl (1*S*,10*bR*)-2-methylene-1,2,3,10*b*-tetrahydrobenzo[*e*] pyrrolo[1,2-*c*][1,2,3] oxathiazine-1-carboxylate 5,5-dioxide (**23ge**)

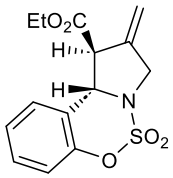

23ge

Prepared following the procedure employed for the synthesis of the cycloadduct **16be**, using ACP **19g** and imine **15e** as starting materials. Reaction carried out for 2 h. Isolated by column chromatography (7-10% EtOAc/Hexane) as a yellowish oil in 63% yield. **^{1}H NMR** (500 MHz, $CDCl_3$) δ (ppm) 7.30 – 7.23 (m, 1H), 7.17 (td, *J* = 7.5, 1.2 Hz, 1H), 7.14 – 7.09 (m, 1H), 6.97 (dd, *J* = 8.3, 1.2 Hz, 1H), 5.58 (s, 1H), 5.25 (q, *J* = 2.2 Hz, 1H), 5.16 (q, *J* = 2.1 Hz, 1H), 4.28 – 4.22 (m, 2H), 4.21 – 4.16 (m, 1H), 4.03 – 3.93 (m, 1H), 3.86 – 3.76 (m, 1H), 1.28 (t, *J* = 7.1 Hz, 3H). **^{13}C NMR** (126 MHz, $CDCl_3$) δ (ppm) 169.5 (C), 150.7 (C), 139.2 (C), 129.8 (CH), 126.8 (CH), 125.9 (CH), 120.1 (C), 119.1 (CH), 112.6 (CH_2), 65.6 (CH), 62.2 (CH_2), 56.7 (CH), 53.2 (CH_2), 14.1 (CH_3). **HRMS** (APCI-TOF): m/z calculated for $C_{17}H_{16}NO_3S^+$ [M + H]$^+$: m/z 314.0845, found 314.0845. Stereochemistry of **23ge** was determined by nOe experiments.

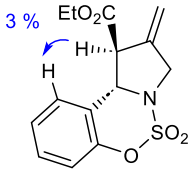

Figure 59. Significant nOe's observed for **23ge**.

Ethyl (4*bR*,5*R*)-6-methylene-4*b*,5,6,7-tetrahydrodibenzo[*d,f*]pyrrolo[1,2-*b*][1,2]thiazepine-5-carboxylate 9,9-dioxide (**23gi**)

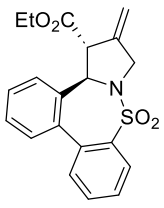

23gi

Prepared following the procedure employed for the synthesis of the cycloadduct **16be**, using ACP **19g** and imine **15i** as starting materials. Isolated by column chromatography (12% EtOAc/Hexane) as a white solid in 60%. Broad signals were detected in NMR at rt and 50 ºC due to the presence of rotamers. Therefore, compound **23gi** was characterized at -50 °C as a mixture 1.5:1 of rotamers. **^{1}H NMR** (500 MHz, $CDCl_3$) δ (ppm) 8.01 (d, *J* = 7.8 Hz, 0.4H), 7.91 (d, *J* = 7.7 Hz, 0.6H), 7.76 (t, *J* = 7.7 Hz, 0.4H), 7.72 (t, *J* = 7.6 Hz, 0.6H), 7.61 (t, *J* = 7.5 Hz, 1.4H), 7.56 – 7.38 (m, 4.6H), 5.24 (s, 0.4H), 5.19 (s, 0.4H), 5.08 (d, *J* = 11.0 Hz, 0.6H), 5.02 (s, 0.6H), 4.94 (s, 0.6H), 4.43 – 4.06 (m, 3.8H), 4.02 – 3.89 (m, 1H), 3.20 (d, *J* = 11.0 Hz, 0.6H), 1.24 (t, *J* = 7.2 Hz, 1.5H), 1.16 (t, *J* = 7.1 Hz, 1.5H). **^{13}C NMR** (126 MHz, $CDCl_3$) δ (ppm) 171.9 (C), 147.3 (C), 139.8 (C), 139.3 (C), 138.5 (C), 134.6 (C), 133.4 (CH), 132.8 (CH), 132.0 (CH), 130.8 (CH), 129.1 (CH), 129.0 (CH), 127.2 (CH), 126.8 (CH), 108.1 (CH_2), 72.6 (CH), 61.8 (CH_2), 59.4 (C), 52.6 (CH_2),

20.2 (CH_3), 14.3 (CH_3). **HRMS** (APCI-TOF): m/z calculated for $C_{20}H_{20}NO_4S^+$ $[M + H]^+$: m/z 370.1108, found 370.1108. Stereochemistry of **23gi** was determined by analogy with that of **23ge**.

Cycloaddition between 19h and 15e: Prepared following the procedure employed for the synthesis of the cycloadduct **16be**. Isomers **23he** and **23he'** are obtained in 97% combined yield and can be easily separated by column chromatography (3-5% EtOAc/Hexane).

(Ethyl (1*R*,10*bR*)-1-methyl- 2-methylene-1,2,3,10*b*- tetrahydrobenzo[*e*] pyrrolo[1,2-*c*][1,2,3]oxathiazine-1-carboxylate 5,5-dioxide (**23he**)

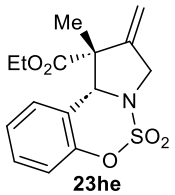

23he

60% yield as a yellowish oil. **^{1}H NMR** (500 MHz, $CDCl_3$) δ (ppm) 7.40 – 7.28 (m, 1H), 7.19 (t, *J* = 7.6 Hz, 1H), 7.07 (t, *J* = 7.8 Hz, 2H), 5.60 (s, 1H), 5.25 – 4.94 (m, 2H), 4.43 – 4.26 (m, 3H), 4.26 – 4.12 (m, 1H), 1.35 (t, *J* = 7.1 Hz, 3H), 1.22 (s, 3H). **^{13}C NMR** (126 MHz, $CDCl_3$) δ (ppm) 172.0 (C), 151.2 (C), 146.0 (C), 129.6 (CH), 127.1 (CH), 125.6 (CH), 119.9 (C), 119.2 (CH), 109.2 (CH_2), 68.1 (CH), 62.1 (CH_2), 57.2 (C), 52.0 (CH_2), 20.1 (CH_3), 14.1 (CH_3). **HRMS** (APCI-TOF): m/z calculated for $C_{15}H_{18}NO_5S^+$ $[M + H]^+$:m/z 324.0900, found 324.0901. Stereochemistry of **23he** was determined by nOe experiments.

(Ethyl (1*R*,10*bS*)-1-methyl-2-methylene-1,2,3,10*b*-tetrahydrobenzo[*e*]pyrrolo[1,2-*c*][1,2,3]oxathiazine-1-carboxylate 5,5-dioxide (**23he'**)

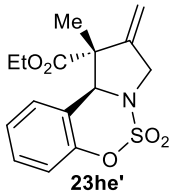

23he'

37% yield as a yellowish oil. **^{1}H NMR** (500 MHz, $CDCl_3$) δ (ppm) 7.41 – 7.28 (m, 1H), 7.20 – 7.12 (m, 2H), 7.05 (dd, *J* = 8.2, 1.1 Hz, 1H), 5.27 (s, 1H), 5.19 – 5.12 (m, 1H), 5.01 (s, 1H), 4.69 (dt, *J* = 12.3, 2.6 Hz, 1H), 4.37 – 4.16 (m, 1H), 3.86 – 3.69 (m, 1H), 3.54 – 3.41 (m, 1H), 1.70 (s, 3H), 0.90 (t, *J* = 7.2 Hz, 3H). **^{13}C NMR** (126 MHz, $CDCl_3$) δ (ppm) 171.0 (C), 151.0 (C), 146.0 (C), 129.6 (CH), 125.8 (CH), 125.7 (CH), 121.6 (C), 119.3 (CH), 110.2 (CH_2), 71.4 (CH), 61.6 (CH_2), 58.6 (C), 56.4 (CH_2), 22.1 (CH_3), 13.5 (CH_3). **HRMS** (APCI-TOF): m/z calculated for $C_{15}H_{18}NO_5S^+$ $[M + H]^+$:m/z 324.0900, found 324.0899. Stereochemistry of **23he'** was determined by nOe experiments.

Cycloaddition between 19h and 15i: Prepared following the procedure employed for the synthesis of the cycloadduct **16be**. Isomers **23hi** and **23hi'** are obtained in 63% combined yield and can be easily separated by column chromatography (10-15% EtOAc/Hexane).

Ethyl (4bS,5S)-5-methyl-6-methylene-4b,5,6,7-tetrahydrodibenzo[d,f]pyrrolo[1,2-b][1,2]thiazepine-5-carboxylate 9,9-dioxide (**23hi**)

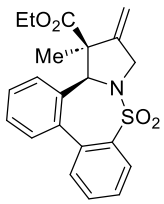

23hi

42% yield as a colourless oil. **^{1}H NMR** (500 MHz, $CDCl_3$) δ (ppm) 7.94 (d, *J* = 7.7 Hz, 1H), 7.63 (t, *J* = 7.6 Hz, 1H), 7.54 (d, *J* = 7.7 Hz, 1H), 7.47 – 7.38 (m, 3H), 7.35 (t, *J* = 7.5 Hz, 1H), 7.29 – 7.20 (m, 1H), 5.77 (s, 1H), 4.98 (s, 1H), 4.88 (s, 1H), 4.36 – 4.15 (m, 3H), 4.08 – 3.93 (m, 1H), 1.30 (t, *J* = 7.1 Hz, 3H), 0.69 (s, 3H). **^{13}C NMR** (126 MHz, $CDCl_3$) δ (ppm) 171.9 (C), 147.3 (C), 139.8 (C), 139.3 (C), 138.5 (C), 134.6 (C), 133.4 (CH), 132.8 (CH), 132.0 (CH), 130.8 (CH), 129.1 (CH), 129.0 (CH), 127.2 (CH), 126.8 (CH), 108.1 (CH_2), 72.6 (CH), 61.8 (CH_2), 59.4 (C), 52.6 (CH_2), 20.2 (CH_3), 14.3 (CH_3). **HRMS** (APCI-TOF): m/z calculated for $C_{21}H_{22}NO_4S^+$ $[M + H]^+$: m/z 384.1264, found 384.1264. Stereochemistry of **23hi** was determined analogy with that of **23he**.

Ethyl (4bS,5R)-5-methyl-6-methylene-4b,5,6,7-tetrahydrodibenzo[d,f]pyrrolo[1,2-b][1,2]thiazepine-5-carboxylate 9,9-dioxide (**23hi'**)

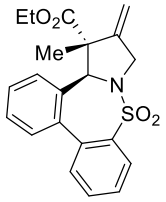

23hi'

21% yield as a colourless oil. **^{1}H NMR** (500 MHz, $CDCl_3$) δ (ppm) 7.94 (d, *J* = 7.7 Hz, 1H), 7.61 (t, *J* = 7.8 Hz, 1H), 7.55 (d, *J* = 7.7 Hz, 1H), 7.48 – 7.36 (m, 4H), 7.29 – 7.24 (m, 1H), 5.16 (s, 1H), 5.05 (s, 1H), 4.83 (s, 1H), 4.29 – 4.09 (m, 2H), 3.67 – 3.55 (m, 1H), 3.31 – 3.13 (m, 1H), 1.42 (s, 3H), 0.74 (t, *J* = 7.1 Hz, 3H). **^{13}C NMR** (126 MHz, $CDCl_3$) δ (ppm) 171.2 (C), 146.7 (C), 138.6 (C), 138.5 (C), 138.3 (C), 134.0 (C), 133.2 (CH), 132.8 (CH), 131.7 (CH), 130.6 (CH), 129.0 (CH), 128.5 (CH), 127.0 (CH), 126.8 (CH), 109.0 (CH_2), 76.5 (CH), 60.9 (CH_2), 57.2 (C), 54.6 (CH_2), 30.3 (CH), 29.7 (CH_2), 20.1 (CH_3), 13.3 (CH_3). **HRMS** (APCI-TOF): m/z calculated for $C_{21}H_{22}NO_4S^+$ [M + H]$^+$: m/z 384.1264, found 384.1264. Stereochemistry of **23hi'** was determined by analogy with that of **23he'**.

Cycloaddition between 19h and 15p: Prepared following the procedure employed for the synthesis of the cycloadduct **16be**. Isomers **23hp** and **23hp'** are obtained in 61% combined yield (dr 1.6:1) and can be easily separated by column chromatography (5-10% EtOAc/Hexane).

Ethyl (1*S*,10*bS*)-1-methyl-2-methylene-10*b*-(trifluoromethyl)-1,2,3,10*b*-tetrahydrobenzo[*e*]pyrrolo[1,2-*c*][1,2,3]oxathiazine-1-carboxylate 5,5-dioxide (**23hp**)

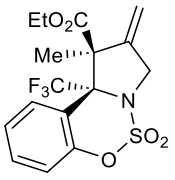

23hp

38% yield as a yellowish oil. **^{1}H NMR** (500 MHz, $CDCl_3$) δ (ppm) 7.66 (d, *J* = 8.1 Hz, 1H), 7.50 (td, *J* = 7.8, 1.5 Hz, 1H), 7.39 – 7.31 (m, 1H), 7.19 (d, *J* = 8.3 Hz, 1H), 5.28 (s, 2H), 4.66 (d, *J* = 14.0 Hz, 1H), 4.41 (d, *J* = 13.9 Hz, 1H), 4.39 – 4.32 (m, 1H), 4.32 – 4.24 (m, 1H), 1.36 (t, *J* = 7.2 Hz, 3H), 1.20 (s, 3H). **^{13}C NMR** (126 MHz, $CDCl_3$) δ (ppm) 169.4 (C), 150.9 (C), 143.3 (C), 131.7 (CH), 128.37 (CH, q, *J* = 3.1 Hz), 126.3 (CH), 124.21 (C, q, *J* = 288.5 Hz), 119.8 (CH), 117.6 (C), 110.4 (CH_2), 78.32 (C, q, *J* = 28.9 Hz), 62.4 (CH_2), 59.0 (C), 53.2 (CH_2), 24.6 (CH_3), 13.7 (CH_3). **^{19}F NMR** (282 MHz, $CDCl_3$) δ (ppm) -71.5 (s). **HRMS** (APCI-TOF): m/z calculated for $C_{16}H_{17}F_3NO_5S^+$ [M + H]$^+$: m/z 392.0761, found 392.0773. Stereochemistry of **23hp** was deduced by comparison with analogue products.

Ethyl (1*R*,10*bS*)-1-methyl-2-methylene-10*b*-(trifluoromethyl)-1,2,3,10*b*-tetrahydrobenzo[*e*]pyrrolo[1,2-*c*][1,2,3]oxathiazine-1-carboxylate 5,5-dioxide (**23hp'**)

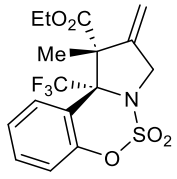

23hp'

23% yield as a yellowish oil. **^{1}H NMR** (300 MHz, $CDCl_3$) δ (ppm) 7.63 (d, *J* = 8.2 Hz, 1H), 7.50 – 7.40 (m, 1H), 7.30 (dd, *J* = 7.6, 1.4 Hz, 1H), 7.13 (dd, *J* = 8.2, 1.4 Hz, 1H), 5.26 (s, 1H), 5.19 (s, 1H), 4.97 – 4.85 (m, 1H), 4.48 – 4.34 (m, 1H), 3.78 (dq, *J* = 10.8, 7.2 Hz, 1H), 3.53 (dq, *J* = 10.8, 7.1 Hz, 1H), 1.74 (q, *J* = 2.6 Hz, 3H), 1.01 (t, *J* = 7.1 Hz, 3H). **^{13}C NMR** (126 MHz, $CDCl_3$) δ (ppm) 169.4 (C), 150.9 (C), 143.3 (C), 131.7 (CH), 128.37 (CH, q, *J* = 3.1 Hz), 126.3 (CH), 124.21 (C, q, *J* = 288.5 Hz), 119.8 (CH), 117.6 (C), 110.4 (CH_2), 78.32 (C, q, *J* = 28.9 Hz), 62.4 (CH_2), 59.0 (C), 53.2 (CH_2), 24.6 (CH_3), 13.7 (CH_3). **^{19}F NMR** (282 MHz, $CDCl_3$) δ (ppm) -69.8 (s). **HRMS** (APCI-TOF): m/z calculated for $C_{16}H_{17}F_3NO_5S^+$ [M + H]$^+$: m/z 392.0761, found 392.0773. Stereochemistry of **23hp'** was deduced by comparison with analogue products.

Cycloaddition between 19i and 15e: Prepared following the procedure employed for the synthesis of the cycloadduct **16be**. Isomers **23ie** and **23ie'** are obtained in 68% combined yield and can be easily separated by column chromatography (20-30% EtOAc/Hexane).

***N*-(((1*S*,10*bS*)-1-methyl -2-methylene-5,5-dioxido -1,2,3,10*b*- tetrahydrobenzo [*e*] pyrrolo[1,2-*c*][1,2,3]oxathiazin-1-yl)methyl)-4-nitrobenzenesulfonamide** (**23ie**)

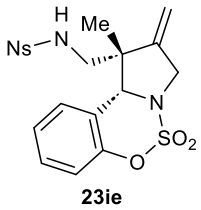

23ie

34% yield as a white solid. **^{1}H NMR** (500 MHz, $CDCl_3$) δ (ppm) 8.29 (d, *J* = 8.8 Hz, 2H), 7.79 (d, *J* = 8.8 Hz, 2H), 7.47 – 7.39 (m, 1H), 7.34 – 7.27 (m, 2H), 7.10 (d, *J* = 8.2 Hz, 1H), 5.34 (s, 1H), 5.23 (s, 1H), 4.75 (s, 1H), 4.42 – 4.20 (m, 2H), 4.11 (d, *J* = 13.4 Hz, 1H), 2.68 (dd, *J* = 12.9, 4.1 Hz, 1H), 2.60 (dd, *J* = 12.9, 9.1 Hz, 1H), 1.45 (s, 3H). **^{13}C NMR** (126 MHz, $CDCl_3$) δ (ppm) 150.9 (C), 150.1 (C), 145.5 (C), 145.5 (C), 130.3 (CH), 127.9 (CH), 126.6 (CH), 126.3 (CH), 124.5 (CH), 119.8 (CH),119.4 (C), 111.6 (CH_2), 70.1 (CH), 52.4 (CH_2), 50.3 (C), 46.0 (CH_2), 19.9 (CH_3). It contains grease. **HRMS** (APCI-TOF): m/z calculated for $C_{19}H_{20}N_3O_7S_2^+$ $[M + H]^+$: m/z 466.0737, found 324.0739. Stereochemistry of **23ie** was determined by comparison with its isomer **23ie'**.

***N*-(((1*S*,10*bR*)-1-methyl -2-methylene-5,5-dioxido- 1,2,3,10*b* -tetrahydrobenzo [*e*] pyrrolo[1,2-*c*][1,2,3]oxathiazin-1-yl)methyl)-4-nitrobenzenesulfonamide (23ie')**

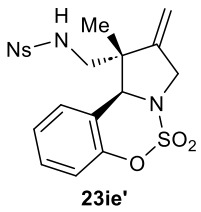

23ie'

34% yield as white solid. **^{1}H NMR** (300 MHz, $CDCl_3$) δ (ppm) 8.37 (t, *J* = 9.4 Hz, 2H), 8.10 (t, *J* = 8.4 Hz, 2H), 7.38 – 7.30 (m, 1H), 7.28 – 7.17 (m, 2H), 7.06 (d, *J* = 8.1 Hz, 1H), 5.32 – 5.19 (m, 1H), 5.15 (s, 1H), 5.09 (s, 1H), 4.91 (s, 1H), 4.35 – 4.24 (m, 1H), 4.19 – 4.02 (m, 2H), 3.30 – 3.12 (m, 1H), 2.04 (s, 3H). **HRMS** (APCI-TOF): m/z calculated for $C_{19}H_{20}N_3O_7S_2^+$ $[M + H]^+$: m/z 466.0737, found 324.0739. Structure of **23ie'** was confirmed by X-ray analysis.

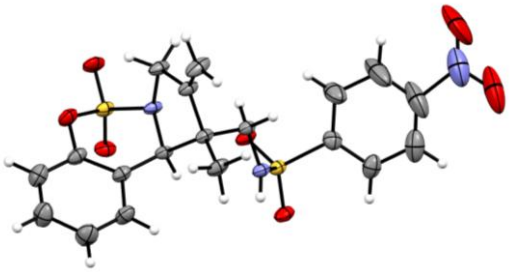

Figure 60. Crystal structure of **23ie'** (**CCDC** 2402103).

Ethyl (4*R*,5*R*)-3-methylene-5-phenyl-1-tosyl-1,2,3,4,5,6-hexahydroindeno[1,2-*b*]azepine-4-carboxylate (24gs)

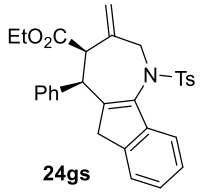

24gs

Prepared following the procedure employed for the synthesis of the cycloadduct **16be**, using ACP **19g** and imine **15s** as starting materials. Reaction carried out at 70 ºC. Isolated by column chromatography (10% EtOAc/Hexane) as a yellow oil in 46% yield, dr 1:0. **^{1}H NMR** (300 MHz, $CDCl_3$) δ (ppm) 7.75 – 7.63 (m, 3H), 7.40 – 7.07 (m, 8H), 6.85 – 6.74 (m, 2H), 5.40 (s, 1H), 5.12 (s, 1H), 4.82 (d, *J* = 15.3 Hz, 1H), 4.10 – 3.92 (m, 2H), 3.80 (d, *J* = 15.3 Hz, 1H), 3.37 (d, *J* = 2.4 Hz, 1H), 3.28 (d, *J* = 23.0 Hz, 1H), 2.98 (s, 1H), 2.79 (d, *J* = 23.1 Hz, 1H), 2.43 (s, 1H), 1.08 (t, *J* = 7.1 Hz, 3H). **^{13}C NMR** (75 MHz, $CDCl_3$) δ (ppm) 171.1 (C), 146.3 (C), 143.5 (C), 142.4 (C), 141.3 (C), 141.2 (C), 140.6 (C), 137.6 (C), 136.8 (C), 129.3 (CH_3), 128.5 (CH), 128.4 (CH), 128.3 (CH), 128.2 (CH), 127.2 (CH), 126.3 (CH), 124.8 (CH), 123.1 (CH), 120.8 (CH), 120.5 (CH_2), 60.9 (CH_2), 53.9 (CH), 52.3 (CH_2), 46.1 (CH), 40.0 (CH_2), 21.5 (CH_3), 13.9 (CH_3). **HRMS** (APCI-TOF): m/z calculated for $C_{30}H_{30}NO_4S^+$ $[M + H]^+$: m/z 500.1890, found 500.1897. Stereochemistry of **24gs** was determined by nOe experiments.

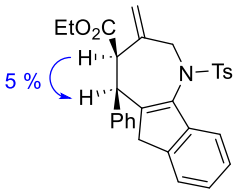

Figure 61. Significant nOe's observed for **24gs**.

Ethyl (4*R*,5*R*)-3-methylene-5-phenyl-1-tosyl-2,3,4,5-tetrahydro-1*H*-benzofuro[3,2*b*] azepine-4-carboxylate (**24gt**+**24gt'**)

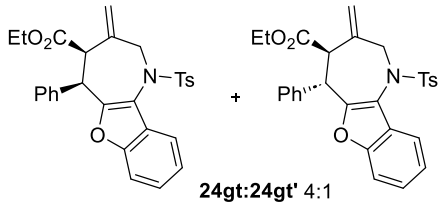

Prepared following the procedure employed for the synthesis of the cycloadduct **16be**, using ACP **19g** and imine **15t** as starting materials. Reaction carried out at 70 ºC. Isolated by column chromatography (10% EtOAc/Hexane) as a yellow oil in 37% yield, dr 4:1. **^{1}H NMR** (500 MHz, $CDCl_3$) δ (ppm) 7.84 (d, *J* = 8.4 Hz, 0.2H), 7.78 (dd, *J* = 7.9, 1.1 Hz, 0.8H), 7.57 (d, *J* = 8.3 Hz, 1.6H), 7.52 – 7.49 (m, 0.2H), 7.38 – 7.33 (m, 0.4H), 7.33 – 7.16 (m, 7.8H), 7.06 – 7.02 (m, 0.4H), 7.01 – 6.96 (m, 1.6H), 5.47 (s, 0.8H), 5.28 (d, *J* = 1.9 Hz, 0.2H), 5.16 (s, 0.8H), 5.05 (m, 0.4H), 4.91 (d, *J* = 15.4 Hz, 0.8H), 4.32 (d, *J* = 15.4 Hz, 0.4H), 4.06 – 3.91 (m, 2.8H), 3.68 (d, *J* = 11.7 Hz, 0.2H), 3.31 – 3.15 (m, 1.6H), 2.48 (s, 0.6H), 2.47 (s, 2.4H), 1.06 (t, *J* = 7.1 Hz, 0.6H), 1.02 (t, *J* = 7.1 Hz, 2.4H). **^{13}C NMR** (126 MHz, $CDCl_3$) δ (ppm) 171.2 (C), 170.2 (C), 153.7 (C), 153.4 (C), 153.3 (C), 153.2 (C), 144.3 (C), 143.9 (C), 140.7 (C), 140.2 (C), 136.8 (C), 136.3 (C), 130.1 (CH), 129.5 (CH), 129.3 (CH), 128.7 (CH), 128.5 (CH), 128.5 (CH), 128.4 (CH), 128.0 (CH), 127.9 (CH), 127.6 (CH), 126.7 (C), 124.7 (CH), 124.2 (CH), 123.5 (CH), 123.1 (CH), 121.7 (CH_2), 120.7 (CH), 120.7 (CH), 118.6 (C), 117.3 (C), 111.5 (CH), 111.5 (CH), 61.1 (CH_2), 61.1 (CH_2), 53.9 (CH), 53.4 (CH_2), 46.4 (CH), 46.3 (CH), 21.8 (CH_3), 21.7 (CH_3), 14.0 (CH_3), 14.0 (CH_3). **HRMS** (APCI-TOF): m/z calculated for $C_{29}H_{28}NO_5S^+$ [M + H]$^+$:m/z 502.1683, found 502.1684. Stereochemistry of **24gt** and **24gt'** was deduced by homology with **35gs**.

Cycloaddition between 19g and 15u: Prepared following the procedure employed for the synthesis of the cycloadduct **16be** at 70 ºC. Isomers **25gu** and **25gu'** are obtained in 58% combined yield (dr 3.5:1) and can be easily separated by column chromatography (20-30% EtOAc/Hexane).

Ethyl (1*R*,2*R*,3*S*)-3-(2,2-dioxidobenzo[*e*][1,2,3]oxathiazin-4-yl)-5-methylene-2-phenylcyclopentane-1-carboxylate (**25gu**)

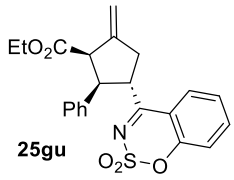

45% as a yellow oil. **^{1}H NMR** (300 MHz, $CDCl_3$) δ (ppm) 7.98 (d, *J* = 8.0 Hz, 1H), 7.70 (t, *J* = 7.8 Hz, 1H), 7.41 (t, *J* = 7.7 Hz, 1H), 7.30 – 7.11 (m, 6H), 5.21 (s, 1H), 5.12 (s, 1H), 4.75 (q, *J* = 9.6 Hz, 1H), 4.23 (dd, *J* = 10.5, 8.1 Hz, 1H), 3.97 – 3.79 (m, 3H), 3.28 (dd, *J* = 16.8, 9.1 Hz, 1H), 2.73 (dd, *J* = 16.7, 9.4 Hz, 1H), 0.94 (t, *J* = 7.1 Hz, 3H). **^{13}C NMR** (126 MHz, $CDCl_3$) δ (ppm) 180.9 (C), 172.5 (C), 153.9 (C), 145.9 (C), 137.4 (C), 137.1 (CH), 128.4 (CH), 128.0 (CH), 127.7 (CH), 127.2 (CH), 126.0 (CH), 119.3 (CH), 116.3 (C), 111.0 (CH_2), 60.5 (CH_2), 55.8 (CH), 51.0 (CH), 45.7 (CH), 39.4 (CH_2), 13.8 (CH_3). **HRMS** (APCI-TOF): m/z calculated for $C_{22}H_{22}NO_5S^+$ [M + H]$^+$:m/z 412.1213, found 412.1219. Stereochemistry of **25gu** was determined by nOe experiments.

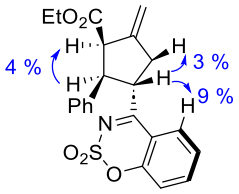

Figure 62. Significant nOe's observed for **25gu**.

Ethyl (1S,2R,3S)-3-(2,2-dioxidobenzo[e][1,2,3]oxathiazin-4-yl)-5-methylene-2-phenylcyclopentane-1-carboxylate (**25gu'**)

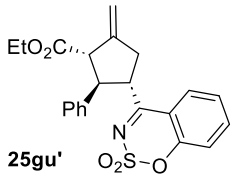

13% as a yellow oil. **^{1}H NMR** (300 MHz, $CDCl_3$) δ (ppm) 7.66 – 7.52 (m, 1H), 7.46 (dd, *J* = 8.0, 1.5 Hz, 1H), 7.25 – 7.12 (m, 7H), 5.28 – 5.21 (m, 1H), 5.19 – 5.13 (m, 1H), 4.31 – 3.98 (m, 3H), 3.94 – 3.67 (m, 2H), 3.18 – 2.86 (m, 2H), 1.22 (t, *J* = 7.1 Hz, 3H). **^{13}C NMR** (126 MHz, $CDCl_3$) δ (ppm) 180.2 (C), 171.3 (C), 153.7 (C), 145.4 (C), 139.5 (C), 136.8 (CH), 128.8 (CH), 127.8 (CH), 127.5 (CH), 127.5 (CH), 125.5 (CH), 119.1 (CH), 116.5 (C), 109.8 (CH_2), 61.1 (CH_2), 56.4 (CH), 53.1 (CH), 50.3 (CH), 39.6 (CH_2), 14.1 (CH_3). **HRMS** (APCI-TOF): m/z calculated for $C_{22}H_{22}NO_5S^+$ $[M + H]^+$:m/z 412.1213, found 412.1219. Stereochemistry of **25gu'** was deduced by homology with **25gu**.

2-(3,3-Dihexyl-4-methylenepyrrolidin-2-yl)phenol (**26de**)

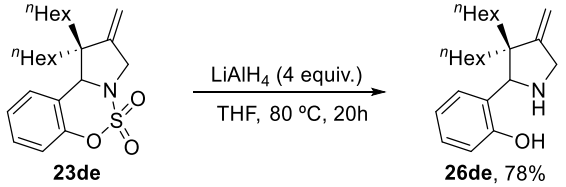

In a dry sealed tube containing a solution of **23de** (40.6 mg, 100 µmol, 1.0 equiv.) and THF (1 mL) at 0 °C, $LiAlH_4$ (6.00 mg, 150 µmol, 1.5 equiv.) was added. The reaction mixture was heated at 80 °C and stirred overnight. The reaction was quenched with H_2O (1 mL) and extracted with Et_2O (3x0.5 mL). The organic phases were concentrated to afford **26de** as a yellow oil (27.0 mg, 78.0 µmol, 78% yield). **^{1}H NMR** (300 MHz, $CDCl_3$) δ (ppm) 7.14 (t, *J* = 7.7 Hz, 1H), 7.03 – 6.68 (m, 3H), 5.08 (s, 1H), 4.76 (s, 1H), 4.42 (s, 1H), 3.87 (d, *J* = 14.6 Hz, 1H), 3.67 (d, *J* = 14.6 Hz, 1H), 1.71 – 1.01 (m, 20H), 0.96 – 0.88 (m, 3H), 0.82 (t, *J* = 6.8 Hz, 3H). **^{13}C NMR** (75 MHz, $CDCl_3$) δ (ppm) 159.5 (C), 150.4 (C), 128.4 (CH), 128.4 (CH), 121.7 (C), 118.3 (CH), 117.0 (CH), 106.2 (CH_2), 68.5 (CH), 52.9 (C), 49.4 (CH_2), 33.3 (CH_2), 32.1 (CH_2), 31.9 (CH_2), 31.8 (CH_2), 30.2 (CH_2), 30.0 (CH_2), 23.9 (CH_2), 23.2 (CH_2), 22.7 (CH_2), 22.6 (CH_2), 14.1 (CH_3), 14.0 (CH_3). **HRMS** (APCI-TOF): m/z calculated for $C_{23}H_{38}NO$ $[M + H]^+$:m/z 344.2948, found 344.2946.

1,1-Dihexyl-1,10*b*-dihydrobenzo[*e*]pyrrolo[1,2-*c*][1,2,3]oxathiazin-2(3*H*)-one 5,5-dioxide (**27de**)

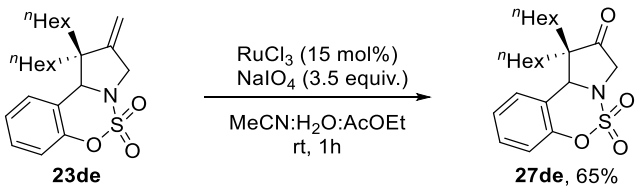

A solution of $NaIO_4$ (73.8 mg, 345 µmol, 3.45 equiv.) in water (0.6 mL) was added to a solution of $RuCl_3$ (7.80 mg, 40%Ru, 15.0 µmol, 0.15 equiv.) in MeCN (0.75 mL), in a dry sealed tube. After stirring for 2 minutes, a solution of **23de** (49.5 mg, 100 µmol, 1.0 equiv.) in EtOAc (0.75 mL) was added dropwise. The mixture was stirred for 1 h, diluted with water (1.5 mL), and extracted with Et_2O (3x1 mL). The combined organic phases were dried, concentrated, and the crude residue was

purified by column chromatography (2% EtOAc/Hexane) to afford **27de** as a colourless oil (26.2 mg, 65.0 μmol, 65% yield). **^{1}H NMR** (300 MHz, $CDCl_3$) δ (ppm) 7.32 (t, *J* = 8.1 Hz, 1H), 7.24 – 7.16 (m, 1H), 7.06 (t, *J* = 8.2 Hz, 2H), 5.13 (s, 1H), 3.99 (d, *J* = 17.0 Hz, 1H), 3.71 (d, *J* = 17.0 Hz, 1H), 2.06 – 1.91 (m, 1H), 1.65 – 1.49 (m, 1H), 1.44 – 0.89 (m, 18H), 0.86 – 0.79 (m, 3H), 0.72 (t, *J* = 7.0 Hz, 3H). **^{13}C NMR** (75 MHz, $CDCl_3$) δ (ppm) 209.2 (C), 151.0 (C), 129.8 (CH), 126.6 (CH), 125.8 (CH), 119.9 (C), 119.5 (CH), 65.4 (CH), 57.9 (C), 53.6 (CH_2), 34.3 (CH_2), 33.7 (CH_2), 31.5 (CH_2), 31.2 (CH_2), 29.7 (CH_2), 29.4 (CH_2), 24.9 (CH_2), 23.3 (CH_2), 22.5 (CH_2), 22.3 (CH_2), 14.0 (CH_3), 13.9 (CH_3). **HRMS** (APCI-TOF): m/z calculated for $C_{22}H_{34}NO_4S^+$ [M + H]$^+$:m/z 408.2203, found 408.2199.

1,1-Dihexyl-2-methyl-1,2,3,10*b*-tetrahydrobenzo[*e*]pyrrolo[1,2-*c*][1,2,3]oxathiazine 5,5-dioxide (**28de** + **28de'**)

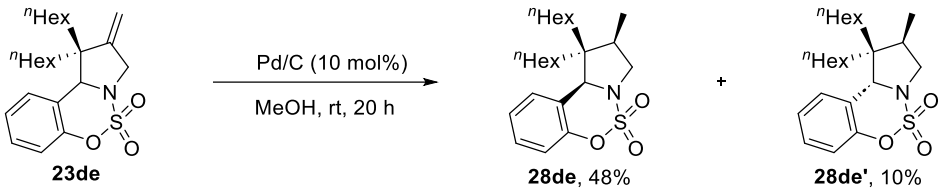

In a dry sealed tube under a N_2 atmosphere, **23de** (40.6 mg, 100 μmol, 1.0 equiv.), Pd/C (10.6 mg, 10 μmol, 0.1 equiv.) and MeOH (3 mL) were added. The black suspension was first purged with a H_2 flow for 30 min and stirred at rt under H_2 atmosphere. After 20 h, the reaction was diluted with EtOAc and filtered through a short pad of Florisil®, eluting with EtOAc. The filtrate was concentrated to yield the mixture of products **28de:28de'** (4.8:1) as a pure colourless oil (23.0 mg, 56.4 μmol, 58% yield). **^{1}H NMR** (300 MHz, $CDCl_3$) δ (ppm) 7.30 (t, *J* = 7.7 Hz, 1H), 7.23 – 6.96 (m, 3H), 4.83 (s, 0.81H), 4.67 (s, 0.19H), 3.85 (dd, *J* = 9.4, 6.2 Hz, 0.19H), 3.77 – 3.58 (m, 0.81H), 3.46 – 3.33 (m, 0.81H), 3.26 (dd, *J* = 9.4, 2.5 Hz, 0.19H), 2.24 (q, *J* = 7.3 Hz, 0.81H), 2.15 – 2.04 (m, 0.19H), 1.72 – 0.86 (m, 25H), 0.80 (t, *J* = 7.1 Hz, 3H), 0.71 – 0.56 (m, 1H). **^{13}C NMR** (75 MHz, $CDCl_3$) δ (ppm) 151.7 (C), 151.4 (C), 129.0 (CH), 128.9 (CH), 127.8 (CH), 127.6 (CH), 125.1 (CH), 125.0 (CH), 122.5 (C), 122.2 (C), 119.5 (CH), 119.2 (CH), 69.6 (CH), 67.9 (CH), 56.2 (CH_2), 55.4 (CH_2), 52.5 (C), 51.9 (C), 39.9 (CH), 38.9 (CH), 34.6 (CH_2), 32.2 (CH_2), 31.8 (CH_2), 31.7 (CH_2), 31.4 (CH_2), 30.3 (CH_2), 30.1 (CH_2), 30.0 (CH_2), 24.5 (CH_2), 24.0 (CH_2), 23.8 (CH_2), 23.7 (CH_2), 22.6 (CH_2), 22.4 (CH_2), 14.7 (CH_3), 14.0 (CH_3), 13.9 (CH_3), 12.8 (CH_3). **HRMS** (APCI-TOF): m/z calculated for $C_{23}H_{38}NO_3S^+$ [M + H]$^+$:m/z 408.2567, found 408.2571. Stereochemistry of **28de** and **28de'** were determined by nOe experiments.

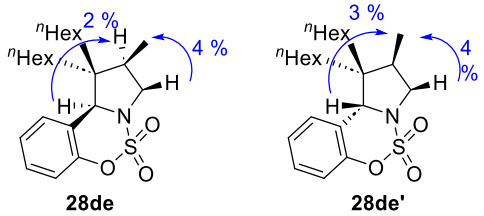

Figure 63. Significant nOe's observed for **28de** and **28de'**.

2-(3,3-Dihexyl-4-methyl-3*H*-pyrrol-2-yl)phenol (**29de**)

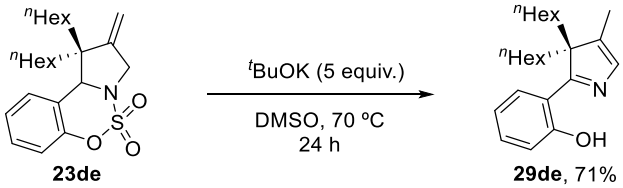

Compound **23de** (53.4 mg, 100 μmol, 1.0 equiv.), *t*BuOK (22.4 mg, 200 μmol, 2.0 equiv.) and dry DMSO (10 mL) were added to a dry Schlenk tube, and the resulting mixture was stirred under heating

at 70 °C for 24 h. Then, the reaction was cooled down to rt, diluted with water (80 mL) and extracted with Et_2O (2x 10 mL). The combined organic phases were dried and concentrated to give a crude residue that was purified by column chromatography (1%EtOAc/Hexane) to afford **29de** as a yellow oil (24.2 mg, 71.0 μmol, 71% yield). **^{1}H NMR** (500 MHz, $CDCl_3$) δ (ppm) 14.58 (s, 1H), 7.65 (dd, *J* = 8.0, 1.6 Hz, 1H), 7.29 (ddd, *J* = 8.5, 7.2, 1.6 Hz, 1H), 7.05 (dd, *J* = 8.3, 1.3 Hz, 1H), 6.86 (ddd, *J* = 8.2, 7.2, 1.3 Hz, 1H), 6.80 (d, *J* = 1.7 Hz, 1H), 2.14 – 1.97 (m, 2H), 1.83 (d, *J* = 1.6 Hz, 3H), 1.79 – 1.69 (m, 2H), 1.20 – 1.02 (m, 12H), 0.78 (t, *J* = 7.1 Hz, 6H), 0.67 (ddq, *J* = 12.1, 10.6, 6.2 Hz, 4H). **^{13}C NMR** (126 MHz, $CDCl_3$) δ (ppm) 182.5 (C), 160.8 (C), 141.1 (C), 135.1 (CH), 131.4 (CH), 126.3 (CH), 118.0 (CH), 118.0 (CH), 117.0 (C), 65.9 (C), 36.9 (CH_2), 31.3 (CH_2), 29.3 (CH_2), 23.1 (CH_2), 22.5 (CH_2), 13.9 (CH_3), 9.7 (CH_3). **HRMS** (APCI-TOF): m/z calculated for $C_{23}H_{36}NO^+$ [M + H]$^+$: m/z 342.2791, found 342.2790.

Phenylboronic acid-d$_2$ (d-33l)

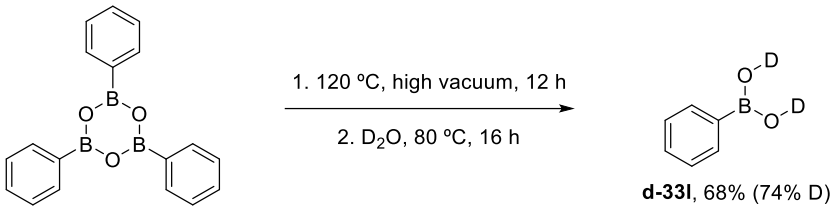

Deuterated phenylboronic acid **d-33l** was prepared following a described procedure with minor modifications.[161] Boroxine (500 mg, 1.60 mmol) and a magnetic stirring bar were added to a 25 mL round bottom flask. The flask was heated to 120ºC under high vacuum for 12 h to remove residual H_2O. Then, the flask was refilled with inert atmosphere and D_2O (6.4 mL) was added. The resulting solution was refluxed at 80 ºC for 16 h in an oil bath. The hot reaction mixture was then filtered to remove the insoluble boroxine. After cooling, a second filtration was performed to isolate the boronic acid as a white solid, which was dried under high vacuum for 5 h (**d-33l**, 136 mg, 1.10 mmol, 68%, 74%D). Deuteration percent (%D) is based on the integral value of the signal at 8.02 ppm, compared to that of phenyl boronic acid **33l**. Spectroscopic data of **d-33l** is in agreement with that reported. **^{1}H NMR** (300 MHz, DMSO) δ (ppm) 8.02 (br. s, 0.38H), 7.93 – 7.70 (m, 2H), 7.44 – 7.24 (m, 3H).

Methyl (1*R*,4*R*,6*R*)-1-methyl-3-oxo-6-(prop-1-en-2-yl)-2-oxabicyclo[2.2.1]heptane-4-carboxylate (35a')

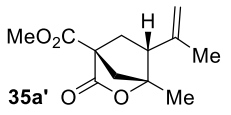

Prepared following the procedure employed for the synthesis of the tandem product **35a'**, using the benzyl alcohol as partner. Isolated by column chromatography (25-40% EtOAc/Hexane) as a colourless oil in 70% yield as a colourless oil. **^{1}H-NMR** (300 MHz, $CDCl_3$) δ (ppm) 4.98 (s, 1H), 4.85 (s, 1H), 3.81 (s, 3H), 2.79 (dd, *J* = 11.1, 5.3 Hz, 1H), 2.51 (dd, *J* = 13.4, 11.1 Hz, 1H), 2.38 (dd, *J* = 10.4, 2.3 Hz, 1H), 2.14 – 1.99 (m, 2H), 1.74 (s, 3H), 1.51 (s, 3H); **^{13}C-NMR** (75 MHz, $CDCl_3$) δ (ppm) 173.5 (C), 168.6 (C), 141.3 (C), 116.2 (CH_2), 90.9 (C), 58.2 (C), 52.8 (CH_3), 52.3 (CH), 48.8 (CH_2), 32.8 (CH_2), 20.8 (CH_3), 17.3 (CH_3). **HRMS** (ESI-TOF): m/z calculated for $C_{12}H_{16}NaO_4$ [M + Na]$^+$: m/z 247.0946, found 247.0937. Stereochemistry of **35a'** was determined by nOe experiments.

[161] He, H.-D.; Chitrakar, R.; Cao, Z.-W.; Wang, D.-M.; She, L.-Q.; Zhao, P.-G.; Wu, Y.; Xu, Y.-Q.; Cao, Z.-Y.; Wang, P. Diphosphine Ligand-Enabled Nickel-Catalyzed Chelate-Assisted Inner-Selective Migratory Hydroarylation of Alkenes. *Angew. Chem. Int. Ed.* **2024**, *63,* e202313336. An alternative using boronic acid as starting material: Shinde, J.; Suresh, S.; Kavala, V.; Yao, C.-F. Pd(II)-catalyzed hydroarylations/hydroalkenylations of terminal alkynes: regioselective synthesis of allylic, homoallylic, and 1,3-diene systems. *Chem. Commun.* **2024**, *60*, 3790-3793.

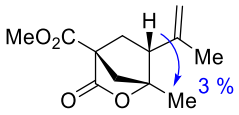

Figure 64. Significant nOe's observed for **35a'**.

Dimethyl 2-(2-((1*R*,4*R*,6*R*)-4-(methoxycarbonyl)-1-methyl-3-oxo-2-oxabicyclo[2.2.1] heptan-6-yl)allyl)malonate (**37aa'**)

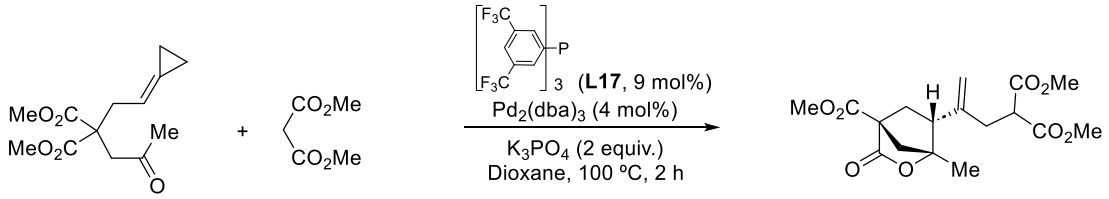

9a **36a**, 2 equiv. **37aa'**

Prepared following general procedure for catalytic reactions (see *Methodology*, page 57), using $Pd_2(dba)_3$ (4.40 mg, 4.80 μmol, 4 mol%), phosphine **L17** (7.20 mg, 10.8 μmol, 9 mol%), keto-ACP **9a** (30.5 mg, 120 μmol, 1.0 equiv.), K_3PO_4 (50.9 mg, 240 μmol, 2.0 equiv.), and dimethyl malonate **36a** (31.7 mg, 27.0 μL, 240 μmol, 2.0 equiv.) in dry 1,4-dioxane (2.4 mL). The reaction crude was purified by flash chromatography (25-40% EtOAc/Hexane) to afford dimethyl 2-(2-((1*R*,4*R*,6*R*)-4-(methoxycarbonyl)-1-methyl-3-oxo-2-oxabicyclo[2.2.1] heptan-6-yl)allyl)malonate (**37aa'**) as colourless oil (38.3 mg, 110 μmol, 90% yield). **^{1}H-NMR** (300 MHz, $CDCl_3$) δ (ppm) 5.03 (s, 1H), 4.99 (d, *J* = 1.5 Hz, 1H), 3.81 (s, 3H), 3.73 (s, 3H), 3.72 (s, 3H), 3.64 (t, *J* = 7.8 Hz, 1H), 2.76 (dd, *J* = 11.1, 5.2 Hz, 1H), 2.68 – 2.53 (m, 3H), 2.40 (dd, *J* = 10.5, 2.4 Hz, 1H), 2.13 (d, *J* = 10.5 Hz, 1H), 2.03 (ddd, *J* = 13.4, 5.3, 2.4 Hz, 1H), 1.53 (s, 3H). **^{13}C-NMR** (75 MHz, $CDCl_3$) δ (ppm) 173.2 (C), 169.3 (C), 169.3 (C), 168.4 (C), 141.8 (C), 115.2 (CH_2), 90.2 (C), 58.2 (C), 52.9 (CH_3), 52.8 (CH_3), 51.0 (CH), 50.7 (CH), 49.2 (CH_2), 34.6 (CH_2), 34.5 (CH_2), 17.5 (CH_3). **HRMS** (ESI-TOF): m/z calculated for $C_{17}H_{23}O_8$ $[M + H]^+$: m/z 355.1393, found 355.1387. Stereochemistry of **37aa'** was determined by nOe experiments.

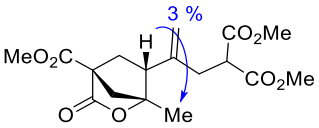

Figure 65. Significant nOe's observed for **37aa'**.

Dimethyl (3*R*,4*R*)-3-hydroxy-4-(5-methoxy-4-(methoxycarbonyl)-5-oxopent-1-en-2-yl)-3-methyl cyclopentane-1,1-dicarboxylate (**37aa**)

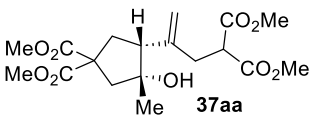

37aa

Prepared following the procedure employed for the synthesis of the tandem product **37aa'**, using K_2CO_3 instead of K_3PO_4. Isolated by column chromatography (25-40% EtOAc/Hexane) as a colourless oil in 70% yield. **^{1}H-NMR** (300 MHz, $CDCl_3$) δ (ppm) 5.03 (s, 1H), 4.99 (s, 1H), 3.78 – 3.68 (m, 13H), 2.83 – 2.66 (m, 2H), 2.67 – 2.53 (m, 2H), 2.46 (dd, *J* = 12.0, 7.1 Hz, 1H), 2.40 – 2.22 (m, 3H), 1.29 (s, 3H). **^{13}C-NMR** (75 MHz, $CDCl_3$) δ (ppm) 173.3 (C), 173.0 (C), 169.8 (C), 169.5 (C), 143.2 (C), 114.07 (CH_2), 79.5 (C), 57.1 (C), 55.1 (CH), 53.0 (CH_3), 52.9 (CH_3), 52.8 (CH_3), 52.7 (CH_3), 50.5 (CH), 48.2 (CH_2), 37.4 (CH_2), 34.5 (CH_2), 25.9 (CH_3). **HRMS** (ESI-TOF): m/z calculated for $C_{18}H_{26}NaO_9$ $[M + Na]^+$: m/z 409.1475, found 409.1472. Stereochemistry of **37aa** was determined by nOe experiments.

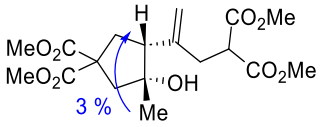

Figure 66. Significant nOe's observed for **37aa**.

Dimethyl 2-(2-((1*R*,4*R*,6*R*)-4-(methoxycarbonyl)-1-methyl-3-oxo-2-oxabicyclo[2.2.1] heptan-6-yl)allyl)-2-(2-oxopropyl)malonate (**37ab'**)

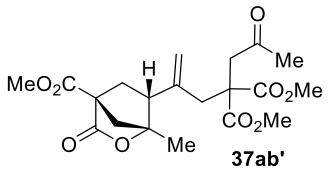

Prepared following the procedure employed for the synthesis of the tandem product **37aa'**, using the substituted malonate **36b** as partner. Isolated by column chromatography (25-40% EtOAc/Hexane) as a colourless oil in 55% yield. **^{1}H-NMR** (300 MHz, $CDCl_3$) δ (ppm) 5.05 (s, 1H), 4.92 (s, 1H), 3.79 (s, 3H), 3.71 (s, 3H), 3.70 (s, 3H), 3.15 (s, 2H), 2.81 (d, *J* = 3.6 Hz, 2H), 2.70 (dd, *J* = 11.1, 4.9 Hz, 1H), 2.59 (dd, *J* = 12.9, 11.1 Hz, 1H), 2.38 (dd, *J* = 10.5, 2.4 Hz, 1H), 2.18 – 2.07 (m, 4H), 1.87 (ddd, *J* = 12.9, 5.0, 2.5 Hz, 1H), 1.53 (s, 3H), **^{13}C-NMR** (75 MHz, $CDCl_3$) δ (ppm) 205.2 (C), 173.5 (C), 171.1 (C), 171.0 (C), 168.4 (C), 141.3 (C), 117.7 (CH_2), 89.9 (C), 58.2 (C), 55.1 (C), 53.1 (CH_3), 53.0 (CH_3), 52.8 (CH_3), 49.5 (CH_2), 49.4 (CH), 46.2 (CH_2), 41.4 (CH_2), 36.0 (CH_2), 30.3 (CH_3), 17.6 (CH_3). **HRMS** (ESI-TOF): m/z calculated for $C_{20}H_{26}NaO_9$ [M + H]$^+$: m/z 433.1475, found 433.1469. Stereochemistry of **37ab'** was determined by nOe experiments.

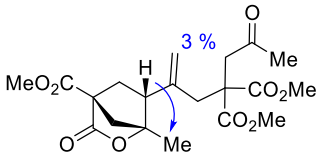

Figure 67. Significant nOe's observed for **37ab'**.

Dimethyl 2-(but-2-yn-1-yl)-2-(2-((1*R*,4*R*,6*R*)-4-(methoxycarbonyl)-1-methyl-3-oxo-2-oxabicyclo [2.2.1]heptan-6-yl)allyl)malonate (**37ac'**)

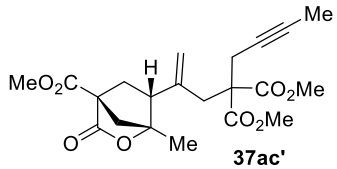

Prepared following the procedure employed for the synthesis of the tandem product **37aa'**, using the substituted malonate **36c** as partner. Isolated by column chromatography (25-40% EtOAc/Hexane) as a colourless oil in 53% yield. **^{1}H-NMR** (300 MHz, $CDCl_3$) δ (ppm) 5.07 (s, 1H), 5.06 (s, 1H), 3.80 (s, 3H), 3.72 (s, 6H), 2.88 (d, *J* = 14.4 Hz, 1H), 2.81 – 2.68 (m, 3H), 2.58 (dd, *J* = 13.2, 11.1 Hz, 1H), 2.39 (dd, *J* = 10.4, 2.4 Hz, 1H), 2.11 (d, *J* = 10.4 Hz, 1H), 1.95 (ddd, *J* = 13.1, 5.2, 2.4 Hz, 1H), 1.76 (t, *J* = 2.5 Hz, 3H), 1.55 (s, 3H), **^{13}C-NMR** (75 MHz, $CDCl_3$) δ (ppm) 173.4 (C), 170.7 (C), 170.5 (C), 168.4 (C), 140.1 (C), 117.7 (CH_2), 89.9 (C), 80.0 (C), 73.5 (C), 58.3 (C), 57.9 (C), 52.9 (CH_3), 49 (CH).8, 49.5 (CH_2), 39.6 (CH_2), 35.9 (CH_2), 23.5 (CH_2), 17.7 (CH_3), 3.6 (CH_3). **HRMS** (ESI-TOF): m/z calculated for $C_{21}H_{27}O_8$ [M + H]$^+$: m/z 407.1706, found 407.1699. Stereochemistry of **37ac'** was determined by analogy with that of **37aa'**.

Dimethyl (3*R*,4*R*)-3-hydroxy-4-(4-(methoxycarbonyl)-5-oxohex-1-en-2-yl)-3-methylcyclopentane-1,1-dicarboxylate (**37ad'+37ad'**)

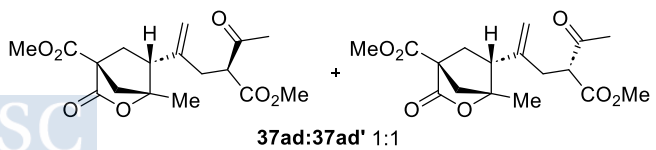

Prepared following the procedure employed for the synthesis of the tandem product **37aa'**, using the 1,3-dicarbonyl partner **36d**. Isolated by column chromatography (25-40% EtOAc/Hexane) as a colourless oil in 69% yield, dr 1:1. **^{1}H-NMR** (300 MHz, $CDCl_3$) δ (ppm) 5.05 (s, 0.5H), 5.04 (s, 0.5H), 4.99 (s, 0.5H), 4.96 (s, 0.5H), 3.83 (s, 3H), 3.79 – 3.70 (m, 4H), 2.85 – 2.73

(m, 1H), 2.72 – 2.47 (m, 3H), 2.48 – 2.35 (m, 1H), 2.27 (s, 3H), 2.20 – 2.11 (m, 1H), 2.10 – 1.99 (m, 1H), 1.56 (d, J = 1.5 Hz, 3H). **^{13}C-NMR** (75 MHz, $CDCl_3$) δ (ppm) 202.1 (C), 202.0 (C), 173.2 (C), 169.7 (C), 168.4 (C), 142.2 (C), 142.1 (C), 115.3 (CH_2), 114.9 (CH_2), 90.3 (C), 90.2 (C), 58.6 (CH), 58.3 (CH), 58.2 (C), 58.2 (C), 52.8 (CH_3), 52.7 (CH_3), 52.6 (CH_3), 51.3 (CH), 51.1 (CH), 49.2 (CH_2), 49.2 (CH_2), 34.56 (CH_2), 34.4 (CH_2), 33.7 (CH_2), 33.6 (CH_2), 29.4 (CH_3), 29.0 (CH_3), 17.5 (CH_3), 17.4 (CH_3). **HRMS** (ESI-TOF): m/z calculated for $C_{17}H_{23}O_7$ $[M + H]^+$: m/z 339.1444, found 339.1442. Stereochemistry of **37ad** and **37ad'** was determined by comparison with analogue products.

Tandem reaction between 9b and 36a: Prepared following the procedure employed for the synthesis of the tandem product **37aa'**, using keto-ACP **9b** as starting material. Isomers **37ba'** and **37ba''** are obtained in 90% combined yield (dr 1:1) and can be easily separated by column chromatography (25-40% EtOAc/Hexane).

Dimethyl 2-(2-((1*R*,4*S*,6*R*)-4-(methoxycarbonyl)-1-methyl-3-oxo-2-oxabicyclo[2.2.2]octan-6-yl) allyl)malonate (**37ba'**)

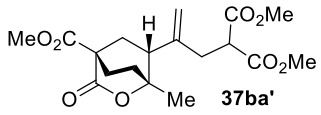

37ba'

45% as a colourless oil. **^{1}H-NMR** (300 MHz, $CDCl_3$) δ (ppm) 5.08 (d, *J* = 1.4 Hz, 1H), 5.06 (s, 1H), 3.80 (s, 3H), 3.75 (s, 3H), 3.73 (s, 3H), 3.67 – 3.60 (m, 1H), 2.79 (dd, *J* = 15.6, 9.1 Hz, 1H), 2.68 – 2.56 (m, 3H), 2.42 (ddt, *J* = 16.0, 12.8, 3.4 Hz, 1H), 2.18 – 2.10 (m, 1H), 2.04 – 1.95 (m, 1H), 1.86 – 1.76 (m, 2H), 1.35 (s, 3H). **^{13}C-NMR** (75 MHz, $CDCl_3$) δ (ppm) 172.4 (C), 170.3 (C), 169.2 (C), 169.1 (C), 144.8 (C), 114.7 (CH_2), 85.3 (C), 53.0 (CH_3), 52.9 (CH_3), 52.8 (CH_3), 50.5 (CH), 49.1 (C), 48.1 (CH), 36.1 (CH_2), 34.0 (CH_2), 27.1 (CH_2), 24.1 (CH_3). **HRMS** (ESI-TOF): m/z calculated for $C_{18}H_{25}O_8$ $[M + H]^+$: m/z 369.1549 , found 369.1545. Stereochemistry of **37ba'** was determined by analogy with that of **37aa'**.

Dimethyl 2-(2-((1*S*,4*R*,6*R*)-4-(methoxycarbonyl)-1-methyl-3-oxo-2-oxabicyclo[2.2.2] octan-6-yl)allyl)malonate (**37ba''**)

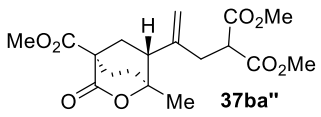

37ba''

45% yield as a colourless oil. **^{1}H-NMR** (300 MHz, $CDCl_3$) δ (ppm) 4.97 (s, 1H), 4.93 (s, 1H), 3.79 (s, 3H), 3.73 (s, 3H), 3.72 (s, 3H), 3.63 (t, *J* = 7.7 Hz, 1H), 2.63 (dd, *J* = 7.7, 1.5 Hz, 2H), 2.54 – 2.35 (m, 2H), 2.35 – 2.23 (m, 2H), 2.03 – 1.79 (m, 3H), 1.34 (s, 3H). **^{13}C-NMR** (75 MHz, $CDCl_3$) δ (ppm) 172.4 (C), 170.3 (C), 169.3 (C), 169.2 (C), 145.7 (C), 114.8 (CH_2), 83.9 (C), 52.9 (CH_3), 52.9 (CH_3), 52.8 (CH_3), 50.4 (CH), 49.1 (C), 46.8 (CH), 34.6 (CH_2), 33.7 (CH_2), 26.2 (CH_2), 22.7 (CH_3). **HRMS** (ESI-TOF): m/z calculated for $C_{18}H_{25}O_8$ $[M + H]^+$: m/z 369.1549, found 369.1547. Stereochemistry of **37ba''** was determined by comparison with its isomer **37ba'**.

Dimethyl 2-(2-((1*R*,2*S*)-2-benzyl-2-hydroxycyclopentyl)allyl)malonate (**37fa**)

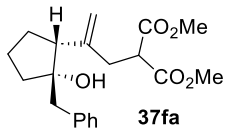

37fa

Prepared following the procedure employed for the synthesis of the tandem product **37aa'**, using keto-ACP **9f** as starting material. Isolated by column chromatography (25-40% EtOAc/Hexane) as a colourless oil in 74% yield. **^{1}H-NMR** (300 MHz, $CDCl_3$) δ (ppm) 7.32 – 7.21 (m, 5H), 5.03 (s, 1H), 4.99 (d, *J* = 1.4 Hz, 1H), 3.82 – 3.72 (m, 7H), 2.92 (d, *J* = 13.4 Hz, 1H), 2.87 – 2.68 (m, 2H), 2.65 (d, *J* = 13.4 Hz, 1H), 2.40 (dd, *J* = 10.8, 8.0 Hz, 1H), 2.02 – 1.67 (m, 5H), 1.64 – 1.40 (m, 2H). **^{13}C-NMR** (75 MHz, $CDCl_3$) δ (ppm) 170.1 (C), 169.7 (C), 145.7 (C), 138.6 (C), 130.3 (CH), 128.2 (CH), 126.4 (CH), 113.7 (CH_2), 82.2 (C), 55.8 (CH), 52.8 (CH_3), 52.7 (CH_3), 50.7 (CH), 46.3 (CH_2), 38.5 (CH_2), 34.5 (CH_2), 29.3 (CH_2), 21.3 (CH_2). **HRMS** (ESI-TOF): m/z calculated for $C_{20}H_{27}O_5$ $[M + H]^+$: m/z 347.1858, found 347.1860. Stereochemistry of **37fa** was deduced by comparison with analogue products.

Dimethyl 2-(2-((3*S*,4*S*)-4-hydroxy-4-methyltetrahydrofuran-3-yl)allyl)malonate (**37ha**)

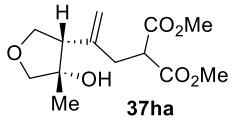

37ha

Prepared following the procedure employed for the synthesis of the tandem product **37aa'**, using keto-ACP **9h** as starting material. Isolated by column chromatography (25-40% EtOAc/Hexane) as a colourless oil in 55% yield. **^{1}H-NMR** (300 MHz, $CDCl_3$) δ 5.03 (d, *J* = 1.9 Hz, 2H), 4.03 – 3.89 (m, 2H), 3.84 (d, *J* = 9.2 Hz, 1H), 3.77 – 3.67 (m, 8H), 2.82 – 2.57 (m, 3H), 2.15 (s, 1H), 1.36 (s, 3H), **^{13}C-NMR** (75 MHz, $CDCl_3$): δ 169.7 (C), 169.4 (C), 141.5 (C), 114.5 (CH_2), 80.2 (CH_2), 78.3 (C), 71.2 (CH_2), 55.4 (CH), 52.9 (CH_3), 52.8 (CH_3), 50.3 (CH), 35.1 (CH_2), 24.5 (CH_3). **HRMS** (ESI-TOF): m/z calculated for $C_{13}H_{22}O_6$ $[M + H]^+$: m/z 273.1338, found 273.1329. Stereochemistry of **37ha** was deduced by comparison with analogue products.

Dimethyl (3*R*,3a*S*,6a*S*)-3a-hydroxy-3-(5-methoxy-4-(methoxycarbonyl)-5-oxopent-1-en-2-yl)hexahydropentalene-1,1(2*H*)-dicarboxylate (**37la**)

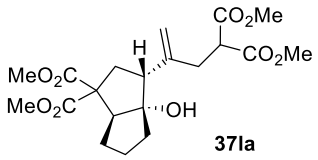

37la

Prepared following the procedure employed for the synthesis of the tandem product **37aa'**, using keto-ACP **9l** as starting material. Isolated by column chromatography (25-40% EtOAc/Hexane) as a colourless oil in 90% yield, dr = 5:1. Characterized as a 4:1 mixture. **^{1}H-NMR** (300 MHz, $CDCl_3$) δ (ppm) 4.93 (d, *J* = 1.1 Hz, 0.8H), 4.92 (d, *J* = 1.5 Hz, 0.8H), 4.82 (d, *J* = 1.3 Hz, 0.2H), 4.76 (d, *J* = 1.6 Hz, 0.2H), 3.78 – 3.76 (m, 1H), 3.75 – 3.70 (m, 8H), 3.69 – 3.67 (m, 3H), 3.20 (dd, *J* = 10.1, 8.4 Hz, 0.8H), 2.92 – 2.73 (m, 1.2H), 2.68 (d, *J* = 7.9 Hz, 1.6H), 2.54 (dd, *J* = 12.9, 6.0 Hz, 0.8H), 2.42 (dd, *J* = 13.9, 5.3 Hz, 0.2H), 2.38 – 2.09 (m, 2H), 2.02 (ddd, *J* = 13.1, 5.4, 2.1 Hz, 0.2H), 1.98 - 1.83 (m, 2H), 1.82 - 1.71 (m, 2.4H), 1.71 – 1.57 (m, 0.8H), 1.37 – 1.07 (m, 2H). **^{13}C-NMR** (75 MHz, $CDCl_3$) δ (ppm) 173.9 (C), 172.7 (C), 171.8 (C), 170.4 (C), 169.7, 169.7 (C), 169.6 (C), 144.3 (C), 143.4 (C), 112.9 (CH_2), 111.0 (CH_2), 90.5 (C), 90.3 (C), 60.2 (C), 59.9 (C), 59.1 (CH), 58.7 (CH), 53.8 (CH), 53.3 (CH), 52.9 (CH_3), 52.9 (CH_3), 52.8 (CH_3), 52.7 (CH_3), 52.68 (CH_3), 52.5 (CH_3), 52.5 (CH_3), 52.2 (CH_3), 50.4 (CH), 50.2 (CH), 40.5 (CH_2), 39.8 (CH_2), 36.6 (CH_2), 34.8 (CH_2), 34.6 (CH_2), 34.3 (CH_2), 30.6 (CH_2), 29.9 (CH_2), 27.5 (CH_2), 25.5 (CH_2). **HRMS** (ESI-TOF): m/z calculated for $C_{20}H_{28}NaO_9$ $[M + Na]^+$: m/z 435.1631, found 435.1632. Stereochemistry of **37la** was determined by nOe experiments.

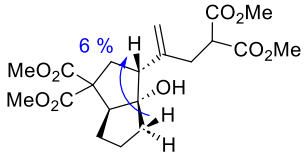

Figure 68. Significant nOe's observed for major isomer **37la**.

Dimethyl (3*R*,4*R*)-3-hydroxy-3-methyl-4-(3-phenoxyprop-1-en-2-yl)cyclopentane-1,1-dicarboxylate (**39aa**)

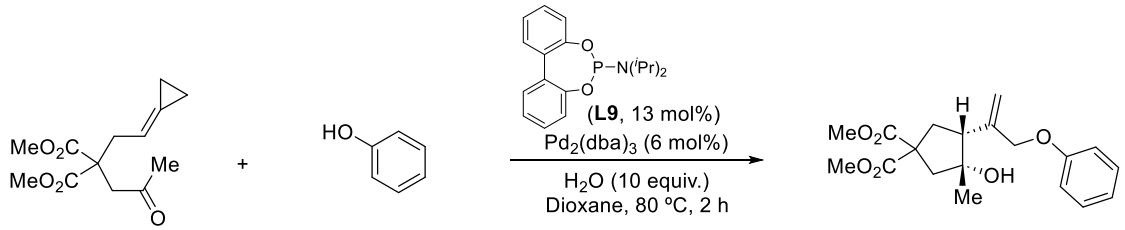

9a **38a**, 2 equiv. **39aa**

Prepared following general procedure for catalytic reactions (see *Methodology*, page 57), using $Pd_2(dba)_3$ (6.60 mg, 7.20 μmol, 6 mol%), phosphoramidite **L9** (4.90 mg, 15.6 μmol, 13 mol%), keto-ACP **9a** (30.5 mg, 120 μmol, 1.0 equiv.), K_3PO_4 (50.9 mg, 240 μmol, 2.0 equiv.), water (21.6 mL, 1.20 mmol, 10 equiv.), and phenol (**38a**, 22.6 mg, 240 μmol, 2.0 equiv.) in dry 1,4-dioxane (2.4 mL). The reaction crude was purified by flash chromatography (25-40% EtOAc/Hexane) to afford dimethyl (3*R*,4*R*)-

3-hydroxy-3-methyl-4-(3-phenoxyprop-1-en-2-yl)cyclopentane-1,1-dicarboxylate (**39aa**) as colourless oil (29.3 mg, 84.0 μmol, 70% yield). **^{1}H-NMR** (300 MHz, $CDCl_3$) δ (ppm) 7.31 – 7.25 (m, 2H), 7.01 – 6.87 (m, 3H), 5.45 (q, *J* = 1.3 Hz, 1H), 5.27 (d, *J* = 1.3 Hz, 1H), 4.57 (d, *J* = 12.2 Hz, 1H), 4.49 (d, *J* = 12.4 Hz, 1H), 3.75 (s, 3H), 3.74 (s, 3H), 2.76 – 2.52 (m, 3H), 2.53 – 2.45 (m, 1H), 2.33 (d, *J* = 14.3 Hz, 1H), 1.33 (s, 3H).**^{13}C-NMR** (75 MHz, $CDCl_3$) δ (ppm) 173.3 (C), 173.3 (C), 158.4 (C), 141.5 (C), 129.6 (CH), 121.3 (CH), 117.8 (CH_2), 115.0 (CH), 79.4 (C), 70.5 (CH_2), 57.2 (C), 53.4 (CH), 53.2 (CH_3), 53.1 (CH_3), 48.6 (CH_2), 37.7 (CH_2), 26.0 (CH_3). **HRMS** (ESI-TOF): m/z calculated for $C_{19}H_{25}O_6$ $[M + H]^+$: m/z 349.1651, found 349.1649. Stereochemistry of **39aa** was determined by nOe experiments.

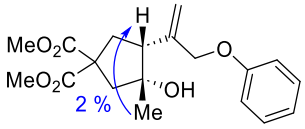

Figure 69. Significant nOe's observed for **39aa**.

Dimethyl (3*R*,4*R*)-4-(3-(2,6-diisopropylphenoxy)prop-1-en-2-yl)-3-hydroxy-3-methylcyclo pentane-1,1-dicarboxylate (**39ab**)

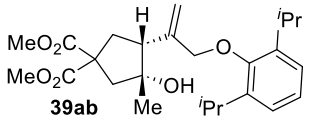

Prepared following the procedure employed for the synthesis of the tandem product **39aa**, using the alcohol **38b** as partner. Isolated by column chromatography (20% EtOAc/Hexane) as a colourless oil in 65% yield. **^{1}H-NMR** (500 MHz, $CDCl_3$) δ (ppm) 7.10 (s, 1H), 5.58 (d, *J* = 1.5 Hz, 0H), 5.41 – 5.13 (m, 0H), 2.80 (t, *J* = 12.9 Hz, 0H), 2.47 (dd, *J* = 13.2, 7.5 Hz, 0H), 2.33 (d, *J* = 14.1 Hz, 0H), 1.32 (s, 1H), 1.23 (d, *J* = 2.3 Hz, 2H), 1.22 (d, *J* = 2.3 Hz, 2H). **^{13}C-NMR** (126 MHz, $CDCl_3$) δ (ppm) 173.4 (C), 173.2 (C), 153.1 (C), 142.5 (C), 142.0 (C), 125.0 (CH), 124.2 (CH), 116.7 (CH_2), 79.0 (C), 76.7 (CH_2), 57.2 (C), 53.7 (CH), 53.1 (CH_3), 48.5 (CH_2), 37.5 (CH_2), 25.8 (CH_3) 24.2 (CH_3). **HRMS** (ESI-TOF): m/z calculated for $C_{25}H_{37}O_6$ $[M + H]^+$: m/z 433.2590, found 433.2585. Stereochemistry of **39ab** was determined by analogy with that of **39aa**.

Dimethyl (3*R*,4*R*)-4-(3-(benzo[*d*][1,3]dioxol-5-yloxy)prop-1-en-2-yl)-3-hydroxy-3-methylcyclo pentane-1,1-dicarboxylate (**39ac**)

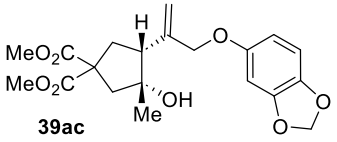

Prepared following the procedure employed for the synthesis of the tandem product **39aa**, using the alcohol **38c** as partner. Isolated by column chromatography (20% EtOAc/Hexane) as a colourless oil in 56% yield. **^{1}H-NMR** (300 MHz, $CDCl_3$) δ (ppm) 6.69 (d, J = 8.5 Hz, 1H), 6.51 (d, J = 2.5 Hz, 1H), 6.34 (dd, J = 8.5, 2.5 Hz, 1H), 5.90 (s, 2H), 5.41 (s, 1H), 5.25 (s, 1H), 4.56 – 4.33 (m, 2H), 3.75 (s, 3H), 3.73 (s, 3H), 2.69 – 2.58 (m, 2H), 2.49 – 2.42 (m, 1H), 2.40 – 2.32 (m, 2H), 1.32 (s, 3H). **^{13}C-NMR** (126 MHz, $CDCl_3$) δ (ppm) 173.1 (C), 173.1 (C), 153.7 (C), 148.2 (C), 142.0 (C), 141.5 (C), 117.6 (CH_2), 107.9 (CH), 106.3 (CH), 101.2 (CH_2), 98.43 (CH), 79.3 (C), 71.2 (CH_2), 57.0 (C), 53.2 (CH), 53.0 (CH_3), 52.9 (CH_3), 48.5 (CH_2), 37.5 (CH_2), 25.8 (CH_3). **HRMS** (ESI-TOF): m/z calculated for $C_{20}H_{25}O_8$ $[M + H]^+$: m/z 393.1549, found 393.1541. Stereochemistry of **39ac** was determined by analogy with that of **39aa**.

Dimethyl (3*R*,4*R*)-3-hydroxy-3-methyl-4-(3-((perfluorophenyl)methoxy)prop-1-en-2-yl)cyclopentane-1,1-dicarboxylate (**3ad**)

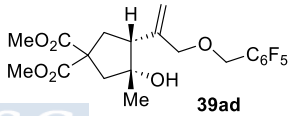

Prepared following the procedure employed for the synthesis of the tandem product **39aa**, using the fluorinated alcohol **38d** as partner. Isolated by column chromatography (20% EtOAc/Hexane) as a colourless oil in 80% yield. **^{1}H-NMR** (300 MHz, $CDCl_3$) δ (ppm) 5.33 (s, 1H), 5.23 (s, 1H), 4.68 – 4.48 (m, 2H), 4.12 (d, *J* = 11.3 Hz, 1H), 3.97 (d, *J* = 11.7 Hz, 1H), 3.75 (s, 3H), 3.72 (s, 3H), 2.73 – 2.52 (m, 3H), 2.38 – 2.25 (m, 2H), 1.25 (s, 3H); **^{13}C-NMR** (75 MHz, $CDCl_3$): δ (ppm) 173.3 (C), 173.2 (C), 141.6 (C), 119.5 (CH_2), 79.1 (C), 73.3 (CH_2), 59.0 (CH_2), 57.2

(C), 53.7 (CH), 53.1 (CH_3), 48.5 (CH_2), 37.3 (CH_2), 25.7 (CH_3). **HRMS** (ESI-TOF): m/z calculated for $C_{20}H_{21}NaO_6$ $[M + H]^+$: m/z 475.1156, found 475.1155. Stereochemistry of **39ad** was determined by analogy with that of **39aa**.

Dimethyl (*E*)-2-(2-((*tert*-butylsulfinyl)imino)ethyl)-2-(2-cyclopropylideneethyl)malonate (**40a**)

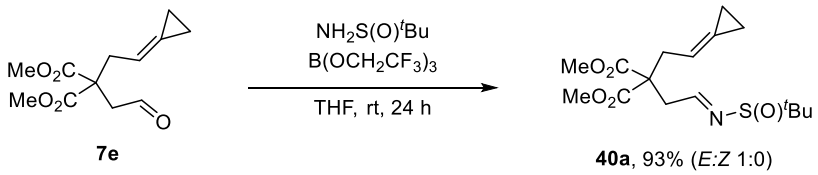

Tris(2,2,2-trifluoroethyl) borate (760 μL, 3.50 mmol, 1.0 equiv.) was added dropwise to a round-bottom flask containing the aldehyde precursor **7e** (845 mg, 3.50 mmol, 1.0 equiv.) and 2-methylpropane-2-sulfinamide (527 mg, 4.20 mmol, 1.2 equiv.) in THF (11 mL). The mixture was stirred at rt for 24 h and then the reaction was quenched with $NH_4Cl_{(sat)}$ (20 mL) and extracted with Et_2O (3x10 mL). The combined organic layers were dried, filtered and concentrated. The product **40a** was obtained after a flash chromatography as a colourless oil (1.12 g, 3.26 mmol, 93% yield). **^{1}H NMR** (300 MHz, $CDCl_3$) δ (ppm) 8.04 (t, *J* = 4.1 Hz, 1H), 5.83 – 5.61 (m, 1H), 3.75 (s, 6H), 3.14 (dd, *J* = 4.2, 2.0 Hz, 2H), 3.09 – 2.87 (m, 2H), 1.22 (s, 9H), 1.18 – 0.94 (m, 4H). **^{13}C NMR** (75 MHz, $CDCl_3$) δ (ppm) 172.0 (C), 168.2 (CH), 128.8 (C), 112.6 (CH), 58.01 (C), 57.5 (C), 53.3 (CH_3), 53.3 (CH_3), 39.9 (CH_2), 37.1 (CH_2), 22.5 (CH_2), 3.4 (CH_2), 2.4 (CH_2). **HRMS** (ESI-TOF): m/z calculated for $C_{13}H_{26}NO_5S$ $[M + H]^+$:m/z 344.1532, found 344.1533.

(*E*)-*N*-(2-((*tert*-Butylsulfinyl)imino)ethyl)-N-(2-cyclopropylideneethyl)-4 methylbenzene sulfonamide (**40c**)

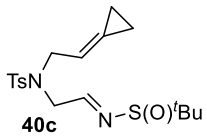

59% yield as a pale-yellow oil. **^{1}H NMR** (300 MHz, $CDCl_3$) δ (ppm) 7.89 (t, *J* = 3.5 Hz, 1H), 7.72 (d, *J* = 8.3 Hz, 2H), 7.30 (d, *J* = 8.1 Hz, 2H), 5.81 – 5.53 (m, 1H), 4.27 – 4.02 (m, 2H), 3.98 (t, *J* = 7.4 Hz, 2H), 2.43 (s, 3H), 1.16 (s, 9H), 1.10 – 0.72 (m, 4H). **^{13}C NMR** (75 MHz, $CDCl_3$) δ (ppm) 165.4 (CH), 143.7 (C), 136.8 (C), 129.9 (CH), 129.1 (C), 127.23 (CH), 112.2 (CH), 57.2 (C), 50.7 (CH_2), 50.1 (CH_2), 22.4 (CH_3), 21.6 (CH_3), 2.8 (CH_2), 1.9 (CH_2). **HRMS** (ESI-TOF): m/z calculated for $C_{18}H_{27}N_2O_5S_2$ $[M + H]^+$:m/z 383.1463, found 383.1471.

Dimethyl 3-((*tert*-butylsulfinyl)amino)-4-(3-(4-methoxyphenyl)prop-1-en-2-yl)cyclopentane-1,1-dicarboxy late (**42aa**+**42aa'**)

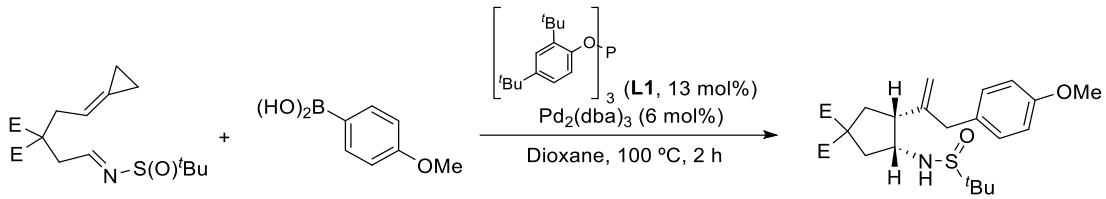

Prepared following general procedure for catalytic reactions (see *Methodology*, page 57), using $Pd_2(dba)_3$ (6.60 mg, 7.20 μmol, 6 mol%), phosphite **L1** (11.0 mg, 15.6 μmol, 13 mol%), imine-ACP **40a** (41.2 mg, 120 μmol, 1.0 equiv.), and 4-methoxyphenylboronic acid **33a** (36.5 mg, 240 μmol, 2.0 equiv.) in dry 1,4-dioxane (2.4 mL). The reaction crude was purified by flash chromatography (8% EtOAc/Hexane) to afford dimethyl 3-((*tert*-butylsulfinyl)amino)-4-(3-(4-methoxyphenyl)prop-1-en-2-yl)cyclopentane-1,1-dicarboxylate (**42aa** + **42aa'**) as a yellow oil (39.1 mg, 110 μmol, 90% yield, dr 1:1). The diastereoisomers **42aa** + **42aa'** were easily separated by column chromatography to be independently characterized. Their respective oxidation reactions with *m*CPBA afforded, in both

cases, the same sulfonamide derivative, confirming that both isomers are epimers at the sulfur center (see below). The stereochemistry at sulfur has not been determined.

(3*R*,4*R*)-Dimethyl 3-(((*S*)-*tert*-butylsulfinyl)amino)-4-(3-(4-methoxyphenyl)prop-1-en-2-yl)cyclo pentane-1,1-dicarboxylate (**42aa**)

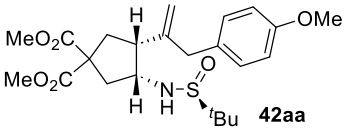

45% yield as a pale-yellow oil. **^{1}H NMR** (300 MHz, $CDCl_3$) δ (ppm) 7.10 (d, *J* = 8.6 Hz, 2H), 6.85 (d, *J* = 8.6 Hz, 2H), 5.04 (s, 1H), 5.02 (s, 1H), 3.93 (s, 1H), 3.81 (s, 3H), 3.71 (d, *J* = 1.2 Hz, 6H), 3.42 (d, *J* = 15.6 Hz, 1H), 3.25 (d, *J* = 15.7 Hz, 1H), 3.25 (s, 1H), 2.73 (d, *J* = 14.8 Hz, 2H), 2.65 (t, *J* = 13.0 Hz, 1H), 2.54 – 2.42 (m, 1H), 2.28 – 2.18 (m, 1H), 1.16 (s, 9H). **^{13}C NMR** (75 MHz, $CDCl_3$) δ (ppm) 173.1 (C), 172.3 (C), 158.4 (C), 146.3 (C), 130.5 (C), 130.3 (CH), 114.8 (CH_2), 114.1 (CH), 57.9 (C), 55.8 (C), 55.4 (CH), 53.4 (CH_3), 53.2 (CH_3), 52.9 (CH_3), 49.0 (CH), 42.0 (CH_2), 40.3 (CH_2), 35.1 (CH_2), 22.7 (CH_3). **HRMS** (ESI-TOF): m/z calculated for $C_{23}H_{34}NO_6S$ $[M + H]^+$: m/z 452.2107, found 452.2103.

(3*R*,4*R*)-Dimethyl 3-(((*R*)-*tert*-butylsulfinyl)amino)-4-(3-(4-methoxyphenyl)prop-1-en-2-yl)cyclo pentane-1,1-dicarboxylate (**42aa'**)

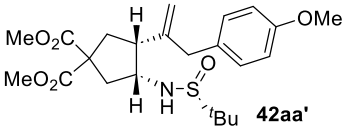

45% yield as a pale-yellow oil. **^{1}H NMR** (300 MHz, $CDCl_3$) δ (ppm) 7.07 (d, *J* = 8.5 Hz, 2H), 6.82 (d, *J* = 8.4 Hz, 2H), 4.86 (d, *J* = 7.9 Hz, 2H), 4.08 – 3.95 (m, 1H), 3.79 (s, 3H), 3.75 (s, 3H), 3.70 (s, 3H), 3.41 (d, *J* = 15.3 Hz, 1H), 3.23 (d, *J* = 15.3 Hz, 1H), 2.67 – 2.36 (m, 5H), 1.21 (s, 9H). **HRMS** (ESI-TOF): m/z calculated for $C_{23}H_{34}NO_6S$ $[M + H]^+$: m/z 452.2107, found 452.2103.

Stereochemistry of **42aa** and **42aa'** was deduced from **43aa**, which was obtained either from **42aa** or **42aa'** by treatment with *m*CPBA:

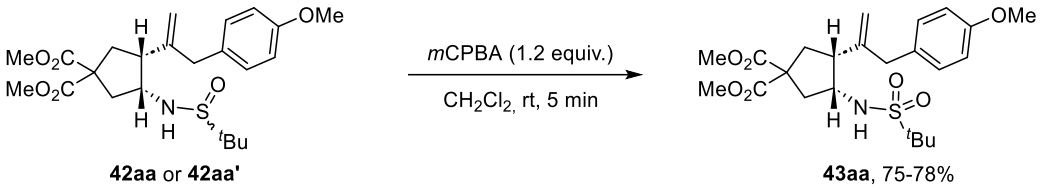

Scheme 145. Conversion of **42aa** and **42aa'** into **43aa** by oxidation of the sulfoxide center.

Tandem reaction between 40a and 33c: Prepared following the procedure employed for the synthesis of the tandem product **42aa**, using imino-ACP **40a** and boronic acid **33c** as starting materials. Isomers **42ac** and **42ac'** are obtained in 93% yield (dr 1:1) and can be separated by column chromatography (8% EtOAc/Hexane).

(3*R*,4*R*)-Dimethyl 3-(3-(4-(*tert*-butyl)phenyl)prop-1-en-2-yl)-4-(((*R*)-*tert*-butylsulfinyl)amino) cyclopentane-1,1-dicarboxylate (**42ac**)

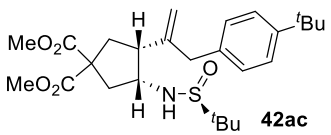

47% yield as a pale-yellow oil. **^{1}H NMR** (500 MHz, $CDCl_3$) δ (ppm) 7.36 – 7.27 (m, 2H), 7.14 – 7.08 (m, 2H), 5.14 – 4.91 (m, 2H), 4.01 – 3.90 (m, 1H), 3.70 (s, 6H), 3.54 – 3.09 (m, 3H), 2.88 – 2.59 (m, 3H), 2.52 – 2.44 (m, 1H), 2.29 – 2.19 (m, 1H), 1.31 (s, 9H), 1.16 (s, 9H). **^{13}C NMR** (126 MHz, $CDCl_3$) δ (ppm) 173.2 (C), 172.3 (C), 149.4 (C), 146.0 (C), 135.4 (C), 128.9 (CH), 125.6 (CH), 115.1 (CH_2), 58.0 (C), 55.8 (C), 53.5 (CH), 53.2 (CH_3), 52.9 (CH_3), 49.0 (CH), 42.4 (CH_2), 40.3 (CH_2), 35.1 (CH_2), 34.6 (C), 31.5 (CH_3), 22.7 (CH_3). **HRMS** (ESI-TOF): m/z calculated for $C_{26}H_{40}NO_5S$ $[M + H]^+$: m/z 478.2627, found 478.2622. Stereochemistry of **42ac** was deduced by NMR homology with **42aa**.

(3*R*,4*R*)-Dimethyl 3-(3-(4-(*tert*-butyl)phenyl)prop-1-en-2-yl)-4-(((*S*)-*tert*-butylsulfinyl)amino)cy clopentane-1,1-dicarboxylate (**42ac'**)

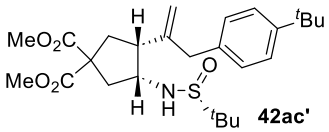

42ac'

46% yield as a pale-yellow oil. **^{1}H NMR** (500 MHz, $CDCl_3$) δ (ppm) 7.30 (d, *J* = 8.0 Hz, 2H), 7.08 (d, *J* = 8.0 Hz, 1H), 4.90 (s, 1H), 4.87 (s, 1H), 4.05 – 3.97 (m, 1H), 3.88 – 3.80 (m, 1H), 3.76 (s, 3H), 3.70 (s, 3H), 3.47 – 3.39 (m, 1H), 3.32 – 3.21 (m, 1H), 2.59 – 2.47 (m, 3H), 2.48 – 2.37 (m, 2H), 1.31 (s, 9H), 1.21 (s, 9H). **^{13}C NMR** (126 MHz, $CDCl_3$) δ (ppm) 174.6 (C), 172.5 (C), 149.3 (C), 146.3 (C), 135.9 (C), 128.8 (CH), 125.5 (CH), 113.6 (CH_2), 58.3 (CH), 57.6 (C), 56.5 (C), 53.5 (CH3), 53.1 (CH_3), 49.0 (CH), 43.0 (CH_2), 42.9 (CH_2), 35.7 (CH_2), 34.5 (C), 31.5 (CH_3), 23.0 (CH_3). **HRMS** (ESI-TOF): m/z calculated for $C_{26}H_{40}NO_5S$ $[M + H]^+$: m/z 478.2627, found 478.2597. Stereochemistry of **42ac'** was deduced by NMR homology with **42aa'**.

Tandem reaction between 40a and 33d: Prepared following the procedure employed for the synthesis of the tandem product **42aa**, using imino-ACP **40a** and boronic acid **33d** as starting materials. Isomers **42ad** and **42ad'** are obtained in 91% combined yield (dr 1:1) and can be separated by column chromatography (8% EtOAc/Hexane).

Dimethyl (3*R*,4*R*)-3-(((*R*)-*tert*-butylsulfinyl)amino)-4-(3-(4-fluorophenyl)prop-1-en-2-yl)cyclo pentane-1,1-dicarboxylate (**42ad**)

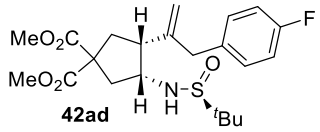

42ad

45% yield as a pale-yellow oil. **^{1}H NMR** (500 MHz, $CDCl_3$) δ (ppm) 7.12 – 7.02 (m, 2H), 6.96 – 6.78 (m, 2H), 4.99 (s, 1H), 4.91 (s, 1H), 3.88 – 3.77 (m, 1H), 3.63 (s, 6H), 3.36 (d, *J* = 17.1, 1H), 3.20 (d, *J* = 17.7 Hz, 1H), 3.15 (s, 1H), 2.78 – 2.61 (m, 1H), 2.59 – 2.48 (m, 1H), 2.47 – 2.33 (m, 1H), 2.23 – 2.08 (m, 1H), 1.08 (s, 9H). **^{13}C NMR** (126 MHz, $CDCl_3$) δ (ppm) 173.1 (C), 172.3 (C), 161.8 (d, *J* = 144.35 Hz, C), 146.0 (C), 134.1 (d, *J* = 3.22 Hz, C), 130.8 (d, *J* = 7.84 Hz, CH), 115.5 (d, *J* = 21.12 Hz, CH), 115.2 (CH_2), 57.9 (C), 55.9 (C), 53.5 (CH_3), 53.2 (CH_3), 52.9 (CH), 49.1 (CH), 42.0 (CH_2), 40.4 (CH_2), 35.2 (CH_2), 22.6 (CH_3). ^{19}F NMR (471 MHz, $CDCl_3$) δ -116.72. **HRMS** (ESI-TOF): m/z calculated for $C_{22}H_{31}FNO_5S$ $[M + H]^+$: m/z 440.1907, found 440.1901. Stereochemistry of **42ad** was deduced by NMR homology with **42aa**.

Dimethyl (3*R*,4*S*)-3-(((*S*)-*tert*-butylsulfinyl)amino)-4-(3-(4-fluorophenyl)prop-1-en-2-yl)cyclo pentane-1,1-dicarboxylate (**42ad'**)

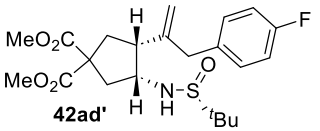

42ad'

46% yield as a pale-yellow oil. **^{1}H NMR** (500 MHz, $CDCl_3$) δ (ppm) 7.07 – 7.01 (m, 2H), 6.93 – 6.85 (m, 2H), 4.81 (s, 1H), 4.79 (s, 1H), 3.95 – 3.87 (m, 1H), 3.84 – 3.76 (m, 1H), 3.69 (s, 3H), 3.64 (s, 3H), 3.43 – 3.16 (m, 2H), 2.50 – 2.46 (m, 2H), 2.44 – 2.29 (m, 3H), 1.14 (s, 9H). **^{13}C NMR** (126 MHz, $CDCl_3$) δ (ppm) 174.5 (C), 172.4 (C), 161.7 (d, *J* = 244.41 Hz, C), 146.1 (C), 134.6 (d, *J* = 3.2 Hz, C), 130.6 (d, *J* = 7.76 Hz, CH), 115.4 (d, *J* = 21.16 Hz, CH), 113.9 (CH_2), 58.1 (CH), 57.6 (C), 56.5 (C), 53.5 (CH_3), 53.1 (CH_3), 49.1 (CH), 43.0 (CH_2), 42.6 (CH_2), 35.7 (CH_2), 23.0 (CH_3). **^{19}F NMR** (471 MHz, $CDCl_3$) δ (ppm) -116.84. **HRMS** (ESI-TOF): m/z calculated for $C_{22}H_{31}FNO_5S$ $[M + H]^+$:m/z 440.1907, found 440.1904. Stereochemistry of **42ad'** was deduced by NMR homology with **42aa'**.

Tandem reaction between 40a and 33f: Prepared following the procedure employed for the synthesis of the tandem product **42aa**, using imino-ACP **40a** and boronic acid **33f** as starting materials. Isomers **42af** and **42af'** are obtained in 99% combined yield (dr 1:1) and can be separated by column chromatography (8% EtOAc/Hexane).

Dimethyl (3*R*,4*R*)-3-(((*R*)-*tert*-butylsulfinyl)amino)-4-(3-(*o*-tolyl)prop-1-en-2-yl)cyclopentane-1,1-dicarboxylate (**42af**)

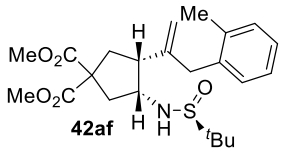

50% yield as a pale-yellow oil. **^{1}H NMR** (500 MHz, $CDCl_3$) δ (ppm) 7.21 – 7.05 (m, 4H), 5.02 (s, 1H), 4.75 (s, 1H), 3.96 (t, *J* = 4.4 Hz, 1H), 3.72 (s, 3H), 3.70 (s, 3H), 3.42 (d, *J* = 16.5 Hz, 1H), 3.29 (d, *J* = 16.8 Hz, 1H), 3.26 (s, 1H), 2.91 – 2.83 (m, 1H), 2.83 – 2.73 (m, 1H), 2.66 (t, *J* = 13.2 Hz, 1H), 2.56 – 2.47 (m, 1H), 2.31 – 2.26 (m, 1H), 2.25 (s, 3H), 1.15 (s, 9H). **^{13}C NMR** (126 MHz, $CDCl_3$) δ (ppm) 173.3 (C), 172.3 (C), 144.9 (C), 137.0 (C), 136.6 (C), 130.4 (CH), 130.3 (CH), 126.8 (CH), 126.3 (CH), 114.4 (CH_2), 57.9 (C), 55.8 (C), 53.4 (CH), 53.2 (CH_3), 52.9 (CH_3), 50.0 (CH), 40.4 (CH_2), 40.3 (CH_2), 35.2 (CH_2), 22.7 (CH_3), 19.6 (CH_3). **HRMS** (ESI-TOF): m/z calculated for $C_{23}H_{34}NO_5S$ [M + H]$^+$: m/z 436.2158, found 436.2151. Stereochemistry of **42af** was deduced by NMR homology with **42aa**.

Dimethyl (3*R*,4*S*)-3-(((*S*)-*tert*-butylsulfinyl)amino)-4-(3-(*o*-tolyl)prop-1-en-2-yl)cyclopentane-1,1-dicarboxylate (42af')

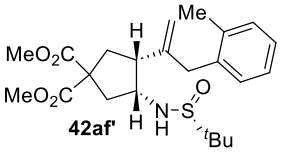

49% yield as a pale-yellow oil. **^{1}H NMR** (500 MHz, $CDCl_3$) δ (ppm) 7.14 (q, *J* = 3.9 Hz, 3H), 7.08 (d, *J* = 4.7 Hz, 1H), 4.88 (s, 1H), 4.68 (s, 1H), 4.09 – 3.98 (m, 1H), 3.86 (d, *J* = 8.0 Hz, 1H), 3.76 (s, 3H), 3.72 (s, 3H), 3.42 (d, *J* = 16.1 Hz, 1H), 3.31 (d, *J* = 16.1 Hz, 1H), 2.58 (s, 2H), 2.49 – 2.39 (m, 1H), 2.29 – 2.21 (m, 4H), 1.22 (s, 9H). **^{13}C NMR** (126 MHz, $CDCl_3$) δ (ppm) 174.6 (C), 172.5 (C), 144.9 (C), 137.2 (C), 137.1 (C), 130.5 (CH), 130.0 (CH), 126.7 (CH), 126.1 (CH), 113.4 (CH_2), 58.2 (CH), 57.5 (C), 56.5 (CH_3), 53.5 (CH), 53.1 (CH_3), 50.0 (CH), 43.0 (CH_2), 40.8 (CH_2), 35.8 (CH_2), 23.1 (CH_3), 19.7 (CH_3). **HRMS** (ESI-TOF): m/z calculated for $C_{23}H_{34}NO_5S$ [M + H]$^+$: m/z 436.2158, found 436.2152. Stereochemistry of **42af'** was deduced by NMR homology with **42aa'**.

Tandem reaction between 40a and 33i: Prepared following the procedure employed for the synthesis of the tandem product **42aa**, using imino-ACP **40a** and boronic acid **33i** as starting materials. Isomers **42ai** and **42ai'** are obtained in 76% combined yield (dr 1:1) and can be separated by column chromatography (8% EtOAc/Hexane).

Dimethyl (3*R*,4*R*)-3-((*R*)-*tert*-butylsulfinyl)amino)-4-(3-(naphthalen-1-yl)prop-1-en-2-yl)cyclo pentane-1,1-dicarboxylate (42ai)

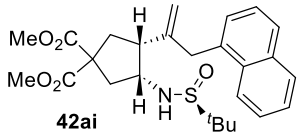

38% yield as a pale-yellow oil. **^{1}H NMR** (500 MHz, $CDCl_3$) δ (ppm) 7.80 – 7.69 (m, 3H), 7.57 (d, *J* = 1.6 Hz, 1H), 7.46 – 7.32 (m, 2H), 7.24 (dd, *J* = 8.4, 1.8 Hz, 1H), 5.03 (s, 1H), 4.99 (s, 1H), 3.98 – 3.86 (m, 1H), 3.62 (s, 3H), 3.59 (s, 3H), 3.55 (d, *J* = 15.7 Hz, 1H), 3.40 (d, *J* = 15.6 Hz, 1H), 3.28 – 3.19 (m, 1H), 2.78 – 2.69 (m, 1H), 2.66 (d, *J* = 14.7 Hz, 1H), 2.59 (t, *J* = 13.1 Hz, 1H), 2.45 – 2.33 (m, 1H), 2.24 – 2.13 (m, 1H), 1.10 (s, 9H). **^{13}C NMR** (126 MHz, $CDCl_3$) δ (ppm) 173.1 (C), 172.3 (C), 145.9 (C), 136.1 (C), 133.7 (C), 132.4 (C), 128.3 (CH), 127.8 (CH), 127.8 (CH), 127.7 (CH), 127.7 (CH), 126.1 (CH), 125.6 (CH), 115.5 (CH_2), 58.0 (C), 55.84(C), 53.5 (CH), 53.2 (CH_3), 52.9 (CH_3), 49.1 (CH), 43.0 (CH_2), 40.4 (CH_2), 35.1 (CH_2), 22.7 (CH_3). **HRMS** (ESI-TOF): m/z calculated for $C_{26}H_{34}NO_5S$ [M + H]$^+$: m/z 472.2158, found 472.2152. Stereochemistry of **42ai** was determined by nOe experiments.

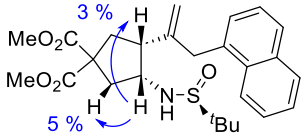

Figure 70. Significant nOe's observed for **42ai**.

Dimethyl (3*R*,4*S*)-3-(((*S*)-*tert*-butylsulfinyl)amino)-4-(3-(naphthalen-1-yl)prop-1-en-2-yl)cyclo pentane-1,1-dicarboxylate (42ai')

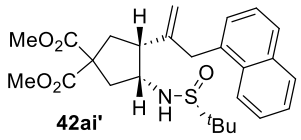

39% yield as a pale-yellow oil. **^{1}H NMR** (500 MHz, $CDCl_3$) δ (ppm) 7.77 – 7.66 (m, 3H), 7.56 – 7.53 (m, 1H), 7.43 – 7.33 (m, 2H), 7.25 – 7.21 (m, 1H), 4.89 (t, *J* = 1.3 Hz, 1H), 4.85 (s, 1H), 4.08 – 3.98 (m, 1H), 3.86 (d, *J* = 8.3 Hz, 1H), 3.68 (s, 3H), 3.59 (s, 3H), 3.57 (d, *J* = 15.4 Hz, 1H), 3.41 (d, *J* = 15.2 Hz, 1H), 2.51 – 2.34 (m, 5H), 1.17 (s, 9H). **^{13}C NMR** (126 MHz, $CDCl_3$) δ (ppm) 174.7 (C), 172.3 (C), 146.1 (C), 136.6 (C), 133.7 (C), 132.4 (C), 128.3 (CH), 127.8 (CH), 127.7 (CH), 127.6 (CH), 127.5 (CH), 126.2 (CH), 125.6 (CH), 114.0 (CH_2), 58.3 (CH), 57.6 (C), 56.5 (C), 53.5 (CH_3), 53.0 (CH_3), 49.2 (CH), 43.7 (CH_2), 43.0 (CH_2), 35.7 (CH_2), 23.0 (CH_3). **HRMS** (ESI-TOF): m/z calculated for $C_{26}H_{34}NO_5S$ [M + H]$^+$: m/z 472.2158, found 472.2142.

Tandem reaction between 40c and 33a: Prepared following the procedure employed for the synthesis of the tandem product **42aa**, using imino-ACP **40c** and boronic acid **33a** as starting materials. Isomers **42ca** and **42ca'** are obtained in 66% combined yield (dr 1:1) and can be separated by column chromatography (8% EtOAc/Hexane).

***R*-*N*-((3*S*,4*S*)-4-(3-(4-Methoxyphenyl)prop-1-en-2-yl)-1-tosylpyrrolidin-3-yl)-2methylpropane-2-sulfinamide** (**42ca**)

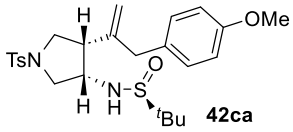

33% yield as a pale-yellow oil. **^{1}H NMR** (500 MHz, $CDCl_3$) δ (ppm) 7.68 (d, *J* = 8.1 Hz, 2H), 7.27 (d, *J* = 8.1 Hz, 2H), 7.04 (d, *J* = 8.5 Hz, 2H), 6.82 (d, *J* = 8.5 Hz, 2H), 5.08 (s, 1H), 4.90 (s, 1H), 3.91 (t, *J* = 4.6 Hz, 1H), 3.79 (s, 3H), 3.58 – 3.44 (m, 2H), 3.41 – 3.35 (m, 2H), 3.21 – 3.18 (m, 1H), 2.81 – 2.69 (m, 1H), 2.40 (s, 3H), 1.05 (s, 9H); **^{13}C NMR** (126 MHz, $CDCl_3$) δ (ppm) 158.6 (C), 143.8 (C), 143.6 (C), 134.7 (C), 130.1 (CH), 129.9 (CH), 129.8 (C), 127.5 (CH), 115.8 (CH_2), 114.2 (CH), 56.0 (C), 55.4 (CH_3), 53.9 (CH_2), 52.3 (CH), 48.5(CH_2), 47.2 (CH), 41.9 (CH_2), 22.5 (CH_3), 21.6 (CH_3). **HRMS** (ESI-TOF): m/z calculated for $C_{25}H_{35}N_2O_4S_2$ [M + H]$^+$: m/z 491.2033, found 491.2033. Stereochemistry of **42ca** was determined by nOe experiments.

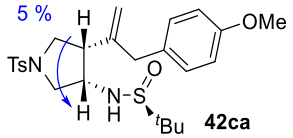

Figure 71. Significant nOe's observed for **42ca**.

***S*-*N*-((3*S*,4*R*)-4-(3-(4-methoxyphenyl)prop-1-en-2-yl)-1-tosylpyrrolidin-3-yl)-methylpropane-2-sulfinamide** (**42ca'**)

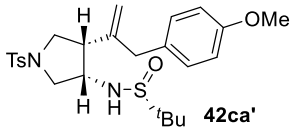

33% yield as a pale-yellow oil. **^{1}H NMR** (500 MHz, $CDCl_3$) δ (ppm) 7.61 (d, *J* = 8.0 Hz, 2H), 7.25 (d, *J* = 8.0 Hz, 2H), 6.95 (d, *J* = 8.5 Hz, 2H), 6.74 (d, *J* = 8.6 Hz, 2H), 4.83 – 4.73 (m, 2H), 3.72 (s, 3H), 3.65 – 3.55 (m, 2H), 3.39 – 3.30 (m, 1H), 3.19 (s, 2H), 3.08 – 2.96 (m, 2H), 2.83 (d, *J* = 6.7 Hz, 1H), 2.51 – 2.43 (m, 1H), 2.37 (s, 3H), 1.01 (s, 9H);. **^{13}C NMR** (126 MHz, $CDCl_3$) δ (ppm) 158.5 (C), 145.7 (C), 143.9 (C), 133.6 (C), 130.5 (C), 130.1 (CH), 130.0 (CH), 127.8 (CH), 114.1 (CH), 113.8 (CH_2), 58.9 (CH), 56.0 (C), 55.4 (CH_3), 53.7 (CH_2), 50.8 (CH_2), 50.0 (CH), 41.6 (CH_2), 22.5 (CH_3), 21.7 (CH_3). **HRMS** (ESI-TOF): m/z calculated for $C_{25}H_{35}N_2NaO_4S_2$ [M + Na]$^+$: m/z 513.1858, found 513.1849. Stereochemistry of **42ca'** was deduced by NMR homology with **42aa'**.

Dimethyl (3*R*,4*R*)-3-((1,1-dimethylethyl)sulfonamido)-4-(3-(4-methoxyphenyl)prop-1-en-2-yl)cy clopentane-1,1-dicarboxylate (**43aa**)

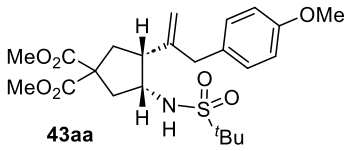

43aa

75-78% as a pale-yellow oil. **^{1}H NMR** (500 MHz, CD_3CN) δ (ppm) 7.06 (d, *J* = 8.6 Hz, 2H), 6.78 (d, *J* = 8.6 Hz, 2H), 4.85 (s, 1H), 4.77 (s, 1H), 4.59 (d, *J* = 9.1 Hz, 1H), 4.14 – 4.00 (m, 1H), 3.69 (s, 3H), 3.63 (s, 3H), 3.57 (s, 3H), 3.40 (d, *J* = 15.6 Hz, 1H), 3.22 (d, *J* = 15.5 Hz, 1H), 2.62 – 2.50 (m, 1H), 2.47 (d, *J* = 1.5 Hz, 1H), 2.46 (s, 1H), 2.27 (d, *J* = 1.6 Hz, 1H), 2.25 (s, 1H), 1.27 (s, 9H). **^{13}C NMR** (126 MHz, CD_3CN) δ (ppm) 173.5 (C), 173.2 (C), 159.2 (C), 148.0 (C), 132.3 (C), 131.3 (CH), 114.7 (CH), 113.8 (CH_2), 60.2 (C), 58.0 (C), 57.4 (CH), 55.8 (CH_3), 53.65 (CH_3), 53.6 (CH_3), 48.8 (CH), 42.6 (CH_2), 42.5 (CH_2), 36.3 (CH_2), 24.6 (CH_3). **HRMS** (ESI-TOF): m/z calculated for $C_{23}H_{33}NO_7SNa$ [M + Na]$^+$: m/z 490.1875, found 490.1855.

Stereochemistry of **43aa** was determined by nOe experiments.

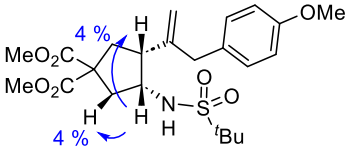

Figure 72. Significant nOe's observed for **43aa**.

(2-Methylenedecyl)benzene (**45bl**)

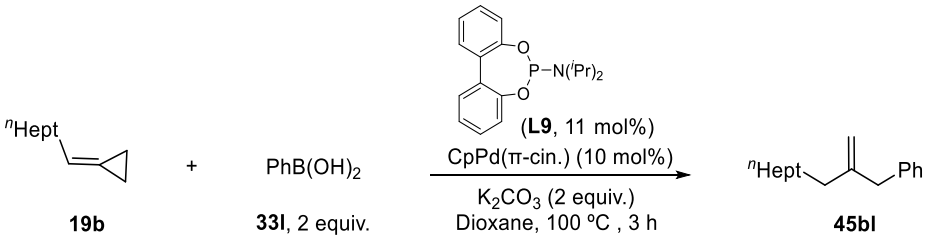

Prepared following general procedure for catalytic reactions (see *Methodology*, page 57), using CpPd(π–cinnamyl) (5.69 mg, 19.7 μmol, 10 mol%), phosphoramidite **L9** (6.80 mg, 21.7 μmol, 11 mol%), octylidenecyclopropane **19d** (30.0 mg, 197 μmol, 1.0 equiv.), and phenylboronic acid **33l** (48.0 mg, 394 μmol, 2.0 equiv.) in dry 1,4-dioxane (2 mL). The reaction crude was purified by flash chromatography (100% Hexane) to afford (2-methylenedecyl)benzene **45bl** as a yellow oil in 90% yield (40.8 mg, 177 μmol, 90% yield). **^{1}H-NMR** (300 MHz, $CDCl_3$) δ (ppm) 7.42 – 7.30 (m, 2H), 7.29 – 7.21 (m, 3H), 4.88 (d, *J* = 2.0 Hz, 1H), 4.79 (d, *J* = 2.1 Hz, 1H), 3.40 (s, 2H), 2.03 (t, *J* = 7.6 Hz, 2H), 1.56 – 1.43 (m, 2H), 1.32 (s, 10H), 0.95 (t, *J* = 6.4 Hz, 3H). **^{13}C-NMR** (75 MHz, $CDCl_3$) δ (ppm) 149.5 (C), 140.1 (C), 129.2 (CH), 128.4 (CH), 126.1 (CH), 111.1 (CH_2), 43.2 (CH_2), 35.6 (CH_2), 32.0 (CH_2), 29.6 (CH_2), 29.5 (CH_2), 29.4 (CH_2), 27.8 (CH_2), 22.8 (CH_2), 14.3 (CH_3). **HRMS** (APCI-TOF): m/z calculated for $C_{17}H_{26}$ [M]$^+$: m/z 230.2035, found 230.2028.

(2-Methylenedecyl-3-d)benzene (**d-45bl**)

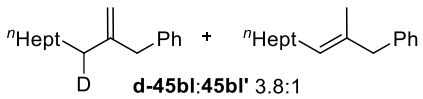

Prepared following the procedure employed for the synthesis of the coupling product **45bl**, using deuterated phenyl boronic acid (**d-33l**) as partner instead **33l**. Isolated by column chromatography (100% Hexane) as a colourless oil in 64% yield, **d-45bl:d-45bl'** = 3.8:1. **^{1}H NMR** (500 MHz, $CDCl_3$) δ 7.45 – 7.32 (m, 2H), 7.30 – 7.23 (m, 3H), 5.34 (t, *J* = 7.2 Hz, 0.2H), 4.89 (s, 0.78H), 4.79 (s, 0.78H), 3.40 (s, 1.56H), 3.35 (s, 0.4H), 2.09 (q, *J* = 7.2 Hz, 0.4H), 2.05 – 1.97 (m, 1.01H), 1.53 – 1.46 (m, 2H), 1.40 – 1.28 (m, 10H), 0.95 (t, *J* = 6.9 Hz, 3H). **^{2}H NMR** (77 MHz, $CDCl_3$) δ 1.99 (br. s, 1D), 1.74 – 1.42 (m, 0.83D).

1-Methoxy-4-(2-methylenedecyl)benzene (**45ba**)

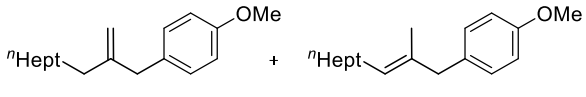

45ba: 45ba' 5:1

Prepared following the procedure employed for the synthesis of the coupling product **45bl**, using boronic acid **33a** as starting material. Isolated by column chromatography (100% Hexane) as a colourless oil in 92% yield, **45ba:45ba'** = 5:1. **^{1}H-NMR** (300 MHz, $CDCl_3$) δ (ppm) 7.12 – 7.08 (m, 2H), 6.85 – 6.81 (m, 2H), 5.27 (m, 0.17 H), 4.80 (d, *J* = 2.0 Hz, 0.83H), 4.71 (d, *J* = 2.1 Hz, 0.83H), 3.80 (s, 3H), 3.28 (s, 1.66H), 3.25 (s, 0.34H), 2.05 (m, 0.51H), 1.96 (t, *J* = 7.6 Hz, 1.66H), 1.48 – 1.38 (m, 2H), 1.28 (d, *J* = 6.8 Hz, 10H), 0.93 – 0.86 (m, 3H). **^{13}C-NMR** (75 MHz, $CDCl_3$) δ (ppm) 158.1 (C), 149.9 (C), 130.0 (CH), 113.8 (CH), 110.7 (CH_2), 55.4 (CH_3), 42.3 (CH_2), 35.5 (CH_2), 32.0 (CH_2), 29.6 (CH_2), 29.5 (CH_2), 29.4 (CH_2), 27.8 (CH_2), 22.8 (CH_2), 14.2 (CH_3). **HRMS** (APCI-TOF): m/z calculated for $C_{18}H_{28}O$ $[M]^+$: m/z 260.2140, found 260.2135.

1-(2-Methylenedecyl)cyclopent-1-ene (**45bb**)

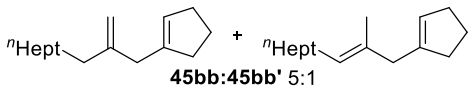

45bb:45bb' 5:1

Prepared following the procedure employed for the synthesis of the coupling product **45bl**, using boronic acid **33b** as starting material. Isolated by column chromatography (100% Hexane) as a colourless oil in 80% yield, **45bb:45bb'** = 5:1. **^{1}H-NMR** (300 MHz, $CDCl_3$) δ (ppm) 5.38 (s, 0.83H), 5.34 (m, 0.17H) 5.17 (t, *J*=7.2 Hz, 0.17 H) 4.75 (s, 0.83H), 4.73 (s, 0.83H), 2.79 (s, 1.67H), 2.73 (s, 0.33H) 2.38 – 2.25 (m, 2H), 2.24 – 2.14 (m, 2.17H), 1.97 (t, *J* = 7.6 Hz, 2H), 1.85 (p, *J* = 7.5 Hz, 2H), 1.48 – 1.33 (m, 2H), 1.32 – 1.21 (m, 10H), 0.92 – 0.80 (m, 3H). **^{13}C-NMR** (75 MHz, $CDCl_3$) δ (ppm) 148.2 (C), 142.7 (C), 125.7 (CH), 110.2 (CH_2), 38.7 (CH_2), 35.8 (CH_2), 34.9 (CH_2), 32.7 (CH_2), 32.1 (CH_2), 29.9 (CH_2), 29.7 (CH_2), 29.6 (CH_2), 29.5 (CH_2), 27.9 (CH_2), 23.8 (CH_2), 22.8 (CH_2), 14.3 (CH_3). **HRMS** (APCI-TOF): HRMS: m/z calculated for $C_{16}H_{29}$ $[M + H]^+$: m/z 221.2269, found 221.2264.

1-Fluoro-4-(2-methylenedecyl)benzene (**45bd**)

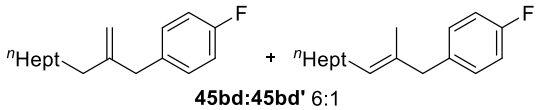

45bd:45bd' 6:1

Prepared following the procedure employed for the synthesis of the coupling product **45bl**, using boronic acid **33d** as starting material. Isolated by column chromatography (100% Hexane) as a colourless oil in 90% yield, **45bd:45bd`** = 6:1. **^{1}H-NMR** (300 MHz, $CDCl_3$) δ (ppm) 7.17 – 7.10 (m, 2H), 7.02 – 6.89 (m, 2H), 5.25 (m, 0.14 H) 4.83 (s, 0.86H), 4.71 (s, 0.86H), 3.30 (s, 1.72H), 3.25 (s, 0.28H), 2.07 – 1.90 (m, 2.14), 1.46 – 1.39 (m, 2H), 1.26 (s, 10H), 0.89 (t, *J* = 6.6 Hz, 3H). **^{13}C-NMR** (75 MHz, $CDCl_3$) δ (ppm) 161.6 (d, *J* = 243.9 Hz, C), 149.3 (C), 130.5 (d, *J* = 8.0 Hz, CH), 115.1 (d, *J* = 21.0 Hz, CH), 111.2 (CH_2), 42.3 (CH_2), 35.5 (CH_2), 32.0 (CH_2), 29.6 (CH_2), 29.5 (CH_2), 29.4 (CH_2), 29.4 (CH_2), 27.8 (CH_2), 22.8 (CH_2), 14.2 (CH_3). **^{19}F-NMR** (282 MHz, $CDCl_3$) δ (ppm) -117.61; **HRMS** (APCI-TOF): m/z calculated for $C_{17}H_{26}F$ $[M + H]^+$: m/z 249.2019, found 249.2013.

Employing *p*-F-C_6H_4OH (**38e**, 2.0 equiv.) instead K_2CO_3, **45bd** is obtained in 60% yield, **45bd:45bd`** = 18:1.

1-Methyl-2-(2-methylenedecyl)benzene (**45bf**)

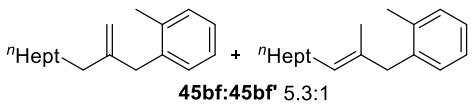

45bf:45bf' 5.3:1

Prepared following the procedure employed for the synthesis of the coupling product **45bl**, using boronic acid **33f** as starting material. Isolated by column chromatography (100% Hexane) as a pale-yellow oil in 50% yield, **45bf:45bf'** = 5.3:1. **^{1}H-NMR** (500 MHz, $CDCl_3$) δ (ppm) 7.22 – 7.04 (m, 4H), 5.15 – 5.00 (m, 0.16H), 4.80 (s, 0.84H), 4.47 (s, 0.84H), 3.31 (s, 1.68H), 3.28 (s, 0.32H), 2.27 (s, 3H), 2.11 – 1.97 (m, 2.16H), 1.51 – 1.42 (m, 2H), 1.46 – 1.16 (m, 10H), 0.89 (t, J = 6.9 Hz, 3H). **^{13}C-NMR** (126 MHz, $CDCl_3$) δ (ppm) 148.3 (C), 138.0 (C), 136.8 (C), 130.1 (CH), 130.0 (CH), 126.2 (CH), 125.8 (CH), 110.4 (CH), 40.2 (CH_2), 36.4 (CH_2), 31.9 (CH_2), 29.5 (CH_2), 29.4 (CH_2), 29.3 (CH_2), 27.9

(CH_2), 22.7 (CH_2), 19.3 (CH_3), 14.1 (CH_3). Signals of **45bf** (major product). **HRMS** (APCI-TOF): m/z calculated for $C_{18}H_{29}$ [M + H]$^+$: m/z 245.2264, found 245.2259.

Employing *p*-F-C_6H_4OH (**38e**, 2.0 equiv.) instead K_2CO_3, **45bf** is obtained in 71% yield, (**45bf:45bf'** = 12:1).

1-(2-Methylenedecyl)naphthalene (**45bi**)

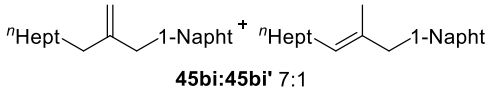

45bi:45bi' 7:1

Prepared following the procedure employed for the synthesis of the coupling product **45bl**, using boronic acid **33i** as starting material. Isolated by column chromatography (100% Hexane) as a pale-yellow oil in 55% yield, **45bi:45bi'** 7:1. **^{1}H-NMR** (500 MHz, $CDCl_3$) δ (ppm) 8.00 (t, *J* = 7.8 Hz, 1H), 7.90 – 7.81 (m, 1H), 7.75 (d, *J* = 8.1 Hz, 1H), 7.52 – 7.44 (m, 2H), 7.42 (t, *J* = 7.6 Hz, 1H), 7.34 (d, *J* = 7.2 Hz, 1H), 5.22 (t, *J* = 7.4 Hz, 0.12H), 4.86 (s, 0.88H), 4.57 (s, 0.88H), 3.79 (s, 1.75H), 3.77 (s, 0.25H), 2.10 (t, *J* = 7.8 Hz, 1.75H), 2.03 (m, 0.37H), 1.55 – 1.44 (m, 2H), 1.37 – 1.13 (m, 10H), 0.90 (t, *J* = 6.7 Hz, 3H). **^{13}C-NMR** (126 MHz, $CDCl_3$) δ (ppm) 148.9 (C), 136.1 (C), 134.0 (C), 132.6 (C), 128.7 (CH), 127.5 (CH), 127.1 (CH), 125.8 (CH), 125.6 (CH), 125.6 (CH), 124.6 (CH), 111.4 (CH_2), 40.1 (CH_2), 36.6 (CH_2), 32.1 (CH_2), 29.9 (CH_2), 29.7 (CH_2), 29.6 (CH_2), 29.4 (CH_2), 28.0 (CH_2), 22.8 (CH_2), 14.3 (CH_3). Signals of **45bi** (major product). **HRMS** (APCI-TOF): m/z calculated for $C_{18}H_{29}$ [M + H]$^+$: m/z 281.2269, found 281.2266.

(4-Methylenedodec-1-en-2-yl)benzene (**45bj**)

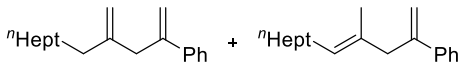

45bj:45bj' 4:1

Prepared following the procedure employed for the synthesis of the coupling product **45bl**, using boronic acid **33j** as starting material. Isolated by column chromatography (100% Hexane) as a colourless oil in 85% yield, **45bj:45bj'** = 4:1. **^{1}H-NMR** (300 MHz, $CDCl_3$) δ (ppm) 7.48 – 7.42 (m, 2H), 7.36 – 7.22 (m, 3H), 5.46 (d, *J* = 1.5 Hz, 0.8H), 5.41 (s, 0.2H), 5.25 (m, 0.2H), 5.14 (d, *J* = 1.5 Hz, 0.8H), 5.09 (s, 0.2H) 4.83 (s, 0.8H), 4.81 (s, 0.8H), 3.25 (s, 1.60H), 3.20 (s, 0.40H), 2.09 – 1.96 (m, 2.20H), 1.55 – 1.39 (m, 2H), 1.36 – 1.20 (s, 10H), 0.91 (t, *J* = 6.8, 3H). **^{13}C-NMR** (75 MHz, $CDCl_3$) δ (ppm) 147.6 (C), 146.0 (C), 141.3 (C), 128.2 (CH), 127.5 (CH), 126.3 (CH), 114.5 (CH_2), 111.6 (CH_2), 42.6 (CH_2), 36.0 (CH_2), 32.1 (CH_2), 29.7 (CH_2), 29.6 (CH_2), 29.4 (CH_2), 27.9 (CH_2), 22.8 (CH_2), 14.3 (CH_3); **HRMS** (APCI-TOF): m/z calculated for $C_{19}H_{29}$ [M + H]$^+$: m/z 257.2269, found 257.2264.

3-(2-methylenedecyl)pyridine (**45bk**)

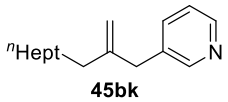

45bk

Prepared following the procedure employed for the synthesis of the coupling product **45bl**, using boronic acid **33k** as starting material. Isolated by column chromatography (100% Hexane) as a colourless oil in 40% yield as a pale-yellow oil (%Conv. **19d** = 75%). **^{1}H-NMR** (300 MHz, $CDCl_3$) δ (ppm) 8.46 (br, *J* = 5.6 Hz, 2H), 7.49 (dt, *J* = 7.8, 2.0 Hz, 1H), 7.21 (dd, *J* = 7.8, 4.8 Hz, 1H), 4.86 (s, 1H), 4.71 (s, 1H), 3.32 (s, 2H), 1.96 (t, *J* = 7.6 Hz, 2H), 1.49 – 1.35 (m, 2H), 1.32 – 1.49 (s, 10H), 0.87 (t, *J* = 6.6 Hz, 3H). **^{13}C-NMR** (75 MHz, $CDCl_3$) δ (ppm) 150.6 (CH), 148.3 (C), 147.8 (CH), 136.5 (CH), 135.4 (C), 123.4 (CH), 111.9 (CH_2), 40.2 (CH_2), 35.7 (CH_2), 32.0 (CH_2), 29.6 (CH_2), 29.4 (CH_2), 29.4 (CH_2), 27.7 (CH_2), 22.8 (CH_2), 14.2 (CH_3). **HRMS** (ESI-TOF): m/z calculated for $C_{16}H_{26}N$ [M + H]$^+$: m/z 232.2065, found 232.2060.

5-(2-Methylenedecyl)benzo[*d*][1,3]dioxole (**45bm**)

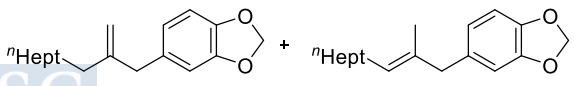

45bm:45bm' 7:1

Prepared following the procedure employed for the synthesis of the coupling product **45bl**, using boronic acid **33m** as starting material. Isolated by column chromatography (100% Hexane) as a colourless oil in 90% yield, **45bm:45bm'** = 7:1. **^{1}H-NMR** (300 MHz, $CDCl_3$) δ (ppm) 6.75 – 6.71 (m, 1H), 6.70 – 6.66 (m, 1H), 6.65 – 6.59 (m, 1H), 5.93 (s, 2H), 5.24 (m, 0.12H) 4.81 (s,

0.88H), 4.74 (s, 0.88H), 3.25 (s, 1.75H), 3.19 (s, 0.25H), 2.02 (m, 0.36H) 1.96 (t, *J* = 7.7 Hz, 1.76H), 1.50 – 1.35 (m, 2H), 1.27 (s, 10H), 0.95 – 0.84 (m, 3H). **^{13}C-NMR** (75 MHz, $CDCl_3$) δ (ppm) 149.6 (C), 147.6 (C), 145.9 (C), 133.9 (C), 121.9 (CH), 111.0 (CH_2), 109.5 (CH), 108.1 (CH), 100.9 (CH_2), 42.8 (CH_2), 35.4 (CH_2), 32.0 (CH_2), 29.6 (CH_2), 29.5 (CH_2), 29.4 (CH_2), 27.7 (CH_2), 22.8 (CH_2), 14.3 (CH_3). **HRMS** (APCI-TOF): m/z calculated for $C_{18}H_{26}O_2$ $[M]^+$: m/z 274.1933, found 274.1927.

Employing *p*-F-C_6H_4OH (**38e**, 2.0 equiv.) instead K_2CO_3, **45bm** is obtained in 56% yield, (**45bm:45bm'** = 18:1).

(3-Hexyl-2-methylenenonyl)benzene (**45dl**)

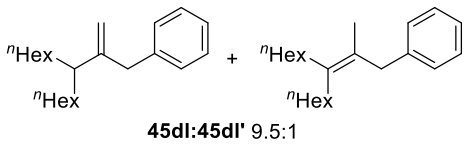

45dl:45dl' 9.5:1

Prepared following the procedure employed for the synthesis of the coupling product **45bl**, using ACP **19d** as starting material. Isolated by column chromatography (100% Hexane) as a colourless oil in 85% yield as a colorless oil, **45dl:45dl'** = 9.5:1. **^{1}H-NMR** (500 MHz, $CDCl_3$) δ (ppm) 7.32 – 7.25 (m, 2H), 7.22 – 7.15 (m, 3H), 4.80 (s, 0.90H), 4.56 (s, 0.90H), 3.40 (s, 0.19H), 3.24 (s, 1.81H), 2.08 – 2.11 (m, 0.30H), 2.07 – 2.00 (m, 0.90 H), 1.41 – 1.33 (m, 4H), 1.33 – 1.15 (m, 16H), 0.89 (t, *J* = 7.0 Hz, 6H).; **^{13}C-NMR** (126 MHz, $CDCl_3$) δ (ppm) 152.1 (C), 140.0 (C), 129.6 (CH), 128.1 (CH), 125.9 (CH), 111.6 (CH_2), 45.9 (CH), 40.0 (CH_2), 34.0 (CH_2), 31.9 (CH_2), 29.5 (CH_2), 27.3 (CH_2), 22.7 (CH_2), 14.1 (CH_3). **HRMS** (APCI-TOF): m/z calculated for $C_{22}H_{36}$ $[M]^+$: m/z 300.2812, found 300.2806.

(2-methylenepropane-1,1,3-triyl)tribenzene (**45el**)

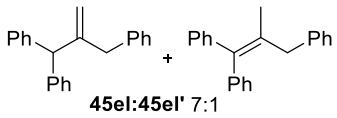

45el:45el' 7:1

Prepared following the procedure employed for the synthesis of the coupling product **45bl**, using ACP **19e** as starting material. The product (**45el**) was partially purified by filtration and directly characterized due its decomposition in silica gel or alumina. The reaction yield and product ratio were determined by ^{1}H-NMR employing TMB as internal standard. 83% as a pale-yellow oil, **45el:45el'** = 7:1. **^{1}H-NMR** (500 MHz, $CDCl_3$) δ (ppm) 7.31 – 7.22 (m, 6H), 7.20 – 7.14 (m, 4H), 7.13 – 7.10 (m, 2H), 7.09 – 7.05 (m, 3H), 5.06 (s, 0.89H), 4.62 (s, 0.89H), 4.54 (s, 0.89H), 3.48 (s, 0.25H), 3.32 (s, 1.75H), 1.66 (s, 0.33H). **^{13}C-NMR** (126 MHz, $CDCl_3$) δ (ppm) 151.4 (C), 142.1 (C), 139.6 (C), 135.6 (CH), 129.3 (CH), 129.2 (CH), 128.4 (CH), 128.3 (CH), 128.2 (CH), 126.3 (CH), 126.2 (CH), 115.8 (CH_2), 56.0 (CH), 43.1 (CH_2). Signals of **45el** (major product). **HRMS** (APCI-TOF): m/z calculated for $C_{22}H_{20}$ $[M]^+$: m/z 284.1560, found 284.1564.

1-Methoxy-4-(2-methylene-3-phenylbutyl)benzene (**45fa**)

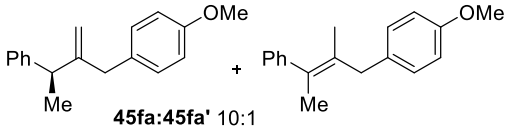

45fa:45fa' 10:1

Prepared following the procedure employed for the synthesis of the coupling product **45bl**, using ACP **19h** and the boronic acid **33a** as starting materials. Isolated by column chromatography (100% Hexane) as a colourless oil in 92% yield as a colourless oil, **45fa:45fa'** = 10:1. **^{1}H-NMR** (300 MHz, $CDCl_3$) δ (ppm) 7.34 (t, *J* = 7.1 Hz, 2H), 7.31 – 7.14 (m, 3H), 7.05 (d, *J* = 8.6 Hz, 2H), 6.86 (d, *J* = 8.6 Hz, 2H), 5.07 (s, 0.91H), 4.9 (s, 0.91H), 3.88 (s, 0.27H) 3.83 (s, 2.72H), 3.38 (q, *J* = 7.1 Hz, 1H), 3.28 (d, *J* = 15.3 Hz, 1.19H), 3.09 (d, *J* = 15.2 Hz, 1H), 1.39 (d, *J* = 7.1 Hz, 3H). **^{13}C-NMR** (75 MHz, $CDCl_3$) δ (ppm) 158.1 (C), 153.1 (C), 145.5 (C), 132.1 (C), 130.2 (CH), 128.5 (CH), 127.8 (CH), 126.3 (CH), 113.8 (CH), 111.0 (CH_2), 55.4 (CH_2), 44.3 (CH), 41.4 (CH_2), 21.0 (CH_3). **HRMS** (APCI-TOF): m/z calculated for $C_{18}H_{21}O$ $[M + H]^+$: m/z 253.1592, found 253.1587.

Ethyl 3-benzylbut-3-enoate (**45gl**)

Prepared following the procedure employed for the synthesis of the coupling product **45bl**, using ACP **19g** as starting material, and *p*-F-C_6H_4OH (**38e**, 2.0 equiv.) instead K_2CO_3. Reaction was carried out at 60 ºC. Isolated by column chromatography (100% Hexane) as a colourless oil in 40% yield

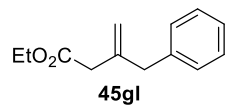

(%Conv. **19g** = 80). **^{1}H-NMR** (500 MHz, $CDCl_3$) δ (ppm) 7.29 (t, *J* = 7.5 Hz, 2H), 7.24 – 7.16 (m, 3H), 5.00 (s, 1H), 4.95 (s, 1H), 4.12 (q, *J* = 7.2 Hz, 2H), 3.46 (s, 2H), 2.97 (s, 2H), 1.30 – 1.14 (m, 3H). It contains grease. **^{13}C-NMR** (126 MHz, $CDCl_3$) δ (ppm) 171.4 (C), 141.9 (C), 138.8 (C), 129.1 (CH), 128.4 (CH), 126.3 (CH), 115.6 (CH_2), 60.6 (CH_2), 42.7 (CH_2), 41.2 (CH_2), 29.7 (CH_2), 14.2 (CH_3). **HRMS** (APCI-TOF): m/z calculated for $C_{13}H_{17}O_2$ $[M + H]^+$: m/z 205.1229, found 205.1225.

Diphenethyl 2-(3-(4-methoxybenzyl)but-3-en-1-yl)malonate (**45la**)

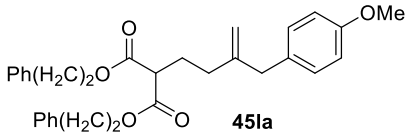

Prepared following the procedure employed for the synthesis of the coupling product **45la**, using ACP **19l** and boronic acid **33a** as starting materials, and *p*-F-C_6H_4OH (**38e**, 2.0 equiv.) instead K_2CO_3. Isolated by column chromatography (100% Hexane) as a colourless oil in 88% yield. **^{1}H-NMR** (300 MHz, $CDCl_3$) δ (ppm) 7.36 – 7.26 (m, 5H), 7.25 – 7.19 (m, 5H), 7.09 (d, *J* = 8.6 Hz, 2H), 6.84 (d, *J* = 8.6 Hz, 2H), 4.79 (s, 2H), 4.32 (t, *J* = 7.0 Hz, 4H), 3.79 (s, 3H), 3.32 (t, *J* = 7.0 Hz, 1H), 3.26 (s, 2H), 2.91 (t, *J* = 7.0 Hz, 4H), 2.08 – 1.91 (m, 4H). **^{13}C-NMR** (75 MHz, $CDCl_3$) δ (ppm) 169.3 (C), 158.2 (C), 147.7 (C), 137.6 (C), 131.5 (C), 130.0 (CH), 129.0 (CH), 128.6 (CH), 126.8 (CH), 113.9 (CH), 112.2 (CH_2), 65.8 (CH_2), 55.4 (CH_3), 51.5 (CH), 42.0 (CH_2), 35.0 (CH_2), 32.8 (CH_2), 26.8 (CH_2). **HRMS** (ESI-TOF): m/z calculated for $C_{31}H_{35}O_5$ $[M + H]^+$: m/z 487.2484, found 487.2476.

1-(3-Ethyl-2-methylenedecyl)-4-methoxybenzene (**45ma**)

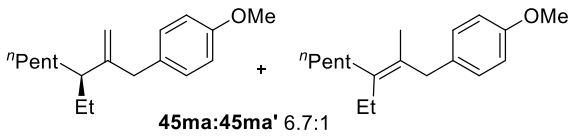

Prepared following the procedure employed for the synthesis of the coupling product **45bl**, using ACP **19m** and the boronic acid **33a** as starting materials. Isolated by column chromatography (100% Hexane) as a colourless oil in 71% yield as a colourless oil, **45ma:45ma'** = 6.7:1. **^{1}H-NMR** (300 MHz, $CDCl_3$) δ (ppm) 7.49 (d, *J* = 8.7 Hz, 0.20H), 7.08 (d, *J* = 8.3 Hz, 1.80H), 6.97 (d, *J* = 8.7 Hz, 0.20H), 6.84 (d, *J* = 8.6 Hz, 1.80H), 4.82 – 4.68 (m, 0.90H), 4.56 (q, *J* = 1.7 Hz, 0.90H), 3.95 (s, 0.30H) 3.80 (s, 2.70H), 3.32 (d, *J* = 4.6 Hz, 0.26H), 3.18 (s, 1.74H), 2.09 (m, 0.20H), 1.93 (p, *J* = 7.2 Hz, 1H), 1.45 – 1.30 (m, 5H), 1.31 – 1.16 (m, 5H), 0.93 – 0.85 (m, 3H), 0.81 (t, *J* = 7.4 Hz, 3H). **^{13}C-NMR** (75 MHz, $CDCl_3$) δ (ppm) 158.0 (C), 152.3 (C), 132.1 (C), 130.6 (CH), 113.7 (CH), 111.6 (CH_2), 55.4 (CH_3), 47.6 (CH), 39.3 (CH_2), 33.7 (CH_2), 32.2 (CH_2), 27.2 (CH_2), 26.7 (CH_2), 22.8 (CH_2), 14.3 (CH_3), 12.0 (CH_3). **HRMS** (APCI-TOF): m/z calculated for $C_{18}H_{29}O$ $[M + H]^+$: m/z 261.2218, found 261.2210.

1-Methoxy-4-((2-methylenedecyl)oxy)benzene (**46ba**)

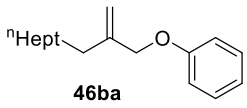

Prepared following the procedure employed for the synthesis of the coupling product **45bl** in absence of boronic acid, using phenol (**38a**, 2.0 equiv.) as additive instead K_2CO_3. Allyl ether **46ba** was obtained as a colourless oil in 55% yield. Spectroscopic data is in agreement the literature.[119d] **^{1}H-NMR** (300 MHz, $CDCl_3$) δ 7.31−7.24 (m, 2H), 6.96−6.82 (m, 2H), 5.12 (s, 1H), 4.98 (s, 1H), 4.45 (s, 2H), 2.13 (t, *J* = 7.7 Hz, 2H), 1.48 (t, *J* = 7.5 Hz, 2H), 1.27 (s, 10H), 0.88 (t, *J* = 6.4 Hz, 3H).

Dimethyl 2-(3-benzylbut-3-en-1-yl)-2-(4-oxopentyl)malonate (**47na**)

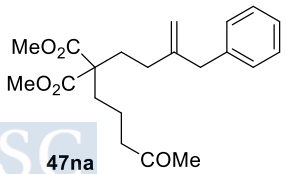

Prepared following the procedure employed for the synthesis of the coupling product **45dl**, using ACP **9n** as starting material, and *p*-F-C_6H_4OH (**38e**, 2.0 equiv.) instead K_2CO_3. Isolated by column chromatography (100% Hexane) as a colourless oil in 85% yield. **^{1}H-NMR** (300 MHz, $CDCl_3$) δ (ppm) 7.24 (t, *J* = 7.3 Hz, 2H), 7.20 – 7.06

[119d] Camacho, D. H.; Nakamura, I.; Saito, S.; Yamamoto, Y. Palladium-Catalyzed Addition of Alcohol Pronucleophiles to Alkylidenecyclopropanes. J. Org. Chem. **2001**, *66*, 1, 270–275.

(m, 3H), 4.84 (s, 1H), 4.76 (s, 1H), 3.64 (s, 6H), 3.32 (s, 2H), 2.35 (t, *J* = 7.1 Hz, 2H), 2.08 (s, 3H), 2.06 – 1.97 (m, 2H), 1.90 – 1.70 (m, 4H), 1.45 – 1.31 (m, 2H). **^{13}C-NMR** (75 MHz, $CDCl_3$) δ (ppm) 207.8 (C), 171.8 (C), 147.8 (C), 139.4 (C), 129.0 (CH), 128.2 (CH), 126.1 (CH), 111.9 (CH_2), 57.3 (C), 52.3 (CH_3), 43.4 (CH_2), 42.8 (CH_2), 31.8 (CH_2), 30.8 (CH_2), 29.8 (CH_3), 29.6 (CH_2), 18.2 (CH_2). **HRMS** (APCI-TOF): m/z calculated for $C_{21}H_{29}O_5$ [M + H]$^+$: m/z 361.2015, found 361.2011.

Dimethyl (5*aR*,9*aR*)-3-(3,5-bis(trifluoromethyl)phenyl)-9*a*-methyl-5-methylene-2-oxooctahydrobenzo[*f*][1,3]oxazepine-7,7(6*H*)-dicarboxylate (**50ba**)

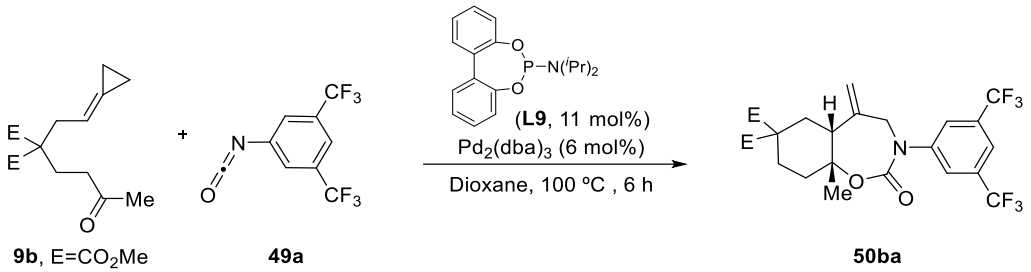

Prepared following general procedure for catalytic reactions (see *Methodology*, page 57), using $Pd_2(dba)_3$ (5.50 mg, 6.00 μmol, 6 mol%), phosphoramidite **L9** (4.10 mg, 13.0 μmol, 13 mol%), keto-ACP **9b** (26.8 mg, 100 μmol, 1.0 equiv.), and aryl isocyanate **2a** (34.6 μL, 200 μmol, 2.0 equiv.) in dry 1,4-dioxane (2 mL). The crude mixture was purified by flash chromatography (25-40% Et_2O/Hexane) to afford (5*a*R,9*a*R)-3-(3,5-bis(trifluoromethyl)phenyl)-9*a*-methyl-5-methylene-2-oxooctahydrobenzo[*f*][1,3] oxazepine-7,7(6*H*)-dicarboxylate (**50ba**) as a colourless solid (39.8 mg, 76.0 μmol, 76%). **^{1}H NMR** (500 MHz, $CDCl_3$) δ (ppm) 7.75 – 7.69 (m, 2H), 7.67 (s, 1H), 5.17 (s, 1H), 5.13 (s, 1H), 4.65 (d, *J* = 14.3 Hz, 1H), 3.73 (s, 3H), 3.68 (d, *J* = 14.4 Hz, 1H), 3.68 (s, 3H), 2.55 (dd, *J* = 12.9, 4.2 Hz, 1H), 2.26 (t, *J* = 13.1 Hz, 1H), 2.21 – 2.05 (m, 4H), 1.55 – 1.45 (m, 1H), 1.42 (s, 3H). **^{13}C NMR** (126 MHz, $CDCl_3$) δ (ppm) 172.0 (C), 171.4 (C), 156.2 (C), 145.1 (C), 141.8 (C), 132.8 (q, *J* = 33.8 Hz, C), 125.8 (CH), 125.8 (CH), 123.0 (d, *J* = 272.9 Hz, C), 120.4 – 120.2 (m, CH), 120.0 (CH_2), 80.9 (C), 54.4 (C), 53.7 (CH_2), 53.1 (CH_3), 52.9 (CH_3), 48.5 (CH), 36.6 (CH_2), 32.3 (CH_2), 26.2 (CH_2), 24.6 (CH_3). **^{19}F NMR** (471 MHz, $CDCl_3$) δ (ppm) -62.9 (s). **HRMS** (APCI-TOF): m/z calculated for $C_{23}H_{24}F_6NO_6^+$ [M + H]$^+$: m/z 524.1502, found 524.1518. Stereochemistry of **50ba** was determined by nOe experiments.

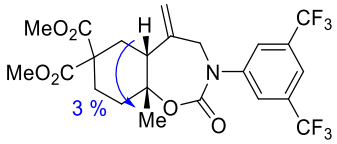

Figure 73. Significant nOe observed for **50ba**.

The structure of **50ba** was confirmed by X-ray analysis:

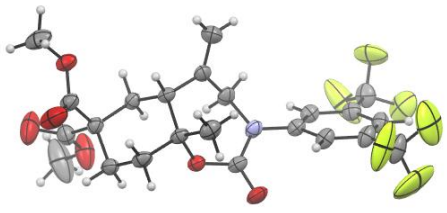

Figure 74. Crystal structure of **50ba** (**CCDC** 2414178).

Enantioselectivity was determined by chiral SFC analysis on Lux 5u Amylose-2 at 40 ºC, (CO_2:MeOH = 98:02, 1 mL/min, λ=254 nm).

Racemic sample:

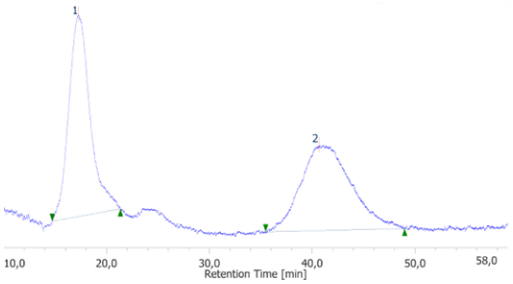

tR [min]	Area [μV·sec]	Height [μV]	Area%	Height%	Quantity	NTP
17,270	741371	5146	50,038	70,173	N/A	366
40,613	740239	2187	49,962	29,827	N/A	311

Using (*R,R,R*)-L12 (65.1:34.9 er; 30% ee):

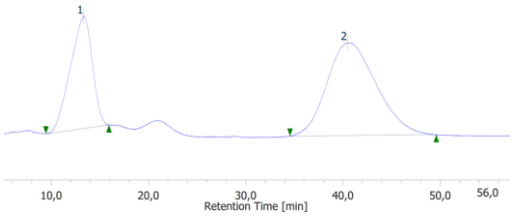

tR [min]	Area [μV·sec]	Height [μV]	Area%	Height%	Quantity	NTP
13,317	2875246	18370	34,891	54,752	N/A	156
40,423	5365410	15182	65,109	45,248	N/A	297

Cycloaddition between 9a and 49a: Prepared following the procedure employed for the synthesis of the cycloadduct **50ba**, using ACP **9a** as starting material. Isomers **50aa** and **50aa'** were obtained in 78% combined yield (dr 7:1) as a yellowish solid. Purification was achieved via flash chromatography (25-40% Et_2O/Hexane). NMR data of **50aa** and **50aa'** was obtained from 10:1 and 4:1 mixtures of these products.

Dimethyl (5*aR*,8*aR*)-3-(3,5-bis(trifluoromethyl)phenyl)-8*a*-methyl-5-methylene-2-oxooctahydro-7*H*-cyclopenta[*f*][1,3]oxazepine-7,7-dicarboxylate (**50aa** + **50aa'**)

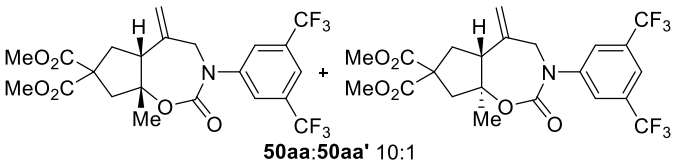

- NMR data of **50aa**, extracted from a **50aa:50aa'** mixture of 10:1. **^{1}H NMR** (500 MHz, $CDCl_3$) δ (ppm) 7.79 (s, 2H), 7.75 (s, 1H), 5.20 (s, 1H), 5.18 (s, 1H), 4.77 (d, *J* = 14.2 Hz, 1H), 3.79 (s, 3H), 3.77 (s, 3H), 3.71 (d, *J* = 14.3 Hz, 1H), 3.02 (dd, *J* = 13.9, 11.6 Hz, 1H), 2.92 (d, *J* = 15.1 Hz, 1H), 2.89 – 2.84 (m, 1H), 2.65 (d, *J* = 14.9 Hz, 1H), 2.29 (dd, *J* = 14.0, 8.5 Hz, 1H), 1.58 (s, 3H). **^{13}C NMR** (126 MHz, $CDCl_3$) δ (ppm) 172.9 (C), 171.8 (C), 155.3 (C), 144.6 (C), 139.8 (C), 132.8 (q, *J* = 33.9 Hz, C), 126.0 –125.9 (m, CH), 123.0 (q, *J* = 272.9 Hz, C), 120.5 – 120.4 (m, CH), 120.0 (CH_2), 90.8 (C), 57.6 (C), 54.9 (CH), 53.4 (CH_3), 53.3 (CH_3), 53.1 (CH_2), 48.8 (CH_2), 38.0 (CH_2), 21.7 (CH_3). **^{19}F NMR** (471 MHz, $CDCl_3$) δ (ppm) -62.9 (s). **HRMS** (APCI-TOF): m/z calculated for $C_{22}H_{22}F_6NO_6^+$ [M + H]$^+$: m/z 510.1346, found 510.1348. Stereochemistry of **50aa** was determined by nOe experiments.

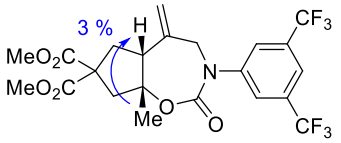

Figure 75. Significant nOe observed for **50aa**.

- **50aa:50aa'** mixture of 4:1: **^{1}H NMR** (300 MHz, $CDCl_3$) δ (ppm) 7.81 (s, 0.4H), 7.79 (s, 1.6H), 7.76 – 7.72 (m, 1H), 5.24 (s, 0.2H), 5.20 (s, 0.8H), 5.18 (s, 0.8H), 5.02 (s, 0.2H), 4.77 (d, *J* = 14.2 Hz, 0.8H), 4.34 (d, *J* = 15.5 Hz, 0.2H), 4.19 (d, *J* = 15.5 Hz, 0.2H), 3.79 (s, 3H), 3.77 – 3.74 (m, 3H), 3.71 (d, *J* = 14.3 Hz, 0.8H), 3.02 (dd, *J* = 13.5, 11.5 Hz, 1H), 2.96 – 2.79 (m, 2H), 2.65 (m, 1H), 2.29 (dd, *J* = 13.5, 8.1 Hz, 0.8H), 2.17 (t, *J* = 13.3 Hz, 0.2H), 1.58 (s, 2.4H), 1.35 (d, *J* = 1.0 Hz, 0.6H). **^{13}C NMR** (75 MHz, $CDCl_3$) δ (ppm) 172.9 (C), 171.8 (C), 155.3 (C), 145.4 (C), 144.6 (C), 140.0 (C), 139.9 (C), 132.8 (q, *J* = 33.9 Hz, C), 126.0 –125.9 (m, CH), 125.5 – 125.3 (m, CH), 123.0 (q, *J* = 272.9 Hz, C), 120.5 –120.4 (m, CH), 119.9 (CH_2), 113.7 (CH_2), 90.8 (C), 57.6 (C), 54.9 (CH), 54.3 (C), 53.5 (CH_3), 53.3 (CH_3), 53.2 (CH_3), 53.1 (CH_2), 48.8 (CH_2), 46.1 (CH_2), 38.0 (CH_2), 32.8 (CH_2), 21.7 (CH_3), 19.9 (CH_3). **^{19}F NMR** (471 MHz, $CDCl_3$) δ (ppm) -62.9 (s). **HRMS** (APCI-TOF): m/z calculated for $C_{22}H_{22}F_6NO_6^+$ $[M + H]^+$: m/z 510.1346, found 510.1348. Stereochemistry of **50aa'** was deduced by analogy with **50aa** and analogue products.

Dimethyl (5*aR*,8*aR*)-8*a*-methyl-5-methylene-2-oxo-3-phenyloctahydro-7*H*-cyclopenta[*f*][1,3]oxazepine-7,7-dicarboxylate (**50ab**)

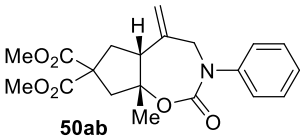

50ab

Prepared following the procedure employed for the synthesis of the cycloadduct **50ba**, using keto-ACP **9a** and phenyl isocyanate (**49b**) as starting materials. Isomers **50b** and **50ab'** are obtained in 75% combined yield (dr 5:1), as a yellow solid. Isomer **50ab** could be independently isolated by column chromatography (25-40% Et_2O/Hexane). **^{1}H NMR** (300 MHz, $CDCl_3$) δ (ppm) 7.37 (t, *J* = 7.6 Hz, 2H), 7.27 (d, *J* = 7.5 Hz, 3H), 5.09 (d, *J* = 4.9 Hz, 2H), 4.71 (d, *J* = 14.1 Hz, 1H), 3.77 (s, 3H), 3.76 (s, 3H), 3.65 (d, *J* = 14.1 Hz, 1H), 3.17 – 2.72 (m, 3H), 2.62 (d, *J* = 14.8 Hz, 1H), 2.36 – 2.14 (m, 1H), 1.60 (s, 3H). **^{13}C NMR** (75 MHz, $CDCl_3$) δ (ppm) 173.1 (C), 171.9 (C), 155.7 (C), 143.4 (C), 140.3 (C), 129.4 (CH), 127.1 (CH), 126.0 (CH), 119.0 (CH_2), 89.6 (C), 57.7 (C), 55.1 (CH), 53.3 (CH_3), 53.2 (CH_2) 53.2 (CH_3), 48.8 (CH_2), 38.1 (CH_2), 21.7 (CH_3). **HRMS** (APCI-TOF): m/z calculated for $C_{20}H_{23}NO_6^+$ $[M + H]^+$: m/z 374.1598, found 374.1602. Stereochemistry of **50ab** and **50ab'** was deducted by comparison with analogue products.

Employing K_2CO_3 (2 equiv.) as additive, **50ab** is obtained in 85% yield, **50ab:50ab'** = 5:1.

Dimethyl (5*aR*,9*aR*)-9a-methyl-5-methylene-2-oxo-3-phenyloctahydrobenzo[*f*][1,3]oxazepine-7,7(6*H*)-dicarboxylate (**50bb**+**50bb'**, 4:1 ratio)

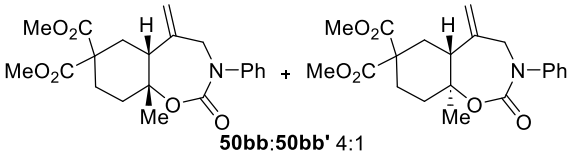

50bb:**50bb'** 4:1

Prepared following the procedure employed for the synthesis of the cycloadduct **50ba**, using phenyl isocyanate (**49b**) as reaction partner. Isomers **50bb** and **50bb'** are obtained in 80% combined yield (dr 4:1), as a yellow solid. Isolated as a 4:1 mixture by column chromatography (25-40% Et_2O/Hexane). **^{1}H NMR** (500 MHz, $CDCl_3$) δ (ppm) 7.40 – 7.34 (m, 2H), 7.31 – 7.21 (m, 3H), 5.16 (s, 0.2H), 5.14 (s, 0.8H), 5.12 (s, 0.8H), 4.97 (s, 0.2H), 4.66 (d, *J* = 14.2 Hz, 0.8H), 4.26 (d, *J* = 14.7 Hz, 0.2H), 4.16 (d, *J* = 14.7 Hz, 0.2H), 3.78 (s, 2.4H), 3.77 (s, 0.6H), 3.74 (s, 0.6H), 3.73 (s, 2.4H), 3.70 (d, *J* = 14.2 Hz, 0.8H), 2.73 – 2.66 (m, 0.2H), 2.56 (dd, *J* = 12.9, 4.1 Hz, 1H), 2.49 (dd, *J* = 13.1, 2.9 Hz, 0.2H), 2.36 (t, *J* = 13.1 Hz, 0.8H), 2.27 – 2.22 (m, 1.6H), 2.21 – 2.12 (m, 1.6H), 2.11 – 2.04 (m, 0.2H), 1.97 – 1.88 (m, 0.4H), 1.81 (t, *J* = 13.3 Hz, 0.2H), 1.57 – 1.51 (m, 0.8H), 1.50 (s, 2.4H), 1.39 (s, 0.6H). **^{13}C NMR** (126 MHz, $CDCl_3$) δ (ppm) 172.1 (C), 172.1 (C), 171.5 (C), 170.9 (C), 156.6 (C), 155.5 (C), 143.9 (C), 143.5 (C), 142.7 (C), 142.4 (C), 129.4 (CH), 128.5 (CH), 126.9 (CH), 126.8 (CH), 125.8 (CH), 125.6 (CH), 119.0 (CH_2), 113.7 (CH_2), 83.3 (C), 79.5 (C), 58.5 (CH_2), 54.7 (C), 54.5 (C), 53.8 (CH_2), 53.1 (CH_3), 53.0 (CH_3), 53.0 (CH_3), 52.9 (CH_3), 52.8 (CH), 48.7 (CH), 36.7 (CH_2), 32.3 (CH_2), 31.7 (CH_2), 28.8 (CH_2), 26.2 (CH_2), 24.4 (CH_3), 17.2 (CH_3). Stereochemistry of **50bb** and **50bb'** was deduced by comparison with analogue products.

Dimethyl (5*aR*,9*aR*)-3-(3,5-dichlorophenyl)-9*a*-methyl-5-methylene-2-oxooctahydrobenzo[*f*][1,3]oxazepine-7,7(6*H*)-dicarboxylate (50bc+50bc')

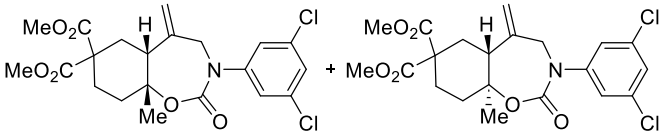

Prepared following the procedure employed for the synthesis of the cycloadduct **50ba**, using the isocyanate **49c** as reaction partner. Isomers **50bc** and **50bc'** are obtained in 65% combined yield (dr 6:1), as a yellow solid. They were isolated as a 4:1 mixture after column chromatography (25-40% Et_2O/Hexane). **^{1}H NMR** (300 MHz, $CDCl_3$) δ (ppm) 7.33 – 7.24 (m, 3H), 5.25 (s, 0.2H), 5.23 (s, 0.8H), 5.21 (s, 0.8H), 5.06 (s, 0.2H), 4.67 (d, *J* = 14.3 Hz, 0.8H), 4.27 (d, *J* = 14.9 Hz, 0.2H), 4.19 (d, *J* = 14.9 Hz, 0.2H), 3.83 (s, 2.4H), 3.82 (s, 0.6H), 3.79 (s, 0.6H), 3.78 (s, 2.4H), 3.72 (d, *J* = 14.3 Hz, 0.8H), 2.70 (s, 0.2H), 2.62 (dd, *J* = 12.8, 4.2 Hz, 1H), 2.36 (t, *J* = 13.3 Hz, 0.8H), 2.30 – 2.08 (m, 3.4H), 2.11 – 1.97 (m, 0.4H), 1.84 (t, *J* = 13.2 Hz, 0.2H), 1.63 – 1.52 (m, 1H), 1.51 (s, 2.4H), 1.41 (s, 0.6H). **^{13}C NMR** (75 MHz, $CDCl_3$) δ (ppm) 172.0 (C), 171.4 (C), 156.2 (C), 145.4 (C), 141.8 (C), 135.4 (C), 127.0 (CH), 126.9 (CH), 124.5 (CH), 124.2 (CH), 119.7 (CH_2), 114.4 (CH_2), 84.3 (C), 80.5 (C), 58.2 (CH_2), 54.4 (C), 53.7 (CH_2), 53.0 (CH_3), 52.9 (CH_3), 48.5 (CH), 36.6 (CH_2), 32.3 (CH_2), 26.2 (CH_2), 24.5 (CH_3), 17.3 (CH_3). **HRMS** (APCI-TOF): m/z calculated for $C_{21}H_{25}Cl_2NO_6^+$ [M + H]$^+$: m/z 456.0975, found 456.0972. Stereochemistry of **50bc** was determined by nOe experiments. Stereochemistry of **50bc'** was deduced by comparison with **50bc** and analogue products.

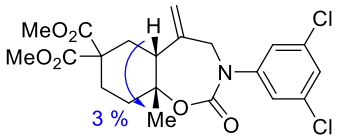

Figure 76. Significant nOe observed for **50bc**.

- NMR data of **50bc** (major isomer), extracted from the 4:1 mixture: **^{1}H NMR** (300 MHz, $CDCl_3$) δ (ppm) 7.33 – 7.24 (m, 3H), 5.23 (s, 1H), 5.21 (s, 1H), 4.67 (d, *J* = 14.3 Hz, 1H), 3.83 (s, 3H), 3.78 (s, 3H), 3.72 (d, *J* = 14.3 Hz, 1H), 2.62 (dd, *J* = 12.8, 4.2 Hz, 1H), 2.36 (t, *J* = 13.3 Hz, 1H), 2.30 – 2.08 (m, 4H), 1.63 – 1.52 (m, 1H), 1.51 (s, 3H). **^{13}C NMR** (75 MHz, $CDCl_3$) δ (ppm) 172.0 (C), 171.4 (C), 156.2 (C), 145.4 (C), 141.8 (C), 135.4 (C), 127.0 (CH), 124.5 (CH), 119.7 (CH_2), 80.5 (C), 54.4 (C), 53.7 (CH_2), 53.0 (CH_3), 52.9 (CH_3), 48.5 (CH), 36.6 (CH_2), 32.3 (CH_2), 26.2 (CH_2), 24.5 (CH_3).

Dimethyl (5*aR*,9*aR*)-3-(2,4-difluorophenyl)-9a-methyl-5-methylene-2-oxooctahydrobenzo[*f*][1,3]oxazepine-7,7(6*H*)-dicarboxylate (50bd+50bd')

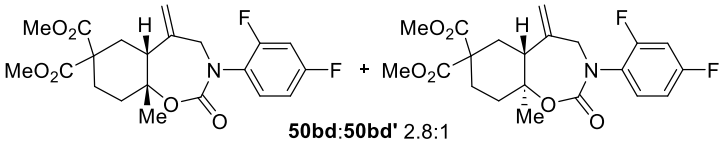

Prepared following the procedure employed for the synthesis of the cycloadduct **50ba**, using the isocyanate **49d** as reaction partner. Isomers **50bd** and **50bd'** are obtained in 45% combined yield (dr 3:1), as a yellow solid. They were isolated as a 2.8:1 mixture by column chromatography (25-40% Et_2O/Hexane). **^{1}H NMR** (300 MHz, $CDCl_3$) δ (ppm) 7.33 – 7.22 (m, 1H), 7.01 – 6.85 (m, 2H), 5.16 (s, 0.74H), 5.13 (s, 0.26H), 5.10 (s, 0.74H), 4.99 (s, 0.26H), 4.69 (d, *J* = 14.2 Hz, 0.74H), 4.26 (d, *J* = 14.6 Hz, 0.26H), 3.97 (d, *J* = 14.6 Hz, 0.26H), 3.85 – 3.71 (m, 6H), 3.47 (d, *J* = 14.2 Hz, 0.74H), 2.76 (d, *J* = 12.8 Hz, 0.26H), 2.59 (dd, *J* = 12.9, 4.2 Hz, 1H), 2.39 (t, *J* = 13.0 Hz, 1H), 2.32 – 2.21 (m, 2H), 2.21 – 2.11 (m, 1H), 1.99 – 1.78 (m, 0.74H), 1.54 (br. s, 3H). **^{13}C NMR** (75 MHz, $CDCl_3$) δ (ppm) 172.2 (C), 172.1 (C), 171.5 (C), 170.9 (C), 161.8 (dd, *J* = 249.8, 11.3 Hz, C), 157.9 (dd, *J* = 253.0, 12.4 Hz, C), 156.4 (C), 155.3 (C), 142.1 (C), 141.7 (C), 129.6 (CH, dd, *J* = 10.0, 2.7 Hz), 127.7 (dd, *J* = 13.2, 4.0 Hz, C), 119.6 (CH_2), 114.4 (CH_2), 111.9 (dd, *J* = 22.4, 3.8 Hz, CH), 161.8 (dd, *J* = 249.8, 11.3 Hz, CH), 83.7 (C), 80.0 (C), 58.7 (CH_2), 54.7 (C), 54.5 (C),

54.0 (CH_2), 53.1 (CH_3), 53.0 (CH_3), 53.0 (CH_3), 52.8 (CH_3), 48.8 (CH), 46.8 (CH), 36.7 (CH_2), 36.7 (CH_2), 32.2 (CH_2), 31.8 (CH_2), 28.9 (CH_2), 26.3 (CH_2), 24.2 (CH_3), 17.0 (CH_3). It contains grease. **^{19}F NMR** (282 MHz, $CDCl_3$) δ (ppm) -109.7 – -110.1 (m), -114.3 – -114.9 (m). **HRMS** (APCI-TOF): m/z calculated for $C_{21}H_{24}F_2NO_6^+$ $[M + H]^+$: m/z 424.1566, found 424.1566. Stereochemistry of **50bd** and **50bd'** was deduced by comparison with analogue products.

- Data extracted for **50bd** (major isomer) from the 2.8:1 mixture: **^{1}H NMR** (300 MHz, $CDCl_3$) δ (ppm) 7.33 – 7.22 (m, 1H), 7.01 – 6.85 (m, 2H), 5.16 (s, 1H), 5.10 (s, 1H), 4.69 (d, *J* = 14.2 Hz, 1H), 3.85 – 3.71 (m, 6H), 3.47 (d, *J* = 14.2 Hz, 0.1H), 2.59 (dd, *J* = 12.9, 4.2 Hz, 1H), 2.39 (t, *J* = 13.0 Hz, 1H), 2.32 – 2.21 (m, 2H), 2.21 – 2.11 (m, 1H), 1.99 – 1.78 (m, 1H), 1.54 (s, 3H). **^{13}C NMR** (75 MHz, $CDCl_3$) δ (ppm) 172.1 (C), 171.5 (C), 161.78 (C, dd, *J* = 249.8, 11.3 Hz), 157.87 (C, dd, *J* = 253.0, 12.4 Hz), 156.4 (C), 141.7 (C), 129.61 (CH, dd, *J* = 10.0, 2.7 Hz), 127.72 (C, dd, *J* = 13.2, 4.0 Hz), 119.6 (CH_2), 111.89 (CH, dd, *J* = 22.4, 3.8 Hz), 161.78 (CH, dd, *J* = 249.8, 11.3 Hz), 80.0 (C), 54.5 (C), 54.0 (CH_2), 53.0 (CH_3), 52.8 (CH_3), 48.8 (CH), 36.7 (CH_2), 32.2 (CH_2), 26.3 (CH_2), 24.2 (CH_3). **^{19}F NMR** (282 MHz, $CDCl_3$) δ (ppm) -109.7 – -110.1 (m), -114.3 – -114.9 (m).

Dimethyl 3-(4-fluorophenyl)-9a-methyl-5-methylene-2-oxooctahydrobenzo[f][1,3]oxazepine-7,7(6H)-dicarboxylate (**50be** + **50be'**)

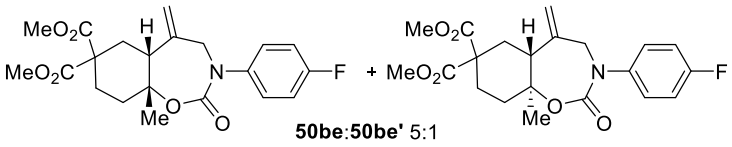

Prepared following the procedure employed for the synthesis of the cycloadduct **50ba**, using the isocyanate **49e** as reaction partner. Isomers **50be** and **50be'** are obtained in 64% combined yield (dr 6:1), as a yellow solid. They were isolated as a 5:1 mixture after column chromatography (25-40% Et_2O/Hexane). **^{1}H NMR** (300 MHz, $CDCl_3$) δ (ppm) 7.29 – 7.20 (m, 2H), 7.05 (td, *J* = 8.5, 0.8 Hz, 1.66H), 6.93 (t, *J* = 8.7 Hz, 0.34H), 5.15 (s, 1H), 5.11 (s, 0.83H), 4.98 (s, 0.17H), 4.65 (d, *J* = 14.2 Hz, 0.83H), 4.23 (d, *J* = 14.7 Hz, 0.17H), 4.10 (d, *J* = 14.8 Hz, 0.17H), 3.78 (s, 2.49H), 3.77 (s, 0.51H), 3.74 (s, 0.51H), 3.73 (s, 2.49H), 3.62 (d, *J* = 14.2 Hz, 0.83H), 2.69 (d, *J* = 13.6 Hz, 0.17H), 2.56 (dd, *J* = 12.8, 4.1 Hz, 0.83H), 2.51 – 2.43 (m, 0.17H), 2.34 (t, *J* = 13.0 Hz, 0.83H), 2.27 – 2.08 (m, 3.66H), 2.06 – 1.92 (m, 0.34H), 1.80 (t, *J* = 13.3 Hz, 0.17H), 1.59 – 1.50 (m, 0.83H), 1.48 (s, 2.49H), 1.37 (s, 0.51H). It contains grease. **^{13}C NMR** (75 MHz, $CDCl_3$) δ (ppm) 172.1 (C), 172.1 (C), 171.4 (C), 162.8 (C), 159.6 (C), 156.8 (C), 142.5 (C), 142.3 (C), 140.0 (C), 127.63 (d, *J* = 8.5 Hz, CH), 127.44 (d, *J* = 8.3 Hz, CH), 119.1 (CH_2), 116.26 (d, *J* = 22.7 Hz, CH), 116.2 (d, *J* = 22.7 Hz, CH), 115.7 (q, *J*=262.3 Hz, C), 115.6 (q, *J* = 22.7 Hz, C), 80.4 (C), 79.8 (C), 58.7 (CH_2), 54.5 (C), 54.1 (CH_2), 53.1 (CH_3), 53.1 (CH_3), 53.0 (CH_3), 52.8 (CH_3), 48.7 (CH), 46.5 (CH), 36.7 (CH_2), 32.3 (CH_2), 31.7 (CH_2), 30.5 (CH_2), 28.9 (CH_2), 26.2 (CH_2), 24.5 (CH_3), 17.2 (CH_3). **HRMS** (APCI-TOF): m/z calculated for $C_{21}H_{25}FNO_6^+$ $[M + H]^+$: m/z 406.1660, found 406.1668. Stereochemistry of **50be** was determined by nOe experiments. Stereochemistry of **50be'** was deduced by comparison with **50be** and analogue products.

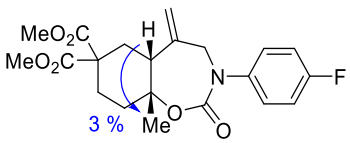

Figure 77. Significant nOe observed for **50be**.

- NMR data extracted for **50be** (major isomer) from the 5:1 mixture: **^{1}H NMR** (300 MHz, $CDCl_3$) δ (ppm) 7.29 – 7.20 (m, 2H), 7.05 (td, *J* = 8.5, 0.8 Hz, 2H), 5.15 (s, 1H), 5.11 (s, 1H), 4.65 (d, *J* = 14.2 Hz, 1H), 3.78 (s, 3H), 3.73 (s, 3H), 3.62 (d, *J* = 14.2 Hz, 1H), 2.56 (dd, *J* = 12.8, 4.1 Hz, 1H), 2.34 (t, *J* = 13.0 Hz, 1H), 2.27 – 2.08 (m, 4H), 1.59 – 1.50 (m, 1H), 1.48 (s, 3H).**^{13}C NMR** (75 MHz, $CDCl_3$) δ (ppm) 172.1 (C), 171.4 (C), 156.8 (C), 142.3 (C), 140.0 (C), 127.63 (d, *J* = 8.5 Hz, CH), 119.1 (CH_2), 116.26 (d, *J* = 22.7 Hz, CH), 115.7 (q, *J* = 262.3 Hz, C), 115.6 (q, *J* = 22.7 Hz, C), 79.8

(C), 54.5 (C), 54.1 (CH_2), 53.0 (CH_3), 52.8 (CH_3), 48.7 (CH), 36.7 (CH_2), 32.3 (CH_2), 26.2 (CH_2), 24.5 (CH_3).

Dimethyl (5*aR*,9*aR*)-3-(4-chlorophenyl)-9*a*-methyl-5-methylene-2-oxooctahydrobenzo[*f*][1,3]oxazepine-7,7(6*H*)-dicarboxylate (**50bf**+**50bf'**)

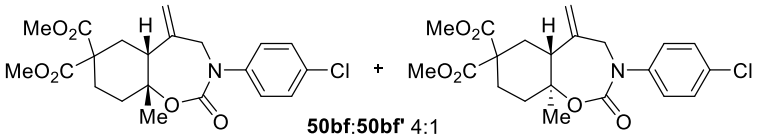

Prepared following the procedure employed for the synthesis of the cycloadduct **50ba**, using the isocyanate **49f** as reaction partner. Isomers **50bf** and **50bf'** are obtained in 60% combined yield (dr 5:1), as a yellow solid. They were isolated as a 4:1 mixture after column chromatography (25-40% Et_2O/Hexane). **^{1}H NMR** (300 MHz, $CDCl_3$) δ (ppm) 7.33 (dd, *J* = 8.8, 0.9 Hz, 2H), 7.23 (dd, *J* = 8.8, 0.9 Hz, 2H), 5.15 (s, 1H), 5.12 (s, 0.8H), 4.98 (s, 0.2H), 4.64 (d, *J* = 14.3 Hz, 0.8H), 4.23 (d, *J* = 14.8 Hz, 0.2H), 4.14 (d, *J* = 14.8 Hz, 0.2H), 3.78 (s, 2.4H), 3.76 (s, 0.6H), 3.74 (s, 0.6H), 3.73 (s, 2.4H), 3.65 (d, *J* = 14.3 Hz, 0.8H), 2.68 (d, *J* = 13.0 Hz, 0.2H), 2.56 (dd, *J* = 12.7, 4.2 Hz, 1H), 2.33 (t, *J* = 13.0 Hz, 1H), 2.28 – 2.08 (m, 3.4H), 2.07 – 1.96 (m, 0.2H), 1.79 (t, *J* = 13.2 Hz, 0.2H), 1.60 – 1.50 (m, 1H), 1.47 (s, 2.4H), 1.36 (s, 0.6H). **^{13}C NMR** (75 MHz, $CDCl_3$) δ (ppm) 172.0 (C), 171.4 (C), 156.5 (C), 142.4 (C), 142.2 (C), 132.4 (C), 132.3 (C), 129.5 (CH), 129.4 (CH), 127.1 (CH), 126.9 (CH), 119.2 (CH_2), 114.0 (CH_2), 84.0 (C), 79.9 (C), 58.4 (CH_2), 54.6 (C), 54.4 (C), 53.8 (CH_2), 53.1 (CH_3), 53.1 (CH_3), 53.0 (CH_3), 52.8 (CH_3), 48.6 (CH), 46.3 (CH), 36.7 (CH_2), 32.3 (CH_2), 31.7 (CH_2), 28.8 (CH_2), 26.2 (CH_2), 24.5 (CH_3), 17.5 (CH_3). **HRMS** (APCI-TOF): m/z calculated for $C_{21}H_{25}ClNO_6^+$ $[M + H]^+$: m/z 422.1365, found 422.1369. Stereochemistry of **50bf** was determined by nOe experiments. Stereochemistry of **50bf'** was deduced by comparison with **50bf** and analogue products.

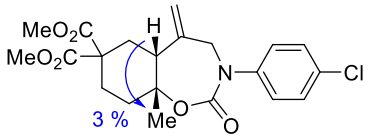

Figure 78. Significant nOe observed for **50bf**.

- NMR data of **50bf** (major isomer) extracted from the 4:1 mixture: **^{1}H NMR** (300 MHz, $CDCl_3$) δ (ppm) 7.33 (dd, *J* = 8.8, 0.9 Hz, 2H), 7.23 (dd, *J* = 8.8, 0.9 Hz, 2H), 5.15 (s, 1H), 5.12 (s, 1H), 4.64 (d, *J* = 14.3 Hz, 1H), 3.78 (s, 3H), 3.73 (s, 3H), 3.65 (d, *J* = 14.3 Hz, 1H), 2.56 (dd, *J* = 12.7, 4.2 Hz, 1H), 2.33 (t, *J* = 13.0 Hz, 1H), 2.28 – 2.08 (m, 4H), 1.60 – 1.50 (m, 1H), 1.47 (s, 3H). **^{13}C NMR** (75 MHz, $CDCl_3$) δ (ppm) 172.0 (C), 171.4 (C), 156.5 (C), 142.4 (C), 142.2 (C), 132.4 (C), 129.5 (CH), 127.1 (CH), 119.2 (CH_2), 79.9 (C), 54.4 (C), 53.8 (CH_2), 53.0 (CH_3), 52.8 (CH_3), 48.6 (CH), 36.7 (CH_2), 32.3 (CH_2), 26.2 (CH_2), 24.5 (CH_3).

(5*aS*,9*aR*)-3-(3,5-bis(trifluoromethyl)phenyl)-9*a*-methyl-5-methylene-7 tosyloctahydropyrido[3,4-*f*][1,3]oxazepin-2(3*H*)-one (**50ca**)

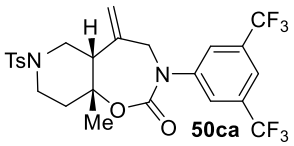

Prepared following the procedure employed for the synthesis of the cycloadduct **50ba**, using ACP **9c** as starting material. Isolated by column chromatography (25-40% Et_2O/Hexane) as a yellowish solid in 36% yield. **^{1}H NMR** (500 MHz, $CDCl_3$) δ (ppm) 7.74 (s, 1H), 7.71 (s, 2H), 7.66 (d, *J* = 8.3 Hz, 2H), 7.35 (d, *J* = 8.3 Hz, 2H), 5.35 (s, 1H), 5.30 (s, 1H), 4.45 (d, *J* = 14.4 Hz, 1H), 3.75 (d, *J* = 14.6 Hz, 1H), 3.72 – 3.67 (m, 1H), 3.64 – 3.53 (m, 1H), 2.79 – 2.73 (m, 2H), 2.72 – 2.65 (m, 1H), 2.46 (s, 3H), 2.29 – 2.16 (m, 1H), 1.95 – 1.82 (m, 1H), 1.52 (s, 3H). **^{13}C NMR** (126 MHz, $CDCl_3$) δ (ppm) 155.6 (C), 144.7 (C), 144.1 (C), 139.3 (C), 133.0 (C), 132.8 (q, *J*=33.6 Hz, C), 130.1 (CH), 127.8 (CH), 125.6 (m, CH) 122.9 (q, *J*=273.1 Hz, C), 121.9 (CH_2), 120.5 (m, CH), 79.6 (C), 54.4 (CH_2), 50.8 (CH), 46.1 (CH_2), 42.3 (CH_2), 38.9 (CH_2), 24.2 (CH_3), 21.7 (CH_3). **^{19}F NMR** (471 MHz, $CDCl_3$) δ (ppm) -63.0 (s). **HRMS** (APCI-TOF): m/z calculated

for $C_{25}H_{25}F_6N_2O_4S^+$ [M + H]$^+$: m/z 463.1434, found 463.1440. Stereochemistry of **50ca** was deduced by analogy with analogue products.

Cycloaddition between 9l and 49a: Prepared following the procedure employed for the synthesis of the cycloadduct **50ba**, using ACP **9l** as starting material. Isomers **50la** and **50la'** were obtained in 41% combined yield (dr 2:1) as a yellowish solid and can be easily separated by column chromatography (25-40% Et_2O/Hexane).

Dimethyl (5*aR*,7*aS*,10*aS*)-3-(3,5-bis(trifluoromethyl)phenyl)-5-methylene-2-oxodecahydro-7*H*-pentaleno[1,6*a*-*f*][1,3]oxazepine-7,7-dicarboxylate (**50la**)

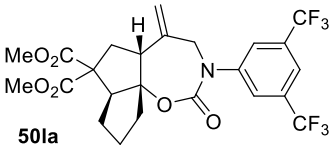

50la

27% yield as a yellowish solid. **^{1}H NMR** (300 MHz, $CDCl_3$) δ (ppm) 7.77 (s, 2H), 7.74 (s, 1H), 5.24 (s, 1H), 5.15 (s, 1H), 4.63 (d, *J* = 14.1 Hz, 1H), 3.82 – 3.68 (m, 7H), 3.11 (dd, *J* = 13.0, 6.6 Hz, 1H), 2.66 (dd, *J* = 13.1, 6.6 Hz, 1H), 2.54 – 2.31 (m, 1H), 2.28 – 2.14 (m, 1H), 2.12 – 1.97 (m, 2H), 1.87 – 1.69 (m, 2H), 1.40 – 1.23 (m, 2H). **^{13}C NMR** (75 MHz, $CDCl_3$) δ (ppm) 171.5 (C), 171.4 (C), 155.3 (C), 144.4 (C), 139.6 (C), 132.6 (q, *J* = 33.7 Hz, C), 125.7 (m, CH), 122.9 (q, *J* = 272.8 Hz, C), 120.2 (m, CH), 119.2 (CH_2), 101.2 (C), 60.6 (C), 58.4 (CH), 53.5 (CH_2), 53.0 (CH_3), 52.4 (CH), 40.8 (CH_2), 33.6 (CH_2), 28.8 (CH_2), 26.6 (CH_2). **^{19}F NMR** (282 MHz, $CDCl_3$) δ (ppm) -63.0 (s). **HRMS** (APCI-TOF): m/z calculated for $C_{24}H_{24}F_6NO_6^+$ [M + H]$^+$: m/z 536.1502, found 536.1505. Stereochemistry of **50la** was deduced by comparison with analogue products.

Dimethyl (5*aR*,7*aR*,10*aR*)-3-(3,5-bis(trifluoromethyl)phenyl)-5-methylene-2-oxodecahydro-7*H*-pentaleno[1,6*a*-*f*][1,3]oxazepine-7,7-dicarboxylate (**50la'**)

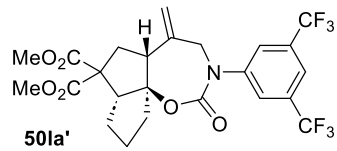

50la'

14% yield as a yellowish solid. **^{1}H NMR** (300 MHz, $CDCl_3$) δ (ppm) 7.86 (s, 2H), 7.81 (s, 1H), 6.51 (s, 1H), 5.12 (d, *J* = 15.7 Hz, 1H), 5.06 – 4.99 (m, 2H), 4.18 (d, *J* = 15.7 Hz, 1H), 3.89 (s, 1H), 3.74 (s, 3H), 3.64 (s, 3H), 3.04 (d, *J* = 15.9 Hz, 1H), 2.33 – 2.13 (m, 1H), 2.08 – 1.74 (m, 4H), 1.47 – 1.25 (m, 2H). **^{13}C NMR** (75 MHz, $CDCl_3$) δ (ppm) 172.1 (C), 171.6 (C), 153.5 (C), 149.4 (C), 142.5 (C), 140.0 (C), 138.7 (C), 132.8 (C, m), 128.5 (m, CH), 126.0 (C), 120.5 (m, CH), 117.1 (CH_2), 60.9 (C), 59.0 (CH), 53.2 (CH_2), 52.9 (CH_3), 52.2 (CH), 46.6 (CH_2), 28.4 (CH_2), 27.9 (CH_2), 25.0 (CH_2). **^{19}F NMR** (282 MHz, $CDCl_3$) δ (ppm) -63.0 (s). **HRMS** (APCI-TOF): m/z calculated for $C_{24}H_{24}F_6NO_6^+$ [M + H]$^+$: m/z 536.1502, found 536.1505. Stereochemistry of **50la'** was deduced by comparison with analogue products.

7. Bibliography

Bibliographic references in this doctoral thesis are provided as footnotes for ease of reading.

Appendix

I. Selected NMR Spectra

^{1}H, DEPT and ^{13}C Spectra of **(*E:Z* 2:1)-1a** in $CDCl_3$

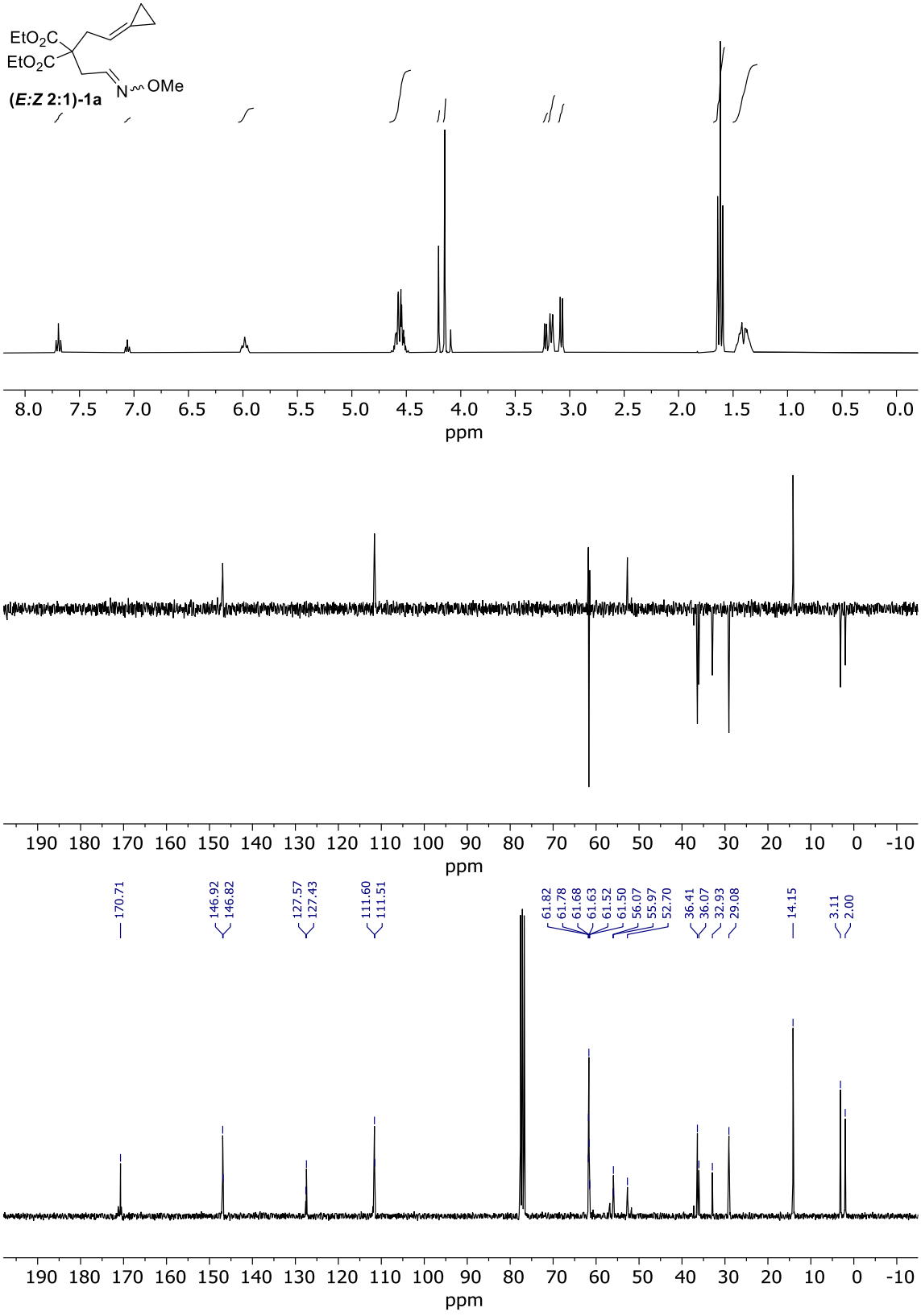

^{1}H, DEPT and ^{13}C Spectra of ***E*-1a** in $CDCl_3$

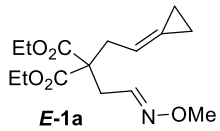

***E*-1a**

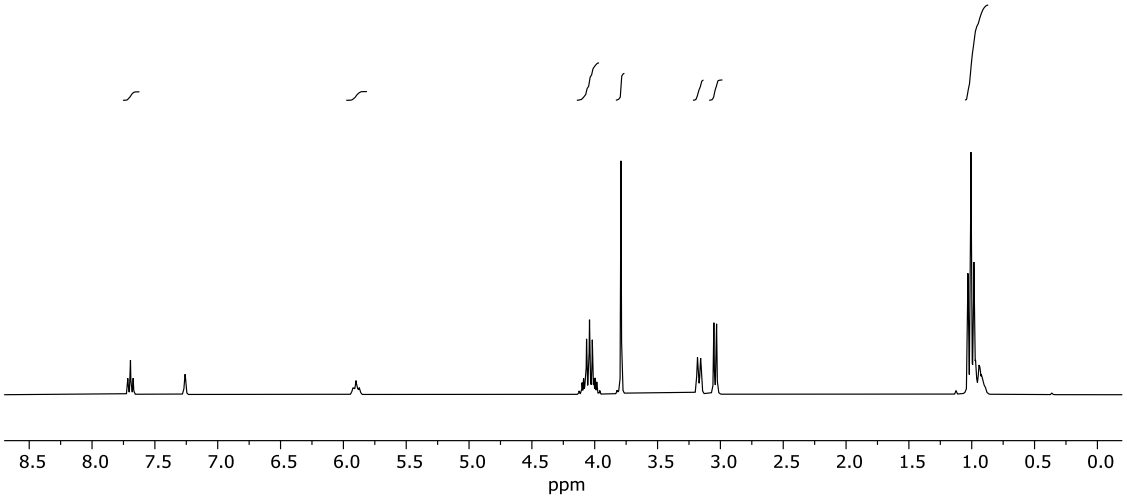

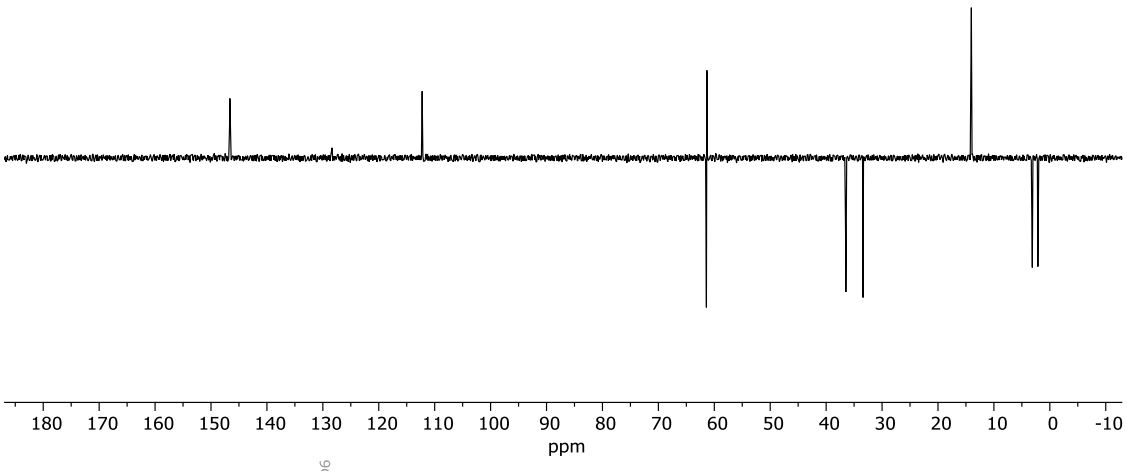

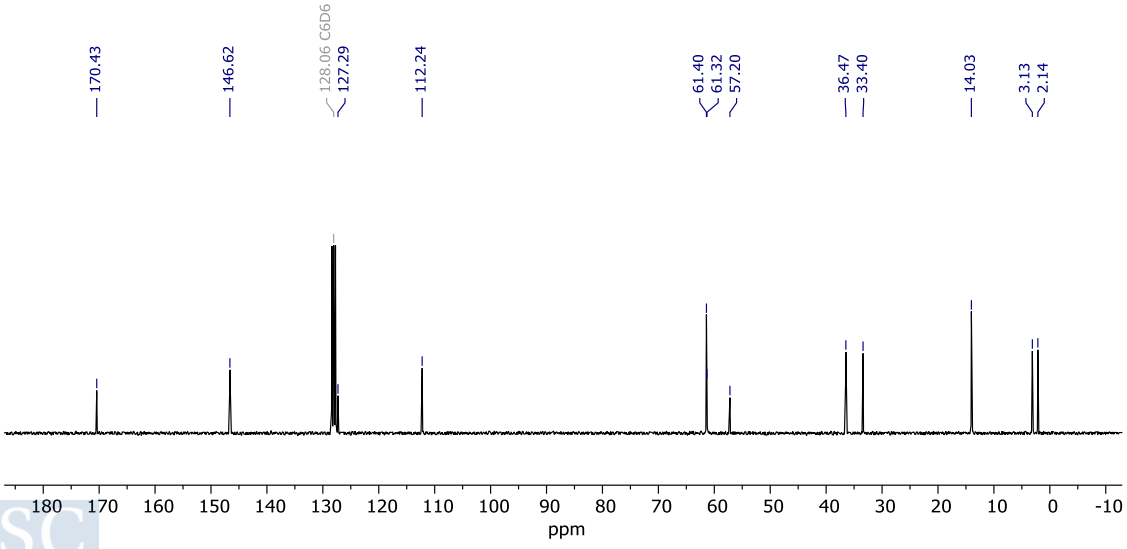

^{1}H, ^{2}H, DEPT and ^{13}C Spectra of ***E*-d$_4$-1a** in CD_3OD

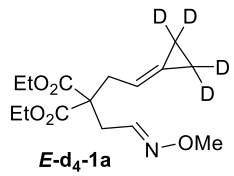

***E*-d$_4$-1a**

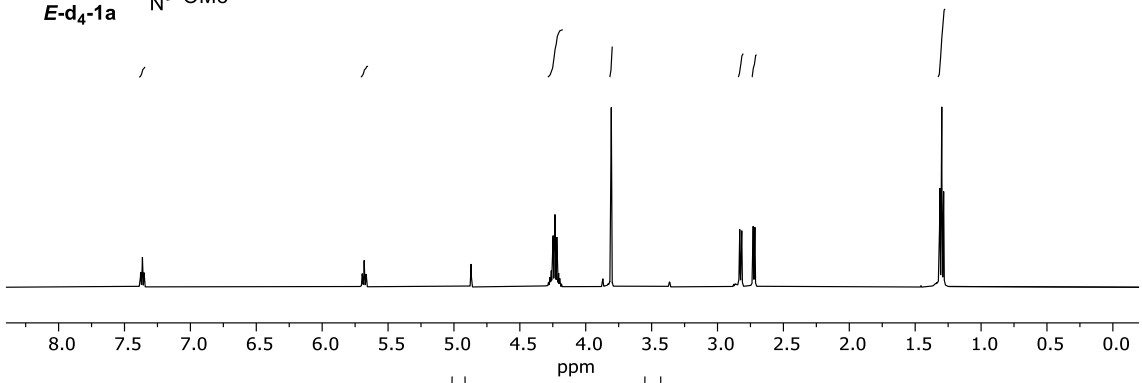

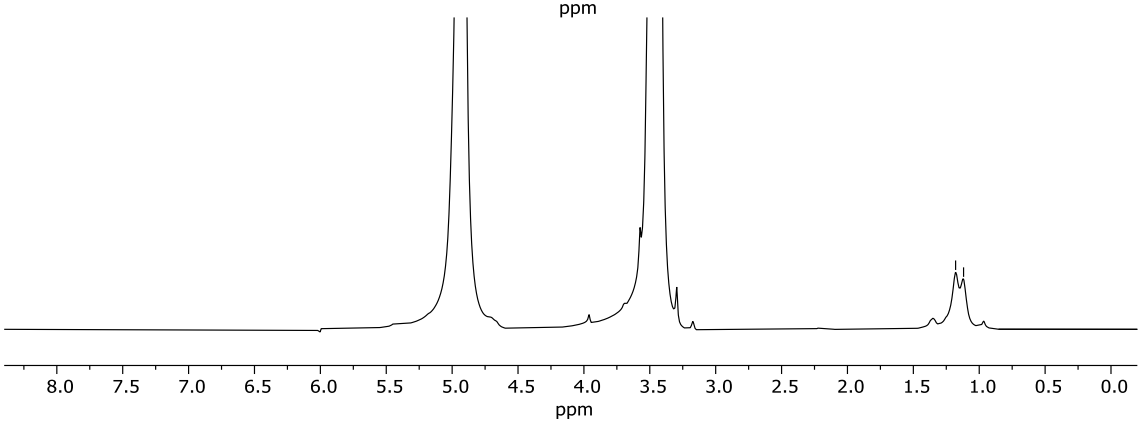

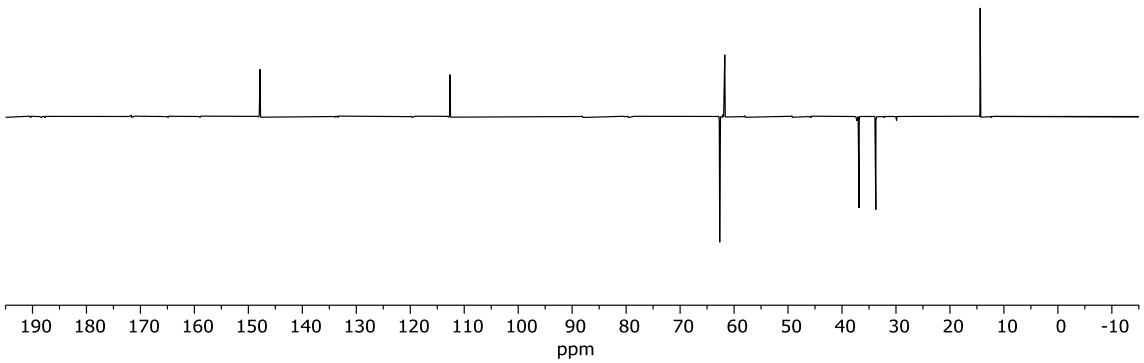

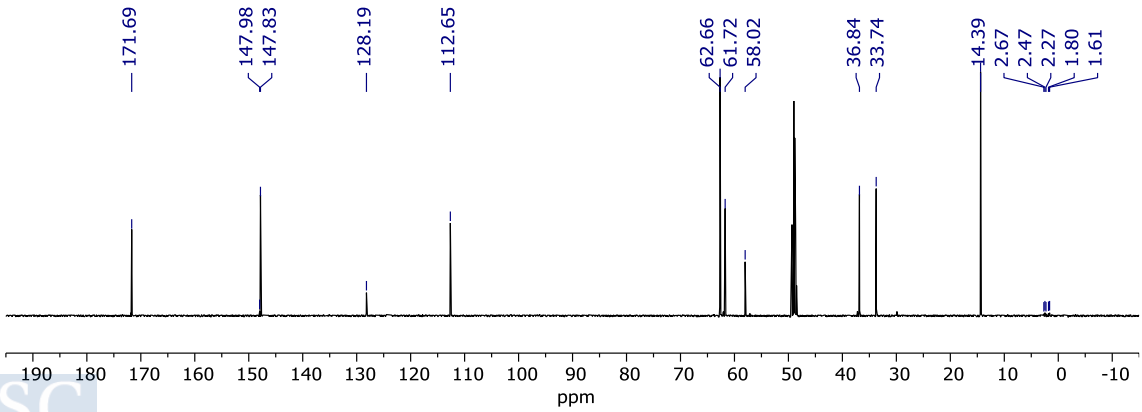

^{1}H, ^{2}H, DEPT and ^{13}C Spectra of ***E*-d$_4$-1a** in CD_3OD

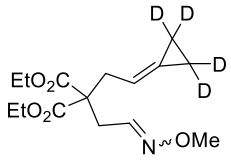

(*E*:*Z* 1:9)-d$_4$-1a

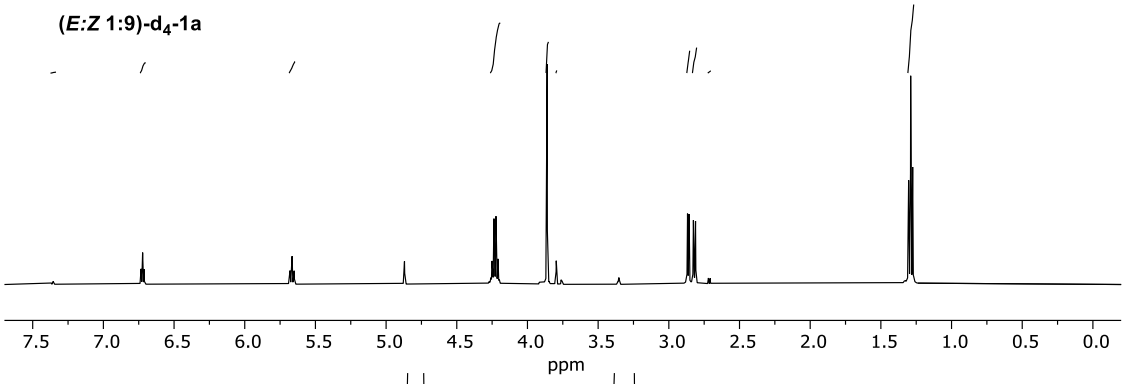

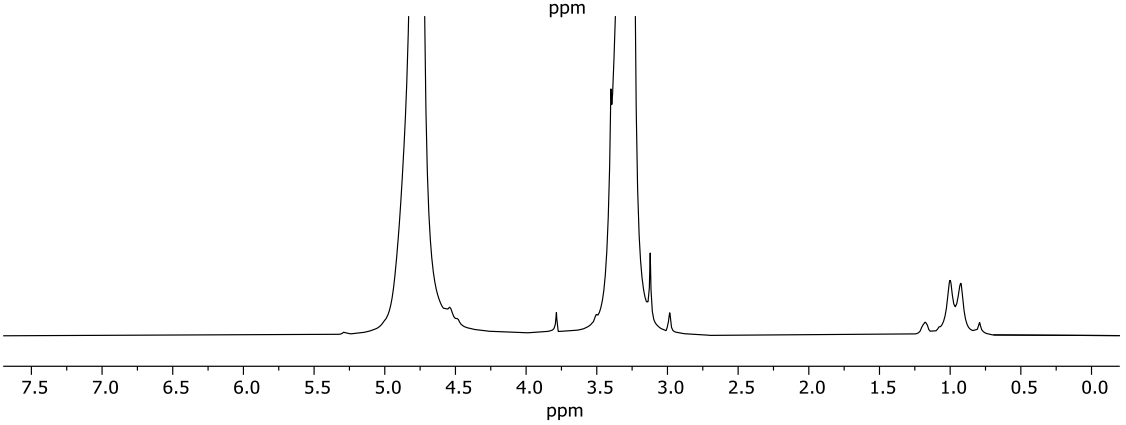

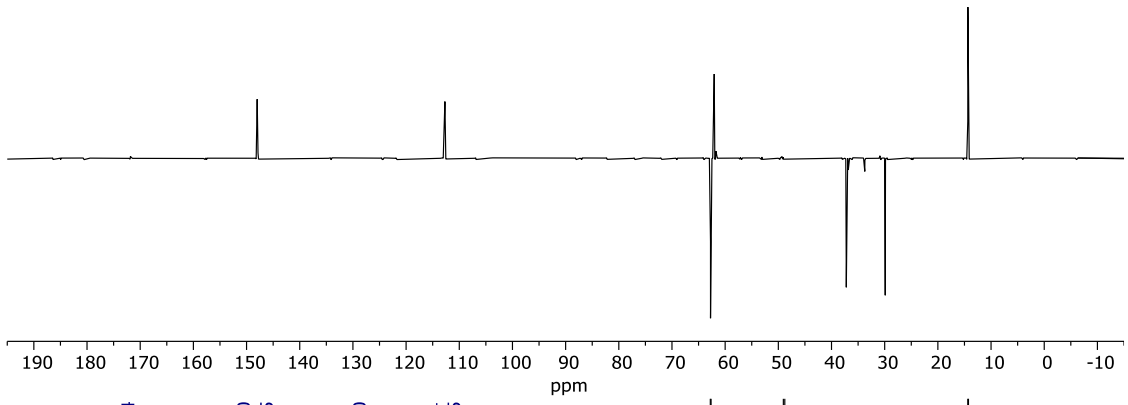

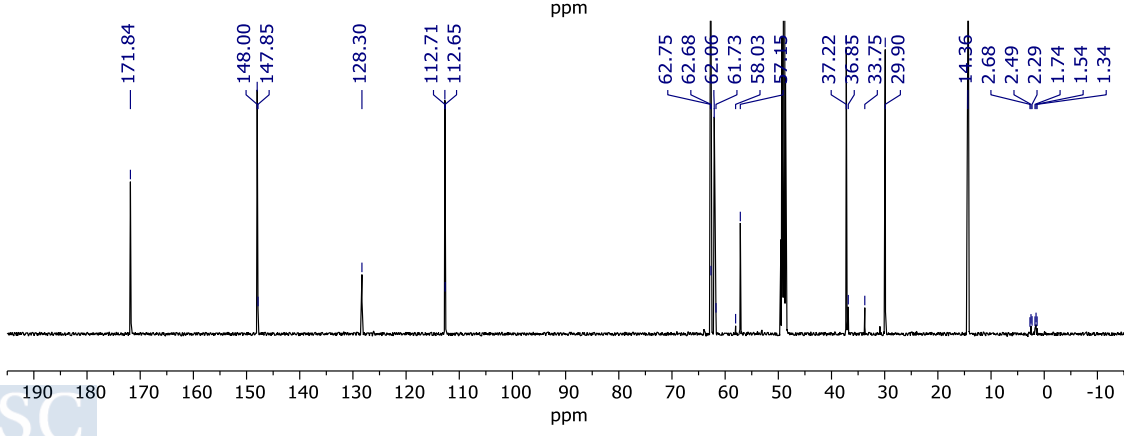

^{1}H, DEPT and ^{13}C Spectra of **(*E:Z* 10:1)-1b** in CD_3OD

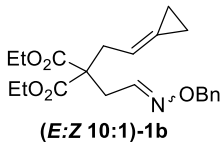

(*E:Z* 10:1)-1b

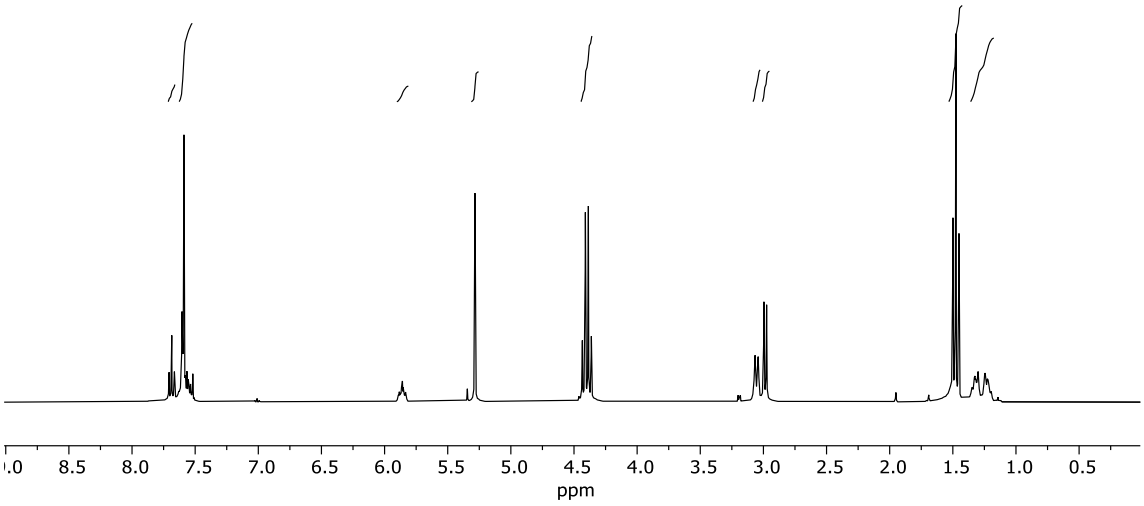

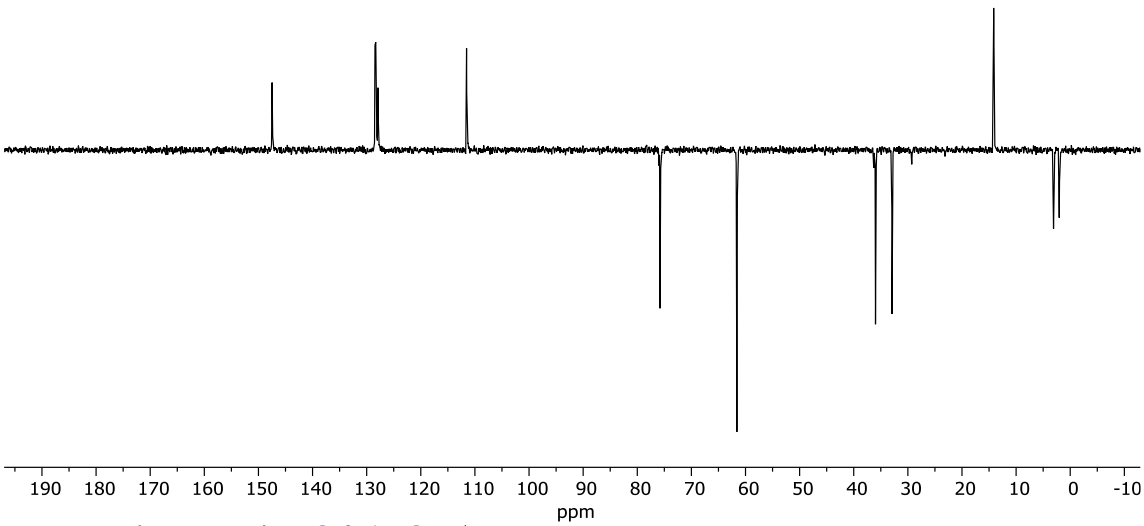

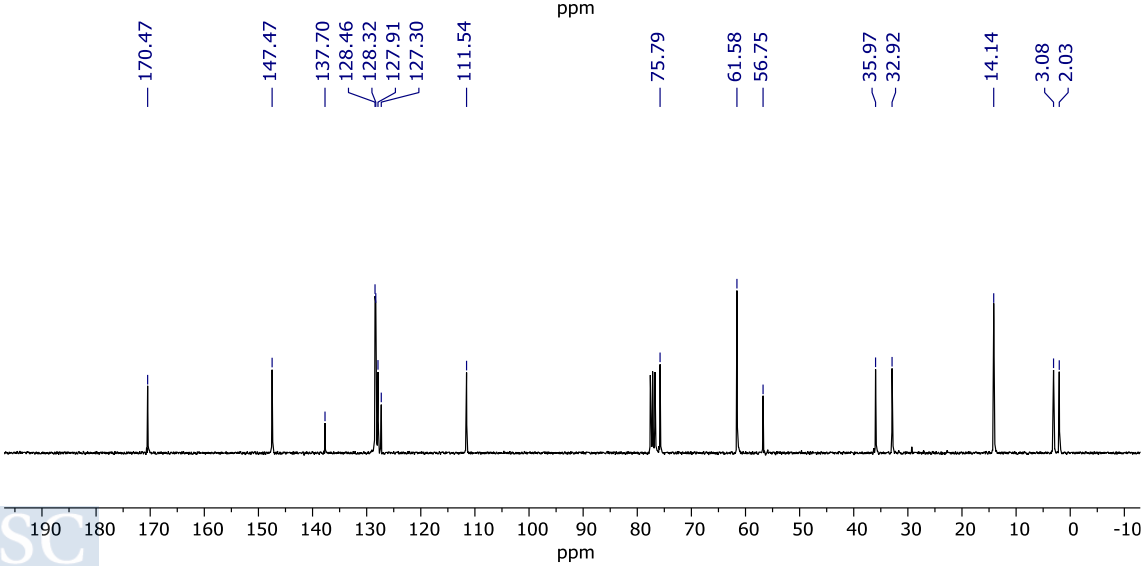

^{1}H, DEPT and ^{13}C Spectra of **(*E:Z* 1:5.7)-1b** in CD_3OD

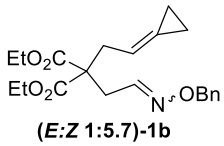

(*E:Z* 1:5.7)-1b

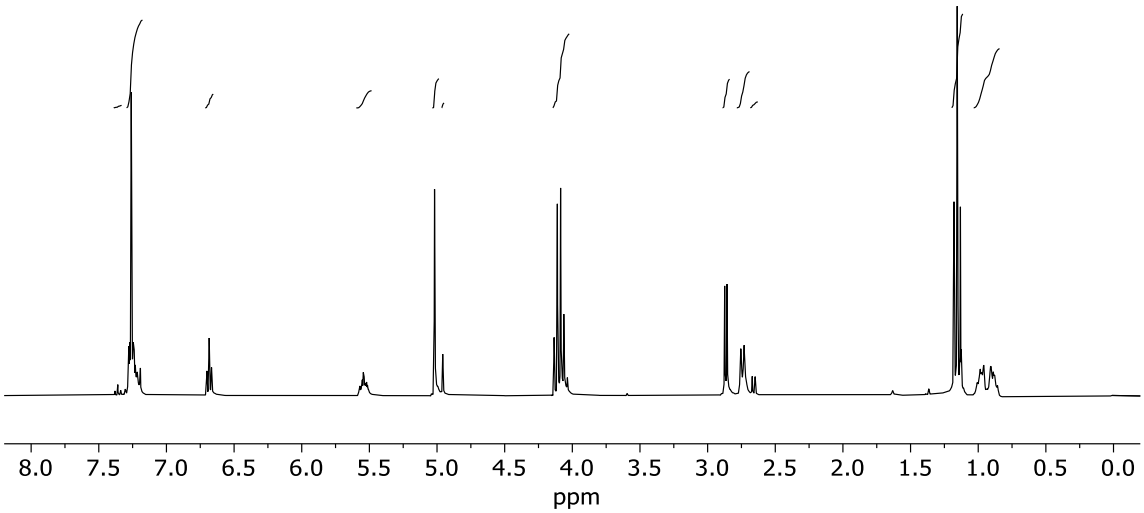

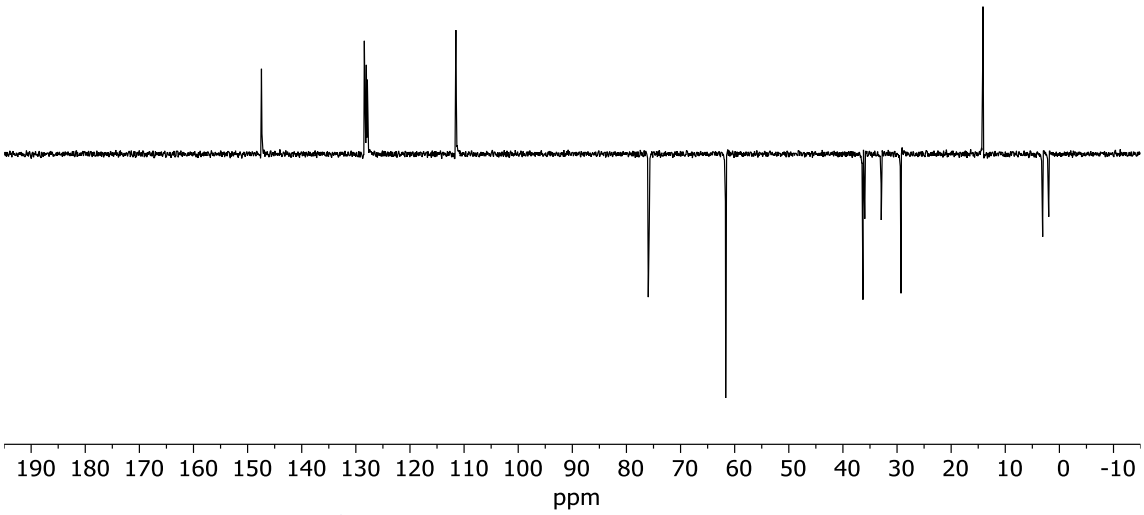

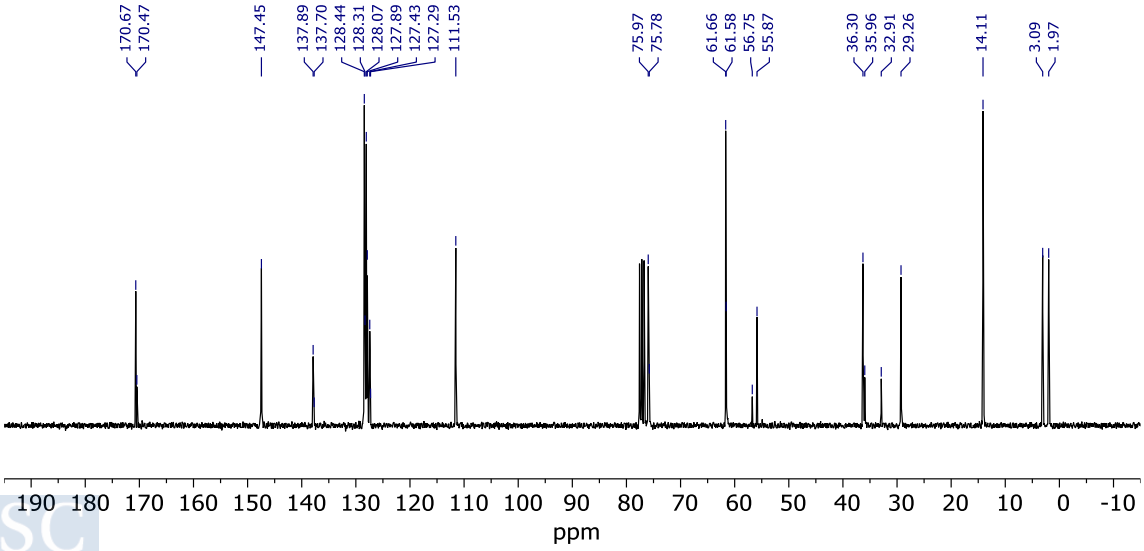

^{1}H, DEPT and ^{13}C Spectra of ***E*-1h** in CD_3OD

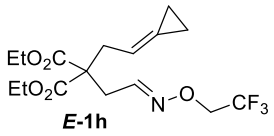

***E*-1h**

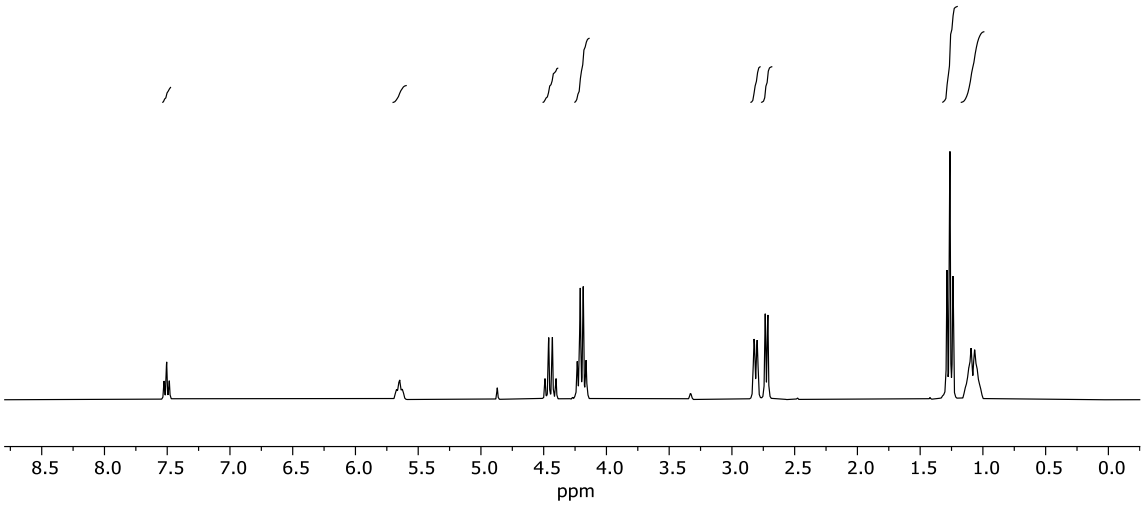

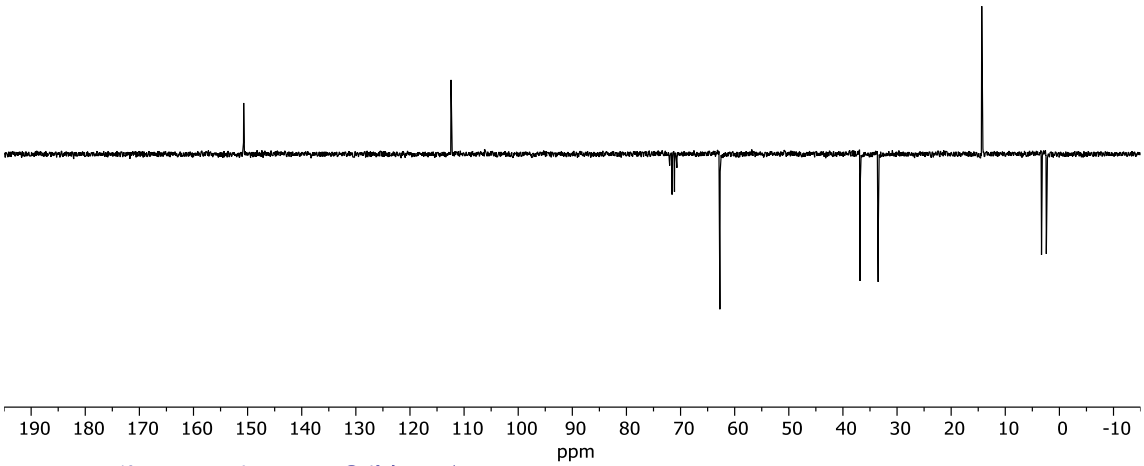

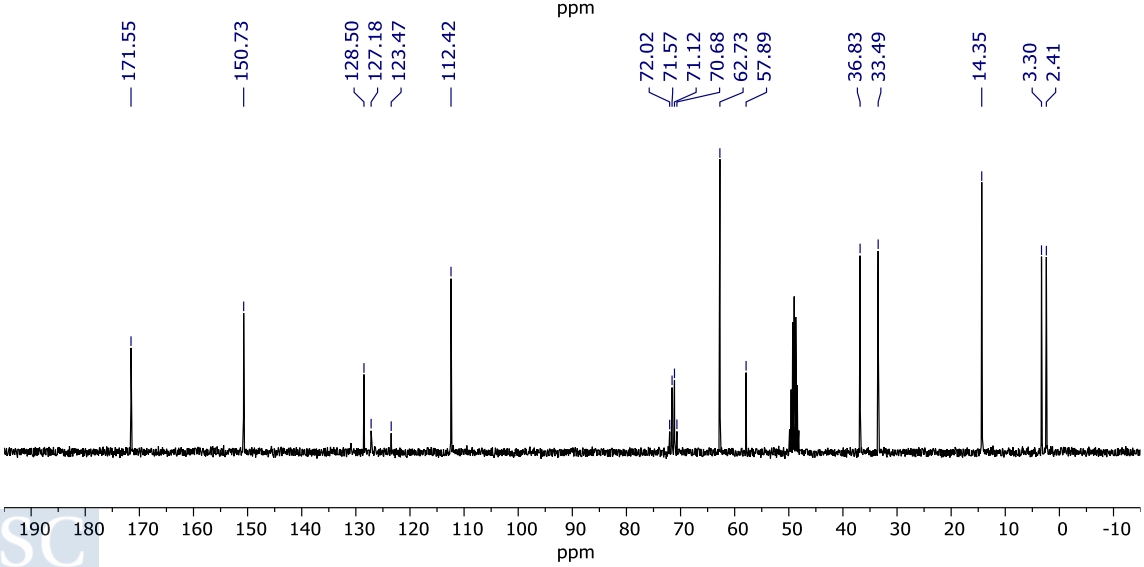

^{1}H, DEPT and ^{13}C Spectra of ***Z*-1h** in CD_3OD

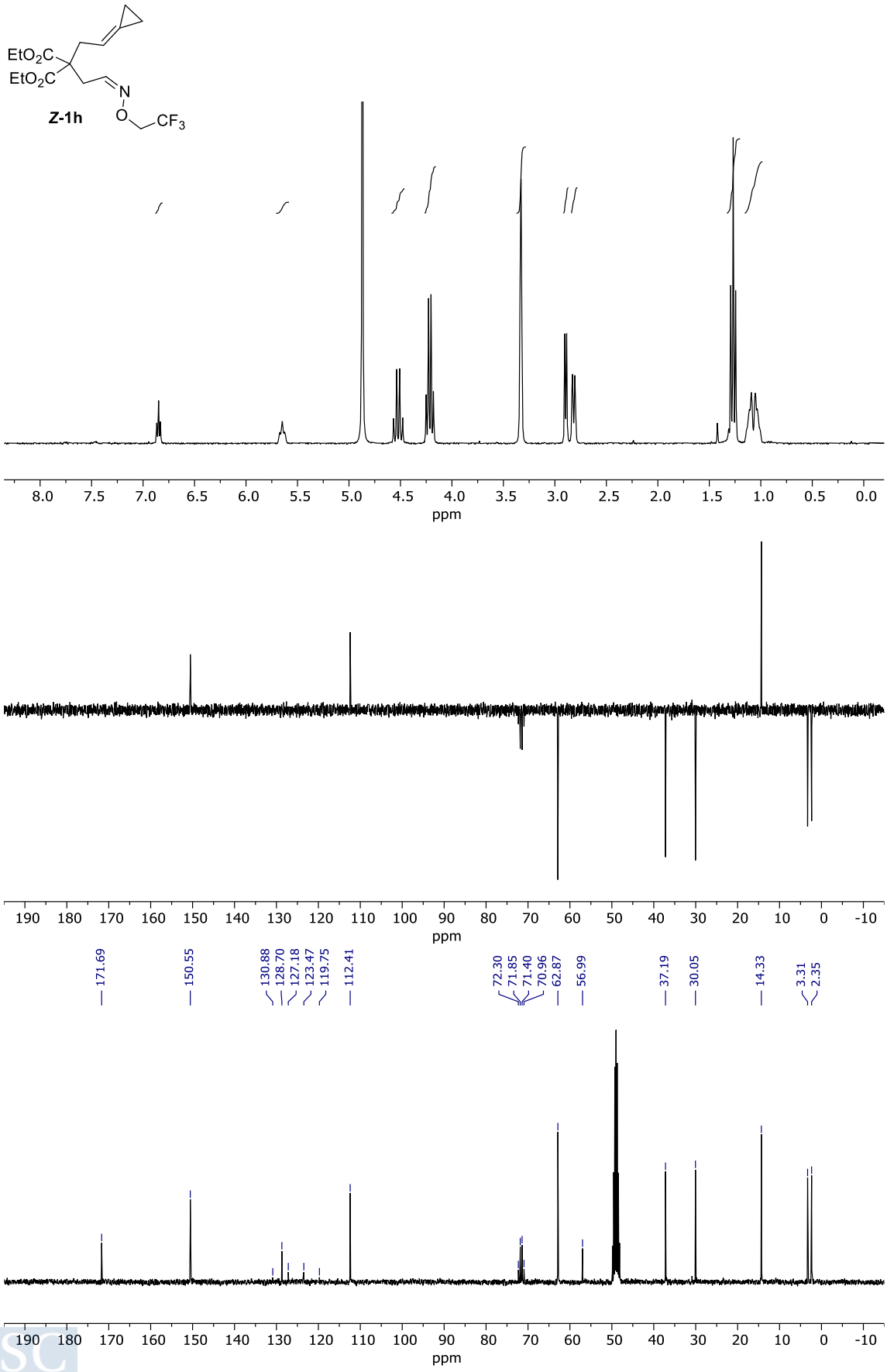

^{1}H, DEPT and ^{13}C Spectra of **2a** in $CDCl_3$

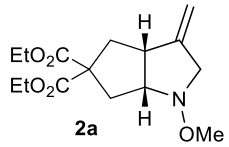

2a

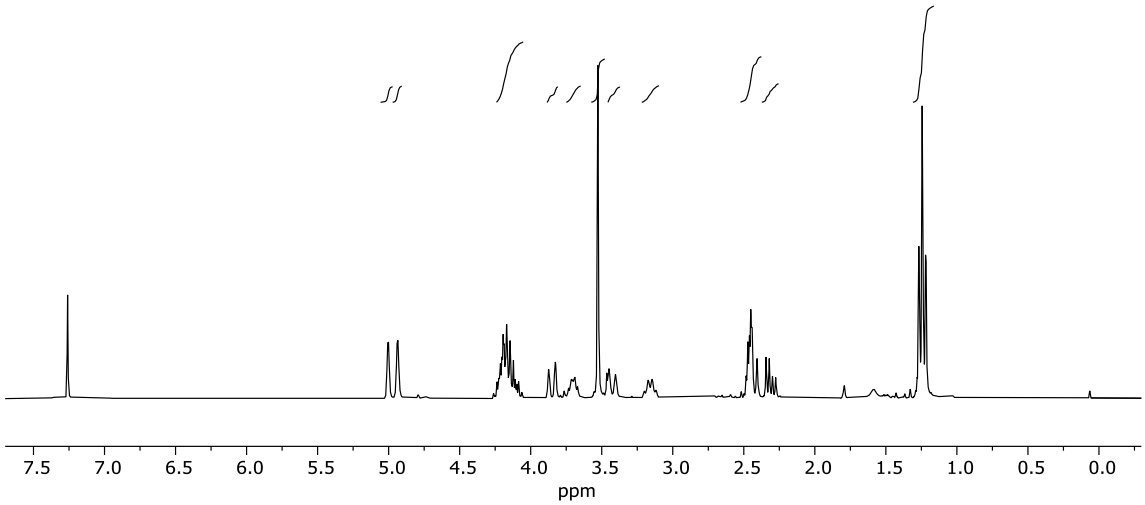

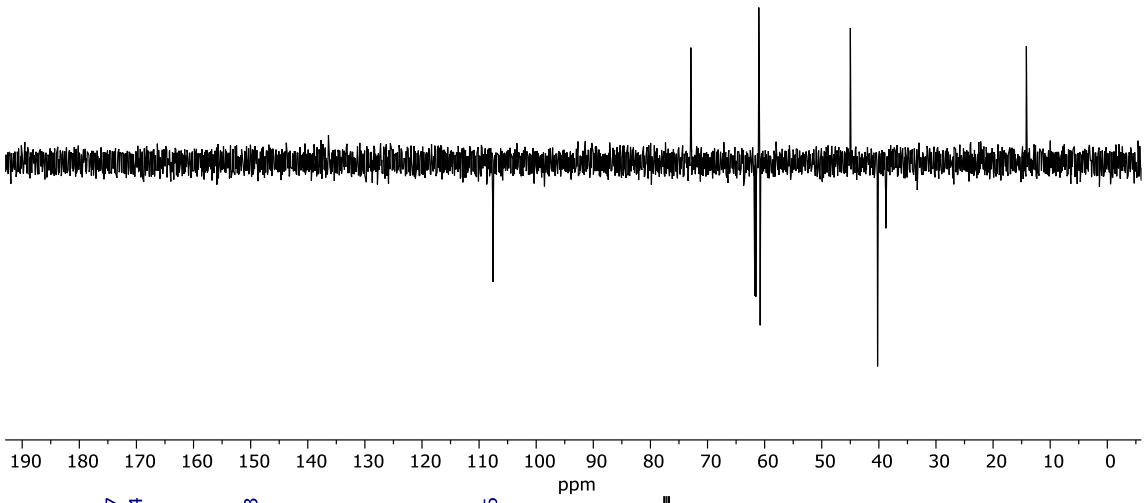

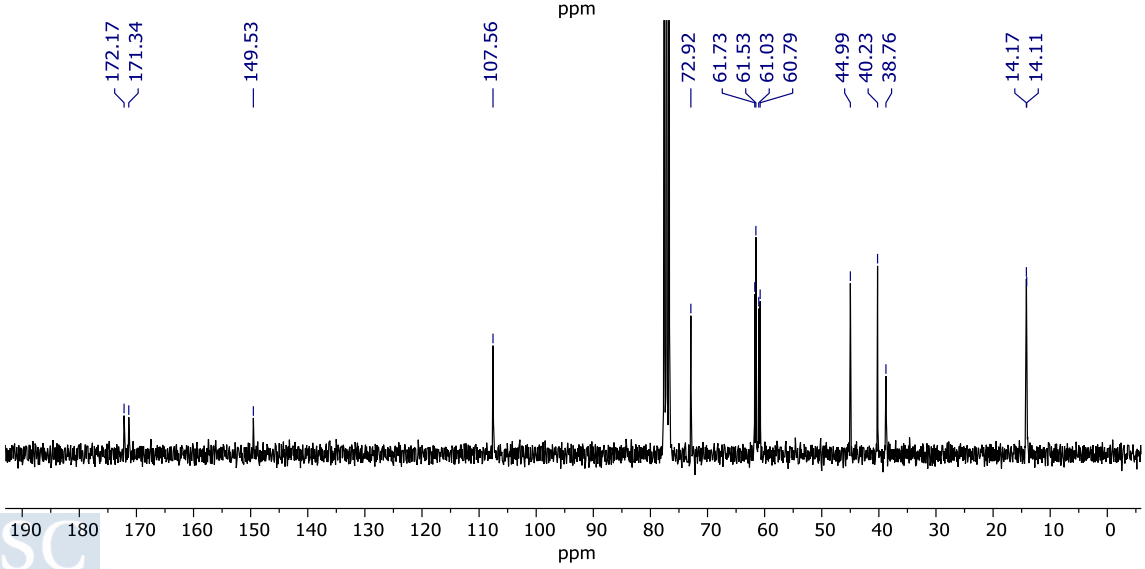

^{1}H, ^{2}H, DEPT and ^{13}C Spectra of **d_4-2a** in $CDCl_3$

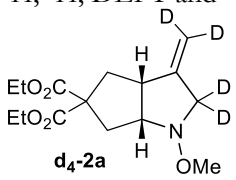

d_4-2a

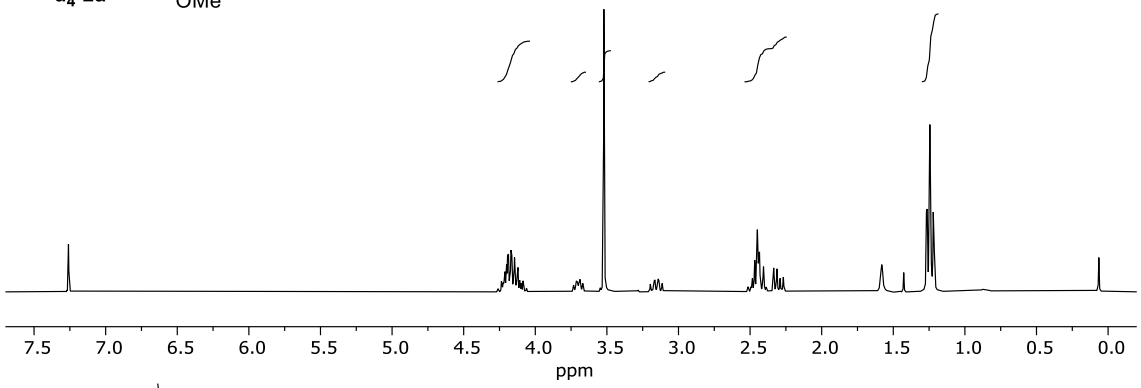

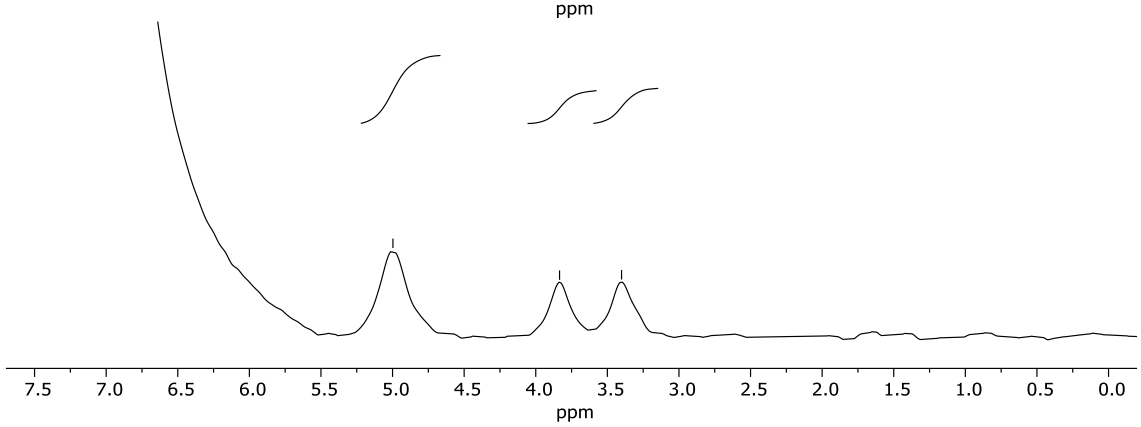

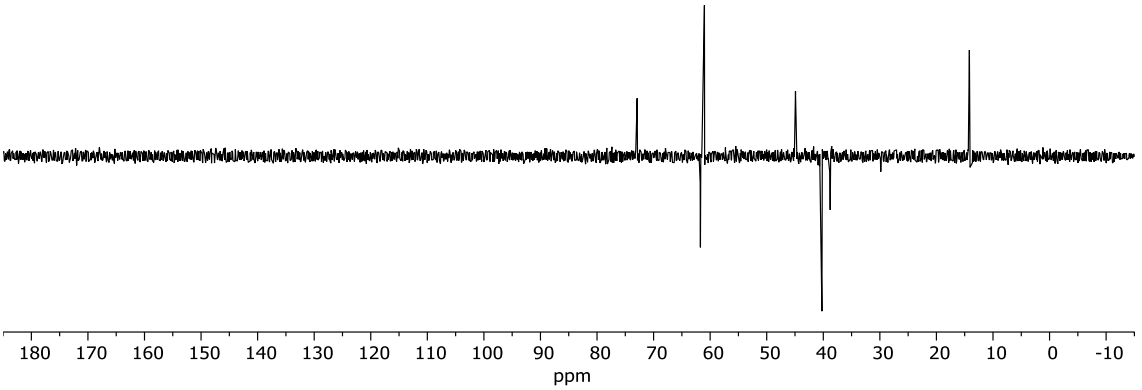

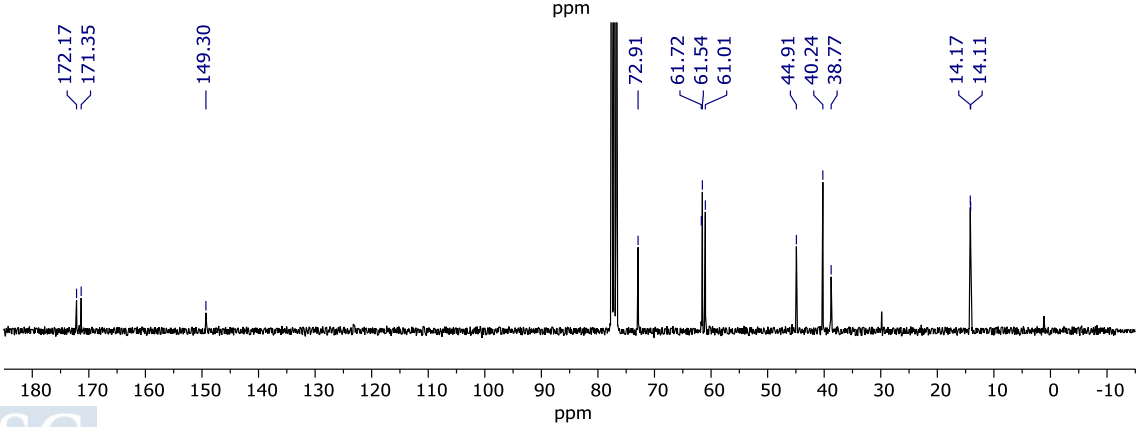

^{1}H, DEPT and ^{13}C Spectra of **2b** in $CDCl_3$

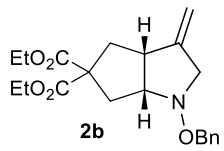

2b

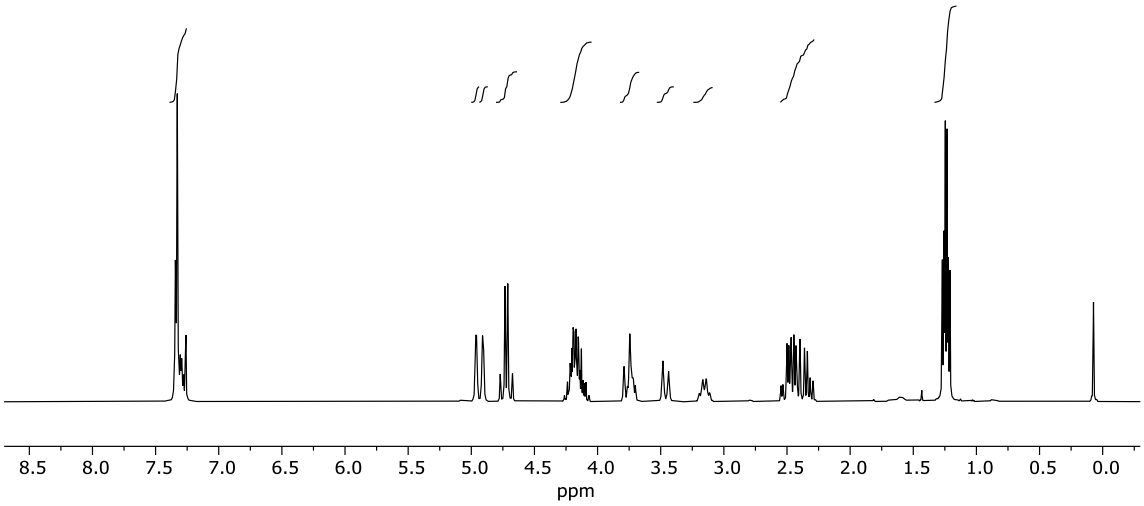

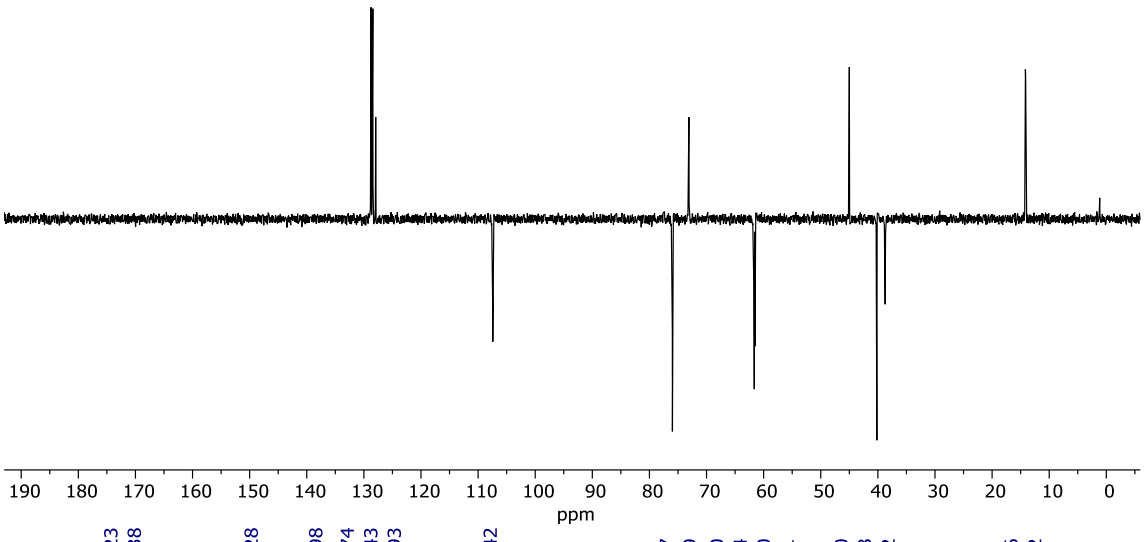

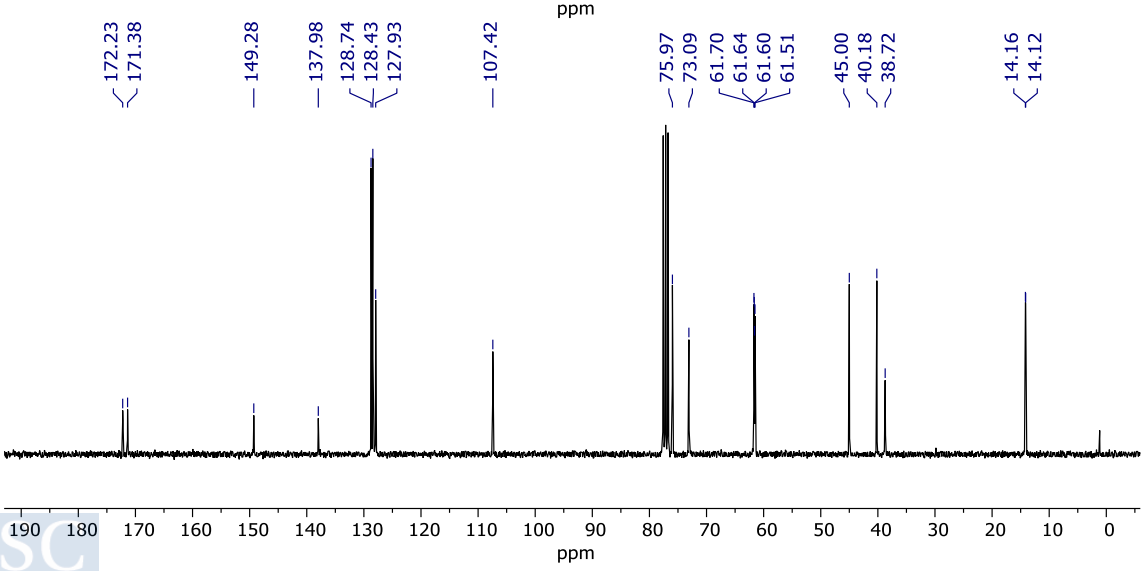

^{1}H, DEPT and ^{13}C Spectra of **2h** in $CDCl_3$

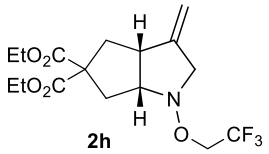

2h

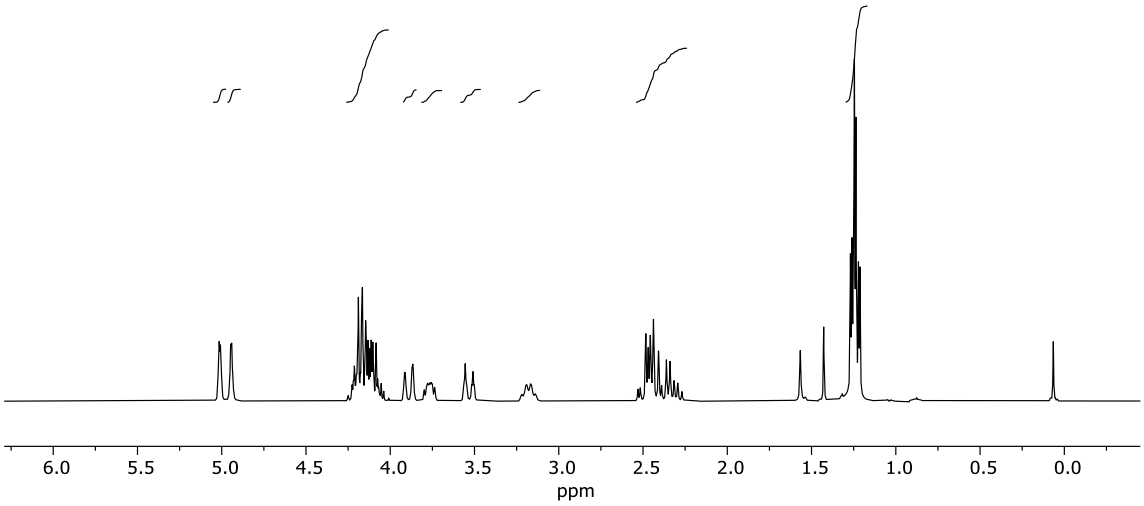

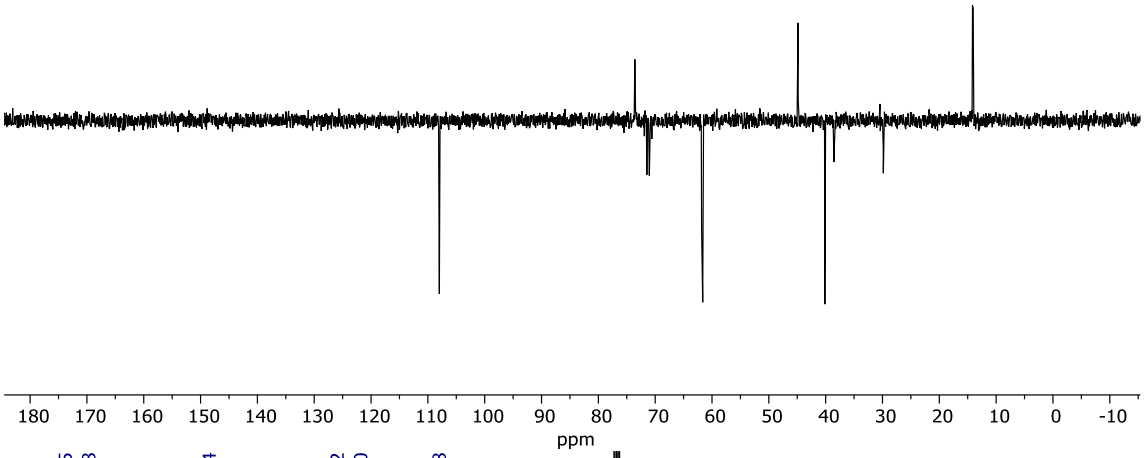

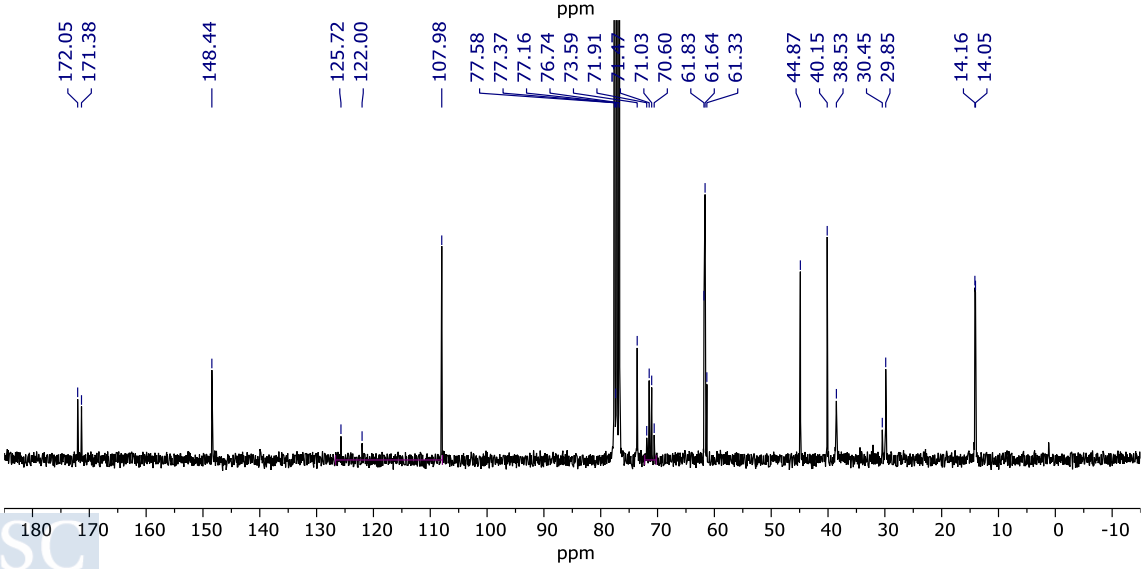

^{1}H, DEPT and ^{13}C Spectra of **(*E:Z* 2:1)-2a** in CD_3OD

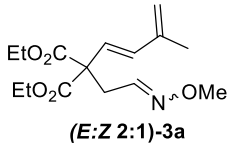

***(E:Z* 2:1)-3a**

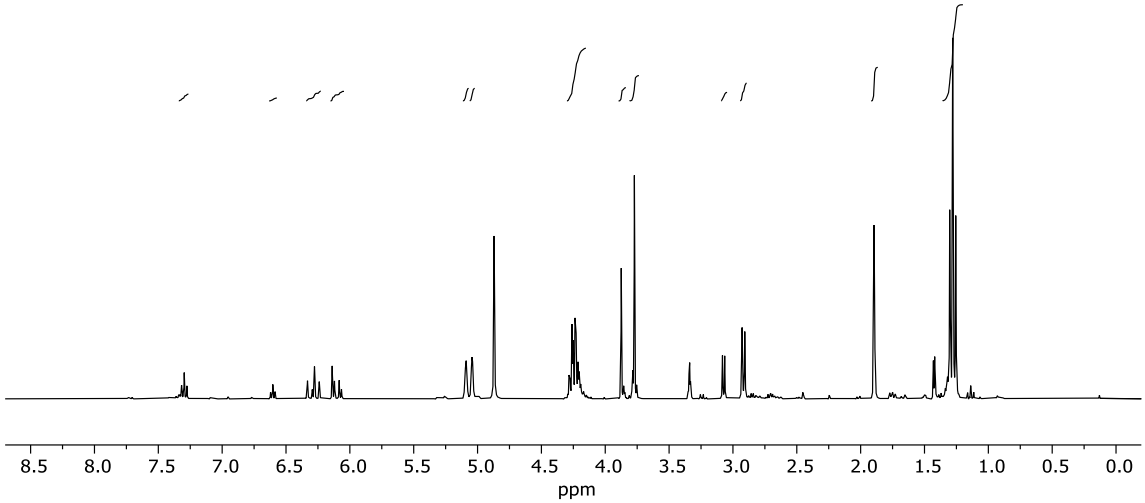

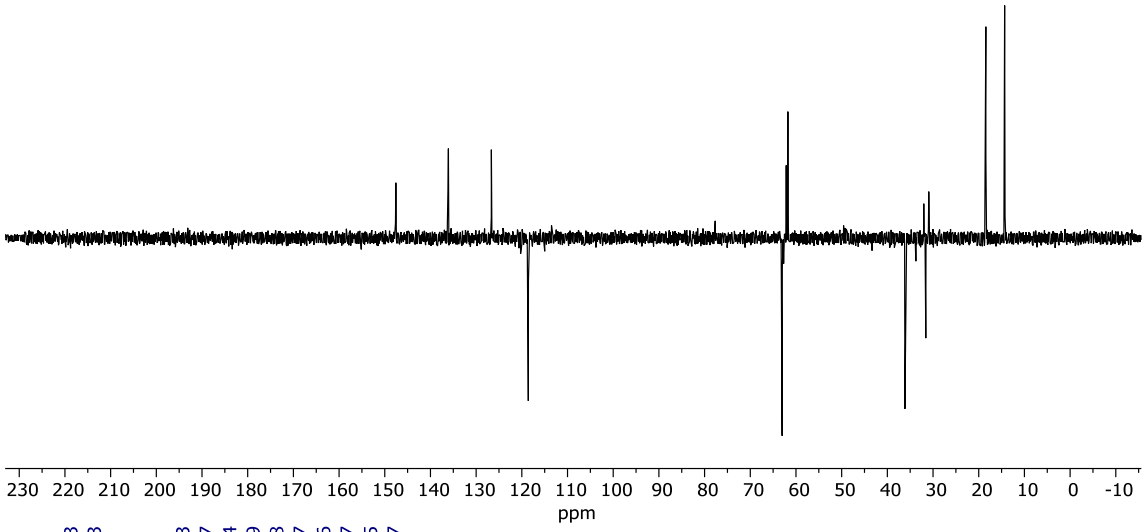

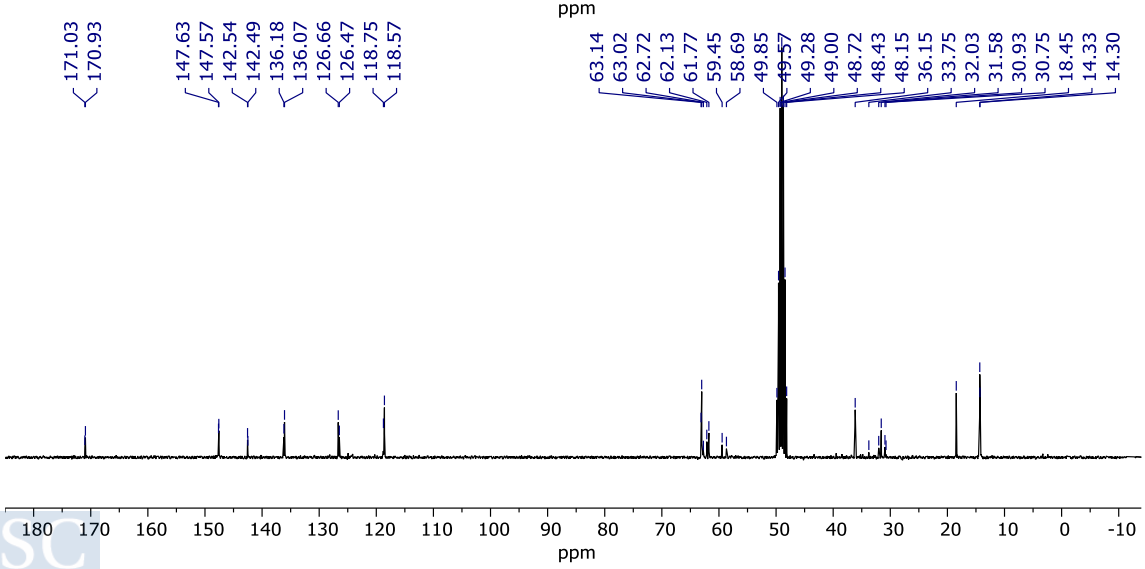

^{1}H, DEPT and ^{13}C Spectra of ***E*-3h** in $CDCl_3$

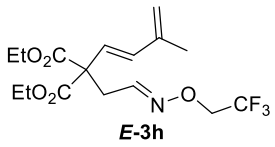

***E*-3h**

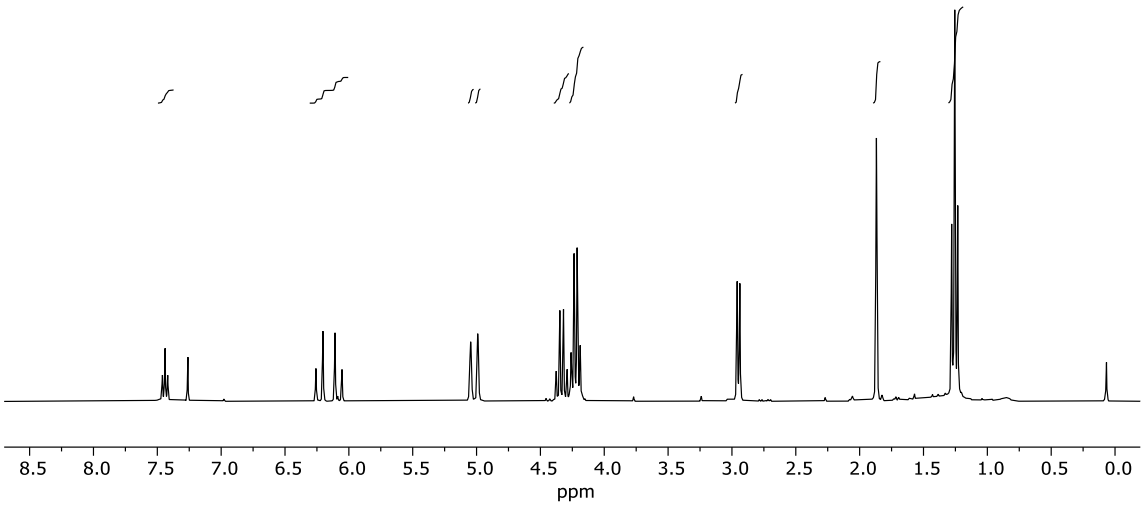

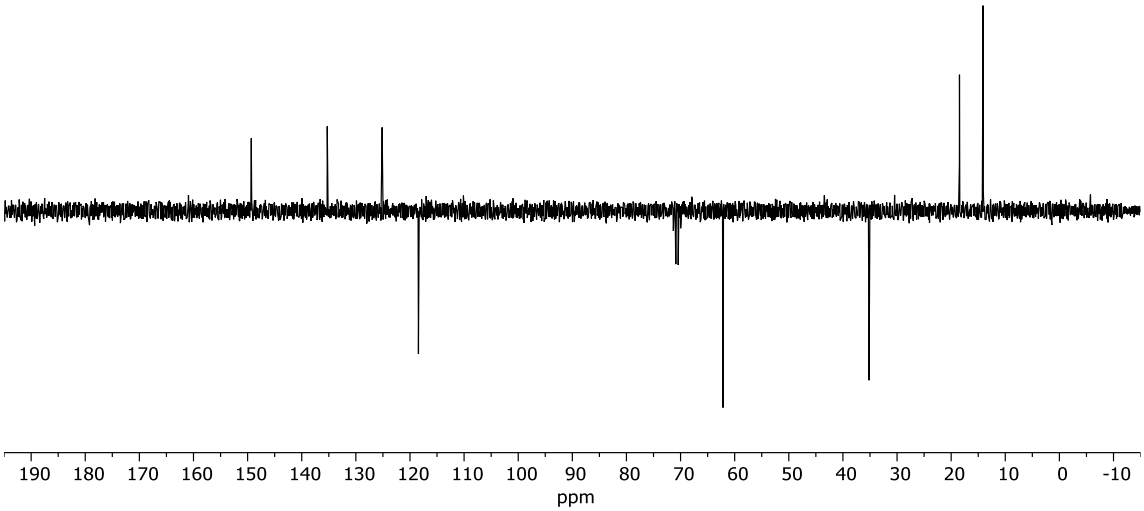

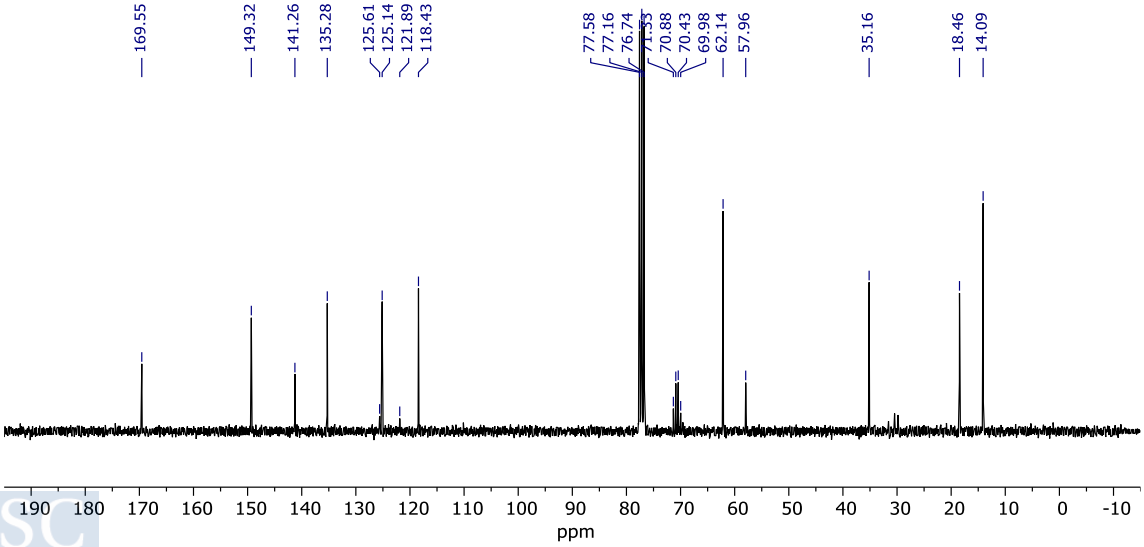

^{1}H, DEPT and ^{13}C Spectra of **(*E:Z* 1:2.3)-4a** in $CDCl_3$

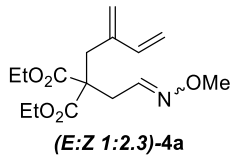

***(E:Z 1:2.3)*-4a**

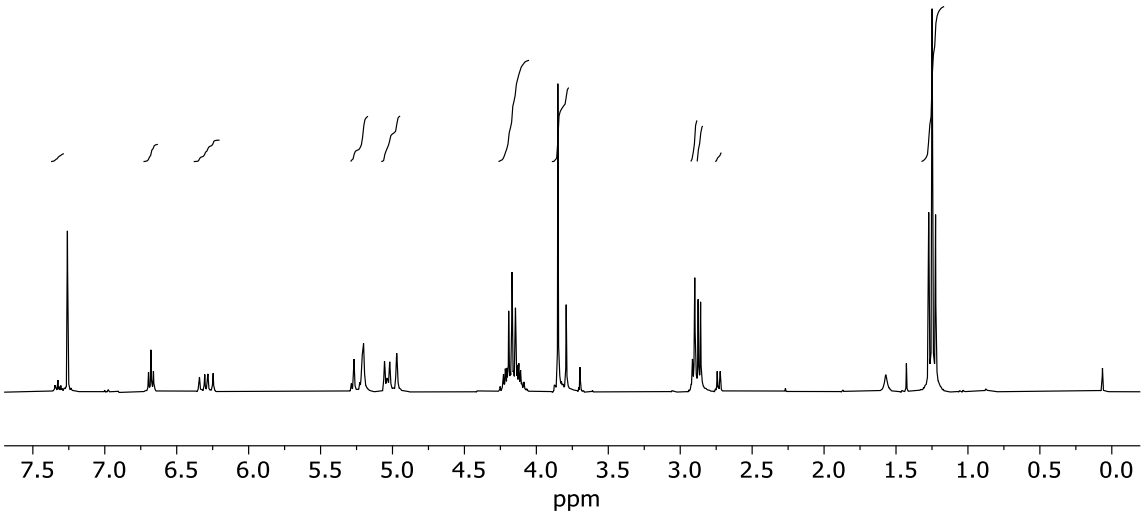

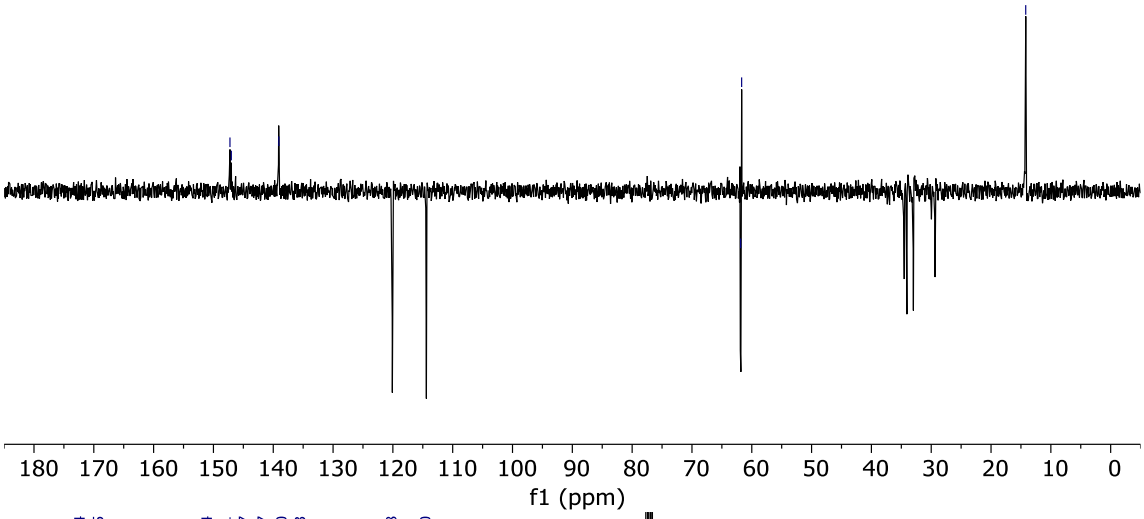

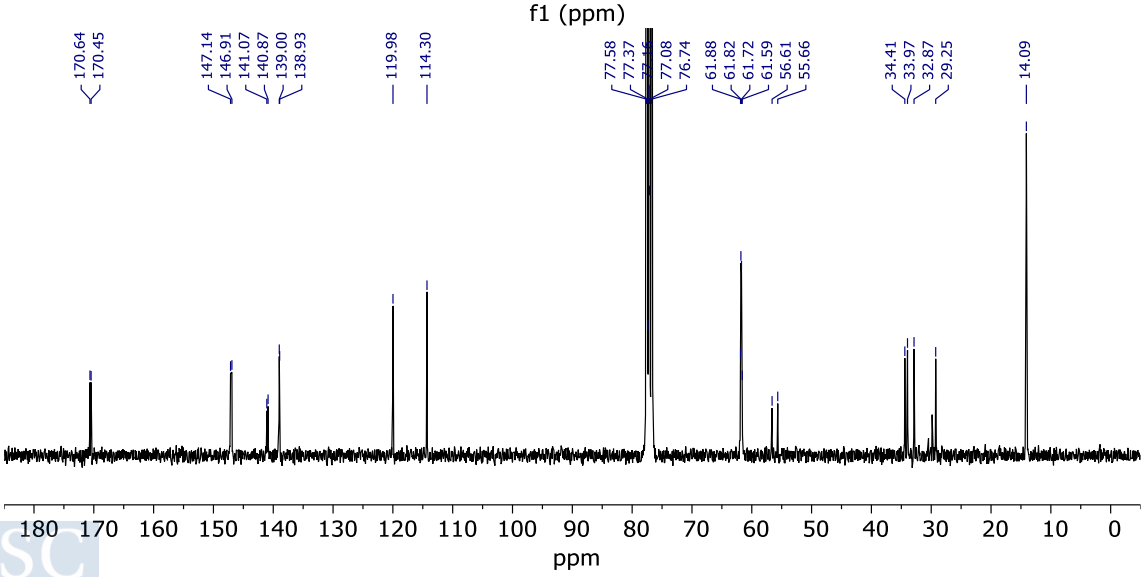

^{1}H, ^{2}H, DEPT and ^{13}C Spectra of **(*E:Z* 4:1)-4a** in CD_3OD

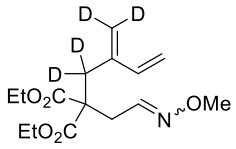

(*E:Z* 4:1)-d_4-4a

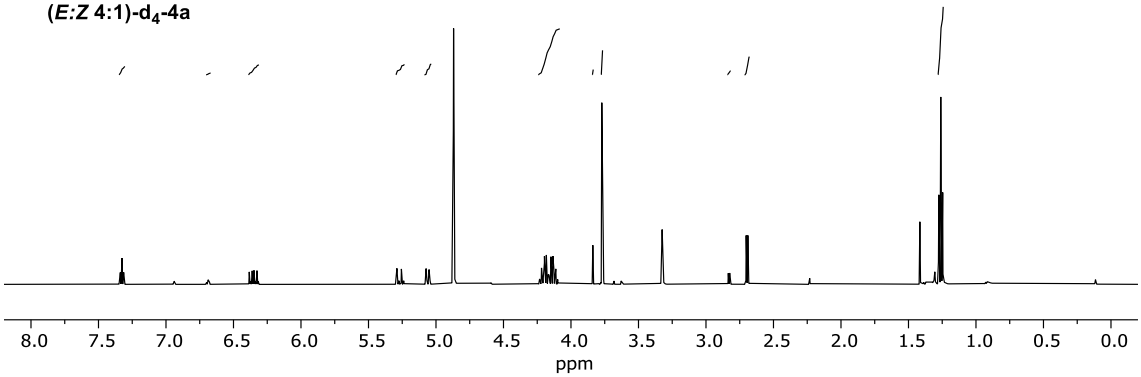

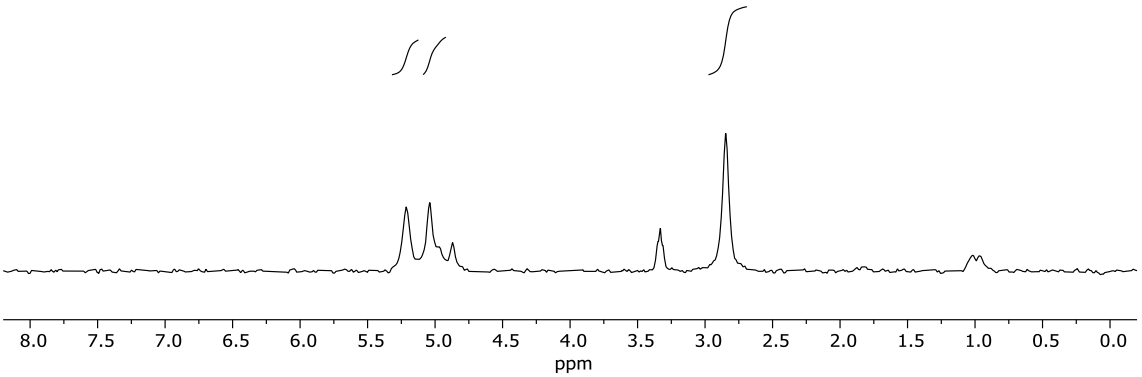

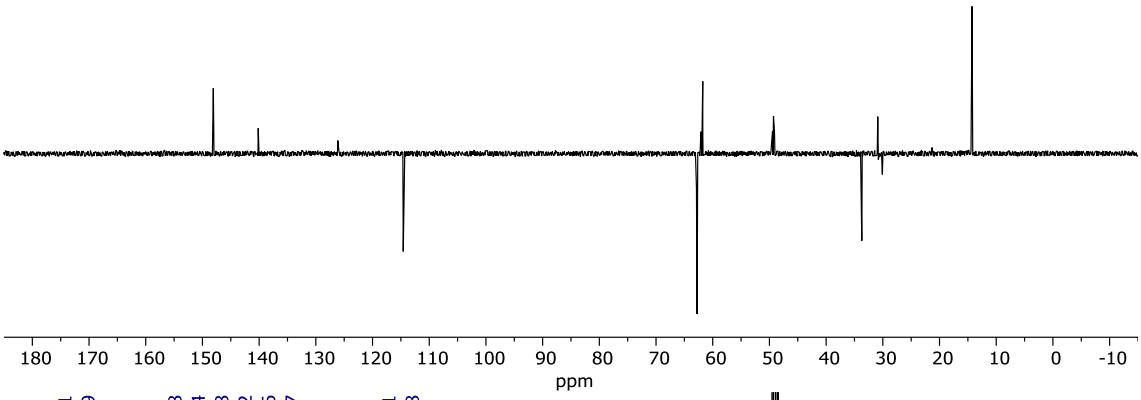

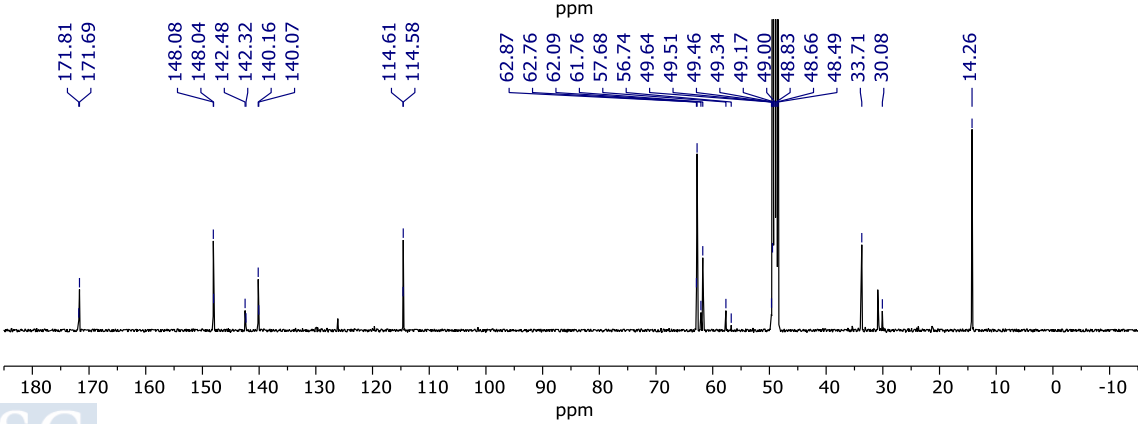

^{1}H, DEPT and ^{13}C Spectra of **9c** in $CDCl_3$

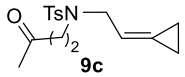

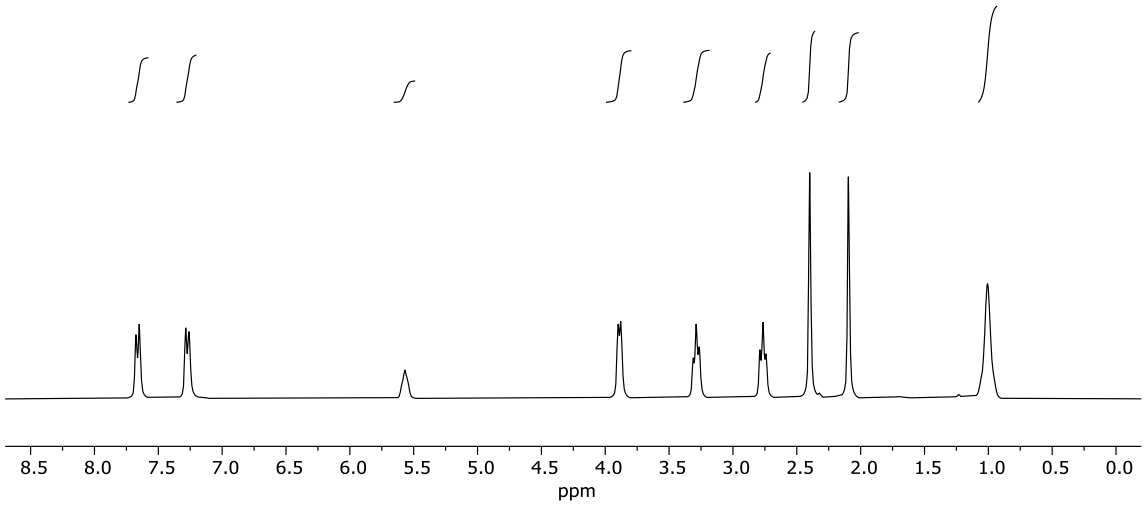

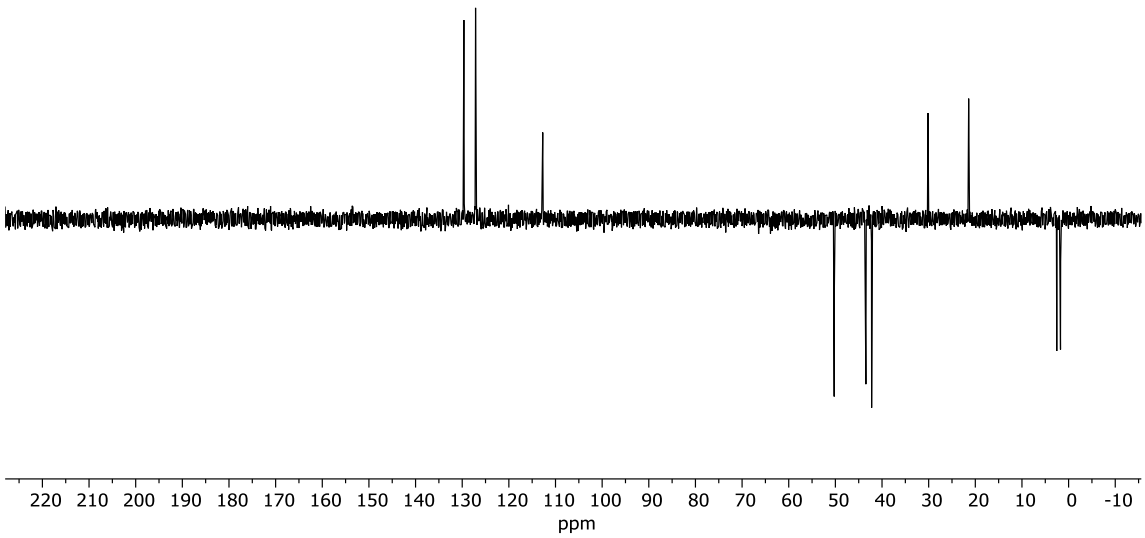

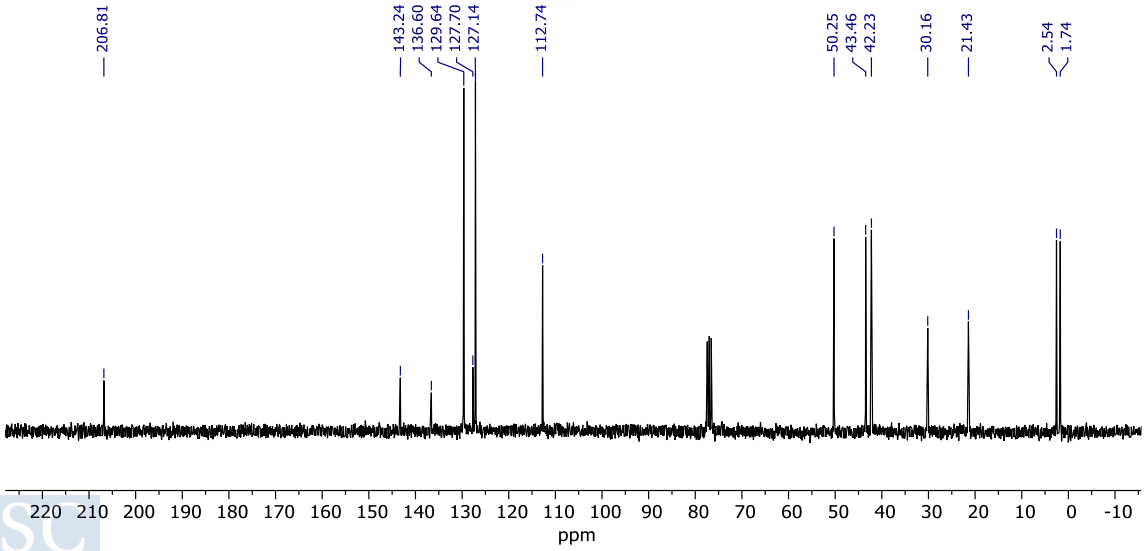

^{1}H, DEPT and ^{13}C Spectra of **15g** in $CDCl_3$

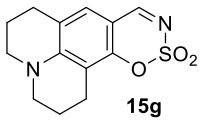

15g

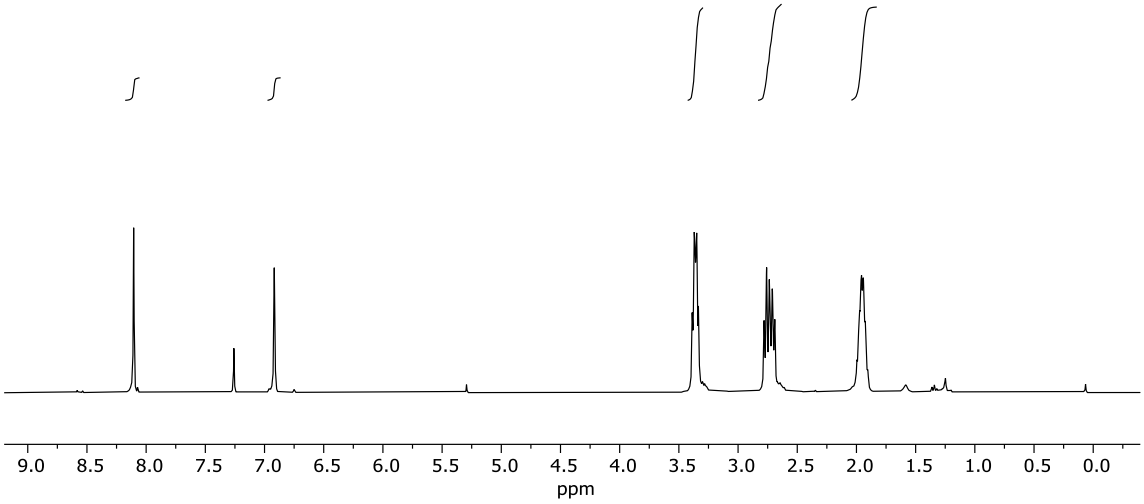

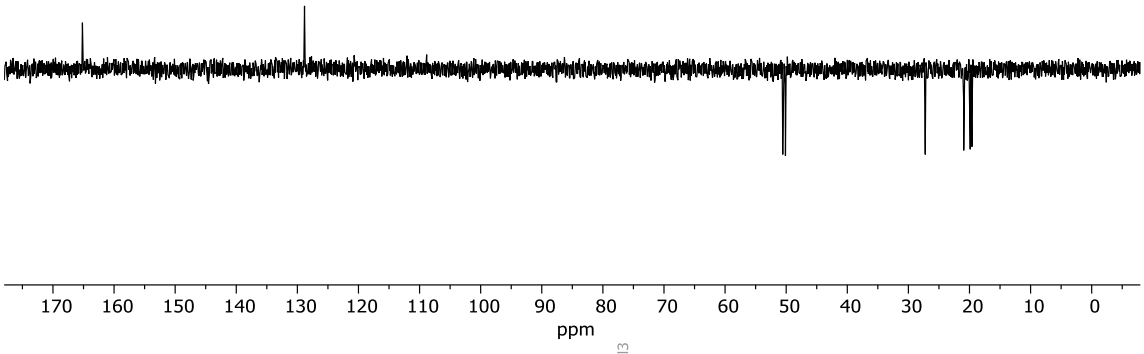

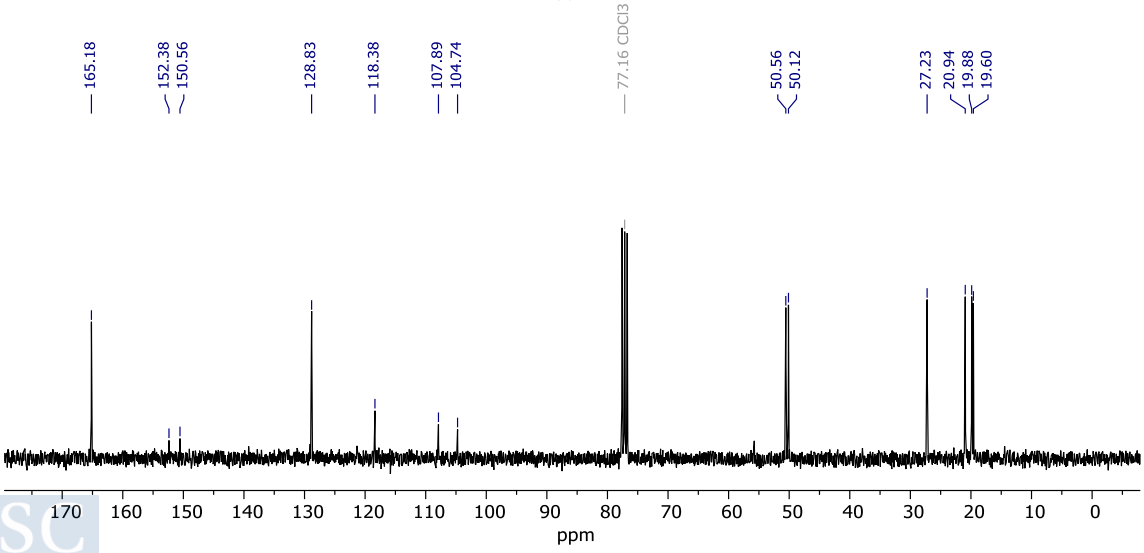

^{1}H, DEPT and ^{13}C Spectra of **16be** in $CDCl_3$

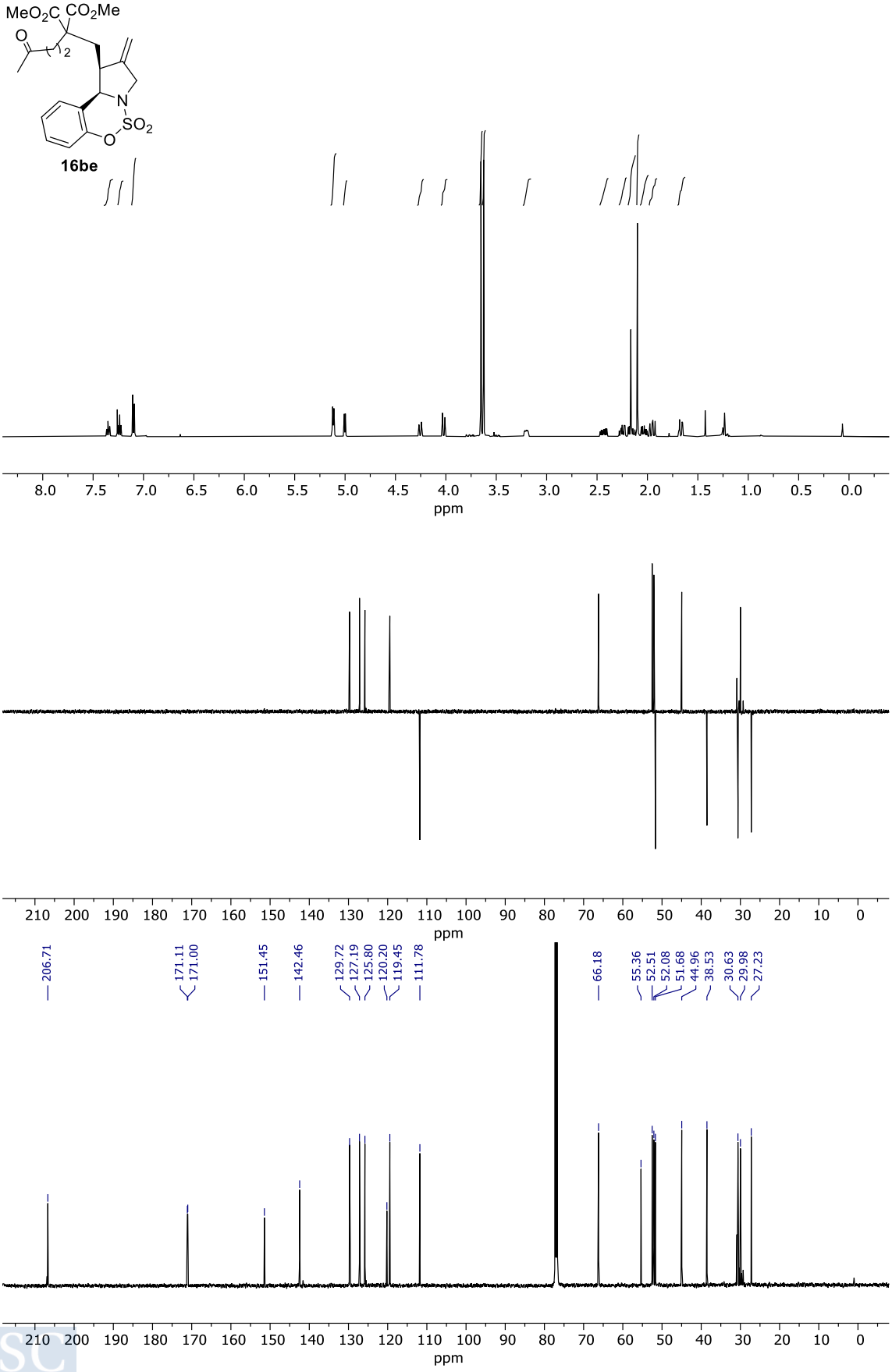

^{1}H, DEPT and ^{13}C Spectra of **16be'** in $CDCl_3$

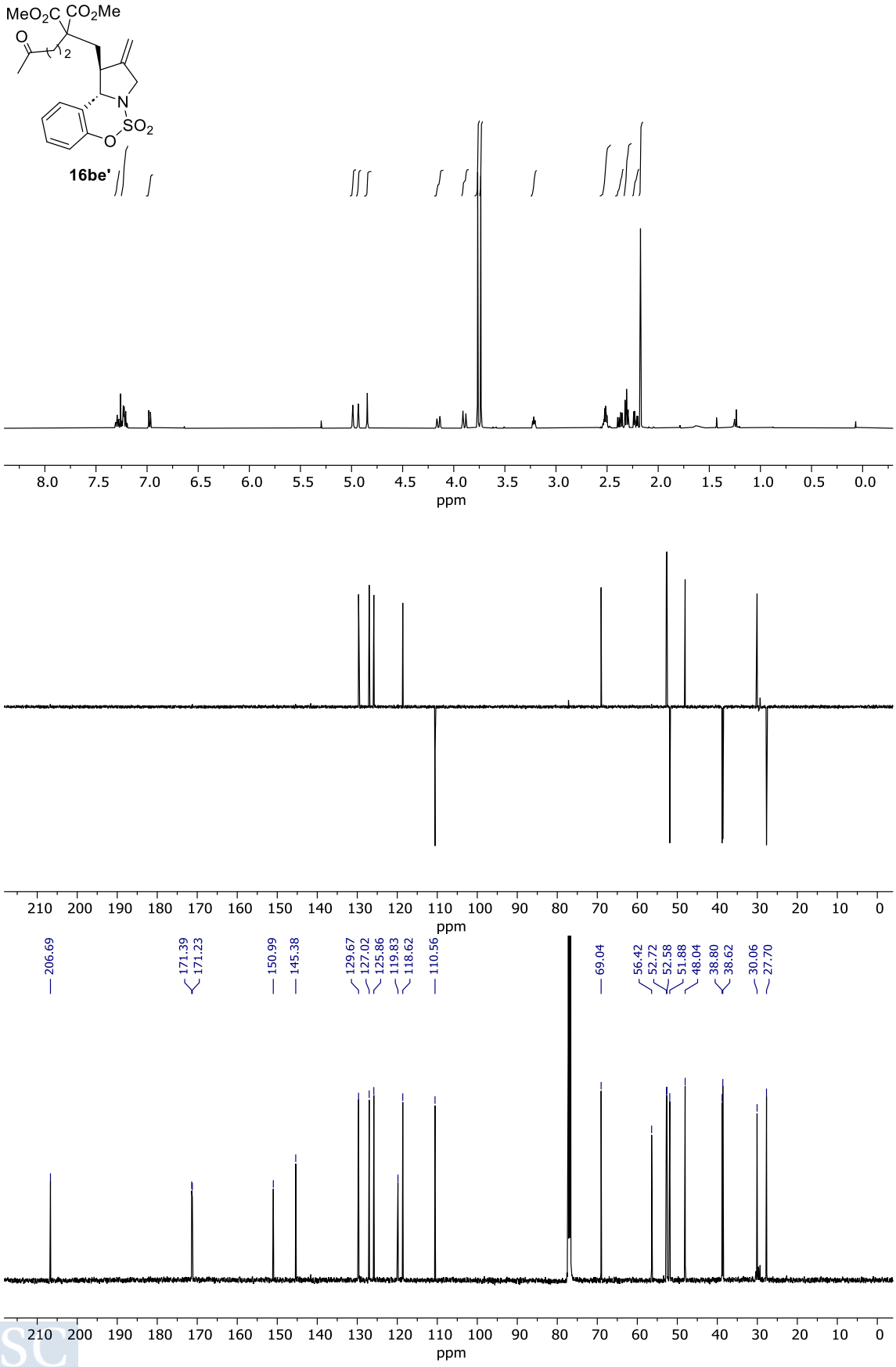

^{1}H, DEPT and ^{13}C Spectra of **23br** in $CDCl_3$

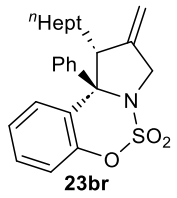

23br

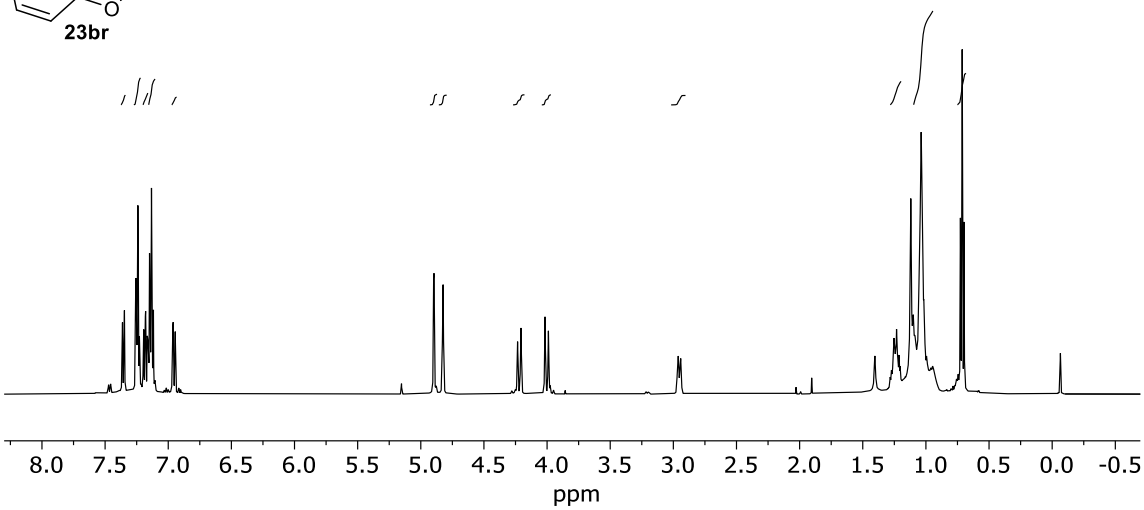

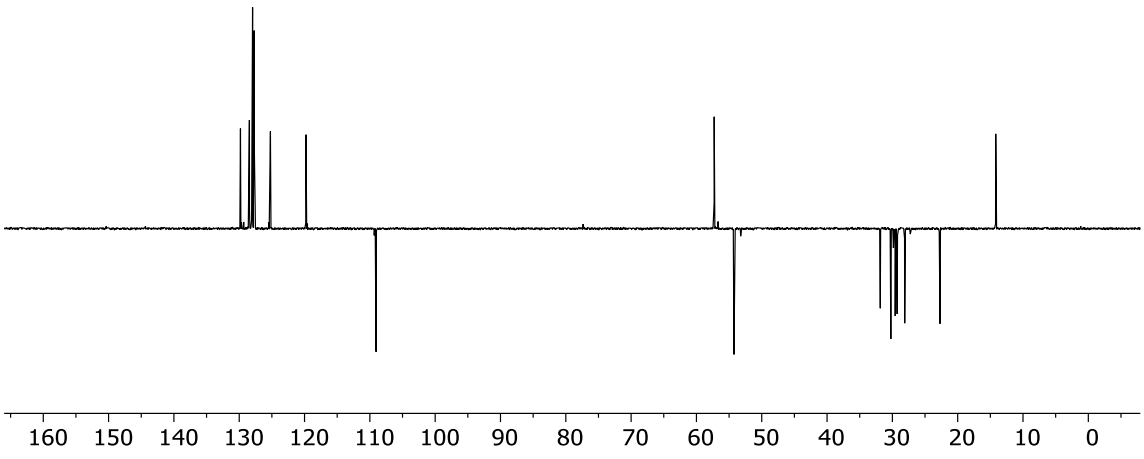

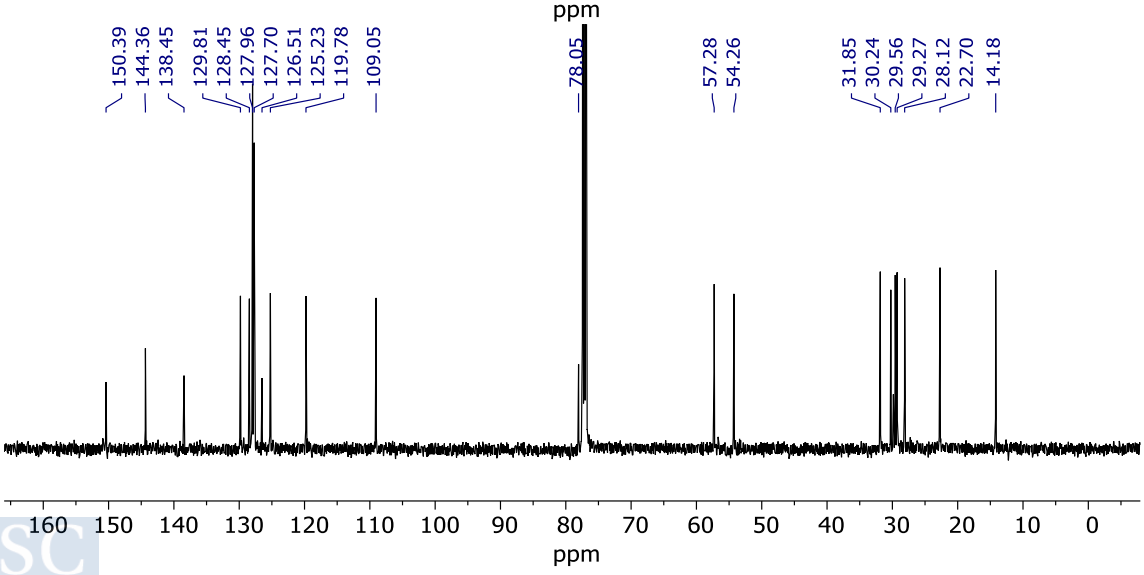

^{1}H, DEPT and ^{13}C Spectra of **23br'** in $CDCl_3$

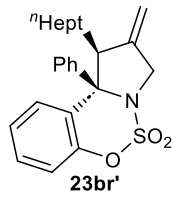

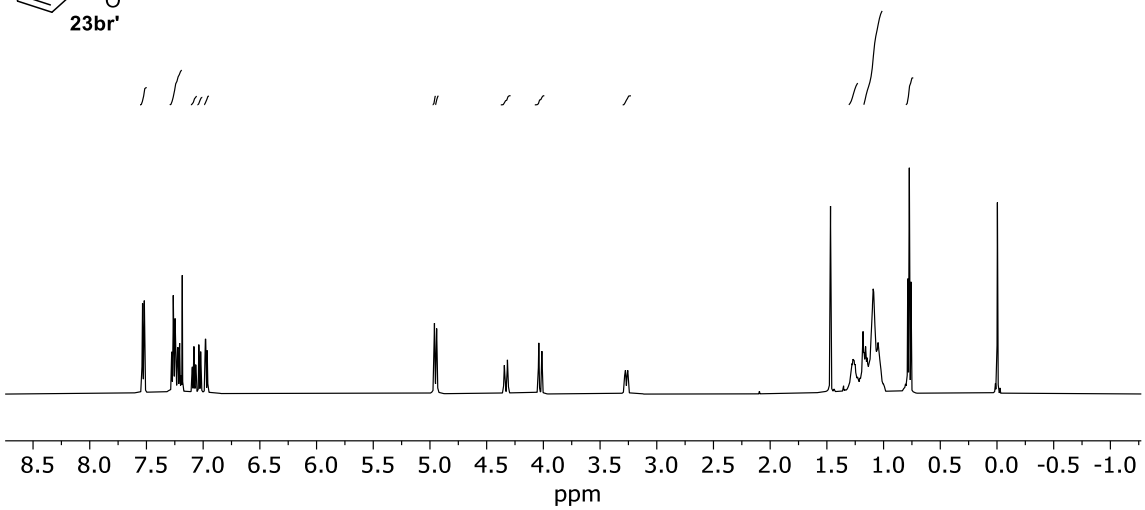

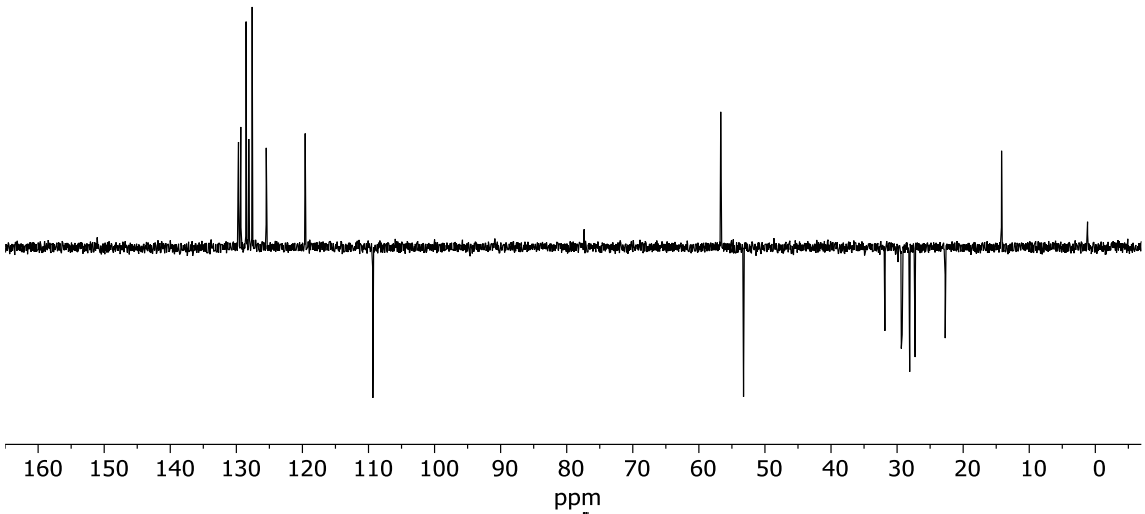

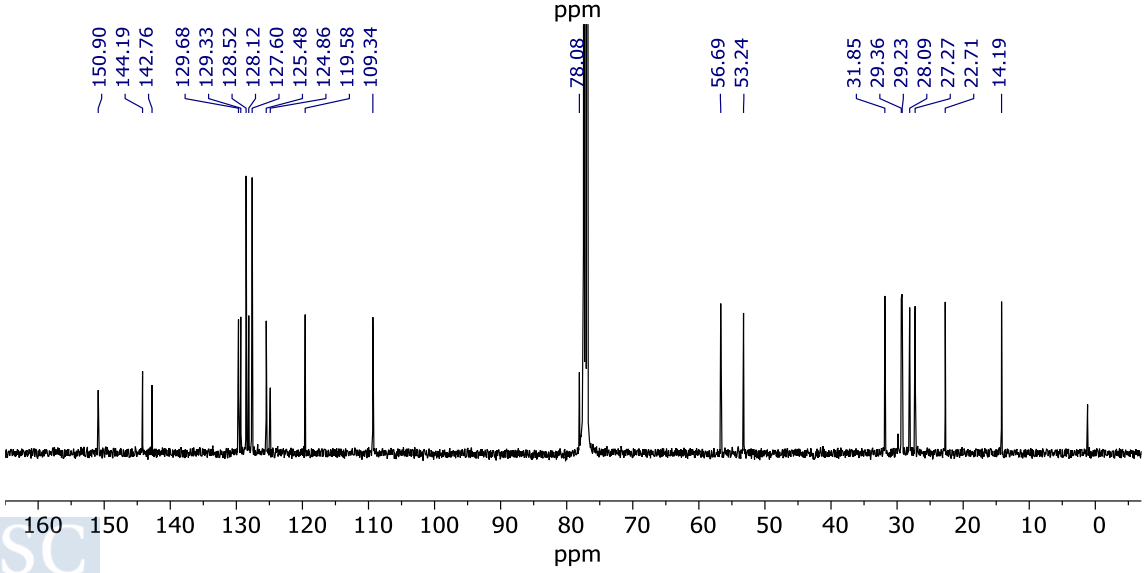

^{1}H, DEPT and ^{13}C Spectra of **23dd** in $CDCl_3$

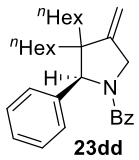

23dd

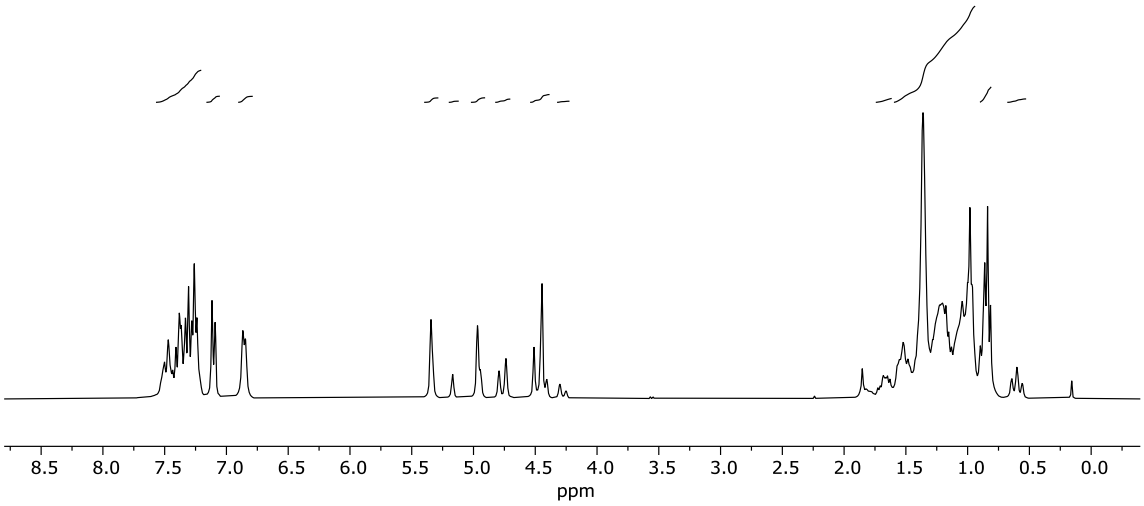

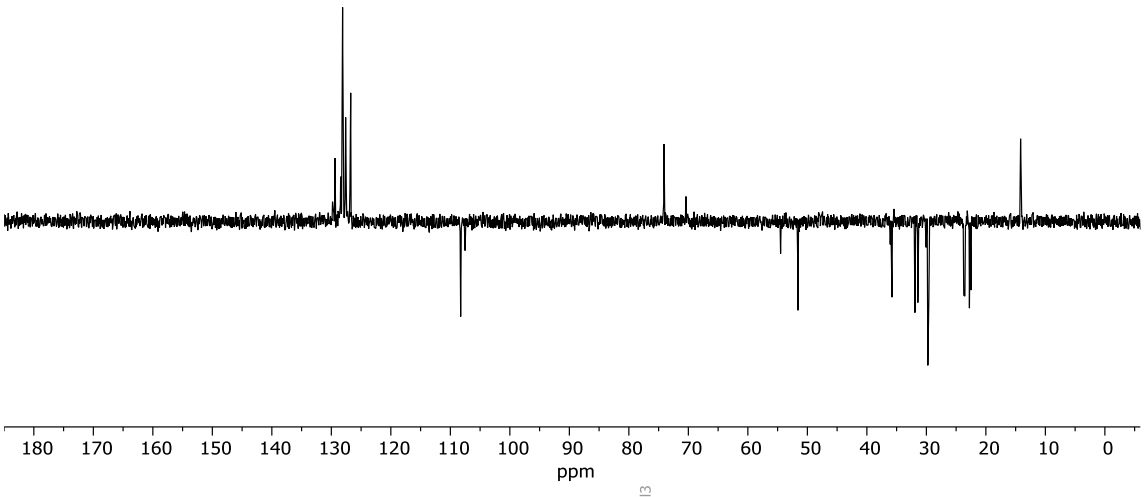

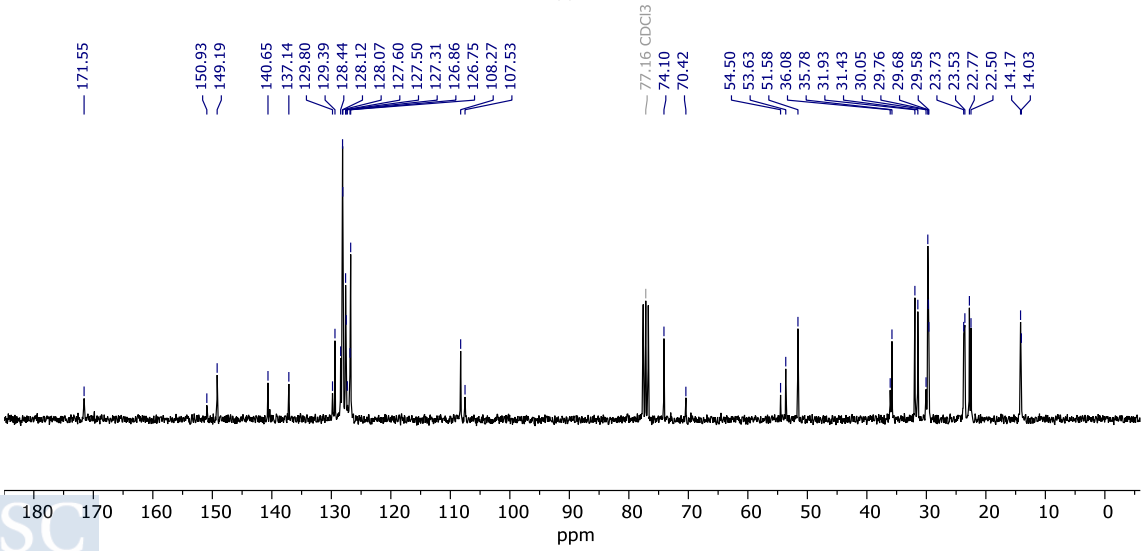

^{1}H, DEPT and ^{13}C Spectra of **23de** in $CDCl_3$

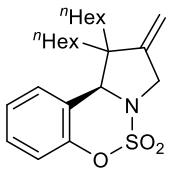

23de

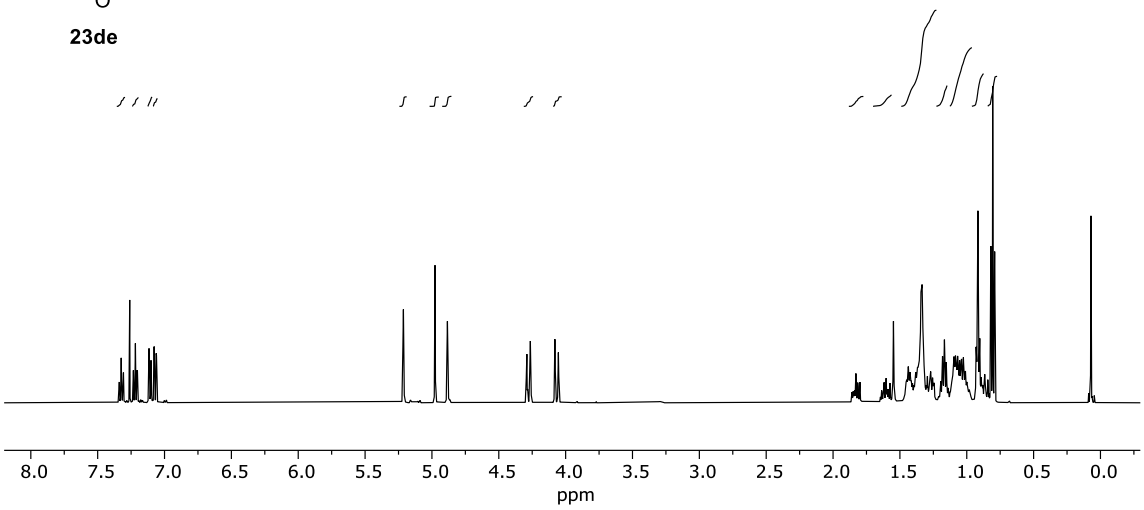

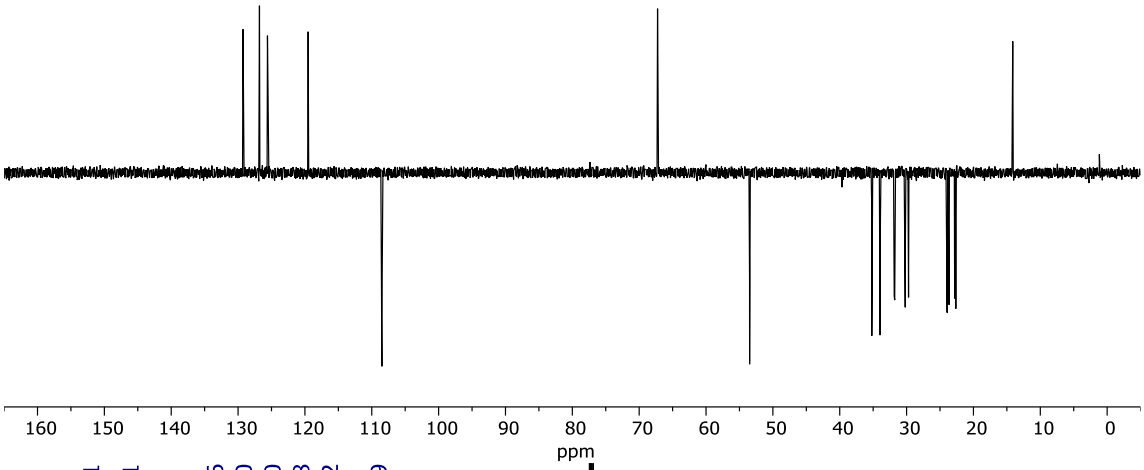

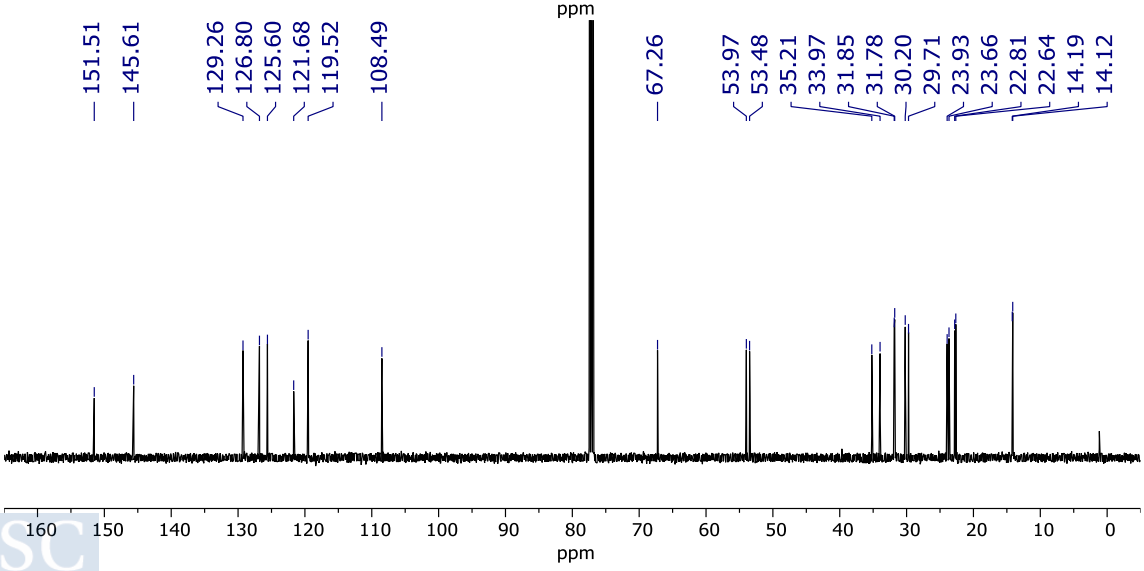

^{1}H, DEPT and ^{13}C Spectra of **23dl** in $CDCl_3$

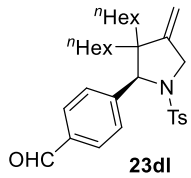

23dl

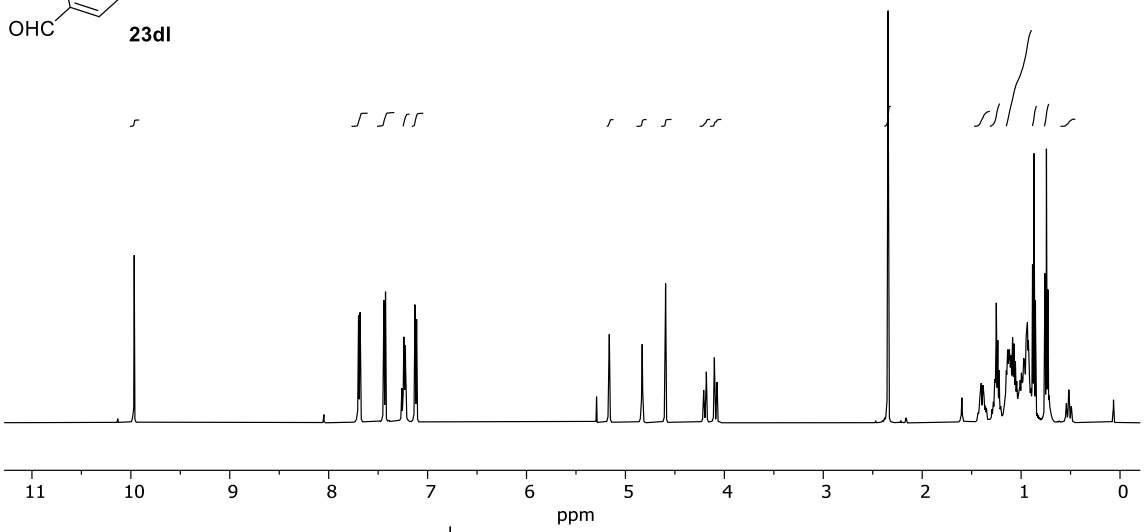

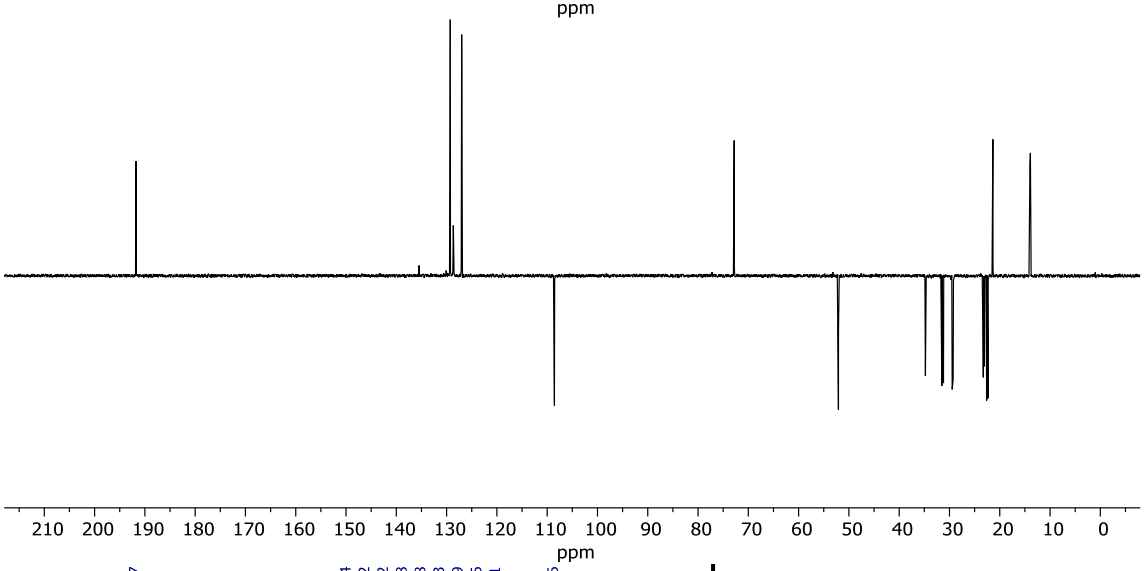

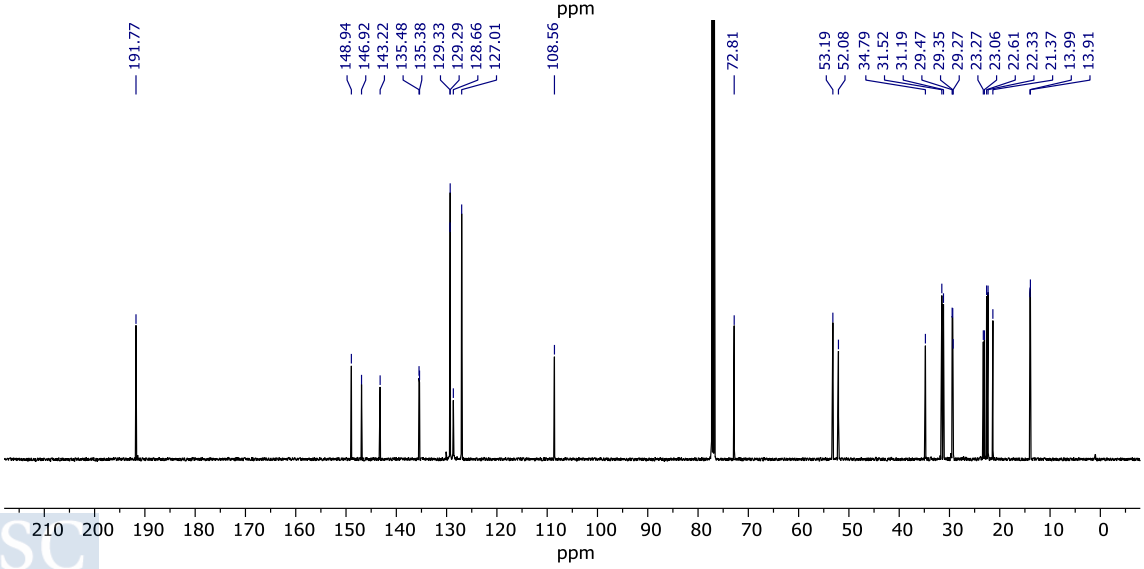

^{1}H, DEPT and ^{13}C Spectra of **23dq** in $CDCl_3$

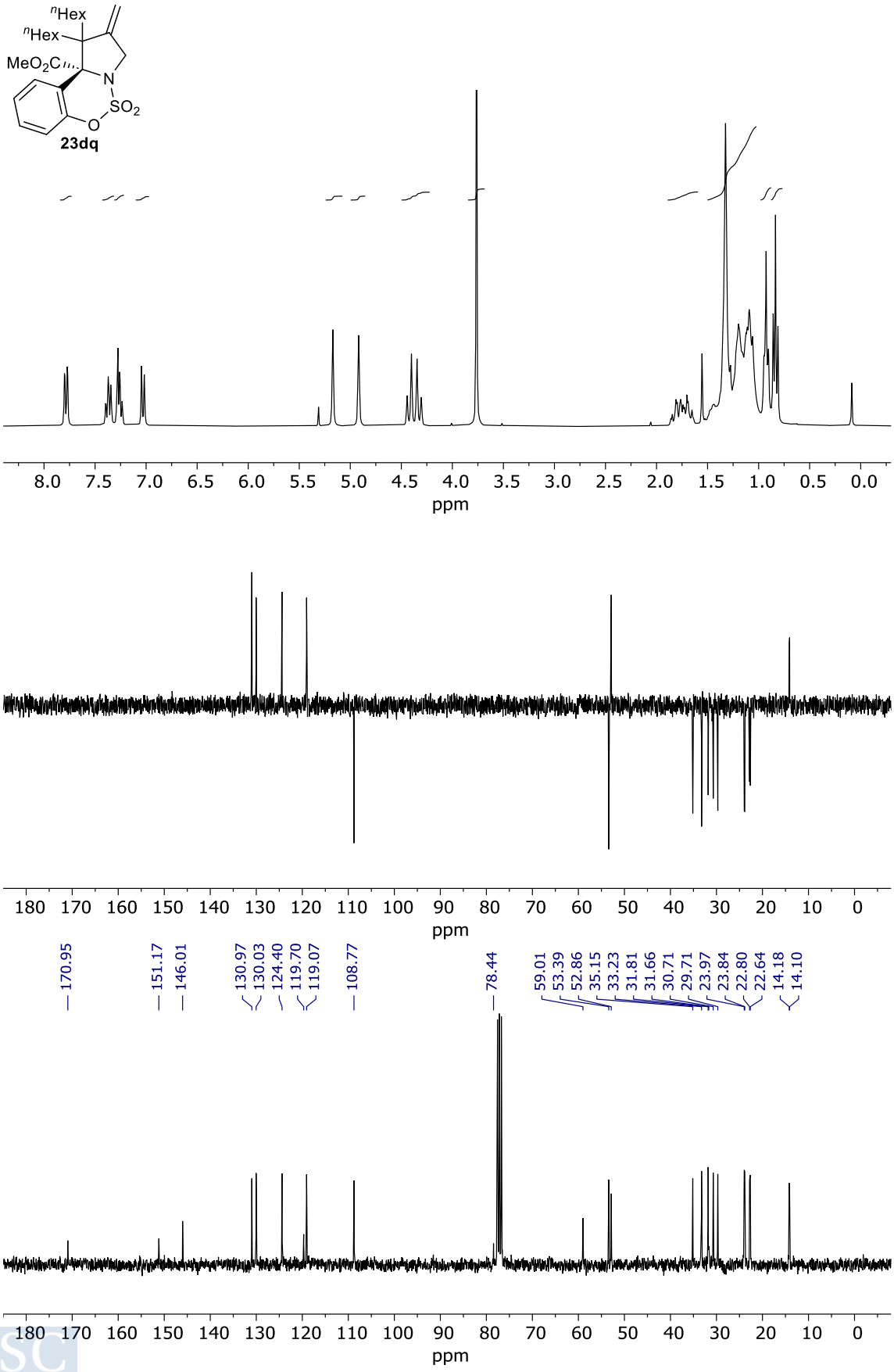

^{1}H, DEPT and ^{13}C Spectra of **23fi** in $CDCl_3$

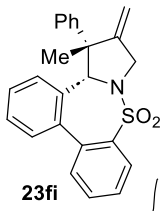

23fi

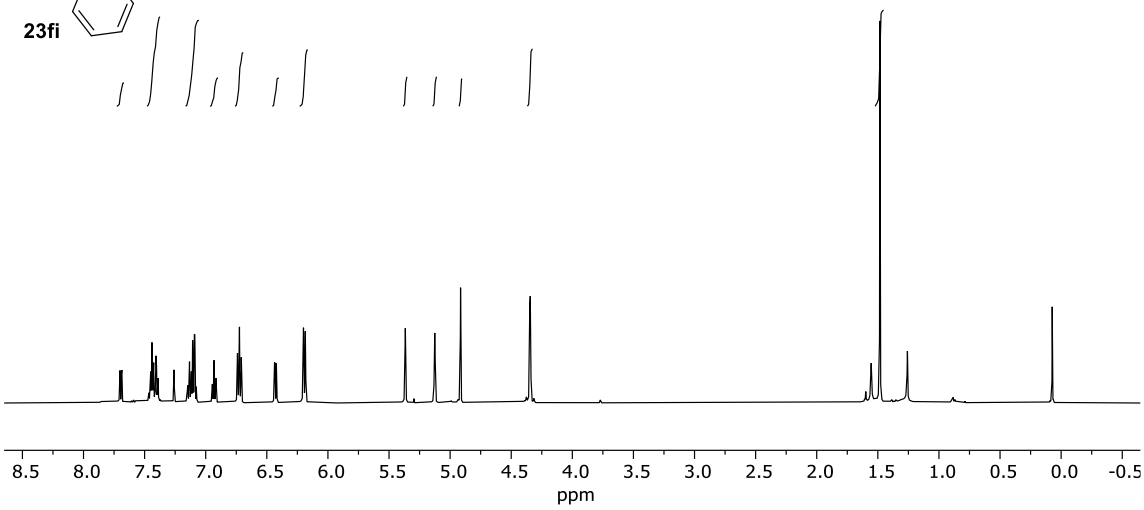

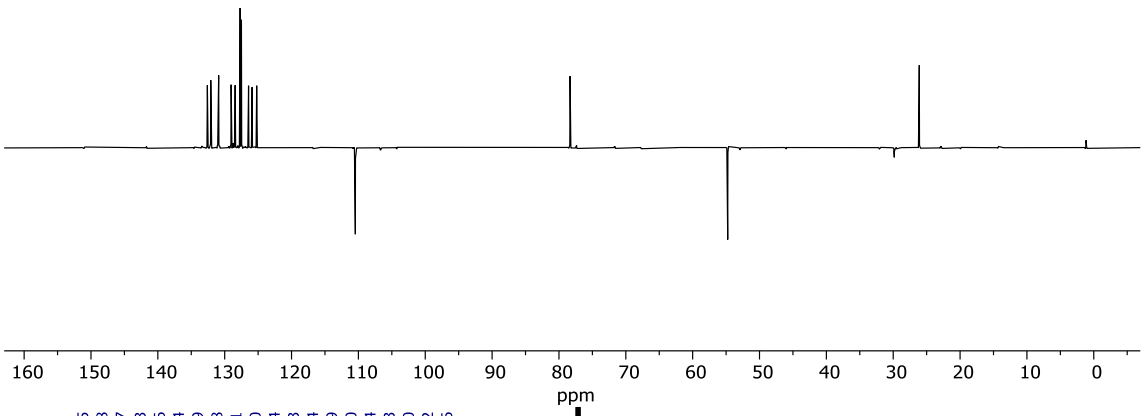

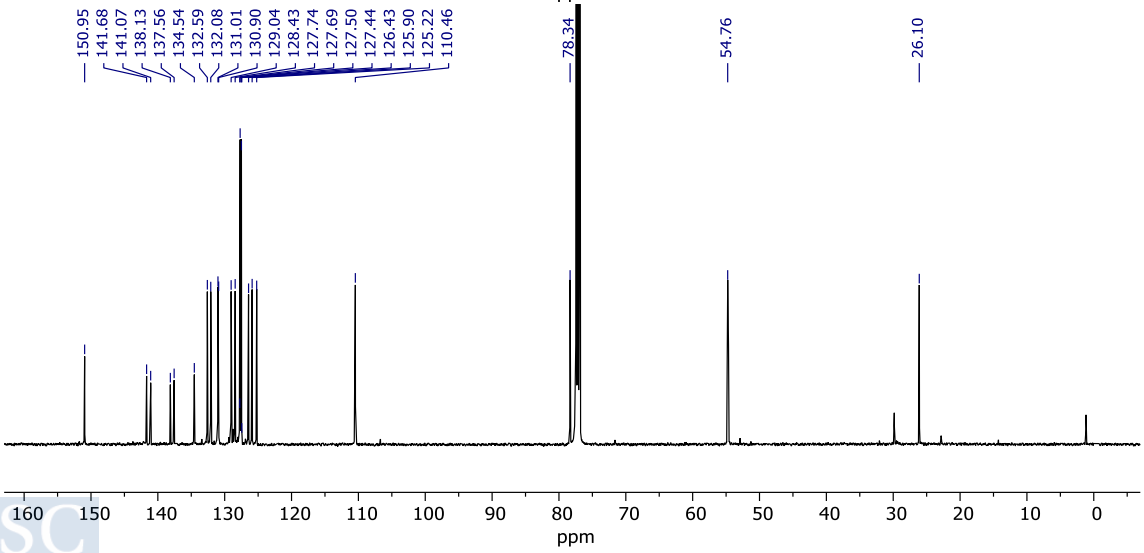

^{1}H, DEPT and ^{13}C Spectra of **23fi'** in $CDCl_3$

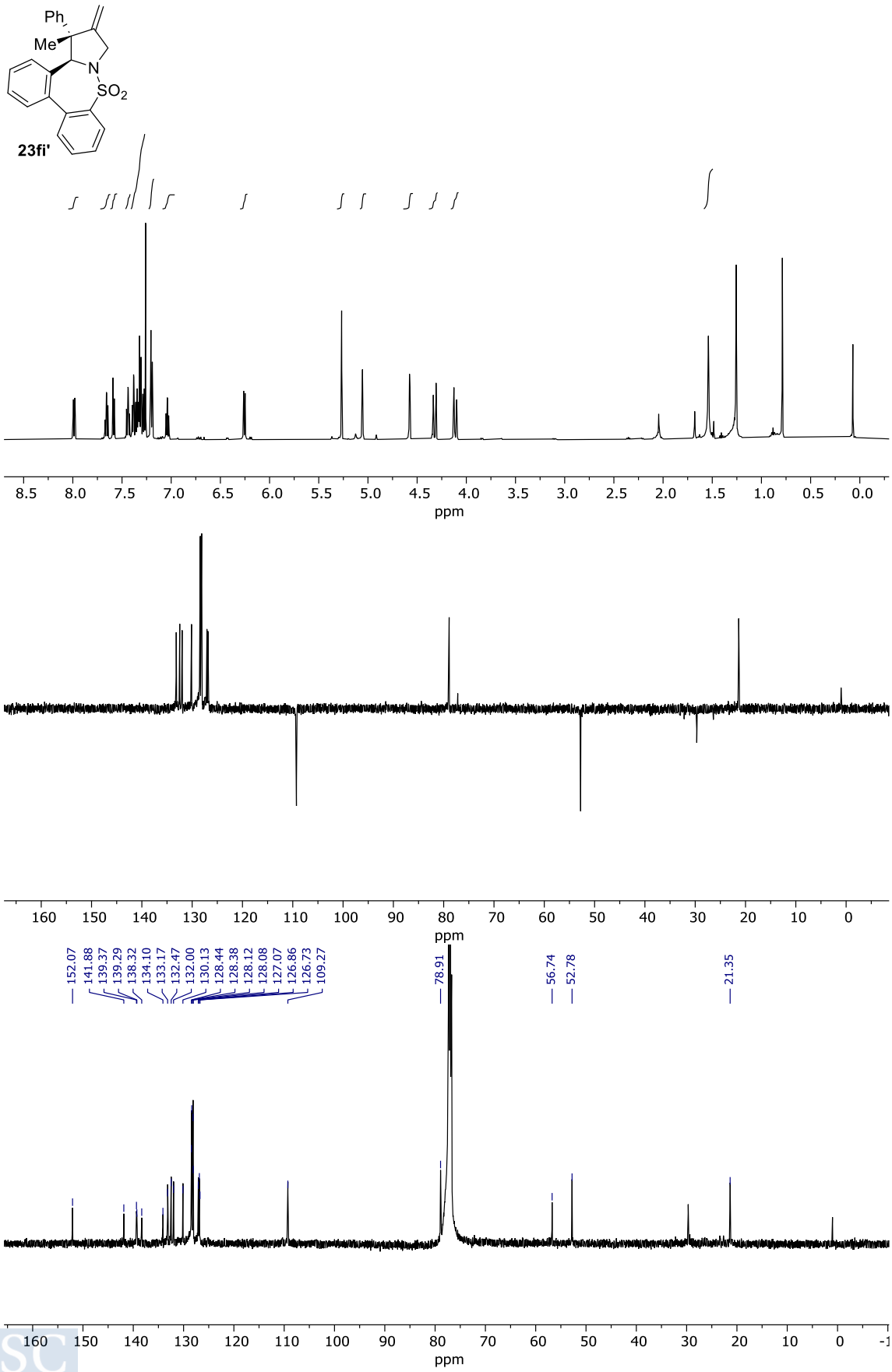

^{1}H, DEPT and ^{13}C Spectra of **23fp:23fp'** ratio 1:1 in $CDCl_3$

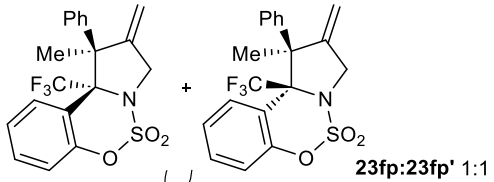

23fp:23fp' 1:1

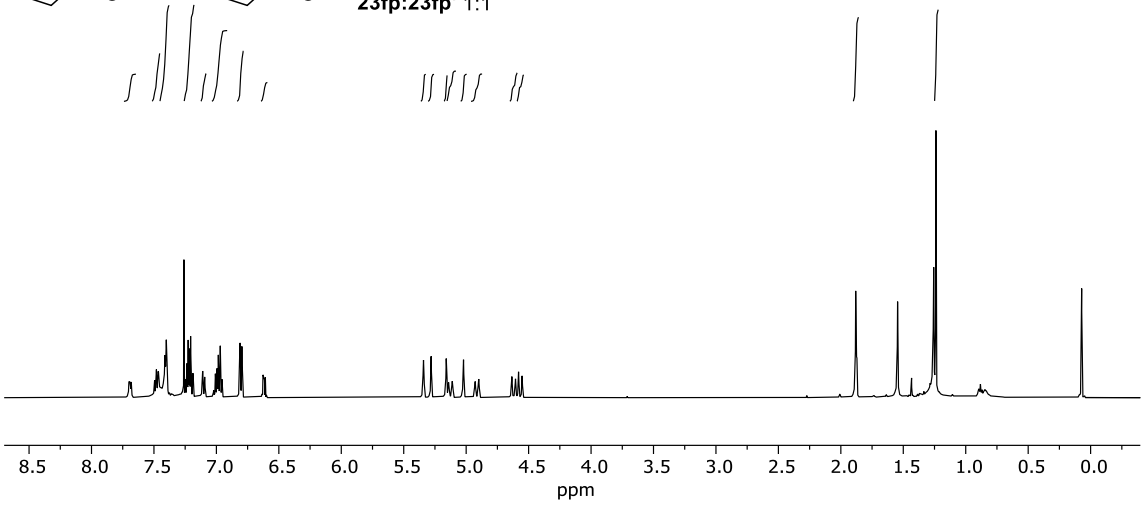

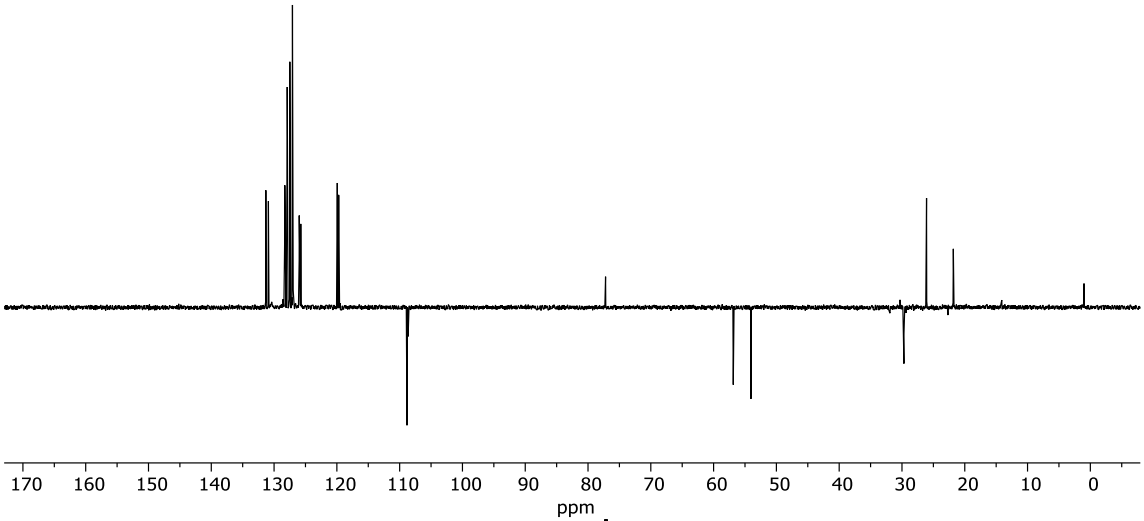

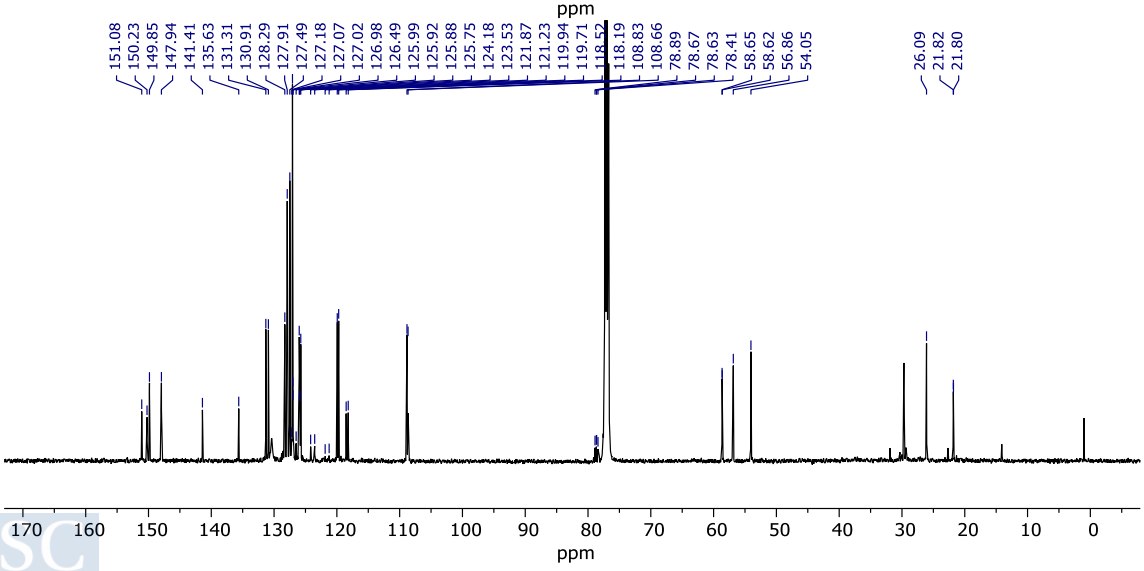

^{1}H, DEPT and ^{13}C Spectra of **24gs** in $CDCl_3$

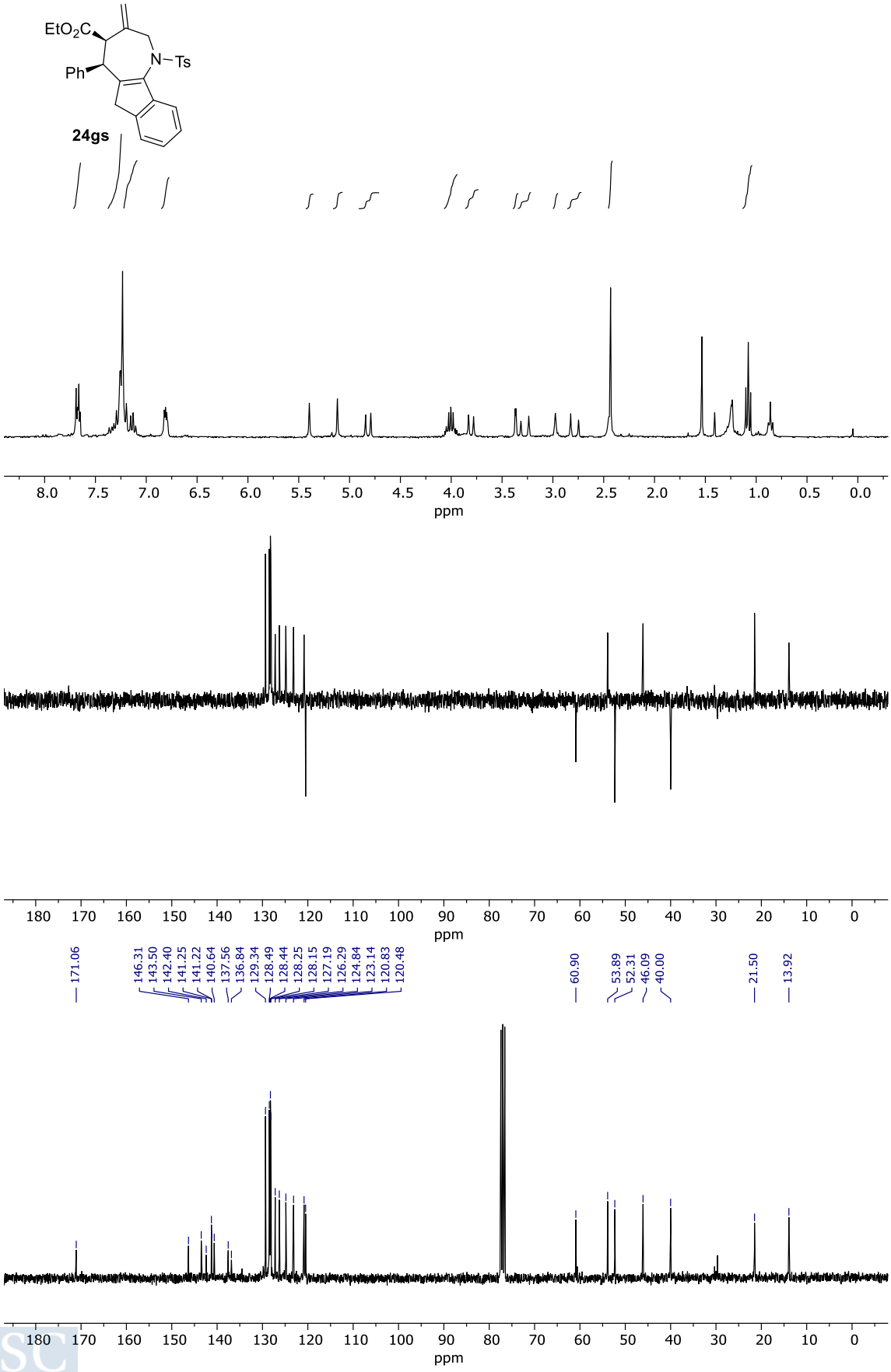

^{1}H, DEPT and ^{13}C Spectra of **25gu** in $CDCl_3$

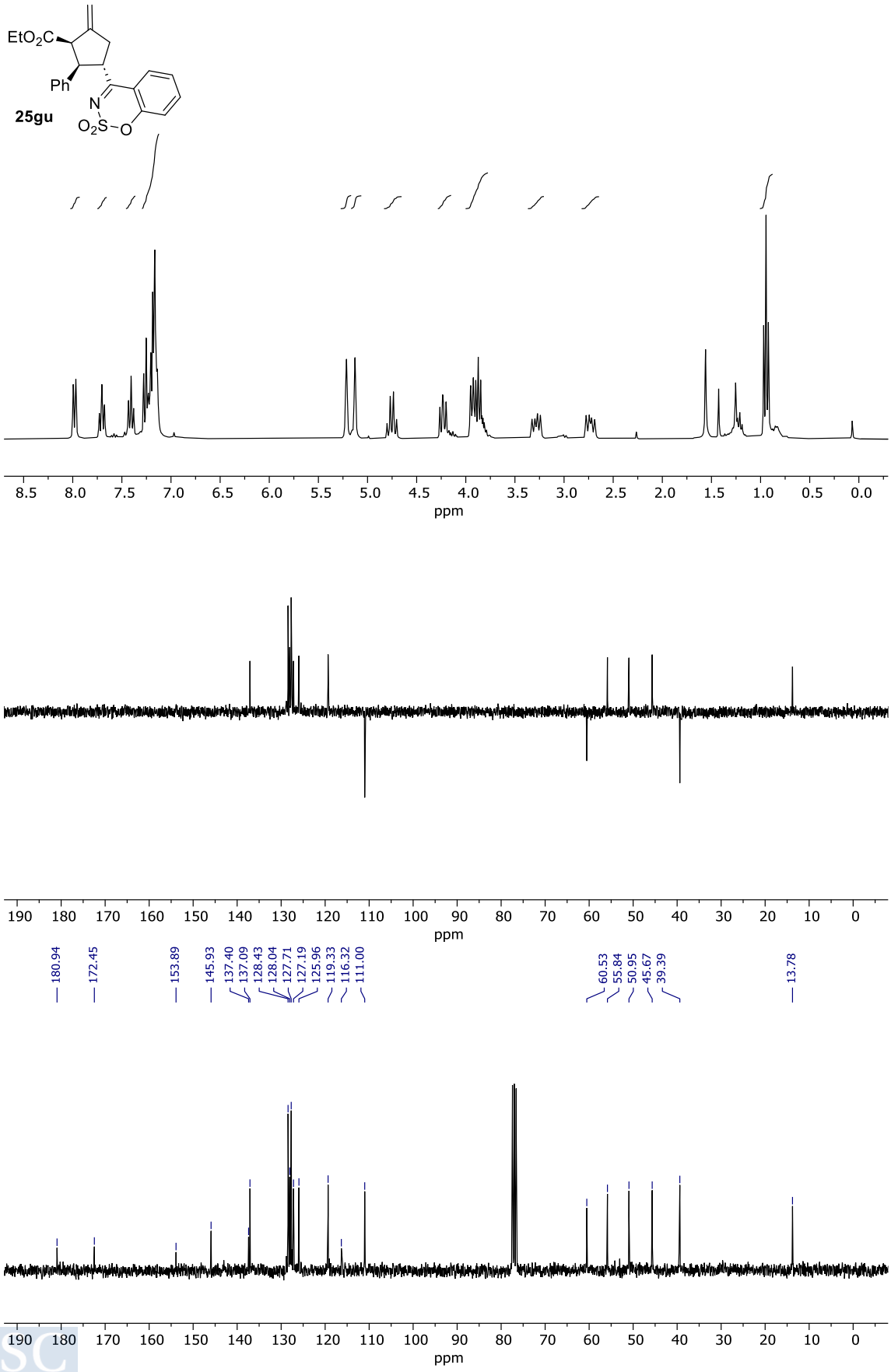

^{1}H, DEPT and ^{13}C Spectra of **25gu'** in $CDCl_3$

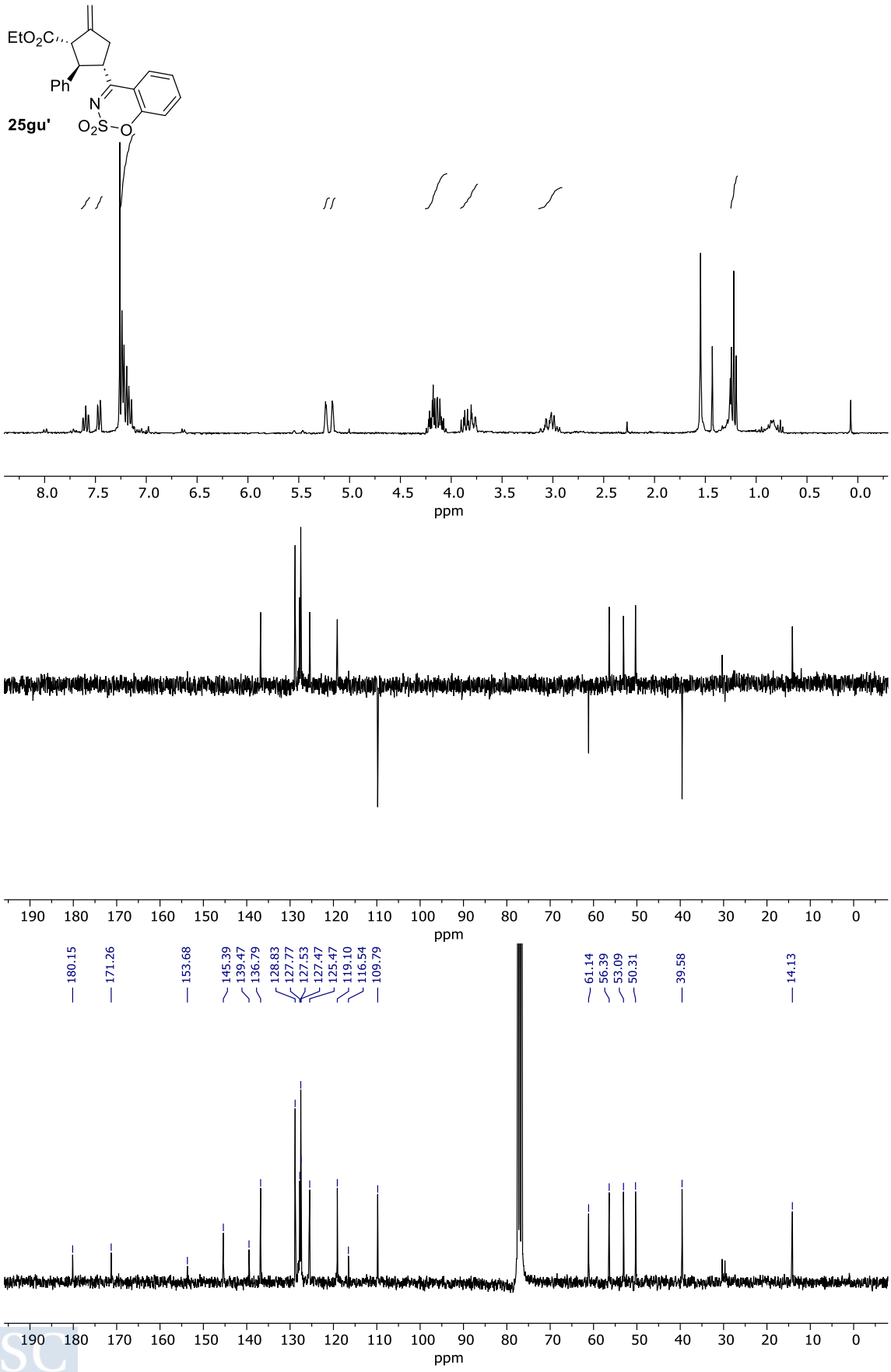

^{1}H, DEPT and ^{13}C Spectra of **29de** in $CDCl_3$

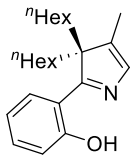

29de

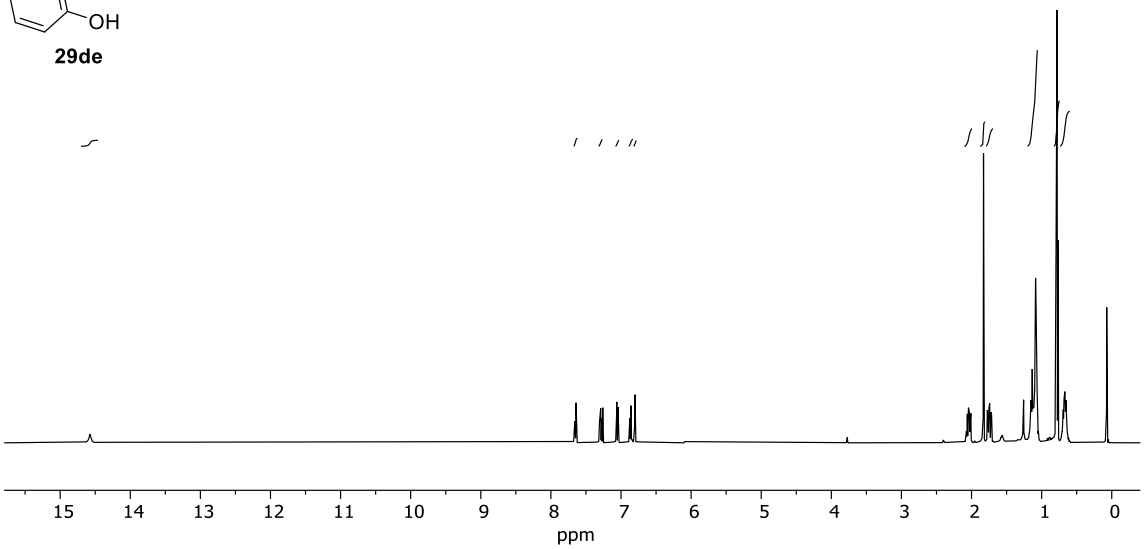

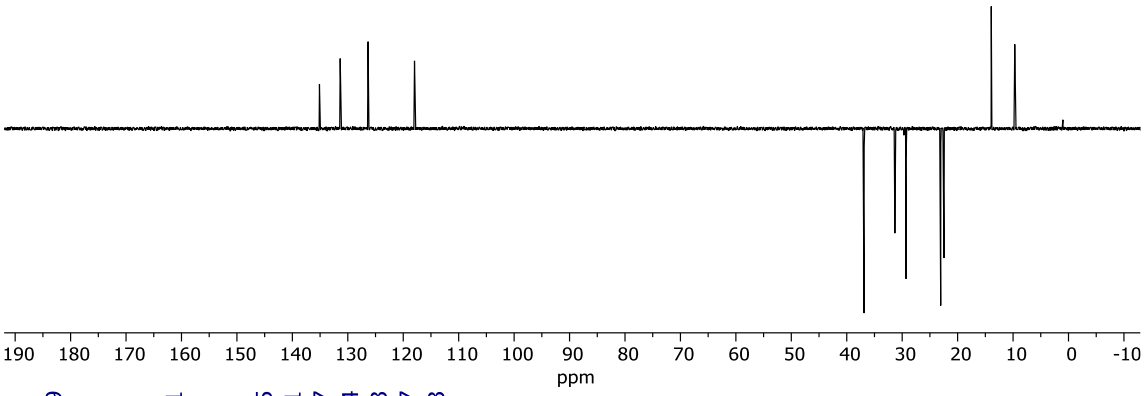

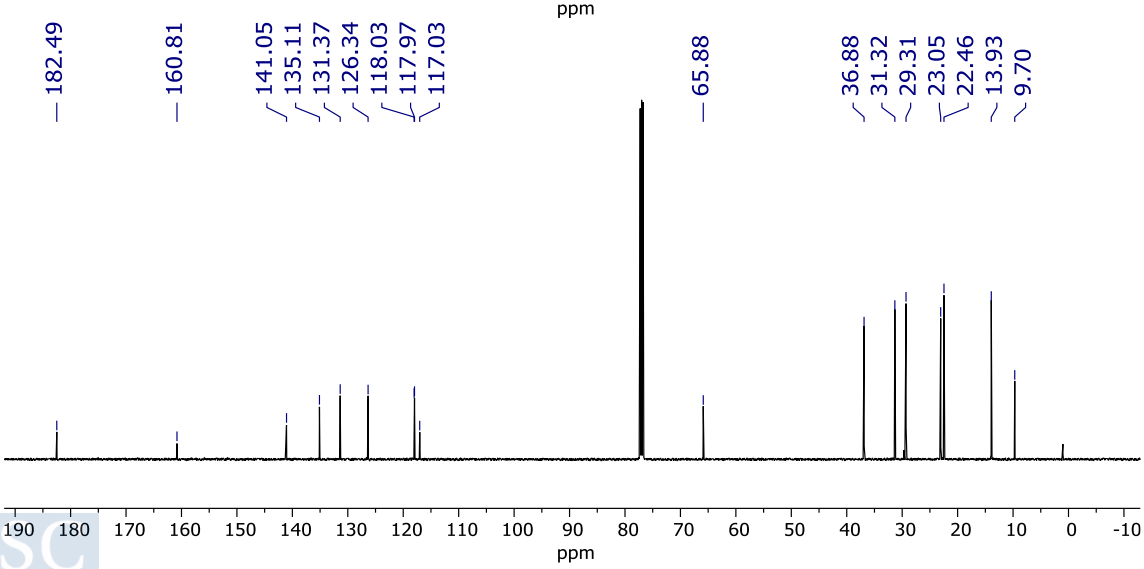

^{1}H, DEPT and ^{13}C Spectra of **37aa** in $CDCl_3$

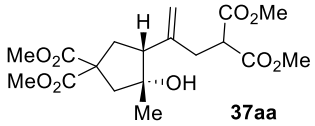

37aa

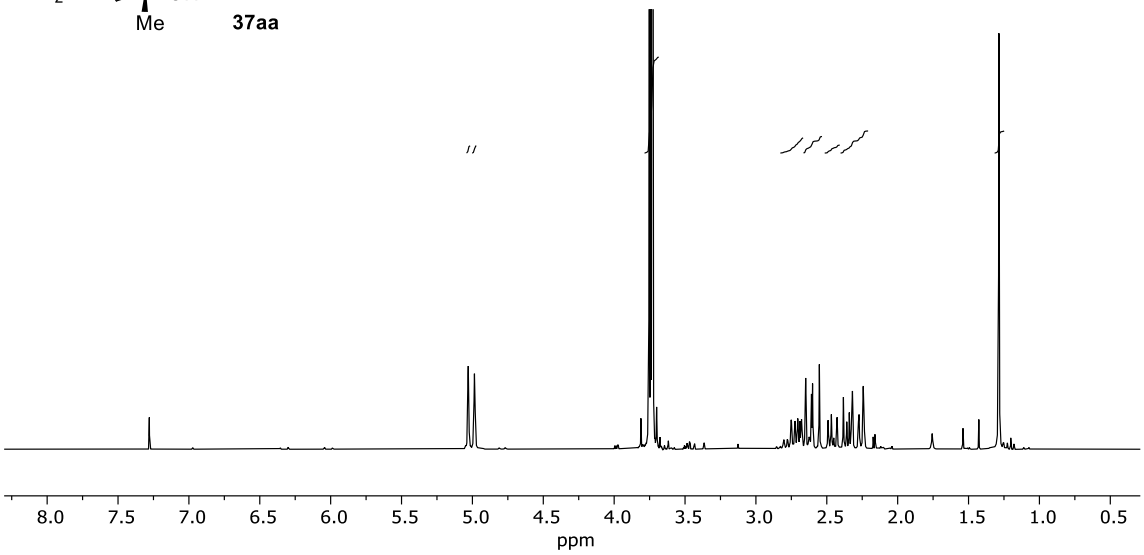

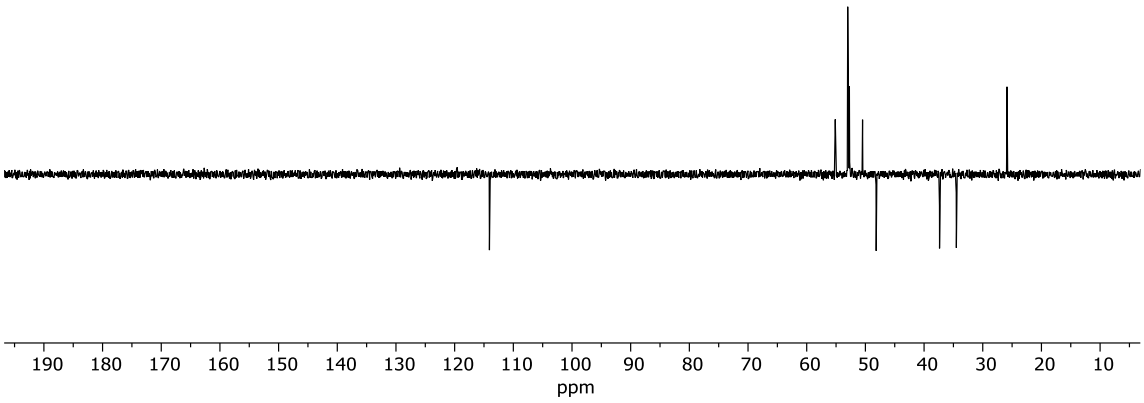

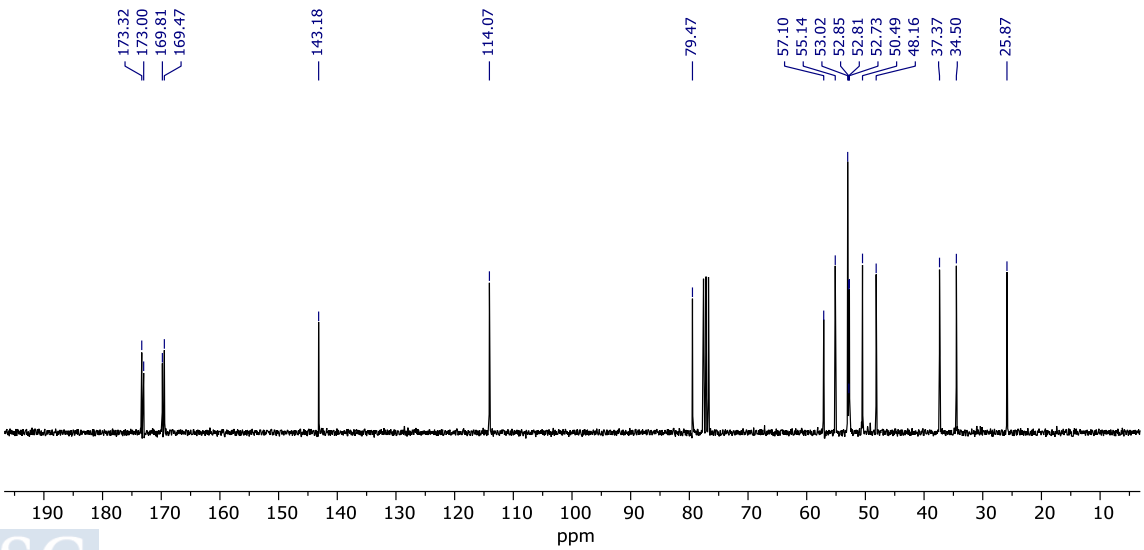

^{1}H, DEPT and ^{13}C Spectra of **37aa'** in $CDCl_3$

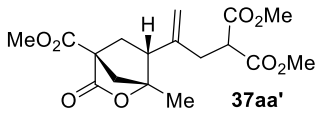

37aa'

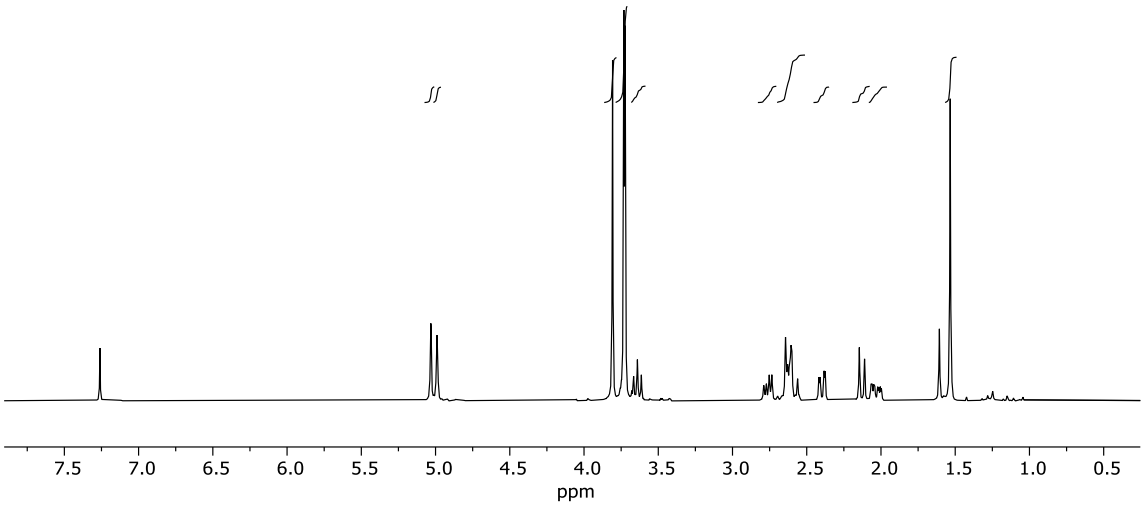

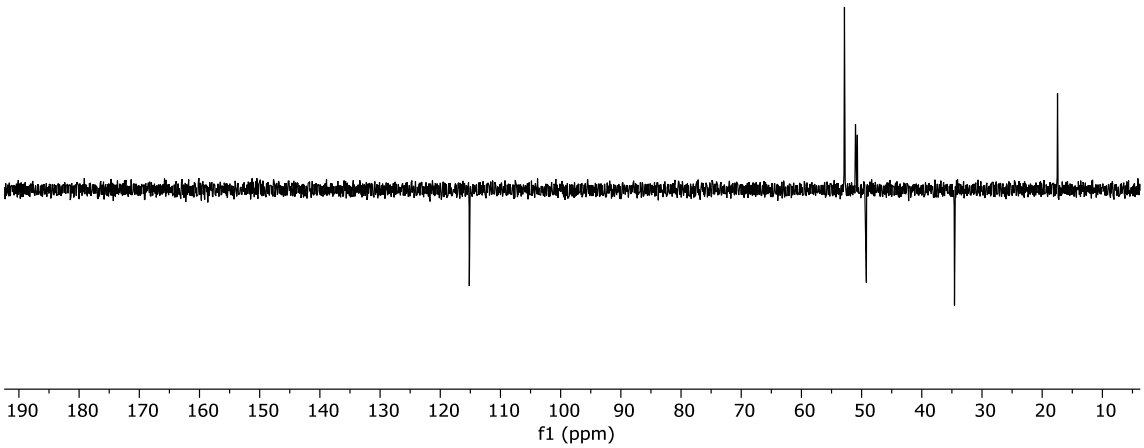

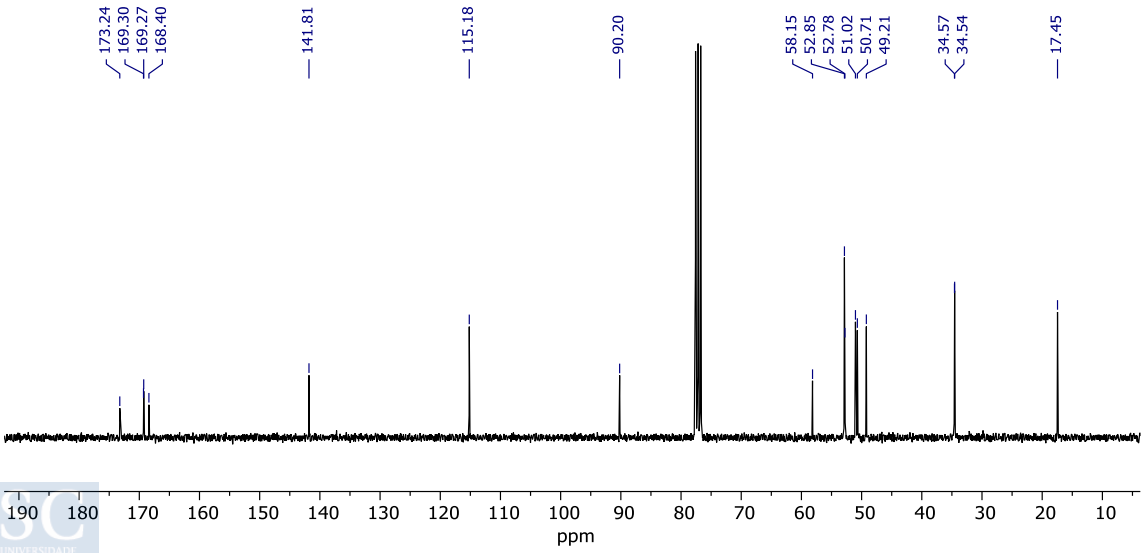

^{1}H, DEPT and ^{13}C Spectra of **39aa** in $CDCl_3$

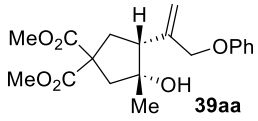

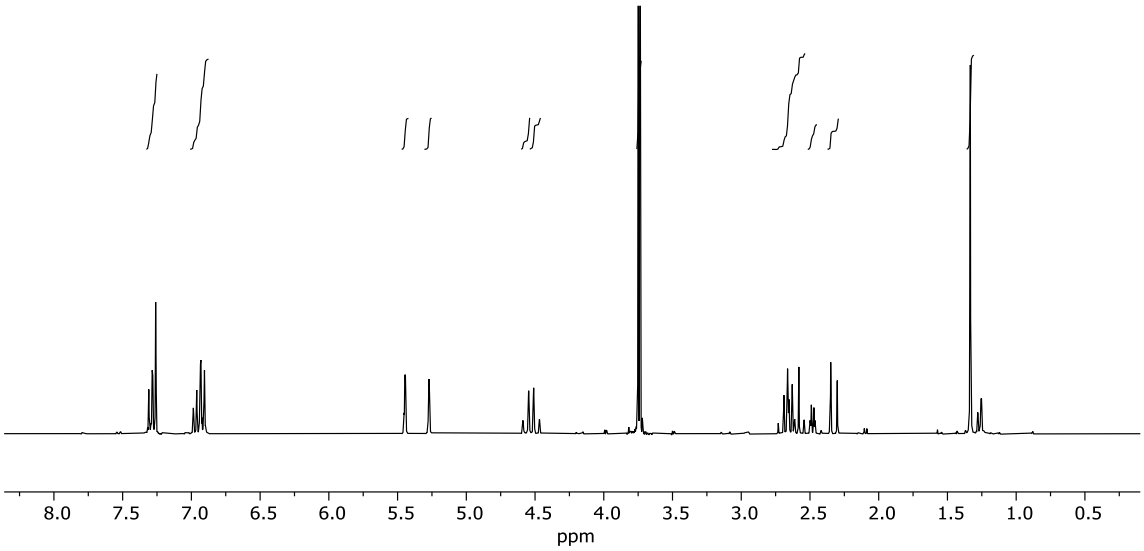

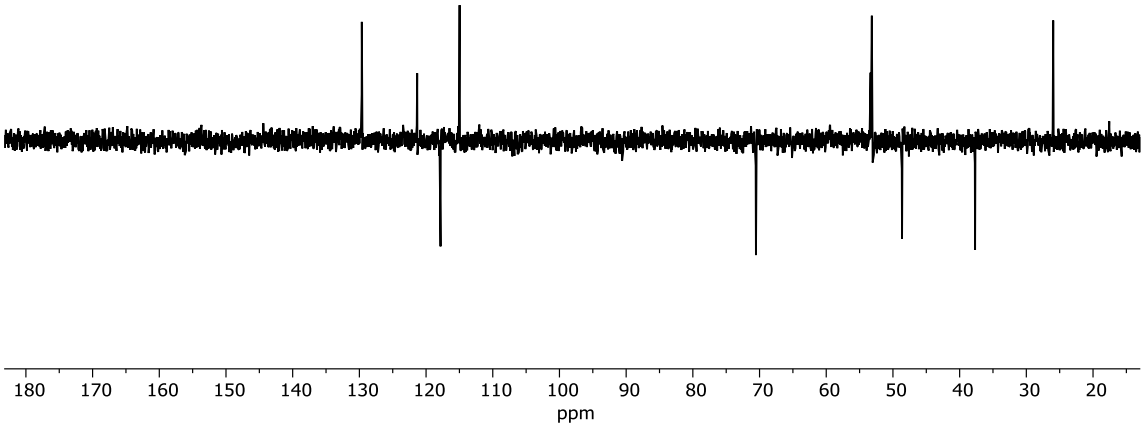

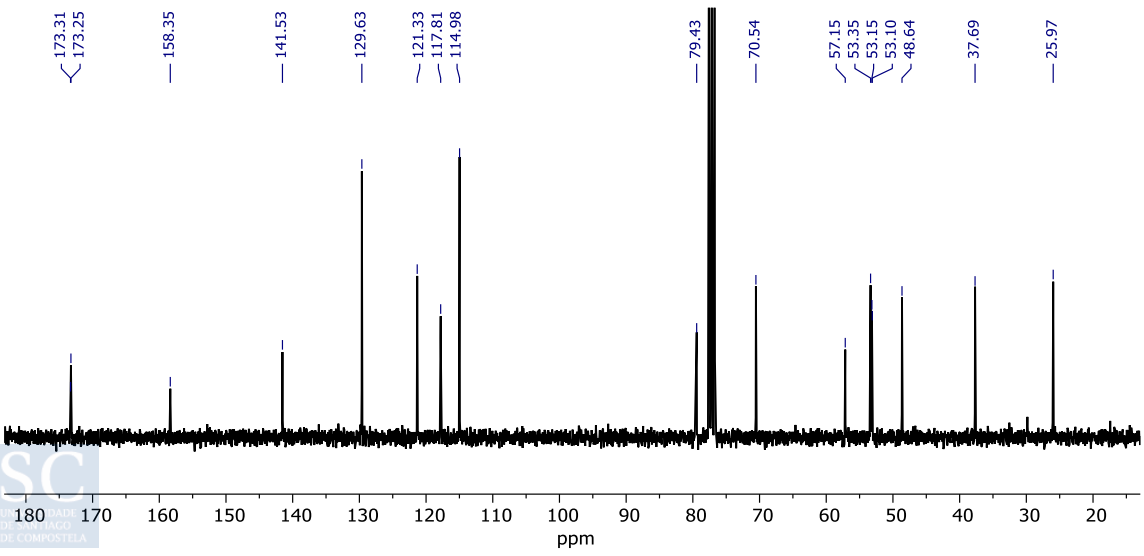

^{1}H, DEPT and ^{13}C Spectra of **39ad** in $CDCl_3$

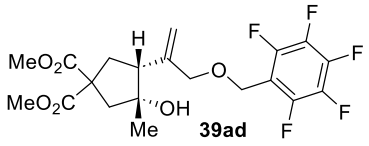

39ad

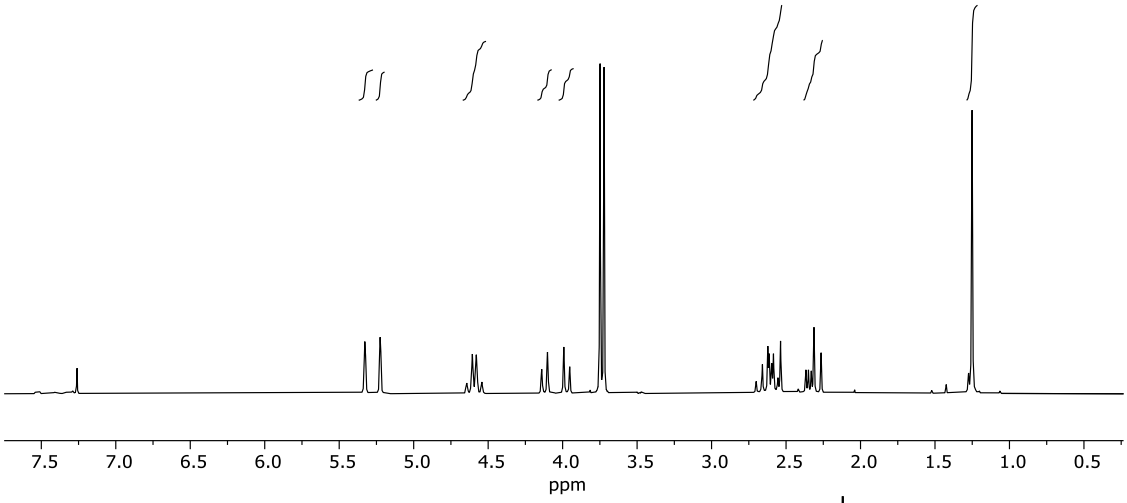

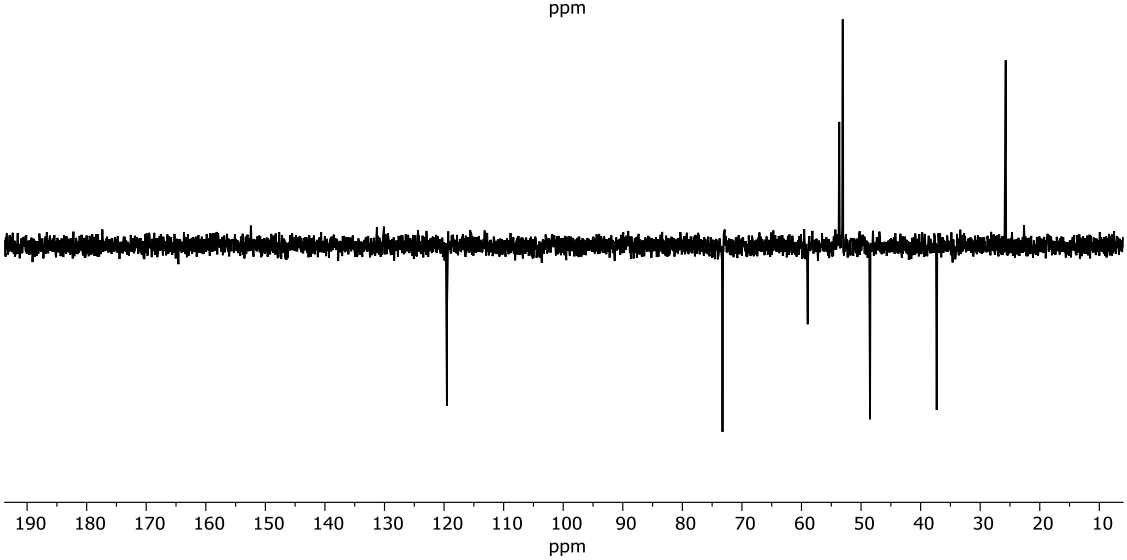

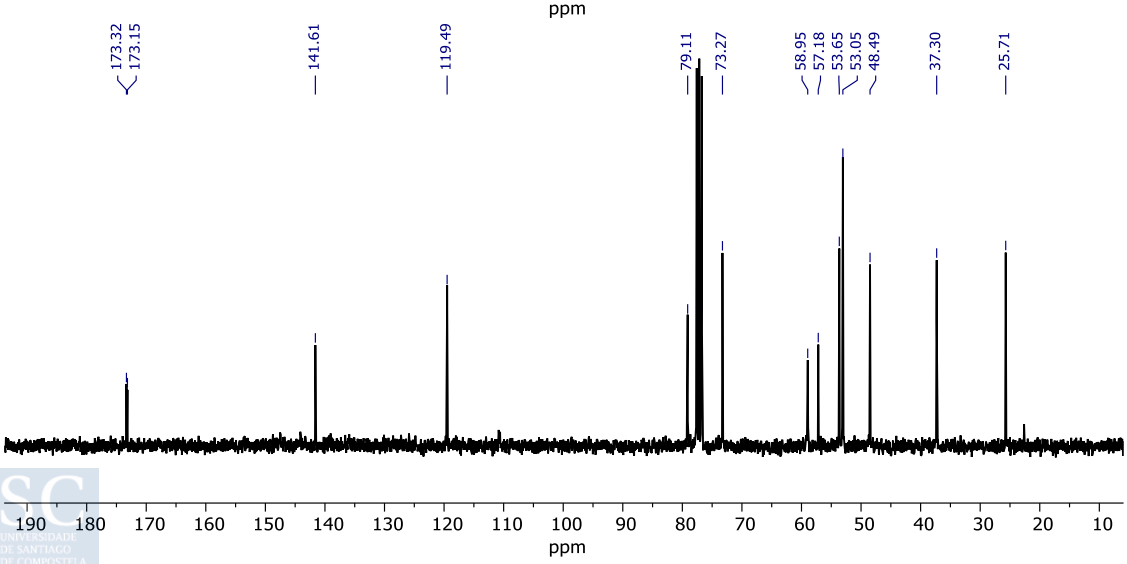

^{1}H, DEPT and ^{13}C Spectra of **40a** in $CDCl_3$

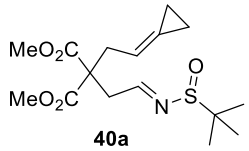

40a

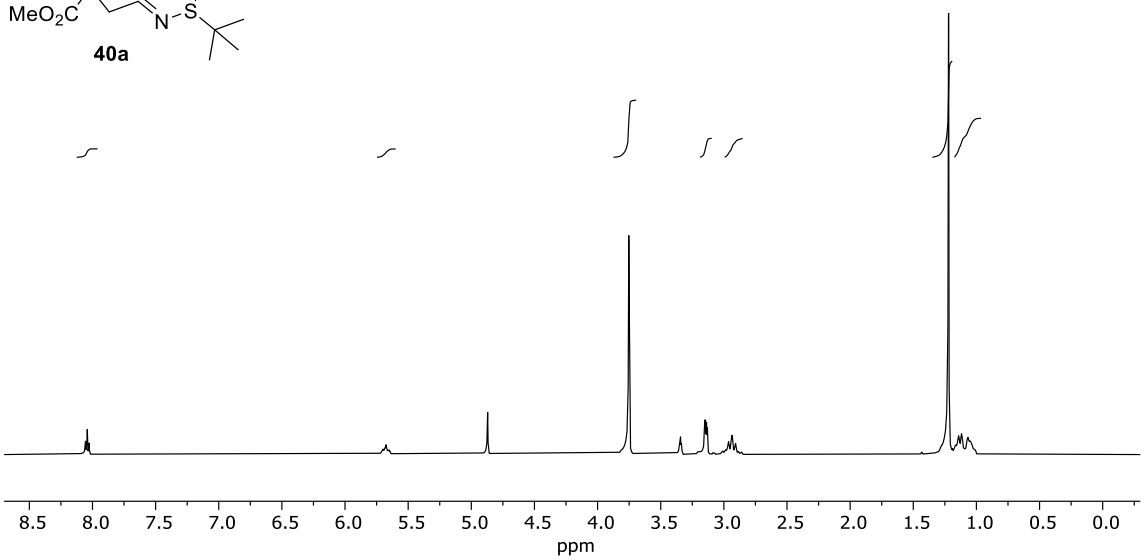

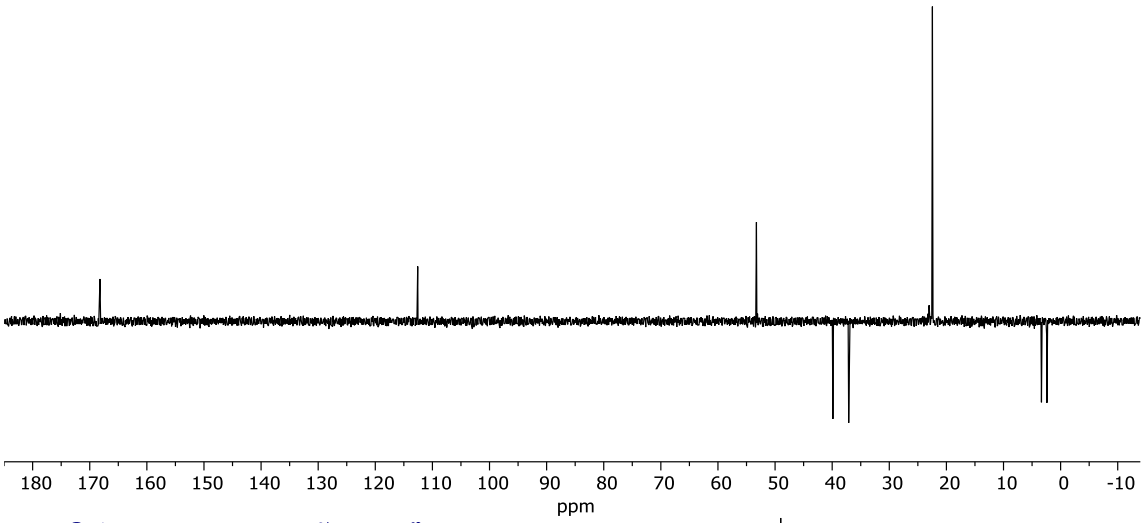

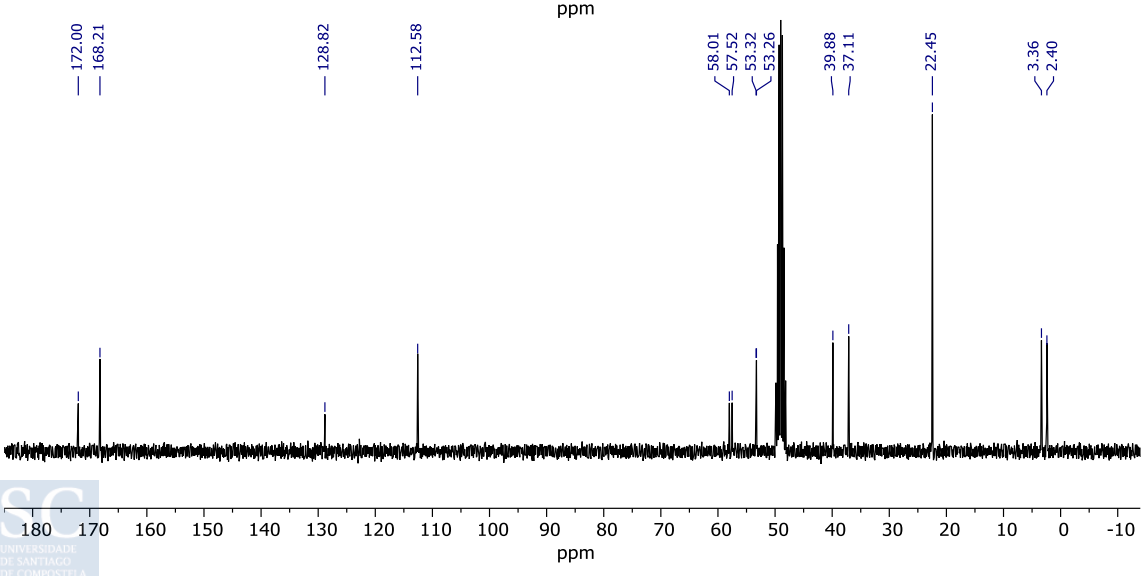

^{1}H, DEPT and ^{13}C Spectra of **42aa** in $CDCl_3$

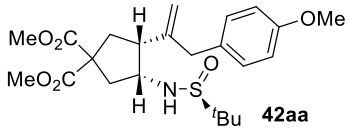

42aa

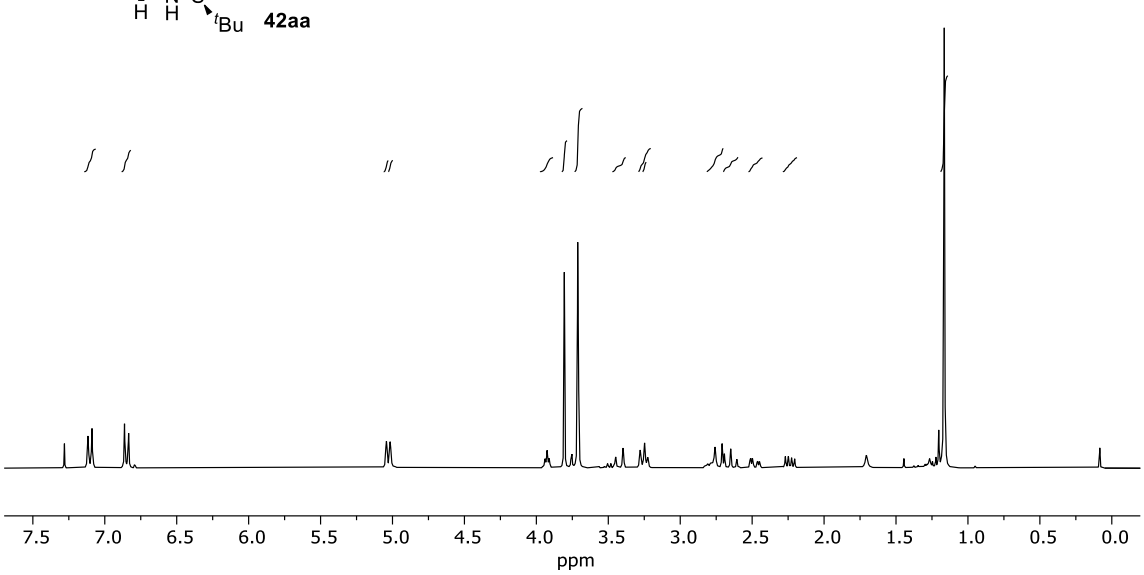

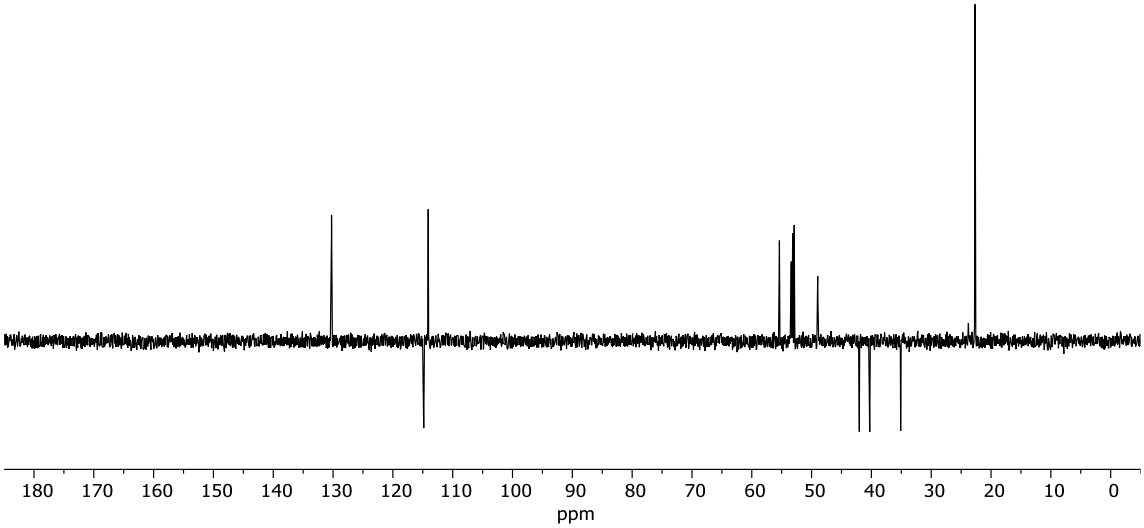

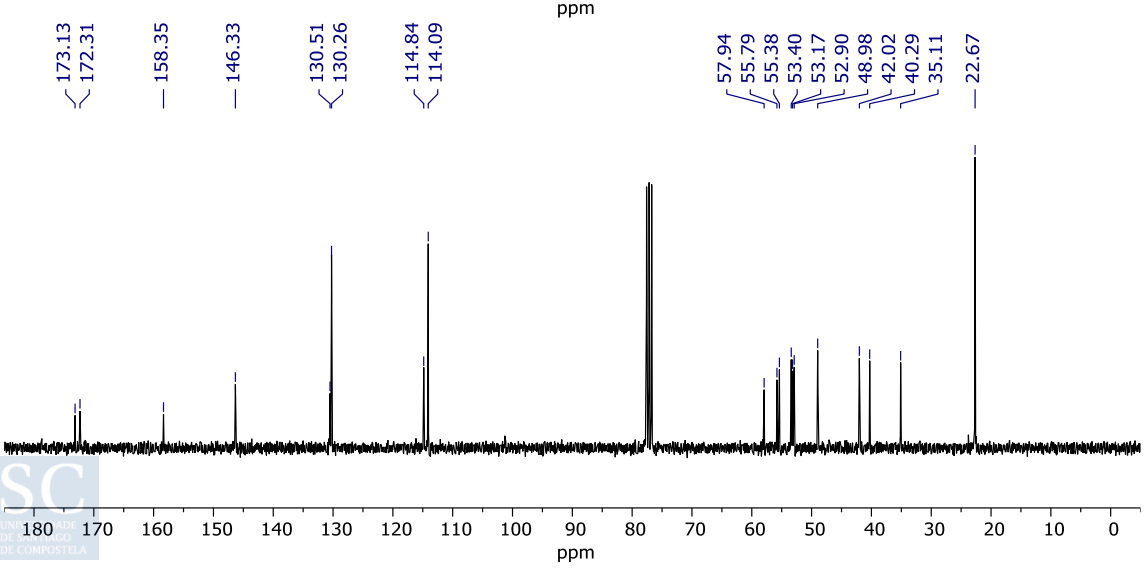

^{1}H, DEPT and ^{13}C Spectra of **42aa'** in $CDCl_3$

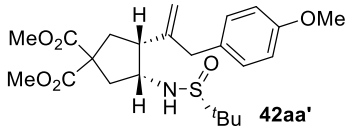

42aa'

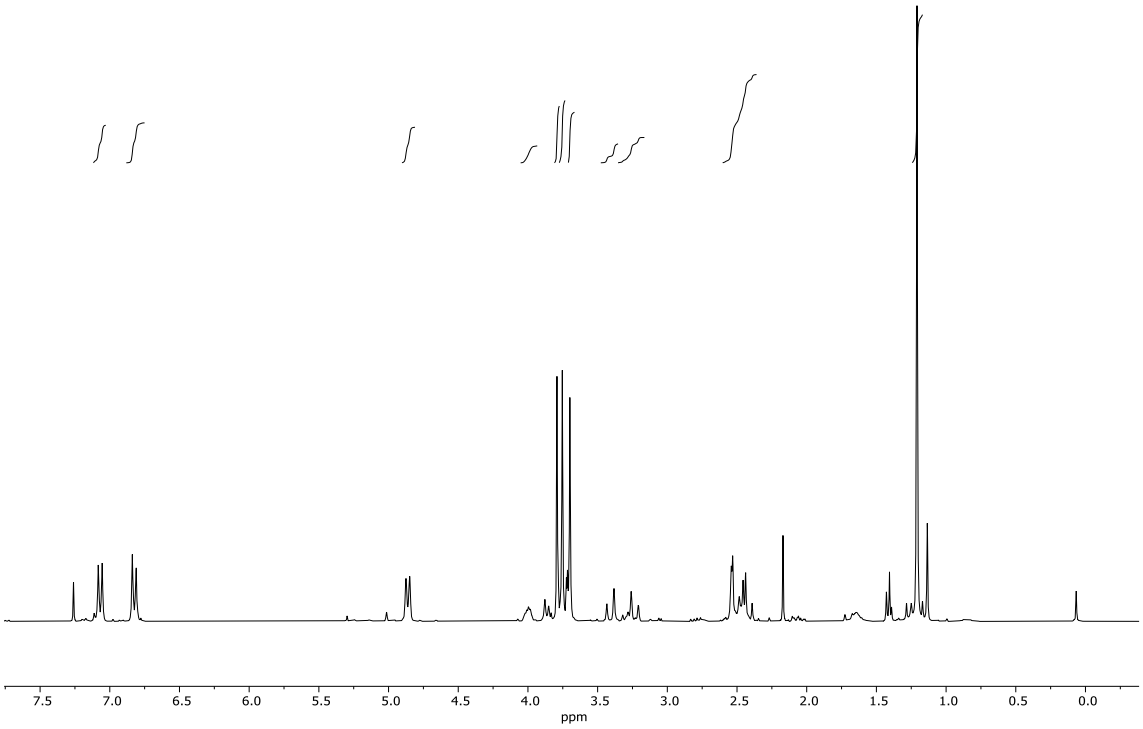

^{1}H, DEPT and ^{13}C Spectra of **42ca** in $CDCl_3$

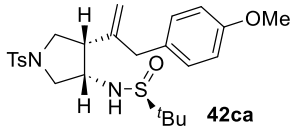

42ca

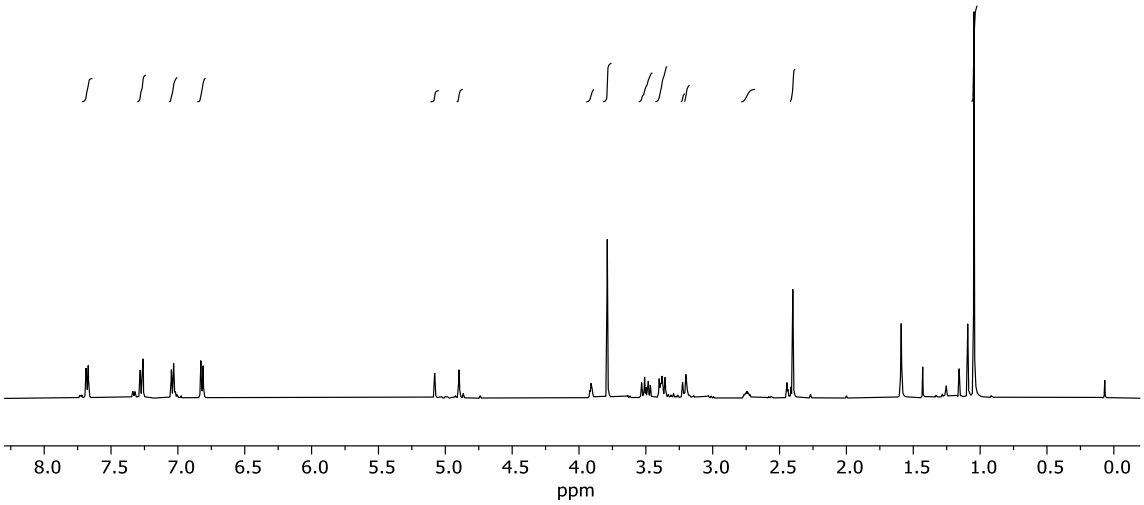

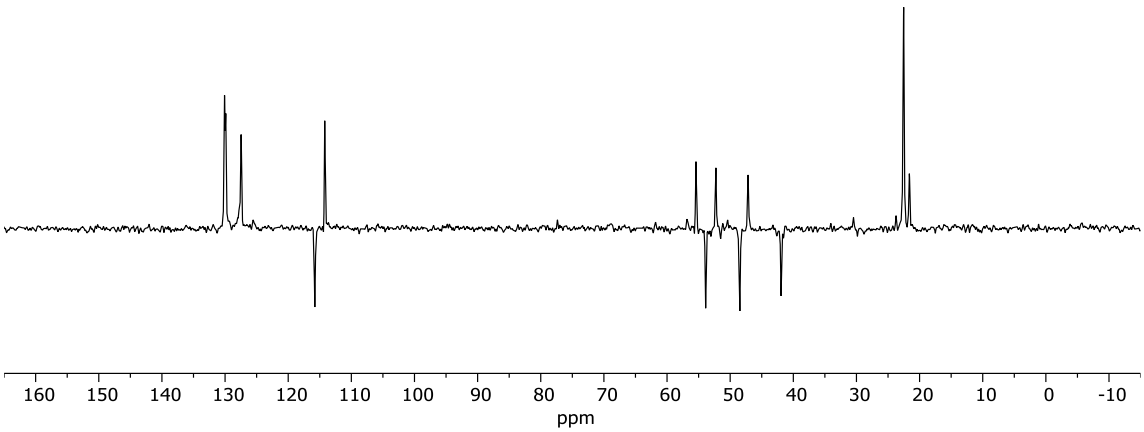

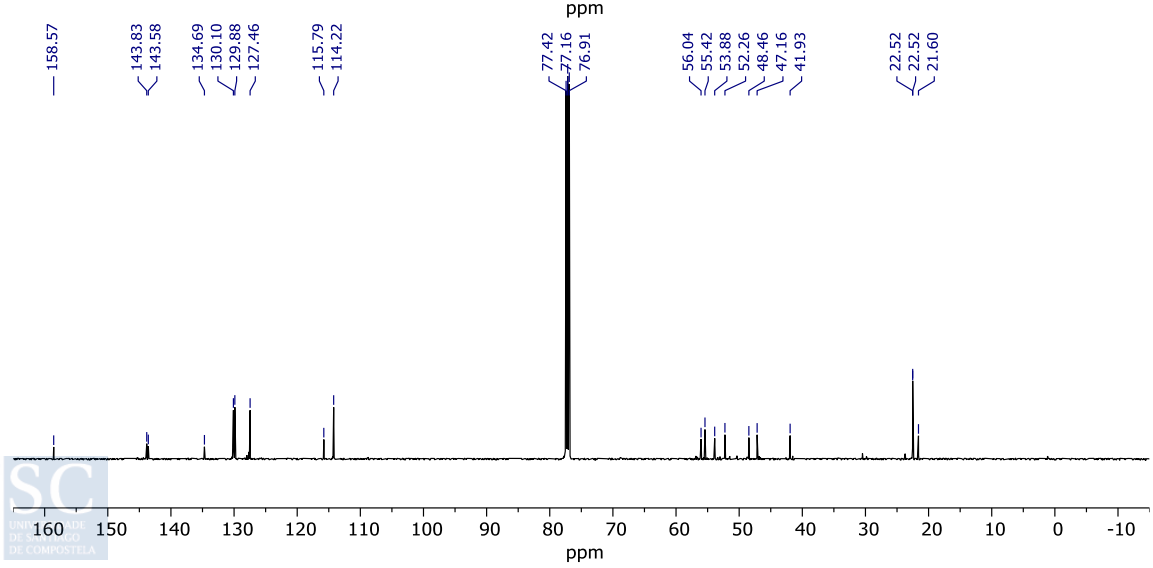

^{1}H, DEPT and ^{13}C Spectra of **42ca** in $CDCl_3$

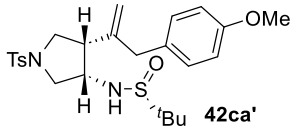

42ca'

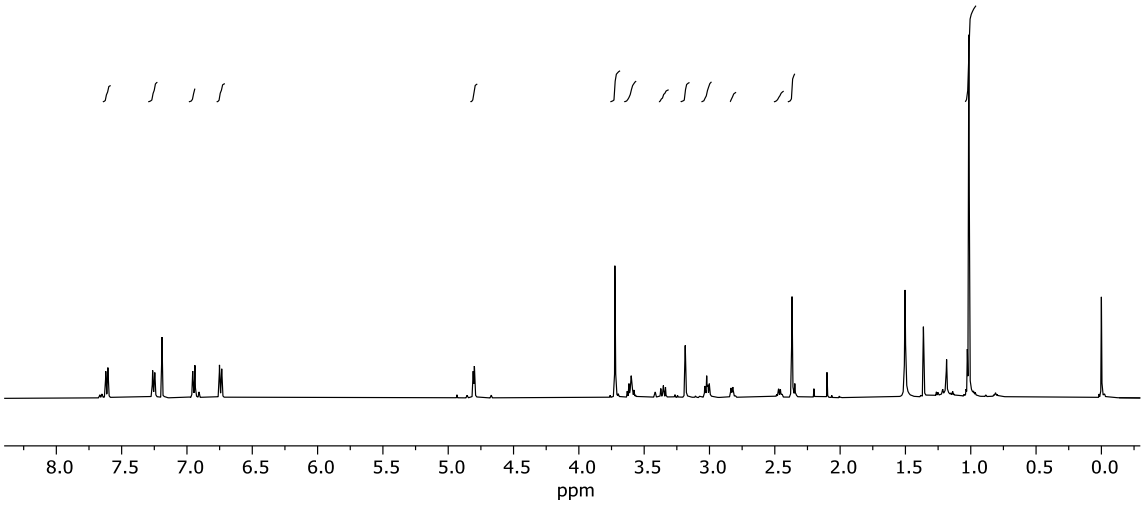

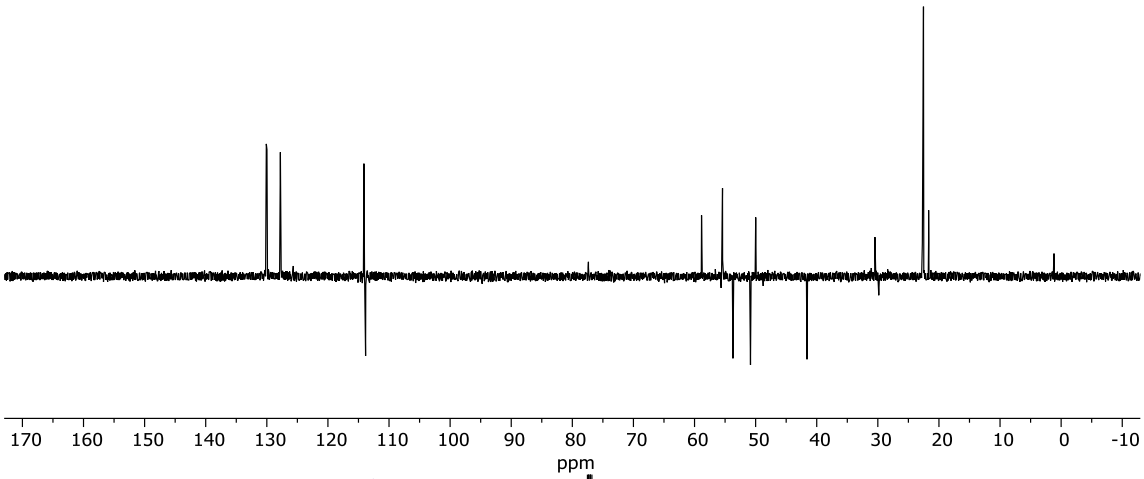

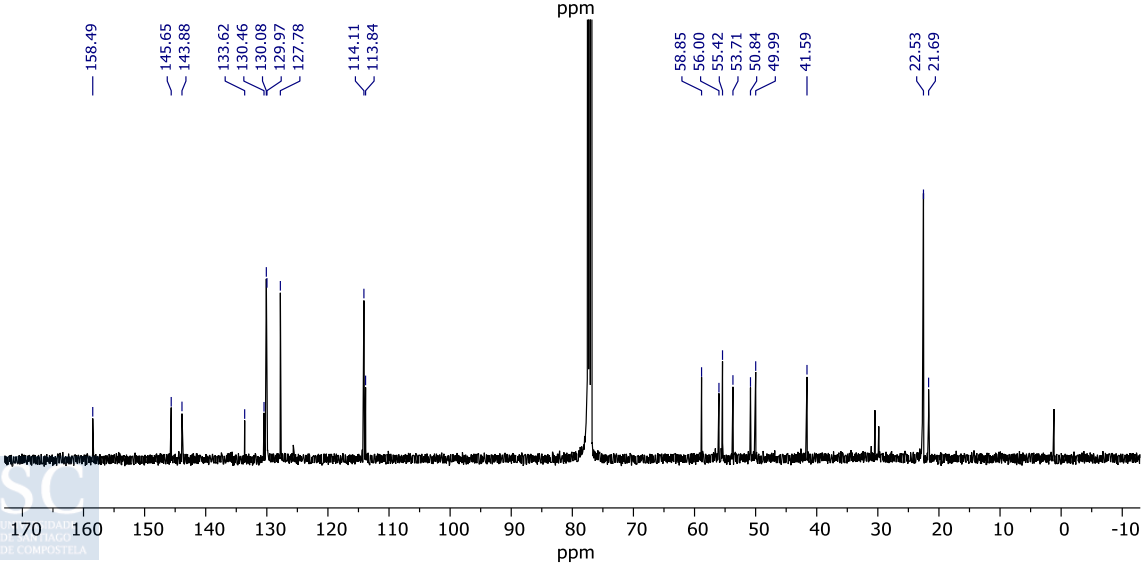

^{1}H, DEPT and ^{13}C Spectra of **43aa** in $CDCl_3$

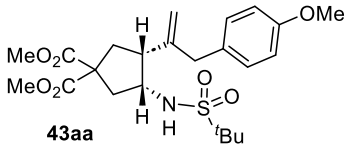

43aa

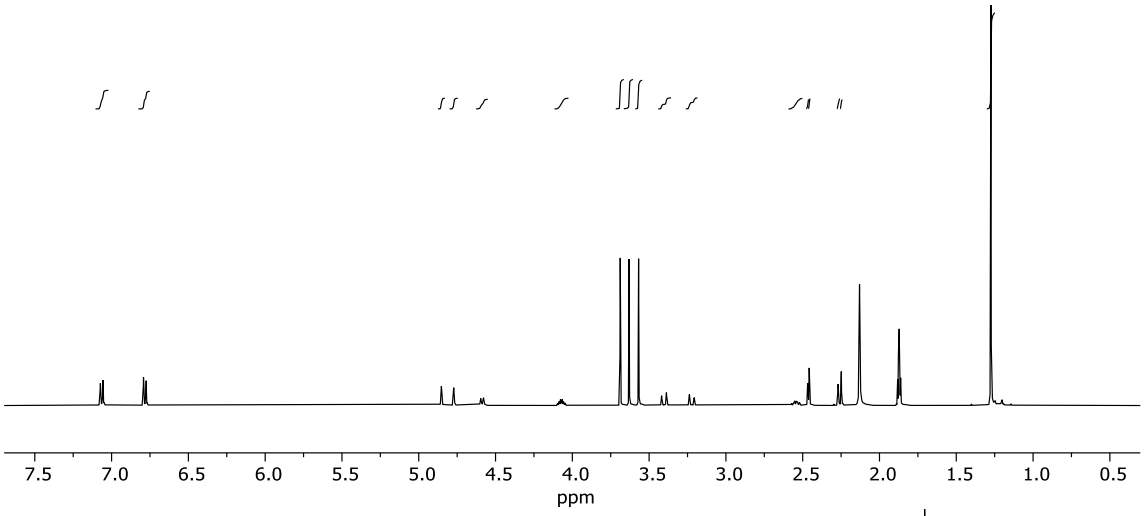

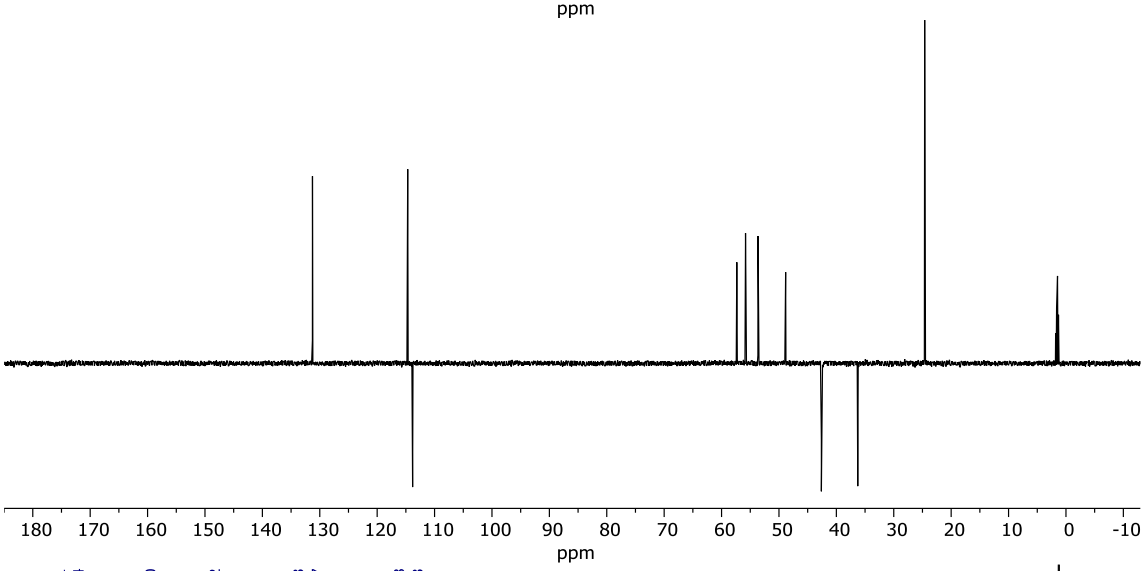

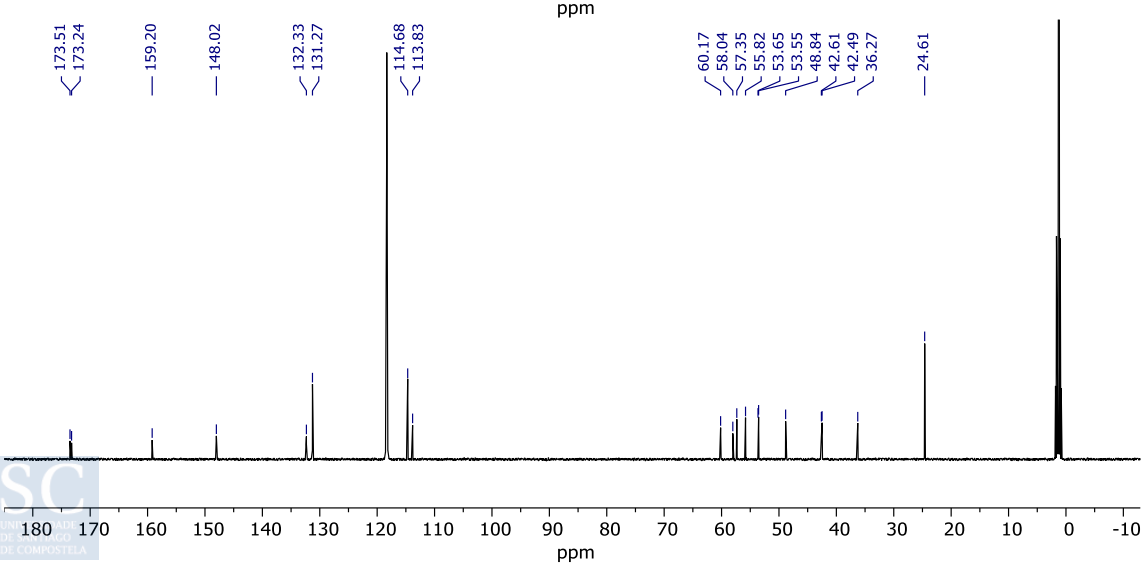

^{1}H, DEPT and ^{13}C Spectra of **45bb:45bb'** ratio 05:1 in $CDCl_3$

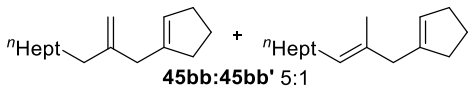

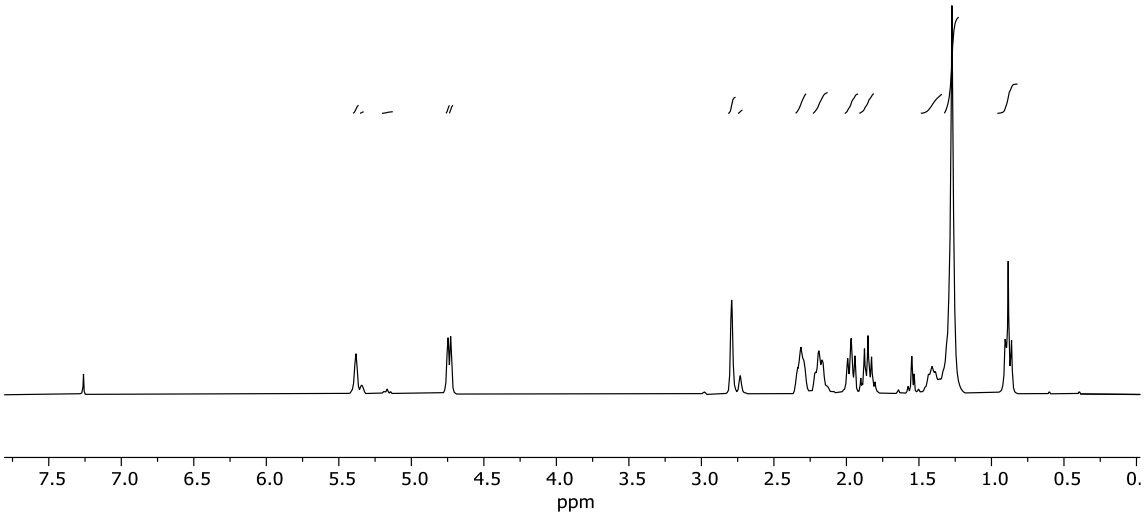

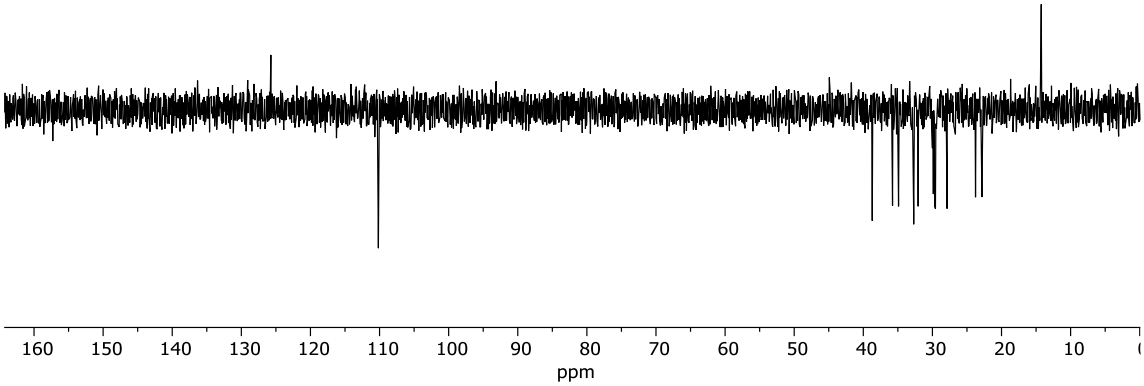

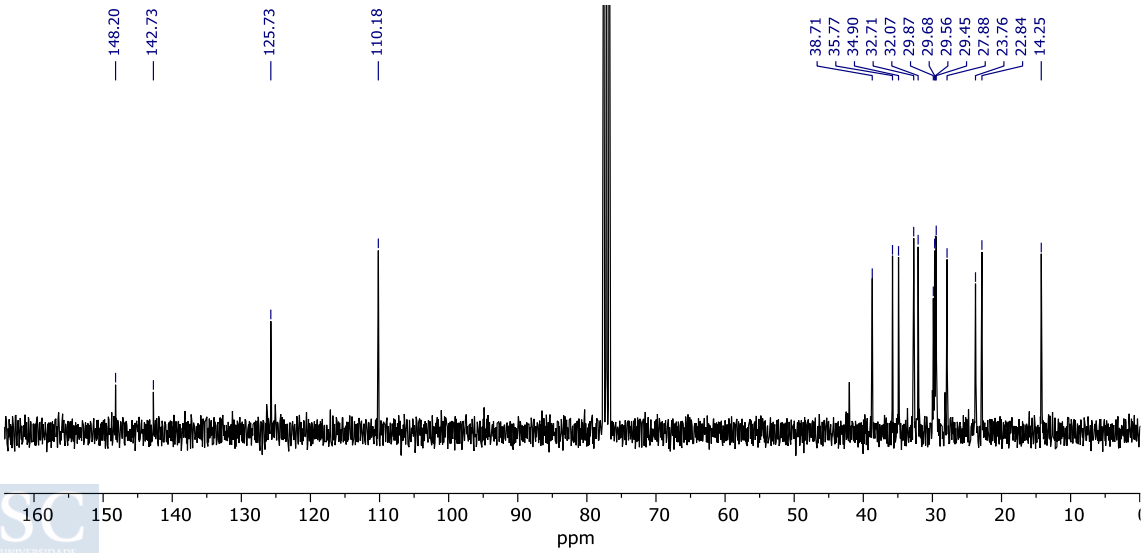

^{1}H, DEPT and ^{13}C Spectra of **45bl** in $CDCl_3$

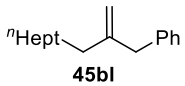

45bl

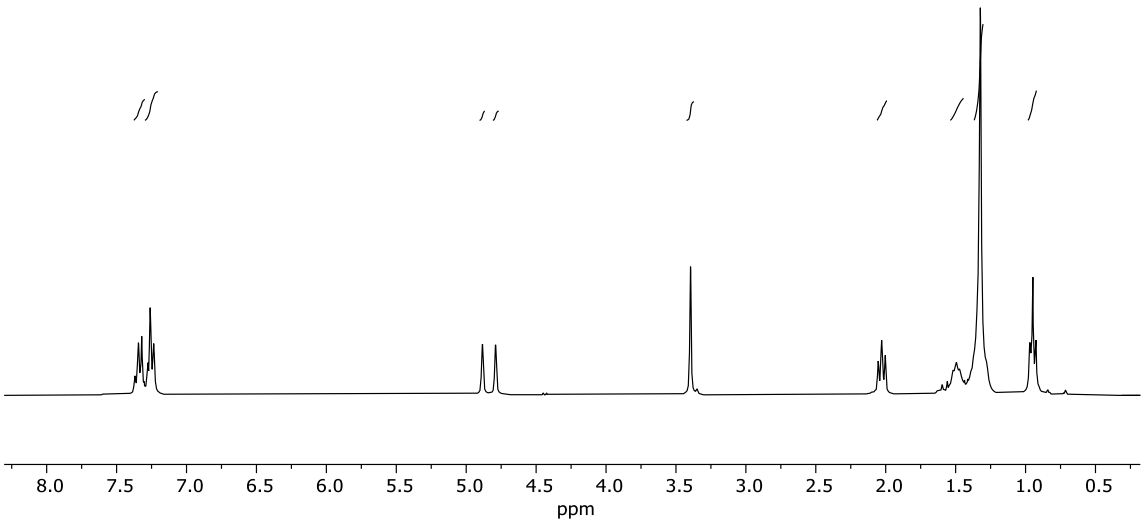

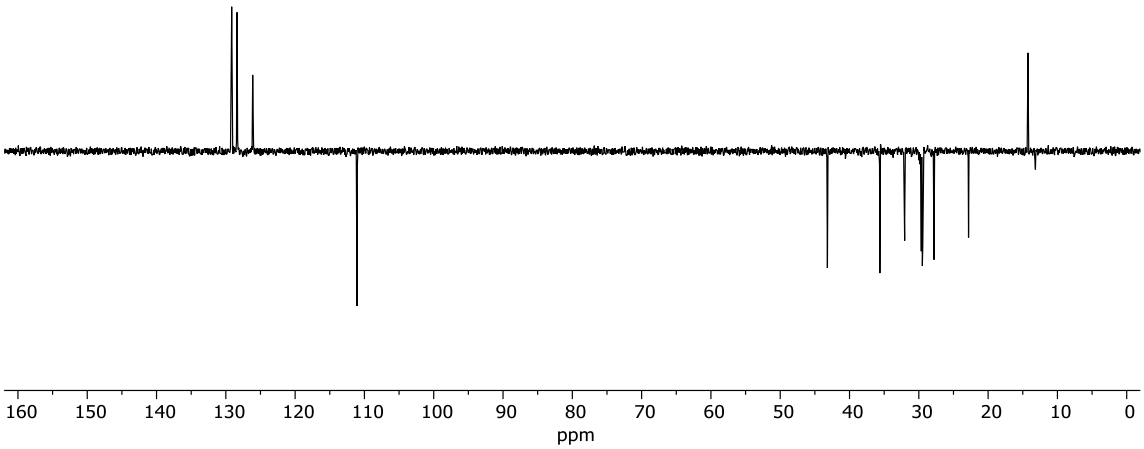

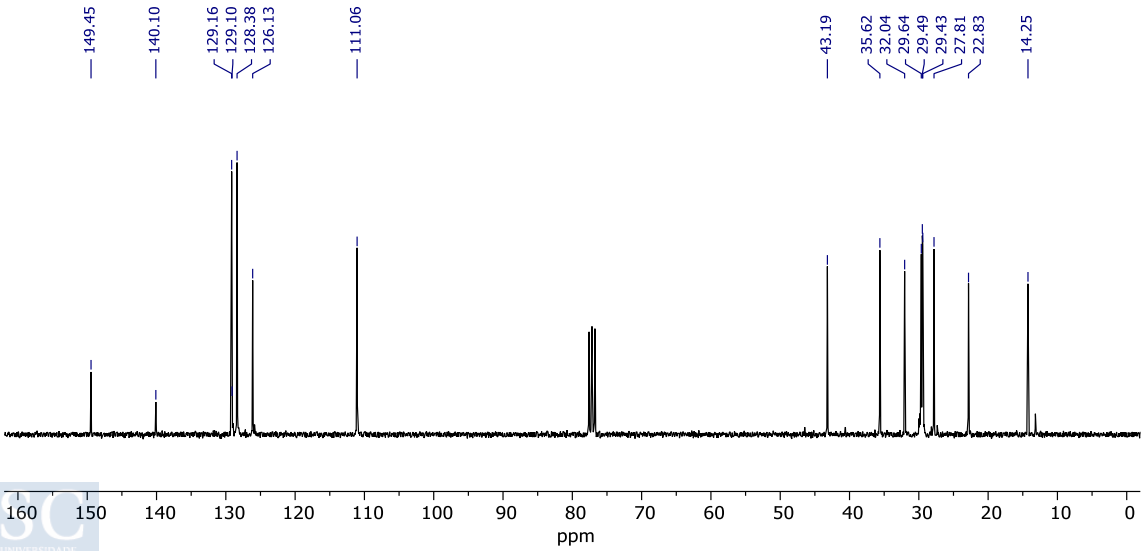

^{1}H, DEPT and ^{13}C Spectra of **45dl:45dl'** ratio 9.5:1 in $CDCl_3$

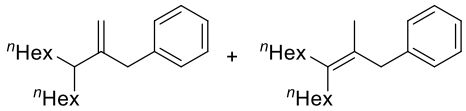

45dl : 45dl' 9.5 : 1

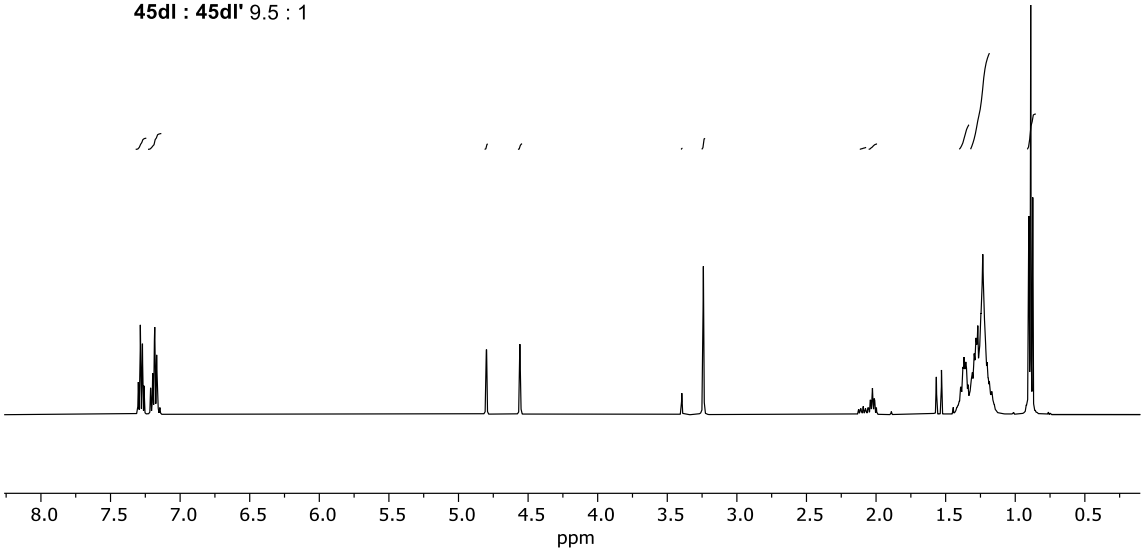

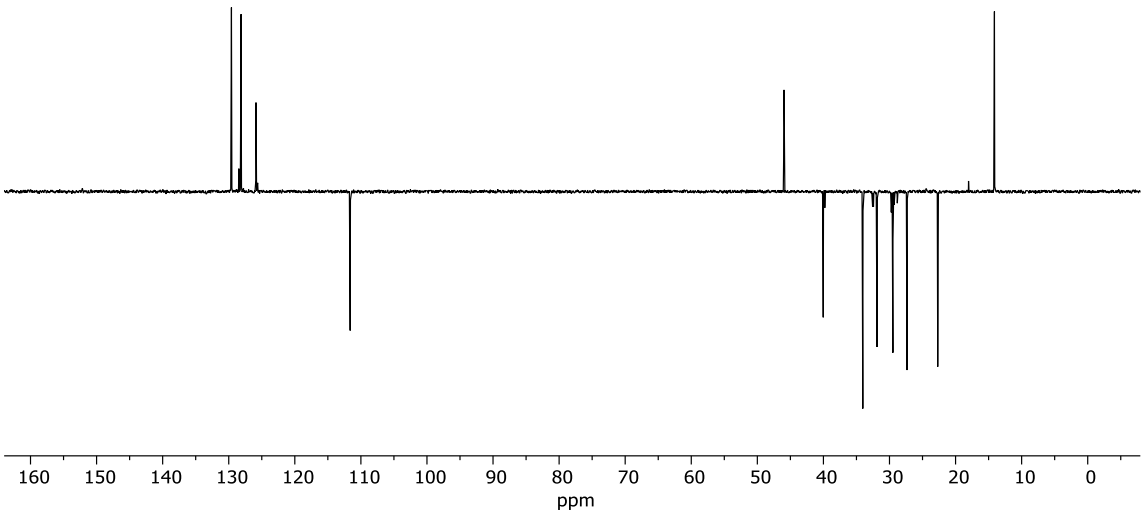

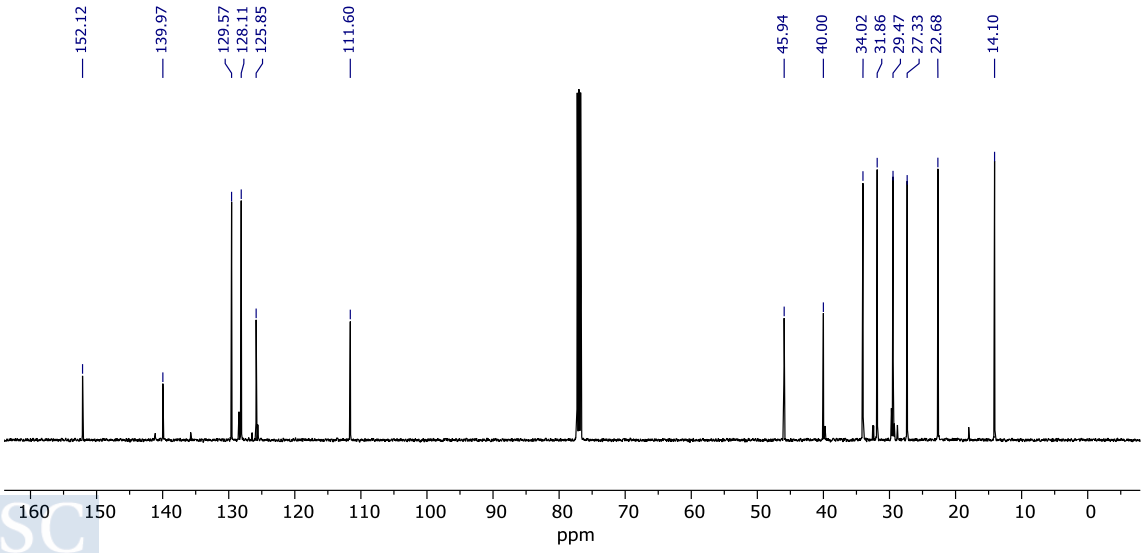

^{1}H, DEPT and ^{13}C Spectra of **50ba** in $CDCl_3$

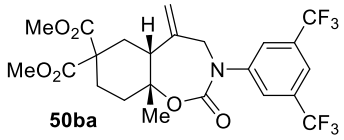

50ba

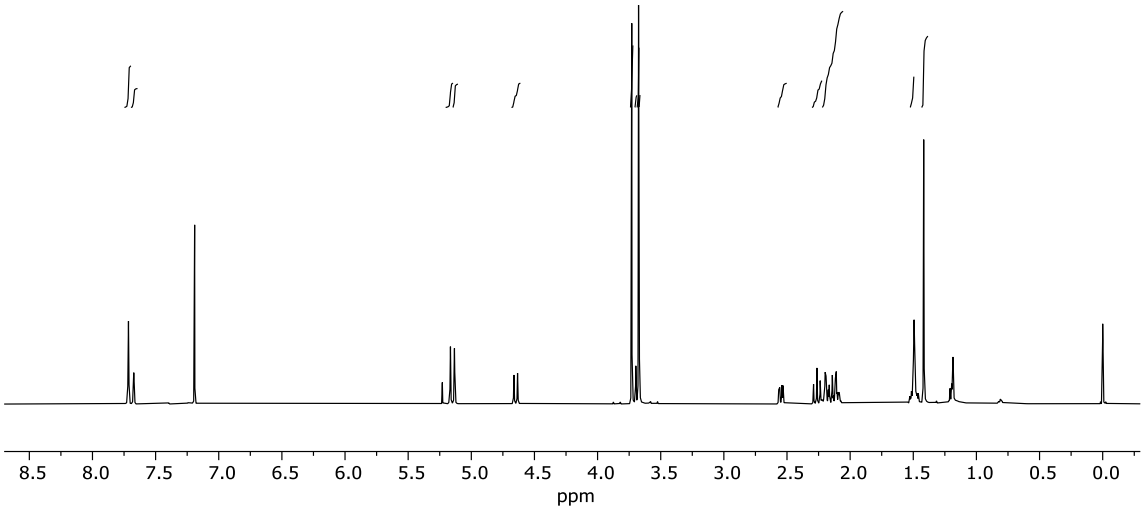

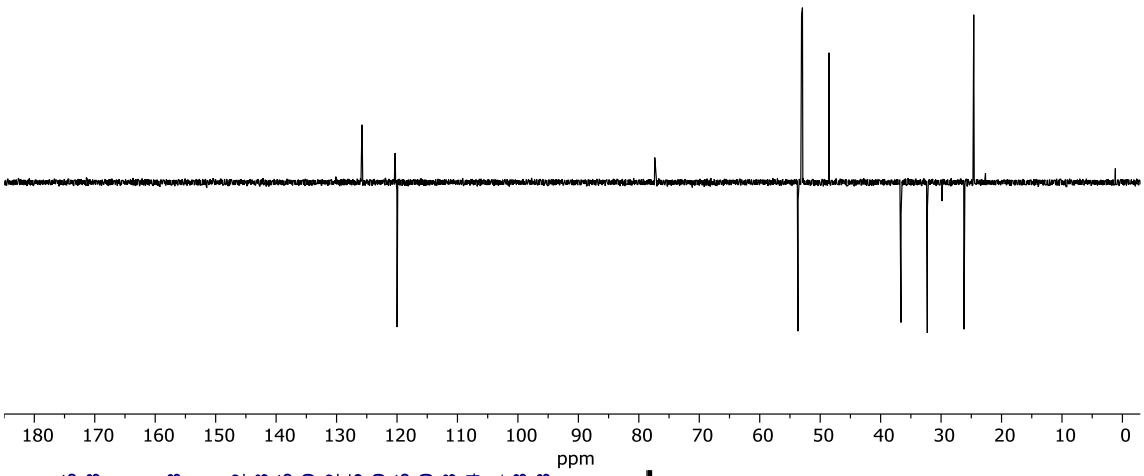

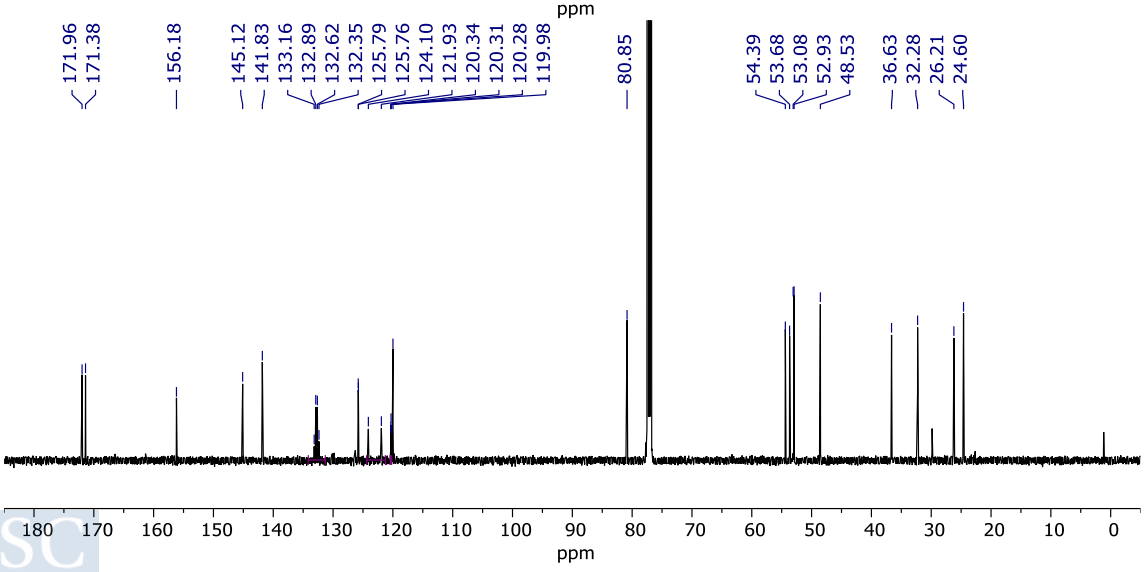

^{1}H, DEPT and ^{13}C Spectra of **50ca** in $CDCl_3$

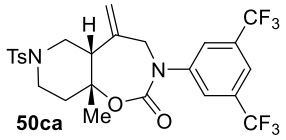

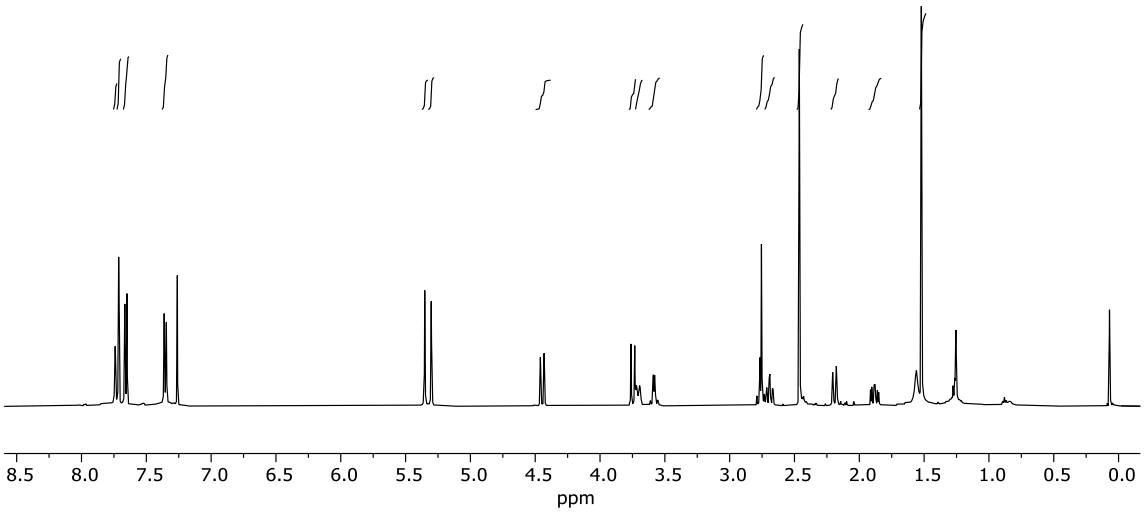

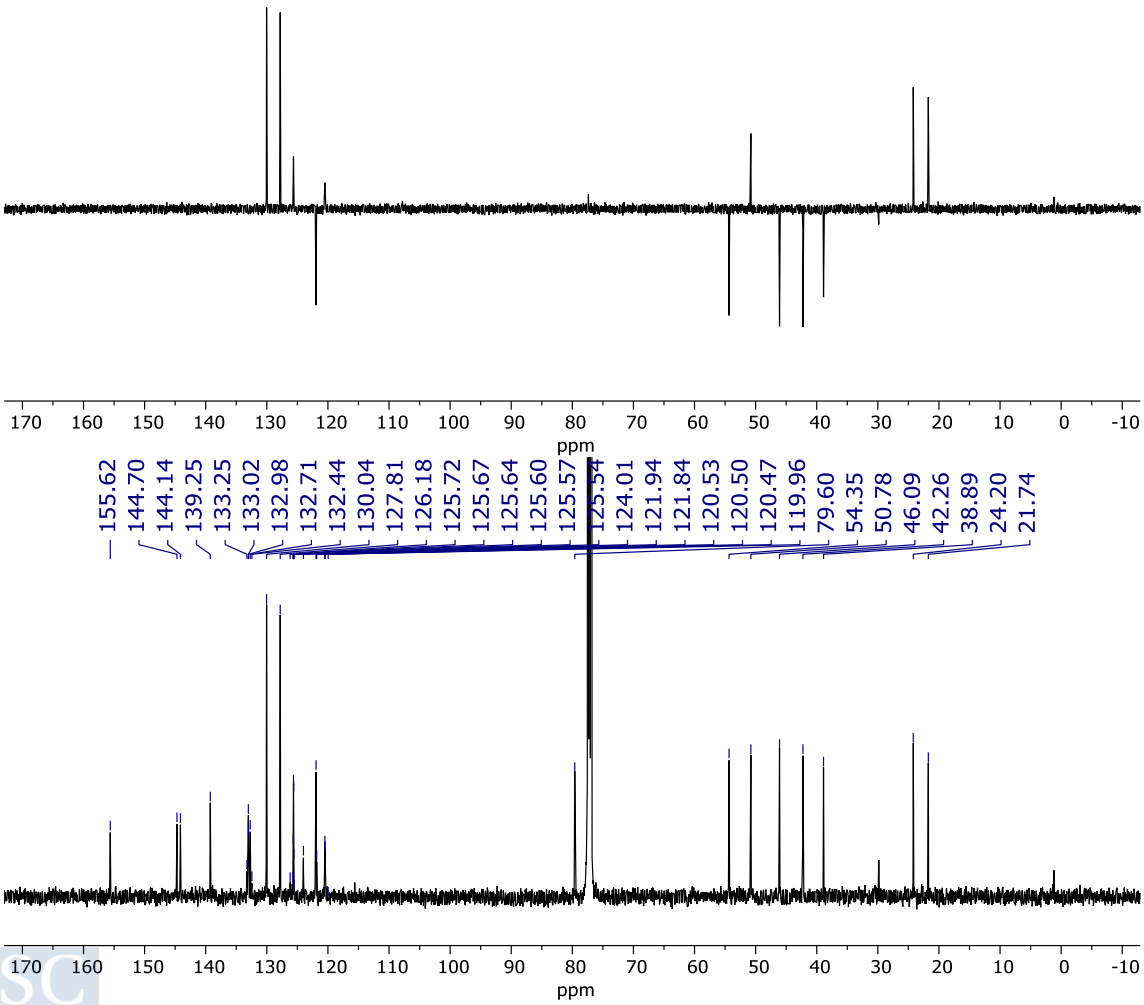

^{1}H, DEPT and ^{13}C Spectra of **50la** in $CDCl_3$

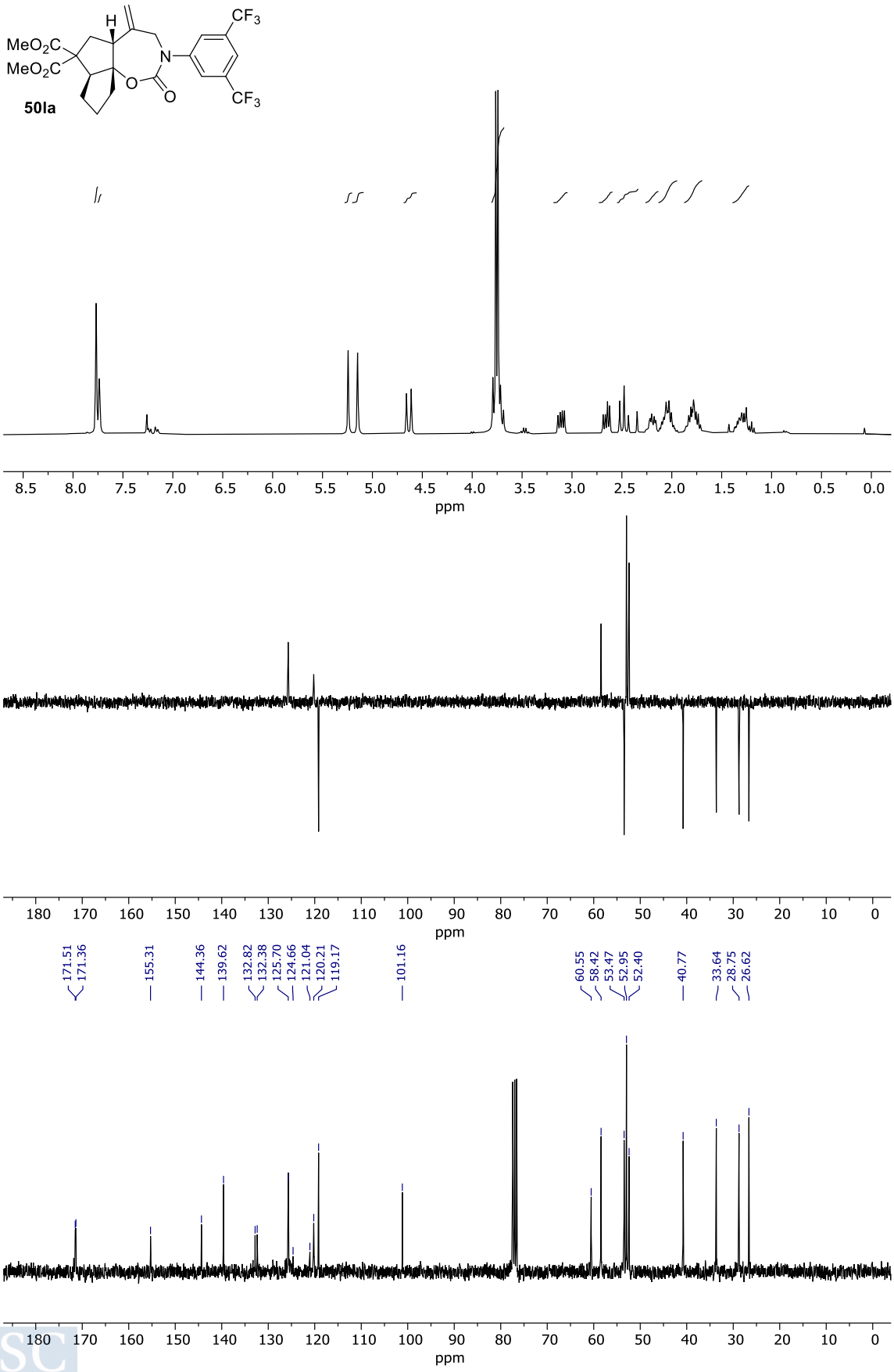

^{1}H, DEPT and ^{13}C Spectra of **50la'** in $CDCl_3$

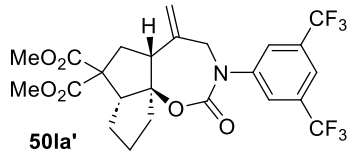

50la'

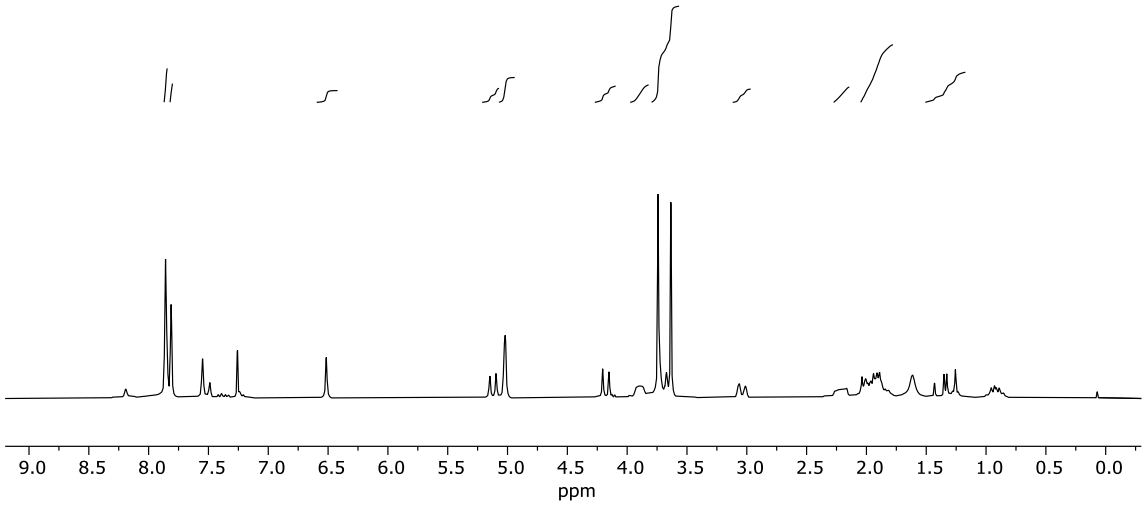

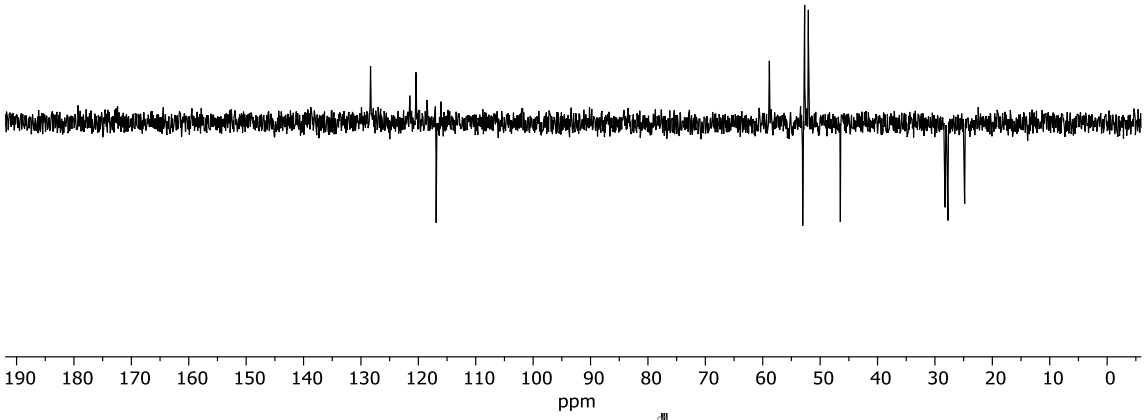

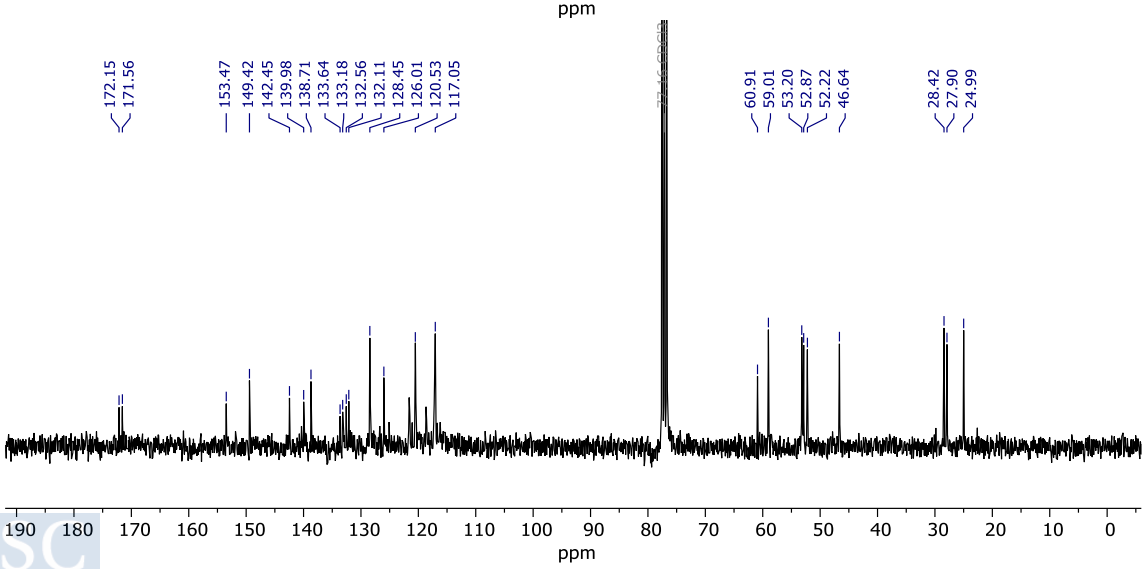

II. Additional DFT Mechanistic Studies

Related to Section 4.2. A DFT Mechanistic Study of Pd(0)-Catalyzed (3+2) Cycloadditions between ACPs and Carbonyls

This part of the appendix contains four additional figures: **Figures A1**, **A2**, **A3** and **A4**

Comments of Figure A1 (see next page)

This profile includes steps with two PH_3 ligands coordinated to the palladium, which were omitted in **Figure 17** for clarity. Therefore, the oxidative addition with two PH_3 ligands takes place through an energy barrier of 21.6 kcal·mol^{-1} (**TS9m-37**). This step is 3.6 kcal·mol^{-1} higher (from **9m**) than when only one PH_3 ligand is attached to the metallic center. The reductive elimination with two PH_3 ligands involves a higher energy barrier than when only one PH_3 is coordinated ($\Delta\Delta G$ = 4.2 kcal·mol^{-1}), although the transition state remains less energetic and still feasible (ΔG = 25.4 kcal·mol^{-1}, **TS38-17m**).

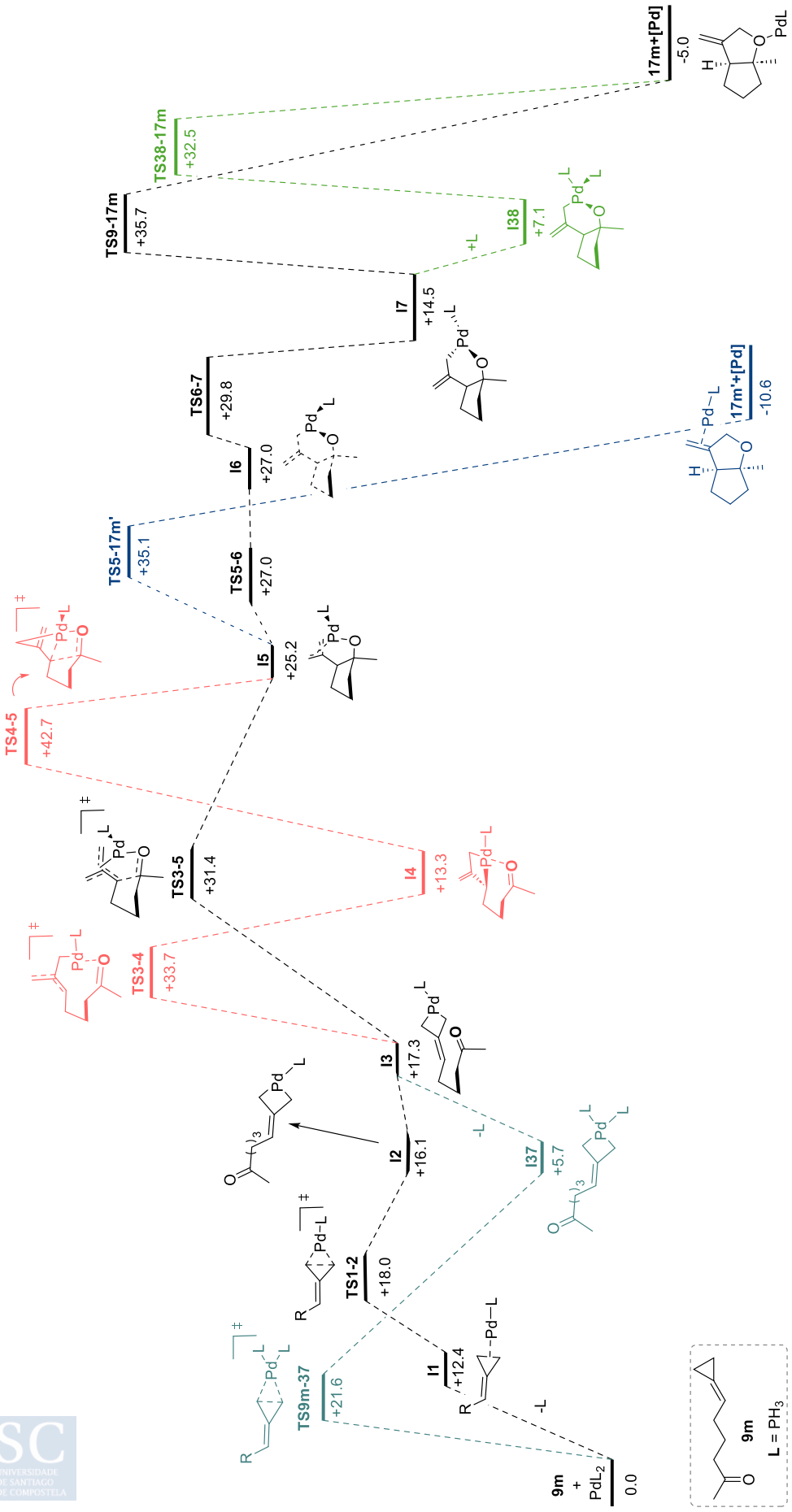

Figure A1. DFT-calculated energy profile ΔG_{solv} (kcal·mol^{-1}) for the cycloaddition of **9m** in toluene. [B3LYP/6-31G(d) (LANL2DZ for Pd)//M06/6–311++g(d,p) (SDD for Pd)].

Comments of Figure A2

Intermediate **I9** holds the alkyl chain of the alkene and the P atom in *syn*-disposition. We also located the isomer in which the alkyl chain of the alkene and the P atom are in *anti*-disposition (denoted as **I9**^{anti}). Its evolution via migratory insertion towards oxapalladacycle **I10** ^{anti} is also feasible, but slightly less favored.

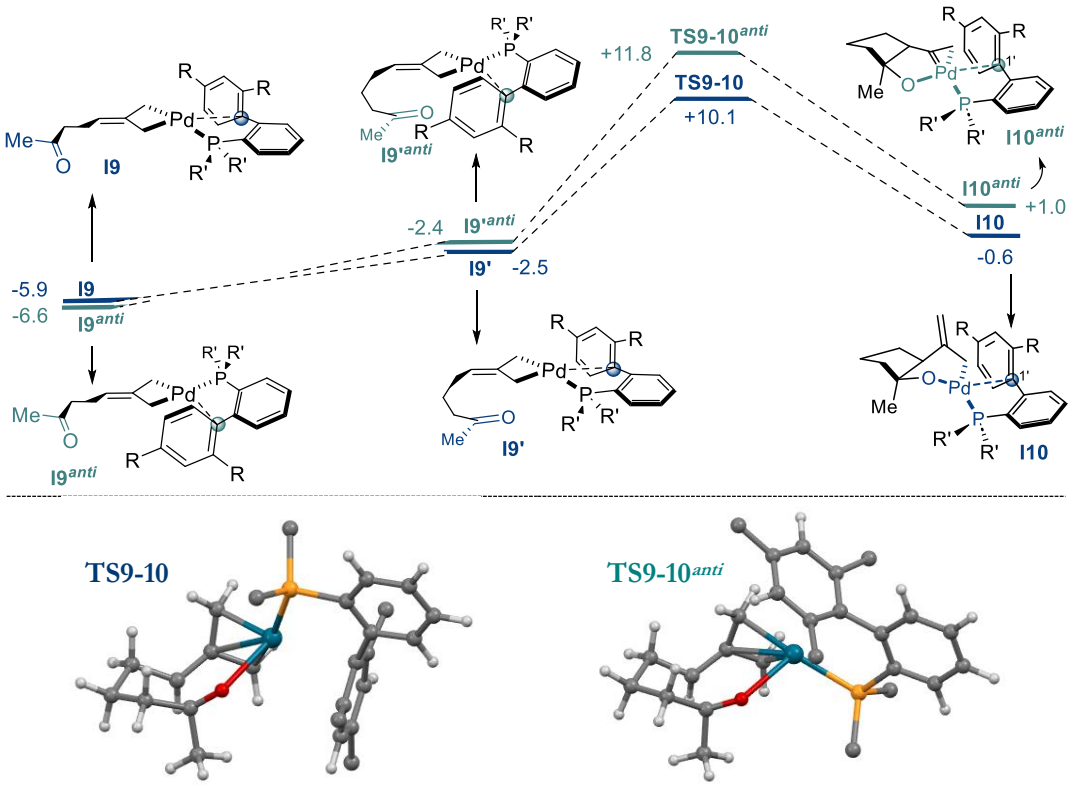

Figure A2. Carbometallation process from isomeric palladacyclobutanes **I9** and **I9**^{anti}.

Comments of Figure A3 (see next page)

Blue pathway: The evolution of **I9** towards **I10** involves an additional step, from **I9** to **I9'**, which was omitted in **Figure 18** for clarity. It involves a conformational change consisting of the folding of the carbonyl chain to enable the subsequent palladaene step. Thus, when the carbonyl is appropriately positioned (**I9'**), the palladaene process involves a barrier of only 12.6 kcal·mol^{-1}.

1. Red pathway: The evolution of **I14** towards **I15** involves an additional step, from **I14** to **I14'**. This step involves a rotation of the phosphine (anticlockwise ≈ 102°). **I14'** also involves a Pd–H γ-agostic interaction. This step has been simplified in the manuscript for clarity.
2. Red pathway: Besides the isomerization/migratory insertion process, **I14** can also evolve to **I16** through an alternative metalloene pathway (via **I14"** and **TS14-16**). **I14"** is also a conformer of **I14** in which the phosphine has rotated (clockwise ≈ 105°). This path is not included in **Figure 18**. Although this path is energetically favored compared to that via **TS14-15**, both are clearly less favorable than the blue pathway, proceeding through **I9**, **I10** and **I12**.

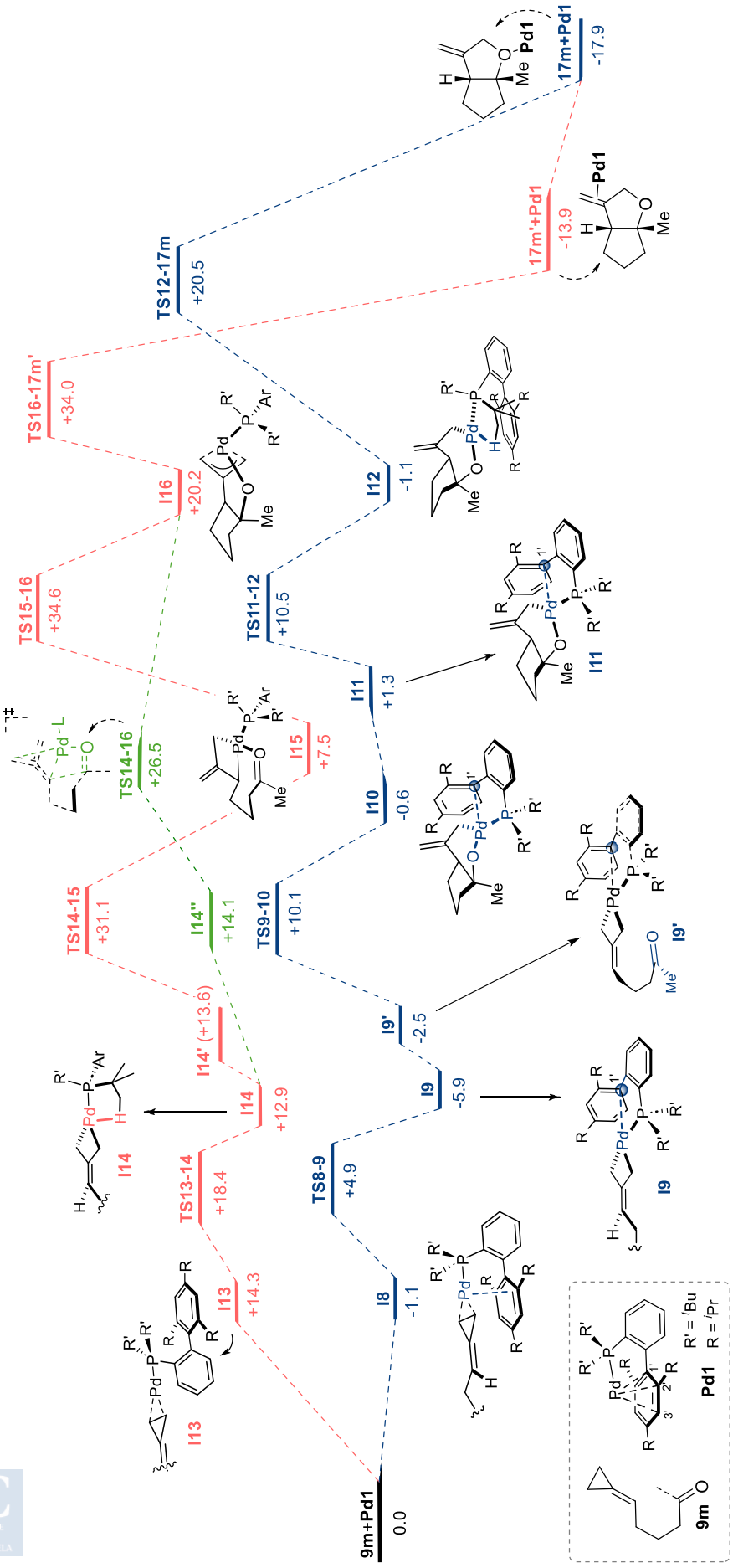

Figure A3. Complete DFT-calculated energy profile ΔG_{solv} (kcal·mol^{-1}) for the (3+2) cycloaddition of **9m** using Pd-*t*BuXPhos (**Pd1**), in toluene. [B3LYP/6-31G(d) (LANL2DZ for Pd)//M06/6–311++g(d,p) (SDD for Pd)].

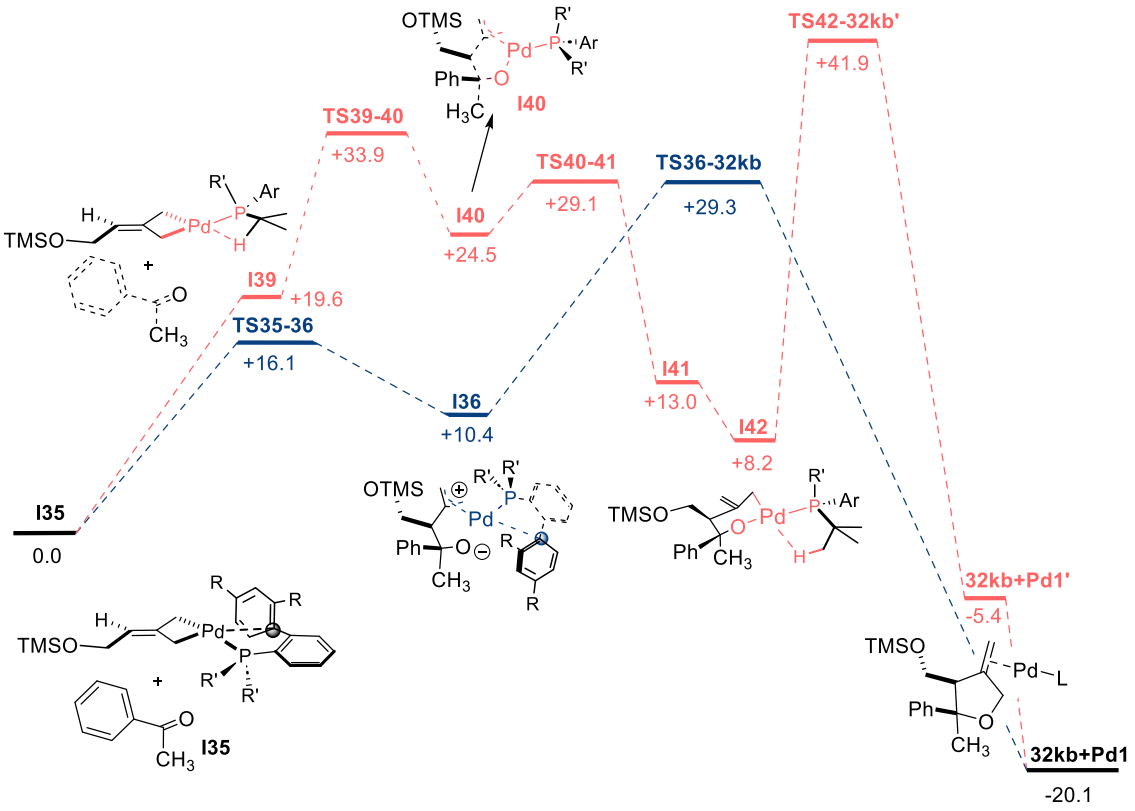

Figure A4. Overall DFT-calculated energy profile ΔG_{solv} (kcal·mol^{-1}) for the (3+2) cycloaddition of **19k** and methyl ketone **31b** using Pd(0)-^{t}BuXPhos (**Pd1**), in toluene. [B3LYP/6-31G(d) (LANL2DZ for Pd)//M06/6–311++g(d,p) (SDD for Pd)].

Related to Section 4.3. Pd(0)-Catalyzed Tandem Cycloisomerization/ Allylic Substitution Reactions of ACPs tethered to Carbonyl and Imine partners

This part of the appendix contains four additional figures: **Figures A5**, **A6**, **A7** and **A8**

Comments of Figure A7.

The use of **L17** as model ligand provided similar results than $P(OMe)_3$ (**Figure 27**, *Section 4.3*, page 157), favoring transmetalation over the reductive elimination that deliver the (3+2) cycloadduct (**17m**). Remarkably, the energy barrier of the migratory insertion in this profile, **TS39-40** from **I38** (ΔG=14.4 kcal·mol^{-1}), is 7.2 kcal·mol^{-1} more energetic than when using $P(OMe)_3$ (**TS5-6**). Regarding the transmetalation and reductive elimination, they imply slightly higher energy barriers than when using $P(OMe)_3$ ($\Delta\Delta G$'s between 0.7 and 1.6 kcal·mol^{-1}). However, all the barriers are consistent with the heating requirements and the experimental results.

Comments of Figure A8.

The use of Pd-PMe_3 as model complex in the reductive elimination step to provide the (3+2) cycloadduct (**TS47-17m**), compared to analogous using $P(OMe)_3$ (**TS6-17m**, **Figure 27**, *Section 4.3*, page 157), involves a higher energy penalty ($\Delta\Delta G$=3.5 kcal·mol^{-1}). The transmetalation steps **TS9-10** (**Figure 27**) and **TS50-51** (**Figure A8**), show similar barriers ($\Delta\Delta G$=0.6 kcal·mol^{-1}). Regarding the next reductive elimination to give the cross-coupling product **34ma**, comparing **TS11-34ma** (**Figure 27**) and **TS52-34ma** (**Figure A8**), the use of $P(OMe)_3$ favors this step with the associated energy penalty differing in 5.9 kcal·mol^{-1}.

The results of **Figures 27**, **A7** and **A8** highlight that the π-acidic character of the monodentate ligand plays a crucial role in the selectivity of the process, favoring the formation of cycloisomerization /cross-coupling products regarding an intramolecular (3+2) cycloaddition proces

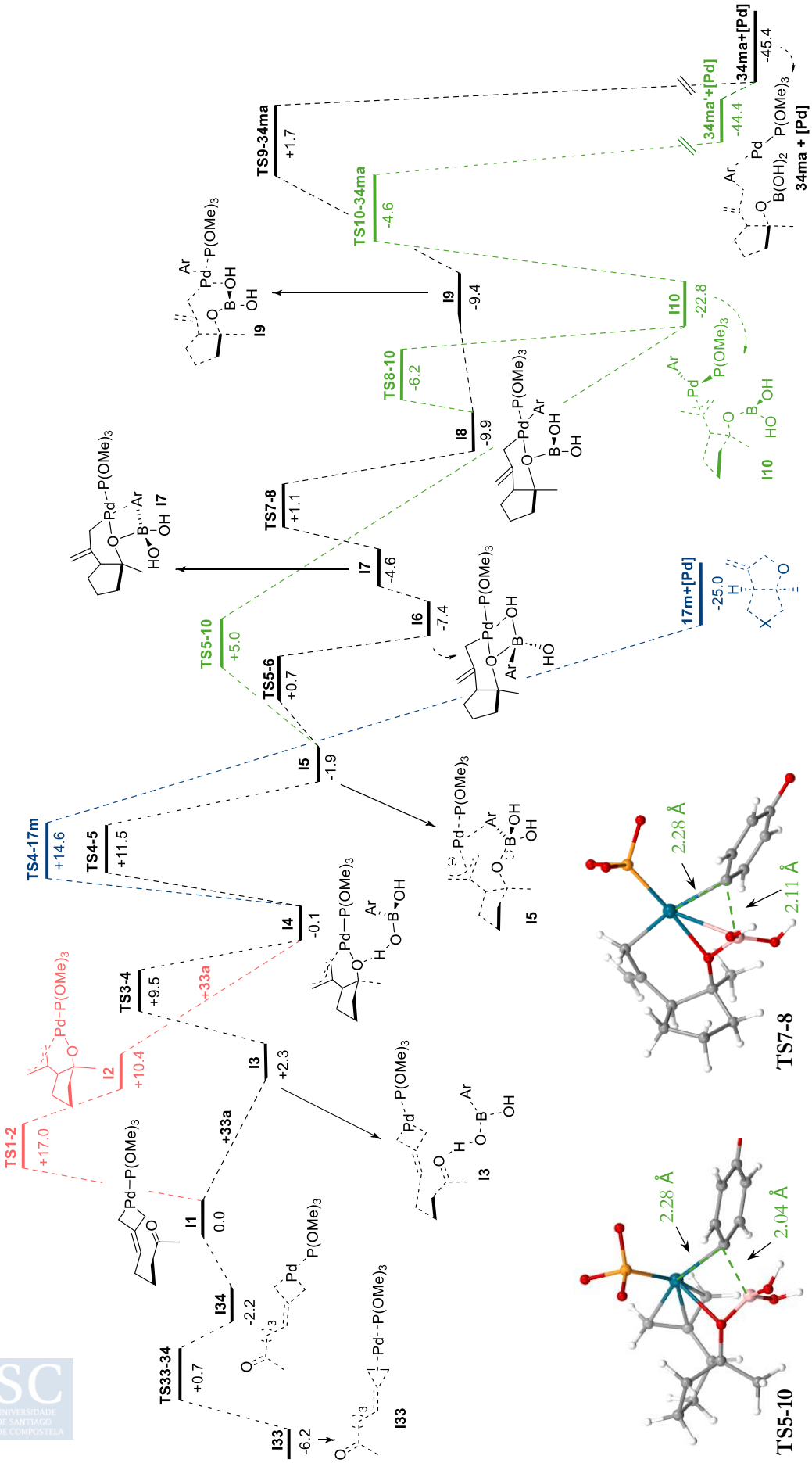

Figure A5. Complete DFT energy profile ΔG_{solv} (kcal·mol^{-1}) for the tandem process between **9m** and boronic acid **33a** using Pd(0)-P(OMe)$_3$, in 1,4-dioxane. [B3LYP/6-31G(d) (LANL2DZ for Pd)//M06/6–311++g(d,p) (SDD for Pd)]. Ar=*p*(MeO)C$_6$H$_4$.

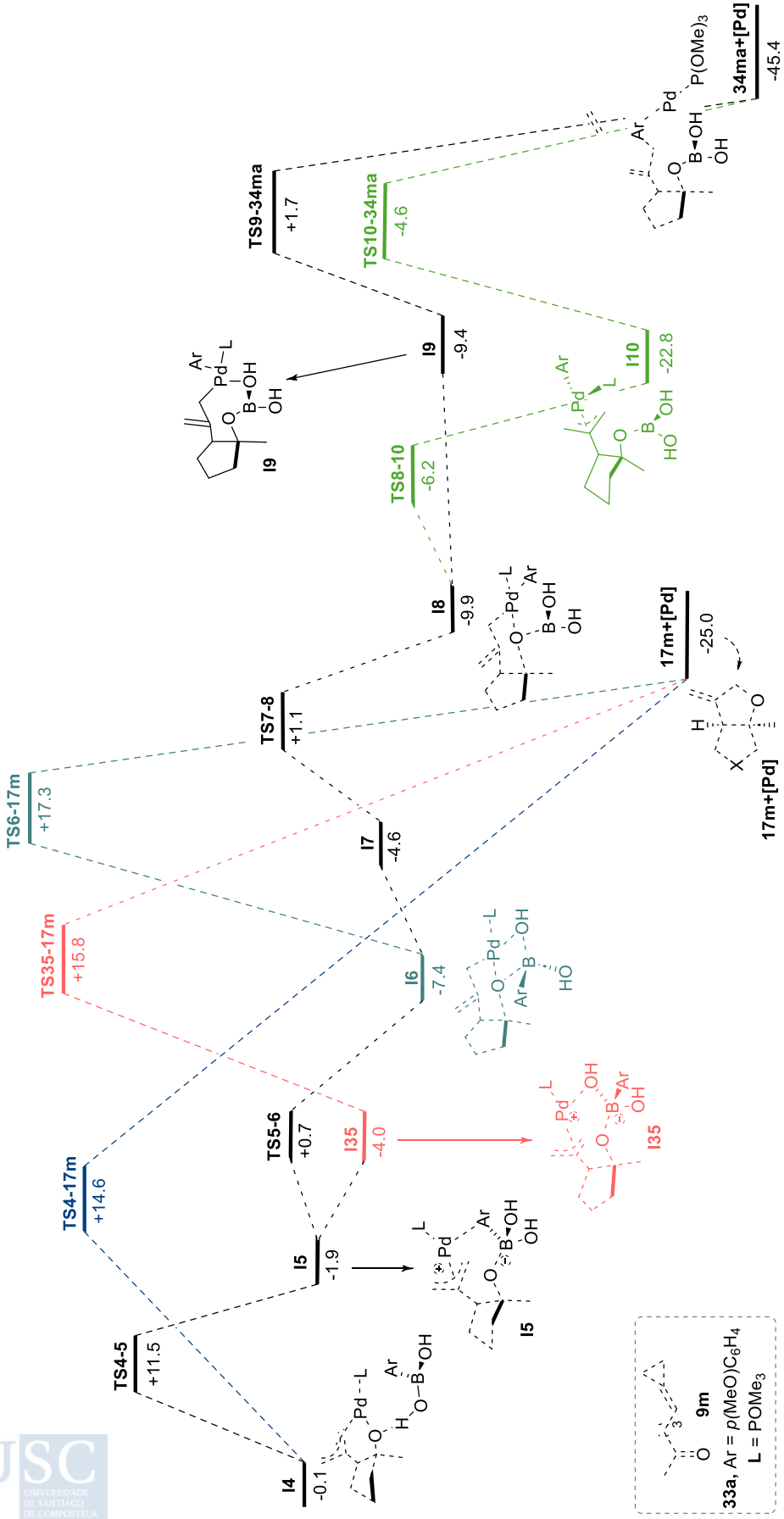

Figure A6. Calculated energy pathways for the formation of the (3 + 2) adduct **17m** through alternative C-O reductive eliminations (kcal·mol^{-1}) using **9m** and boronic acid **33a** with Pd(0)-P(OMe)$_3$, in 1,4-dioxane. [B3LYP/6-31G(d) (LANL2DZ for Pd)//M06/6–311++g(d,p) (SDD for Pd)]. Ar=*p*(MeO)C$_6$H$_4$.

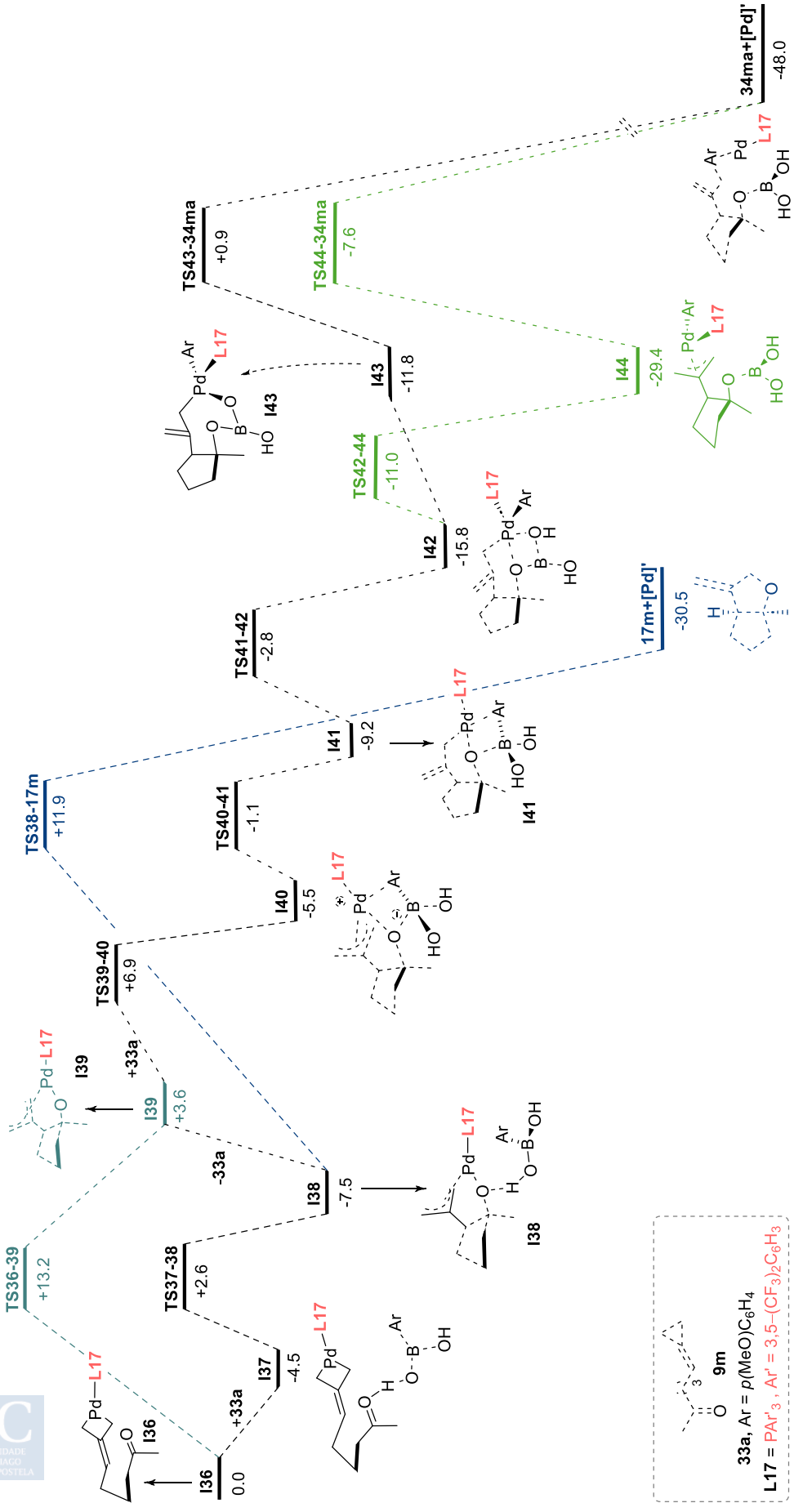

Figure A7. Analysis of the cycloisomerization/cross-coupling pathway using **L17** as ligand. Energy profile ΔG_{solv} (kcal·mol^{-1}) using **9m** and boronic acid **33a** with Pd(0)-**L17**, in 1,4-dioxane. [B3LYP/6-31G(d) (LANL2DZ for Pd)//M06/6–311++g(d,p) (SDD for Pd)]. Ar=*p*(MeO)C_6H_4.

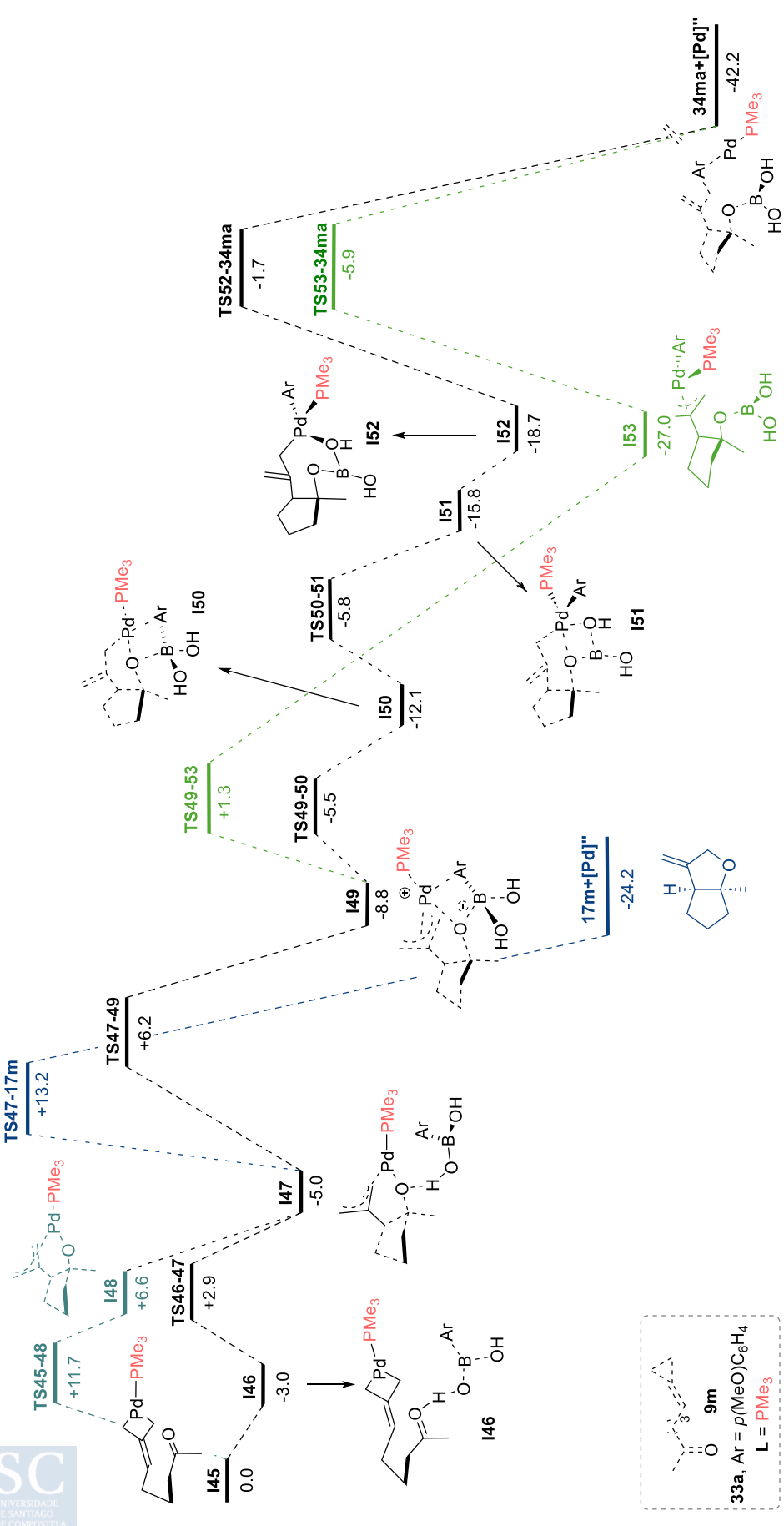

Figure A8. Analysis of the cycloisomerization/cross-coupling pathway using $\mathbf{PMe_3}$ as ligand. Energy profile ΔG_{solv} (kcal·mol^{-1}) using **9m** and boronic acid **33a** with Pd(0)- $\mathbf{PMe_3}$, in 1,4-dioxane. [B3LYP/6-31G(d) (LANL2DZ for Pd)//M06/6–311++g(d,p) (SDD for Pd)]. [Ar=*p*(MeO)C$_6$H$_4$].

Related to Section 4.4. Pd(0)-Catalyzed Cross-Coupling between ACPs and Boronic Acids

This part of the appendix contains three additional figures: **Figures A9**, **A10** and **A11**

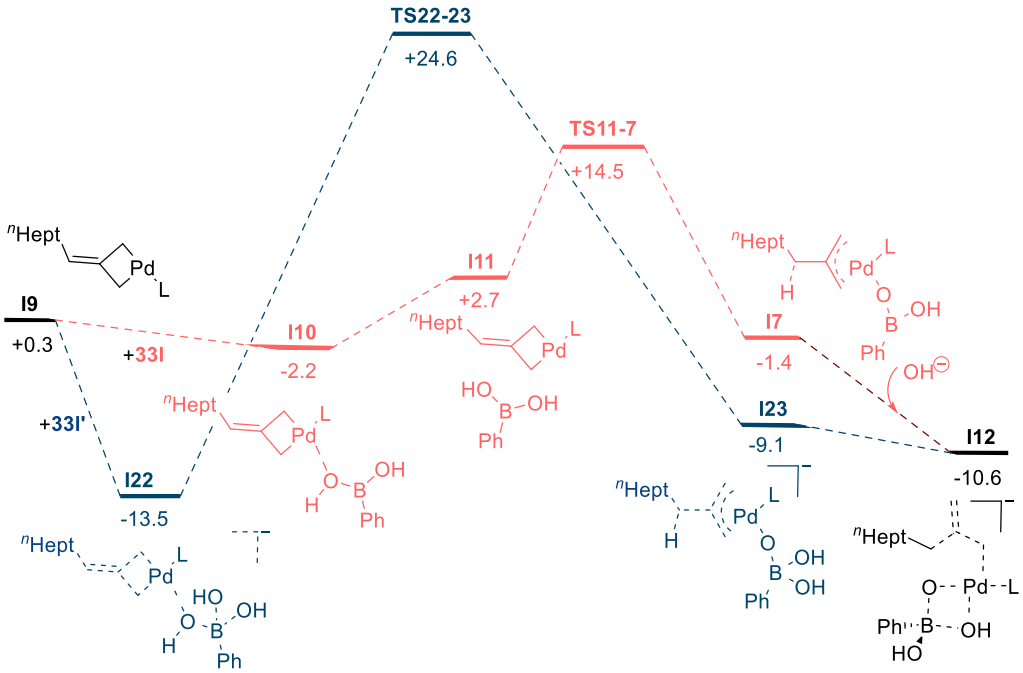

Figure A9. Energy profile ΔG_{solv} (kcal·mol^{-1}) for the model reaction involving **19b**, phenyl boronic acid (**33l**), trihydroxy(phenyl)borate (**33l'**) and Pd(0)-P(OPh)$_3$, in 1,4-dioxane. [B3LYP/6-31G(d) (LANL2DZ for Pd)//B3LYP-GD3/6–311++g(d,p) (SDD for Pd)].

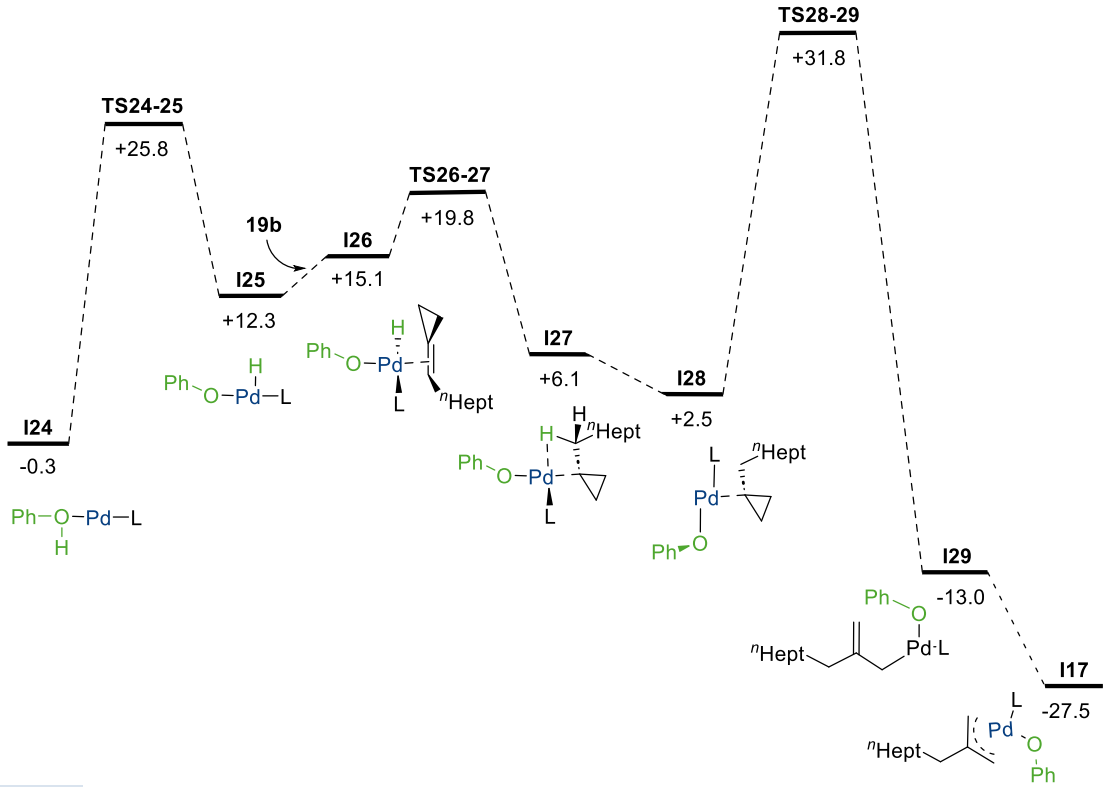

Figure A10. Energy profile ΔG_{solv} (kcal·mol^{-1}) for the model reaction involving **19b**, phenol and Pd(0)-P(OPh)$_3$, in 1,4-dioxane. [B3LYP/6-31G(d) (LANL2DZ for Pd)//B3LYP-GD3/6–311++g(d,p) (SDD for Pd)].

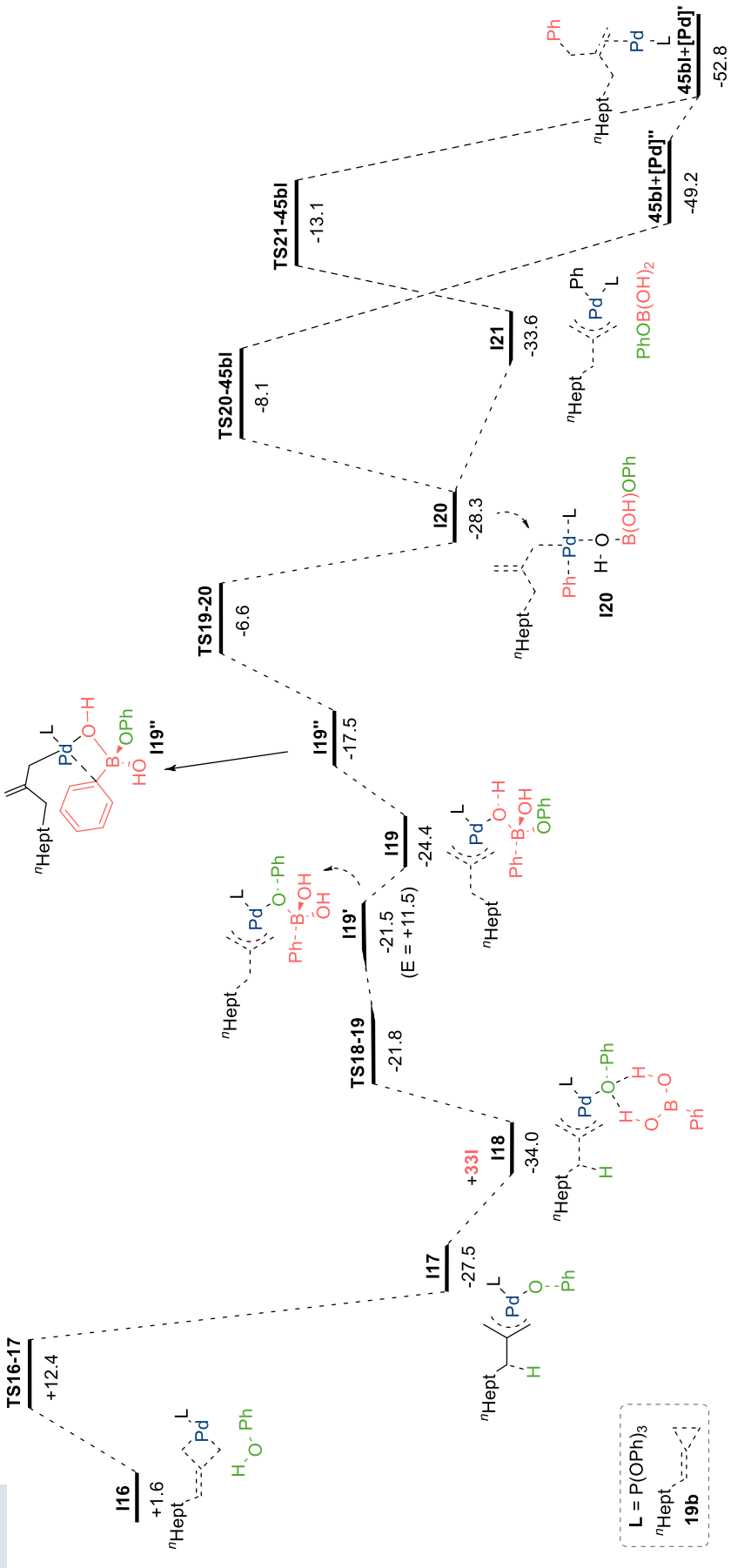

Figure A11. Energy profile ΔG_{solv} (kcal·mol^{-1}) for the model reaction involving **19b**, phenyl boronic acid (**33l**), phenol and Pd(0)-P(OPh)$_3$, in 1,4-dioxane. [B3LYP/6-31G(d) (LANL2DZ for Pd)//B3LYP-GD3/6–311++g(d,p) (SDD for Pd)].

Related to Section 4.5. Pd(0)-Catalyzed (3+2+2) Cycloaddition between ACPs tethered to Carbonyl Moieties and Isocyanates

For clarity, some steps were omitted in the **Figure 39**. See the next page for a full energy profile (**Figure A12**).

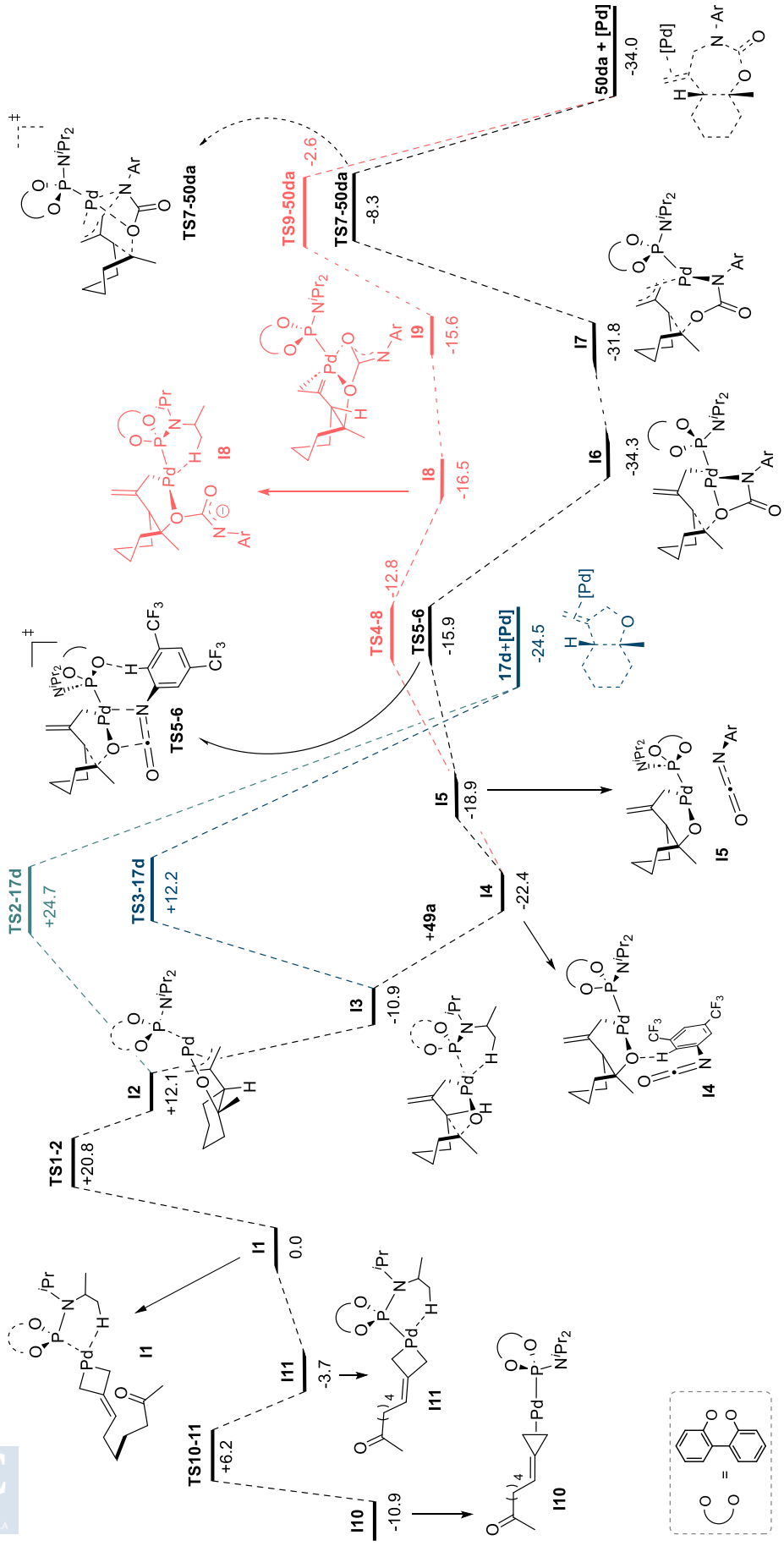

Figure A12. Complete DFT energy profile ΔG_{soln} (kcal·mol^{-1}) for the (3+2+2) cycloaddition of **9d** and **49a** using Pd(0)-**L9**, in 1,4-dioxane. [B3LYP/6-31G(d) (LANL2DZ for Pd)//M06/6–311++g(d,p) (SDD for Pd)]. Ar = 3,5-bis(trifluoromethyl)phenyl.

III. List of Publications

Results and Discussion 4.2:

Title:	Pd-Catalysed (3+2) Heterocycloadditions between Alkylidenecyclopropanes and Carbonyls: Straightforward Assembly of Highly Substituted Tetrahydrofurans
Authors:	Felipe Verdugo, Eduardo da Concepción, Ricardo Rodiño, Martín Calvelo, Jose Luis Mascareñas, Fernando López
Affiliation:	Centro Singular de Investigación en Química Biolóxica e Materiais Moleculares (CIQUS) and Departamento de Química Orgánica, Universidade de Santiago de Compostela, 15782 Santiago de Compostela (Spain)
Journal:	ACS Catalysis
Year:	2020
Volume, pages:	10, 7710-7718
Impact factor:	13.084 (2020)
PhD student contribution:	Study of the reaction mechanism through DFT computations; Discussion of the results and revision of the manuscript

Results and Discussion 4.3:

Title:	Palladium-Catalyzed Tandem Cycloisomerization/Cross-Coupling of Carbonyl- and Imine-Tethered Alkylidenecyclopropanes
Authors:	Felipe Verdugo, Ricardo Rodiño, Martín Calvelo, Jose Luis Mascareñas, Fernando López
Affiliation:	Centro Singular de Investigación en Química Biolóxica e Materiais Moleculares (CIQUS) and Departamento de Química Orgánica, Universidade de Santiago de Compostela, 15782 Santiago de Compostela (Spain)
Journal:	Angewandte Chemie International Edition
Year:	2022
Volume, pages:	61, e202202295
Impact factor:	16.6 (2022)
PhD student contribution:	Discovery of the reaction; Synthesis of starting materials; Screening of conditions; Synthesis and characterization of all compounds; Manipulation of the products; Study of the reaction mechanism through DFT computations; Discussion of the results and revision of the manuscript

Results and Discussion 4.4:

Title:	Palladium-Catalyzed Cross-Coupling between Alkylidenecyclopropanes and Boronic Acids
Authors:	Ricardo Rodiño, Fernando Mardones, Krishna Paredes, Claudio A. Jiménez, Ronald Nelson, Jose Luis Mascareñas, Fernando López, Felipe Verdugo
Affiliation:	Centro Singular de Investigación en Química Biolóxica e Materiais Moleculares (CIQUS) and Departamento de Química Orgánica, Universidade de Santiago de Compostela, 15782 Santiago de Compostela (Spain)
Journal:	Advanced Synthesis & Catalysis
Year:	2024
Volume, pages:	Online version (https://doi.org/10.1002/adsc.202400657)
Impact factor:	4.4 (2023)
PhD student contribution:	Synthesis of starting materials; Screening of conditions; Synthesis and characterization of compounds; Manipulation of the products; Study of the reaction mechanism through DFT computations; Discussion of the results and revision of the manuscript

IV. Copyright Permissions

All figures, graphs and schemes of this thesis are of original design, with some elements inspired by the publications related to the research. Copyright permissions for these publications are provided below.

Results and Discussion 4.2:

Pd-Catalyzed (3 2) Heterocycloadditions between Alkylidenecyclopropanes and Carbonyls: Straightforward Assembly of Highly Substituted Tetrahydrofurans

Author: Felipe Verdugo, Eduardo da Concepción, Ricardo Rodiño, et al
Publication: ACS Catalysis
Publisher: American Chemical Society
Date: Jul 1, 2020

Results and Discussion 4.3:

Palladium-Catalyzed Tandem Cycloisomerization/Cross-Coupling of Carbonyl- and Imine-Tethered Alkylidenecyclopropanes

Author: Felipe Verdugo, Ricardo Rodiño, Martín Calvelo, et al
Publication: Angewandte Chemie International Edition
Publisher: John Wiley and Sons
Date: Apr 14, 2022

Licensed Content

Licensed Content Publisher	John Wiley and Sons
Licensed Content Publication	Angewandte Chemie International Edition
Licensed Content Title	Palladium-Catalyzed Tandem Cycloisomerization/Cross-Coupling of Carbonyl- and Imine-Tethered Alkylidenecyclopropanes
Licensed Content Author	Felipe Verdugo, Ricardo Rodiño, Martín Calvelo, et al
Licensed Content Date	Apr 14, 2022
Licensed Content Volume	61
Licensed Content Issue	24
Licensed Content Pages	7

Order Details

Type of use	Dissertation/Thesis
Requestor type	Author of this Wiley article
Format	Print and electronic
Portion	Full article
Will you be translating?	No

Results and Discussion 4.4:

Palladium-Catalyzed Cross-Coupling between Alkylidenecyclopropanes and Boronic Acids

Author: Ricardo Rodiño, Fernando Mardones, Krishna Paredes, et al
Publication: Advanced Synthesis & Catalysis
Publisher: John Wiley and Sons
Date: Oct 15, 2024

Licensed Content

Licensed Content Publisher	John Wiley and Sons
Licensed Content Publication	Advanced Synthesis & Catalysis
Licensed Content Title	Palladium-Catalyzed Cross-Coupling between Alkylidenecyclopropanes and Boronic Acids
Licensed Content Author	José L. Mascareñas, Fernando López, Felipe Verdugo, et al
Licensed Content Date	Oct 15, 2024
Licensed Content Volume	366
Licensed Content Issue	24
Licensed Content Pages	7

Order Details

Type of use	Dissertation/Thesis
Requestor type	Author of this Wiley article
Format	Print and electronic
Portion	Full article
Will you be translating?	No

In this PhD thesis, we explored the reactivity of alkylidenecyclopropanes (ACPs) using Pd-catalysis. We developed Pd-catalyzed (3+2) heterocycloadditions between ACP precursors, and imine and carbonyl partners, providing access to tetrahydrofuran and pyrrolidine scaffolds. Furthermore, a formal Pd-catalyzed (3+2+2) cycloaddition of ACPs tethered to carbonyl moieties with aryl isocyanates was reported. We also developed Pd-catalyzed tandem cycloisomerization/allylic substitution reactions, where Pd(II)-allylic intermediates generated from ACPs tethered to unsaturated moieties were intercepted by various nucleophiles to yield functionalized cyclic alcohols and amines. Moreover, we described a Pd- catalyzed allylic cross-coupling reaction between ACPs and boronic acids, to construct 1,1-disubstituted alkenes.